Extraction and Recovery of Metals from Waste Electrical and Electronic Equipment (WEEE) using Both Traditional and Designer Solvents

A Thesis Submitted for the Degree of Doctor of Philiosophy

by

Aghogho Blessing Obukohwo

College of Health, Medicine and Life Sciences (CHMLS)

Department of Life Science

Division of Environmental Sciences

Brunel University London

April 2022

Declaration of Work

I declare that this thesis 'Extraction and Recovery of Metals from Waste Electrical and Electronic Equipment (WEEE) using Both Traditional and Designer Solvents is entirely my work and where materials in this work could be construed as work of others, it is completely cited and also referenced, and/or with appropriate acknowledgement given.

Signature: 

Name of Student: Aghogho Blessing Obukohwo

Name of 1st Supervisor: Dr Abdul Chaudhary

Name of 2nd Supervisor: Prof Rakesh Kanda

ACKNOWLEDGEMENT

I extend my sincere gratitude to God who gave me the strength to carry on through my PhD research. I appreciate Dr. Abdul Chaudhary and Prof Rakesh Kanda for their guidance, skills and general support through this thesis. I will not forget to thank all the supportive staff of the Environmental sciences in Brunel University London, e^3 Recycling Limited, Neath, United Kingdom for supplying the samples used in this research. Finally, to my sponsor Petroleum Development Trust Fund (PTDF) Nigeria, my wife (Ejedafeta Obukohwo), my son (Simeon Obukohwo), my parents (Mr & Mrs Obukohwo Godwin) thank you for all your prayers and support.

TABLE OF CONTENT

CHAPTER FOUR

FIGURES

TABLES

ACRONYMS

AAS	-	Atomic Absorption Spectrometer
AILs	.-	Anion aprotic ionic liquids
AQ	-	*Aqua-regia* (1:3, HNO_3: HCl)
AQ1 – AQ3	-	*Aqua-regia* (hotplate method)
AQ4 – AQ6	-	*Aqua-regia* (microwave method)
BFR	-	Brominated flame retardant
CA	-	Citric acid
CA1 – CA3	-	Citric acid (hotplate method)
CA4 – CA6	-	Citric acid (microwave method)
COSHH	-	Control of Substances Hazardous to Health
CRT	-	cathode ray tubes
DI	-	Deionized
Dim	-	Dimension
EAA	-	Ethylammonium acetate
EAF	-	Ethylammonium Formate
EDTA	-	Ethylenediaminetetraacetate acid
FAAS	-	Flame Atomic Absorption Spectrometer
HA1 – HA3	-	Hydrochloric acid (hotplate method)
HA4 – HA6	-	Hydrochloric acid (microwave method)
HCl	-	Hydrochloric acid
HCL	-	Hollow Cathode Lamp
HNO_3	-	nitric acid
H_2SO_4	-	sulphuric acid
IL	-	Ionic liquid
IL A	-	1-butyl pyridinium bromide
IL B	-	1-butyl-3-methylimidazolium hexafluorophosphate
IL C	-	1-butyl-3-methylimidazolium bromide
IL D	-	1-(1-cyanoethyl)-3-methylimidazolium bromide
IL E	-	1-(3-cyanopropyl)-3-methylimidazolium bromide
IL F	-	1-[2-(2-hydroxyethoxy)]-3-methylimidazolium chloride
IL G	-	1-(2-cyanoethyl)-3-methylimidazolium bromide
ILA1 – ILA3	-	1-butyl pyridinium bromide (hotplate method)
ILA4 – ILA6	-	1-butyl pyridinium bromide (microwave method)
ILB1 – ILB3	-	1-butyl-3-methylimidazolium hexafluorophosphate (hotplate method)

ILB4 – ILB 6	-	1-butyl-3-methylimidazolium hexafluorophosphate (microwave method)
ILC1 – ILC3	-	1-butyl-3-methylimidazolium bromide (hotplate method)
ILC4 – ILC6	-	1-butyl-3-methylimidazolium bromide (microwave method)
ILD1 – ILD3	-	1-(1-cyanoethyl)-3-methylimidazolium bromide (hotplate method)
ILD4 – ILD6	-	1-(1-cyanoethyl)-3-methylimidazolium bromide (microwave method)
ILE1 – ILE3	-	1-(3-cyanopropyl)-3-methylimidazolium bromide (hotplate method)
ILE4 – ILE6	-	1-(3-cyanopropyl)-3-methylimidazolium bromide (microwave method)
ILF1 – ILF3	-	1-[2-(2-hydroxyethoxy)]-3-methylimidazolium chloride (hotplate method)
ILF4 – ILF6	-	1-[2-(2-hydroxyethoxy)]-3-methylimidazolium chloride (microwave method)
ILG1 – ILG3	-	1-(2-cyanoethyl)-3-methylimidazolium bromide (hotplate method)
ILG4 – ILG6	-	1-(2-cyanoethyl)-3-methylimidazolium bromide (microwave method)
L_D	-	Limit of Detection
LCD	-	liquid crystal display
LOL	-	Limit of Linearity
L_Q	-	Limit of Quantitation
LS	-	Leaste Squares
MA	-	Malic Acid
MA1 – MA3	-	Malic acid (hotplate method)
MA4 – MA6	-	Malic acid (microwave method)
MAF	-	Methylammonium Formate
MSDS	-	Material Safety Data Sheet
NA1 – NA3	-	Nitric acid (hotplate method)
NA4 – NA6	-	Nitric acid (microwave method)
PC	-	Principal components
PCA	-	Principal component analysis
PCB	-	Printed circuit boards
PILs	-	Protic ionic liquid
PPE	-	Personal Protective Equipment
RTIL	-	Room-temperature ionic liquid
SA1 – SA3	-	Sulphuric acid (hotplate method)
SA4 – SA6	-	Sulphuric acid (microwave method)
SEM	-	Scanning Electron Microscope
SME	-	Small or Medium-Sized Enterprise
SD	-	Standard deviation
TA	-	Tartaric acid
TA1 – TA3	-	Tartaric acid (hotplate method)
TA4 – TA6	-	Tartaric acid (microwave method)
USEPA	-	United States Environmental Protection Agency

W1 – W3	-	Deionized water (hotplate method)
W4 – W6	-	Deionized water (microwave method)
WEEE	-	Waste Electrical and Electronic Equipment
XRD	-	X-ray diffraction

Abstract

Waste Electrical and Electronic Equipment (WEEE) are electrical and electronic gadgets known to have reached their end-of-life. They are made of printed circuit boards (PCBs) containing valuable metals like copper, gold, iron, lead nickel, silver, tin and zinc which can leach into the environment when landfilled. Current extraction methods for the recovery and recycling of metals from WEEE uses various solvents which are not selective, releases toxic gases and recover metals in a mixed form which requires further purification steps to recover individual metals.

The main aim of this project is to design and optimise a recycling process which can be regarded as the best available technique (BAT) for the extraction and recovery of metals from WEEE. Two metal extraction methods namely hotplate and microwave were used in this research. The extraction solvents were divided into three categories namely i) inorganic, ii) organic and iii) designer solvents. For clarity, all experiments conducted using hotplate extraction method were labelled as 1-3 and microwave extraction method as 4-6.

The extraction process optimisation was conducted by investigating the effects of various parameters on the extraction of five metals (Cu, Zn, Fe Ni and Pb) from WEEE under identical experimental conditions. The parameters were effect of dose of WEEE used, particle-size, H_2O_2, as an oxidising agent, temperature, extraction time and concentration of solvents. In total, fifteen solvents were used for the extraction of metals from WEEE, four inorganic solvents (*aqua-regia*, nitric acid, hydrochloric acid, sulfuric acid), three organic solvents (citric acid, malic acid, tartaric acid), seven ionic liquids as designer solvents and water. Three of these designer solvents were purchased (1-butyl pyridinium bromide, 1-butyl-3-methylimidazolium hexafluorophosphate and 1-butyl-3-methylimidazolium bromide) while the remaining four designer solvents were synthesized in our laboratory (1-(1-cyanoethyl)-3-methylimidazolium bromide, 1-(3-cyanopropyl)-3-methylimidazolium bromide), 1-[2-(2-hydroxyethoxy)]-3-methylimidazolium chloride and 1-(2-cyanoethyl)-3-methylimidazolium bromide). Flame atomic absorption spectrometer (FAAS) was used for the analysis of metal concentrations.

The limit of detection (L_D) and limit of quantitation (L_Q) were calculated for each metal using the calibration design method. The composition of metals in the WEEE sample was determined using *aqua-regia* at 70 ^{0}C for 6 hours and the composition of the metals were Cu (43.9 %), Zn (22.4 %), Fe (7.3 %), Ni (1.3 %), Pb (1.7 %) and other materials (23.4 %). The results revealed that inorganic solvents were more aggressive than the organic and designer solvents for the extraction of Cu, Zn, Fe, Ni and Pb from WEEE. The optimum conditions for the extraction of metals were 70^{0}C leaching temperature, 120 minutes leaching time, 0.5 g dose, 2 mol/L concentration for inorganic solvents, 25 g/L for organic solvents, 100 g/L for designer solvents and 4.0 mm particle-size. For the data quality assessment (DQA), principal component analysis (PCA) was used as this is the most widely used multivariate data analysis technique. The highest PCA contributors for the effect of dose, particle-sizes, H_2O_2, temperature and time were *aqua-regia*, nitric acid and hydrochloric acid. For concentration effect, it was *aqua-regia* and nitric acid. Apart from *aqua-regia*, the best leaching solvents for each of the metals are as follows: Cu (nitric acid), Zn (all solvents), Fe (hydrochloric acid), Ni (nitric acid) and Pb (nitric acid). The best parameter used was the effect of H_2O_2 which increased the extraction of the metals for most solvents. The extraction efficiency based on the solvents was in the order inorganic > organic > designer solvents. *Aqua-regia* was the best performing solvent followed by nitric acid and sulfuric acid. The organic acids and designer solvents were generally considered to have similar performance. The metals were recovered using electrochemical recovery method. Approximately 82 % of Cu and 30 % of Zn were recovered in 17 hours.

Keywords: Hydrometallurgy, metals extraction, metal recovery, solvents, inorganic acids, organic acids, ionic liquids, citric acid, malic acid, tartaric acid, e-waste, mixed metal wastes, waste electrical electronic equipment.

CHAPTER ONE

Introduction

1.1 Introduction

When wastes have the potential to be recycled and converted to useful materials they are considered as secondary raw materials with great value. Rich ores for the refining of metals are getting scarce gradually and other materials such as low-grade ores and other secondary sources such as tailings, solid and liquid wastes are now considered as economical sources of metal by metallurgical industries. Urban mining is a term widely used to describe the recovery of metals from anthropogenic wastes. In other words, it is a process of recovering elements or compounds from wastes (RPA, 2012; Reuter *et al.*, 2013; Witt *et al*., 2021). Some examples of such wastes are Waste Electrical and Electronic Equipment (WEEE), electroplating wastes and tannery waste. The metals present in these mixed waste streams include both hazardous, transition and precious group metals (mercury, lead, lithium, antimony, beryllium, cadmium, copper, silver, platinum, gold, nickel, zinc). When WEEE and other metal bearing wastes are sent to landfills they may contaminate groundwater due to leaching of metals; they may also pollute soil and air due to fire outbreak or release of hazardous components; they can also fill up landfill volume. (Sum, 1991; Spalvins, 2008; Adediran & Abdulkarim, 2012; Damodaran *et al.*, 2013; Ghandi, 2014; He and Xu, 2014; Kumar *et al.*, 2014; Letsrecycle, 2020; Zhang & Xu, 2016; Das *et al*., 2021; Hsu *et al*., 2019; Tuncuk , 2019; Sabzkoohi *et al*., 2021; Witt *et al*., 2021).

Wastes containing valuable or hazardous metals may need to be sorted for reuse or recycling. In WEEE, the mixture of metals and other materials is heterogenous and this has led to a serious challenge in selective recovery of desired materials. The recovery is low as metals are lost in slag and gaseous effluents is high. However, researchers have also combined complexants and oxidants to study the dissolution of metals. It has been reported by Kumar *et al*., 2014 that 100 % of zinc and copper were dissolved when a combination of 2 mol/L H_2SO_4 and 0.2 mol/L H_2O_2 were used to leach printed circuit board (PCB) at 85 ^{0}C for 8 hours. According to Dhawan *et al.*, 2009, HNO_3 is more effective than HCl and H_2SO_4 in leaching metals from PCB and these mineral acids are known to be really aggressive for metal recovery they are disadvantaged as they release toxic gases (NO_x, Cl_2 & SO_2). Metal recovery through this process is non-selective as the metals are extracted in a mix and a

further purification step is required (Sum, 1991; Oh *et* al, 2003; Veit *et al.,* 2005; Dalrymple, 2007; Oishi *et al* 2007; Eswaraiah *et al.,* 2008; Wu *et al.,* 2008; Dhawan *et al.,* 2009; Damodaran *et al.,* 2013; He and Xu, 2014; Kumar *et al*., 2014; Jadhav & Hocheng, 2015; Wang *et al.* 2016; Zhang & Xu, 2016; Hsu *et al*., 2019; Tuncuk , 2019; Witt *et al*., 2021). Various types of organic acids are considered as environmentally friendly leaching agents and have been used for the extraction of Pb and PbO from scrap battery paste by Sonmez & Kumar, 2009. Citric acid and acetic acid were used to leach large PCB but poor metal slubilization was observed as only 9.89 % and 19.57 % of copper respectively was recovered. However, 100 % Li and 90 % Co have been recovered using 1.25 M citric acid and 1 % vol H_2O_2 at 90 ^{0}C for 30 min and a solid to liquid ratio of 20 g/L. (Seal *et al.,* 2003; Chen *et al.,* 2004; Chen & Tsai, 2004; Du *et al.,* 2004; Pandija *et al*. 2007; Sonmez & Kumar, 2009; Li *et al.,* 2010; Jadhav & Hocheng, 2015; Wang *et al.* 2016; Okwu *et al*., 2021).

I have reported some of the extraction and leaching methods which are currently being used for the extraction of metal values from various types of mixed materials. However, all these methods have their advantages and disadvantages. There is a need to develop new extraction methods, or optimise the existing methods by the synergistic combination, for the extraction and recovery of metals from mixed material like WEEE. The predictions are with the current use of metals like copper, tin and zinc will lead to a situation of non-sustainability within 10 to 20 years time. However, these predictions may be pessimistic and don't take into account the development in the extraction and recovery techniques but we need to take these prediction very seriously (Seal *et al.,* 2003; Chen *et al.,* 2004; Chen & Tsai, 2004; Du *et al.,* 2004; Pandija *et al*. 2007; Sonmez & Kumar, 2009; Li *et al.,* 2010; Jadhav & Hocheng, 2015; Wang *et al.* 2016; Okwu *et al*., 2021).

1.2 WEEE Directive

The WEEE Directive (2012/19/EU) regulates the practice of WEEE recycling in the UK and and this is done by using an environmentally aware approach which involves designing products that is easy for dismantling, reusing, recycling, recoverying and treatmenting of WEEE. It aims to reduce the hazardous substances and quantity of WEEE that goes to landfills yearly and ensures that producers of WEEE setup a national WEEE collection point and system for processing WEEE. This enables easy collection of WEEE from consumers which leads to accountability and reporting to the national enforcement authority. The collection point is known as the Distributor Takeback Scheme (DTS) which is don through

Designated Collection Facilities (DCFs) while the system for processing WEEE is known as the Authorized Treatment Facility (ATF). Organisations wishing to treat WEEE must have the ATF licence and operate within the terms of the licence. The consumers, vendors, distributors, electronics manufacturers, local and national government are involved in implementing the national WEEE scheme. However, military products and largescale industrial tools are excluded from this process. To economically and effectively reuse or recycle WEEE, the Producer Compliance Scheme enables producers to comply with the WEE regulations. It is compulsory for every producer of WEEE to join the scheme as it establishes a link between the Environment Agency, some services and the producers. For newer electronic products entering the market, the amount and types of electronics put into the market is reported, information showing how the end user can dispose the product when it reaches its end-of-life is placed on the new electronics products. The manufacturer has to declare compliance collection compliance and provide evidence in support of the declaration. The treatment facility is updated to ensure they efficiently reprocess the new products (WEEE Regulations, 2013; WEEE Directive, 2012; HSE, 2021).

1.3 WEEE Problems in Nigeria

It has been reported that almost 50 % of WEEE in Africa comes from Europe and only 12 % of global e-waste are recycled yearly. Akuru and Okoro, 2010 and Bonn, 2018 reported that Nigeria gets 60,000 - 71,000 metric tonnes of used electronics with a 10 % rise yearly. However, Iwenwanne, 2019 reported that Nigeria got 56, 000 metric tonnes of WEEE in 2015. Adediran & Abdulkarim, 2012 reported that 75 % of these WEEE are already junk, they are irrepairable, do not function properly and are already near their end-of-life. A third world country like Nigeria, which has fewer landfill sites spread across the country compared to the western nations in Europe and America, struggles to manage various types of waste materials like WEEE (Sum, 1991; Spalvins, 2008; Akuru and Okoro 2010; Adediran & Abdulkarim, 2012; Damodaran *et al.*, 2013; Ghandi, 2014; He and Xu, 2014; Kumar *et al.*, 2014; Zhang & Xu, 2016; Letsrecycle, 2020). Also, Terada, 2012 reported that there is no computer recycling facility in Lagos, Nigeria and the e-waste is dumped across different sites in Lagos. Nigeria is currently plagued with WEEE all over the country and due to the level of poverty most people cannot buy new gadgets hence they turn to buying these ‘e-wastes’ as second-hand products but they do not last long and they are soon discarded indiscriminately. These e-wastes begin to form heap of mixed metals which exposes the environment to metals from the printed circuit boards (PCBs) such as mercury, lead, lithium, antimony, beryllium,

cadmium, copper, silver, platinum, gold, nickel and zinc. Since these e-wastes are in abundance all over the country, some of the locals, particularly young boys, scavenge for valuable component from the waste (**Figure 1.1 a**), collect them and sell the collection at $2. Some locals also resort to recovering metals from the PCBs thereby dismantling and burning (**Figure 1.1 b**) in the open indiscriminately. There is usually clouds of black smoke hanging over such dump sites and when lead solder in these wastes melts it produces toxic lead fumes in the environment which can lead to lead posioning. Also, when plastics melts dioxin and furans are produced. These processes pollutes the entire ecosystem as wildlife and humans are exposed to health risks, air is polluted and the soil gets toxic (Adediran & Abdulkarim, 2012; Terada, 2012; Ogunseitan, 2013). The government of Nigeria is very concerned about these WEEE problems in the country and has sponsored this research to provide an alternative means for small or medium-sized enterprise (SME) to be able to recycle their WEEE in a more environmentally friendly way.

Figure 1.1 (a) Indiscriminate dumping (b) Open indiscriminate burning
Source: (George, 2019; Velis & Cook, 2021)

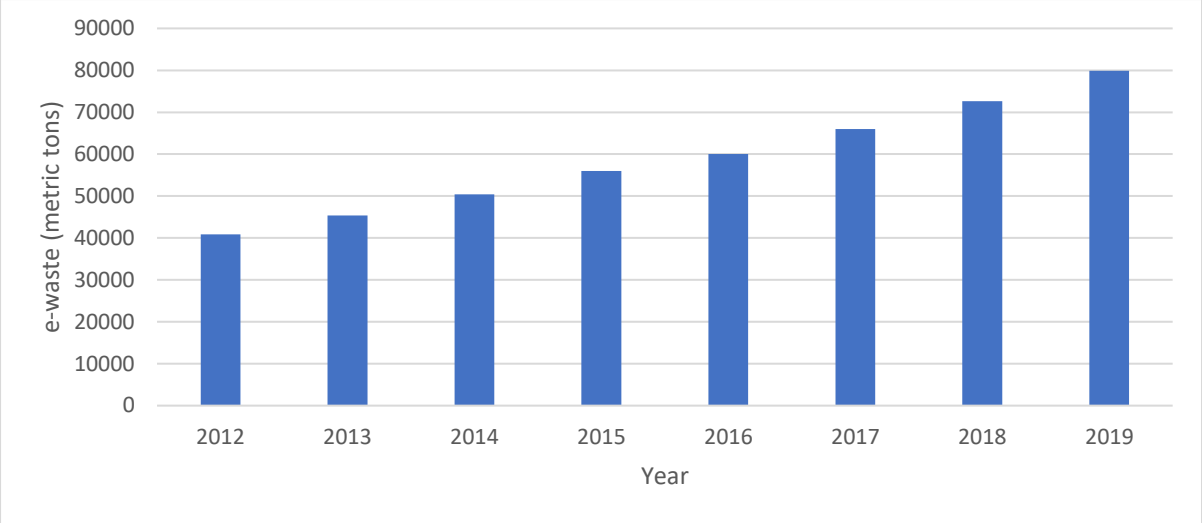

Figure 1.2 Estimated e-waste imported into Nigeria yearly

Adapted from: (Akuru & Okoro, 2010; Bonn, 2018 and Iwenwanne, 2019)

The main focus of this research project is to synthesize, characterize and optimise novel ionic liquids (ILs) and compare the extraction of these designer solvents to traditional solvents (mineral and organic acids) for the extraction and recovery of five metals (Cu, Zn, Fe, Ni and Pb) from WEEE. It has been reported that the use of ionic liquid (ILs) as leaching agents is environmentally-friendly and they do not release toxic substances. Extraction of metals is also task-specific, selective and faster than traditional solvents. Less energy is spent in the process and the desired properties can be designed from ionic liquids (Seal *et al.,* 2003; Chen *et al.,* 2004; Chen & Tsai, 2004; Du *et al.*, 2004; Pandija *et al*. 2007; Sonmez & Kumar, 2009; Li *et al.*, 2010; Jadhav *et al*., 2016; Wang *et al.* 2016; Schaeffera *et al*., 2018; Witt *et al*., 2021).

1.3 Aim and Objectives

The main aim of this project is to compare the extraction and recovery of metals from WEEE, a secondary source of mixed metals, using both traditional and designer solvents.

The objectives are:

- To review the problems associated with the current management of WEEE in Nigeria and highlight the problems associated with the recovery of metals from this secondary waste material.

- To prepare and use some novel ionic liquids (IL), as designer solvents, suitable for the selective extraction and recovery of metals from WEEE.
- To compare the extractions of these novel ionic liquids (ILs) with other traditional solvents such as inorganic (HNO_3, HCl and H_2SO_4) and organic solvents (citric, malic and tartaric acids) for the extraction and recovery of five metals (Cu, Zn, Fe, Ni and Pb) from WEEE.
- To use an electrochemical method for the recovery of individual metals from some selective leaching solutions containing mixed metals.

CHAPTER TWO

Literature Review

2.1. Waste Electrical and Electronic Equipment (WEEE)

Waste Electrical and Electronic Equipment (WEEE) is defined as equipment that require the use of electricity for its function and they are also regarded as equipment which works with electrical networks. Examples are cell phones, computers, televisions, batteries, refrigerators which have reached their end-of-life. These gadgets are made up of wires, printed circuit boards (PCBs), cathode ray tubes (CRT) and liquid crystal display (LCD). Some of the valuable materials WEEE is made up of are metals, plastics, glass and other materials (**Figure 2.1** and **Table 2.1**). These materials contain precious group metals like gold and silver, heavy metals like iron, copper, nickel, lead, cobalt, chromium, cadmium along with other hazardous materials like brominated flame retardant (BFR). **Table 2.2** shows some useful and hazardous components present in WEEE. Every year, between 34 - 54 million metric tons of Waste Electrical and electronic equipment (WEEE) are generated globally and this figure is growing yearly (Habashi, 1999; EU, 2003; Huang, 2009; Terada, 2012; Ogunseitan, 2013; He and Xu, 2014; Zhang & Xu, 2016; Statista, 2021). The research by Kiddee *et al.,* 2013 showed that 500 million tons of computers were discarded in the United States while at the end of 2010 about 610 million tons of computers became outdated in Japan (Kiddee *et al*., 2013; Park *et al*., 2014; Hadi *et al.*, 2015; Zhang & Xu, 2016). In Nigeria for instance, 60,000 – 71,000 tons of used equipment are imported yearly and the largest market for computers in Ikeja, Lagos and the Computer and Allied Product Dealers Association stated that about 75 % of the electronics shipped to the country are considered wastes from the source country; 19 % of these electronics do not function properly and are already near their end-of-life but they become useful to the Nigerian second-hand market as the level of poverty does not allow the people to afford new gadgets hence the reason for the large market of e-waste. The solid waste heap is a source for mixed metals (Adediran & Abdulkarim, 2012; Letsrecycle, 2020; Okwu *et al*., 2021).

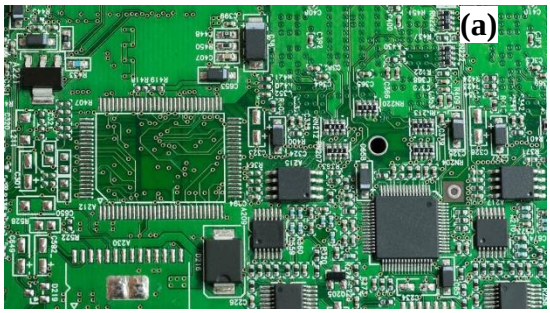
(a)


(b)

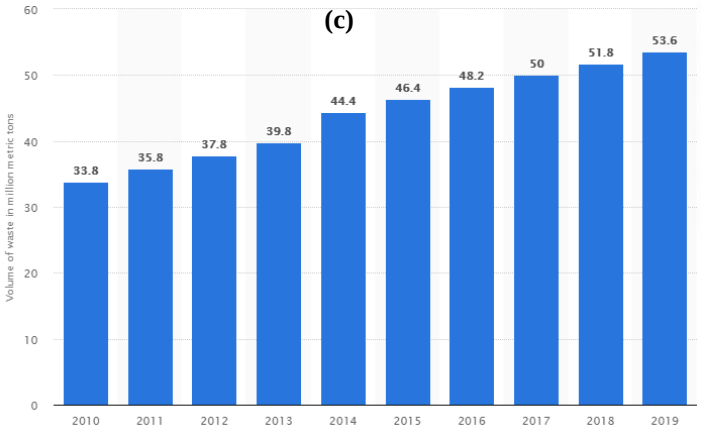

Figure 2.1 (a & b) PCB boards **(c)** Electronic waste generated worldwide (million metric tons)

Source: (Statista, 2021)

Table 2.1. Main components of WEEE

WEEE	Main components
Cell phone	LCDs, PCBs, wires, battery
Computer	LCDs, PCBs, wires, CRTs, speakers, battery
Television	LCDs, PCBs, wires, CRTs, speakers, demagnetized coil, deflection yoke
Refrigerator	Refrigerant, wires, tubes, liners

Adapted from: (He and Xu, 2014; Zhang & Xu, 2016)

Table 2.2. Useful and Hazardous Components in WEEE

Component	Useful components	Hazardous materials
PCBs	Resin, copper, glass, fibre	Brominated flame retardant, heavy metals
CRT	Glass	Pb (PbO)
LCD	Glass, In_2O_3	Liquid crystal, TAC, PVA
Wire	Plastic, copper, aluminium	Polychlorinated biphenyls

Adapted from: (He and Xu, 2014)

The United States Environmental Protection Agency (USEPA) stated that e-waste of 80 – 85 % by weight ends up in landfills and when they are leached the soil gets contaminated along with groundwater in adjacent regions. The study by Splavins *et al*., 2008 showed that when e-waste is mixed with municipal wastes the leaching of lead increased due to more aggressive

acidic conditions. It has been reported by Vehlow *et al.,* 2000 that the incineration of e-waste with municipal waste will lead to the formation of brominated and chlorinated dioxins and furans which are extremely toxic chemicals. Therefore, the use of open indiscriminate dumping, burning (**Figure 2.2 a-b**), landfill and incineration for the management of WEEE are not environmentally friendly options and don't comply with the sustainability principles (Vehlow *et al*., 2000; Splavin *et al*., 2008; Adediran & Abdulkarim, 2012; Tuncuk *et al.,* 2012; Hadi *et al.*, 2015; Wang and Xu, 2015; Okwu *et al*., 2021).

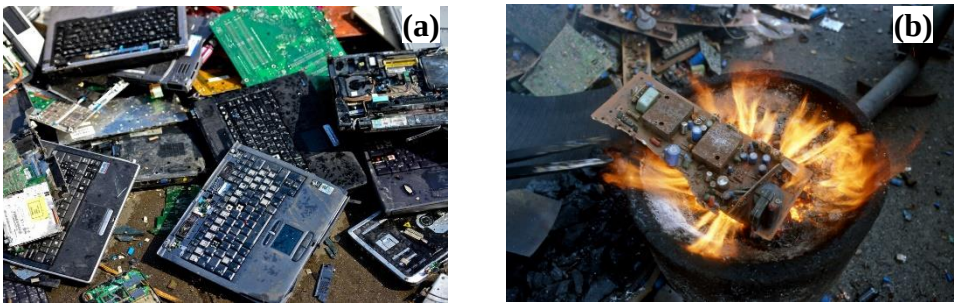

Figure 2.2 (a) Discarded WEEE (b) Burning of e-waste
Source: (Haqshenas, 2018; Tribuneonlineng, 2018)

There is high value of precious metals in e-wastes and PCBs contains larger portions of precious metals since microelectronic components like capacitors and semiconductor chips are mounted on them. Most electric and electronic equipment contain PCBs which make up 3 % of all WEEE produced. Nearly 160 – 210 kg of copper and 80 – 1,500 g of gold can be contained in one metric ton of circuit boards and, when compared to mining in the United States, the amount of gold is 40 – 800 times and the amount copper is 30 – 40 times the amounts present in the ores which are currently being processed. PCBs are the most economically attractive portion of WEEE but as they are mixed with both hazardous and precious materials such as metals, organics, fibre glass, plastics in small volumes it poses difficulty in extraction, recovery and recycling of materials of interest. **Table 2.3** shows the composition of materials in a populated PCB. The separation techniques also limit the exploitation of the materials that can be recovered. There is a growing opportunity in metal recovery in Nigeria and it will be useful to have a safe simple method which industries or individuals can easily use to recover valuable metals from mixed metallic wastes. When the value of resale for a metal can cover the cost of recovery it is given a high priority (Yordanov, 1998; Grossman, 2007; Adediran & Abdulkarim, 2012; Tuncuk *et al.,* 2012;

Canal *et al.*, 2013; He & Xu 2014; Hadi *et al.*, 2015; Wang and Xu, 2015; Akbari, 2019; Das *et al*., 2021; Sabzkoohi *et al*., 2021; Witt *et al*., 2021).

Table 2.3 Composition of Materials in Populated PCBs

Component	Mass (%)
Gold	0.03
Copper	16
Silver	0.05
Nickel	2
Iron	3
Palladium	0.01
Lead	4
Glass-reinforced plastic	> 70

Adapted from: (Bizzo *et al.*, 2014; Hadi *et al.*, 2015)

2.2 Pretreatment of PCBs

In recycling WEEE, a pretreatment step is carried out and this is a physical process of mechanically breaking and then crushing the PCBs. At first, the electronic components are dismantled and are further concentrated based on their physical properties. The physical properties mainly considered are metals and non-metals and this is achieved by using one of the following methods: magnetic separation, eddy current separation, screening, pneumatic separation and electrostatic separation. To completely separate magnetic fractions of the crushed PCBs it is best to use the magnetic separation. However, some non-ferrous metals might be included as a result of insufficient liberation. Eddy-current is more suitable for aluminium fractions and sieving crushed PCBs is necessary as this will help to prevent the influence of different particle sizes during separation. The hazardous components on PCBs are selectively disassembled as this would reduce the amount of toxic elements ending up in the mainstream of the recycling process. During the crushing of PCBs the local temperature of the PCBs increase and some researchers have argued that this process may result in agglomeration and localized pyrolysis of plastics. However, Yuan *et al*. 2007 researched on the using low temperature for crushing PCBs but the method involved high energy cost (Zhang *et al.*, 2012; Havlik *et al.*, 2014; Ghosh *et al*., 2015; Silvas, 2015; Hsu *et al*., 2019; Tuncuk , 2019; Witt *et al*., 2021).

2.3 Hydrometallurgy

Hydrometallurgy process uses a procedure known as leaching where a solution is used to solubilize the crushed metal waste. It also involves purification (solvent extraction or ion exchange) and metal recovery. Hydrometallurgy has one or more aqueous phase and it has been studied as an independent discipline from the alchemist's days. Over the years researches have been conducted to determine hydrometallurgical processes with less setup costs which may be suitable for small scale with high metal yields. Hydrometallurgy is cheap since it requires less capital and high metal recovery but it is disadvantaged by the high level of toxic pollutants such as NO_x, Cl_2 & SO_2. Hydrometallurgy is more suitable method of metal extraction as the primary ores needed for metal refining has become lower in grade (Conard, 1992; Salgado *et al*., 2003; Mooiman *et al*., 2005; Arens & Chernyak, 2008; Sepulveda, 2010; Jadhav & Hocheng, 2015; Jadhav *et al*., 2016). Hydrometallurgy involves the use of acid or base for leaching; it may be combined with electrowinning. Examples of these acidic and basic solvents used for hydrometallurgy are hydrochloric acid (HCl), nitric acid (HNO_3), sulfuric acid (H_2SO_4), thiosulphate ($S_2O_3^{2-}$), thiourea ($(NH_2)_2CS$), sodium cyanide (NaCN). They are known to have several effects on health and environment because the acids solubilize metals and the use of sulfates to remove metals from its solid phase produces harmful sulfate-rich by-product. A large-scale release of this by-product could affect drainage systems. The use of H_2SO_4, HCl and HNO_3 or *aqua-regia* have been investigated by several researchers as very effective leaching agent for heavy metals but the gases released through this process comprises Cl_2, SO_2 and NO_x which poses threat to the persons involved in the experiment and the environment. Other hydrometallurgical problems include the impact of impurities during purification and the time it takes to recover high amount of metals (Li et al., 2010, Park et al., 2013, Park et al., 2014; Tuncuk , 2019; Das *et al*., 2021).

$$M + 4HNO_3 \rightarrow M(NO_3)_{2(aq)} + 2H_2O_{(l)} + 2NO_{2\,(g)}$$

General metal reaction with nitric acid

$$M_{(s)} + 2HCl_{(aq)} \rightarrow MCl_{2\,(aq)} + H_{2\,(g)}$$

General metal reaction with nitric acid

$$M_{(s)} + H_2SO_{4\,(aq)} \rightarrow MSO_{4\,(aq)} + H_{2\,(g)}$$

General metal reaction with sulphuric acid

Where *M* is metal

Some researchers have considered microwave-assisted leaching as a way of improving metal extraction yield and also reducing the process time. Connel & Moe 1966 were the earliest to research the use of microwave energy for heating minerals. Microwave technology is a type of electromagnetic energy which moves through high frequency waves. The microwave energy is a non-contact form of heating also known in the family of electro-heat techniques like infrared heating, radio frequency, direct resistance and induction. It is a very selective heating that is rapid with very efficient energy transfer. It initiates quickly and also terminates quickly. Microwave energy operates within a wavelength of 1 mm to 1 m and a frequency between 300 MHz to 300 GHz. The frequency used the most for the purpose of heating is 915 MHz to 2.45 GHz. In the dissolution stage, metals can be separated if one metal is insoluble in the solvent used. To remove components from the mixture selectively the leaching process usually follows the separation process (Connell & Moe, 1966; Fleming, 1992; Mooiman *et al*., 2005; Demim *et al*, 2013a; Demim *et al*, 2013b; Demim *et al*, 2014; Leyma *et al*, 2016; Yang *et al*., 2016).

2.4 Solvents for Leaching

Common solvents for recovery of metals as reported by other researchers are HNO_3, HCl, H_2SO_4 and *aqua-regia*. Other solvents which are reported in the literature for the extraction of different metals consist of ionic liquids (ILs), cyanide (CN), thiosulfates, thiourea, and Ethylenediaminetetraacetic acid (EDTA). The rate of leaching can be affected by adjusting factors like temperature, stirring intensity, granularity, solid to solution ratio, acid-adding method and acid concentration. A typical leaching setup is shown in **Figure 2.3**. Recycling cost would benefit from reducing the sizes of the PCB as this was reported in the research by Dalrymple, 2007. (Dalrymple, 2007; Oishi *et al* 2007; Dhawan *et al.*, 2009; Jadhav & Hocheng, 2015). Acid, base and salts may be combined in varying proportions to enhance the leaching efficiency of various types of leaching agents. Consequently, the addition of reducing agents such as SO_2 & Fe^{2+} and oxidizing agents like HClO, H_2O_2, NaClO & Cl_2 can also be used to enhance leaching process. One of the most widely used oxidizing agents is H_2O_2 because of its good properties; it is relatively versatile, powerful. It is known to be

stronger than potassium permanganate, chlorine and chlorine dioxide (Oh *et al.,* 2003; Havlik *et al*, 2005; Oustadakis *et al*., 2010; Shawabkeh, 2010; Jadhav & Hocheng, 2015; Wu *et al*., 2015). A general oxidation of the metals is follows:

$$M_{(s)} + H_2O_{2(aq)} \rightarrow M^{2+} + OH + OH^-$$

$$M_{(s)} + OH \rightarrow M^{2+}_{(aq)} + OH^-$$

Where *M* is metal

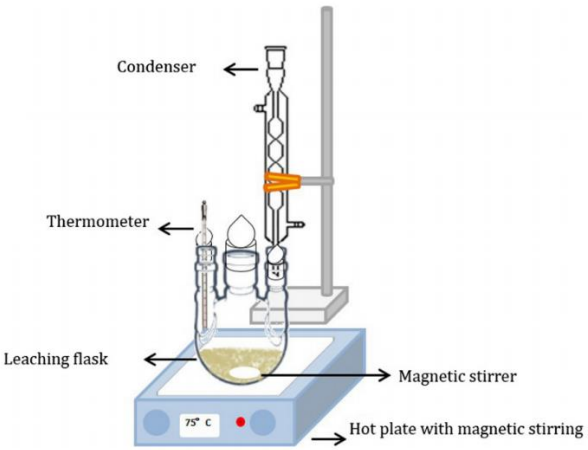

Figure 2.3 A Typical Leaching setup

Source: (Silvas *et al.,* 2015)

2.4.1 Traditional Solvents - Mineral Acids

Mineral acids are formed from inorganic compounds and when dissolved in water they form conjugate base and hydrogen ion. Dhawan *et al.,* 2009's report suggested that HNO_3 is more effective than HCl and H_2SO_4 in leaching metals from PCB. Oishi *et al* 2007 reported that a leach liquour of 45 – 50 g/L was obtained when ammonium sulphate and chloride solutions with oxidizing agent (copper ammine complexes) were used to leach PCB. Almost 100 % of zinc and copper were dissolved when a combination of 2 mol/L H_2SO_4 and 0.2 mol/L H_2O_2 were used to leach PCB at 85 ^{0}C for 8 hours. Although Habbache *et al*, 2009 reported nitrate, chloride and sulfate ions as really aggressive for metal recovery but these inorganic acids are disadvantaged as they release toxic gases (NO_x, Cl_2 & SO_2) and further purification steps are required. When PCBs were shredded to less than 1mm, 95 % aluminium, iron and nickel were leached within 12 hours. Ground PCBs have also been researched by Veit *et al.,* 2005, Eswaraiah *et al.,* 2008, Wu *et al.,* 2008. Other researchers have also combined complexants and oxidants to study the dissolution of copper (Oh *et* al, 2003; Du, 2004; Veit *et al.*, 2005;

Dalrymple, 2007; Oishi *et al* 2007; Eswaraiah *et al.,* 2008; Wu *et al.,* 2008; Dhawan *et al.,* 2009; Kumar *et al*., 2014; Jadhav & Hocheng, 2015; Wang *et al.* 2016).

2.4.2 Traditional Solvents - Organic Acids

Organic acids are compounds composed mainly of carbon and hydrogen atoms. Examples of organic acids used for leaching are citric acid, malic, tartaric acid, and EDTA. Researchers have studied the dissolution behaviour of copper in citric acid using H_2O_2 as oxidizer. Also, glycine as complexing agent and H_2O_2 as oxidizing agent has been used for copper dissolution; copper dissolution was also studied using oxalic acid and H_2O_2 by Pandija *et al.* 2007. Organic acids are attracting attention as they are biodegradable. The recovery of Pb and PbO from scrap battery paste has been studied by Sonmez & Kumar, 2009 using citric acid monohydrate; 4 M of citric acid monohydrate with H_2O_2 was sufficient to leach PbO_2. Citric acid is a natural acid, biodegradable and can dissolve in water with ease; it degrades in both aerobic and anaerobic conditions as it has also been used for the recovery of metals from sewage sludge. Jadhav & Hocheng, 2015 research showed that citric acid and acetic acid were used to leach large PCB for 96 hours and 364 hours but poor metal solubilization was observed as only 9.89 % and 19.57 % of copper respectively was recovered. However, Li *et al.,* 2010 research recovered 100 % Li and 90 % Co using 1.25 M citric acid and 1 % vol H_2O_2 at 90 ^{0}C for 30 min and a solid to liquid ratio of 20 g/L (Seal *et al.,* 2003; Chen *et al.,* 2004; Chen & Tsai, 2004; Du *et al.,* 2004; Pandija *et al*. 2007; Sonmez & Kumar, 2009; Li *et al.,* 2010; Jadhav & Hocheng, 2015; Wang *et al.,* 2016).

Biswas & Mulaba-Bafubiandi, 2016 leached oxidized ores using citric acid, oxalic and gluconic acid, 83.6 % Cu and 77.2 % Co were obtained with 0.15 M citric acid at 80 ^{0}C. Other organic acids that have been studied with H_2O_2 as reducing agent are oxalic acid by Sun & Qui, 2012 and malic acid. Ascorbic acid has been used as reducing agent along with citric acid and in the research sintered metal oxides (Cr-substituted hematites) were dissolved. **Table 4.1** shows the best leaching conditions of different metals in organic acids (Manjanna *et al.,* 2001; Li *et al.,* 2012; Li *et al.,* 2013; Sun & Qui, 2012; Biswas & Mulaba-Bafubiandi, 2016).

Table 2.4 Best leaching conditions of metals in different organic acids

Leaching agent	Experimental Condition	% Extraction	Reference
1.25M Ascobic acid	70 ^{0}C, 20 min	98 % Li & 95 % Co	Li *et al.*, 2012
1M Oxalic Acid + 15 vol % H_2O_2	80 ^{0}C, 120 min	98 % Li & 68 % Co	Sun & Qju, 2012
0.1M Citric acid + 0.02M Ascobic acid	80 ^{0}C, 360 min	100 % Li & 80 % Co	Nayaka *et al.*, 2015
1.5M Succinic acid + 4 vol % H_2O_2	70 ^{0}C, 40 min	96 % Li & 100 % Co	Li *et al.*, 2015
1.25M Citric acid + 1 vol % H_2O_2	90 ^{0}C, 30 min	100 % Li & 90 % Co	Li *et al.*, 2013
0.1M Citric acid + 0.02M Ascobic acid	80 ^{0}C, 360 min	100 % Li & 80 % Co	Li *et al.*, 2013
1.5M Aspartic acid + 4 vol % H_2O_2	90 ^{0}C, 120 min	60 % Li & 60 % Co	Li *et al.*, 2013

Adapted from: (Li *et al.*, 2012; Sun and Qiu 2012; Li *et al.*, 2013; Li *et al.*, 2015; Nayaka *et al.*, 2015; Nayaka *et al.*, 2016)

2.4.3 Designer Solvents - Ionic Liquids (ILs)

Ionic liquid (IL) is a molten salt made of cations and anions with melting points below 100 ^{0}C. ILs with below 25 ^{0}C is regarded as a room-temperature ionic liquid (RTIL). ILs have non-flammable property and a negligible low vapour pressure. They also have properties that can be tuned to suit specific purpose or design. ILs also have distribution coefficients that is enhanced. The distribution coefficient is the ratio of concentration of a substance in one phase to the concentration in another phase when both concentrations are in equilibrium. Ionic liquids have specific properties that make them unique and some of these properties are miscibility with water and organic solvents, high solubility which means they only need small reactor volumes; they have good extractability for metal ions and organic compounds, good thermal stability up to 200 ^{0}C, large spectra transparency and good solvating properties; they are easy to prepare and relatively cheap. Other properties of ILs include exhibition of Franklin acidity, Bronsted Lewis and super-acidity. ILs are very good solvents as they do not dissolve glass or polythene and are good for organic, inorganic and polymeric materials. A researcher like Kenneth R Seddon earlier predicted that IL has the potentials to revolutionize activities where liquids are used. It is a task-specific method which is faster than using traditional solvents and the process does not release toxic gases (Seddon, 1997; Suarez *et al*,

1998; Welton,1999; Visser *et al*, 2001a; Berthod *et al*, 2008; Domanska & Rekawek, 2009; Leyma *et al*, 2016).

The most common ionic liquids used for the separation of metal ions is 1-butyl-3-methylimidazolium hexafluorophosphate, [BMIM][PF6], 1-butyl-3-methylimidazolium hexafluorophosphate, [BMIM][PF6], or 1-hexyl-3-methylimidazolium hexafluorophosphate, [HMIM][PF6] or other ILs with hexafluorophosphate, PF^{-}_{6} , or bis[(trifluoromethyl)sulfonyl]imide, NTf^{-}_{2}, anions. Ionic liquids have a character that is hydrophobic and this enables them to extract compounds that are also hydrophilic in biphase separation. However, in a system that is biphasic the extractant would remain in the hydrophobic phase to enable the removal of the metal ion from the aqueous phase. There is a challenge of determining new classes of solvents for traditional separation with the ability to partition the solvent phase quantitatively and can also complex target metal ions readily or even identifying suitable conditions for which specific metal ion species could be extracted selectively from aqueous streams which contains complexing ions that are inorganic (Seddon, K.R., 1997; Visser *et al*, 2001a; Domanska & Rekawek, 2009).

Due to the unique physical and chemical properties of ionic liquids they have been used as alternatives for solvents in various applications. ILs are also used particularly in clean technology in place of conventional solvents. The most common formulation of ILs are the imidazolium or pyridilium cations which bears a simple appendage of the alkyl cation group. The physical properties of these ILs have been achieved by altering length of the alkyl group in the ring. This allows modifying the melting points, viscosity and hydrophobicity (Gordon *et al*., 1998; Visser *et al*., 2001a; Visser *et al*., 2001b; Domanska & Rekawek, 2009).

Other aspects of ILs formulation include appendage of side chains like ions and heterocyclic aromatic molecules with complex functions and structures. However, some research has shown that the use of ILs is faced with the challenge of recovering the extracted metal ions and solubilization losses. ILs can be prepared by combining bulky organic cations like 1-butyl-3-methylimidazolium or 1-butylpyridinium with a wide variety of anions with different types of anions. The variation in the anions and cations of ILs are used to control the properties of ILs. Altering the anion of ILs has been well investigated and the effect has been understood. An example is the preparation of salts based on aluminium (III) chloride which are basic, acidic and very water sensitive while those anions based like triflate and hexafluorophosphate are highly hydrophobic and neutral. However, chemical modification

effect of cations in ILs has been less studied and not well understood. An increase in cation chain length is expected to alter the melting point as well as the hydrophobicity and viscosity of the liquids. Liquid crystalline phase on melting point could be formed as a further effect. 1-butyl-3-methylimidazolium hexafluorophosphate, [bmim][PF6] has found an increasing use as it is easy to produce and almost insoluble in water (Gordon *et al*., 1998; Visser *et al*., 2001a; Visser *et al*., 2001b; Domanska & Rekawek, 2009; Schaeffera *et al*., 2018).

Table 2.5 and **2.6** shows the generic structure of common ILs and some selected properties. The choice of anion and the length of the alkyl chain in the cation determines the properties of alkylimidazolium ILs. The anion chosen determines the water miscibility of the IL which in turn affects the property of the liquid. Increasing the length of the cation chain from butyl to hexyl or butyl to octyl increases the viscosity and hydrophobicity of the ILs while the surface tension and density is decreased (Stepnowski, 2006).

Table 2.5 Common ionic liquids

Type of Ionic liquid & Structure	Type of Ionic liquid Structure
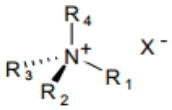 Alkyammonium	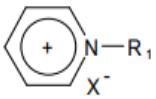 Alkylpyridinium
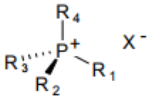 Alkylphosphonium	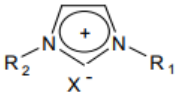 Alkylimidazolium

Where R_x: -CH_3 to -C_9H_{19}; **X^-:** $AlCl_4^-$, SbF_6^-, $CF_3SO_3^-$, PF_6^-, $(CF_3SO_2)_2N^-$

Source: (Stepnowski, 2006)

Table 2.6 Selected properties of 1-butyl- and 1-hexyl-3-methylimidazolium chlorides, tetrafluoroborates and hexafluorophosphates

Ionic Liquid	Water Solubility	Melting Point (^{0}C)	Viscosity (cP)	Temperature Limit (^{0}C)	Density g/ml)
[BMIM][PF_6]	NS	10	371	349	1.37
[BMIM][Cl]	S	41	716	254	1.08
[BMIM][BF_4]	S	-81	219	360	1.12
[HMIM][PF_6]	NS	-61	582	376	1.30
[HMIM][Cl]	S	-70	-	253	1.03
[HMIM][BF_4]	PS	-82	314	-	1.21

Where S: Soluble, NS: non-soluble, PS: Partly soluble

Source: (Stepnowski, 2006)

Imidazolium cations commonly used for the preparation of ILs can be made to possess functions that is task-specific. An example is metal legating group which could enhance the partitioning of target metal ions from water into the ILs phase. When imidazolium cations are used in less expensive ILs it also improves the partitioning of target metals. **Table 2.7** shows some physicochemical properties of selected ionic liquids (Gordon *et al*., 1998; Visser *et al*., 2001a; Visser *et al*., 2001b; Domanska & Rekawek, 2009). Due to the unique properties like negative vapour pressure and flame resistance possessed by ionic liquids they have been highlighted as green solvents which are also alternative to conventional solvents. By combining the ion pairs of ionic liquids their physicochemical properties can be readily tunable. Also, the development of extractant compatibility with hydrophobic ILs have been developed by researchers. However, difficulty has been encountered in discovering a commercial extractant that would be soluble in ILs or in stripping metals ions from extracting ILs phase. Typical examples are the organophosphorus extractants like the di(2-ehtylhexyl) phosphoric acid (D2EHPA) and PC-88A (2-ethylhexylphosphonic acid mono-2-ethylhexyl ester) are used as extractant which separates and purifies rare earth metals since they exhibit high extraction and selectivity for rare earth metals but the solubility of these extractants in ionic liquids are still poor. However, N, N-dioctyldiglycol amic acid (DODGAA) is a phosphorus-free green extractant which works well as a carrier for an IL-based membrane or as an extractant of rare earth metal in ILs.

Researchers like Yang *et al*., 2012 previously confirmed that DODGAA should be suitable for extracting rare earth metals using imidazolium based IL (Freemantle, 1998; Renner, 2001;

Binnemans, 2005; Sun *et al.*, 2012; Baba *et al.*, 2011; Naganawa, *et al*., 2007; Shimojo *et al*., 2007; Kubota, *et al.*, 2010; Kubota *et al.*, 2011; Yang *et al*., 2012; Yang *et al*, 2013).

Alternative leaching agents which do not release toxic substances are gaining more attention. Ionic liquids (ILs) and organic solvents are some of the solvents useful for hydrometallurgy. There are a good number of literature of the study of aprotic ILs but there are limited literatures on the ionicity of protic ILs. Rogers and Coworkers used 1-butyl-3-methylimidazolium hexafluorophosphate [C4mim][PF6] as extractant for Hg^{2+} and Cd^{2+} (Wei *et al.*, 2003; Li *et al.*, 2010, Park *et al*., 2013, Park *et al.*, 2014; Schaeffera *et al*., 2018).

Table 2.7 Physicochemical properties of selected ionic liquids

Class	Ionic liquid	Cation name	Melting point (^{0}C)	Density (25 ^{0}C)	Viscosity (25 ^{0}C) (cP)	Solubility in water
Bis(trifluoro methylsulfonyl) amide	EMIM $NTfO_2$	1-Ethyl-3-methyl imidazolium	-17	1.52	18	N
	MM2PMIM $NtfO_2$	1,2- Dimethyl-3-propylimidazolium	15	1.46	41	N
Halogenate	EMIM Cl	1-Ethyl-3-methyl imidazolium	89	1.12	Solid	S
	BMIM Cl	1-Butyl-3-methyl imidazolium	65	1.10	Solid	S
	Na Cl	Sodium	801	2.16	-	S
	Na Br	Sodium	747	2.17	-	S
	Na I	Sodium	661	3.66	-	S
	Na F	Sodium	993	2.56	-	S
Dicyanamide	EMIM DCA	1-ethyl-3-methyl imidazolium	-21	1.06	21	-
	BMIM DCA	1-butyl-3-methyl immidazolium	-6	1.06	27	S
Tetrafluoroborate	EMIM BF_4	1-ethyl-3-methyl imidazolium	6	1.248	66	S
	BMIM BF_4	1-butyl-3-methyl imidazolium	-82	1.208	233	S
Hexafluorophosphate	BMIM PF_6	1-butyl-3-methyl imidazolium	10	1.373	400	18g/L
	HMIM PF_6	1-Hexyl-3-methyl imidazolium	-61	1.304	800	N
Perfluroalkylsulfate	EMIM TfO	1-ethyl-3-methyl imidazolium	-9	1.39	45	S
	EEIM TfO	1,3-diethyl imidazolium	23	1.33	53	-

Formate (methanoate)	EAF	Ethyl ammonium	-10	0.990	11.5	S
	BAF	Butyl ammonium	-10	0.973	22.2	S
Acetate (ethanoate)	EMIM Act	1-ethyl-3-methyl imidazolium	-20	1.03	91	S
	BMIM Act	1-butyl-3-methyl imidazolium	-20	1.06	525	S
Thiocyanate	BA SCN	Butylammonium	20.5	0.949	97	S
	DPA SCN	Dipropylammonium	5.5	0.964	86	S
Nitrate	EA NO_3	Ethylammonium	12.5	1.122	32	S
	PA NO_3	Propylammonium	4	1.157	67	S

Where S: soluble, N: non-soluble, Tfo: triflate anion or trifluoromethyl sulfate

Adapted from: (Welton,1999; Liu *et al*, 2005; Stepnowski, 2006; Berthod *et al*, 2008)

Anion aprotic ionic liquids (AILs) have been widely studied for their physicochemical and electrochemical properties like density, melting point, chemical reactivity, electrochemical window and ionic conductivity and high thermal stability properties but the protic ionic liquid (PILs) which is relatively cheaper and easier to synthesize lack sufficient literatures as their use in metal extraction is not yet well studied. The mixing of ionic liquids with conventional solvents which improves its properties have also been studied. A recent ionicity study on aprotic and protic ionic liquids in three different molecular solvents by Thawarkar *et al.* (2016) revealed that aprotic ionic liquids displayed 100 % ionicity in water and ethyl glycol while protic ionic liquids also had good ionicity in water and ethyl glycol. A higher ionicity was observed in the aprotic ionic liquids. The study focused on examining properties such as conductivity, viscosity and self-diffusion coefficients (Mennea *et al.*, 2013; Ghandi, 2014; Park *et al.*, 2014; Thawarkar *et al.*, 2016). Leyma *et al.*, 2016 research synthesized novel ammonium and phosphonium ionic liquids with thiosalicylate derivates as anoins. The Ils showed good extraction rates for cadmium and copper but moderate rates for zinc after 24 hours which was a limiting factor. However, the increase in cation size is a reason for higher ionic conductivity for some imidazolium-based PILs; similarly, increase in cation size is a reason for higher conductivity of methyl formate over butyl ammonium formate. There are a few akylammonium based PILs which have a high ion conductivity more than 10 mS.cm-1 at 25 ^{0}C and examples are: methylammonium formate (MAF), ethylammonium acetate (EAA), ethylammonium formate (EAF) (Ghandi, 2014).

2.5 Metal Recovery

Electrochemical method is one of the metal recovery methods which is currently being used for the recovery of metals from different types of leachates. This method has been optimised within our research group for the recovery of different metals from both single and mixed metal solutions (Javaid, 2006).

The types of electrochemical reactors include batch electrochemical reactor, plug flow electrochemical reactor and continuous stirred-tank electrochemical reactor. Electrochemical approach is a clean and simple method of metal recovery and it deals mainly with the process of transferring charges at the interface of a material that is electrically conductive and an ionic conductor. This form of removal has a number of advantages such as safety, affordability and versatility. Equipments required for electrochemical recovery process include electroplating bath, suitable electrodes such as a cathode and an anode that is insoluble. When electricity is introduced to the electrodes which are immersed in the electrolyte it causes oxidation and reduction to occur. The metal ions are reduced at the anode and at the cathode the reaction is very competitive, for example, hydrogen ions are reduced to hydrogen gas. The anode to be used has to be carefully selected such that it would not react with the electrolyte. The metal to be recovered will be deposited at the cathode and this process is referred to as electrochemical deposition. Some other advantages of electrochemical recovery is that it is highly selective and it costs less to operate. Some disadvantages include the solution composition and the rate of deposition causes loose deposits; there is also interference from the evolution hydrogen reaction (Chen & Lim, 2005; Lister *et al*., 2014). This thesis seeks to prepare four novel ionic liquids and compare their extraction efficiencies with three other ionic liquids and traditional solvents.

CHAPTER THREE

Methodology

3.1 Source of WEEE as mixed metal materials

The materials for this research include WEEE containing mixed metals (**Figure 3.1a & b**). The WEEE samples were provided by e^3 Recycling Limited, Neath, SA11 2HZ, United Kingdom, and it was used as supplied. This WEEE sample was made up of 4 mm crushed PCBs and it contains higher percentage of metals as large portions of plastics were physically removed to concentrate the metals. After the sample arrived further sieving to much smaller sizes like < 1 mm, 2 mm, 3 mm and 4 mm was carried out to get different particle sizes for this research.

Figure 3.1 a & b WEEE samples from scrap computers.

3.2 Other materials

The materials used for this experiment were obtained from the Department of Life Science, Division of Environmental Sciences, Brunel University London. All stock standard solutions containing 1,000 mg/L of metal (Cu, Zn, Fe, Ni and Pb) and the leaching solvents mainly inorganic acids, organic acids and ionic liquids were acquired from Sigma-Aldrich and Fisher Scientific. Deionized water (DI) was used as a control leaching agent. The solvents were inorganic acids (HNO_3, H_2SO_4, HCl), organic acids (citric acid, malic acid, tartaric acid) and ionic liquids, IL, (1-butyl-3-methylimidazolium bromide, 1-butyl-3-methylimidazolium hexafluorophosphate, 1-butylpyridinium bromide, 1-(1-cyanoethyl)-3-methylimidazolium bromide, 1-(3-cyanopropyl)-3-methylimidazolium bromide, 1-[2-(2-hydroxyehoxy)]-3-methylimidazolium chloride and 1-(2-cyanoethyl)-3-methylimidazolium bromide)). For ease

of identification in this research the ionic liquids were categorized using alphabets (A, B, C, D, E, F & G) as follows:

- IL A – (1-butyl pyridinium bromide)
- IL B – (1-butyl-3-methylimidazolium hexafluorophosphate)
- IL C – (1-butyl-3-methylimidazolium bromide)
- IL D – (1-(1-cyanoethyl)-3-methylimidazolium bromide)
- IL E – (1-(3-cyanopropyl)-3-methylimidazolium bromide)
- IL F – (1-[2-(2-hydroxyethoxy)]-3-methylimidazolium chloride)
- IL G – (1-(2-cyanoethyl)-3-methylimidazolium bromide)

The following are the chemical structures of the seven ionic liquids (IL A - G):

a)

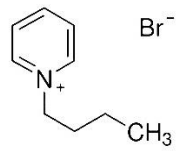

1-butyl pyridinium bromide

b)

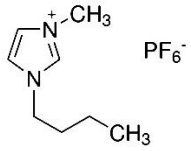

1-butyl-3-methylimidazolium hexafluorophosphate

c)

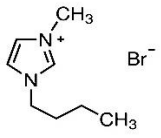

1-butyl-3-methylimidazolium bromide

d)

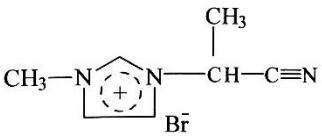

1-(1-Cyanoethyl)-3-methylimidazolium bromide

e)

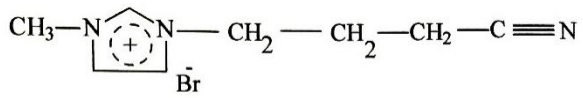

1-(3-Cyanopropyl)-3-methylimidazolium bromide

f)

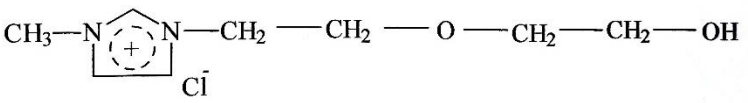

1-[2-(2-hydroxyethoxy)]-3-methylimidazolium chloride

g)

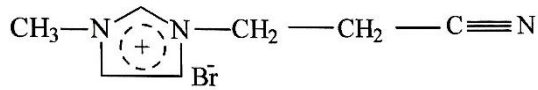

1-(2-cyanoethyl)-3-methylimidazolium bromide

Source: (Javaid, 2006; Merck, 2021a; Merck, 2021b; Merck, 2021c)

Three of the ionic liquids (A, B & C) were purchased from Sigma-Aldrich and Fisher Scientific while the remaining 4 ionic liquids (D, E, F & G) were synthesised using the protocol developed in our laboratory (Javaid, 2006; Faivre, 2009). The starting materials for preparing the ionic liquids (D, E, F & G) were also bought from Sigma-Aldrich and Fisher Scientific . The starting materials were made up of a cation (1 methylimidazole) and an anion which was one of the following: 2 bromopropionitrile, 4 bromobutyronitrile, 2(2-chloroethoxyethanol, 3 bromopropionitrile). DI water was obtained from within the laboratory, glass wares such as flasks and beakers were washed, decontaminated with 3% HNO_3 and rinsed with deionized water, micro-pipette, regular microwave, microwave for digestion or leaching, magnetic hot plates and magnetic followers as well as Flame Atomic Absorption Spectrometer (FAAS), and Scanning Electron Microscope (SEM), were available

in our laboratories. Personal Protective Equipment (PPE) such as buttoned lab coat, gloves, fume cupboard and safety goggles were also provided by the department (See **Figures 3.2 - 3.7**). The reagents used in this research were risk assessed and a control of substances hazardous to health (COSHH) form was prepared using material safety data sheet (MSDS).

Figure 3.2 (a) Fume cupboard for leaching experiments (b) Hotplate for leaching experiment (c) Filteration process using a butchner funnel for leaching experiments (d) Samples from leaching (Leachate) (e) Diluted leachates from leaching experiments

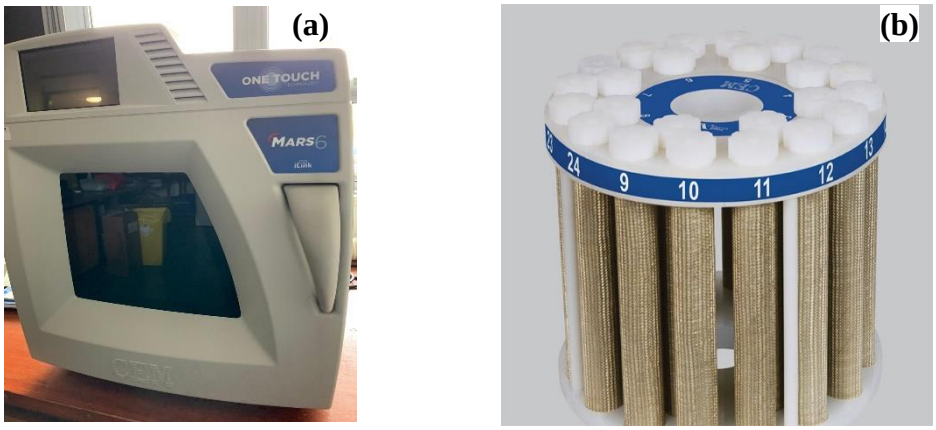

Figure 3.3 (a) MAR-6 CEM Microwave for leaching (b) CEM vessels for holding samples

3.2.1 Extraction Method

All metal extraction experiments were carried out using two methods namely: i) a hotplate method and ii) a microwave leaching method. The process of optimisation for the hotplate method was conducted by investigating the effects of particle-size (1, 2, 3 & 4 mm), temperature (25, 40 & 70 ^{0}C), solvent concentration (inorganic solvents (1, 2, 3 mol/L), organic solvents (15, 25 & 50 g/L) and designer solvents (50, 100 & 250 g/L)), extraction time (30, 60, 90, 120, 150 & 180 minutes) and dosage (0.2, 0.5, 0.7, 1.5, 2.0 & 3.0 g of WEEE). The process of optimisation for the microwave method was conducted by investigating the effects of particle-size (1, 2, 3 & 4 mm), temperature (150 ^{0}C), solvent concentration (inorganic solvents (1, 2, 3 mol/L), organic solvents (15, 25 & 50 g/L) and designer solvents (50, 100 & 250 g/L)), extraction time (20 minutes) and dosage (0.2, 0.5, 0.7, 1.5, 2.0 & 3.0 g of WEEE). Metal bearing waste (WEEE) and leaching solvents were conducted in a 100 ml reaction flask using a magnetic hotplate, magnetic follower and a thermometer to monitor the temperature. The rotation of the stirrer was set to 340 rpm. In this project the amount of WEEE required was first weighed out using a Precisa 400 M Weighing Balance and then transferred into the reaction flask before adding the leaching agent. At the end of the experiment, the solid residue was filtered using a butchner funnel and various dilutions were prepared from the leachate for FAAS analysis.

The composition of metals in the WEEE sample was conducted by dissolving the sample in *aqua-regia* and after the dissolution, all metals were completely dissolved leaving behind plastics and other materials. The process optimisation for the microwave method was conducted by investigating the effects of particle-size (1, 2, 3 & 4 mm), temperature (150 ^{0}C),

solvent concentration (inorganic solvents (1, 2, 3 mol/L), organic solvents (15, 25 & 50 g/L) and designer solvents (50, 100 & 250 g/L)), extraction time (20 minutes) and dosage (0.2, 0.5, 0.7, 1.5, 2.0 & 3.0 g). The amount of WEEE required was weighed out using a Precisa 400 M Weighing Balance. Metal bearing waste (WEEE) and leaching solvents (10 ml) were conducted using the microwave (MARS-6 CEM) vessels. At the end of the experiment, the solid residue was filtered using a butchner funnel and various dilutions were prepared from the leachate for FAAS analysis.

3.2.2 Standard and sample preparation

All standards solutions of known concentration were prepared from a stock solution containing 1,000 mg/L of Cu, Zn, Fe, Ni and Pb. The linearity of these metals according to the FAAS reference guide were 5.0, 6.0, 15.0, 20.0 & 1.0 mg/L respectively. This is the maximum concentration the FAAS can detect for each metal respectively. The FAAS uses the absorbance readings from these prepared standard solutions with known concentration to plot a calibration graph and it then uses the calibration curve to determine the concentration of a sample. The formula $C_1V_1 = C_2V_2$ was used to determine the volume required to prepare 100 ml from the stock solution of each metal standards. An adjustable micropipette was used to measure the calculated volume which was poured into a 100 ml volumetric flask before using deionized water to make up the volume of each corresponding measurement. The samples were prepared by making various dilutions and using micropipette to measure a calculated amount from leachates; this was done to make sure that the metal concentration fall within the limit of quantitation (LOQ) and the limit of linearity (LOL) for each metal.

3.2.3 Blank Preparation

In this experiment deionized water was obtained from the laboratory, Brunel University London, in a clean beaker. The deionized water was used as the blank at the start of every analysis on the FAAS before analysing the standards followed by the sample solutions.

3.3 Synthesis of Ionic Liquids

The method used for the preparation of different types of ionic liquids has already been developed within our own laboratories by Javaid (2006) and Faivre (2009). The research by Varma & Namboodiri (2001) used a regular microwave to synthesis ILs and in this research,

a regular microwave was also used for the synthesis of four ionic liquids (ILs). This was achieved by adjusting the anion chain length. The cation used was 1-methylimidazole (MIM) and the anions were 2 bromopropionitrile, 4 bromobutyronitrile, 2(2-chloroethoxyethanol), 3-bromo propionitrile. These selections were based on the alkyl group length and the metal complexing group. The regular microwave (**Figure 3.4 a-d**) was a Beko microwave oven (Model: MOC 20100W); it was set to 120 Watt (defrost mode) for the synthesis experiment. This method uses microwave heating system to tranfer energy to the reactants directly and this results in product formation (Varma & Namboodiri, 2001; Javaid, 2006; Faivre, 2009).

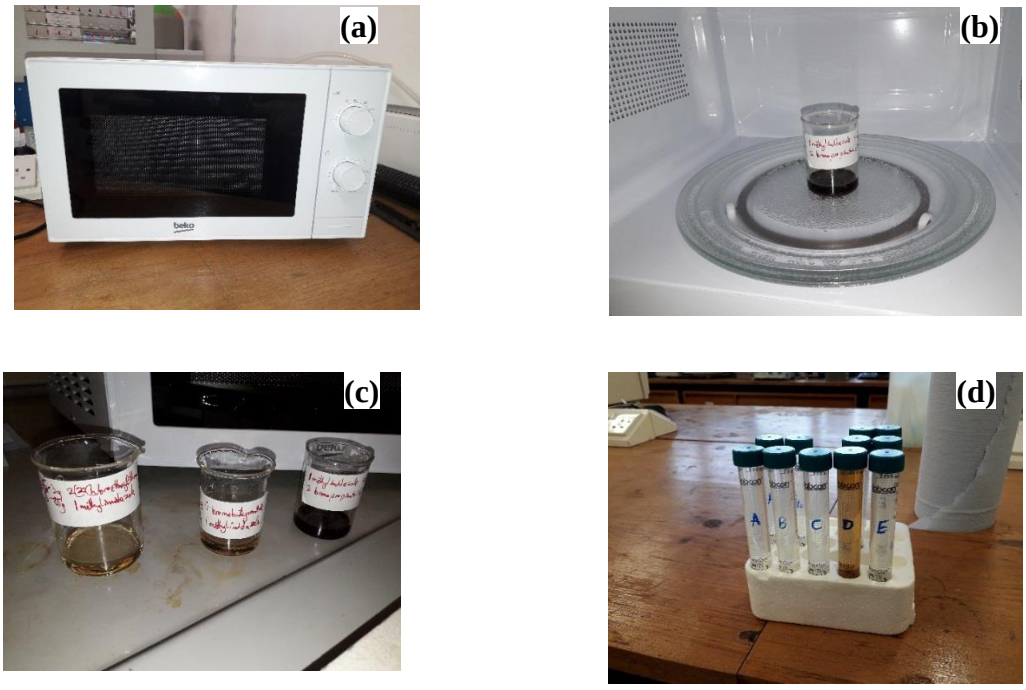

Figure 3.4 (a) Beko microwave oven (Model: MOC 20100W) synthesis of ionic liquids (b - d) samples of prepared ionic liquids

Javaid (2006) synthesised, characterised and optimised the application of these ionic liquids (D–G) on the recovery of copper and zinc compounds from spent catalysts. The starting materials, cation and anion, were mixed in a 1:1.25 ratio respectively (5 g of cation and 6.25 g of anion). Both cation and anion were mixed in a 150 ml beaker and then heated in the beko microwave oven following the sequence in **Table 3.1.** The reaction was complete when a viscous liquid was achieved. Temperature recorded was between 70 ^{0}C and 100 ^{0}C. The newly formed ionic liquid was allowed to cool to room temperature and the product was washed with ether three times to remove any starting materials that did not react then it was allowed to dry. The new product was stored in sample bottles at room temperature.

Table 3.1 Preparation of Ionic Liquids

Ionic Liquids (IL)	Starting materials (Reactant)	Different Heating Time (seconds)	Product (ionic liquid)
D	1-methylimidazole + bromopropionitrile	20, 20, 10, 10 & 10	1-(1-Cyanoethyl)-3-methylimidazolium bromide
E	1-methylimidazole + 4 bromobutyronitrile	20 & 10	1-(3-Cyanopropyl)-3-methylimidazolium bromide
F	1-methylimidazole + 2(2-chloroethoxyethanol)	20, 20, 20, 20, 20, 20 & 20	1-[2-(2-hydroxyethoxy)]-3-methylimidazolium chloride
G	1-methylimidazole + 3 bromopropionitrile	Formed without heating	1-(2-cyanoethyl)-3-methylimidazolium bromide

ILs D – G are not commercially available and they do not have enough information regarding their health and safety. The review by Gonçalves *et al*, 2021 indicated that ionic liquids have been previously considered as green solvents which is safe for human life, health and the environment as they have low vapor pressure. However, some ILs have shown that their biodegradability in the environment is relatively poor as these ionic liquids are produced from energy sources that are non-renewable. ILs could be toxic to one organism and it could be also non-toxic to another organism (Bubalo *et al*., 2014; Neumann *et al*., 2014; Pawłowska *et al*., 2019; Gonçalves *et al*, 2021)

3.4 Instrumentation

The analytical instruments used for the analysis were Perkin Elmer A Analyst 100 Flame Atomic Absorption Spectrometer (FAAS) and the Scanning Electron Microscope.

3.4.1 Atomic Absorption Spectrometer

The FAAS uses the appropriate Hollow Cathode Lamp (HCL) as source of light for the metal. The FAAS makes use of acetylene gas and air as fuel source to power the burner also known as a flame atomizer which excites atoms in the samples (**Figure 3.5 a - d**). The

amount of light absorbed in the process is sent to the detector from the constant frequency emitted through the Lamp. The instrument was turned on, current, wavelength and slit adjusted accordingly to match the reference book. The air and fuel regulators were turned on to ignite the flame and deionized water was aspirated for 10 minutes which was the warm up time for the instrument. The prepared standards were aspirated and the flow optimized by adjusting the aspiration rate until it reached maximum. The oxidant and fuel ratio were also adjusted to obtain optimum fuel to allow the flame colour for each of the metals appear as indicated in the method book for FAAS. This will allow maximum readout of absorbance.

Figure 3.5 (a) Perkin Elmer A Analyst 100 Flame Atomic Absorption Spectrometer (FAAS)

(b) acetylene fuel regulator (c) prepared samples for analysis (d) air regulator

3.4.2 Scanning Electron Microscope

Scanning Electron Microscope (SEM) creates an image by using a focused beam over an image (**Figure 3.6**). An interaction takes place between the electron and the sample and

signals produced can be used to obtain information on the composition and surface topography of the sample. Types of signals produced include, back-scattered electron, reflected, secondary electrons x-ray, light (cathodoluminescence), transmitted electron and absorbed current. Secondary electrons are emitted close to the surface of the specimen when secondary electron imaging is done and very high image resolution can be produced showing up to < 1 nm size of sample surface. Back-scattered electrons are electrons from beam reflected from the sample by elastic scattering and they come from locations that are deep within the sample; its intensity is related strongly to the specimen's atomic number but the resolution from back scattered electron images are lesser than that of secondary electron images. When an electron beam removes an inner shell electron from the sample characteristic x-rays are emitted and energy is released as higher energy electron fills the shell. Wavelength Dispersive Spectroscopy X-ray or an Energy Dispersive Spectroscopy (EDS) measures the wavelength or energy of the characteristic x-ray.

Figure 3.6 Scanning Electron Microscope (LEO 1455VP)
Source: (ETC-Brunel, 2021)

3.4.3 Electrochemical Recovery

Electrochemical recovery process (**Figure 3.7 a -d**) recovers metals values from leached solution and in this process electrodeposition occurs. The control or adjustment of pH is important in the recovery of specific metals, for example $Al(OH)_3$ is used in ensuring the pH is adjusted to the desired level and the presence of one metal might influence the deposition of another metal. The voltage (V) and current (A) are set to achieve the best results. Two anode electrodes and one cathode electrode made of steel are used. The ISO-TECH (model

number IPS-606D) as in **Figure 3.7a** is used to introduce electricity to the electrodes which are immersed in the electrolyte and this causes oxidation and reduction to occur. The ions in the electrolyte flow towards one of the electrodes thereby causing electrochemical deposition to occur. The electrolyte used was HNO_3 from the leaching process, pH was 1, current was set to 1.5 A and voltage was set to 2.9 V. The initial concentration of the metals in the electrolyte was taken at the 0^{th} hour using the FAAS. The time for the experiment was 17 hours (Huyen *et al*., 2016; Zhang & Xu, 2016; Demir *et al*., 2017).

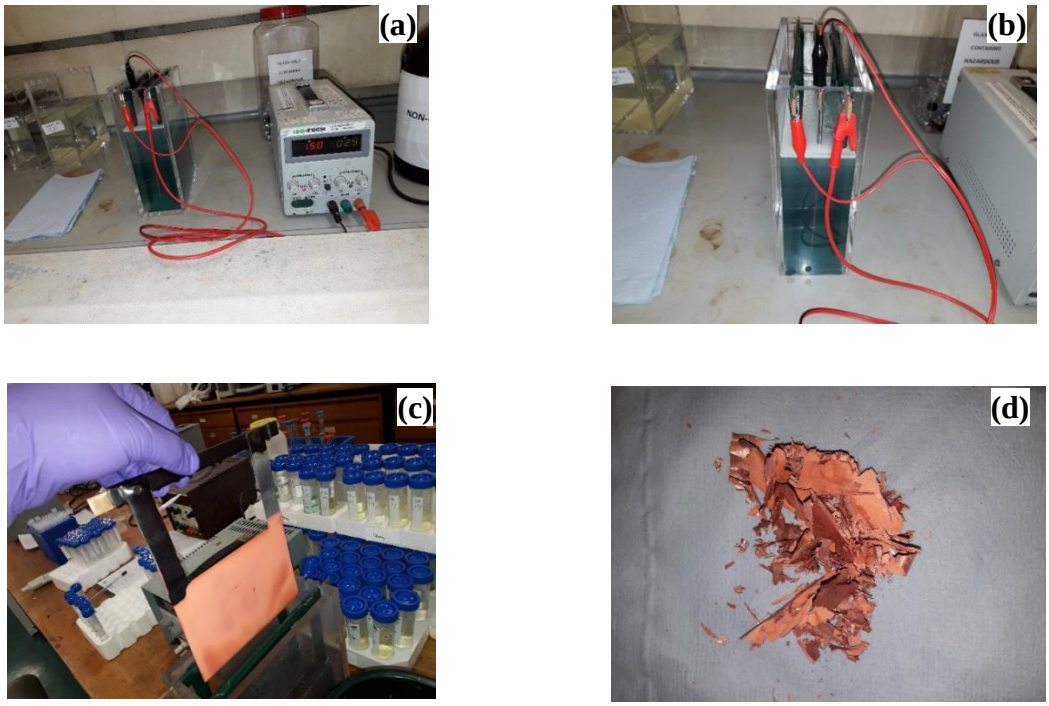

Figure 3.7 a & b Electrochemical Recovery Setup for Metals using the ISO-TECH (model number IPS-606D) (c) Copper deposits on electrode (d) Scrapes of recovered copper from electrodes

3.5 Analysis of Standard and Sample Solutions

The Perkin Elmer A Analyst 100 Atomic Absorption Spectrometer (AAS) was switched on followed by the computer. The lamp required for a metal analysis was then inserted in the FAAS. The air pump (oxidant) and acetylene (fuel) were opened and adjusted to the appropriate level. A method for each metal was developed using the AA Winlab software for the FAAS. The lamp settings were checked and set to the correct wavelength, operating current and slit; this was followed by turning on the flame. Consequently, the analysis began

by aspirating the blank solution to get a 0.000 absorbance reading. Each of the metal standard solutions were analysed starting from the lowest to the highest concentrations respectively and this was followed by aspirating all the available samples while the readings were also recorded.

3.6 Limit of detection (L_D) and limit of quantitation (L_Q) by calibration design method

It is important to know the lowest detectable concentration for the FAAS as the highest detectable concentration (limit of linearity) for each metal was already provided by the manufacturer in the FAAS (PerkinElmer A Analyst 100) user guide book. **Figure 3.8** shows the relationship between instrument calibration curve & analyte detection. The critical limit (L_C) is the signal of the instrument that can be attributed to the presence of an analyte which is different from a baseline noise or zero. The Limit of detection (L_D) is the lowest concentration at which an analyte can be detected confidently. The Limit of quantitation (L_Q) is the lowest concentration that can be quantitatively determined with precision and accuracy. The limit of linearity (LOL) is the highest detectable concentration that would produce a linear response. The linear range is the range between the limit of quantitation and the limit of linearity (Patel *et al.*, 2011; Gaines, 2021).

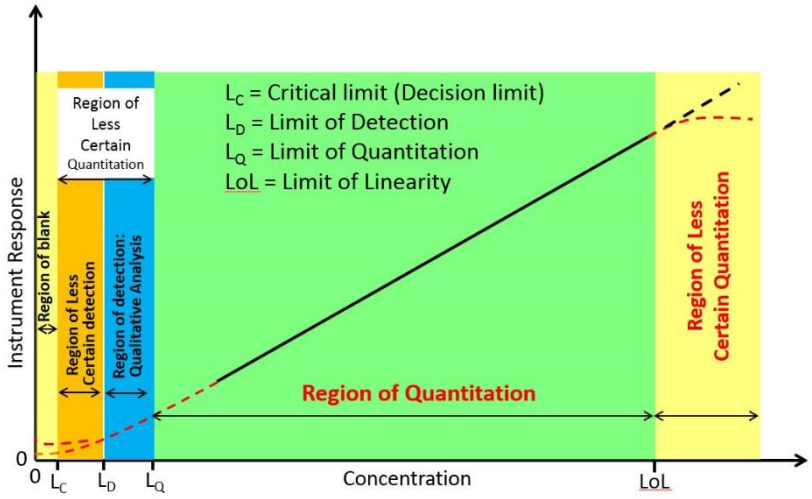

Figure 3.8 Relationship of instrument calibration curve & analyte detection

The standard deviation of the blank and signal-to-noise ratio are the two most commonly used methods for determining the L_D and L_Q of an analytical instrument. This research used the standard deviation of the blank method in determining the L_D and L_Q. For the purpose of

illustration, **Figure 3.9, Table 3.2** and the calculations below would be used to show how the L_D and L_Q could be derived. First, seven standard solutions are prepared starting with a blank solution and six other standard solutions (0.1 – 0.6 mg/L) of a metal (Cu, Zn, Fe, Ni & Pb). The solutions are analysed with the FAAS to get the absorbance reading. The calibration curve (**Figure 3.9**) is plotted and the regression equation from the plot is used to calculate the $\bar{y}$ value (**Table 3.2**) for each of the seven standard solutions. The regression equation is as follows:

$$\bar{y} = bx + a$$

Where $\bar{y}$ = regression equation , b = gradient slope, x = known concentration of standard (mg/L), a = y-intercept

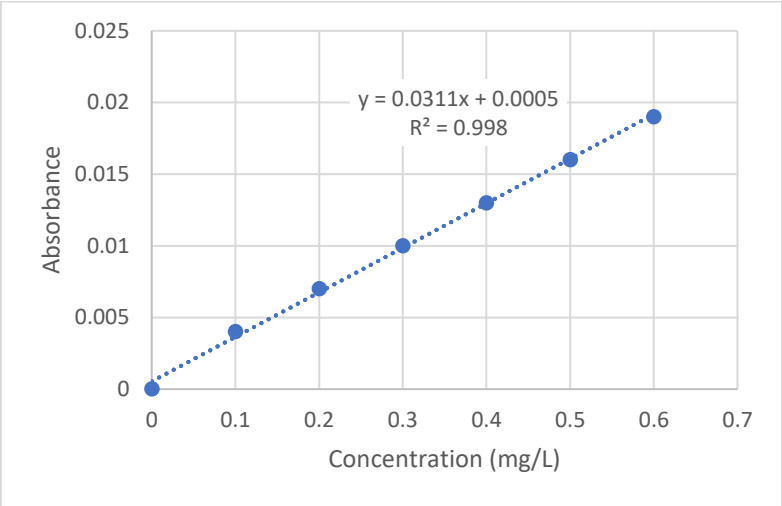

Figure 3.9 Sample of calibration plot for L_D

From **Figure 3.9**, the values for the formula, $\bar{y} = bx + a$, can be derived as *b = 0.0311*, *a = 0.0005* while *x = known standard concentrations as seen in **Table 3.2.*** To the determine the L_D and L_Q, the formulae below are used:

$$Y_{LD} = Y_{blank} + 3S_{blank}$$

$$Y_{LQ} = Y_{blank} + 10S_{blank}$$

Table 3.2 Standard deviation of regression

n	x	y	b	a	$\bar{y}$	$(y - \bar{y})^2$
1	0.0	0.0000	0.0311	0.0005	0.0005	2.5×10^{-7}
2	0.1	0.0040	0.0311	0.0005	0.0036	1.52×10^{-7}
3	0.2	0.0070	0.0311	0.0005	0.0067	7.84×10^{-8}
4	0.3	0.0100	0.0311	0.0005	0.0098	2.89×10^{-8}
5	0.4	0.0130	0.0311	0.0005	0.0129	3.6×10^{-9}
6	0.5	0.0160	0.0311	0.0005	0.0161	2.56×10^{-9}
7	0.6	0.0190	0.0311	0.0005	0.0192	2.56×10^{-8}
$\sum(y - \bar{y})^2$						5.411×10^{-7}

Where n = number of standards, x = known standard concentrations (mg/L), y = absorbance readings from FAAS, b = gradient slope from plot, a = y-intercept from plot

The standard deviation of regression $S_{y/x}$ would be calculated as follows:

$$S_{y/x} = \sqrt{\frac{\sum(y - \bar{y})^2}{n - 2}}$$

From **Table 3.2** above, $S_{y/x}$ would be:

$$S_{y/x} = \sqrt{\frac{5.411 \times 10^{-7}}{7-2}} = 0.00033$$

$S_{y/x}$ is used in place of S_{blank} while the y-intercept, a, is used in place of Y_{blank}. Therefore,

if $S_{y/x} = S_{blank}$ and $a = Y_{blank}$ then, $Y_{LD} = Y_{blank} + 3S_{blank}$ could be re-written as

$$Y_{LD} = a + 3S_{y/x}$$

$$Y_{LD} = 0.0005 + (3 \times 0.00033)$$

$$Y_{LD} = 0.00149$$

The limit of detection would be determined using the regression equation, $\bar{y} = bx + a$ (see **Table 3.2** above)

$$0.00149 = 0.0311x + 0.0005$$

$$x = \frac{0.00149 - 0.0005}{0.0311} = 0.0318\ mg/L$$

The L_D is 0.0318 mg/L

Similarly, the limit of quantitation, L_Q would be calculated using the formula

$$Y_{LQ} = Y_{blank} + 10S_{blank}$$

Remember that $S_{y/x} = S_{blank}$ and $a = Y_{blank}$ therefore $Y_{LQ} = Y_{blank} + 10S_{blank}$ could be re-written as $Y_{LQ} = a + 10S_{y/x}$

$Y_{LQ} = 0.0005 + (10 \times 0.00033)$

$Y_{LD} = 0.0038$

The limit of quantitation would be determined using the regression equation, $\bar{y} = bx + a$ (see **Table 3.2** above)

$$0.0038 = 0.0311x + 0.0005$$

$$x = \frac{0.0038 - 0.0005}{0.0311} = 0.1061\ mg/L$$

The L_Q is 0.1061 mg/L

In summary, from the illustration above, the calculated limit of detection was 0.0318 mg/L and the calculated limit of quantitation was 0.1061 mg/L. So if the analytical instrument detects a concentration less than the limit of detection (< 0.0318 mg/L in this case), the calculated limit of detection (0.0318 mg/L) would be used instead.

CHAPTER 4

Results and Discussions

4.1. Qualitative determination of WEEE samples

Four SEM specimen stubs were used to hold small portions of the WEEE samples. These samples were not coated and they were examined using the SEM-EDS (LEO 1455 VP) to identify the different types of metals present in them. The various metals present are seen in the four spectra images (**Figure 4.1 a-d**). The Energy Dispersive Spectroscopy (EDS) spectra image from the SEM in **Figure 4.1** shows the peaks for the elements (a) Cu & Zn, (b) Fe, Pb & Sn, (c) Au & Ni, (d) Ag present in the WEEE samples.

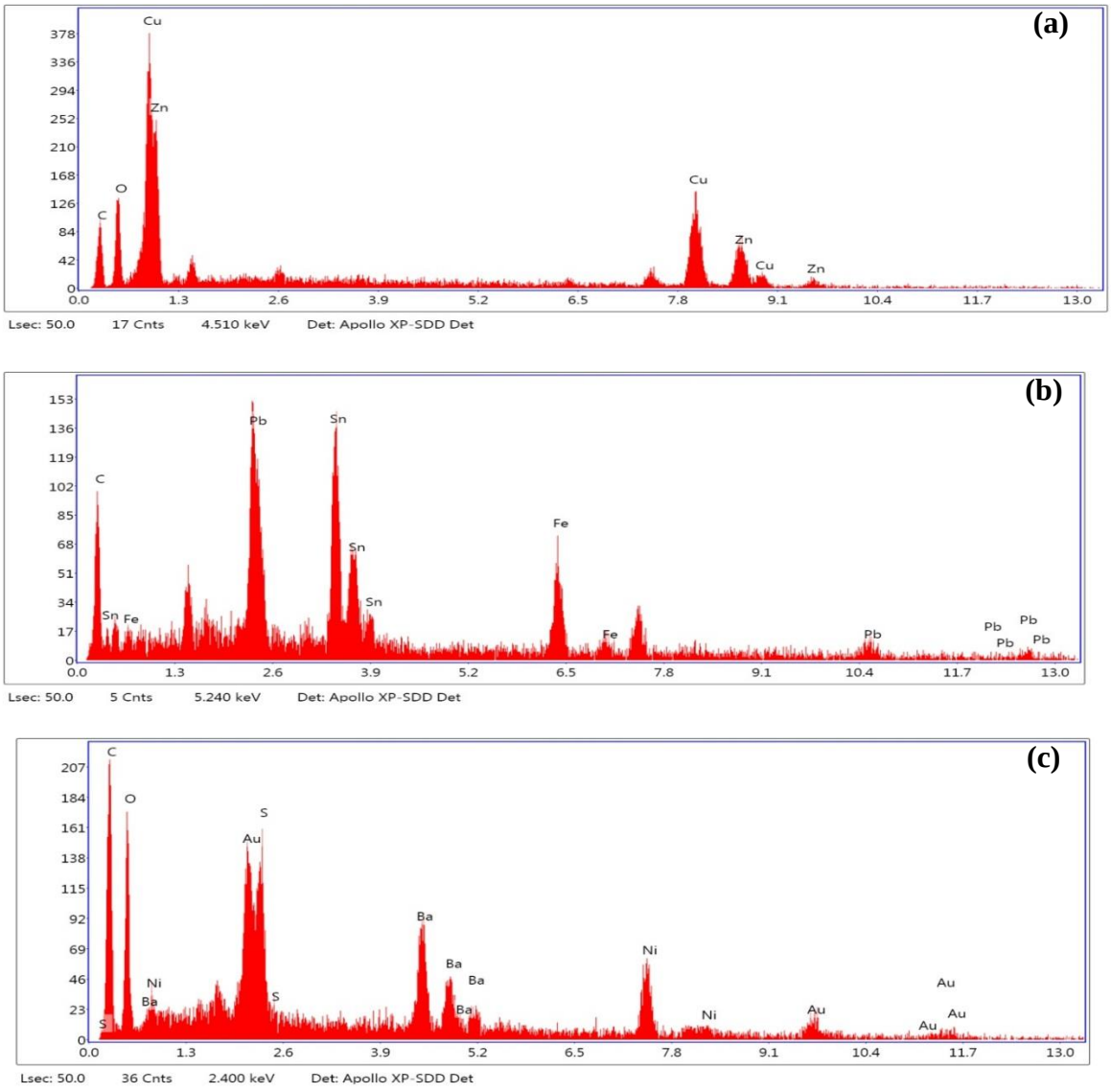

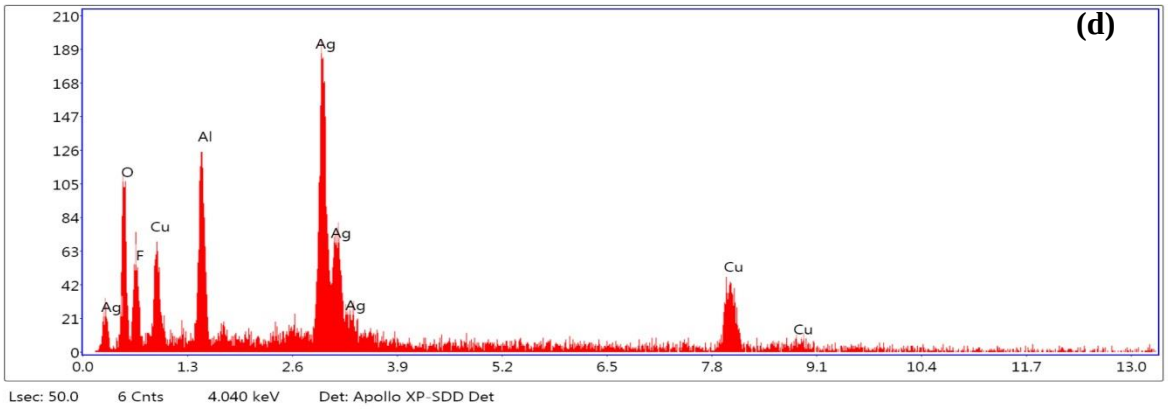

Figure 4.1 Spectra images from SEM-EDS showing peaks of elements present in WEEE samples before leaching (a) Cu & Zn, (b) Fe, Pb & Sn, (c) Au & Ni, (d) Ag.

4.2 Quantitative analysis

The quantitative analysis in this project was done to determine how much metals were present in the WEEE samples and this was carried out using the PerkinElmer A Analyst 100 Flame Atomic Absorption Spectrometer (FAAS). For each of the metals (Cu, Zn, Fe, Ni and Pb) analysed, the instrument was set to the standard operating condition in the manufacturer's guide and these operating conditions can be seen in **Table 4.1**.

Table 4.1 Operating condition of the FAAS used in this research

Analysed Element	Wavelength (nm)	Slit (nm)	Fuel	Operating current (mA)	Linear Range (mg/L)
Cu	324.8	0.7	Air - acetylene	25.0	5.0
Zn	213.9	0.7	Air - acetylene	15.0	1.0
Fe	248.3	0.2	Air - acetylene	30.0	6.0
Ni	232.0	0.2	Air - acetylene	2.0	15.0
Pb	283.3	0.7	Air - acetylene	7.0	20.0

4.2.1 Determination of Limit of Detection (L_D) and Limit of Quantitation (L_Q) using the Calibration Design Method

The limit of detection (L_D) and limit of quantitation (L_Q) are the lowest concentrations that can be reliably detected and quantified when a sample is analysed. This also shows how precisely the instrument (FAAS) responds. The absorbance readings of blank and standard obtained to determine the limit of detection and limit of quantitation for each of the metals

are shown in **Table 4.2.** The calculated values for L_D & L_Q are given in **Table 4.3**. This was done to know the lowest concentration detectable by the FAAS as the highest best detectable concentration (limit of linearity) for each metal was already provided in the FAAS (PerkinElmer A Analyst 100) user guide book by the manufacturer. The L_D and L_Q were done by calculating the standard deviation of regression. The formula $Y_{LD} = Y_{blank} + 3S_{blank}$ was used to calculate the L_D while L_Q was calculated using the formula $Y_{LQ} = Y_{blank} + 10S_{blank}$ **Figures 4.2 - 4.6** show the Leaste Squares (LS) regression line used to calculate L_D & L_Q for Cu, Zn, Ni, Fe & Pb.

Table 4.2 Absorbance readings from analysis of calibration design method for FAAS

	Elements				
Concentration (mg/L)	**Cu (absorbance)**	**Zn (absorbance)**	**Fe (absorbance)**	**Ni (absorbance)**	**Pb (absorbance)**
0.0	0.000	0.000	0.000	0.000	0.000
0.1	0.001	0.012	0.001	0.003	0.009
0.2	0.003	0.031	0.004	0.006	0.018
0.3	0.004	0.046	0.007	0.010	0.029
0.4	0.006	0.057	0.010	0.014	0.036
0.5	0.007	0.070	0.013	0.015	0.039
0.6	0.008	0.081	0.015	0.018	0.051

Table 4.3 Calculated L_D & L_Q using calibration design method for FAAS

Element	L_D (mg/L)	L_Q (mg/L)
Cu	0.111	0.371
Zn	0.057	0.192
Fe	0.108	0.360
Ni	0.087	0.209
Pb	0.820	2.732

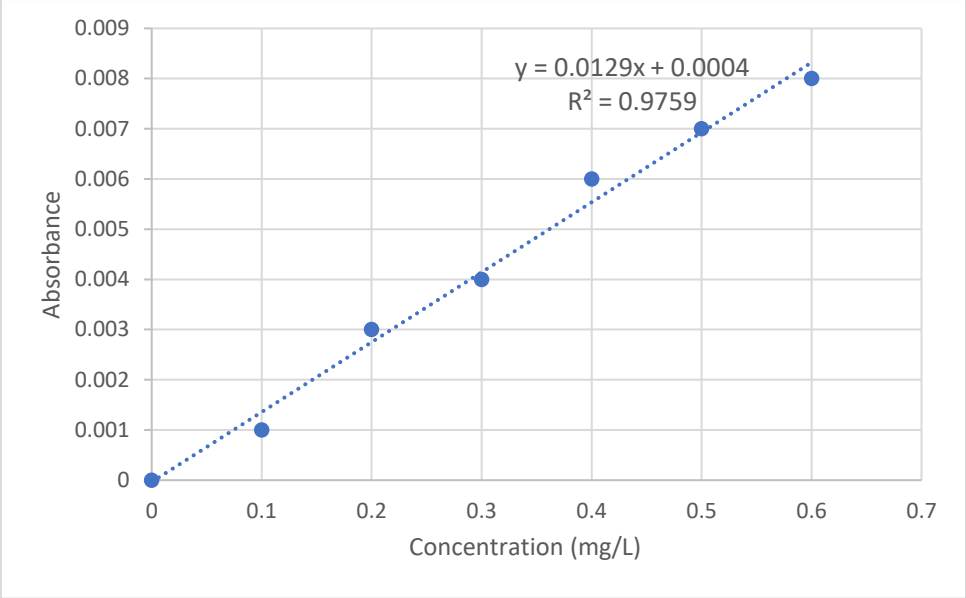

Figure 4.2 LS regression line used to calculate L_D & L_Q for copper (Cu)

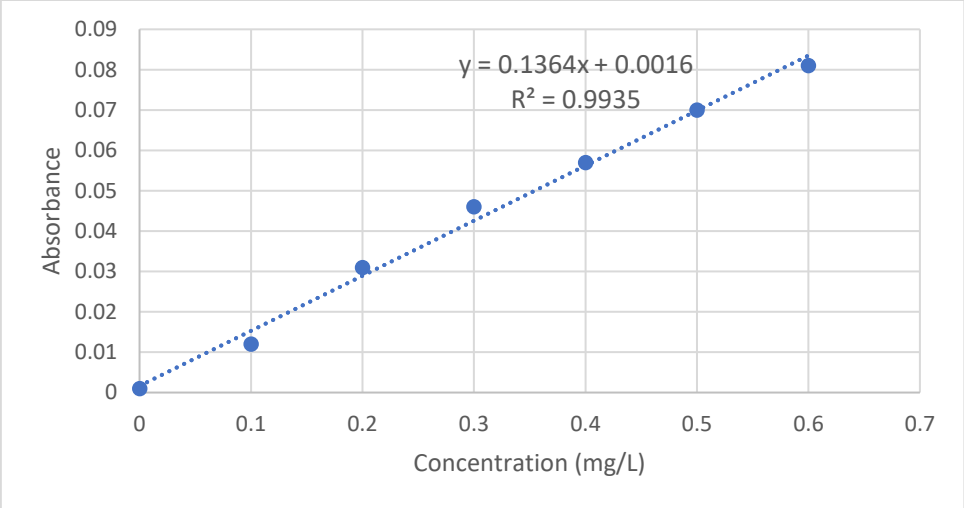

Figure 4.3 LS regression line used to calculate L_D & L_Q for zinc (Zn)

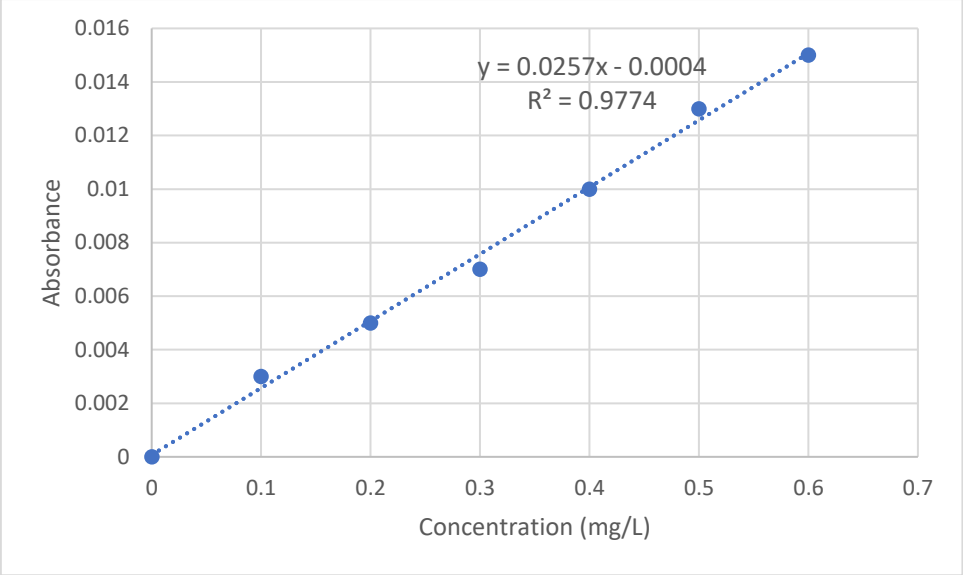

Figure 4.4 LS regression line used to calculate L_D & L_Q for iron (Fe)

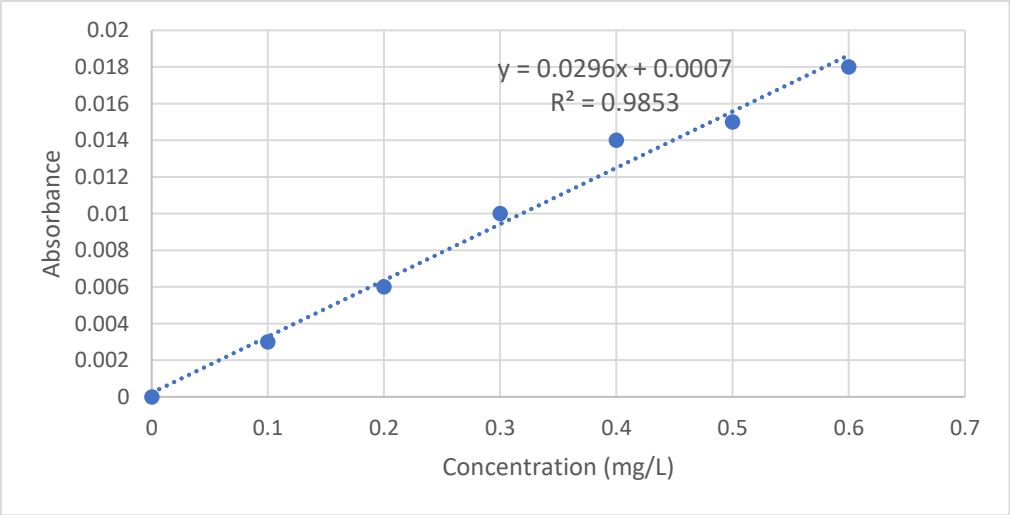

Figure 4.5 LS regression line used to calculate L_D & L_Q for nickel (Ni)

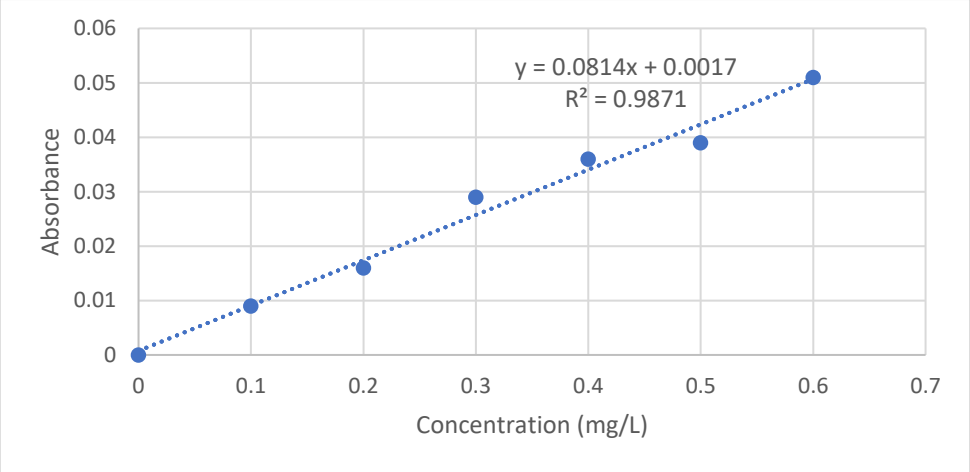

Figure 4.6 LS regression line used to calculate L_D & L_Q for lead (Pb)

4.2.2 Determination of Standard Calibration Curve

The FAAS reads absorbance from prepared standard solutions as described in section **3.2.1**. The known concentrations of the prepared standard solutions and the absorbance readings are used by the FAAS to plot a calibration graph. Subsequently, the calibration graph is used by the FAAS to determine the concentration of an analysed sample. **Tables 4.4 – 4.8** shows the known concentrations of prepared standards for the metals (Cu, Zn, Fe, Ni & Pb) and the absorbance readings from the FAAS while **Figures 4.7 – 4.11** shows the calibration graphs produced.

4.2.3 Determination of Standard Calibration Curve for Copper (Cu)

The calibration curve was determined from the analysis of the standards prepared from stock solution (1,000 mg/L) of copper. From the **Table 4.4** and **Figure 4.7**, the correlation value, R^2, was 0.9998 with a slope of 0.0543. From the calibration curve, concentration of the sample analysed is determined. The correlation value of 0.9998 was good enough to predict the concentration of Cu in the leachate.

Table 4.4 Absorbance for Copper Standard

Concentration (mg/L)	Absorbance
0.0	0.000
1.0	0.058
2.0	0.110
3.0	0.166
4.0	0.220
5.0	0.272

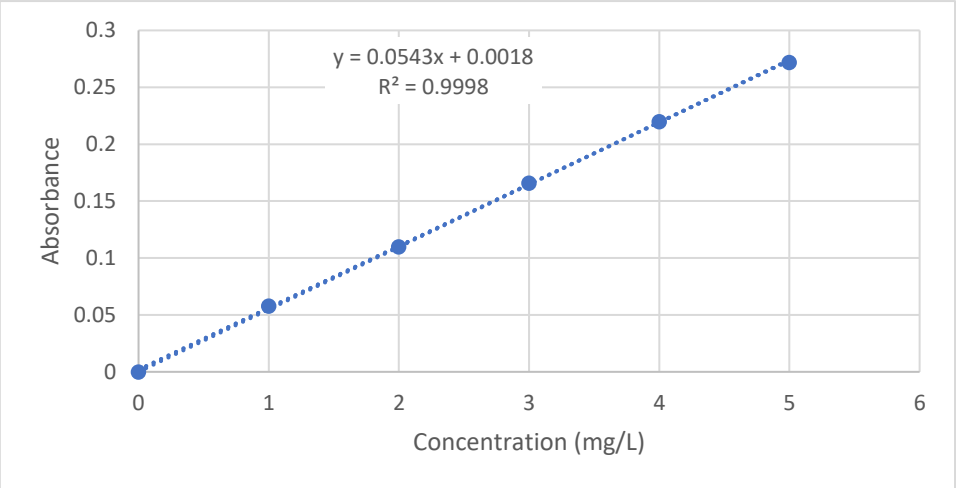

Figure. 4.7 Calibration curve for copper determination

4.2.4 Determination of Standard Calibration Curve for Zinc (Zn)

The calibration curve was determined from the analysis of the standards prepared from stock solution (1000 mg/L) of zinc. From **Table 4.5** and **Figure 4.8**, the correlation value, R^2, was 0.9989 with a slope of 0.3026. From the calibration curve, concentration of the sample analysed is determined. The correlation value of 0.9989 was good enough to predict the concentration of Zn in the leachate.

Table 4.5 Absorbance for zinc standard

Concentration (mg/L)	Absorbance
0.0	0.000
0.2	0.063
0.4	0.131
0.6	0.188
0.8	0.245
1.0	0.303

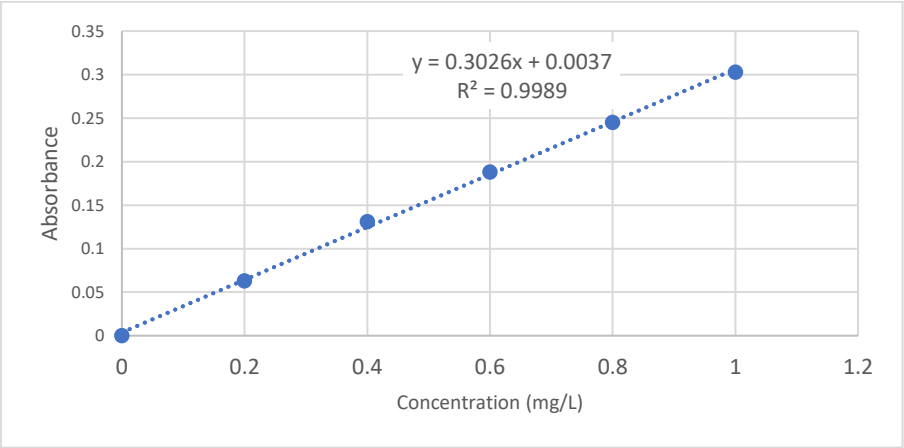

Figure 4.8 Calibration curve for zinc determination

4.2.5 Determination of Standard Calibration Curve for Iron (Fe)

The calibration curve was determined from the analysis of the standards prepared from stock solution (1000 mg/L) of iron. From the **Table 4.6** and **Figure 4.9** the correlation value, R^2, was 0.9951 with a slope of 0.0377. From the calibration curve, concentration of the sample analysed is determined. The correlation value of 0.9951 was good enough to predict the concentration of Fe in the leachate.

Table 4.6 Absorbance for iron standard

Concentration (mg/L)	Absorbance
0.0	0.000
1.0	0.045
2.0	0.084
3.0	0.124
4.0	0.163
5.0	0.185
6.0	0.232

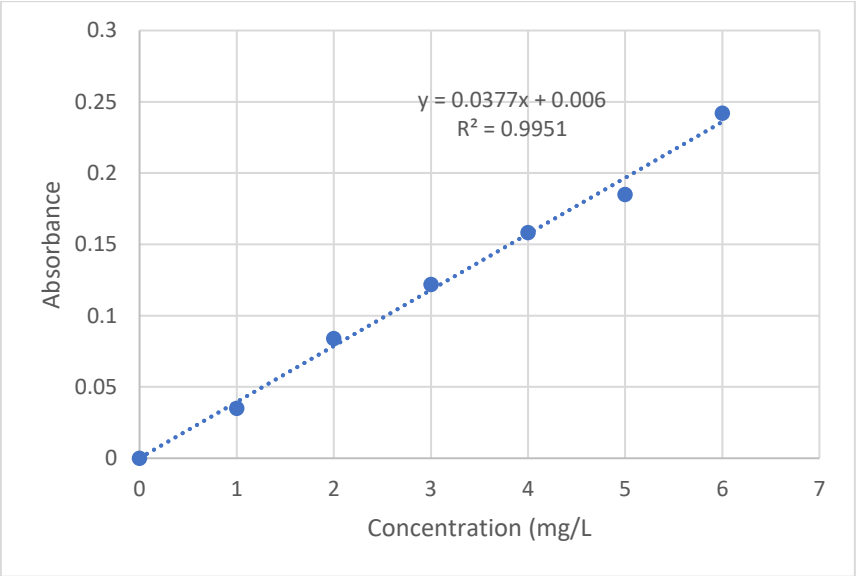

Figure 4.9 Calibration curve for iron determination

4.2.6 Determination of Standard Calibration Curve for Nickel (Ni)

The calibration curve was determined from the analysis of the standards prepared from stock solution (1000 mg/L) of nickel. From **Table 4.7** and **Figure 4.10**, the correlation value, R^2, was 0.9984 with a slope of 0.0404. The correlation value of 0.9984 was good enough to predict the concentration of Ni in the leachate.

Table 4.7 Absorbance for nickel standard

Concentration (mg/L)	Absorbance
0.0	0.000
0.5	0.021
1.0	0.039
1.5	0.059
2.0	0.082

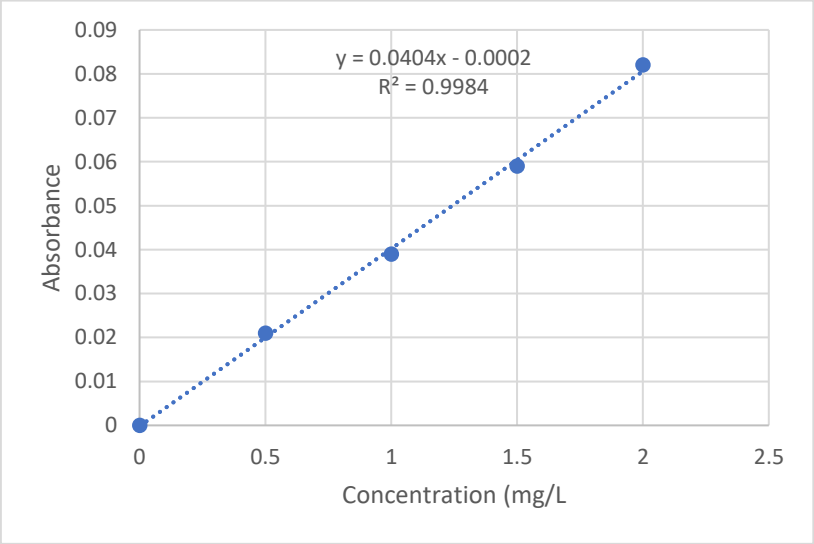

Figure 4.10 Calibration curve for nickel determination

4.2.7 Determination of Standard Calibration Curve for lead (Pb)

The calibration curve was determined from the analysis of the standards prepared from stock solution (1000 mg/L) of lead. From **Table 4.8** and **Figure 4.11**, the correlation value, R^2, was 0.9974 with a slope of 0.0063. The correlation value of 0.9974 was good enough to predict the concentration of Pb in the leachate.

Table 4.8 Absorbance for lead standard

Concentration (mg/L)	Absorbance
0.0	0.000
5.0	0.027
10.0	0.058
15.0	0.09
20.0	0.126

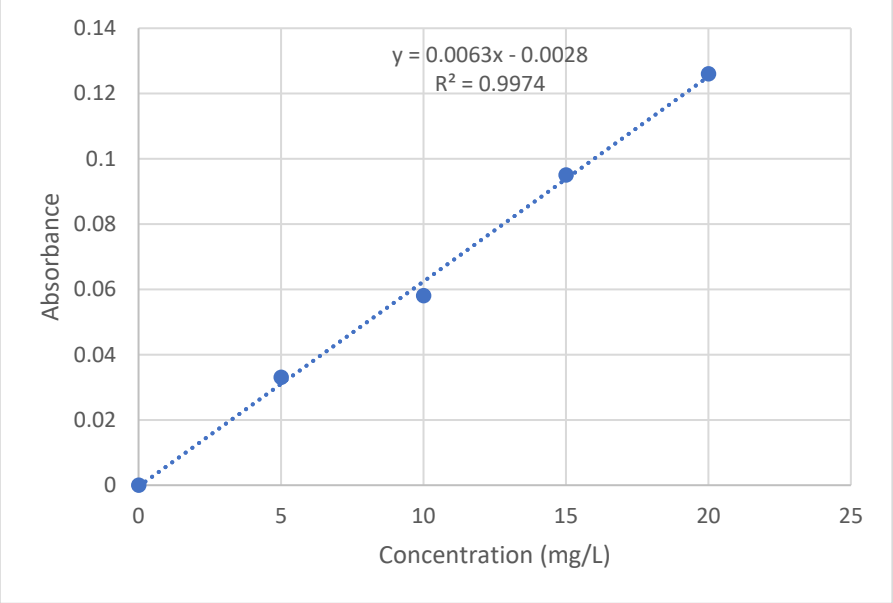

Figure 4.11 Calibration curve for lead determination

4.3 Determination of metal composition in WEEE using *aqua-regia*

To determine the composition of metals in the WEEE samples used for this research, *aqua-regia* was used for the dissolution experiment as it was the most aggressive solvent. The 3.0 g WEEE sample (**Figure 4.17 (a)**) was first examined using X-ray from the SEM (LEO 1455 VP) to identify the metals present. The metals are seen in the x-ray fluorescence (XRF) image from SEM in **Figure 4.17 (b)**. The figure shows the presence of Cu, Zn, Fe, Ni & Pb in the WEEE sample. The dissolution experiment carried out within 6 hours to allow the complete dissolution of metals in *aqua-regia*. The sample was then analysed using the Perkin Elmer A Analyst 100 Flame Atomic Absorption Spectrometer and the concentration was calculated in mg/g while the metal composition was calculated in percentage (%). The formula used can be seen below:

$$Metal\ concentration\ (mg/g) = \frac{Analysed\ concentration\ (mg/L) \times volume\ (L)}{Sample\ weight\ (g)}$$

$$Metal\ composition\ (\%) = \frac{Analysed\ concentration\ \left(\frac{mg}{L}\right) \times volume\ (L)}{Sample\ weight\ (mg)} \times 100$$

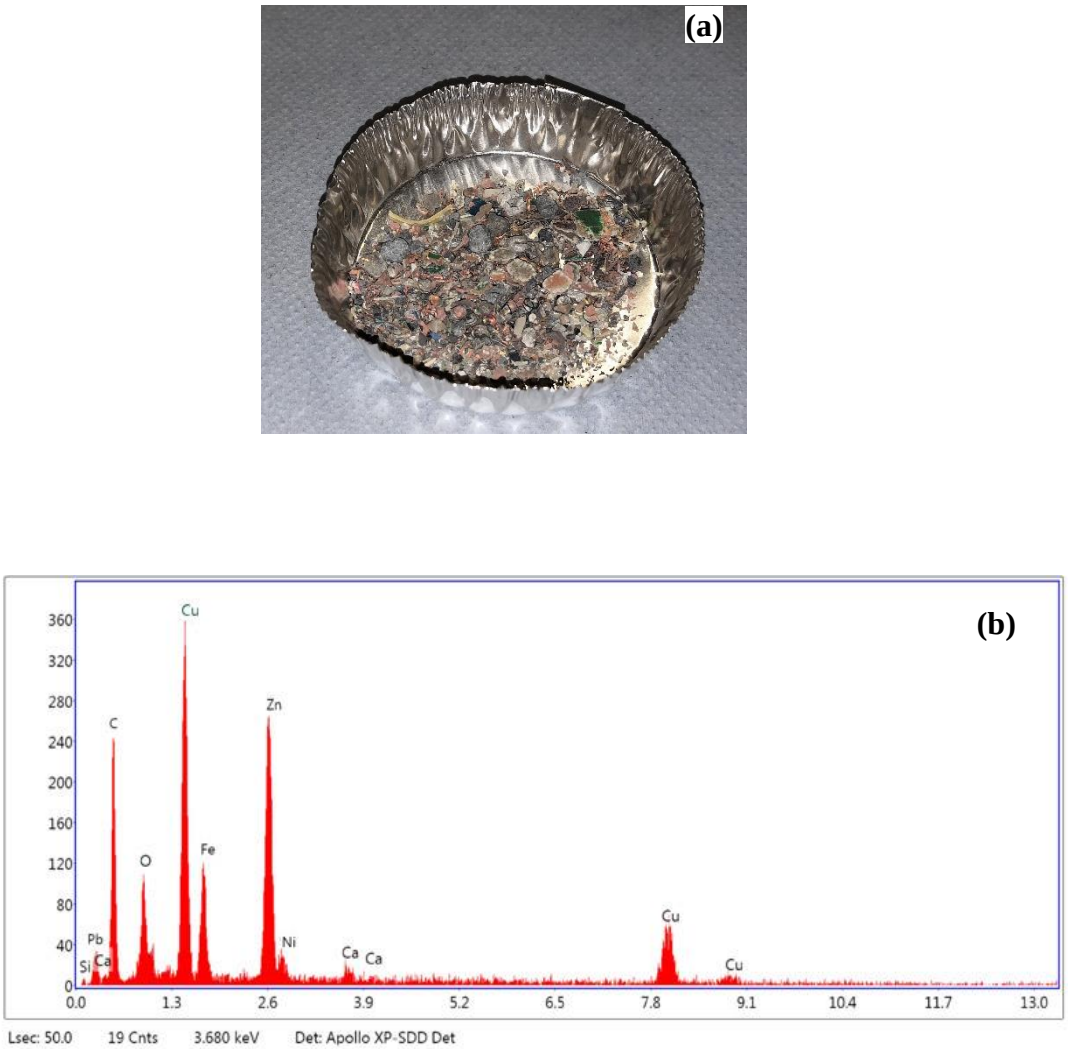

Figure 4.17 (a) WEEE sample (3.0 g) before dissolution (b) XRF image before dissolution of WEEE in *aqua-regia*

Table 4.14 and **Figure 4.18 (a)** shows the metals concentrations (mg/g) dissolved by *aqua-regia* and their composition (%). The metal from the highest composition to the lowest are in

the order Cu (44 %) > Zn (22 %) > Fe (7.3 %) > Pb (1.7 %) > Ni (1.3 %). The total composition of these metals was 76.6 % as seen in **Table 4.14** and **Figure 4.18 (a)**. The residue or WEEE sample left after the dissolution (**Figure 4.18 (b)**) weighed 0.08 g and its composition was 23.4 % (**Table 4.14**). This residue was then examined using X-ray from the SEM-EDS (LEO 1455 VP) and **Figure 4.18 (c)** shows that the dissolution by *aqua-regia* completely dissolved all metals and only plastics and other materials were left.

Table 4.14 Composition of metals in *aqua-regia* after 6 hours dissolution at 70 ^{0}C

Metal	Concentration (mg/g)	Percentage composition (%)
Cu	438.9 ± 36.4	43.9
Zn	224.1 ± 29.9	22.4
Fe	73.1 ± 7.2	7.3
Ni	13.2 ± 2.2	1.3
Pb	16.9 ± 1.6	1.7
	Total metal composition	76.6
	Remaining composition (other materials)	23.4

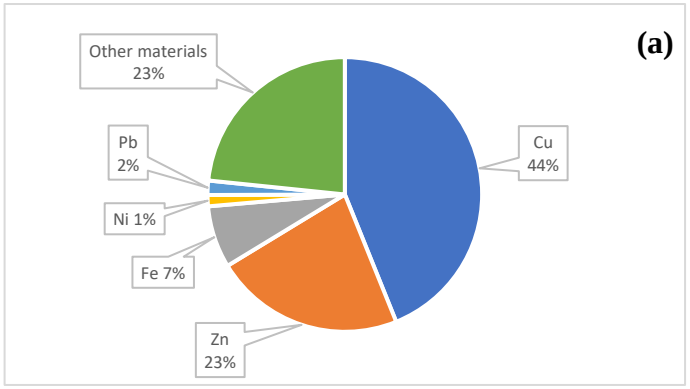

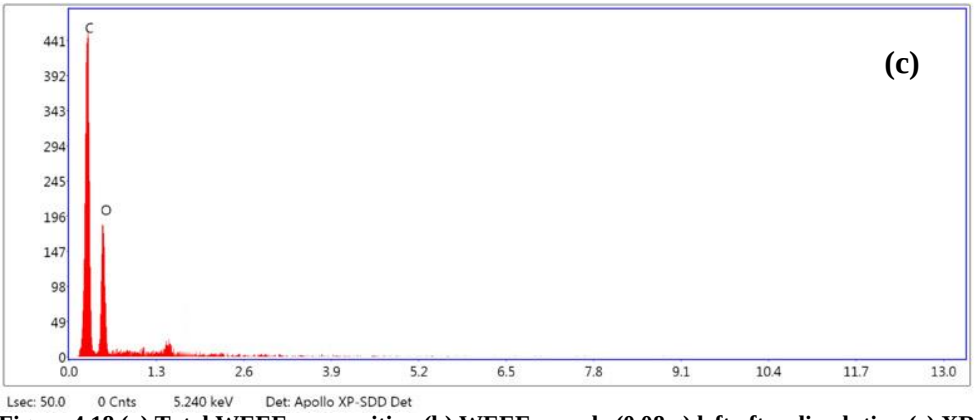

Figure 4.18 (a) Total WEEE composition (b) WEEE sample (0.08 g) left after dissolution (c) XRF image after 6 hours dissolution of metals with *aqua-regia*

4.4. WEEE leaching effect

The main focus of this project is to evaluate the extraction of five metals (Cu, Zn, Fe, Ni and Pb) from WEEE. It was decided to use *aqua-regia* as the best available leaching solution to extract these metals to establish the baseline conditions for the remaining leaching solvents. In other words, concentration from *aqua-regia* was taken as 100 % as it always gave the highest concentrations. The EDS images for both pre and post *aqua-regia* leaching show that almost all metals have been removed from the WEEE samples. Each experiment was conducted three times (triplicate) under the same experimental conditions to evaluate the reproducibility of the method. The mean concentrations in mg/g as well as the standard deviations (as the error bars) were calculated for each metal. This was done to show repeatability of the experiment. The two methods used for the experiments were i) hotplate and ii) microwave methods. The parameters for experiments were particle-size, temperature, reaction time, concentration, dose and H_2O_2 effects. The following leaching solvents were used in this research :

1. Inorganic solvents

1) *Aqua-regia* (1:3, HNO_3 : HCl)
2) Nitric acid (HNO_3)
3) Hydrochloric acid (HCl)
4) Sulfuric acid (H_2SO_4)

2. Organic solvents

1) Citric acid ($C_6H_8O_7$)
2) Malic acid ($C_4H_6O_5$)
3) Tartaric acid ($C_4H_6O_6$)

3. Designer solvents

1) IL-A – (1-butyl pyridinium bromide)
2) IL-B – (1-butyl-3-methylimidazolium hexafluorophosphate)
3) IL-C – (1-butyl-3-methylimidazolium bromide)
4) IL-D – (1-(1-cyanoethyl)-3-methylimidazolium bromide)
5) IL-E – (1-(3-cyanopropyl)-3-methylimidazolium bromide)
6) IL-F – (1-[2-(2-hydroxyethoxy)]-3-methylimidazolium chloride)
7) IL-G – (1-(2-cyanoethyl)-3-methylimidazolium bromide)

4). Control solvent

1) Deionised water (DI)

The designer solvents were chosen as they have been previously reported to have dissolved metal compounds (Javaid, 2006; Faivre, 2009). However, gold and silver were not considered in this research because they do not dissolve in acids and the focus was to extract these five metals (Cu, Zn, Fe, Ni & Pb) which is the major interest of the Nigerian government.

The leaching concentration (mg/g) from the analyzed leachate was calculated using the formula:

$$Metal\ concentration\ (mg/g) = \frac{Analysed\ concentration\ (mg/L) \times volume\ (L)}{Sample\ weight\ (g)}$$

The optimisation was determined by converting the above concentration (mg/g) to percentage extraction (%) and this was determined using the formula:

$$Extraction\ (\%) = \frac{Leaching\ concentration\ (mg/g)}{Aqua - regia\ leaching\ concentration\ (mg/g)} \times 100$$

4.4.1 Principal Component Analysis

Principal component analysis (PCA) was also used to analyse the dataset in this research as the data was relatively large and contained many variables. PCA is a multivariate analysis suitable for analysing dataset with multiple variables. It helps to summarize and visualize the dataset as well as extract the most important information thereby presenting them as new variables also known as principal components (PC) or dimensions (Dim). In other words, PCA is used to reduce the dimensionality of a dataset that is multivariate into two or three dimensions which can be graphically visualized; also retaining the most important information with little loss of information. This means that a very good portion of the dataset can be well explained using a few dimension. PCA correlates all redundant data in the dataset to help explain most of the variance. Other researchers considered the process of reducing dimensionality and redundancy in the data as removing noise from the data (Kohla & Luniak, 2005; Reris & Brooks, 2015; Statisticshowto, 2021; STHDA, 2021; Towardsdatascience, 2021).

In PCA, the data is first normalized or standardized such that the mean = 0 and the standard deviation = 1. This is also called scaling of the data because it would make all the variables comparable. The formular for normalizing PCA data is as follows:

$$PCA\ normalization = \frac{x_i - mean(x)}{SD}$$

Where x_i is the variable value, x is the mean, sd is the standard deviation (SD)

The generated dimensions are sorted from the highest to the lowest (Dim.1 >Dim.2 > Dim.3 > …) in line with the standard deviation. In other words, Dim.1 accounts for the highest variability in the data and this was followed by Dim.2, Dim.3 and so on. The proportion of variance are used to measure the amount of variance in the dimension. The variability in the data is the difference between the actual value and estimated value (normalized value). The cumulative proportion is the accumulated amount of variance that is explained in the data. So for example, if only three dimensions are chosen then the cumulative proportion (value in percentage) at Dim.3 would account for the total variance in the data. Also, since the data is normalized it means that only the dimensions with SD > 1 would be used as any dimension with SD < 1 would be discarded. This method is used as a cutoff point for the number of dimensions to retain for the PCA. Generally, 70 % or above of the total variance would be suitable to explain the data. The data in this research was analysed using R 4.0.3 and RStudio as the integrated development environment (Kohla & Luniak, 2005; Reris & Brooks, 2015; Statisticshowto, 2021; STHDA, 2021; Towardsdatascience, 2021).

The PCA results were generated using the following:

i) The coordinates of variables (y) are used to create a scatter plot. It is also the correlation between variables and dimension.

ii) The quality of representation also called squared cosine or Cos2 for the variables is calculated as squared coordinates:

$$Quality\ of\ representation = y \times y \text{ or } y^2$$

where y = coordinates of variables

iii) Contributions of the variables is how much percentage a variable is contributing to a particular principal component and it is calculated using:

$$Contributions\ of\ the\ variables = \frac{y^2 \times 100}{total\ y^2\ of\ the\ component}$$

where y = coordinates of variables

A biplot is the relationship between the variables and the observations. Also, the angle of variable vectors represents the correlation between variables. High positive correlation occurs when the angles between variables are small; there is no correlation when the variable vectors form an angle 90 degree (right angle); high negative correlation occurs when the variable vector angle is opposite or (around 180 degree). The longest vector represents the highest variance. In other words, the longer vector show more variable variability in a dimension but the shorter vectors are represented in the other dimensions. Lastly, variable vectors parallel to a dimension contributes more to that dimension (Kohla & Luniak, 2005; Reris & Brooks, 2015; Statisticshowto, 2021; STHDA, 2021; Towardsdatascience, 2021).

The following abbreviations (**Table 4.15**) were used for different leaching solvents in order to highlight the outcomes of the PCA.

Table 4.15 Abbreviations were used for different leaching solvents in PCA

Leaching solvent	Name	Abbreviation	Hotplate method	Microwave method
Inorganic solvents	*Aqua-Regia*	AQ	AQ1 – AQ3	AQ4 – AQ6
	Nitric acid	NA	NA1 – NA3	NA4 – NA6
	Hydrochloric acid	HA	HA1 – HA3	HA4 – HA6
	Sulfuric acid	SA	SA1 – SA3	SA4 – SA6
Organic solvents	Citric acid	CA	CA1 – CA3	CA4 – CA6
	Malic acid	MA	MA1 – MA3	MA4 – MA6
	Tartaric acid	TA	TA1 – TA3	TA4 – TA6
Designer solvents	1-butyl pyridinium bromide	IL A	ILA1 – ILA3	ILA4 – ILA6
	1-butyl-3-methylimidazolium hexafluorophosphate	IL B	ILB1 – ILB3	ILB4 – ILB6
	1-butyl-3-methylimidazolium bromide	IL C	ILC1 – ILC3	ILC4 – ILC6
	1-(1-cyanoethyl)-3-methylimidazolium bromide	IL D	ILD1 – ILD3	ILD4 – ILD6
	1-(3-cyanopropyl)-3-methylimidazolium bromide	IL E	ILE1 – ILE3	ILE4 – ILE6
	1-[2-(2-hydroxyethoxy)]-3-methylimidazolium chloride	IL F	ILF1 – ILF3	ILF4 – ILF6
	1-(2-cyanoethyl)-3-methylimidazolium bromide	IL G	ILG1 – ILG3	ILG4 – ILG6
Control solvent	Deionized water	W	W1 – W3	W4 – W6

4.5 Determination of Dose effect

The hotplate and microwave methods were used to determine the effect of dose (0.2, 0.5, 0.7, 1.5, 2.0, 3.0 g of WEEE) on the extraction of Cu, Zn, Fe, Ni & Pb. For the hotplate method, the experimental conditions were temperature (70 ^{0}C), particle-size (4 mm), concentration (2 mol/L for inorganic acids, 25 g/L for organic acids and 100 g/L for ionic liquids), time (120 minutes) and rotation speed (340 rpm). For the microwave method, the experimental conditions were time (20 minutes), particle-size (4.0 mm), temperature (150 ^{0}C), concentration (2 mol/L for inorganic acids, 25 g/L for organic acids and 100 g/L for ionic liquids). **Appendices 1 a - e** shows tables of the mean concentrations of dose effect for Cu, Zn, Fe, Ni and Pb (mg/g) from three different experiments and the SD as the error bar.

4.5.1 Effect of Dose on Leaching Cu

Table 4.16 a shows the percentage extraction of Cu with dose and this is also represented in **Figure 4.19**. In the hotplate method (**Figure 4.19**), as the dose increased from 0.2 – 3.0 g there was no significant change in Cu extraction for NA. The peak Cu extraction was 41 % at 0.2 g. For the other solvents, HA, IL-E and IL-G the best extraction was at 0.2 g (10, 11 and 22 % respectively) and the extraction decreased as the dose increased. However, all other solvents showed < 1.5 % extraction. Consequently, in the microwave method (**Figure 4.19**), as the dose increased from 0.2 g to 3.0 g the best Cu extraction was NA (52 % at 0.2 g), there was no significant change for 0.2 – 0.7 g but it decreased till 3.0 g. The remaining solvents had Cu extraction < 1.5 %.

Comparing the hotplate method with microwave method, two sample independent t-test was done for each of the solvents. The null hypothesis (H_0) stated that the mean of both methods are equal while the alternative hypothesis (H_1) stated that the mean of both methods are not equal. In **Table 4.16 b** it shows that at 95 % confidence level the independent t-test for NA, HA, IL-E & IL-G had p-values > 0.05 and this shows that the means for both methods are equal so the hotplate and microwave methods have the same efficiencies.

Table 4.16a Percentage concentration values for effect of dose on leaching Cu

	Dosage (g)	Extraction (%)														
		AQ	NA	HA	SA	CA	MA	TA	IL-A	IL-B	IL-C	IL-D	IL-E	IL-F	IL-G	W
Hotplate Method	0.20	100.00	40.99	9.59	0.18	1.36	0.40	0.16	0.01	0.01	0.09	0.24	11.07	0.66	22.48	0.00
	0.50	100.00	34.78	3.06	0.09	0.51	0.06	0.05	0.01	0.02	0.04	0.14	1.43	0.30	18.45	0.00
	0.70	100.00	36.41	1.26	0.07	0.14	0.04	0.03	0.00	0.01	0.03	0.12	0.88	0.12	9.65	0.00
	1.50	100.00	33.90	0.26	0.02	0.03	0.01	0.00	0.00	0.01	0.01	0.05	0.35	0.05	1.27	0.00
	2.00	100.00	35.60	0.06	0.01	0.02	0.01	0.00	0.00	0.02	0.01	0.03	0.27	0.02	0.43	0.00
	3.00	100.00	39.93	0.04	0.02	0.02	0.00	0.00	0.00	0.00	0.01	0.03	0.09	0.01	0.17	0.00
Microwave Method	0.20	100.00	52.24	1.12	0.02	0.02	0.15	0.07	0.04	0.05	0.05	0.05	0.56	0.05	0.78	0.01
	0.50	100.00	50.00	0.81	0.02	0.02	0.12	0.05	0.04	0.04	0.04	0.05	0.43	0.05	0.64	0.02
	0.70	100.00	50.61	0.20	0.03	0.02	0.08	0.03	0.03	0.03	0.03	0.03	0.32	0.03	0.53	0.03
	1.50	100.00	36.15	0.15	0.06	0.03	0.06	0.02	0.03	0.03	0.03	0.03	0.34	0.03	0.46	0.04
	2.00	100.00	15.57	0.14	0.09	0.03	0.02	0.01	0.03	0.03	0.03	0.03	0.31	0.03	0.47	0.04
	3.00	100.00	9.60	0.10	0.06	0.03	0.01	0.01	0.02	0.02	0.02	0.02	0.21	0.02	0.32	0.14

Table 4.16b Independent t-test between hotplate and microwave methods at 95% confidence level (dose effect in Cu)

	NA	HA	IL-E	IL-G
p-value	0.88	0.23	0.28	0.07
Hotplate Mean (%)	36.94	2.38	2.35	8.74
Microwave Mean (%)	35.70	0.42	0.36	0.53

Note: There were no t-tests for < 1.5 % extractions as they were considered insignificant

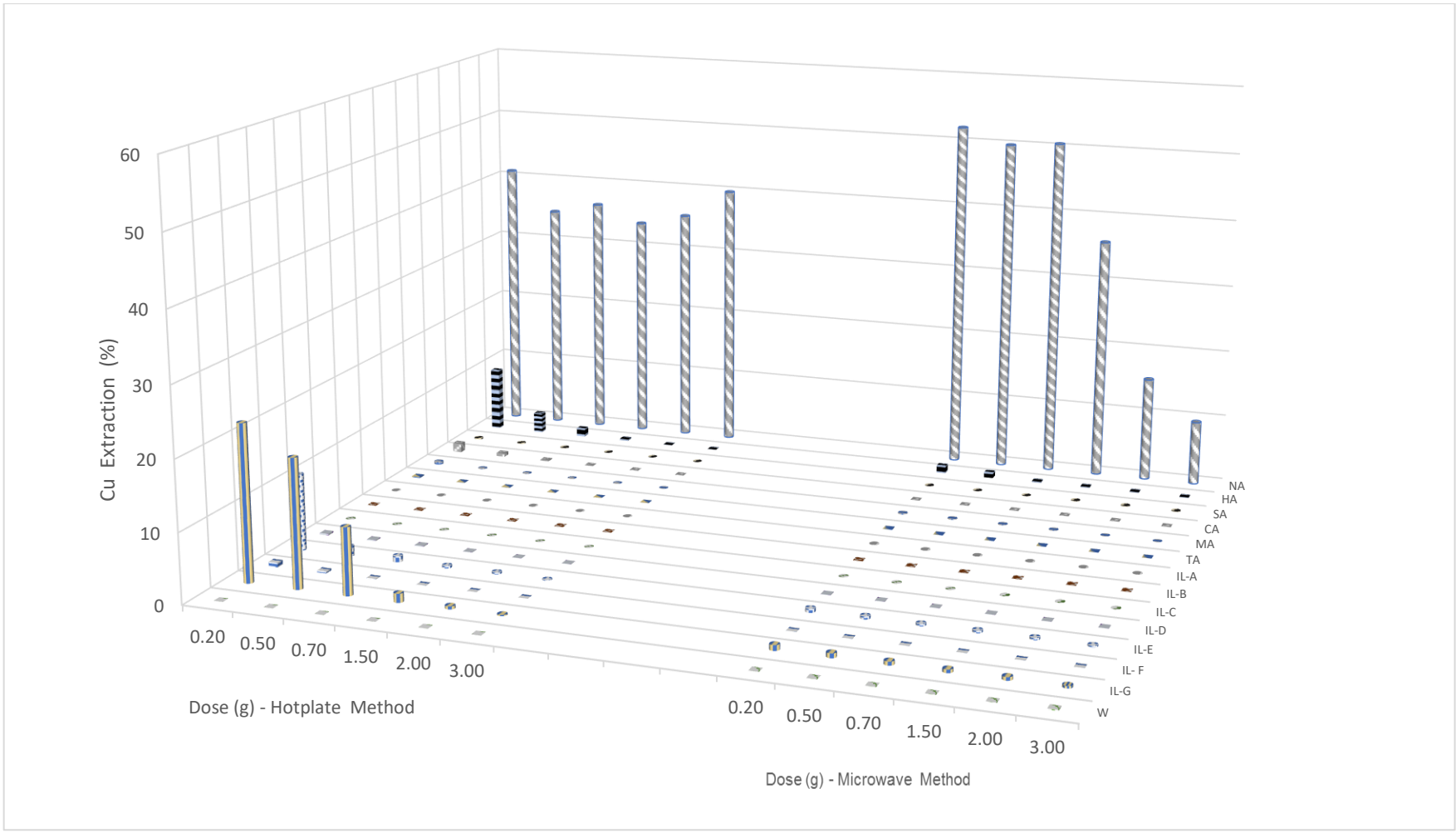

Figure 4.19 Percentage concentration for the effect of sample dose on leaching Cu

4.5.2 Effect of Dose on Leaching Zn

Table 4.17 shows the percentage extraction of Zn with dose and this is also represented in **Figure 4.20**. In the hotplate method (**Figure 4.20)**, as the dose increased from 0.2 – 3.0 g the Zn extraction in NA increased to 74 % at 0.7 g before decreasing. In HA, it increased to 98 % at 0.7 g before decreasing. In SA and CA, the Zn extraction increased to the best dose of 0.5 g (65 and 53 % respectively) before decreasing. In MA, the Zn extraction increased to 62 % at 1.5 g before decreasing while in TA, IL-D, IL-E, IL-F, IL-G the best Zn extraction was at 0.2 g (19, 13, 10, 12 and 12 % respectively) before decreasing. The other solvents had < 2 % of Zn extraction. In the microwave method (**Figure 4.20**), as the dose increased from 0.2 g to 3.0 g the Zn extraction was best at 0.7 g for NA (81 %), HA (84 %), SA (65 %). Zn extraction was best at 3.0 g for CA (77 %), 1.5 g for MA (68 %) and TA (69 %) Zn extraction was best at 0.2g for IL-A (57 %), IL-B (65 %), IL-C (79 %), IL-E (71 %), IL-F (92 %), IL-G (71 %) except IL-D at 0.5 g (65 %). In general, extraction of Zn using the microwave method was relatively effective as every solvent reached a peak extraction > 55 % of Zn.

Comparing the hotplate method with microwave method, two sample independent t-test was done for each of the solvents. The null hypothesis (H_0) stated that the mean of both methods are equal while the alternative hypothesis (H_1) stated that the mean of both methods are not equal. In **Table 4.17 b** it shows that at 95 % confidence level the independent t-test for NA, HA, SA, CA and MA had p-values > 0.05 and this shows that the means for both methods are equal so the hotplate and microwave methods have the same efficiencies. However, TA and ILs A – G had p-values < 0.05 which shows that the means for both methods are not equal and the microwave method which had the higher mean was better.

Table 4.17a Percentage concentration values for effect of dose on leaching Zn

	Dosage (g)	Extraction (%)														
		AQ	NA	HA	SA	CA	MA	TA	IL-A	IL-B	IL-C	IL-D	IL-E	IL-F	IL-G	W
Hotplate Method	**0.20**	100.00	43.14	49.93	34.40	28.57	35.34	19.17	0.06	0.05	0.18	12.78	9.61	12.03	12.03	0.01
	0.50	100.00	72.59	92.98	65.39	53.13	32.69	14.05	0.04	1.06	0.12	6.74	6.79	8.79	12.06	0.01
	0.70	100.00	74.39	97.69	52.34	52.34	61.47	15.16	0.03	0.74	0.09	3.78	5.82	7.81	10.13	0.01
	1.50	100.00	65.69	85.87	53.41	51.38	61.98	13.25	0.95	0.72	0.15	1.52	7.83	7.42	9.95	0.01
	2.00	100.00	47.23	52.16	30.92	26.59	26.78	6.69	0.01	0.01	0.05	0.26	3.87	3.46	9.97	0.00
	3.00	100.00	41.32	40.33	22.76	16.15	17.56	3.52	0.01	0.01	0.03	0.05	1.60	2.41	5.85	0.00
Microwave Method	**0.20**	100.00	40.45	50.29	31.92	12.24	10.93	46.43	57.14	64.80	79.08	53.57	70.92	91.84	71.43	0.01
	0.50	100.00	66.19	67.71	55.87	22.77	25.05	37.65	41.30	55.87	75.30	64.78	53.04	87.04	62.75	0.01
	0.70	100.00	81.08	83.78	64.86	31.35	34.59	33.87	46.49	47.57	59.46	55.86	46.85	70.27	61.26	0.01
	1.50	100.00	73.34	80.67	44.69	60.50	67.84	68.75	33.35	45.03	58.79	53.63	47.10	61.88	60.16	0.01
	2.00	100.00	76.52	69.13	35.87	75.65	63.48	39.13	36.20	43.04	57.39	52.17	44.67	66.85	45.65	0.01
	3.00	100.00	66.05	63.71	29.38	76.80	56.45	40.32	36.29	43.78	50.40	48.10	36.86	51.84	50.40	0.01

Table 4.17b Independent t-test between hotplate and microwave methods at 95% confidence level (dose effect in Zn)

	NA	HA	SA	CA	MA	TA	IL-A	IL-B	IL-C	IL-D	IL-E	IL-F	IL-G
p-value	0.27	0.99	0.95	0.53	0.76	1.96×10^{-4}	4.28×10^{-7}	6.44×10^{-8}	7.66×10^{-8}	1.27×10^{-8}	3.90×10^{-6}	1.41×10^{-6}	$1.95s \times 10^{-7}$
Hotplate Mean (%)	57.39	69.83	43.20	38.03	39.30	11.97	0.18	0.43	0.10	4.19	5.92	6.99	10.00
Microwave Mean (%)	67.27	69.61	43.77	46.55	43.06	44.36	41.80	50.02	63.40	54.69	49.91	71.62	58.61

Note: There were no t-tests for < 0.1 % extractions as they were considered insignificant

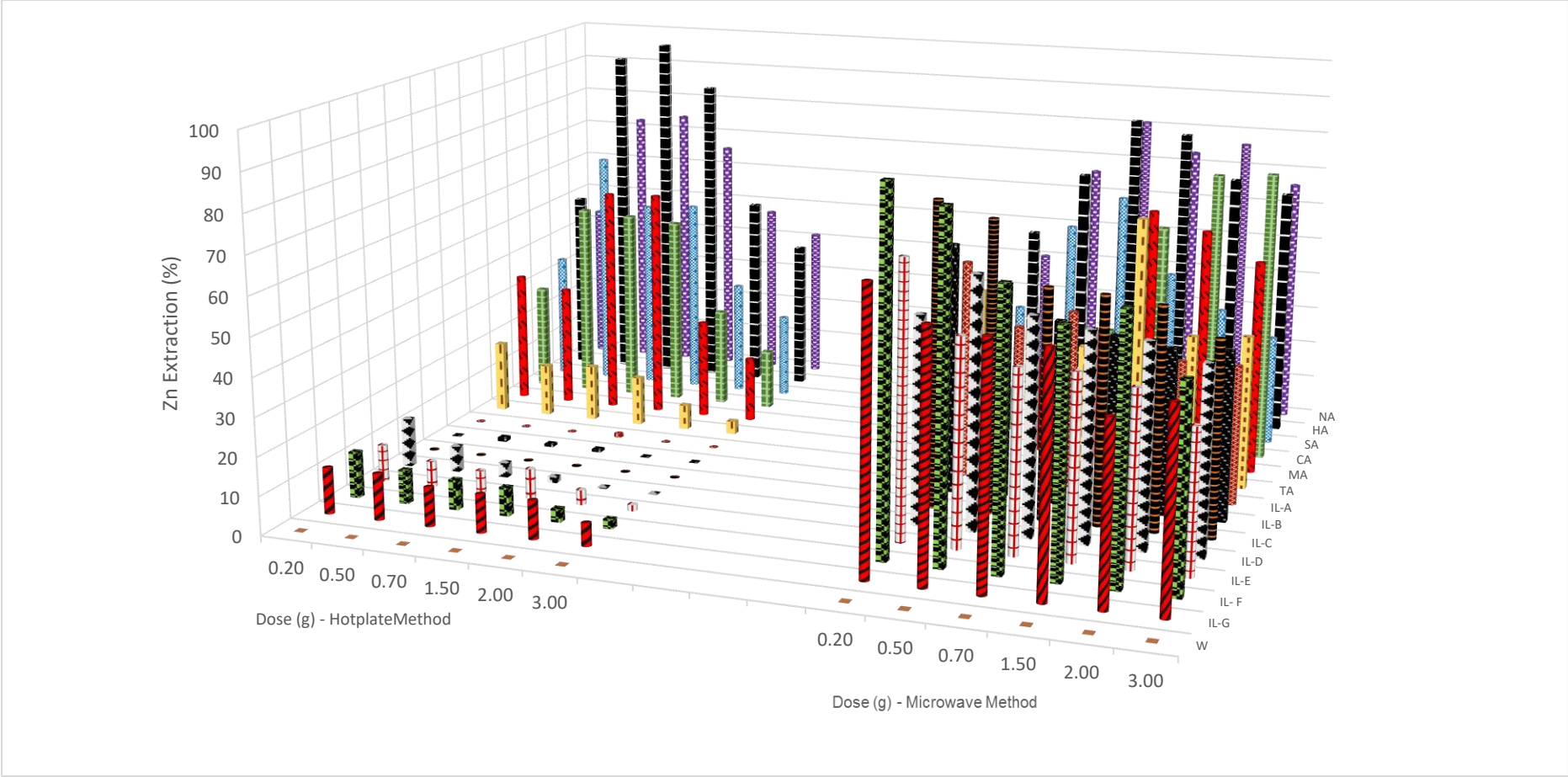

Figure 4.20 Percentage concentration for the effect of sample dose on leaching Zn

4.5.3 Effect of Dose on Leaching Fe

Table 4.18 a shows the percentage extraction of Fe with dose and this is also represented in **Figure 4.21**. In the hotplate method (**Figure 4.21**), as the dose increased from 0.2 – 3.0 g the Fe extractions for NA was best at 0.2 g (59 %), HA was best at 0.5g (68 %) and the extraction across the dose range was not stable while SA was best at SA 46 % before decreasing. The organic acids had Fe extractions < 3 % while the ionic liquids (ILs A - G) showed no significant extractions. In the microwave method (**Figure 4.21**), as the dose increased from 0.2 g to 3.0 g the best Fe extraction were NA (46 % at 0.2 g), HA (43 % at 0.2 g), SA (25 % at 0.5 g) had no significant change (0.2 – 1.5 g) before decreasing. The organic acids had Fe extractions < 3 % while the ionic liquids (ILs A - G) showed no significant extractions.

Comparing the hotplate method with microwave method, two sample independent t-test was done for each of the solvents. The null hypothesis (H_0) stated that the mean of both methods are equal while the alternative hypothesis (H_1) stated that the mean of both methods are not equal. In **Table 4.18 b** it shows that at 95 % confidence level the independent t-test for HNO_3, HCl and tartaric acids had p-values > 0.05 and this shows that the means for both methods are equal so the hotplate and microwave methods have the same efficiencies. However, the solvents with p-value < 0.05 shows that the mean of both methods are not equal therefore the hotplate method was better for H_2SO_4 while the microwave method was better for citric and malic acids.

Table 4.18a Percentage concentration values for effect of dose on leaching Fe

	Dosage (g)	Extraction (%)														
		AQ	NA	HA	SA	CA	MA	TA	IL-A	IL-B	IL-C	IL-D	IL-E	IL-F	IL-G	W
Hotplate Method	**0.20**	100.00	59.48	42.14	37.90	2.12	0.74	1.68	0.01	0.01	0.01	0.01	0.01	0.01	0.01	0.01
	0.50	100.00	56.55	67.80	46.10	1.95	1.23	1.96	0.00	0.00	0.00	0.00	0.00	0.00	0.00	0.00
	0.70	100.00	28.55	58.75	26.49	1.29	0.92	0.79	0.00	0.00	0.00	0.00	0.00	0.00	0.00	0.00
	1.50	100.00	47.24	23.28	33.91	1.62	1.53	1.44	0.00	0.00	0.00	0.00	0.00	0.00	0.00	0.00
	2.00	100.00	27.79	51.02	33.73	1.85	0.94	1.73	0.00	0.00	0.00	0.00	0.00	0.00	0.00	0.00
	3.00	100.00	31.85	60.79	15.84	1.41	0.36	0.90	0.00	0.00	0.00	0.00	0.00	0.00	0.00	0.00
Microwave Method	**0.20**	100.00	46.08	42.50	24.36	2.44	2.56	1.73	0.01	0.01	0.01	0.01	0.01	0.01	0.01	0.00
	0.50	100.00	45.42	42.02	25.22	2.98	2.35	2.80	0.01	0.01	0.01	0.01	0.01	0.01	0.01	0.01
	0.70	100.00	30.24	41.21	20.90	2.55	2.42	1.89	0.00	0.00	0.00	0.00	0.00	0.00	0.00	0.01
	1.50	100.00	28.92	42.56	21.27	2.43	2.31	2.67	0.00	0.00	0.00	0.00	0.00	0.00	0.00	0.01
	2.00	100.00	18.62	28.60	17.64	1.94	7.88	2.16	0.00	0.00	0.00	0.00	0.00	0.00	0.00	0.00
	3.00	100.00	18.79	34.80	9.07	1.62	8.22	0.89	0.00	0.00	0.00	0.00	0.00	0.00	0.00	0.01

Table 4.18b Independent t-test between hotplate and microwave methods at 95% confidence level (dose effect in Fe)

	NA	HA	SA	CA	MA	TA
p-value	0.20	0.11	0.03	0.03	0.02	0.11
Hotplate mean (%)	41.91	50.63	32.33	1.71	0.95	1.42
Microwave mean (%)	31.35	38.62	19.74	2.33	4.29	2.02

Note: There were no t-tests for < 0.1 % extractions as they were considered insignificant

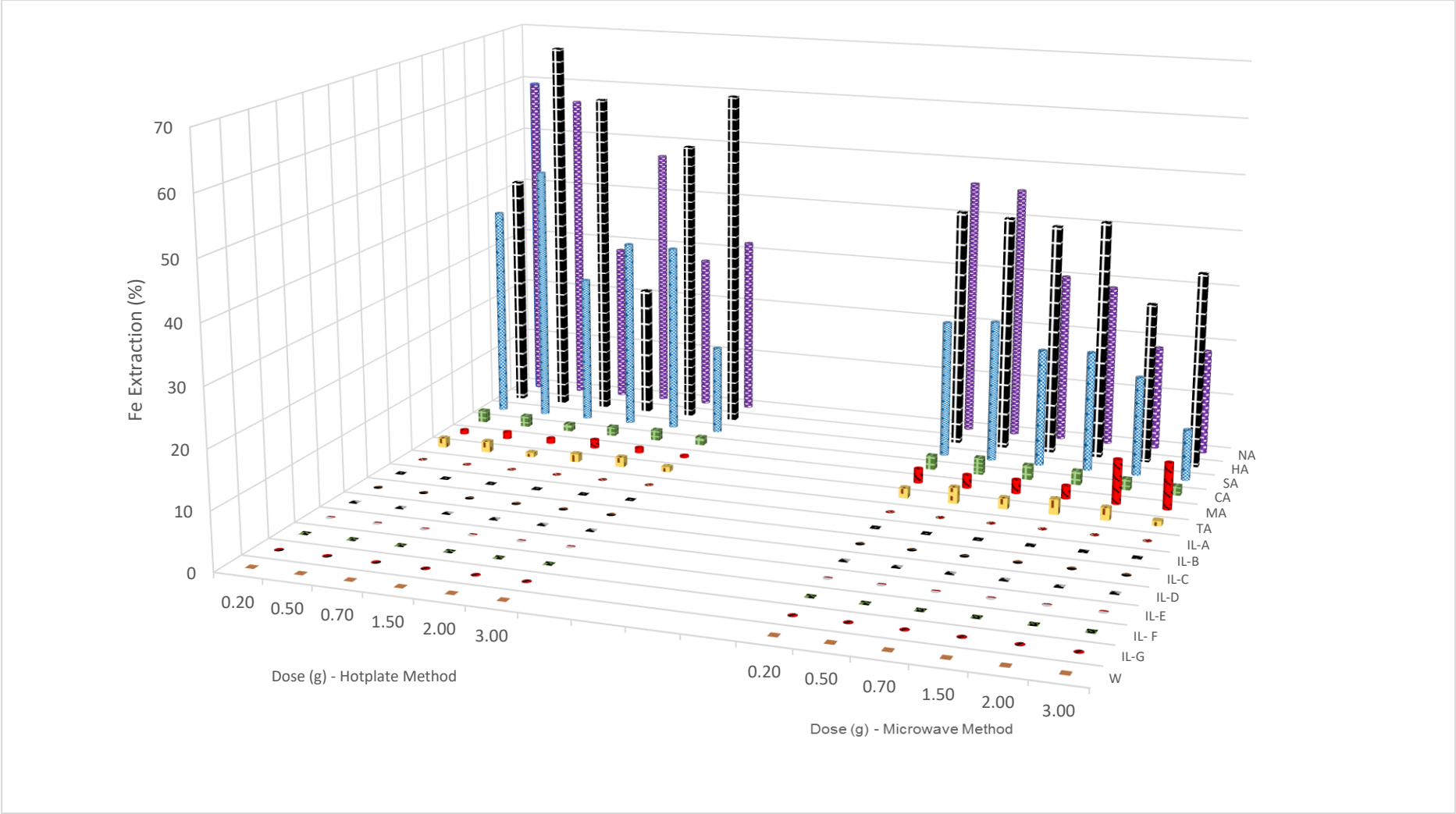

Figure 4.21 Percentage concentration on the effect of sample dose on leaching Fe

4.5.4 Effect of Dose on Leaching Ni

Table 4.19 a shows the percentage extraction of Ni with dose and this is also represented in **Figure 4.22**. In the hotplate method (**Figure 4.22**), as the dose increased from 0.2 – 3.0 g NA and HA increased except SA and TA which showed no significant change. The best Ni extraction were NA (7 % at 2.0 g), HA (7 % at 2.0 g), SA (3 % at 1.5 g), CA (5 % at 2.0 g), TA (3 % at 0.5 g). MA and ILs A - G did not show any significant extractions. In the microwave method (**Figure 4.22)**, as the dose increased from 0.2 g to 3.0 g the Ni extraction only increased in NA but decreased in HA. Ni extraction did not show any significant change in SA. The solvents peak extractions were NA (12 % at 3.0 g), HA (9 % at 0.2 g), SA (4 % at 1.5 g). The organic acids and ILs A - G did not show any significant extractions.

Comparing the hotplate method with microwave method, two sample independent t-test was done for each of the solvents. The null hypothesis (H_0) stated that the mean of both methods are equal while the alternative hypothesis (H_1) stated that the mean of both methods are not equal. In **Table 4.19 b** it shows that at 95 % confidence level the independent t-test for HA & SA had p-values > 0.05 and this shows that the means for both methods are equal so the hotplate and microwave methods have the same efficiencies. However, the solvents with p-value < 0.05 shows that the mean of both methods are not equal therefore the hotplate method was better for CA and TA while the microwave method was better for NA.

Table 4.19a Percentage concentration values on effect of dose on leaching Ni

	Dosage (g)	Extraction (%)														
		AQ	NA	HA	SA	CA	MA	TA	IL-A	IL-B	IL-C	IL-D	IL-E	IL-F	IL-G	W
Hotplate Method	**0.20**	100.00	2.76	3.03	2.37	1.84	0.83	1.97	0.01	0.01	0.01	0.01	0.01	0.01	0.01	0.01
	0.50	100.00	3.63	3.13	2.75	2.31	0.60	2.50	0.01	0.01	0.01	0.01	0.01	0.01	0.01	0.01
	0.70	100.00	5.95	5.02	2.79	1.86	0.48	2.14	0.00	0.00	0.00	0.00	0.00	0.00	0.00	0.00
	1.50	100.00	7.17	6.30	3.04	1.65	0.49	2.26	0.00	0.00	0.00	0.00	0.00	0.00	0.00	0.00
	2.00	100.00	7.42	7.20	2.62	5.45	0.45	2.04	0.00	0.00	0.00	0.00	0.00	0.00	0.00	0.00
	3.00	100.00	6.79	6.79	2.39	1.29	0.43	1.89	0.00	0.00	0.00	0.00	0.00	0.00	0.00	0.00
Microwave Method	**0.20**	100.00	7.16	8.84	3.16	0.88	0.54	0.36	0.03	0.03	0.03	0.03	0.03	0.03	0.03	0.01
	0.50	100.00	7.78	4.00	3.11	0.51	0.28	0.19	0.01	0.01	0.01	0.01	0.01	0.01	0.01	0.01
	0.70	100.00	10.66	2.85	2.96	0.44	0.24	0.16	0.01	0.01	0.01	0.01	0.01	0.01	0.01	0.02
	1.50	100.00	11.41	2.17	3.59	0.55	0.35	0.23	0.01	0.01	0.01	0.01	0.01	0.01	0.01	0.03
	2.00	100.00	11.57	1.34	2.77	0.44	0.28	0.18	0.01	0.01	0.01	0.01	0.01	0.01	0.01	0.03
	3.00	100.00	12.13	0.86	2.35	0.38	0.23	0.15	0.01	0.01	0.01	0.01	0.01	0.01	0.01	0.04

Table 4.19b Independent t-test between hotplate and microwave methods at 95% confidence level (dose effect in Ni)

	NA	HA	SA	CA	TA
p-value	0.00	0.21	0.13	0.01	2.09×10^{-09}
Hotplate mean (%)	5.62	5.24	2.66	2.40	2.13
Microwave mean (%)	10.11	3.34	2.99	0.53	0.21

Note: There were no t-tests for < 1.0 % extractions as they were considered insignificant

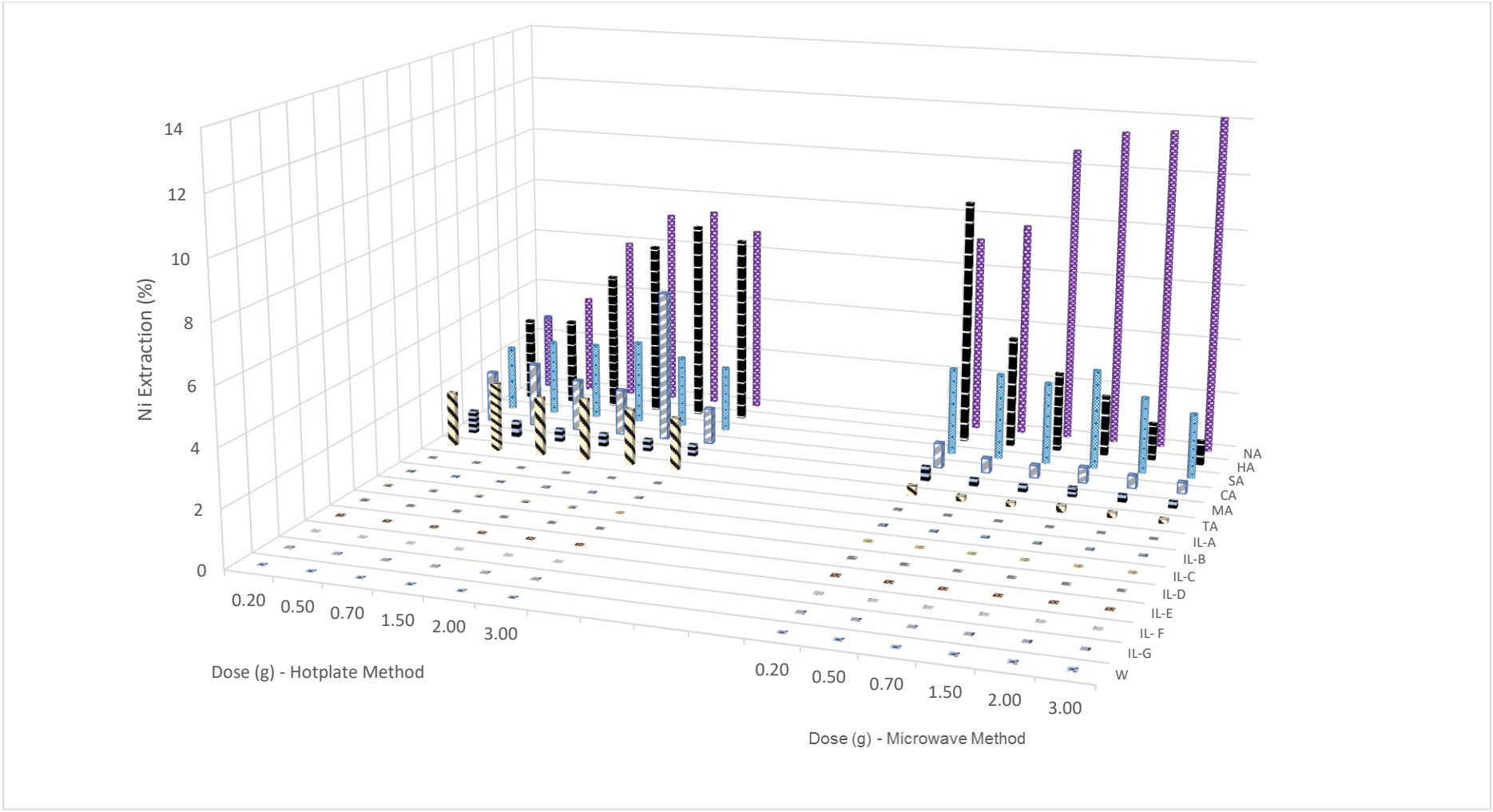

Figure 4.22 Percentage concentration for the effect of sample dose on leaching Ni

4.5.5 Effect of Dose on Leaching Pb

Table 4.20 a shows the percentage extraction of Pb with dose and this is also represented in **Figure 4.23**. In the hotplate method (**Figure 4.23)**, the dose increased from 0.2 – 3.0 g the Pb extraction increased for NA and HA but decreased for SA, the organic acids and IL D. The best extraction for Pb were NA (63 % at 3.0 g), HA (55 % at 2.0 g), SA (2 % at 0.2 g), CA (6 % at 0.2 g), MA (11 % at 0.2 g), TA (4 % at 0.2 g), IL D (4 % at 0.2 g) and IL G (1 % at 0.2 g). ILs A, B, C, E & F did not show any significant extractions. In the microwave method **(Figure 4.23)**, the dose increased from 0.2 g to 3.0 g the Pb extraction decreased. The solvents peak extractions for NA (67 % at 0.2 g) and HA (52 % at 0.2 g). SA, the organic acids and ILs A – G did not show any significant extractions.

To compare the hotplate method with microwave method, two sample independent t-test was done for each of the solvents. The null hypothesis (H_0) stated that the mean of both methods are equal while the alternative hypothesis (H_1) stated that the mean of both methods are not equal. In **Table 4.20 b** it shows that at 95 % confidence level the independent t-test for NA, HA and IL G had p-values > 0.05 and this shows that the means for both methods are equal so the hotplate and microwave methods have the same efficiencies. However, the solvents with p-value < 0.05 shows that the mean of both methods are not equal therefore the hotplate method was better for SA, CA, MA and TA.

Table 4.20a Percentage concentration values for effect of dose on leaching Pb

	Dosage (g)	Extraction (%)														
		AQ	NA	HA	SA	CA	MA	TA	IL-A	IL-B	IL-C	IL-D	IL-E	IL-F	IL-G	W
Hotplate Method	**0.20**	100.00	22.06	20.43	1.61	6.24	11.40	3.66	0.34	0.24	0.25	4.47	0.36	0.23	1.46	0.00
	0.50	100.00	41.42	47.87	1.01	3.30	5.11	1.86	0.15	0.12	0.12	1.87	0.17	0.11	0.77	0.00
	0.70	100.00	47.15	45.45	0.71	3.13	3.13	1.57	0.15	0.14	0.12	1.37	0.16	0.10	0.65	0.00
	1.50	100.00	59.82	51.22	1.02	3.22	2.93	1.41	0.14	0.12	0.11	1.21	0.15	0.09	0.41	0.00
	2.00	100.00	56.07	54.55	0.95	1.73	1.73	1.30	0.14	0.12	0.11	0.52	0.13	0.00	0.29	0.00
	3.00	100.00	63.00	38.50	0.83	1.30	1.37	0.90	0.10	0.08	0.08	0.43	0.05	0.04	0.06	0.00
Microwave Method	**0.20**	100.00	66.67	52.44	0.14	0.17	0.17	0.17	0.45	0.52	0.44	0.34	0.00	0.57	0.55	0.05
	0.50	100.00	59.56	39.89	0.09	0.17	0.17	0.17	0.33	0.37	0.33	0.21	0.00	0.37	0.36	0.09
	0.70	100.00	51.67	26.67	0.07	0.19	0.19	0.21	0.25	0.26	0.28	0.16	0.00	0.29	0.28	0.10
	1.50	100.00	58.10	20.34	0.05	0.23	0.22	0.22	0.17	0.17	0.18	0.12	0.00	0.18	0.19	0.15
	2.00	100.00	53.03	12.60	0.04	0.18	0.18	0.20	0.17	0.15	0.17	0.11	0.00	0.16	0.16	0.16
	3.00	100.00	48.58	13.53	0.03	0.16	0.16	0.16	0.13	0.11	0.13	0.08	0.00	0.13	0.13	0.19

Table 4.20b Independent t-test between hotplate and microwave methods at 95% confidence level (dose effect in Pb)

	NA	HA	SA	CA	MA	TA	IL-D	IL-G
p-value	0.26	0.09	2.26×10^{-05}	0.00	0.02	0.00	0.04	0.15
Hotplate mean (%)	48.25	43.00	1.02	3.15	4.28	1.78	1.65	0.61
Microwave mean (%)	56.27	27.58	0.07	0.18	0.18	0.19	0.17	0.28

Note: There were no t-tests for < 1.0 % extractions as they were considered insignificant

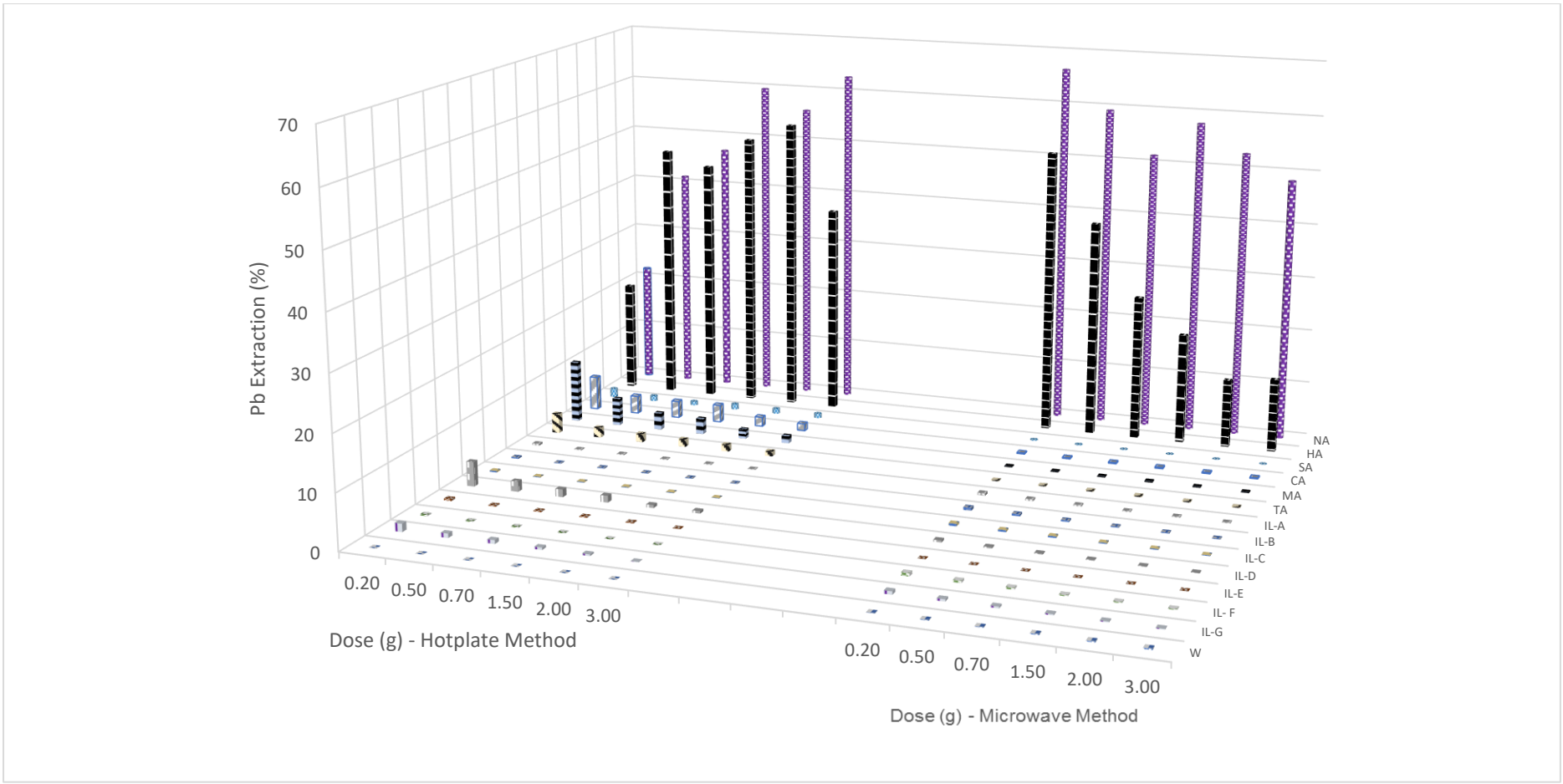

Figure 4.23 Percentage concentration for the effect of sample dose on leaching Pb

4.6 PCA for dose effect

4.6.1 PCA Scree Plot for Dose Effect

The dose effect experiment involved 30 variables and 90 observations. The variables were made up of five metals (Cu, Zn, Fe, Ni and Pb) with each of these metals having results from six different samples of WEEE dose (0.2, 0.5, 0.7, 1.5, 2.0, 3.0 g). The observations were results from each of the fifteen solvents with three replicates each from the hotplate and microwave methods used in the experiment. **Table 4.21** shows the summarized data of the first six principal components extracted from both the hotplate and microwave methods (mg/g) in **Appendices 1 a – e**. **Figure 4.24** shows the scree plot of variance for the dimensions from dose effect data and they are in the order of highest to the lowest with Dim.1 as 80.4 % and Dim.2 as 8.3 %. From this scree plot we can infer that Dim.1 explains the most part of the dose effect data as it is larger than the other dimensions. From **Table 4.21**, we can see that Dim.1 & 2 showed a SD > 1.0 as SD = 1 is the cutoff point. Therefore, we can accept the first two dimensions (Dim.1 & 2) with a proportion of variance of 80.4 & 8.3% respectively. Consequently, the cumulative proportion in Dim.1 & 2 also showed 80.4, 88.7 & 94.3 % respectively. This means that with Dim.2 having a SD of 1.6 , about 88.7 % of the data can be accounted for while the remaining 11.3 % of the data can be disregarded as they fall below SD < 1.0.

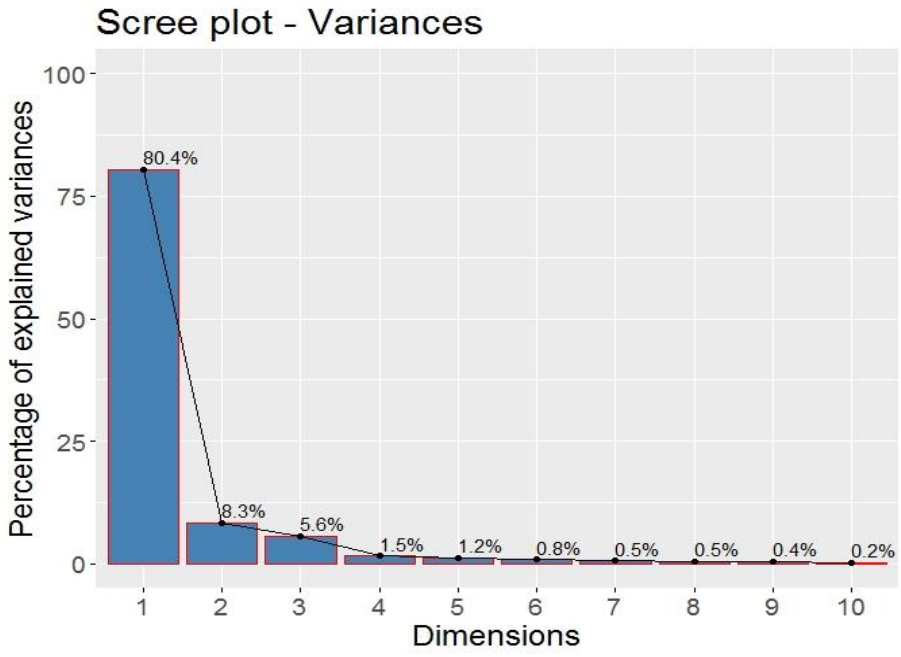

Figure 4.24 Scree plot showing variance for dose effect

Table 4.21 Summarized Principal Components for Dose Effect

Principal Components	Dim.1	Dim.2	Dim.3	Dim.4	Dim.5	Dim.6
Standard deviation	4.911	1.577	0.294	0.678	0.611	0.492
Proportion of Variance	0.804	0.083	0.558	0.015	0.012	0.008
Cumulative Proportion	0.804	0.887	0.943	0.958	0.971	0.979

Figure 4.25 shows the biplot for dose effect data which is the relationship between the variables and the observations in the dose data. It also shows the structure of variables correlations and clustered observations. From the PCA plot, we can see the variables with the longest vector projections. They represent the highest variations in the data and they have occured in Zn0.7, Cu0.2, Zn0.5, Zn1.5, Zn 2.0 and Cu0.7. The replicate observations formed clusters, for example, in the hotplate method (1, 2 & 3) the observations AQ1, AQ2 & AQ3 which represents the hotplate result for *aqua-regia* formed a cluster which means that the three replicated experiments showed similarity in the result from dose effect. Also, this behaviour was observed in AQ4, AQ5 & AQ6 (microwave method) showing that the replicated results were similar. The *aqua-regia* observations AQ1-3 and AQ4-6 are considered outliers on the PCA as they were clearly outside the group clustering and also far away from the other observations. However, they were not treated as outliers or removed as they were needed in this research inorder to clearly differentiate the best performing solvents or observations. Other observation clusters were seen in (HA1, HA2 & HA3), (NA1, NA2 & NA3), (NA4, NA5 & NA6) and (SA1, SA2 & SA3). The above stated clusters had various degrees of euclidean distance (distance between observations) and the observations from *aqua-regia* (AQ1-3) was the farthest followed by *aqua-regia* (AQ4-6). However, NA1-3 and NA4-6 were next before SA1-3. Consequently, SA4-6, the organic acids and ionic liquids all seemed to have clustered together as their euclidean distance were relatively close.

We can see that the variables vectors were pointing towards AQ1-3, AQ4-6, HA1-3, NA1-3 and NA4-6. This shows a high degree of association between the variables and the observations but the reverse was the case for the other observations such as SA1-3, SA4-6, the organic acids and ionic liquids as the PCA plot (**Figure 4.25**) clearly shows the variable vectors pointing away from them and this implies very low association between the variables and these observations. Also, the variables were pointing towards the hotplate method (red) showing high variable association with the hotplate method. However, more than half of the

variables were pointing away from the microwave method (blue) showing lesser variable association with the microwave method except for Cu0.2, Cu0.7 Cu0.5, Fe2.0 and Pb0.2 which showed high association with the microwave method.

The variable vectors closest to each other showed high correlation amongst themselves, for example Fe3.0 and Fe0.7 or Zn0.2 and Zn3.0 formed angles around 30 degrees. Negative correlation was observed between Zn0.7 and Cu0.2 as their vectors formed angles around 180 degrees. No correlation was observed between Pb0.7 and Zn0.7 as their vectors form angle of 90 degrees. The x-axis which is Dim.1 (80.4 % of variation explained) shows that all the variable vectors are positioned on the left side of the plot thereby revealing negative correlation for all variables. So we would expect that the lower the values of Dim.1 the higher values for each of the variables. The y-axis which is Dim.2 (8.3 % of variation explained) shows that half of the variables postioned at the top were positive correlation and the other half at the bottom were negative correlation (Kohla & Luniak, 2005; Reris & Brooks, 2015; Statisticshowto, 2021; STHDA, 2021; Towardsdatascience, 2021).

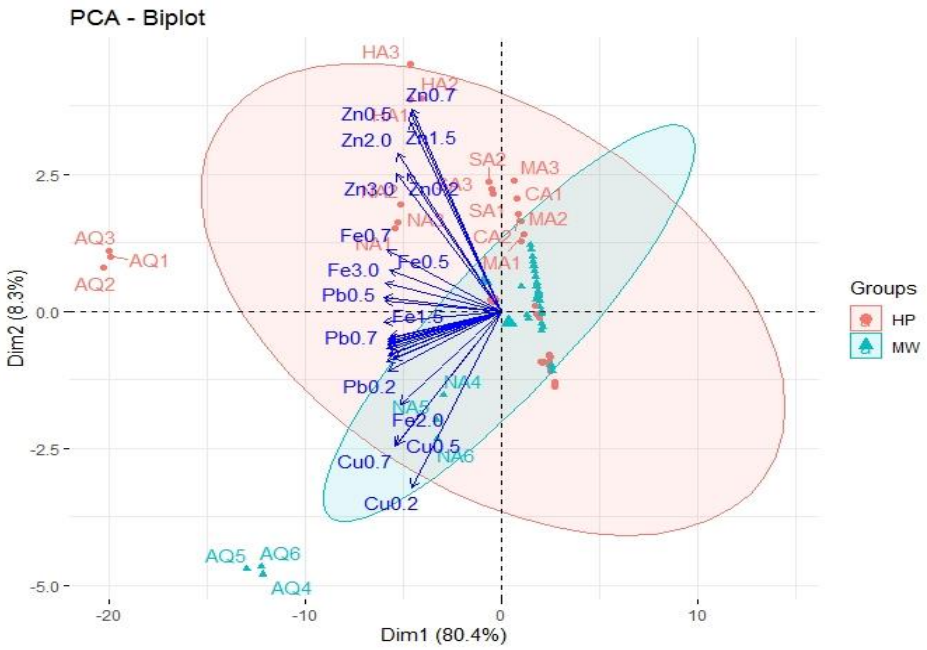

Figure 4.25 Biplot of variables and observations for Dose Effect

4.6.2 PCA Result for Variable Coordinates in Dose Effect

Figure 4.26 a shows the plot for the variable coordinates for Dim.1 & 2 which are representing of the position of the dose effect variables on the plot. The coordinates are correlation between a variable and a dimension. **Figure 4.26 b** shows a three-dimensional view of variable coordinates for the three dimensions (Dim.1, 2 & 3) with Dim.1 (80.4 %) on the x-axis, Dim.2 (8.3 %) on the z-axis and Dim.3 (5.6 %) on the y-axis. **Figure 4.26 c** shows the variable coordinates visualization with spots of different colour intensity. The strongest or darkest colour represent the highest correlation values and the correlation values decreases with decrease in the colour intensity of the spots in the visualization. Also, the positive correlated values are in blue while the negative correlated values are in red. Here, Dim.1 - 5 are represented by Dim.1 - 5. The order of importance decreased from Dim.1 - 5. We can see that Dim.1 showed the highest colour intensity and this was followed by Dim.2 - 5. However, all the coordinates in Dim.1 showed strong negative correlation. In Dim.2, moderate positive correlation occurred in Zn 0.5, Zn 0.7, Zn 1.5. The other variables showed weak positive and negative correlation.

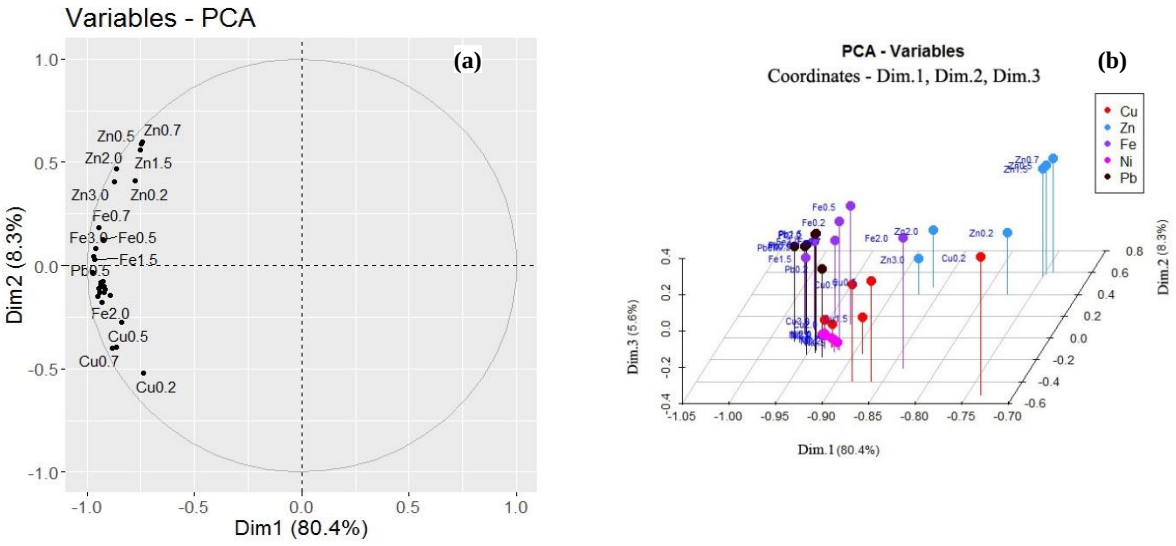

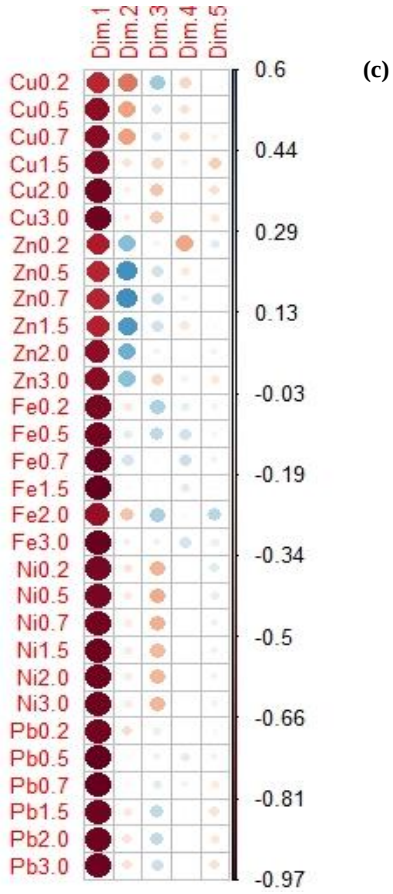

(c)

Figure 4.26: (a) Variable Coordinates Correlation Plot (dose effect) (b) Variable Coordinates 3D Plot (dose effect) (c) Variable Coordinates Dim Plot (dose effect)

4.6.3 PCA Result for Variable Cos2 Quality of Representation in Dose Effect

Figure 4.27 a shows the Cos2 plot of variable with the highest Cos2 value which are in orange while the mid cos2 variables value are in blue. The variables in orange are the most represented in the plot as they are closest to the circle of correlation with very high values and this is followed by the yellow and then the blue spots. All the variables indicated in this Cos2 plot **(Figure 4.27 a)** show very good representation for Dim.1 as all the variables are far from the centre of the circle and none is close to the centre of the circle. **Figure 4.27 b&c** shows another visualization of the Cos2 variables in the form of bar plots. We can see that the Cos2 variables for Dim.1 in **Figure 4.27 b** are the highest which shows that the quality of representation is good. The variables in the bar plots are arranged from highest to lowest. Consequently, all negative values have been cancelled out and **Figure 4.27 d** shows the Cos2 variables visualization with spots of different colour intensity. The strongest or darkest colour

represent the highest Cos2 variables and the Cos2 variables decreased with decrease in the colour intensity of the spots in the visualization. We can see that Dim.1 variables showed the highest colour intensity and this was followed by Dim.2. In Dim.1 (**Figure 4.27 b**), the data visualized explains 80.4% of the dose effect experiment and the best five represented variables were Pb0.7, Pb0.5, Fe1.5, Fe 3.0 and Pb3.0. In Dim.2 (**Figure 4.27 c**), the visualized data explains 8.3 % of the dose effect experiment and the best three correlated variables were Zn0.7, Zn0.5 and Zn1.5.

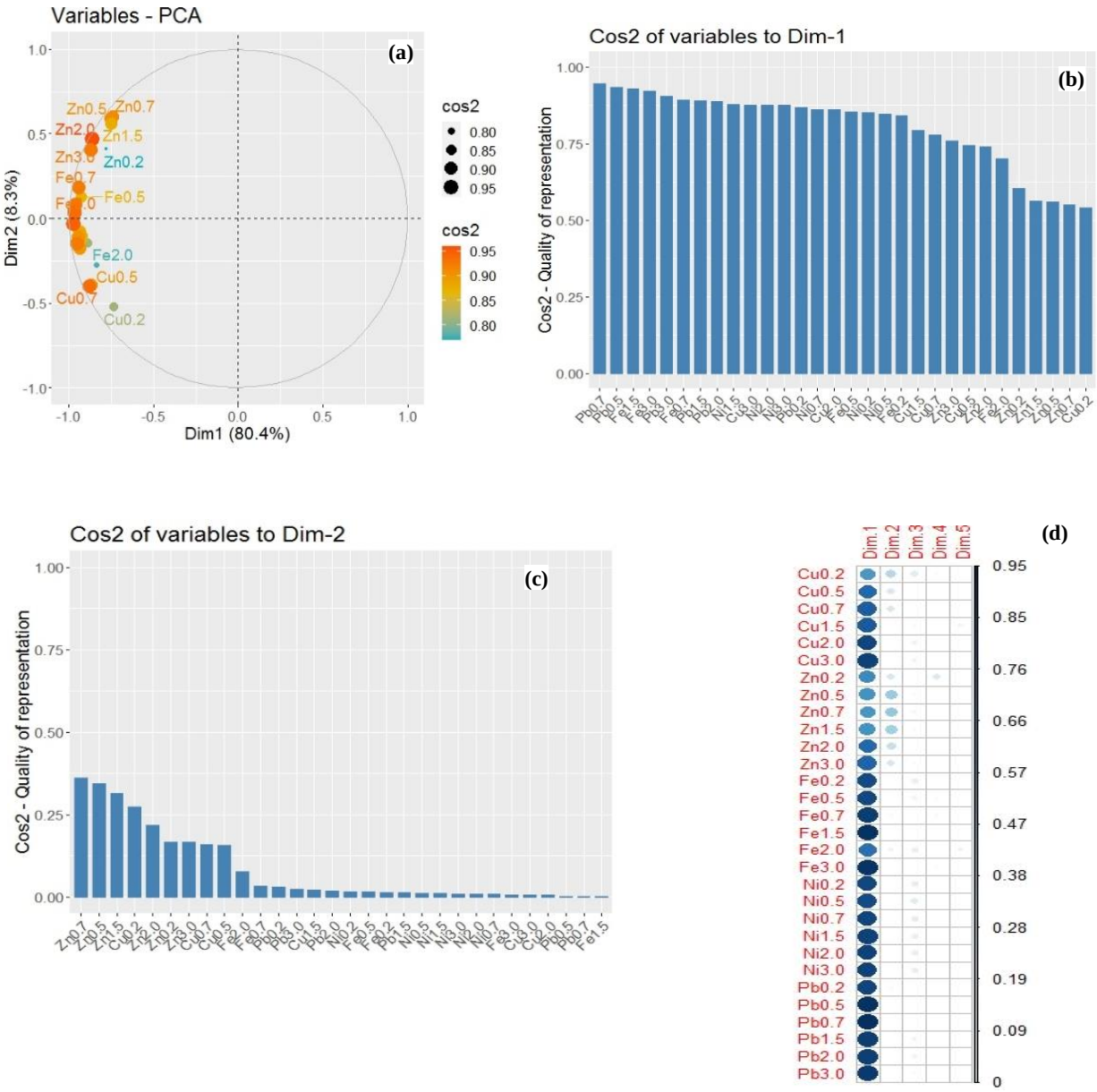

Figure 4.27 (a) Cos2 quality of representation (dose effect) (b) Dim.1 quality of representation (dose effect) (c) Dim.2 quality of representation (dose effect) (d) Cos2 quality of representation plot (dose effect)

4.6.4 PCA Result for Variables Contribution in Dose Effect

Figure 4.28 a shows the contribution of variable correlation plot with the most contributing variables indicated in red and the least contributing variables indicated in blue. From **Figure 4.28 b - c**, we can see the contribution of variables represented in bar plots with red dotted lines which indicates the expected average contribution. Dim.1 and Dim.2 are the most important to be considered in explaining the contribution while Dim.3, 4 & 5 are less important. In Dim.1 (**Figure 26 b**), most contribution of variables values were slightly above the expected average contribution. **Table 4.22** shows the actual values for the best contribution of variables and **Figure 4.28 d** shows the contribution of variables plot with spots of different colour intensity. The darker colours indicate higher contribution while the lighter color indicate low contribution. The contribution of variables for a particular dimension are measured in percentages. Correlated variables in the contribution of variables for Dim.1 & Dim.2 explains 80.4 % and 8.3 % respectively. Contributions from Dim.1 are the most important as they contribute more than other variables and this is followed by Dim.2. Even though the contributions from other dimensions are highly correlated (Dim.3, Dim.4 & Dim.5), they would not be considered since they are not as important as in Dim.1 & 2. The order of importance in the contribution for the dimensions are Dim.1 > Dim.2 > Dim.3 > Dim.4 > Dim.5. A variable with large contribution value contributes more to the component. Dim.1 which explains 80.4 % of the variation is represented in **Figure 4.28 b.** We can see the bar chart for Dim.1 contributions arranged in descending order and the best five contributing variables were Pb0.7 (3.92 %), Pb0.5 (3.87 %), Fe 1.5 (3.86 %), Fe 3.0 (3.82 %) & Pb 3.0 (3.75 %). Dim.2 which explains 8.3 % of the variation is represented in **Figure 4.28 c**. We can see the bar chart for Dim.2 contributions also arranged in descending order and the best three contributing variables were Zn 0.7 (14.48 %), Zn 0.5 (13.83 %), Zn 1.5 (12.68 %). The best contributing variables for dose effect from highest to lowest are in the order Pb 0.7 > Pb 0.5 > Fe 1.5 > Fe 3.0 > Pb 3.0 > Zn 0.7 > Zn 0.5 > Zn 1.5.

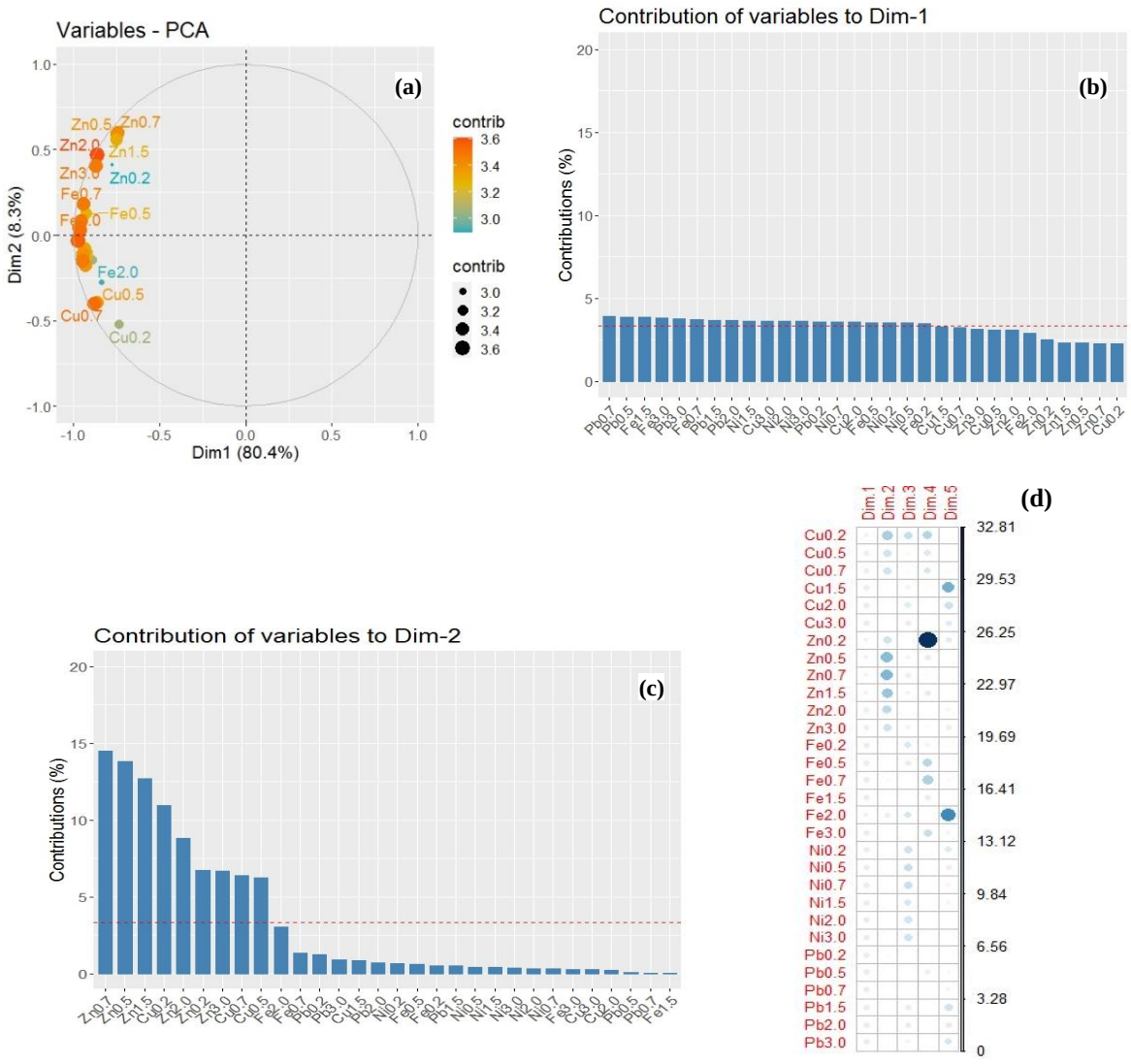

Figure 4.28 (a) Contribution of Variable Correlation Plot (dose effect) (b) Dim.1 Contribution of Variable Bar Plots (dose effect) (c) Dim.2 Contribution of Variable Bar Plots (dose effect) (d) Variable Contribution Plot (dose effect)

Table 4.22 Best Contributing Variables for Dose Effect (in bold)

	Dim 1 (%)	Dim 2 (%)
Zn 0.5	2.32	**13.83**
Zn 0.7	2.28	**14.48**
Zn 1.5	2.33	**12.68**
Fe 1.5	**3.86**	0.04
Fe 3.0	**3.82**	0.28
Pb 0.5	**3.87**	0.07
Pb 0.7	**3.92**	0.04
Pb 1.5	**3.69**	0.50
Pb 3.0	**3.75**	0.92

4.6.5 PCA Result for Observation Coordinates in Dose Effect

Figure 4.29 a shows the plot for the observation coordinates which are representing the position of the solvents used in dose effect experiment for both the hotplate and microwave methods. **Figure 4.29 b - e** shows the three-dimensional plots of inorganic acids, organic acids, ionic liquid (a - c) and ionic liquid (d - g). Dim.1 on the x-axis, Dim.2 on the z-axis and Dim.3 on the y-axis. These three dimensional plots shows the coordinates or positioning of the solvents used for the dose effect experiment. **Figure 4.30 a – d** shows the observation coordinate visualization plot for inorganic acids, organic acids, ionic liquid (a - c) and ionic liquid (d - g). The observation coordinates for the inorganic acids all showed very good negative correlation except SA4 - 6 (sulphuric acid) which showed positive correlation. AQ1-6 (*aqua-regia*) had the strongest negative correlation values followed by NA1-3 (nitric acid) then HA 1-3 (hydrochloric acid). The strength of correlation can be seen on Dim.1 in **Figure 4.30 a** as very dark red colours. Dim.2 also had good correlation values except for SA5 which showed relatively weak negative correlation. The organic acid, Dim.1 (**Table 4.18 b**), all showed strong positive correlation and the strength of correlation can be seen in Dim.1 in **Figure 4.30 b** while the Dim.2 showed good positive correlation except for CA5, CA6, MA4 & TA1. The coordinates in ionic liquids (a - c) all showed strong positive correlation in Dim.1 and the strength of correlation can be seen on Dim.1 in **Figure 4.30 c** while Dim.2 showed strong negative and positive correlations. The weakest correlations were in ILA4, ILA5 & ILA6. The coordinates in ionic liquids (d - g) all showed strong positive correlation in Dim.1 and the strength of correlation can be seen on Dim.1 in **Figure 4.30 d** while Dim.2 showed strong negative and positive correlations.

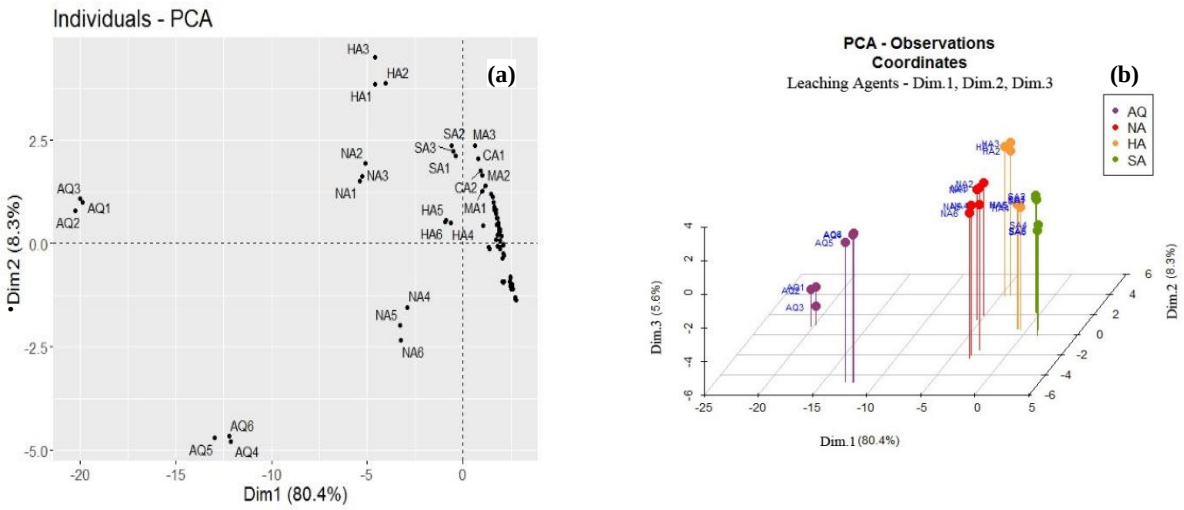

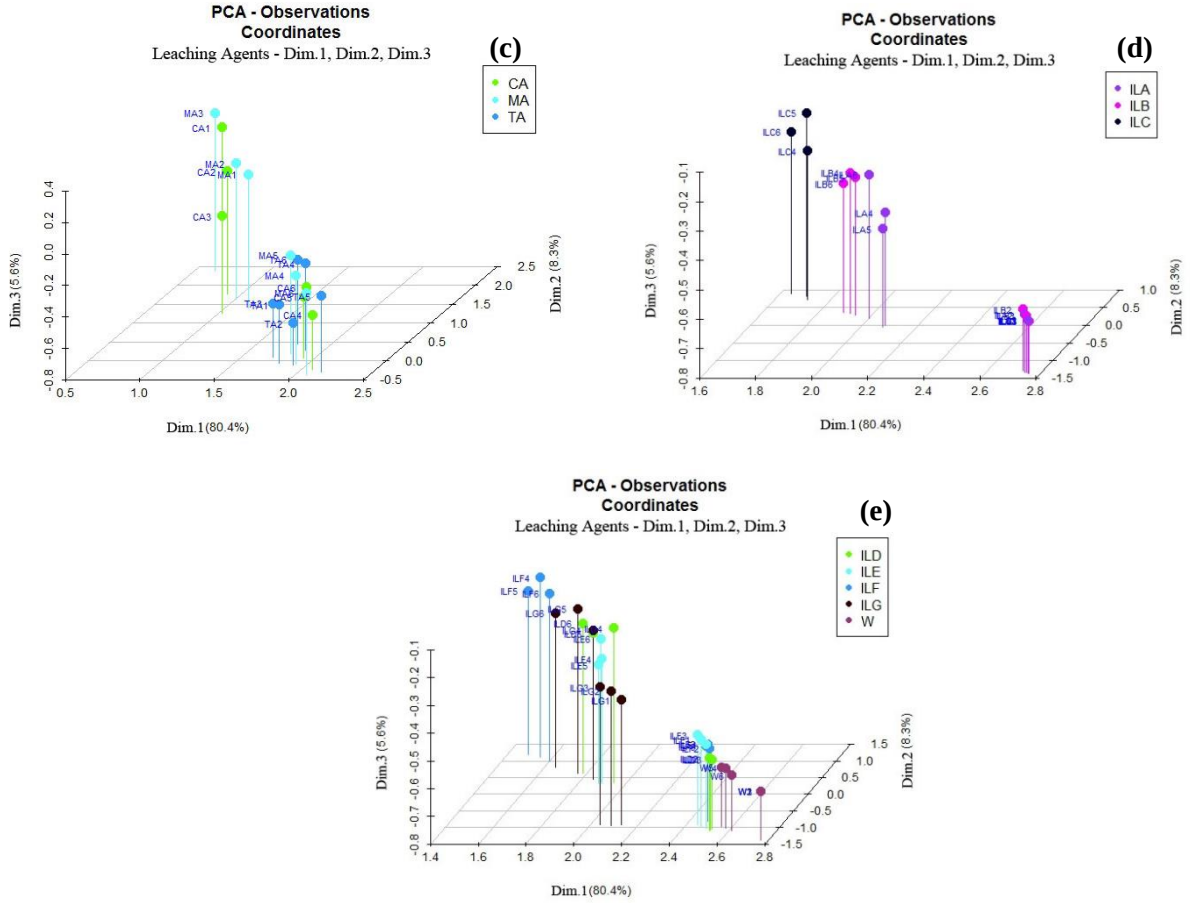

Figure 4.29: (a) observation coordinate correlation plot (dose effect) (b) observation coordinate for inorganic acids (dose effect) (c) observation coordinate for organic acids (dose effect) (d) observation coordinate for IL a-c (dose effect) (e) observation coordinate for IL d-g (dose effect)

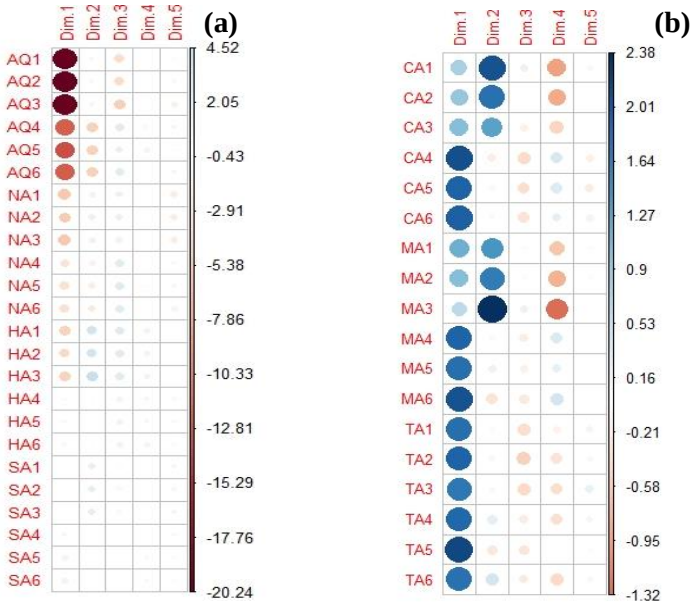

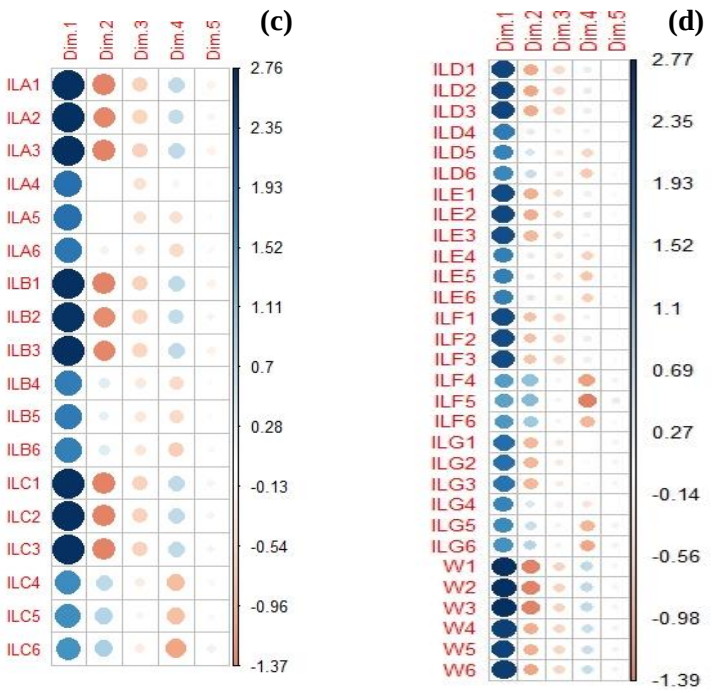

Figure 4.30: (a) Observation coordinate plot for inorganic acids (dose effect) (b) observation coordinate plot for organic acids (dose effect) (c) observation coordinate plot for IL a – c (dose effect) (d) observation coordinate plot for IL d - g (dose effect)

4.6.6 PCA Result for Observation Cos2 Quality of Representation in Dose Effect

Figure 4.31 a shows the Cos2 plot of observation with the highest Cos2 value which are in orange while the mid cos2 observation value are in blue. The observations in orange are the most represented in the plot as they have very high values and this is followed by the yellow and then the blue spots. **Figure 4.31 b - e** shows the three-dimensional plots Cos2 observation for inorganic acids, organic acids, ionic liquid (a - c) and ionic liquid (d - g). Dim.1 on the x-axis, Dim.2 on the z-axis and Dim.3 on the y-axis. These three dimensional plots shows the coordinates or positioning of the solvents used for the dose effect experiment. **Figure 4.32 a - d** shows the Cos2 observations visualization with spots of different colour intensity. The strongest or darkest colour represent the highest Cos2 observations and the Cos2 observations decreased with decrease in the colour intensity of the spots in the visualization. Dim.1 (inorganic acids) showed good quality of representation. AQ1-6 had good quality of representation followed by NA1-3. The poorest quality of representation were found in HA4, SA1, 2 & 3. In Dim.2 (inorganic acids), only moderate quality of representation were found in SA1,2 & 3. Dim.1 in Figure 4.32b (organic acids) showed good quality of representation. CA4-5, MA4-6 & TA1-6 had good quality of representation. The poorest quality of representation were found in CA1 & MA3. In Dim.2 (organic acids), only

moderate quality of representation were found in CA1, 2 & MA3. The good quality of representation with strong colour intensity can be seen in Dim.1 (**Figure 4.32 b**). The quality of representation in Dim.1 (ionic liquids (a - c)) showed good quality of representation. In Dim.2, IL a – c, poor quality of representation were observed all through. Dim.1 in Figure 4.32 c (IL(a - c)) showed good quality of representation. In Dim.2 (IL (a - c)), poor quality of representation were found. The good quality of representation with strong colour intensity can be seen in Dim.1 (**Figure 4.32 d**).

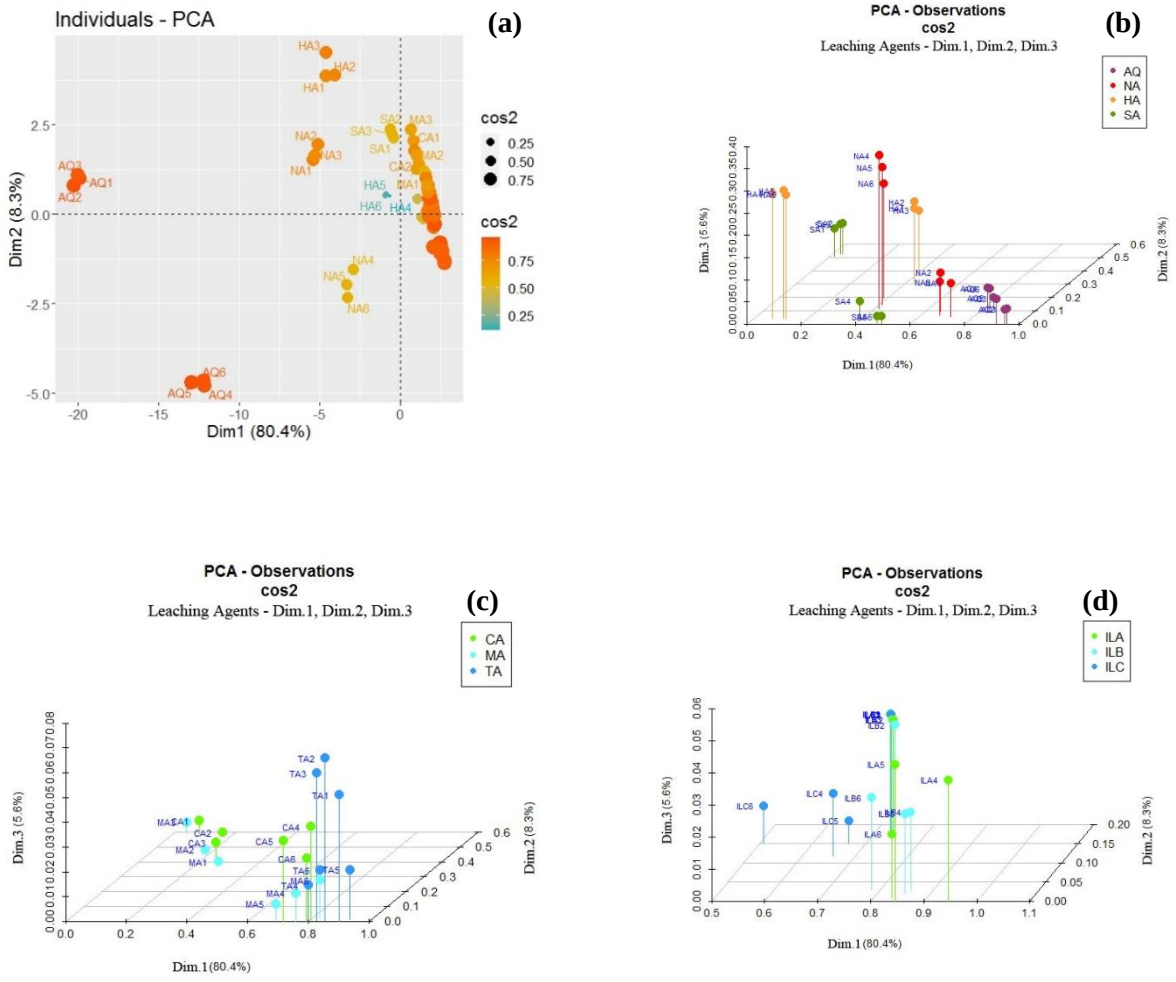

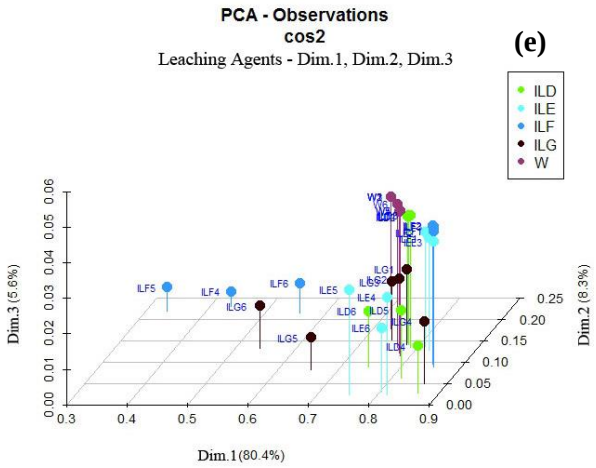

Figure 4.31: (a) Observation cos2 correlation plot (dose effect) (b) Observation cos2 for inorganic acids (dose effect) (c) Observation cos2 for organic acids (dose effect) (d) Observation cos2 for IL a-c (dose effect) (e) Observation cos2 for IL d-g (dose effect)

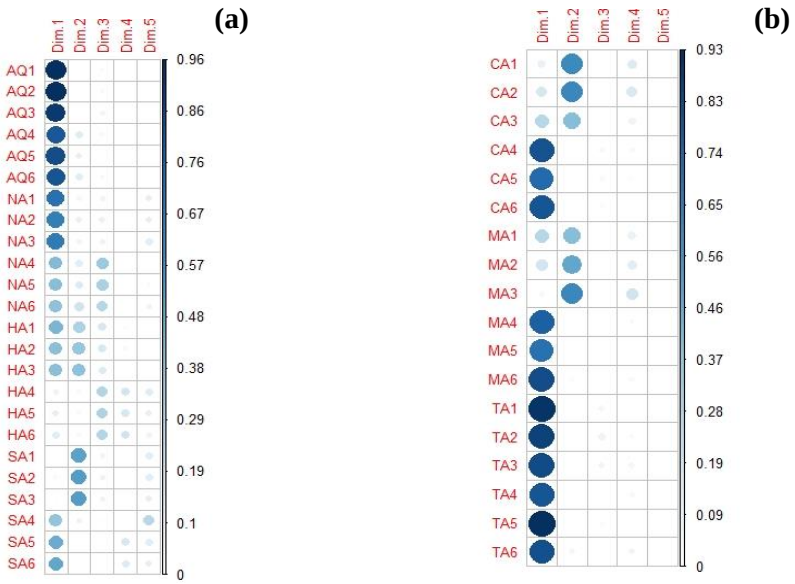

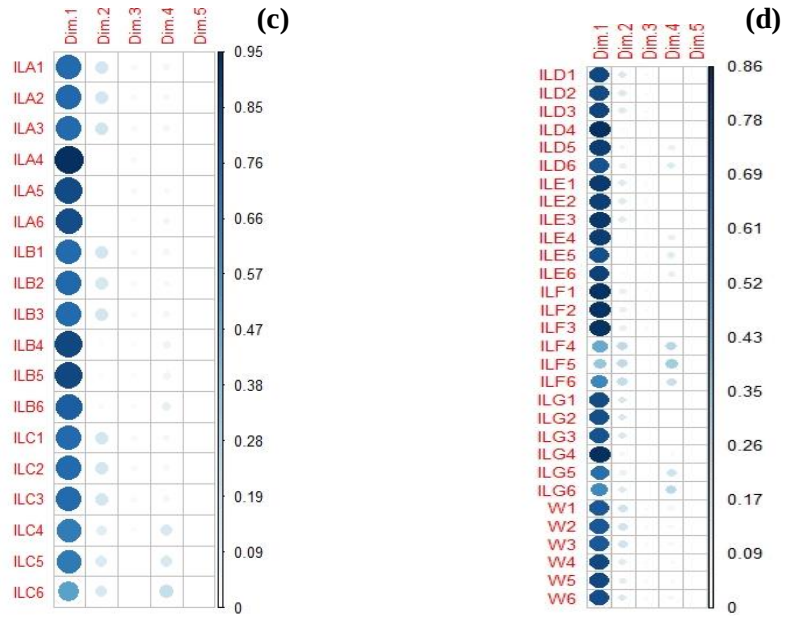

Figure 4.32: (a) Observation cos2 Dim plot for inorganic acids (dose effect) (b) observation cos2 Dim plot for organic acids (dose effect) (c) observation cos2 Dim plot for IL a – c (dose effect) (d) observation cos2 Dim plot for IL d - g (dose effect)

4.6.7 PCA Result for Observation Contribution in Dose Effect

Figure 4.33 a shows the contribution plot of observation with the highest contribution values which are in orange while the mid contribution value are in blue. In the figure, more labelling priority is given to the highest contributing observation with the least contributing observations not appearing. The observations in orange are the most represented in the plot as they have very high values and this is followed by the yellow and then the blue spots. **Figure 4.33 b - e** shows the three-dimensional plots of observation contribution for inorganic acids, organic acids, ionic liquid (a - c) and ionic liquid (d - g). Dim.1 on the x-axis, Dim.2 on the z-axis and Dim.3 on the y-axis. These three dimensional plots shows the positioning of the solvents contribution on the plot. **Table 4.23** shows the observation contribution values in percentages. **Figure 4.34 a -d** shows the observation contribution visualization with spots of different colour intensity. The strongest or darkest colour represent the highest observation contribution and the observation contribution decreased with decrease in the colour intensity of the spots in the visualization. The observation contribution in Dim.1 for inorganic acids (**Table 4.23**), shows observation contribution and the best five were solvents that contributed to this Dim.1 were AQ1 (18.19 %), AQ2 (18.87 %), AQ3 (18.45 %), AQ4 (6.77 %), AQ5 (7.73 %), AQ6 (6.85 %) and it was followed by NA1 - 6 & HA1-3 (approximately 1.0 %). In

Dim.2 (inorganic acids), the best three observation contributions were AQ4 (10.29), AQ5 (9.88), AQ6 (9.73), HA3 (9.14).The best observation contribution with strong colour intensity can be seen in Dim.1 (**Figure 4.34 a**). The best contributing solvents from highest to lowest are in the order AQ2 > AQ3 > AQ1 > AQ5 > AQ6 > AQ4 > NA1 - 6 > HA1 - 3. The observation contributions with strong colour intensity can be seen in Dim.1 & 2 (**Figure 4.34 b**).

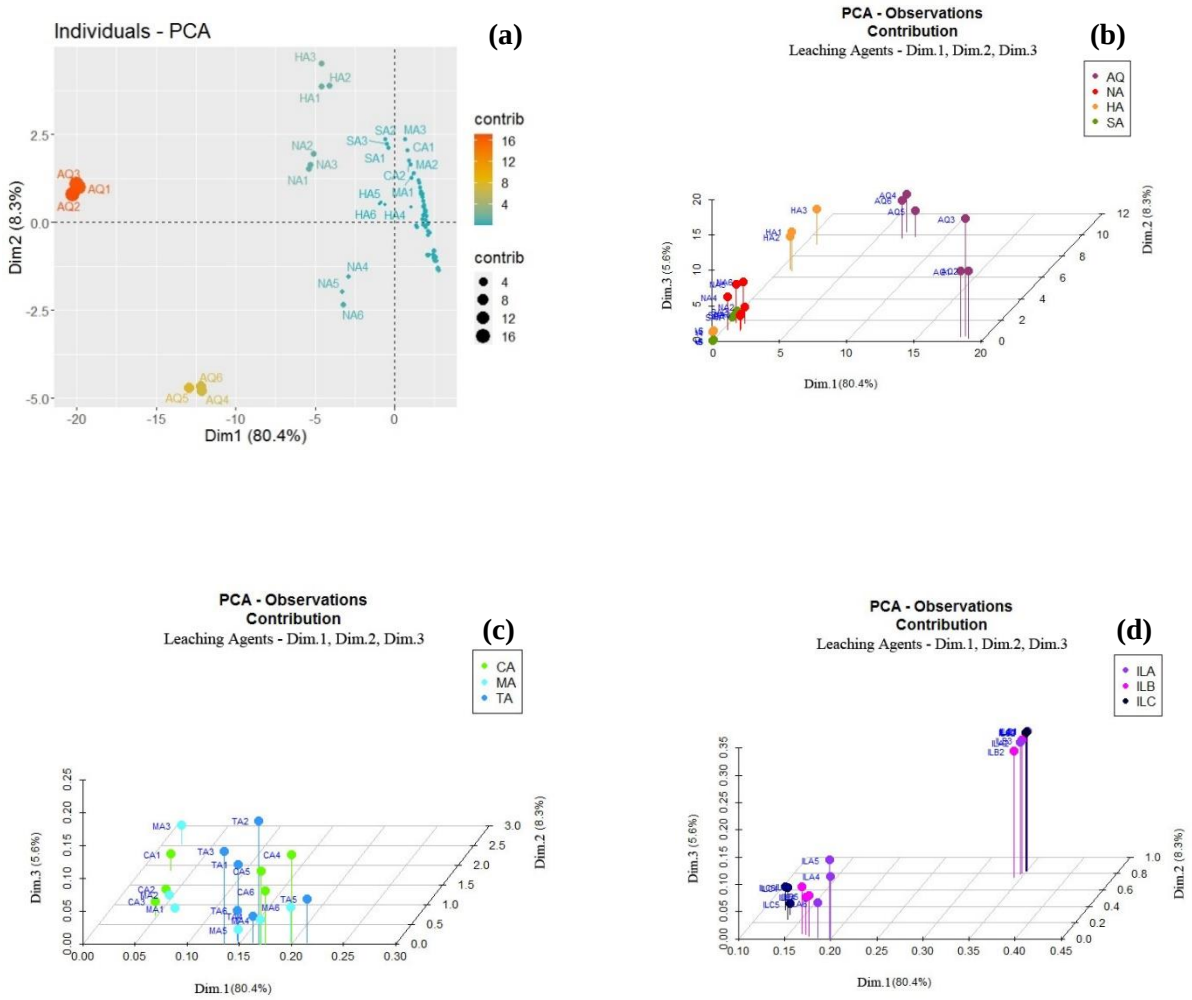

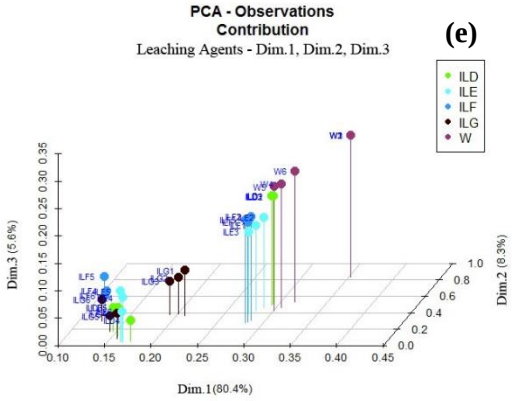

Figure 4.33: (a) Observation contribution plot (dose effect) (b) Observation contribution for inorganic acids (dose effect) (c) Observation contribution for organic acids (dose effect) (d) Observation contribution for IL a-c (dose effect) (e) Observation contribution for IL d-g (dose effect)

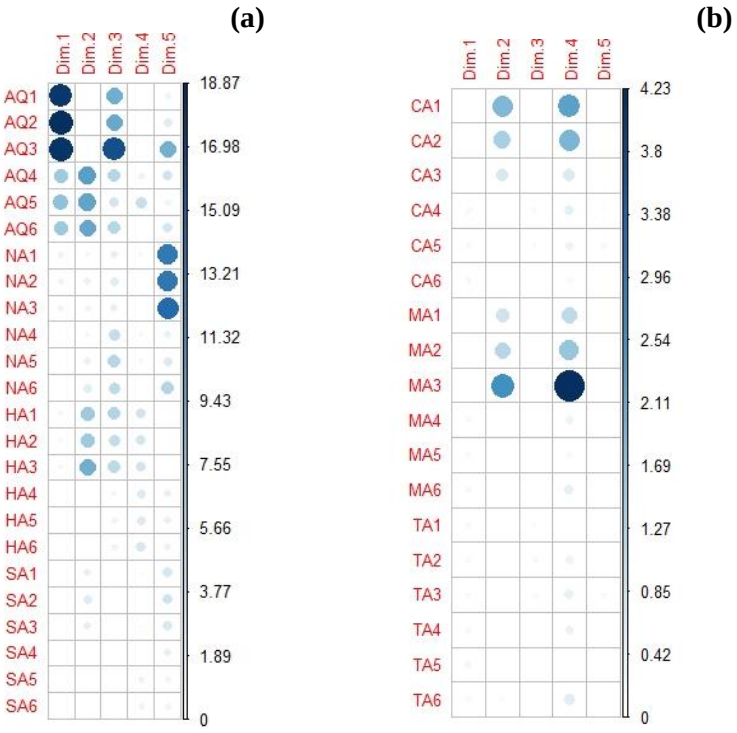

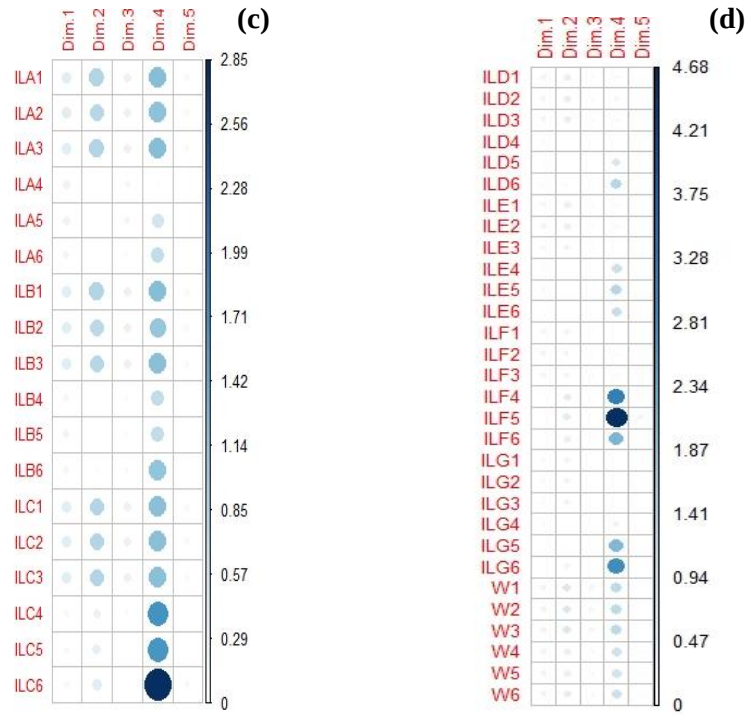

Figure 4.34: (a) Observation contribution Dim plot for inorganic acids (dose effect) (b) observation contribution Dim plot for organic acids (dose effect) (c) observation contribution Dim plot for IL a – c (dose effect) (d) observation contribution Dim plot for IL d - g (dose effect)

Table 4.23 Best Contributing Observations for Dose Effect (in bold)

	Dim 1 (%)	Dim 2 (%)
AQ1	**18.19**	0.44
AQ2	**18.87**	0.28
AQ3	**18.45**	0.54
AQ4	**6.77**	**10.29**
AQ5	**7.73**	**9.88**
AQ6	**6.85**	**9.73**
NA1	**1.34**	1.03
NA2	**1.20**	1.69
NA3	**1.28**	1.18
NA4	0.39	1.06
NA5	0.50	1.76
NA6	0.49	2.45
HA1	0.97	6.64
HA2	0.76	6.75
HA3	0.97	9.14

4.7. Determination of Particle-size Effect

Two methods, hotplate (HP) and microwave (MW) methods, were used to determine the effect of particle-sizes (1, 2, 3 & 4 mm) on the extraction of Cu, Zn, Fe, Ni and Pb. For the hotplate method, the experimental conditions were time (120 minutes), temperature (70 ^{0}C), concentration (2 mol/L for inorganic acids, 25 g/L for organic acids and 100 g/L for ionic liquids), sample weight (0.5 g) and rotation speed (340 rpm). For the microwave method, the experimental conditions were time (20 minutes), temperature (150 ^{0}C), concentration (2mol/L for inorganic acids, 25 g/L for organic acids and 100 g/L for ionic liquids) and sample weight (0.5 g). **Appendices 2 a - e** shows tables of the mean concentrations of particle-size effect for Cu, Zn, Fe, Ni and Pb (mg/g) with dose from three different experiments and the standard deviation as the error bar.

4.7.1 Effect of Particle-size on Leaching Cu

Table 4.24 a shows the percentage extraction of Cu for the hotplate method and this is also represented in **Figure 4.35.** In the hotplate method (**Figure 4.35**), the particle-size increased from 1mm to 4mm the Cu extraction also increased for HA and IL-G while NA and IL-E did not show significant changes. The peak extractions for the solvents were NA (66 % at 3 mm), HA (34 % at 4 mm), IL-E (3 % at 1 mm) and IL-G (29 % at 4 mm). The other solvents had < 1 % Cu extraction. In the microwave method (**Figure 4.35**)**,** the particle-size increased from 1 mm to 4 mm the Cu extraction did not show much significant change. The peak extraction was NA (49 % at 3 mm) and the other solvents did not show any significant Cu extractions.

Comparing the hotplate method with microwave method, two sample independent t-test was done for NA, HA, IL-G and IL-E. The null hypothesis (H_0) stated that the mean of both methods are equal while the alternative hypothesis (H_1) stated that the mean of both methods are not equal. In **Table 4.24 b** it shows that at 95 % confidence level the independent t-test for NA, HA, IL-G and IL-E had p-values < 0.05 and this shows that the means for both methods are not equal so the hotplate method which had the higher mean values is a better method.

Table 4.24a Percentage concentration for effect of particle-size on leaching Cu

	Particle-size (mm)	Extraction (%)														
		AQ	NA	HA	SA	CA	MA	TA	IL-A	IL-B	IL-C	IL-D	IL-E	IL-F	IL-G	W
Hotplate Method	1.00	100.00	55.09	11.21	0.10	0.33	0.14	0.08	0.00	0.00	0.00	0.02	3.25	0.12	8.30	0.00
	2.00	100.00	55.67	15.93	0.15	0.29	0.17	0.08	0.01	0.01	0.00	0.04	2.65	0.15	11.15	0.00
	3.00	100.00	65.94	28.38	0.32	0.23	0.31	0.36	0.01	0.01	0.01	0.03	2.17	0.05	15.92	0.00
	4.00	100.00	63.43	34.08	0.58	0.20	0.48	0.60	0.01	0.01	0.01	0.13	2.23	0.11	29.15	0.00
Microwave Method	1.00	100.00	46.59	0.50	0.01	0.02	0.07	0.04	0.03	0.03	0.03	0.03	0.42	0.04	0.48	0.01
	2.00	100.00	47.62	0.46	0.01	0.01	0.08	0.05	0.03	0.03	0.03	0.04	0.40	0.04	0.51	0.02
	3.00	100.00	49.15	0.44	0.01	0.01	0.10	0.05	0.03	0.03	0.04	0.04	0.41	0.04	0.62	0.03
	4.00	100.00	47.39	0.46	0.02	0.01	0.10	0.05	0.04	0.04	0.04	0.04	0.39	0.04	0.67	0.04

Table 4.24b Independent t-test between hotplate and microwave methods at 95% confidence level (particle-size effect on Cu)

	NA	HA	IL-E	IL-G
p-value	0.00	0.01	0.01×10^{-2}	1.50×10^{-2}
Hotplate mean (%)	60.03	22.40	2.58	16.13
Microwave mean (%)	47.69	0.47	0.41	0.57

Note: There were no t-tests for < 1.0 % extractions as they were considered insignificant

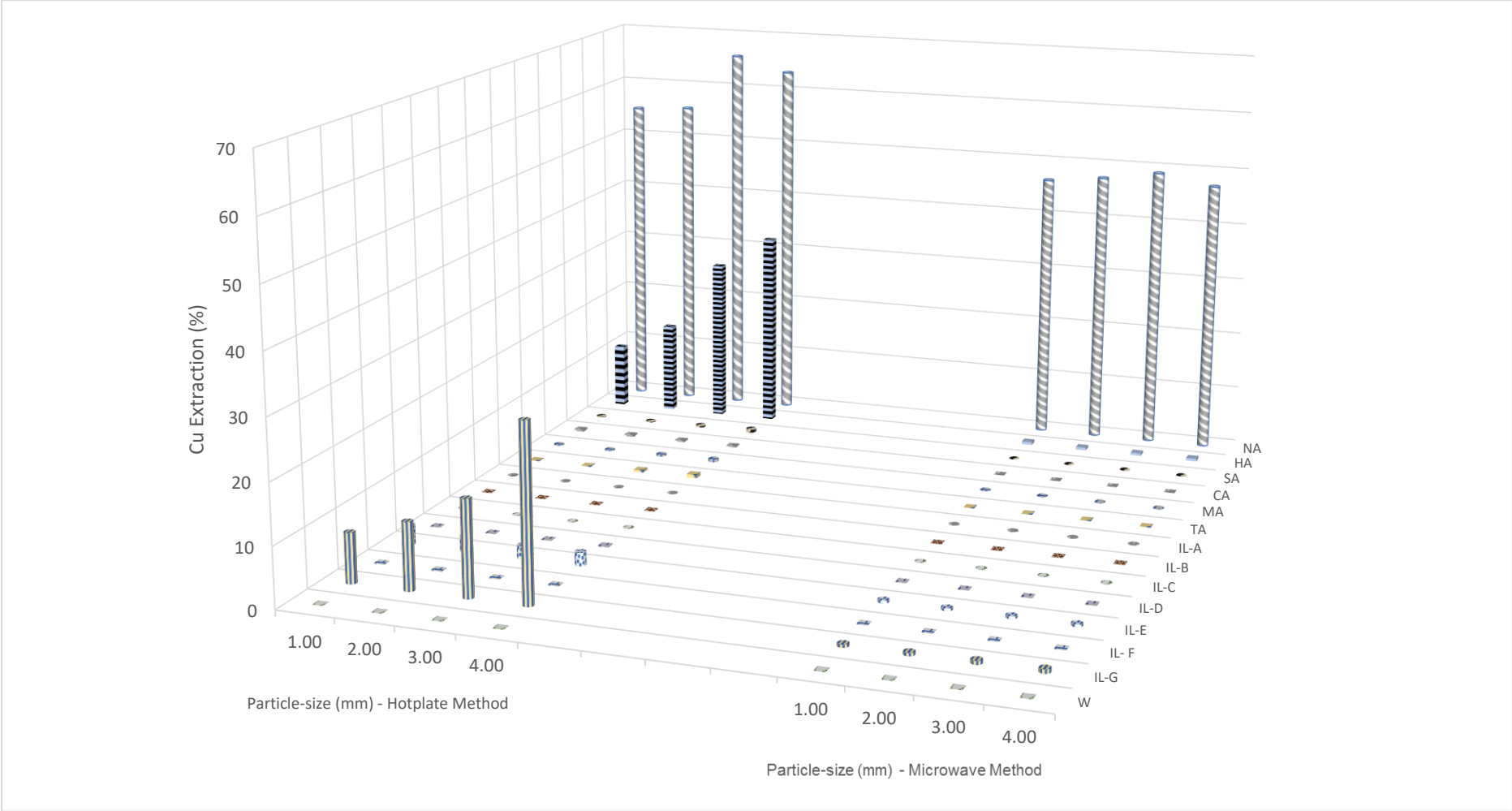

Figure 4.35 Percentage concentration for the effect of particle-size on leaching Cu

4.7.2 Effect of Particle-size on Leaching Zn

Table 4.25 a shows the percentage extraction of Zn for the hotplate method and this is also represented in **Figure 4.36.** For the hotplate method, in **Figure 4.36** the particle-size increased from 1 mm to 4 mm the Zn extraction also increased for the inorganic and organic acids. However, the HA extraction decreased while the ionic liquids did not show any significant change in extractions. The peak extractions for the solvents were HA (93 % at 1 mm), NA (79 % at 3 mm), SA (77 % at 3 mm), CA (63 % at 4 mm), TA (54 % at 4 mm), MA (34 % at 4 mm), ILs D, E, F & G had extractions in the range of 6 – 10 %. The other solvents had < 1 % Zn extraction. In the microwave method (**Figure 4.36**), the particle-size increased from 1 mm to 4 mm the Zn extraction showed little significant changes. The peak extractions were IL-F (84 % at 1 mm), IL-C (81 % at 1 mm), HA (80 % at 1 mm), SA (80 % at 1 mm), NA (76 % at 4 mm), IL-E (71 % at 1 mm), IL-A (70 % at 1 mm), IL-B (58 % at 1 mm), IL-G (58 % at 1 mm), TA (56 % at 1 mm), IL-D (54 % at 1 mm), MA (29 % at 1 mm), CA (25 % at 1 mm).

Comparing the hotplate method with microwave method, two sample independent t-test was done for each of the solvents. The null hypothesis (H_0) stated that the mean of both methods are equal while the alternative hypothesis (H_1) stated that the mean of both methods are not equal. In **Table 4.25 b** it shows that at 95 % confidence level the independent t-test for NA, HA, SA, CA, MA and TA had p-values > 0.05 and this shows that the means for both methods are equal so both methods for these solvents are the same. However, ILs A – G had p-values < 0.05 meaning the mean both methods are not equal therefore the microwave method with larger mean is better.

Table 4.25a Percentage concentration for effect of particle-size on leaching Zn

	Particle-size (mm)	Extraction (%)														
		AQ	NA	HA	SA	CA	MA	TA	IL-A	IL-B	IL-C	IL-D	IL-E	IL-F	IL-G	W
Hotplate Method	**1.00**	100.00	27.78	93.33	25.11	22.22	23.11	24.33	0.01	0.01	0.03	7.38	6.76	8.62	9.07	0.00
	2.00	100.00	76.29	65.98	68.56	28.35	27.84	38.66	0.02	0.01	0.08	8.45	8.35	8.66	10.21	0.01
	3.00	100.00	79.03	71.51	73.12	39.80	28.23	44.03	0.02	0.02	0.10	8.82	9.25	7.74	9.03	0.01
	4.00	100.00	77.90	65.75	77.35	62.98	34.25	53.70	0.03	0.03	0.13	8.62	9.50	7.96	7.51	0.01
Microwave Method	**1.00**	100.00	64.12	76.95	79.87	25.32	29.22	56.49	70.13	57.79	80.52	53.90	71.43	84.42	58.44	0.01
	2.00	100.00	77.44	62.88	72.84	23.77	33.35	55.21	56.23	56.23	81.28	51.12	53.16	79.23	49.07	0.01
	3.00	100.00	71.50	58.13	62.80	23.01	29.38	40.41	51.81	47.67	66.74	50.98	48.08	80.83	47.67	0.01
	4.00	100.00	75.68	61.45	62.59	20.20	26.03	40.97	49.31	45.14	65.24	50.07	42.48	80.42	51.21	0.01

Table 4.25b Independent t-test between hotplate and microwave methods at 95% confidence level (particle-size effect on Zn)

	NA	HA	SA	CA	MA	TA	IL-A	IL-B	IL-C	IL-D	IL-E	IL-F	IL-G
p-value	0.61	0.28	0.53	0.14	0.69	0.33	1.81×10^{-5}	3.09×10^{-6}	2.66×10^{-6}	5.05×10^{-9}	0.37×10^{-4}	9.86×10^{-10}	2.35×10^{-6}
Hotplate mean (%)	65.25	74.14	61.04	38.34	28.36	40.18	0.02	0.02	0.09	8.32	8.47	8.25	8.96
Microwave mean (%)	72.19	64.85	69.53	23.08	29.50	48.27	56.87	51.71	73.45	51.52	53.79	81.23	51.60

Note: There were no t-tests for < 0.1 % extractions as they were considered insignificant

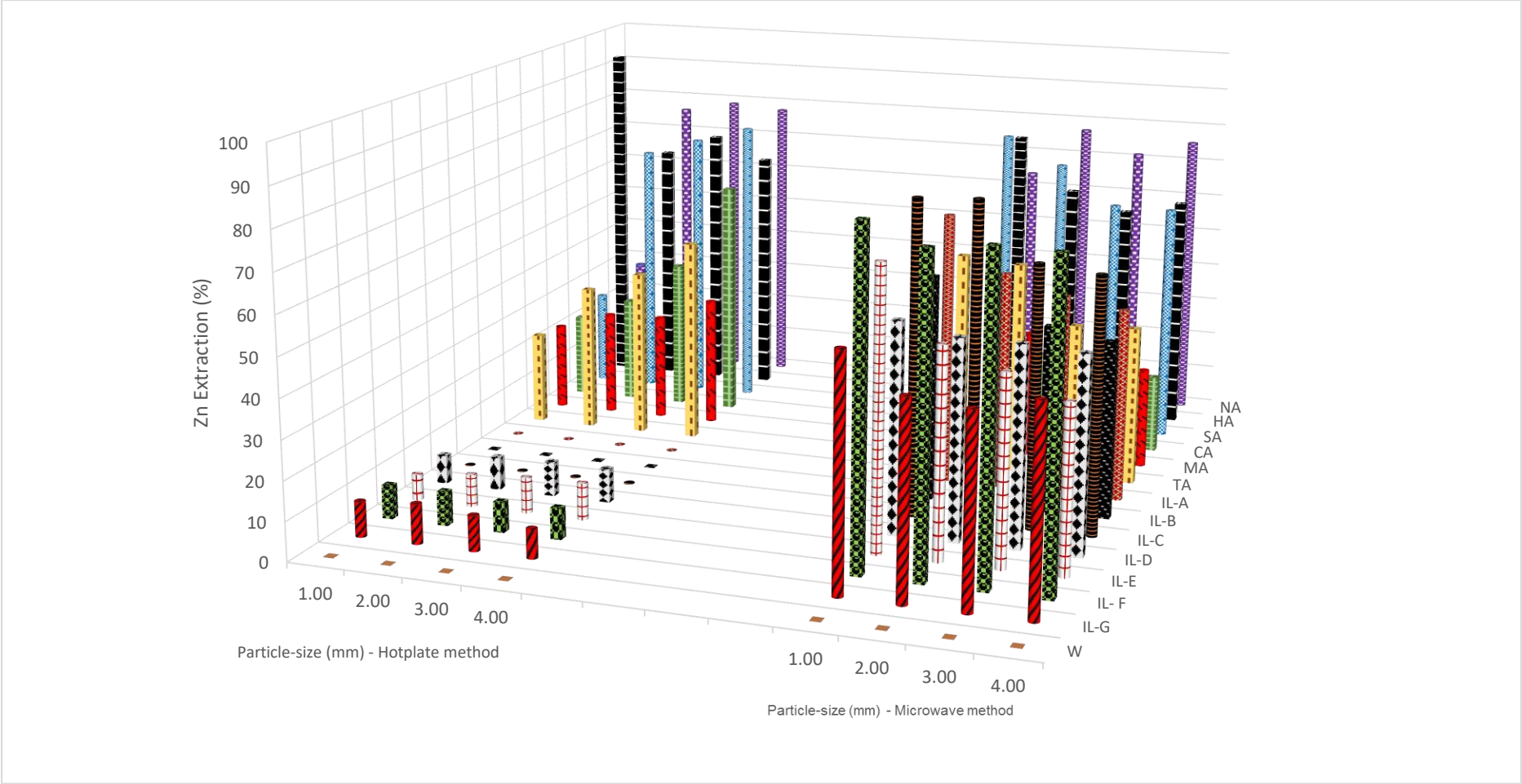

Figure 4.36 Percentage concentration for the effect of particle-size on leaching Zn

4.7.3 Effect of Particle-size on Leaching Fe

Table 4.26 a shows the percentage extraction of Fe for the hotplate method and this is also represented in **Figure 4.37**. In the hotplate method (**Figure 4.37)** the particle-size increased from 1 mm to 4 mm the Fe extraction also increased for the inorganic acids, Zn extractions for the organic acids decreased. The peak extractions for the solvents were HA (98 % at 4 mm), NA (70 % at 4 mm), SA (56 % at 4 mm), MA (5 % at 1 mm), CA (4 % at 1 mm), TA (3 % at 1 mm), ILs A to G showed no significant Fe extractions. In the microwave method (**Figure 4.37**) the particle-size increased from 1 mm to 4 mm the Fe extraction also increased for the inorganic acids, Zn extractions for the organic acids decreased. The peak extractions for the solvents were NA (52 % at 4 mm), HA (47 % at 4 mm), SA (24 % at 4 mm), CA (5 % at 1 mm), MA (5 % at 1 mm), TA (3 % at 1 mm), ILs A to G showed <1 % extractions.

To compare the hotplate method with microwave method, two sample independent t-test was done for each of the solvents. The null hypothesis (H_0) stated that the mean of both methods are equal while the alternative hypothesis (H_1) stated that the mean of both methods are not equal. In **Table 4.26 b** it shows that at 95 % confidence level the independent t-test for NA, SA, CA, MA and TA had p-values > 0.05 and this shows that the means for both methods are equal so the hotplate and microwave methods have the same efficiencies. However, HA had p-value < 0.05 meaning the mean of both methods are not equal therefore the hotplate method with larger mean (73 %) is better.

Table 4.26a Percentage concentration values for effect of particle-size on leaching Fe

	Particle-size (mm)	Extraction (%)														
		AQ	NA	HA	SA	CA	MA	TA	IL-A	IL-B	IL-C	IL-D	IL-E	IL-F	IL-G	W
Hotplate Method	**1.00**	100.00	18.69	55.96	16.07	4.32	4.77	2.58	0.01	0.01	0.01	0.01	0.01	0.01	0.01	0.01
	2.00	100.00	44.32	54.44	17.37	2.53	3.09	1.74	0.01	0.01	0.01	0.01	0.01	0.01	0.01	0.01
	3.00	100.00	54.03	81.86	47.06	1.60	1.95	1.31	0.00	0.00	0.00	0.00	0.00	0.00	0.00	0.00
	4.00	100.00	70.38	98.26	55.54	0.85	1.20	0.92	0.00	0.00	0.00	0.00	0.00	0.00	0.00	0.00
Microwave Method	**1.00**	100.00	39.16	45.13	15.27	4.58	4.94	2.72	0.01	0.01	0.01	0.01	0.01	0.01	0.01	0.00
	2.00	100.00	37.89	40.66	15.41	3.79	3.84	2.18	0.01	0.01	0.01	0.01	0.01	0.01	0.01	0.00
	3.00	100.00	41.11	44.07	19.98	3.39	3.26	1.90	0.01	0.01	0.01	0.01	0.01	0.01	0.01	0.00
	4.00	100.00	51.57	46.94	24.39	2.84	2.82	1.92	0.00	0.00	0.00	0.00	0.00	0.00	0.00	0.00

Table 4.26b Independent t-test between hotplate and microwave methods at 95% confidence level (particle-size effect on Fe)

	NA	HA	SA	CA	MA	TA
p-value	0.71	0.04	0.19	0.16	0.33	0.23
Hotplate mean (%)	46.86	72.63	34.01	2.33	2.75	1.64
Microwave mean (%)	42.43	44.20	18.76	3.65	3.72	2.18

Note: There were no t-tests for < 1.0 % extractions as they were considered insignificant

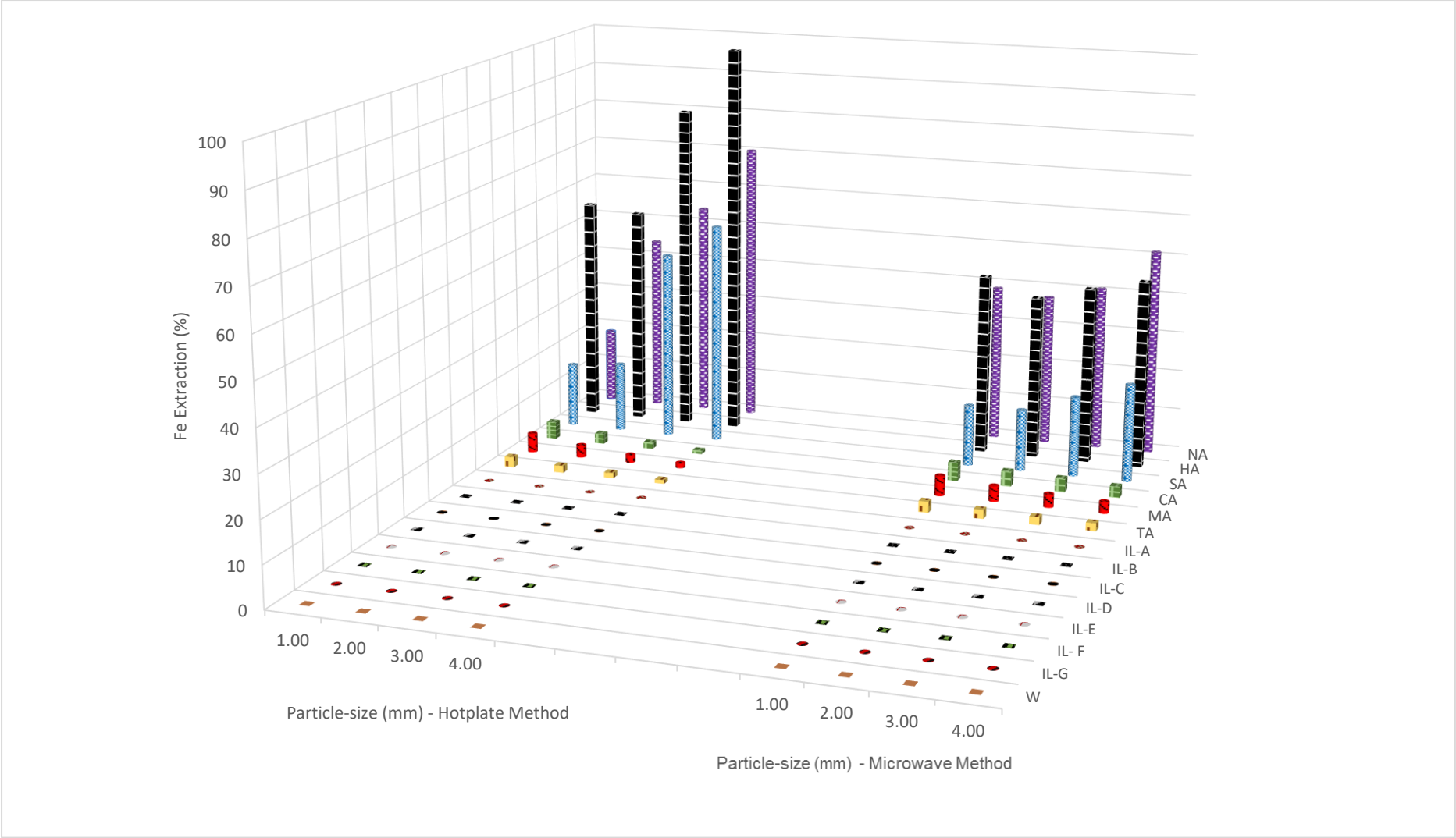

Figure 4.37 Percentage concentration for the effect of particle-size on leaching Fe

4.7.4 Effect of Particle-size on Leaching Ni

Table 4.27 a shows the percentage extraction of Ni for the hotplate method and this is also represented in **Figure 4.38**. For the hotplate method, in **Figure 4.38** the particle-size increased from 1 mm to 4 mm the Ni extractions did not show any significant change for the inorganic and organic acids. The solvents peak extractions for the solvents in this research were NA (5 % at 4 mm), HA (2 % at 4 mm), SA (3 % at 4 mm), CA (2 % at 3 mm) and TA (3 % at 3 mm). MA and ILs A - G did not show any significant Ni extractions. In the microwave method (**Figure 4.38**), the particle-size increased from 1 mm to 4 mm the Ni extractions did not show any significant change for the inorganic. The solvents peak extractions for the solvents were NA (10 % at 2 mm), SA (5 % at 3 mm), HA (4 % at 3 mm). The organic acids and ILs A - G did not show any significant Ni extractions.

To compare the hotplate method with microwave method, two sample independent t-test was done for each of the solvents. The null hypothesis (H_0) stated that the mean of both methods are equal while the alternative hypothesis (H_1) stated that the mean of both methods are not equal. In **Table 4.27 b** it shows that at 95 % confidence level the independent t-test for HA had p-value > 0.05 and this shows that the means for both methods are equal so the hotplate and microwave methods have the same efficiency. However, NA, HA, SA and TA had p-value < 0.05 meaning the mean of both methods are not equal therefore the hotplate method with larger mean was better TA while the microwave method was better for NA, HA, SA.

Table 4.27 a Percentage concentration values for effect of particle-size on leaching Ni

	Particle-size (mm)	Extraction (%)														
		AQ	NA	HA	SA	CA	MA	TA	IL-A	IL-B	IL-C	IL-D	IL-E	IL-F	IL-G	W
Hotplate Method	**1.00**	100.00	3.43	0.86	1.19	0.50	0.54	0.48	0.01	0.01	0.01	0.00	0.01	0.01	0.01	0.01
	2.00	100.00	3.69	1.13	1.20	0.90	0.71	1.16	0.01	0.01	0.01	0.00	0.01	0.01	0.01	0.01
	3.00	100.00	3.89	1.50	1.83	1.28	0.73	1.75	0.01	0.01	0.01	0.00	0.01	0.01	0.01	0.01
	4.00	100.00	4.61	2.15	2.79	1.82	0.71	2.58	0.01	0.01	0.01	0.00	0.01	0.01	0.01	0.01
Microwave Method	**1.00**	100.00	9.49	3.30	3.96	0.59	0.28	0.26	0.02	0.02	0.02	0.02	0.02	0.02	0.02	0.00
	2.00	100.00	9.90	3.68	4.42	0.75	0.26	0.26	0.02	0.02	0.02	0.02	0.02	0.02	0.02	0.01
	3.00	100.00	8.74	4.18	4.74	0.75	0.38	0.24	0.02	0.02	0.02	0.02	0.02	0.02	0.02	0.01
	4.00	100.00	8.15	4.13	4.26	0.89	0.33	0.24	0.01	0.01	0.01	0.01	0.01	0.01	0.01	0.01

Table 4.27 b Independent t-test between hotplate and microwave methods at 95% confidence level (particle-size effect on Ni)

	NA	HA	SA	CA	TA
p-value	3.16×10^{-5}	4.46×10^{-4}	7.35×10^{-4}	0.24	0.03
Hotplate mean (%)	3.91	1.41	1.75	1.13	1.49
Microwave mean (%)	9.07	3.82	4.35	0.75	0.25

Note: There were no t-tests for < 0.8 % extractions as they were considered insignificant

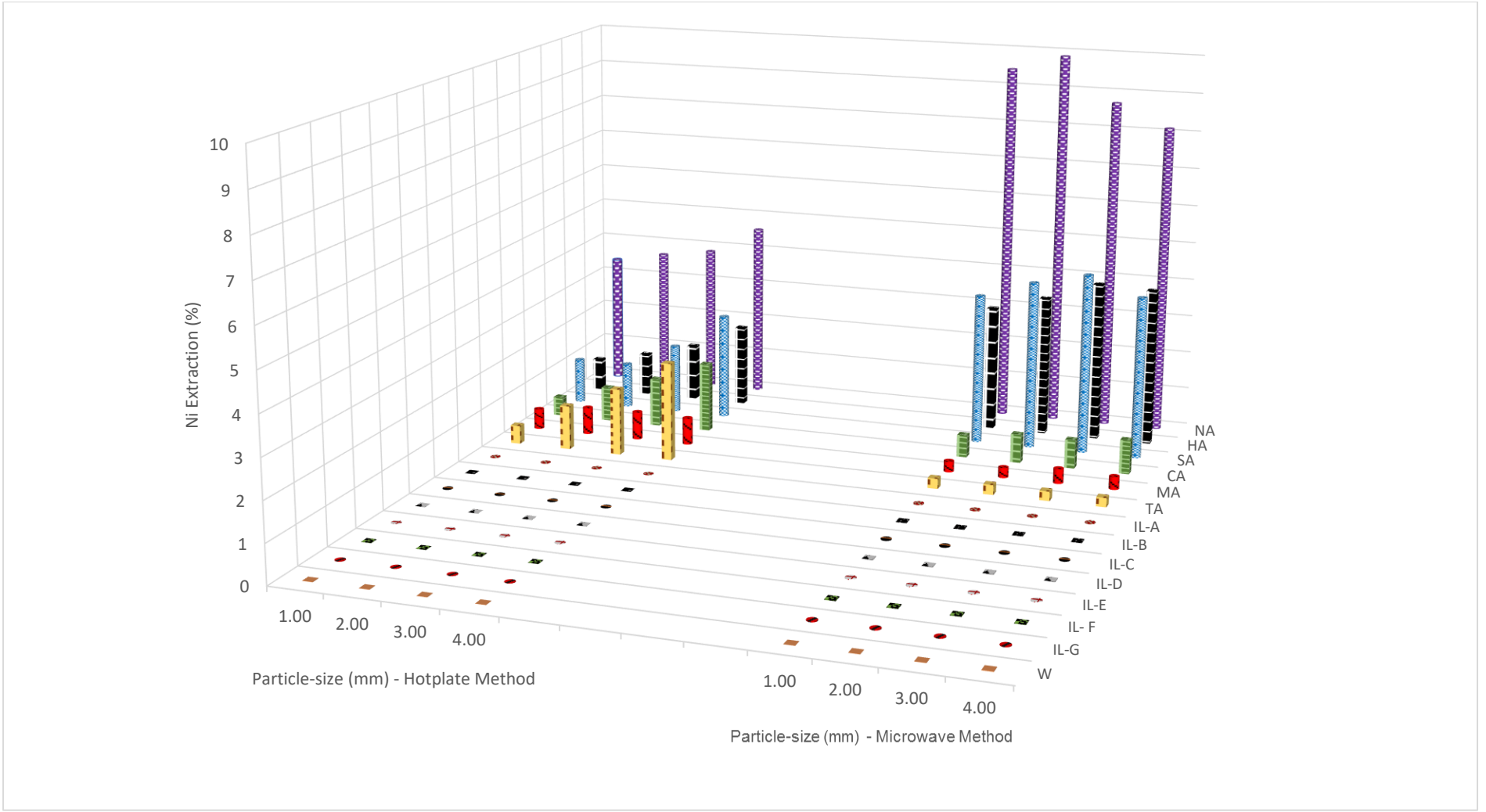

Figure 4.38 Percentage concentration for the effect of particle-size on leaching Ni

4.7.5 Effect of Particle-size on Leaching Pb

Table 4.28 a shows the percentage extraction of Pb for the hotplate method and this is also represented in **Figure 4.39.** In the hotplate method, in **Figure 4.39** the particle-size increased from 1 mm to 4 mm the Pb extraction in NA and CA decreased while the other solvents did not show significant changes. The solvents peak extractions in this research were NA (88 % at 1 mm), HA (73 % at 1 mm), SA (2 % at 1 mm), CA (13 % at 1 mm), MA (6 % at 1 mm), TA (4 % at 1 mm), IL D (3 % at 4 mm). ILs A, B, C, E, F & G did not show any significant Pb extractions. In the microwave method (**Figure 4.39**), as the particle-size increased from 1 mm to 4 mm the Pb extraction in NA increased while in HA there was no significant change. The solvents peak extractions were NA (70 % at 4 mm), HA (37 % at 4 mm). SA, the organic acids and ILs A- G did not show any significant Pb extractions.

To compare the hotplate method with microwave method, two sample independent t-test was done for each of the solvents. The null hypothesis (H_0) stated that the mean of both methods are equal while the alternative hypothesis (H_1) stated that the mean of both methods are not equal. In **Table 4.28b** it shows that at 95 % confidence level the independent t-test for NA, HA, SA, CA, MA and TA and IL D had p-value < 0.05 meaning the mean of both methods are not equal therefore the hotplate method with larger mean is better.

Table 4.28 a Percentage concentration values for effect of particle-size on leaching Pb

	Particle-size (mm)	Extraction (%)														
		AQ	NA	HA	SA	CA	MA	TA	IL-A	IL-B	IL-C	IL-D	IL-E	IL-F	IL-G	W
Hotplate Method	**1.00**	100.00	87.50	72.50	2.05	13.33	6.00	4.25	0.17	0.17	0.17	1.20	0.20	0.16	0.44	0.16
	2.00	100.00	73.68	63.16	1.52	8.21	4.21	3.32	0.23	0.24	0.24	1.47	0.29	0.13	0.51	0.10
	3.00	100.00	75.00	70.83	1.24	6.17	5.67	2.75	0.19	0.19	0.19	2.47	0.24	0.20	0.52	0.08
	4.00	100.00	67.31	66.25	0.97	4.62	5.77	2.40	0.15	0.14	0.14	2.56	0.19	0.16	0.87	0.06
Microwave Method	**1.00**	100.00	44.74	31.58	0.32	0.32	0.32	0.32	0.32	0.32	0.32	0.22	0.32	0.32	0.32	0.02
	2.00	100.00	37.50	28.57	0.15	0.15	0.15	0.15	0.15	0.15	0.15	0.10	0.15	0.15	0.15	0.04
	3.00	100.00	39.18	30.61	0.10	0.10	0.10	0.10	0.10	0.10	0.10	0.07	0.10	0.10	0.10	0.04
	4.00	100.00	70.45	37.12	0.09	0.09	0.09	0.09	0.09	0.09	0.09	0.06	0.09	0.09	0.09	0.06

Table 4.28 b Independent t-test between hotplate and microwave methods at 95% confidence level (particle-size effect on Pb)

	NA	HA	SA	CA	MA	TA	IL-D
p-value	0.02	1.16×10^{-05}	1.66×10^{-03}	5.87×10^{-05}	1.40×10^{-05}	3.13×10^{-04}	1.99×10^{-05}
Hotplate mean (%)	75.87	68.45	1.45	8.08	5.41	3.18	1.93
Microwave mean (%)	47.97	31.97	0.17	0.17	0.17	0.17	0.11

Note: There were no t-tests for < 1.0 % extractions as they were considered insignificant

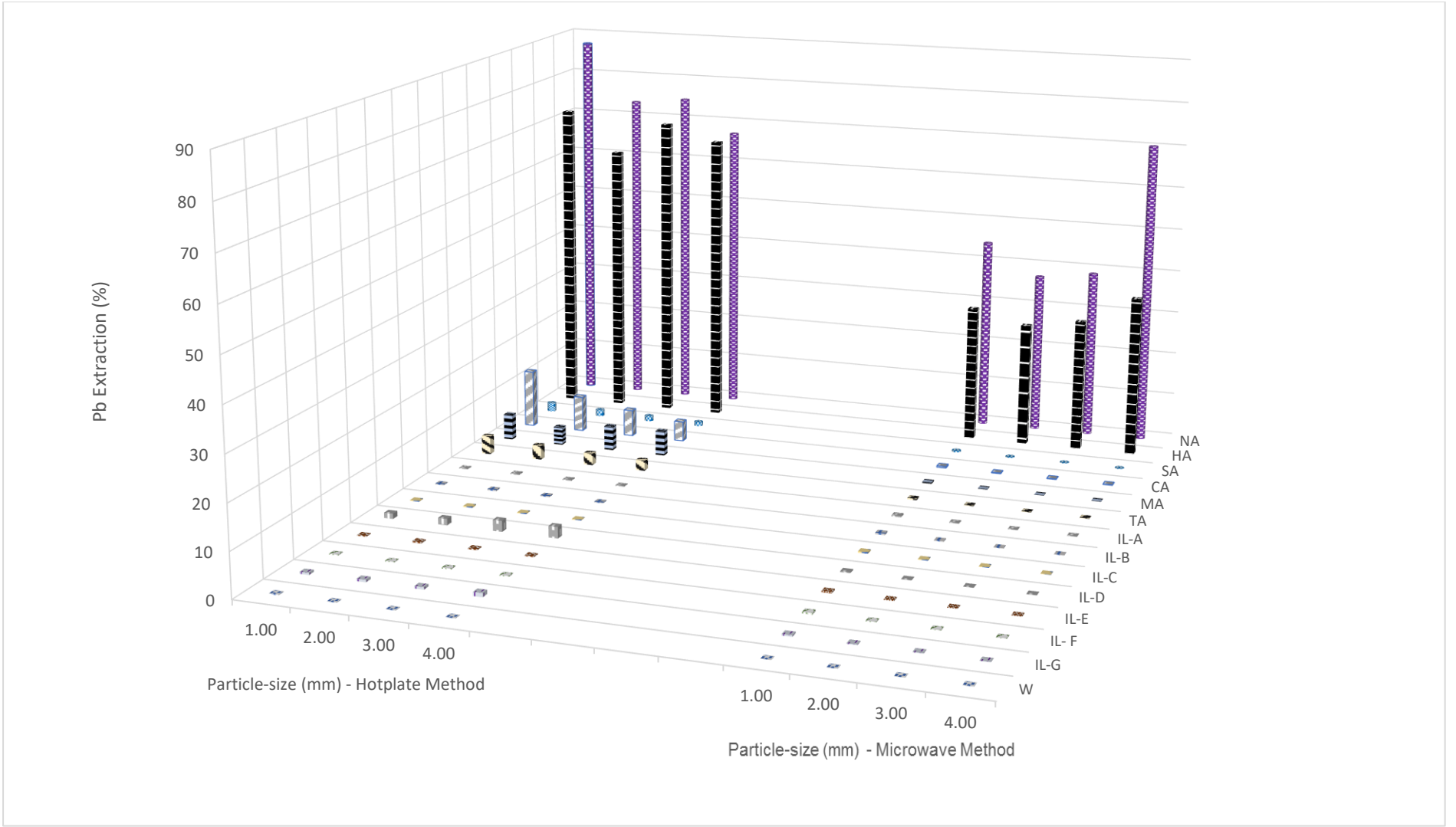

Figure 4.39 Percentage concentration for the effect of particle-size on leaching Pb

4.8 PCA for Particle-size Effect

4.8.1 PCA Scree Plot for Particle-size Effect

This particle-size effect experiment involved 20 variables and 90 observations. The variables were made up of five metals (Cu, Zn, Fe, Ni and Pb) with each of these metals having results from four different samples of WEEE particle-sizes (1, 2, 3 & 4 mm). The observations were results from each of the fifteen solvents with three replicates each from the hotplate and microwave methods used in the experiment. **Table 4.29** shows the summarized data of the first six principal components extracted from both the hotplate and microwave methods (mg/g) in **Appendices 2 a – e** and **Figure 4.40** shows the scree plot of variance for the dimensions from particle-size effect data and they are in the order of highest to the lowest with Dim.1 as 75.2 %, Dim.2 as 11.1 % and Dim.3 as 7.5 %. From this scree plot we can infer that Dim.1 explains the most part of the particle-size effect data as it is larger than the other dimensions. From **Table 4.29**, we can see that Dim.1, 2 & 3 showed a SD > 1.0 as SD = 1 is the cutoff point. Therefore, we can accept the first three dimensions (Dim.1, 2 & 3) with a proportion of variance of 75.2 & 11.1 & 7.5 % respectively. Consequently, the cumulative proportion in Dim.1, 2 & 3 also showed 75.2, 86.4 & 93.9 % respectively. This shows that with Dim.3 having a SD of 1.2, about 93.9 % of the data can be accounted for while the remaining 6.1 % of the data can be disregarded as they fall below SD < 1.0.

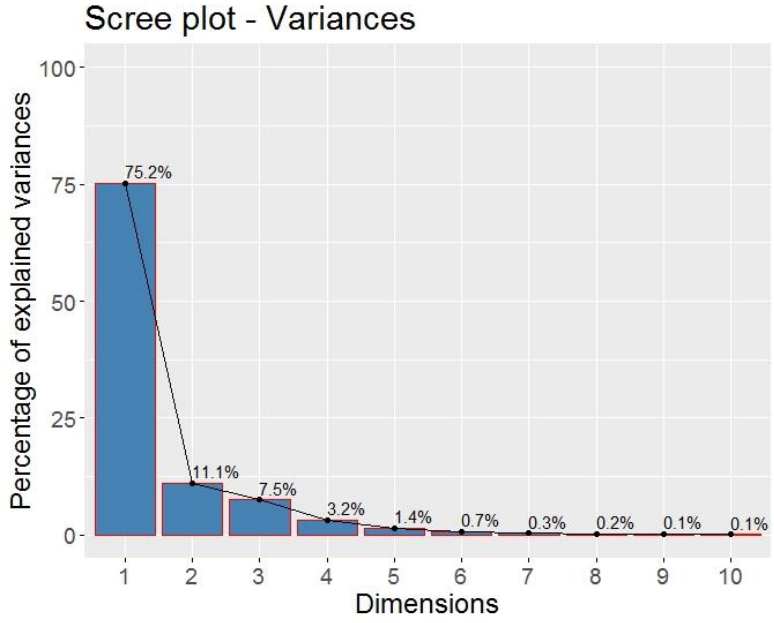

Figure 4.40 Scree plot for particle size effect

Table 4.29 Summarized principal components for particle-size

Principal Components	Dim.1	Dim.2	Dim.3	Dim.4	Dim.5	Dim.6
Standard deviation	3.879	1.493	1.224	0.802	0.522	0.384
Proportion of Variance	0.752	0.111	0.075	0.032	0.014	0.007
Cumulative Proportion	0.752	0.864	0.939	0.971	0.944	0.992

Figure 4.41 shows the biplot for particle-size effect data which is the relationship between the variables and the observations in the particle-size data. It also shows the structure of variables correlations and clustered observations. From the PCA plot, we can see the variables with the longest vector projections. They represent the highest variations in the data and they have occured in Zn1, Zn2, Zn3, Zn4, Cu1, Cu2, Cu3 and Cu4. The replicate observations formed clusters, for example, in the hotplate method (1, 2 & 3) the observations AQ1, AQ2 & AQ3 which represents the hotplate result for *aqua-regia* formed a cluster which means that the three replicated experiments showed similarity in the result from particle-size effect. Also, this behaviour was observed in AQ4, AQ5 & AQ6 (microwave method) showing that the replicated results were similar. The *aqua-regia* observations AQ1-3 and AQ4-6 are considered outliers on the PCA as they were clearly outside the group clustering and also far away from the other observations. However, they were not treated as outliers or removed as they were needed in this research inorder to clearly differentiate the best performing solvents or observations. Other observation clusters were seen in (HA1, HA2 & HA3),(NA1, NA2 & NA3) and (SA1, SA2 & SA3). The above stated clusters had various degrees of euclidean distance (distance between observations) and the observations from *aqua-regia* (AQ1-3) was the farthest followed by *aqua-regia* (AQ4-6). However, NA1-3 and NA4-6 were next before, HA1-3 and SA1-3. Consequently, SA4-6, the organic acids and ionic liquids all seemed to have clustered together as their euclidean distance were relatively close.

We can see that the variables vectors were pointing towards AQ1-3, AQ4-6, HA1-3, NA1-3 and NA4-6. This shows a high degree of association between the variables and the observations but the reverse was the case for the other observations such as HA4-6, SA4-6, the organic acids and ionic liquids as the PCA plot (**Figure 4.41**) clearly shows the variable vectors pointing away from them and this implies very low association between the variables and these observations. Also, the variables were pointing towards the hotplate method (red) except Cu1, Cu2, Cu3 & Cu4 showing high variable association with the hotplate method.

However, Cu1, Cu2, Cu3 & Cu4 variables were pointing towards the microwave method (blue) showing more variable association with the microwave method.

The variable vectors closest to each other showed high correlation amongst themselves, for example Pb2 and Pb3, Ni1 and Ni2, Fe3 and Fe4 formed angles around 30 degrees. Negative correlation was observed between Zn1 and Cu3 as their vectors formed angles around 180 degrees. No correlation was observed between Fe4 and Cu4 as their vectors formed angle 90 degrees. The x-axis which is Dim.1 (75.2 % of variation explained) shows that all the variable vectors are positioned on the left side of the plot thereby revealing negative correlation for all variables. So we would expect that the lower the values of Dim.1 the higher high values for each of the variables. The y-axis which is Dim.2 (11.1 % of variation explained) shows that half of the variables postioned at the top were positive correlation and the other half at the bottom were negative correlation. (Kohla & Luniak, 2005; Reris & Brooks, 2015; Statisticshowto, 2021; STHDA, 2021; Towardsdatascience, 2021).

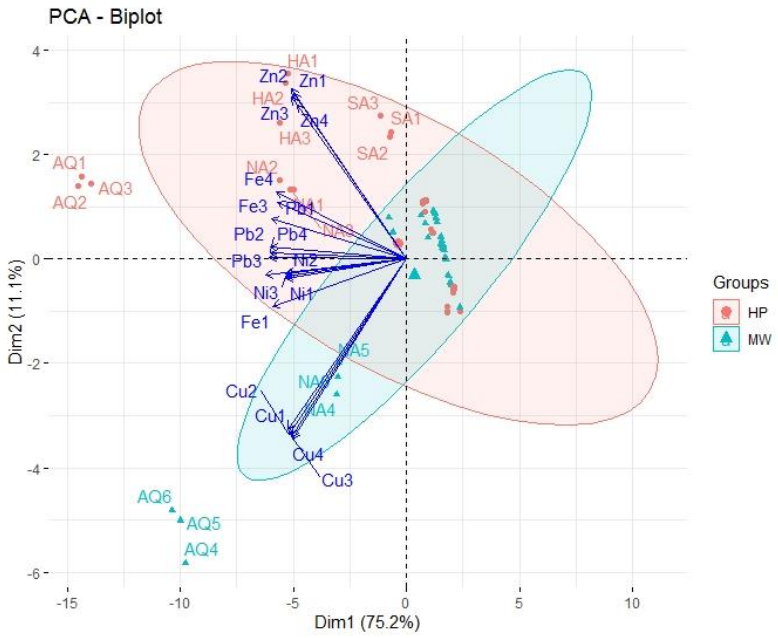

Figure 4.41 Biplot for particle size effect

4.8.2 PCA Result for Variable Coordinates in Particle-Size Effect

Figure 4.42 a shows the plot for the variable coordinates for Dim.1 & 2 which are representation of the position of the particle-size effect variables on the plot. The coordinates are correlation between a variable and a dimension. **Figure 4.42 b** shows a three-dimensional view of variable coordinates for the three dimensions (Dim.1, 2 & 3) with Dim.1 (75.2 %) on the x-axis, Dim.2 (11.1 %) on the z-axis and Dim.3 (7.5 %) on the y-axis. **Figure 4.42 c** shows the variable coordinates visualization with spots of different colour intensity. The strongest or darkest colour represent the highest correlation values and the correlation values decreases with decrease in the colour intensity of the spots in the visualization. Also, the positive correlated values are in blue while the negative correlated values are in red. Here, Dim.1, 2, 3, 4 & 5 are represented by Dim.1, 2, 3, 4 & 5. The order of importance decreased from Dim.1 to 5. We can see that Dim.1 showed the highest colour intensity and this was followed by Dim.2, 3, 4 & 5. However, all the coordinates in Dim.1 showed strong negative correlation**.** Moderate positive and negative correlation was observed in Dim.2.

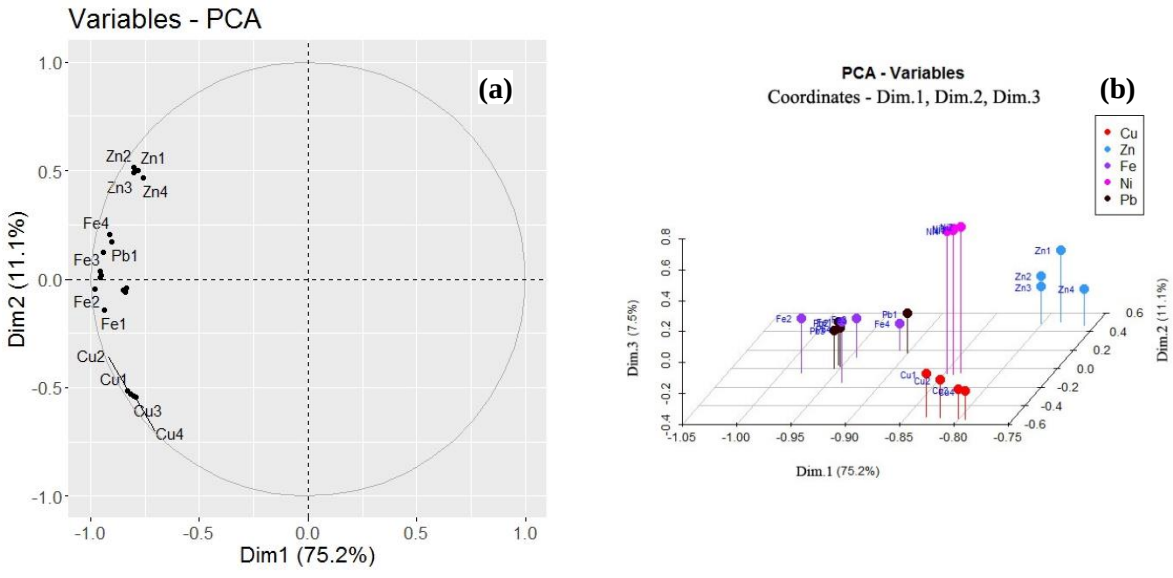

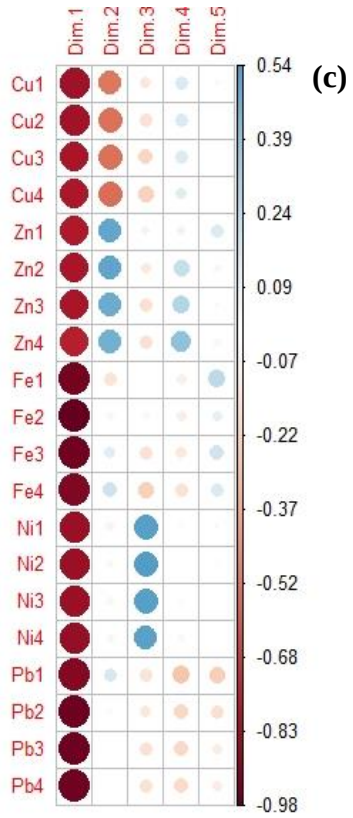

Figure 4.42: (a) Variable Coordinates Correlation Plot (particle-size effect) (b) Variable Coordinates 3D Plot (particle-size effect) (c) Variable Coordinates Dim Plot (particle-size effect)

4.8.3 PCA Result for Variable Cos2 Quality of Representation in Particle-size Effect

Figure 4.43 a shows the Cos2 plot of variable with the highest Cos2 value which are in orange while the mid cos2 variables value are in blue. The variables in orange are the most represented in the plot as they are closest to the circle of correlation with very high values and this is followed by the yellow and then the blue spots. All the variables indicated in this Cos2 plot **(Figure 4.43 a)** show very good representation for Dim.1 as all the variables are far from the centre of the circle and none is close to the centre of the circle. **Figure 4.43 b & c** shows another visualization of the Cos2 variables in the form of bar plots. We can see that the Cos2 variables for Dim.1 in **Figure 4.43 b** are the highest which also supports the fact that the quality of representation is good. The variables in the bar plots are arranged from highest to lowest. **Figure 4.43 d** shows the Cos2 variables visualization with spots of different colour intensity. The strongest or darkest colour represent the highest Cos2 variables and the Cos2 variables decreased with decrease in the colour intensity of the spots in the visualization. We

can see that Dim.1 variables showed the highest colour intensity and this was followed by Dim.2. In Dim.1 (**Figure 4.43 b**), the data visualized explains 75.2 % of the particle-size effect data and the best five represented variables were Fe2, Pb3, Pb2, Pb4 and Fe3 while the least three correlated variables in Dim.1 were Cu4, Zn1 and Zn4. In Dim.2 (**Figure 4.43 c**), the visualized data explains 11.1 % of the particle-size effect experiment and the best three correlated variables were Cu4, Cu3 and Cu2.

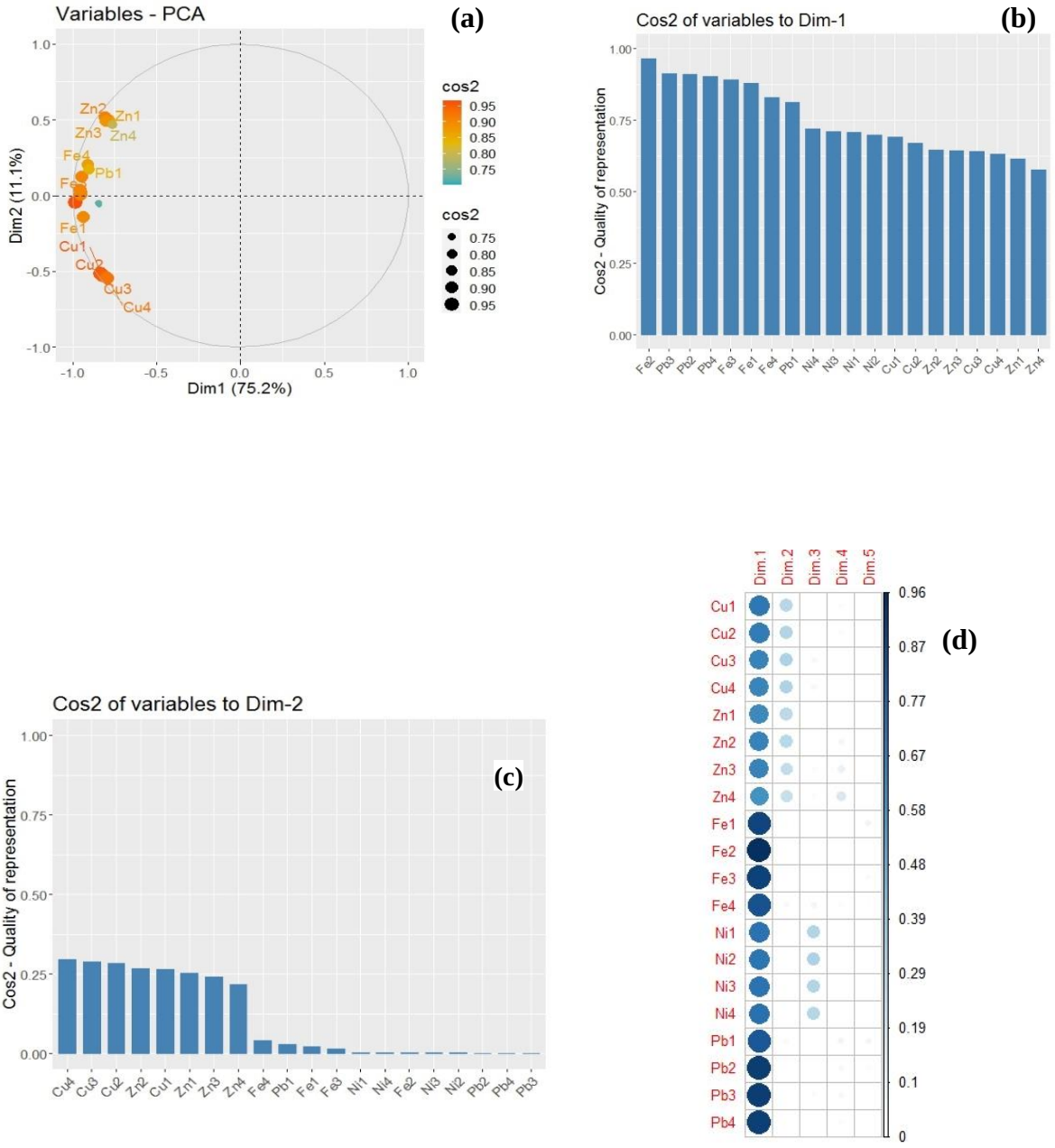

Figure 4.43: (a) Variable Cos2 quality of representation (particle-size effect) (b) Dim.1 quality of representation (particle-size effect) (c) Dim.2 quality of representation (particle-size effect) (d) Cos2 quality of representation plot (particle-size effect)

4.8.4 PCA Result for Variables Contribution in Particle-size Effect

Figure 4.44 a shows the contribution of variable correlation plot with the most contributing variables indicated in red and the least contributing variables indicated in blue. From **Figure 4.44 b & c**, we can see the contribution of variables represented in bar plots with red dotted lines which indicates the expected average contribution. Dim.1 and Dim.2 are the most important to be considered in explaining the contribution while Dim.3, 4 & 5 are less important. In Dim.1 (**Figure 43 b**), most contribution of variables values were slightly above the expected average contribution. **Table 4.30** shows the actual values for contribution of variables and **Figure 4.44 d** shows the contribution of variables plot with spots of different colour intensity. The darker colours indicate higher contribution while the lighter color indicate low contribution. The contribution of variables for a particular dimension are measured in percentages. Correlated variables in the contribution of variables for Dim.1 & Dim.2 explains 75.2 % and 11.1 % respectively. Contributions from Dim.1 are the most important as they contribute more than other variables and this is followed by Dim.2. Even though the contributions from other dimensions are high (Dim.3, Dim.4 & Dim.5), they would not be considered since they are not as important as contributions from Dim.1 & 2. The order of importance in the contribution for the dimensions are Dim.1 > Dim.2 > Dim.3 > Dim.4 > Dim.5. A variable with large contribution value contributes more to the component. Dim.1 which explains 75.2 % of the variation is represented in **Figure 4.44 b.** We can see the bar chart for Dim.1 contributions arranged in descending order and the best five contributing variables were Fe2 (6.40 %), Pb3(6.07 %), Pb2 (6.05 %), Pb4 (6.01 %) and Fe3 (5.92 %). Dim.2 which explains 11.2 % of the variation is represented in **Figure 4.44 c.** We can see the bar chart for Dim.2 contributions also arranged in descending order and the best three contributing variables were Cu4 (13.29 %), Cu3 (12.98 %) and Cu2 (12.67 %). The best contributing variables for particle-size effect from highest to lowest are in the order Fe2 > Pb3 > Pb2 > Pb4 > Fe3> Cu4 > Cu3 > Cu2.

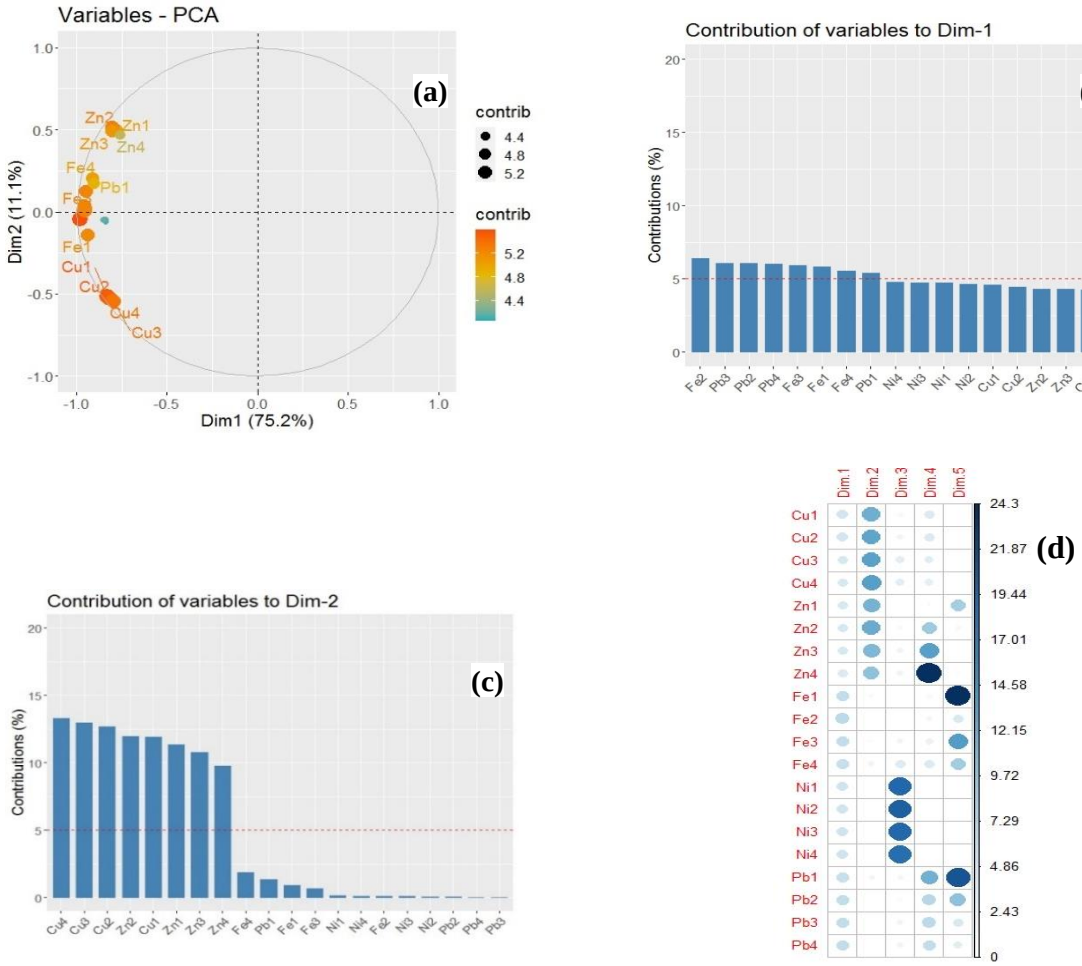

Figure 4.44: (a) Contribution of Variable Correlation Plot (particle-size effect) (b) Dim.1 Contribution of Variable Bar Plots (particle-size effect) (c) Dim.2 Contribution of Variable Bar Plots (particle-size effect) (d) Variable Contribution Plot (particle-size effect)

Table 4.30 Best Contributing Variables for Particle-size (in bold)

	Dim 1 (%)	Dim 2 (%)
Cu 2	4.44	**12.67**
Cu 3	4.26	**12.99**
Cu 4	4.19	**12.29**
Fe 2	**6.40**	0.10
Fe 3	**5.92**	0.67
Pb 2	**6.05**	0.06
Pb 3	**6.07**	1.06
Pb 4	**6.01**	0.02

4.8.5 PCA Result for Observation Coordinates in Particle-size Effect

Figure 4.45 a shows the plot for the observation coordinates which are representing the position of the solvents used in particle-size effect experiment for both the hotplate and microwave methods. **Figure 4.45 d - e** shows the three-dimensional plots of inorganic acids, organic acids, ionic liquid (a - c) and ionic liquid (d - g). Dim.1 on the x-axis, Dim.2 on the z-axis and Dim.3 on the y-axis. These three dimensional plots shows the coordinates or positioning of the solvents used for the particle-size effect experiment. **Figure 4.46 a – d** shows the observation coordinate visualization plot for inorganic acids, organic acids, ionic liquid (a - c) and ionic liquid (d - g). In Dim.1 the observation coordinates for the inorganic acids all showed very good negative correlation except SA4 - 6 (sulphuric acid) which showed positive correlation. AQ1-6 (*aqua-regia*) had the strongest negative correlation values followed by NA1-3 (nitric acid) then HA 1-3 (hydrochloric acid). The strength of correlation can be seen on Dim.1 in **Figure 4.46 a** as very dark red colours. Dim.2 also had good positive and negative correlation values except for HA4, HA6 and SA4 which showed relatively weak negative correlation values. The organic acid Dim.1 all showed strong positive correlation and the strength of correlation can be seen on Dim.1 in **Figure 4.46 b** while the Dim.2 showed good positive and negative correlation except for TA4. The coordinates in ionic liquids (a - c) seen in **Table 4.25 c** all showed strong positive correlation in Dim.1 and the strength of correlation can be seen on Dim.1 in **Figure 4.31 c** while Dim.2 showed strong negative and positive correlations. The weakest correlations were in ILB5 & ILB6. The coordinates in ionic liquids (d - g) in **Table 4.25 d** all showed strong positive correlation in Dim.1 and the strength of correlation can be seen on Dim.1 in **Figure 4.31 d** while Dim.2 showed strong negative and positive correlations. The weakest correlations were in ILE4, ILE5, ILG5 and ILG6.

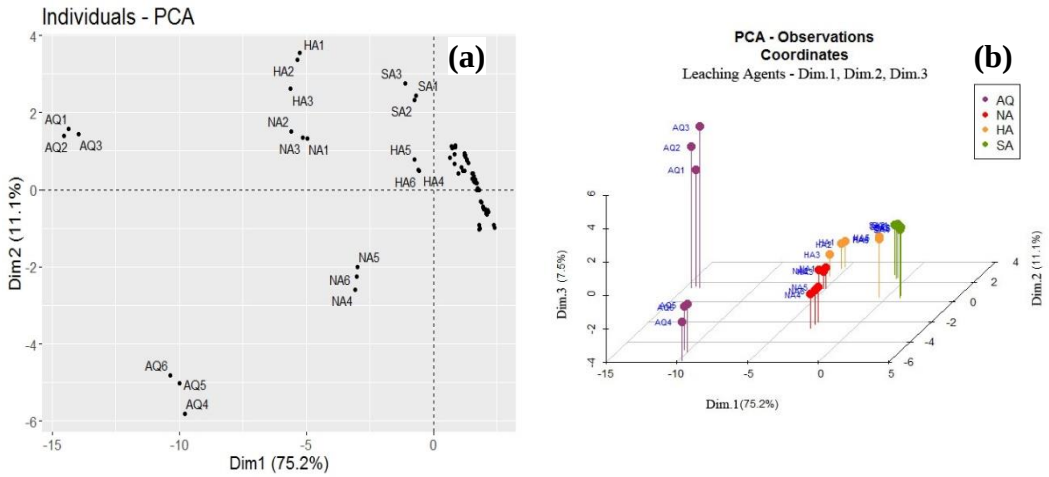

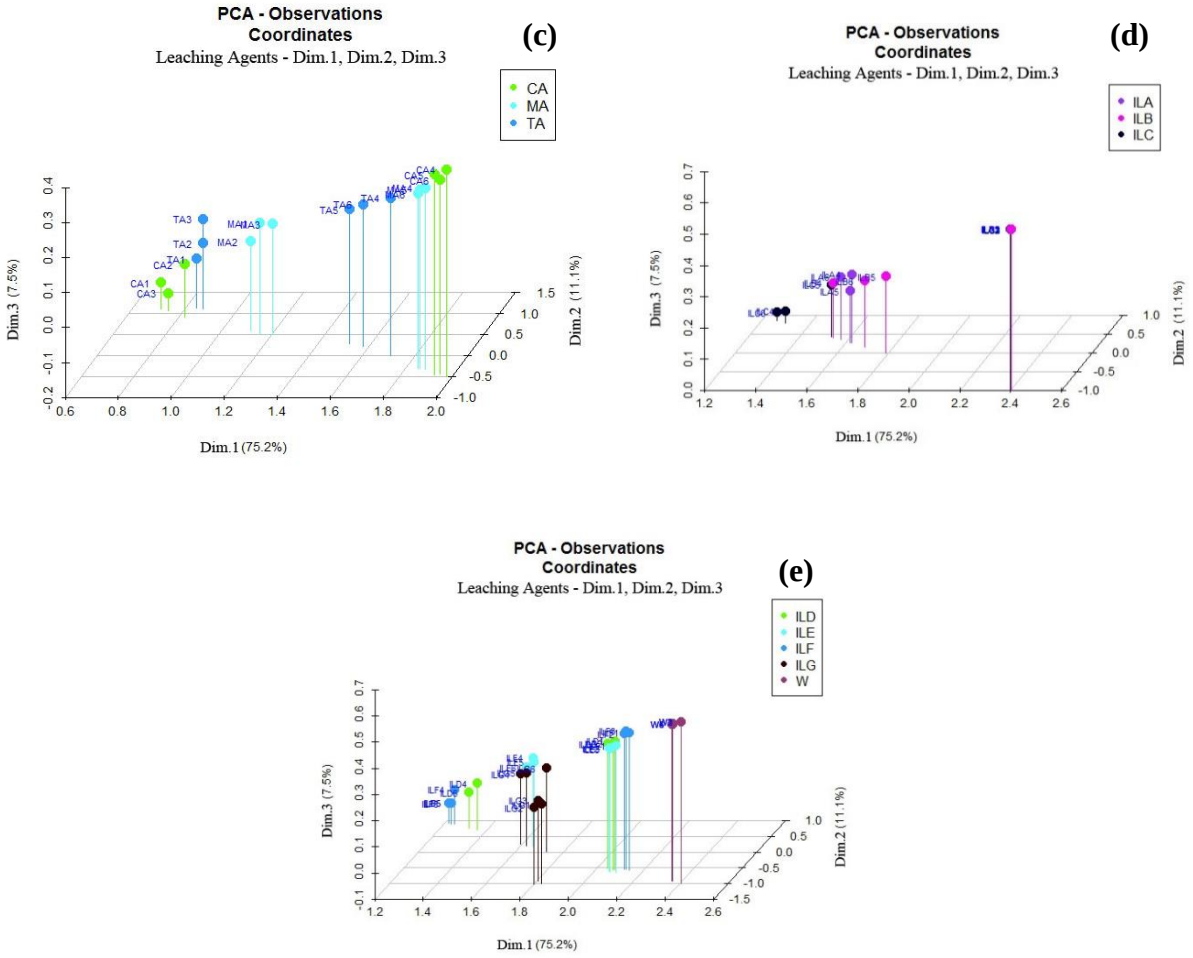

Figure 4.45: (a) observation coordinate correlation plot (dose effect) (b) observation coordinate for inorganic acids (dose effect) (c) observation coordinate for organic acids (dose effect) (d) observation coordinate for IL a-c (dose effect) (e) observation coordinate for IL d-g (dose effect)

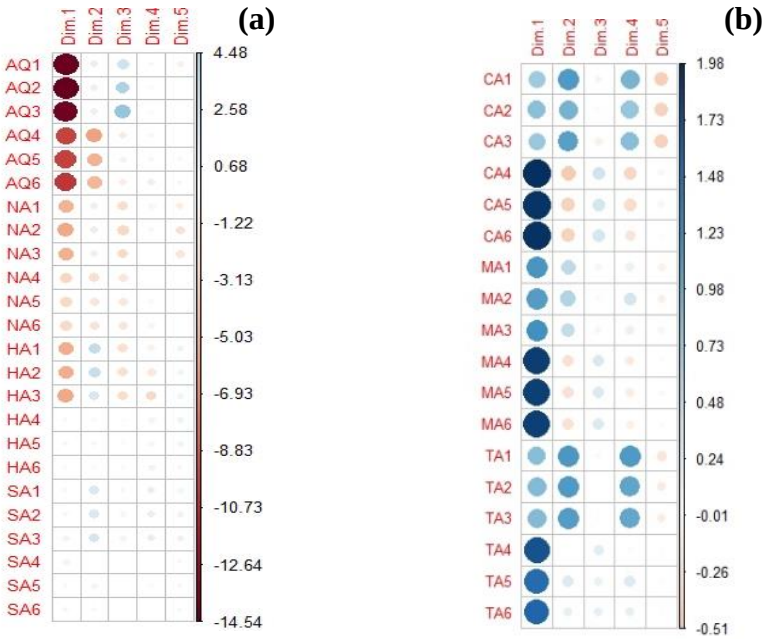

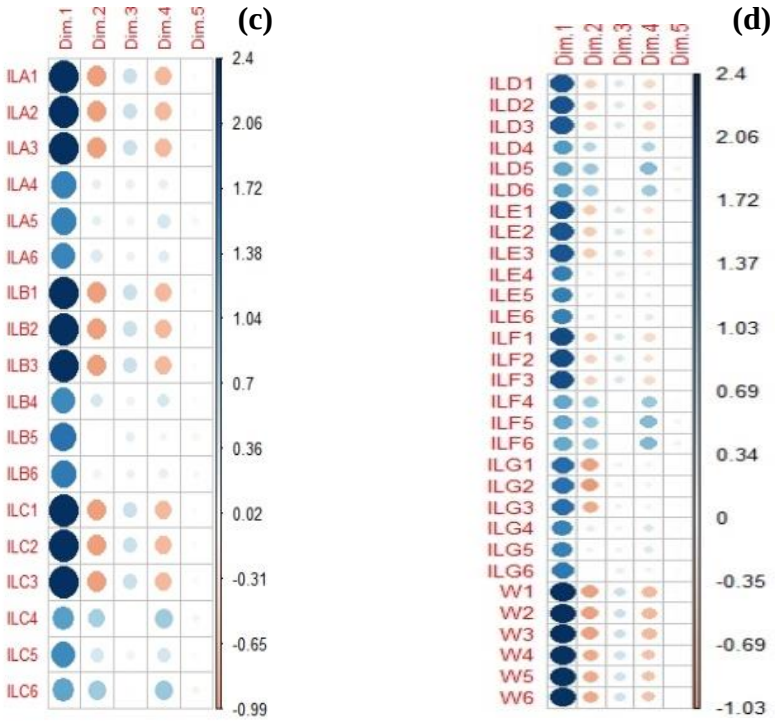

Figure 4.46: (a) Observation coordinate plot for inorganic acids (dose effect) (b) observation coordinate plot for organic acids (dose effect) (c) observation coordinate plot for IL a – c (dose effect) (d) observation coordinate plot for IL d - g (dose effect)

4.8.6 PCA Result for Observation Cos2 Quality of Representation in Particle-size Effect

Figure 4.47 a shows the Cos2 plot of observation with the highest Cos2 value which are in orange while the mid cos2 observation value are in blue. The observations in orange are the most represented in the plot as they have very high values and this is followed by the yellow and then the blue spots. **Figure 4.47 b - e** shows the three-dimensional plots Cos2 observation for inorganic acids, organic acids, ionic liquid (a - c) and ionic liquid (d - g). Dim.1 on the x-axis, Dim.2 on the z-axis and Dim.3 on the y-axis. These three dimensional plots shows the coordinates or positioning of the solvents used for the particle-size effect experiment. Consequently, all negative values have been cancelled out and **Figure 4.48 a -d** shows the Cos2 observations visualization with spots of different colour intensity. The strongest or darkest colour represent the highest Cos2 observations and the Cos2 observations decreased with decrease in the colour intensity of the spots in the visualization. The quality of representation in Dim.1 (inorganic acids) showed good quality of representation. AQ1-6 had good quality of representation followed by NA1-3. The poorest quality of representation were found in SA1, SA2, SA3. In Dim.2 (inorganic acids), only moderate quality of representation were found in SA2, SA3. The quality of representation with strong colour intensity can be

seen in Dim.1 (**Figure 4.48 a**). The quality of representation in Dim.1 (organic acids) showed good quality of representation TA4 , TA6, MA5, MA6, MA4 had good quality of representation. The poorest quality of representation were found in CA1 and CA3. In Dim.2 (organic acids), only moderate quality of representation were found in TA1 -3. Dim.1 (IL (a - c)), showed good quality of representation except for ILC4 and ILC6 which showed moderate quality of represention. The good quality of representation with strong colour intensity can be seen in Dim.1 (**Figure 4.48 c**). Dim.1 (IL (d - g)) showed good quality of representation. In Dim.2 (IL (a - c)), poor quality of representation. The good quality of representation with strong colour intensity can be seen in Dim.1 (**Figure 4.48 d**).

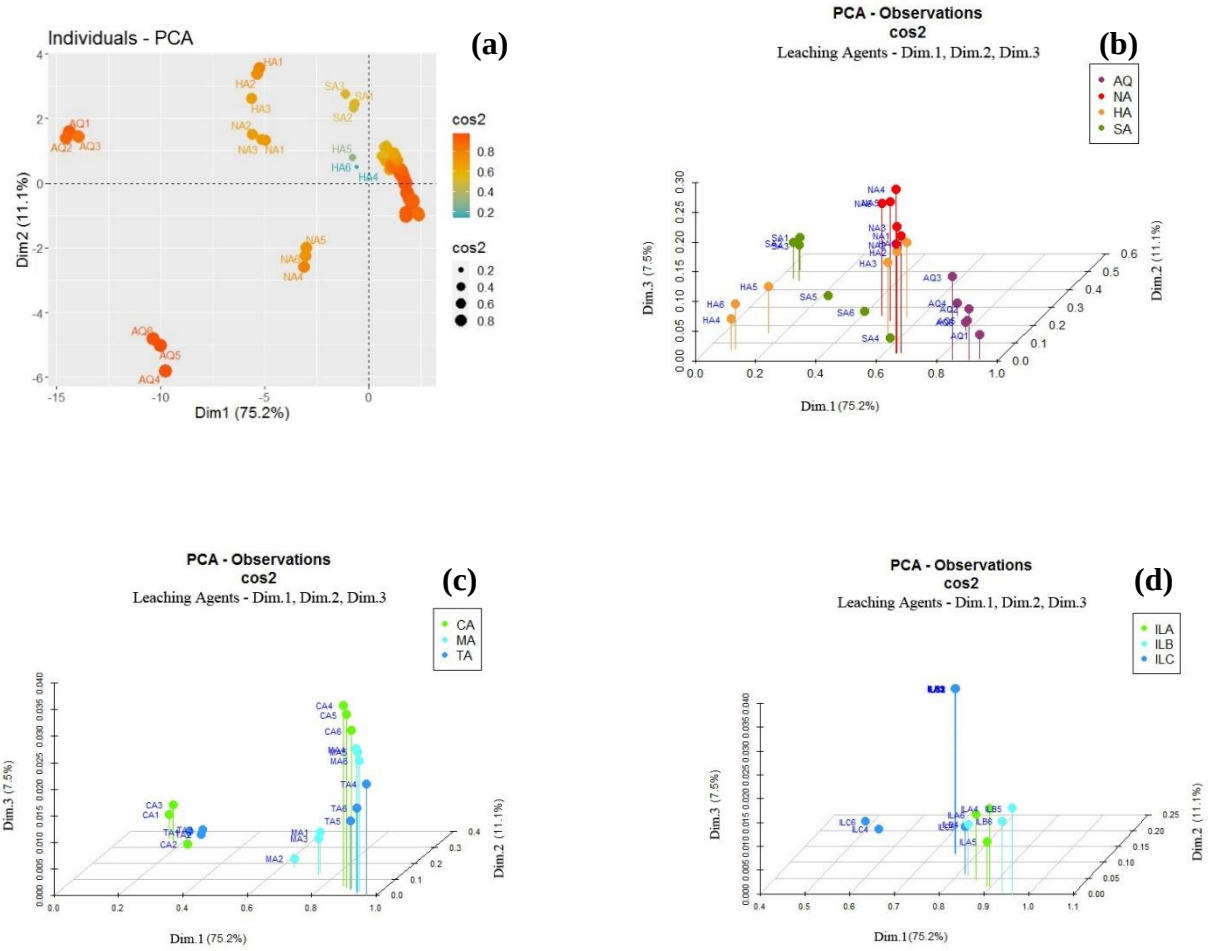

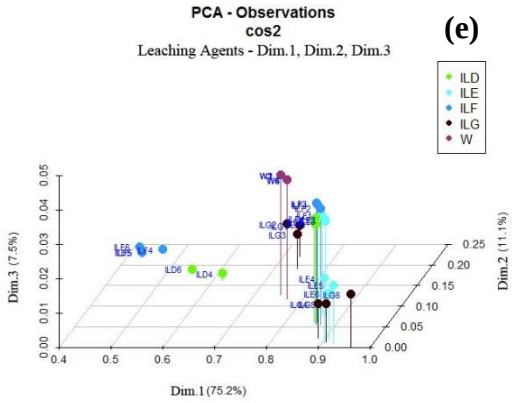

Figure 4.47: (a) Observation cos2 correlation plot (dose effect) (b) Observation cos2 for inorganic acids (dose effect) (c) Observation cos2 for organic acids (dose effect) (d) Observation cos2 for IL a-c (dose effect) (e) Observation cos2 for IL d-g (dose effect)

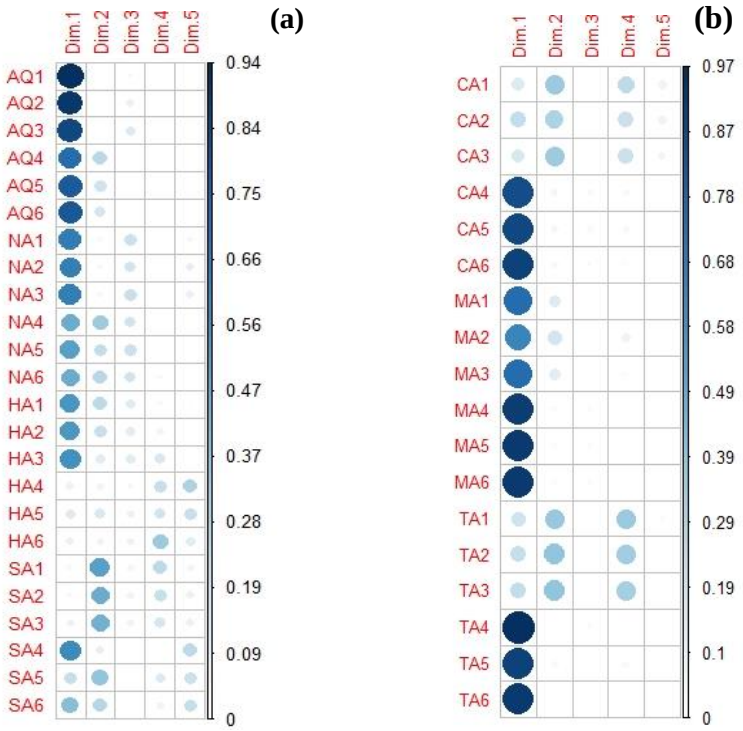

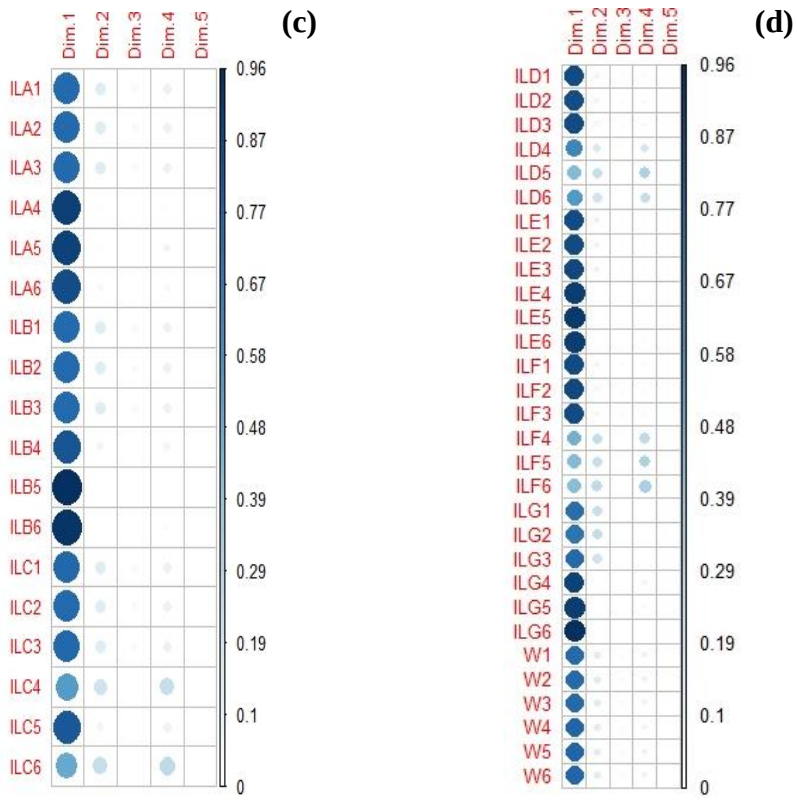

Figure 4.48: (a) Observation cos2 Dim plot for inorganic acids (dose effect) (b) observation cos2 Dim plot for organic acids (dose effect) (c) observation cos2 Dim plot for IL a – c (dose effect) (d) observation cos2 Dim plot for IL d - g (dose effect)

4.8.7 PCA Result for Observation Contribution in Particle-size Effect

Figure 4.49 a shows the contribution plot of observation with the highest contribution values which are in orange while the mid contribution value are in blue. In the figure, more labelling priority is given to the highest contributing observation with the least contributing observations not appearing. The observations in orange are the most represented in the plot as they have very high values and this is followed by the yellow and then the blue spots. **Figure 4.49 b - e** shows the three-dimensional plots of observation contribution for inorganic acids, organic acids, ionic liquid (a - c) and ionic liquid (d - g). Dim.1 on the x-axis, Dim.2 on the z-axis and Dim.3 on the y-axis. These three-dimensional plots shows the positioning of the solvents contribution on the plot. **Table 4.31** shows the observation contribution values in percentages. **Figure 4.50 a - d** shows the observation contribution visualization with spots of different colour intensity. The strongest or darkest colour represent the highest observation contribution and the observation contribution decreased with decrease in the colour intensity of the spots in the visualization. The observation contribution in Dim.1 for inorganic acids (**Table 4.31**), shows observation contribution and the best solvents that contributed to this

Dim.1 were AQ2 (15.61 %), AQ1 (15.21 %), AQ3 (14.39 %), AQ6 (7.92 %), AQ5 (7.40 %), AQ4 (7.05 %) and it was followed by NA2, HA3, HA2, HA1, NA3, NA1 (approximately 2.00 %). In Dim.2 (inorganic acids), the best three observation contributions were AQ4 (16.88 %), AQ5 (12.51 %), AQ6 (11.53 %), HA1 (6.30 %), HA2 (5.67 %). The best observation contribution with strong colour intensity can be seen in Dim.1 (**Figure 4.50a**). The best contributing solvents from highest to lowest are in the order AQ2 > AQ1 > AQ3 > AQ6 > AQ5 > AQ4 > NA2 > HA3 > HA2 > HA1 > NA3 > NA1. The observation contributions with strong colour intensity can be seen in Dim.1 & 2 (**Figure 4.50b**).

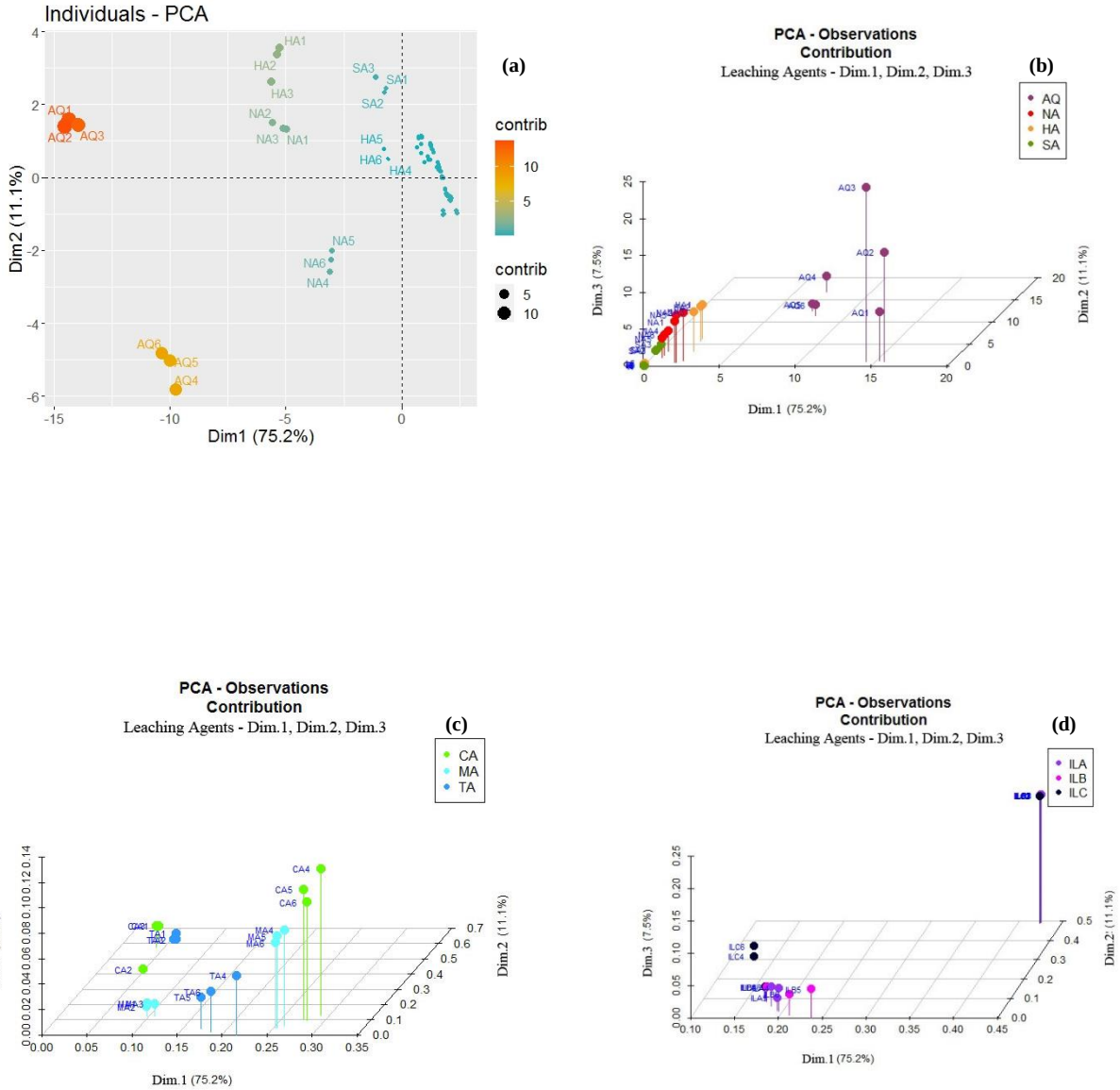

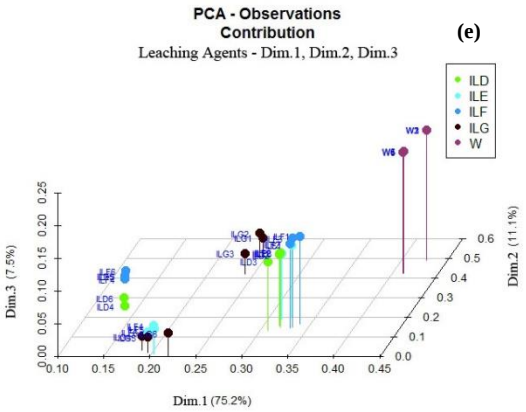

Figure 4.49: (a) Observation contribution plot (dose effect) (b) Observation contribution for inorganic acids (dose effect) (c) Observation contribution for organic acids (dose effect) (d) Observation contribution for IL a-c (dose effect) (e) Observation contribution for IL d-g (dose effect)

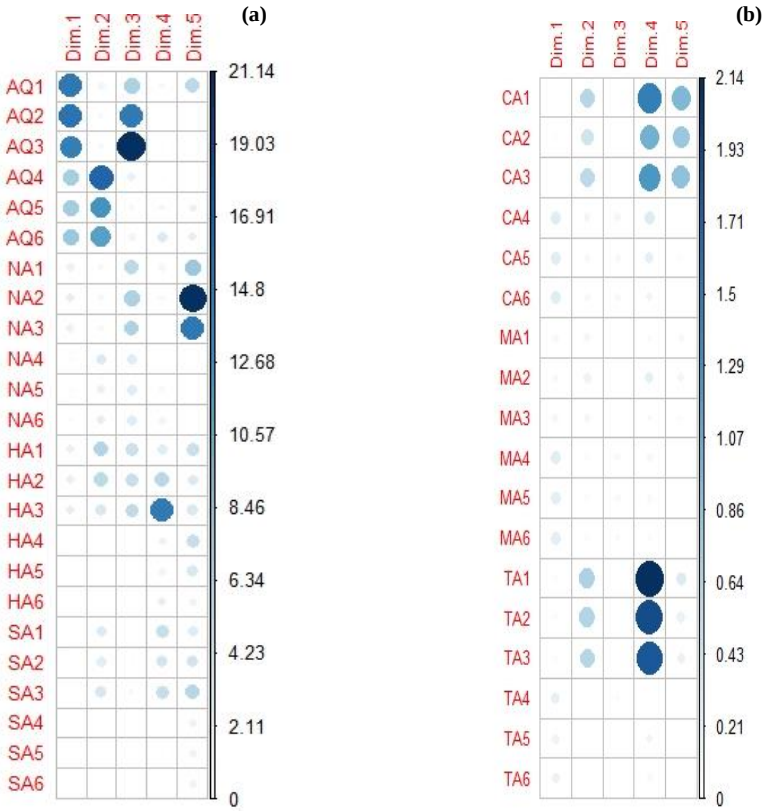

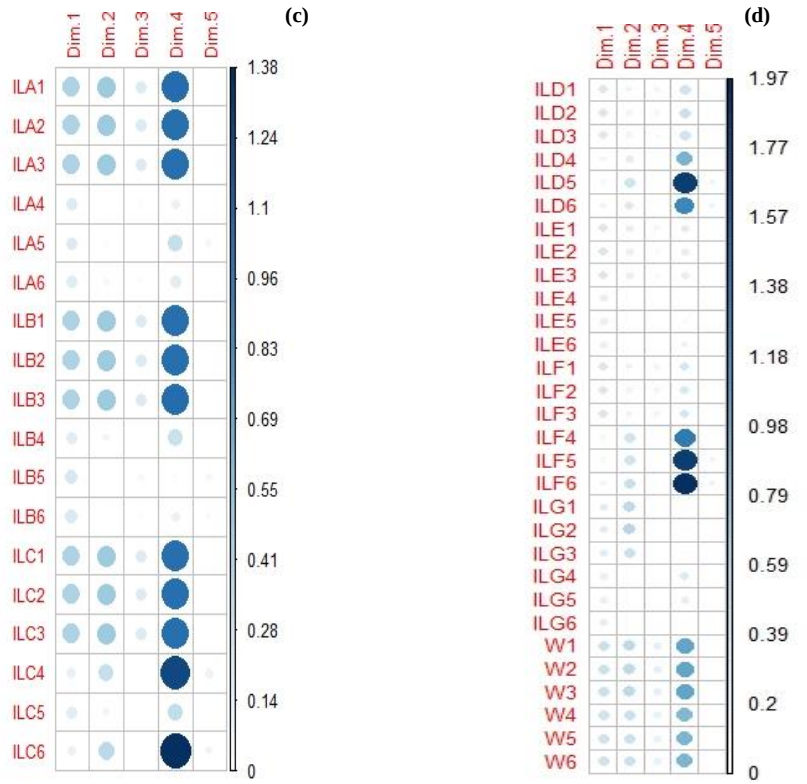

Figure 4.50 (a) Observation contribution Dim plot for inorganic acids (dose effect) (b) observation contribution Dim plot for organic acids (dose effect) (c) observation contribution Dim plot for IL a – c (dose effect) (d) observation contribution Dim plot for IL d - g (dose effect)

Table 4.31 Best Contributing Observations for Particle-size Effect

	Dim 1 (%)	**Dim 2 (%)**
AQ1	**15.2**	1.3
AQ2	**15.6**	1.0
AQ3	**14.4**	1.0
AQ4	**7.1**	**16.9**
AQ5	**7.4**	**12.5**
AQ6	**7.9**	**11.5**
NA1	**1.8**	0.9
NA2	**2.3**	1.1
NA3	**1.9**	0.9
HA1	**2.0**	**6.3**
HA2	**2.1**	**5.7**
HA3	**2.3**	**3.4**

4.9 Determination of H_2O_2 Effect

Two methods, hotplate and microwave methods, were used to determine the effect of H_2O_2 amount (5, 15 & 25 %) on the extraction of Cu, Zn, Fe, Ni and Pb. For the hotplate method, the experimental conditions were particle-size (4 mm), time (120 minutes), temperature (70 ^{0}C), concentration (2 M for inorganic acids, 25 g/L for organic acids and 100 g/L for ionic liquids), sample weight (0.5g) and rotation speed (340 rpm). For the microwave method, the experimental conditions were particle-size (4 mm), time (20 minutes), temperature (150 ^{0}C), concentration (2 M for inorganic acids, 25 g/L for organic acids and 100 g/L for ionic liquids) and sample weight (0.5 g). **Appendices 3 a - e** shows tables of the mean concentrations of H_2O_2 effect for Cu, Zn, Fe, Ni and Pb (mg/g) with H_2O_2 concentrations from three different experiments and the standard deviation as the error bar.

4.9.1 Effect of H_2O_2 amount on Leaching Cu

Table 4.32 a shows the percentage extraction of Cu with H_2O_2 amount and this is also represented in **Figure 4.51.** In the hotplate method (**Figure 4.51**), the H_2O_2 amount increased from 5 – 25 % Cu extraction increased in HA while NA did not show any significant difference. The peak extractions of Cu were HA (77 % at 25 % H_2O_2), NA (39 % at 15 % H_2O_2), CA (7 % at 5 % H_2O_2), MA (6 % at 5 % H_2O_2) and SA (1 % at 25 % H_2O_2). The other solvents had < 2 % Cu extraction. In the microwave method (**Figure 4.51**), the H_2O_2 increased from 5 – 25 % the Cu extraction did not change significantly. The peak extractions of Cu were HA (74 % at 25 % H_2O_2), NA (62 % at 25 % H_2O_2), CA (7 % at 5 % H_2O_2) and MA (7 % at 5 % H_2O_2). The other solvents had < 2 % Cu extraction.

To compare the hotplate method with microwave method, two sample independent t-test was done for each of the solvents. The null hypothesis (H_0) stated that the mean of both methods are equal while the alternative hypothesis (H_1) stated that the mean of both methods are not equal. In **Table 4.32 b** it shows that at 95 % confidence level the independent t-test for HA and MA had p-values > 0.05 and this shows that the means for both methods are equal so the hotplate and microwave methods have the same efficiencies. However, NA, SA and CA with p-value < 0.05 shows that the mean of both methods are not equal therefore the microwave method was better for HA while the the hotplate method was better for NA, SA and CA.

Table 4.32a Percentage concentration values for effect of H_2O_2 amount on leaching Cu

	H_2O_2 Amount (%)	Extraction (%)														
		AQ	NA	HA	SA	CA	MA	TA	IL-A	IL-B	IL-C	IL-D	IL-E	IL-F	IL-G	W
Hotplate Method	5.00	100.00	37.50	67.30	1.10	6.54	5.97	0.28	0.09	0.06	0.27	0.14	0.54	0.20	0.50	0.01
	15.00	100.00	39.37	69.84	1.16	1.56	6.73	0.24	0.08	0.07	0.29	0.14	0.57	0.21	0.54	0.02
	25.00	100.00	38.70	76.83	1.25	0.83	7.30	0.22	0.07	0.07	0.31	0.16	0.62	0.21	0.60	0.03
Microwave Method	5.00	100.00	57.78	67.78	0.69	6.67	6.72	0.14	0.07	0.08	0.05	0.07	0.15	0.02	0.14	0.01
	15.00	100.00	58.89	71.67	0.63	0.95	5.94	0.09	0.10	0.07	0.06	0.09	0.16	0.02	0.15	0.02
	25.00	100.00	61.67	74.44	0.49	0.49	1.48	0.07	0.14	0.07	0.06	0.09	0.18	0.02	0.16	0.03

Table 4.32 b Independent t-test between hotplate and microwave methods at 95 % confidence level (H_2O_2 effect on Cu)

	NA	HA	SA	CA	MA
p-value	7.05×10^{-05}	0.99	0.00	0.00	0.31
Hotplate mean (%)	38.52	71.32	1.17	1.17	6.67
Microwave mean (%)	59.45	71.30	0.60	0.60	4.71

Note: There were no t-tests for < 1.0 % extractions as they were considered insignificant

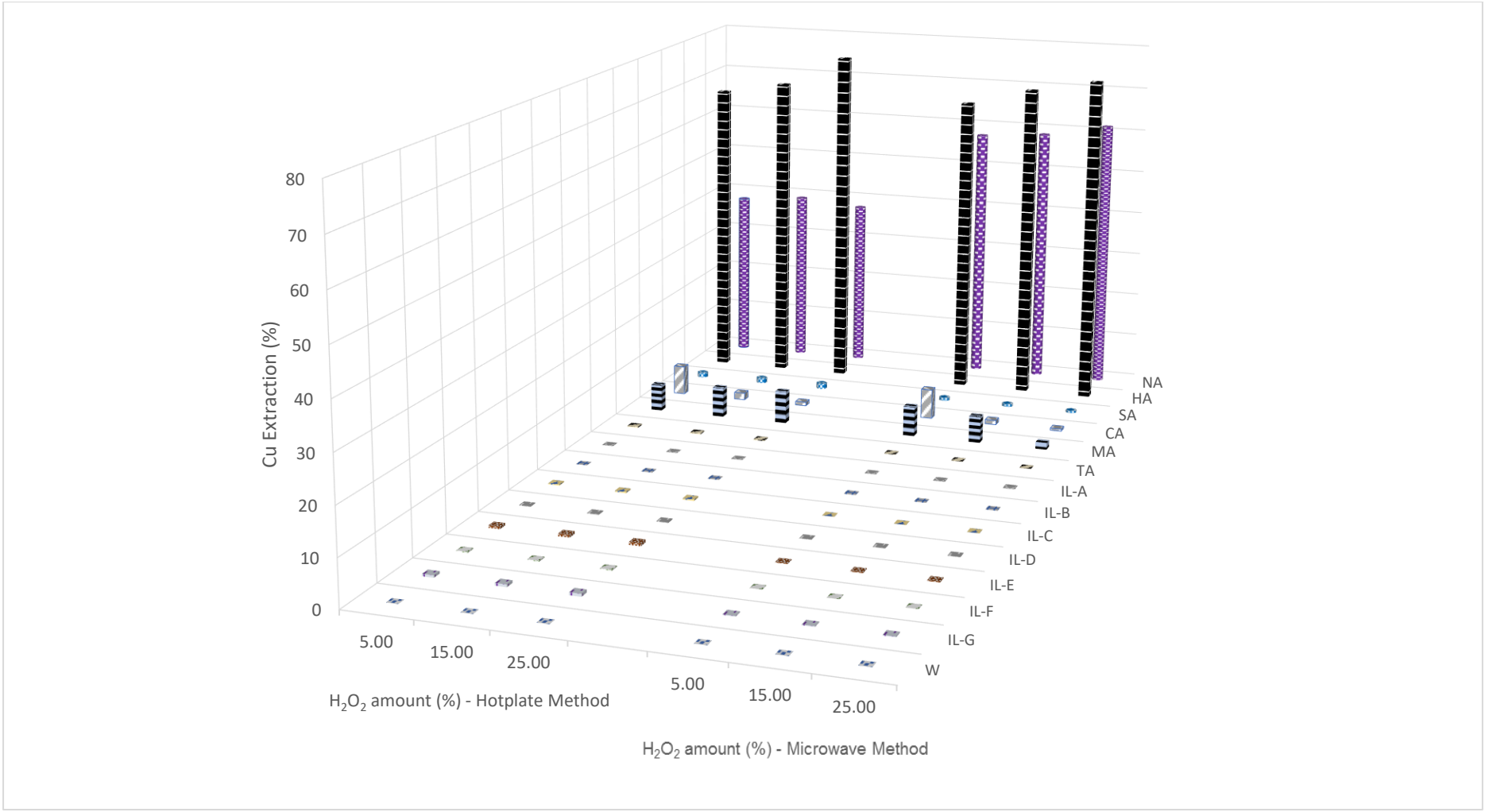

Figure 4.51 Percentage concentration for the effect of H_2O_2 amount on leaching Cu

4.9.2 Effect of H_2O_2 amount on Leaching Zn

Table 4.33a shows the percentage extraction of Zn with H_2O_2 amount and this is also represented in **Figure 4.52**. In the hotplate method (**Figure 4.52**), the H_2O_2 amount increased from 5 – 25 % the Zn extractions did not show any significant change. The peak extractions of Zn were NA (86 % at 15 % H_2O_2), HA (24 % at 5 % H_2O_2), SA (24 % at 25 % H_2O_2), CA (16 % at 5 % H_2O_2), MA (20 % at 25 % H_2O_2), TA (17 % at 5 % H_2O_2), IL A (56 % at 5 % H_2O_2), IL B (70 % at 5 % H_2O_2), IL C (72 % at 5 % H_2O_2), IL D (71 % at 5 % H_2O_2), IL E (61 % at 5 % H_2O_2), IL F (69 % at 5 % H_2O_2), IL G (66 % at 5 % H_2O_2). In the microwave method (**Figure 4.52**), the H_2O_2 increased from 5 – 25 % the Zn extractions did not show any significant change. The peak extractions of Zn were NA (51 % at 25 % H_2O_2), HA (50 % at 25 % H_2O_2), SA (45 % at 25 % H_2O_2), CA (43 % at 25 % H_2O_2) and MA (37 % at 25 % H_2O_2), TA (31 % at 5 % H_2O_2), IL A (19 % at 25 % H_2O_2), IL B (17 % at 5 % H_2O_2), IL C (22 % at 5 % H_2O_2), IL D (22 % at 5 % H_2O_2), IL E (20 % at 25 % H_2O_2), IL F (21 % at 5 % H_2O_2), IL G (21 % at 25 % H_2O_2) had extraction range between 17 % to 22 %.

To compare the hotplate method with microwave method, two sample independent t-test was done for each of the solvents. The null hypothesis (H_0) stated that the mean of both methods are equal while the alternative hypothesis (H_1) stated that the mean of both methods are not equal. In **Table 4.33 b** it shows that at 95 % confidence level the independent t-test for TA had p-values > 0.05 and this shows that the means for both methods are equal so the hotplate and microwave methods have the same efficiencies. However, the other solvents with p-value < 0.05 shows that the mean of both methods are not equal therefore the hotplate method was better for NA and ILs A – G while the microwave method was better for HA, SA, CA and MA

Table 4.33a Percentage concentration values for effect of H_2O_2 amount on leaching Zn

	H_2O_2 Amount (%)	Extraction (%)													
		AQ	NA	HA	SA	CA	MA	TA	IL-A	IL-B	IL-C	IL-D	IL-E	IL-F	IL-G	W
Hotplate Method	5.00	100.00	84.21	23.68	15.92	15.79	18.06	16.86	55.53	70.13	70.66	70.89	58.42	66.45	62.66	0.01
	15.00	100.00	85.53	21.38	20.71	15.16	19.40	6.82	54.41	69.93	72.04	68.09	57.63	67.76	63.32	0.01
	25.00	100.00	84.87	21.76	23.79	12.89	19.70	0.01	53.16	68.68	69.08	68.82	60.82	68.59	66.12	0.01
Microwave Method	5.00	100.00	44.38	43.08	41.21	37.18	29.37	30.67	17.74	17.30	21.53	21.46	19.03	21.30	20.18	0.01
	15.00	100.00	48.71	49.33	44.22	38.98	33.62	5.54	17.50	16.99	20.68	21.88	19.23	21.24	20.58	0.01
	25.00	100.00	51.48	49.86	44.84	42.70	36.76	0.00	18.47	16.73	20.90	20.98	20.08	20.86	20.83	0.01

Table 4.33b Independent t-test between hotplate and microwave methods at 95 % confidence level (H_2O_2 effect on Zn)

	NA	HA	SA	CA	MA	TA	IL-A	IL-B	IL-C	IL-D	IL-E	IL-F	IL-G
p-value	6.32×10^{-05}	3.91×10^{-04}	7.98×10^{-04}	1.73×10^{-04}	2.97×10^{-03}	0.71	1.04×10^{-06}	4.26×10^{-05}	6.29×10^{-07}	6.80×10^{-07}	2.57×10^{-06}	2.13×10^{-07}	2.25×10^{-06}
Hotplate mean (%)	84.87	22.27	20.14	14.61	19.05	7.89	54.37	69.58	70.59	69.27	58.96	67.60	64.03
Microwave mean (%)	48.19	47.42	43.42	39.62	33.25	12.07	17.90	17.01	21.04	21.44	19.45	21.13	20.53

Note: There were no t-tests for < 1.0 % extractions as they were considered insignificant

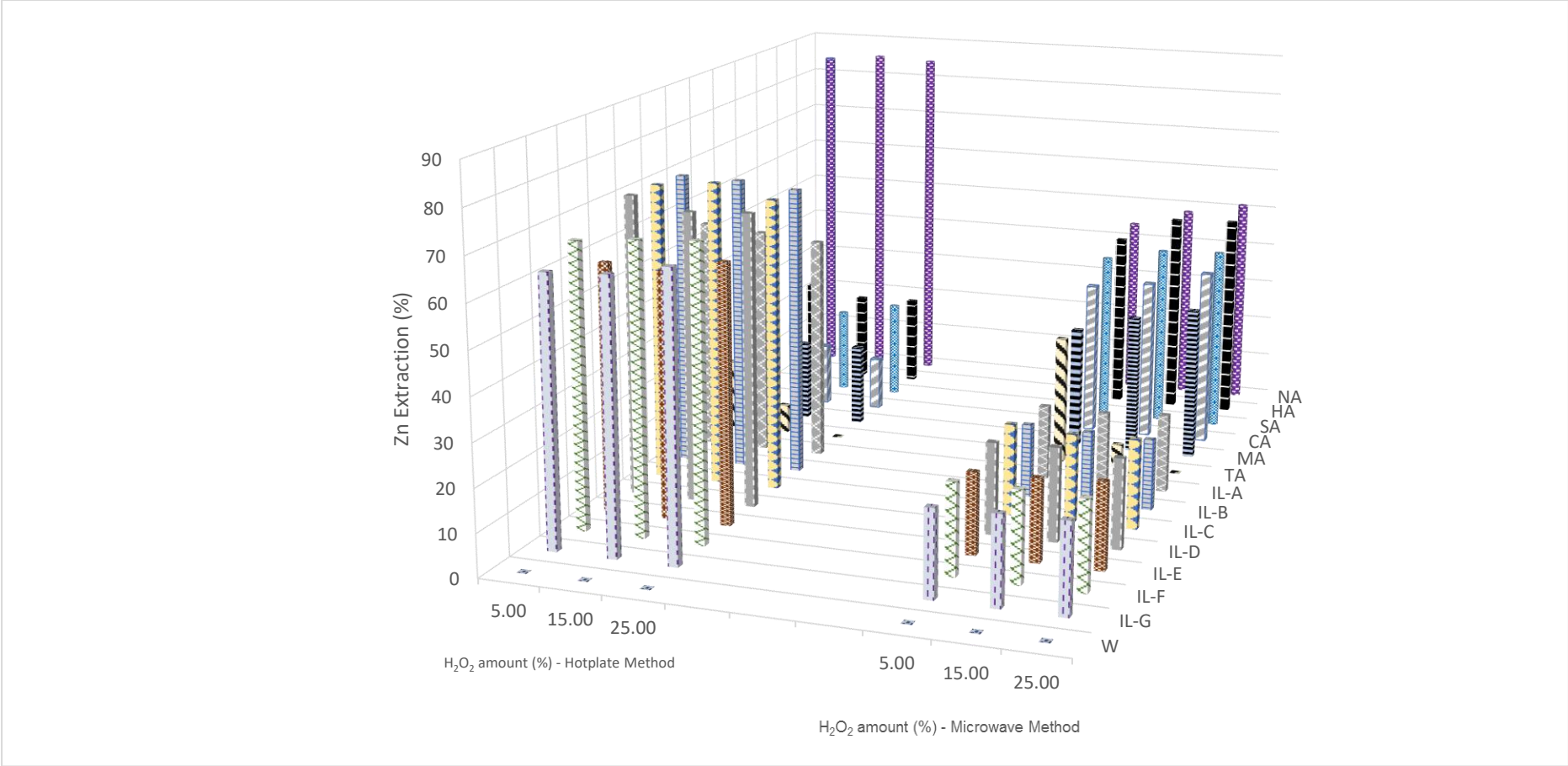

Figure 4.52 Percentage concentration for the effect of H_2O_2 amount on leaching Zn

4.9.3 Effect of H_2O_2 amount on Leaching Fe

Table 4.34 a shows the percentage extraction of Fe with H_2O_2 amount and this is also represented in **Figure 4.53.** In the hotplate method (**Figure 4.53**) the H_2O_2 amount increased from 5 – 25 % Fe extraction in HNO_3 did not show any significant difference, HCl extraction decreased while H_2SO_4 increased. The solvents peak extractions of Fe in this research were NA (6 % at 25 % H_2O_2), HA (36 % at 5 % H_2O_2), SA (48 % at 25 % H_2O_2), IL-F (4 % at 25 % H_2O_2). The other solvents did not show any significant extractions. In the microwave method (**Figure 4.53**), the H_2O_2 increased from 5 – 25 % the Fe extraction peaked at 15 % H_2O_2 and then decreased for the inorganic acid except for SA which decreased. The solvents peak extractions of Fe were NA (2 % at 15 % H_2O_2), HA (85 % at 15 % H_2O_2) and SA (5 % at 5 % H_2O_2). ILs E & F had < 2 % Fe extractions while the other solvents did not show any significant extractions.

To compare the hotplate method with microwave method, two sample independent t-test was done for each of the solvents. The null hypothesis (H_0) stated that the mean of both methods are equal while the alternative hypothesis (H_1) stated that the mean of both methods are not equal. In **Table 4.34b** it shows that at 95 % confidence level the independent t-test for HA and SA had p-values > 0.05 and this shows that the means for both methods are equal so the hotplate and microwave methods have the same efficiencies. However, the solvents with p-value < 0.05 shows that the mean of both methods are not equal therefore the hotplate method was better for NA and IL-F while the microwave method was better for IL-E.

Table 4.34a Percentage concentration values for effect of H_2O_2 amount on leaching Fe

	H_2O_2 Amount (%)	Extraction (%)														
		AQ	NA	HA	SA	CA	MA	TA	IL-A	IL-B	IL-C	IL-D	IL-E	IL-F	IL-G	W
Hotplate Method	5.00	100.00	4.59	36.02	30.59	0.00	0.51	0.23	0.00	0.00	0.12	0.00	0.00	3.43	0.26	0.00
	15.00	100.00	5.19	27.27	37.06	0.00	0.13	0.05	0.00	0.00	0.13	0.00	0.00	3.86	0.28	0.00
	25.00	100.00	6.20	4.68	48.05	0.00	0.15	0.06	0.00	0.00	0.14	0.00	0.00	4.18	0.33	0.00
Microwave Method	5.00	100.00	1.99	7.70	84.88	0.00	0.00	0.00	0.05	0.64	0.11	0.39	1.42	1.34	0.10	0.00
	15.00	100.00	2.25	85.35	56.25	0.00	0.03	0.03	0.06	0.68	0.13	0.42	1.61	1.54	0.12	0.00
	25.00	100.00	0.03	1.67	29.99	0.00	0.00	0.00	0.06	0.68	0.13	0.46	1.86	1.70	0.14	0.00

Table 4.34b Independent t-test between hotplate and microwave methods at 95 % confidence level (H_2O_2 effect on Fe)

	NA	HA	SA	IL-E	IL-F
p-value	0.01	0.77	0.33	2.15×10^{-4}	6.76×10^{-4}
Hotplate mean (%)	5.33	22.66	38.57	0.00	3.82
Microwave mean (%)	1.42	31.57	57.20	1.63	1.53

Note: There were no t-tests for < 1.0 % extractions as they were considered insignificant

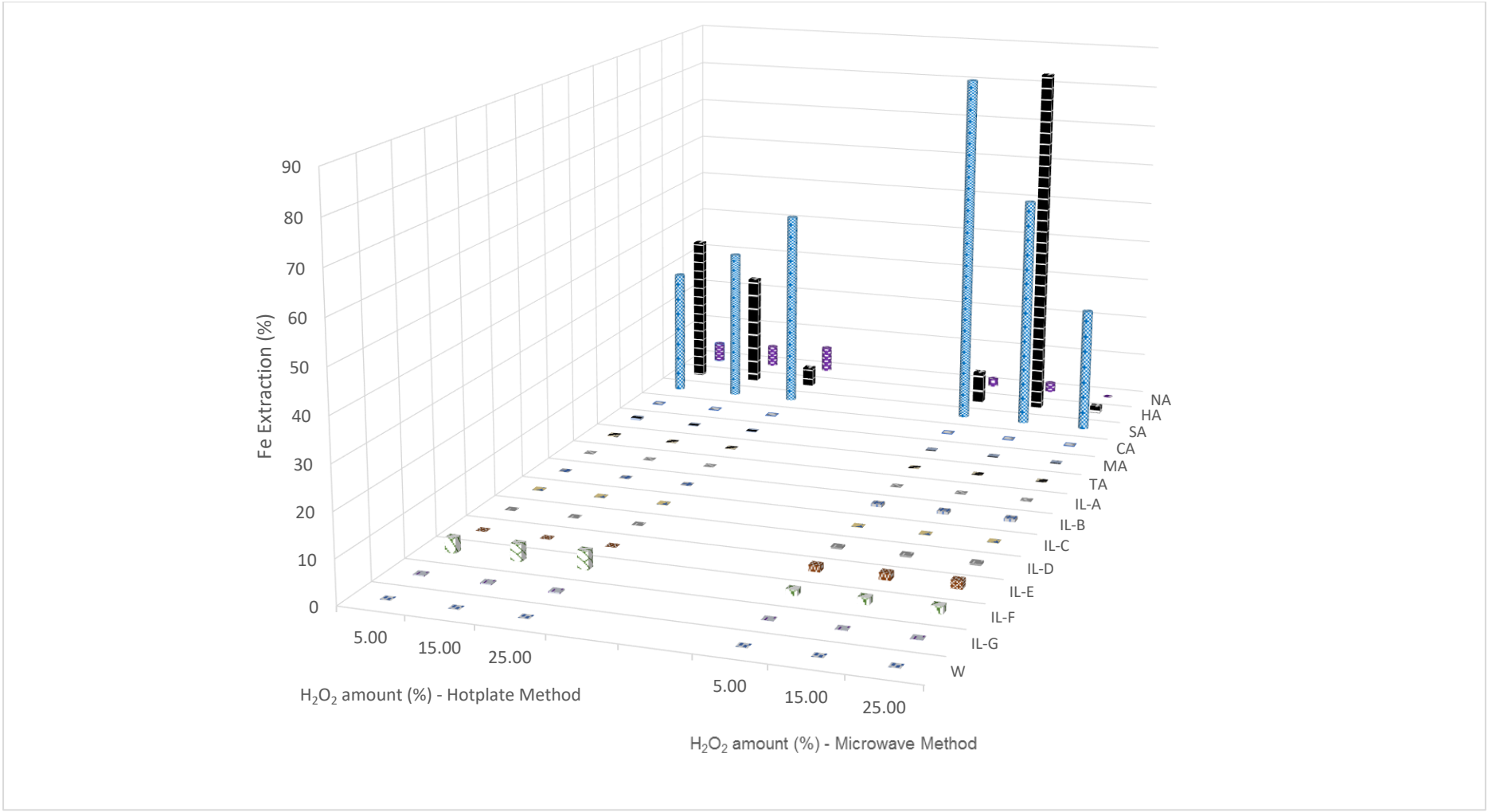

Figure 4.53 Percentage concentration for the effect of H_2O_2 amount on leaching Fe

4.9.4 Effect of H_2O_2 amount on Leaching Ni

Table 4.35 a shows the percentage extraction of Ni with H_2O_2 amount and this is also represented in **Figure 4.54.** In the hotplate method (**Figure 4.54**), the H_2O_2 amount increased from 5 – 25 % Ni extraction decreased in the inorganic acids. The solvents peak extractions of Ni in this research were NA (26 % at 5 % H_2O_2), HA (34 % at 15 % H_2O_2). The organic acids and ILs A - G did not show any significant extractions. In the microwave method (**Figure 4.54**), the H_2O_2 amount increased from 5 – 25 % the Ni extraction only decreased in NA. The solvents peak extractions of Ni were NA (82 % at 5 % H_2O_2), HA (78 % at 15 % H_2O_2) and SA (96 % at 15 % H_2O_2). The organic acids and ILs A - G did not show any significant extractions.

To compare the hotplate method with microwave method, two sample independent t-test was done for each of the solvents. The null hypothesis (H_0) stated that the mean of both methods are equal while the alternative hypothesis (H_1) stated that the mean of both methods are not equal. In **Table 4.35 b** it shows that at 95 % confidence level the independent t-test for NA, HA and SA had p-values < 0.05 and this shows that the mean of both methods are not equal therefore the microwave method was better the solvents.

Table 4.35a Percentage concentration values for effect of H_2O_2 amount on leaching Ni

	H_2O_2 Amount (%)	Extraction (%)														
		AQ	NA	HA	SA	CA	MA	TA	IL-A	IL-B	IL-C	IL-D	IL-E	IL-F	IL-G	W
Hotplate Method	**5.00**	100.00	25.53	23.40	0.65	0.04	0.35	0.01	0.01	0.01	0.01	0.01	0.01	0.01	0.01	0.00
	15.00	100.00	23.57	34.04	0.50	0.06	0.00	0.01	0.01	0.01	0.01	0.01	0.01	0.01	0.01	0.01
	25.00	100.00	22.26	0.65	0.39	0.01	0.13	0.01	0.01	0.01	0.01	0.01	0.01	0.01	0.01	0.01
Microwave Method	**5.00**	100.00	82.12	63.89	29.86	0.04	0.16	0.01	0.01	0.13	0.02	0.02	0.02	0.04	0.16	0.00
	15.00	100.00	64.06	78.30	95.83	0.06	0.14	0.02	0.01	0.15	0.02	0.02	0.02	0.04	0.17	0.01
	25.00	100.00	55.42	48.61	44.97	0.02	0.15	0.01	0.02	0.13	0.02	0.02	0.02	0.03	0.18	0.01

Table 4.35b Independent t-test between hotplate and microwave methods at 95 % confidence level (H_2O_2 effect on Ni)

	NA	HA	SA
p-value	0.01	0.03	0.048
Hotplate mean (%)	23.77	19.36	0.51
Microwave mean (%)	67.20	63.60	56.89

Note: There were no t-tests for < 0.5 % extractions as they were considered insignificant

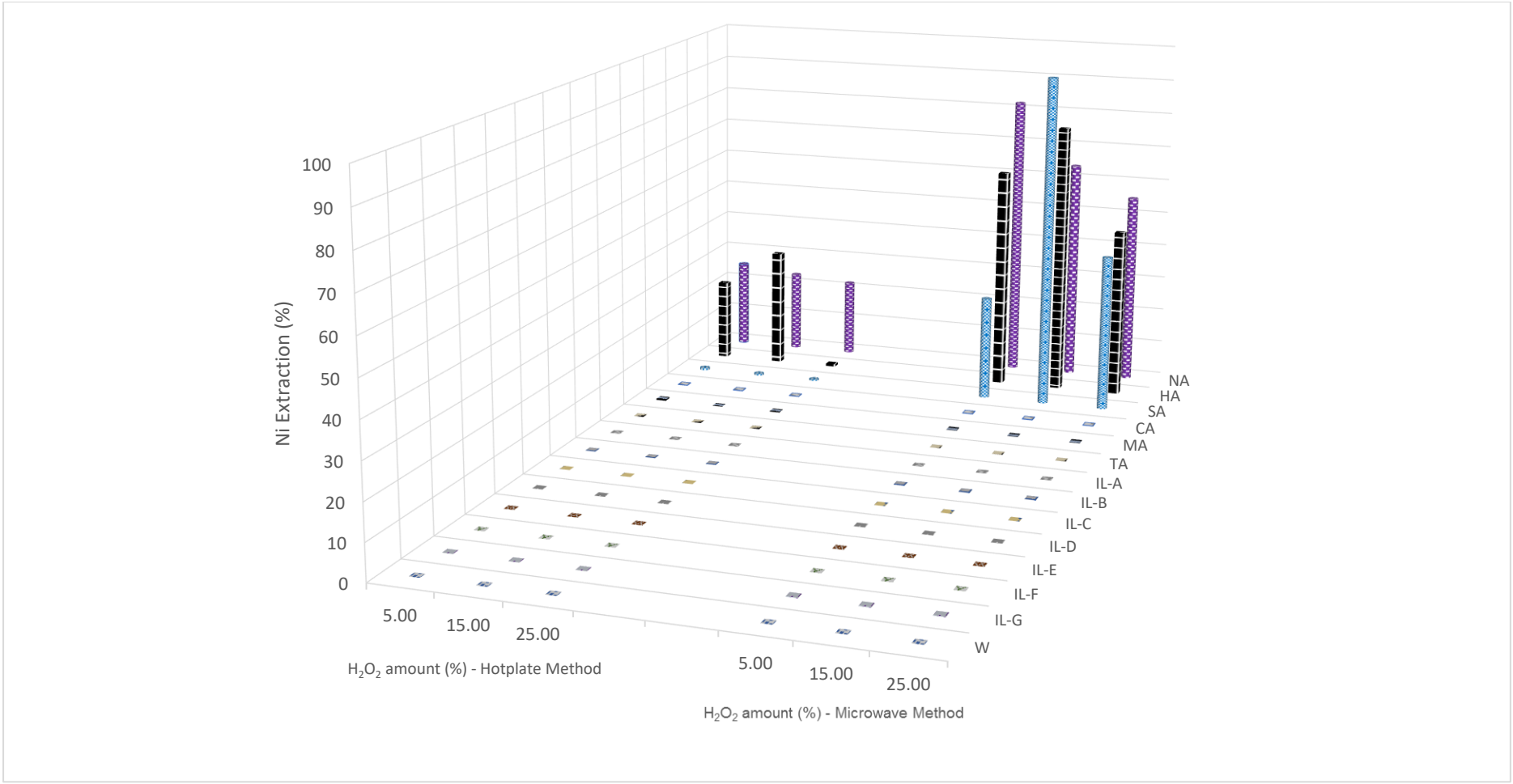

Figure 4.54 Percentage concentration for the effect of H_2O_2 amount on leaching Ni

4.9.5 Effect of H_2O_2 amount on Leaching Pb

Table 4.36a shows the percentage extraction of Pb with H_2O_2 amount and this is also represented in **Figure 4.55.** In the hotplate method (**Figure 4.55**), the H_2O_2 amount increased from 5 – 25 % Pb extraction decreased. The solvents peak extractions of Pb in this research were NA (4 % at 5 % H_2O_2), HA (7 % at 5 % H_2O_2). SA, the organic acids and ILs A - G did not show any significant extractions. In the microwave method (**Figure 4.55),** the H_2O_2 increased from 5 – 25 % Pb extraction increased. The peak extractions of Pb were NA (43 % at 25 % H_2O_2), HA (24 % at 25 % H_2O_2). SA, the organic acids and ILs A- G did not show any significant extractions.

To compare the hotplate method with microwave method, two sample independent t-test was done for each of the solvents. The null hypothesis (H_0) stated that the mean of both methods are equal while the alternative hypothesis (H_1) stated that the mean of both methods are not equal. In **Table 4.36 b** it shows that at 95 % confidence level the independent t-test for HA had p-values > 0.05 and this shows that the means for both methods are equal so the hotplate and microwave methods have the same efficiencies. However, the solvents (NA and SA) with p-value < 0.05 shows that the mean of both methods are not equal therefore the microwave method with higher mean was better for NA and SA.

Table 4.36a Percentage concentration values for effect of H_2O_2 amount on leaching Pb

	H_2O_2 Amount (%)	Extraction (%)													
		AQ	NA	HA	SA	CA	MA	TA	IL-A	IL-B	IL-C	IL-D	IL-E	IL-F	IL-G	W
Hotplate Method	5.00	100.00	3.70	6.94	0.37	0.28	0.49	0.28	0.54	0.39	0.44	0.34	0.42	0.54	0.26	0.02
	15.00	100.00	2.16	4.81	0.43	0.25	0.34	0.32	0.42	0.43	0.43	0.37	0.43	0.56	0.22	0.04
	25.00	100.00	1.85	3.24	0.52	0.22	0.34	0.37	0.37	0.43	0.37	0.37	0.43	0.31	0.25	0.04
Microwave Method	5.00	100.00	28.15	1.09	1.33	0.67	1.11	0.56	0.63	0.44	0.10	0.10	0.11	0.15	0.14	0.02
	15.00	100.00	36.11	18.89	1.11	0.67	0.93	0.37	0.59	0.41	0.11	0.10	0.10	0.16	0.15	0.04
	25.00	100.00	42.59	23.89	1.07	0.33	0.52	0.33	0.41	0.37	0.12	0.07	0.11	0.16	0.16	0.04

Table 4.36b Independent t-test between hotplate and microwave methods at 95 % confidence level (H_2O_2 amount on Pb)

	NA	HA	SA
p-value	0.00	0.24	0.00
Hotplate mean (%)	2.57	5.00	0.44
Microwave mean (%)	35.62	14.62	1.17

Note: There were no t-tests for < 1.0 % extractions as they were considered insignificant

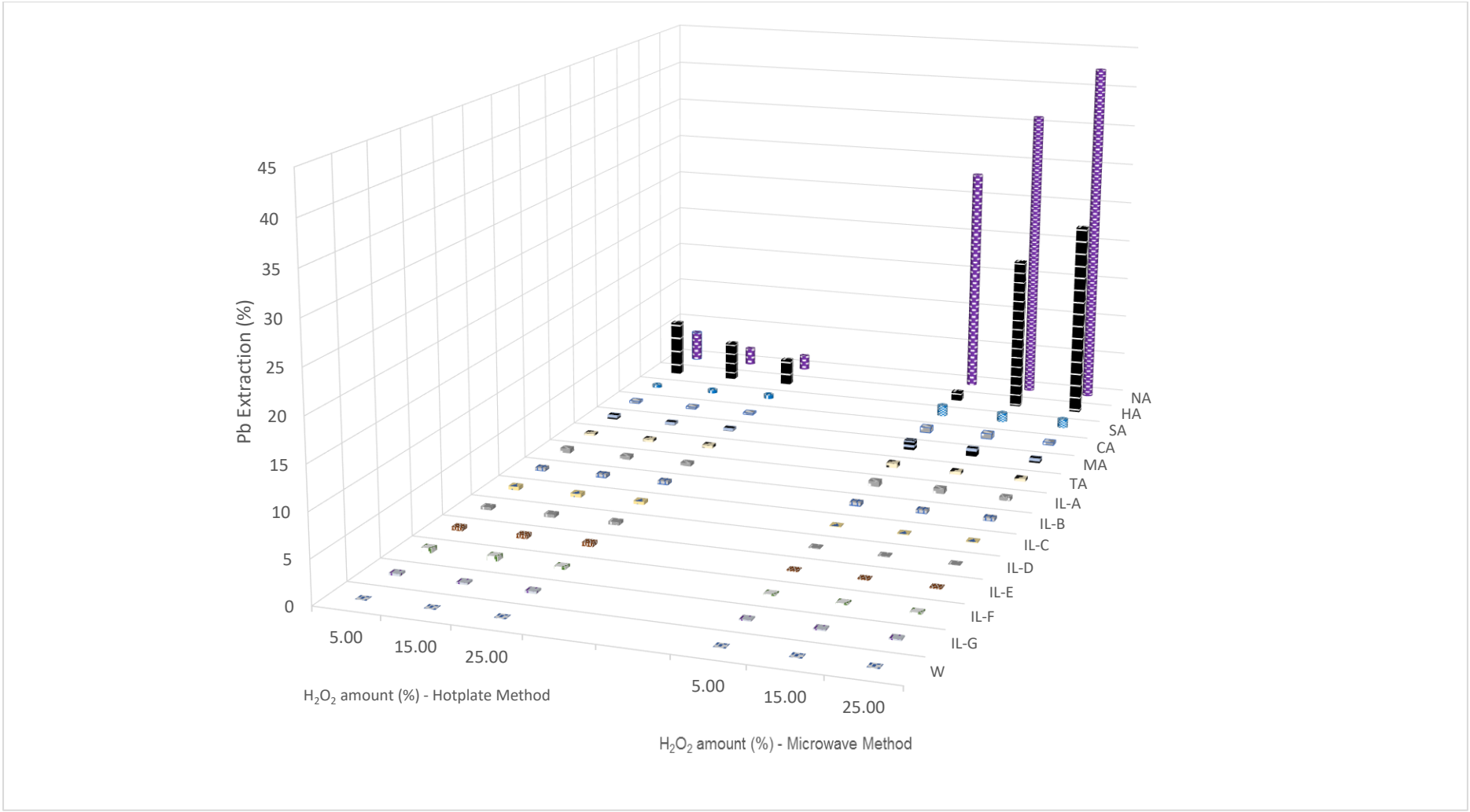

Figure 4.55 Percentage concentration for the effect of H_2O_2 amount on leaching Pb

4.10 PCA for H_2O_2 Effect

4.10.1 PCA Scree Plot for H_2O_2 Effect

The H_2O_2effect experiment involved 15 variables and 90 observations. The variables were made up of five metals (Cu, Zn, Fe, Ni and Pb) with each of these metals having results from three different experiments on effect of H_2O_2 amount (5, 15 & 25 %). The observations were results from each of the fifteen solvents with three replicates each from the hotplate and microwave methods used in the experiment. **Table 4.37** shows the summarized data of the first six principal components extracted from both the hotplate and microwave methods (mg/g) in **Appendices 3 a – e**. **Figure 4.56** shows the scree plot of variance for the dimensions from dose effect data and they are in the order of highest to the lowest with Dim.1 as 72.4 %, Dim.2 as 13.9 % and Dim.3 as 8.4 %. From this scree plot we can infer that Dim.1 explains the most part of the dose effect data as it is larger than the other dimensions. From **Table 4.19**, we can see that Dim.1, 2 & 3 showed a SD > 1.0 as SD = 1 is the cutoff point. Therefore, we can accept the first three dimensions (Dim.1, 2 & 3) with a proportion of variance of 72.4, 13.9 & 8.4 % respectively. Consequently, the cumulative proportion in Dim.1, 2 & 3 also showed 72.4, 86.2 & 94.6 % respectively. This shows that with Dim.3 having a SD of 1.1, about 94.6 % of the data can be accounted for while the remaining 5.4 % of the data can be disregarded as they fall below SD < 1.0.

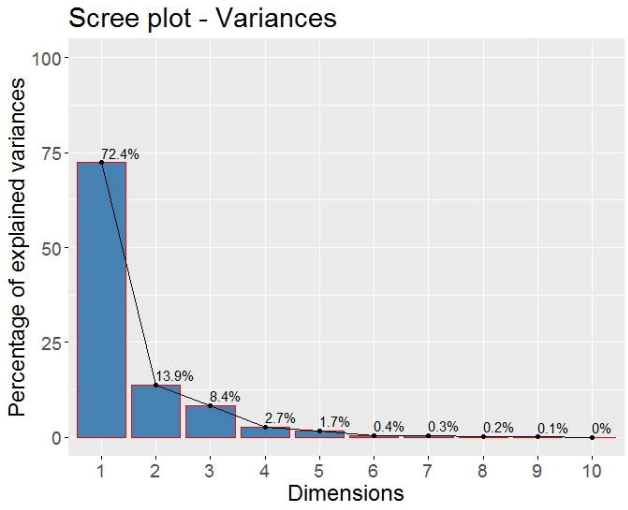

Figure 4.56 Scree plot for H_2O_2 effect

Table 4.37 Summarized principal components for H_2O_2 effect

Principal Components	Dim.1	Dim.2	Dim.3	Dim.4	Dim.5	Dim.6
Standard deviation	3.295	1.442	1.121	0.631	0.502	0.257
Proportion of Variance	0.724	0.139	0.084	0.027	0.017	0.004
Cumulative Proportion	0.724	0.862	0.946	0.972	0.989	0.994

Figure 4.57 shows the biplot for H_2O_2 effect data which is the relationship between the variables and the observations in the H_2O_2 data. It also shows the structure of variables correlations and clustered observations. From the PCA plot, we can see the variables with the longest vector projections. They represent the highest variations in the data and they have occured in Zn15, Zn25, Zn5 and Ni25. The replicate observations formed clusters, for example, in the hotplate method (1, 2 & 3) the observations AQ1, AQ2 & AQ3 which represents the hotplate result for *aqua-regia* formed a cluster which means that the three replicated experiments showed similarity in the result from H_2O_2 effect. Also, this behaviour was observed in AQ4, AQ5 & AQ6 (microwave method) showing that the replicated results were similar. The *aqua-regia* observations AQ1-3 and HA1-3 (hydrochloric acid) are considered outliers on the PCA as they were clearly outside the group clustering and also far away from the other observations. However, they were not treated as outliers or removed as they were needed in this research inorder to clearly differentiate the best performing solvents or observations. Other observation clusters were seen in (NA1, NA2 & NA3). The above stated clusters had various degrees of euclidean distance (distance between observations) and the observations from *aqua-regia* (AQ1-3) was the farthest followed by hydrochloric acid (HA1-3). However, NA1-3 and AQ4-6 were next. Consequently, NA4-6, HA4-6, SA1-3, SA4-6, organic acids and ionic liquids all seemed to have clustered together as their euclidean distance were relatively close.

We can see that the variables vectors were pointing towards AQ1-3, AQ4-6 and HA1-3. This shows a high degree of association between the variables and the observations but the reverse was the case for the other observations such as NA4-6, HA4-6, SA1-3, SA4-6, the organic acids and ionic liquids as the PCA plot (**Figure 4.57**) clearly shows the variable vectors pointing away from them and this implies very low association between the variables and these observations. Also, all the variables were pointing towards the hotplate method (red) showing high variable association with the hotplate method. However, the variables were all

pointing away from the microwave method (blue) showing less variable association with the microwave method. The variable vectors closest to each other showed high correlation amongst themselves, for example Zn15, Zn 25 and Zn5. No correlation was observed between Zn15 and Ni25 as their vectors formed angle close to 90 degrees. The x-axis which is Dim.1 (72.4 % of variation explained) shows that all the variable vectors are positioned on the left side of the plot thereby revealing negative correlation for all variables. So we would expect that the lower the values of Dim.1 the higher high values for each of the variables. The y-axis which is Dim.2 (13.9 % of variation explained) shows that half of the variables positioned at the top were positive correlation and the other half at the bottom were negative correlation. (Kohla & Luniak, 2005; Reris & Brooks, 2015; Statisticshowto, 2021; STHDA, 2021; Towardsdatascience, 2021).

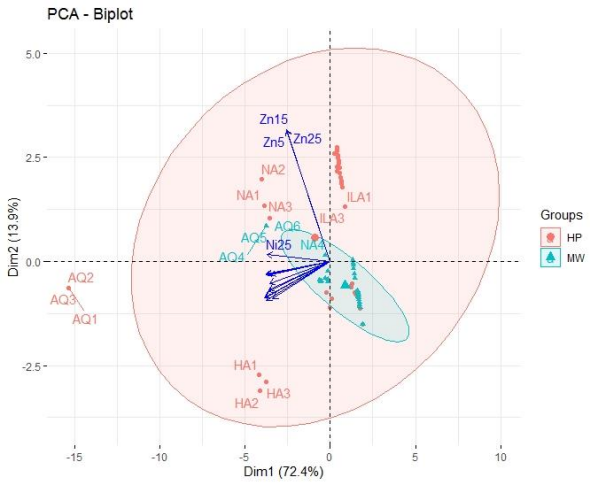

Figure 4.57 Biplot for H_2O_2 effect

4.10.2 PCA Result for Variable Coordinates in H_2O_2 Effect

Figure 4.58 a shows the plot for the variable coordinates for Dim.1 & 2 which are representing of the position of the H_2O_2 effect variables on the plot. The coordinates are correlation between a variable and a dimension. **Figure 4.58 b** shows a three-dimensional view of variable coordinates for the three dimensions (Dim.1, 2 & 3) with Dim.1 (72.4 %) on the x-axis, Dim.2 (13.9 %) on the z-axis and Dim.3 (8.4 %) on the y-axis. **Figure 4.58 c** shows the variable coordinates visualization with spots of different colour intensity. The strongest or darkest colour represent the highest correlation values and the correlation values decreases with decrease in the colour intensity of the spots in the visualization. Also, the positive correlated values are in blue while the negative correlated values are in red. Here,

Dim.1, 2, 3, 4 & 5 are represented by Dim.1, 2, 3, 4 & 5. The order of importance decreased from Dim.1 to 5. We can see that Dim.1 showed the highest colour intensity and this was followed by Dim.2, 3, 4 & 5. However, all the coordinates in Dim.1 showed strong negative correlation. In Dim.2, moderate negative correlation occurred in Ni15. The other variables showed weak positive and negative correlation. Dim.3 showed relatively weak positive and negative correlations.

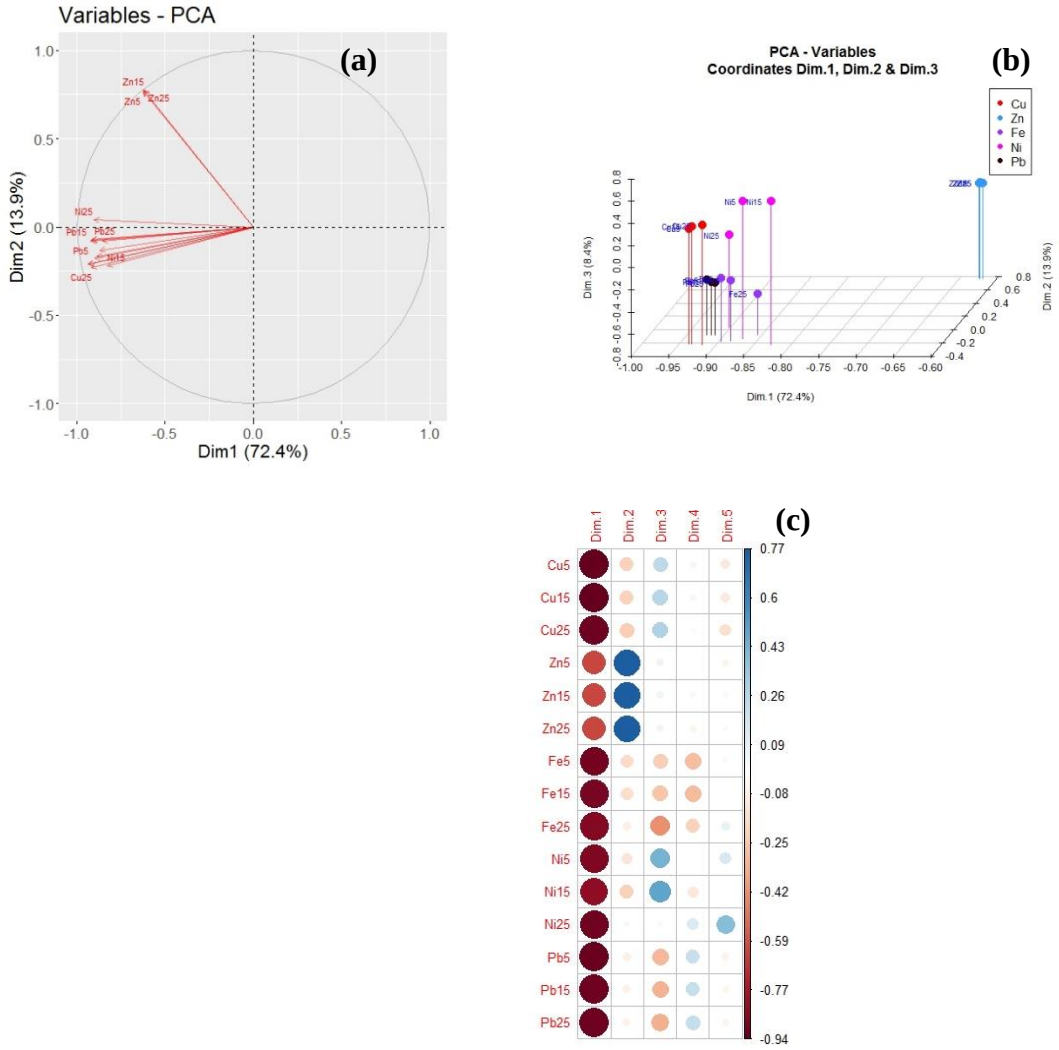

Figure 4.58: (a) Variable Coordinates Correlation Plot (H_2O_2 effect) (b) Variable Coordinates 3D Plot (H_2O_2 effect) (c) Variable Coordinates Dim Plot (H_2O_2 effect)

4.10.3 PCA Result for Variable Cos2 Quality of Representation in H_2O_2 Effect

Figure 4.59 a shows the Cos2 plot of variable with the highest Cos2 value which are in orange while the mid cos2 variables value are in blue. The variables in orange are the most represented in the plot as they are closest to the circle of correlation with very high values and this is followed by the yellow and then the blue spots. All the variables indicated in this Cos2 plot **(Figure 4.59 a)** show very good representation for Dim.1 as all the variables are far from the centre of the circle and none is close to the centre of the circle. **Figure 4.59b & c** shows another visualization of the Cos2 variables in the form of bar plots. We can see that the Cos2 variables for Dim.1 in **Figure 4.59 b** are the highest which also supports the fact that the quality of representation is good. The variables in the bar plots are arranged from highest to lowest. Consequently, all negative values have been cancelled out and **Figure 4.59 d** shows the Cos2 variables visualization with spots of different colour intensity. The strongest or darkest colour represent the highest Cos2 variables and the Cos2 variables decreased with decrease in the colour intensity of the spots in the visualization. We can see that Dim.1 variables showed the highest colour intensity and this was followed by Dim.2. In Dim.1 (**Figure 4.59 b**), the data visualized explains 72.4 % of the H_2O_2 effect experiment and the five best represented variables were Cu5, Cu15, Pb5, Cu25 and Pb15. In Dim.2 (**Figure 4.59 c**), the visualized data explains 13.9 % of the H_2O_2 effect experiment and the three best represented variables were Zn15, Zn25 and Zn5.

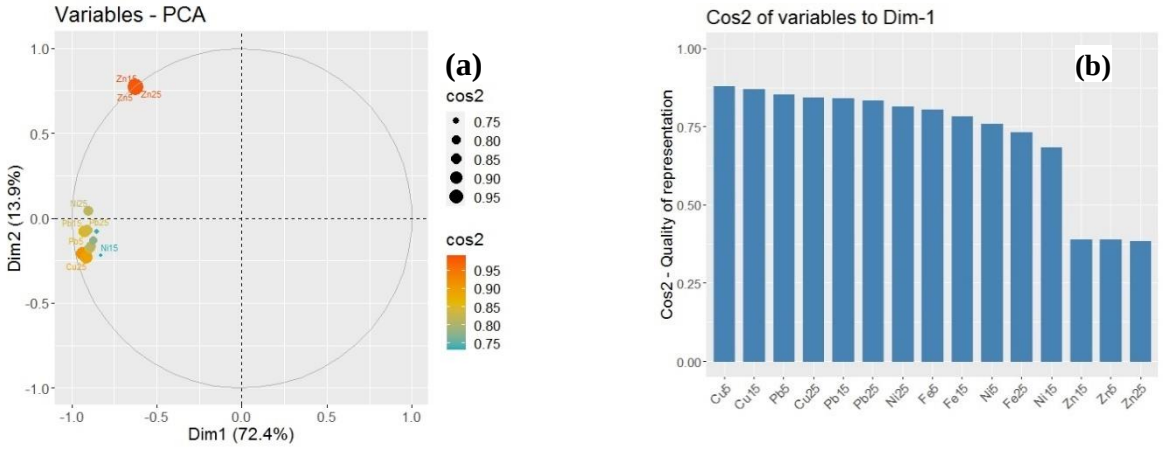

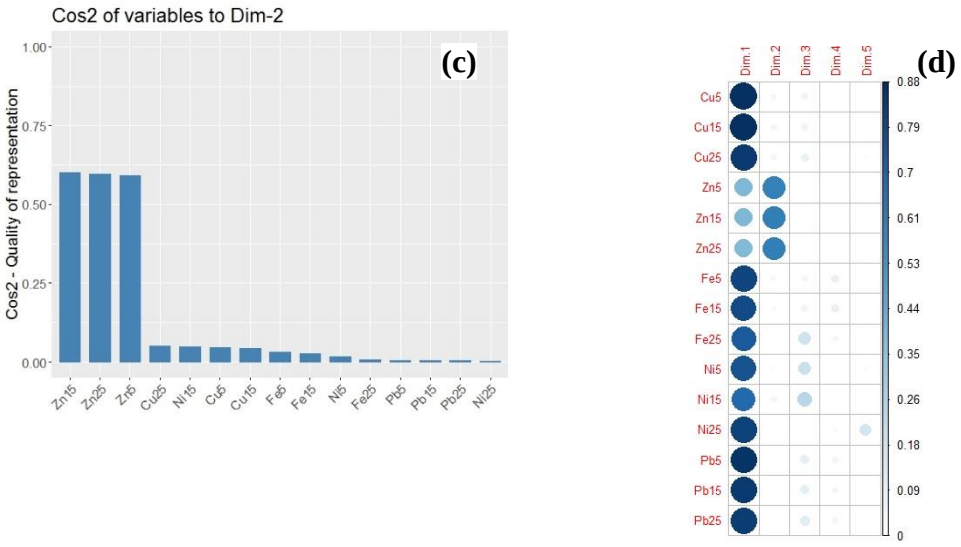

Figure 4.59: (a) Variable Cos2 quality of representation (H_2O_2 effect) (b) Dim.1 quality of representation (H_2O_2 effect) (c) Dim.2 quality of representation (H_2O_2 effect) (d) Cos2 quality of representation plot (H_2O_2 effect)

4.10.4 PCA Result for Variables Contribution in H_2O_2 Effect

Figure 4.60 a shows the contribution of variable correlation plot with the most contributing variables indicated in red and the least contributing variables indicated in blue. From **Figure 4.60 b & c**, we can see the contribution of variables represented in bar plots with red dotted lines which indicates the expected average contribution. Dim.1 and Dim.2 are the most important to be considered in explaining the contribution while Dim.3, 4 & 5 are less important. In Dim.1 (**Figure 60 b**), most contribution of variables values were slightly above the expected average contribution. **Table 4.38** shows the actual values for contribution of variables and **Figure 4.60 d** shows the contribution of variables plot with spots of different colour intensity. The darker colours indicate higher contribution while the lighter color indicate low contribution. The contribution of variables for a particular dimension are measured in percentages. Correlated variables in the contribution of variables for Dim.1 & Dim.2 explains 72.4 % and 13.9 % respectively. Contributions from Dim.1 are the most important as they contribute more than other variables and this is followed by Dim.\2. Even though the contributions from other dimensions are high (Dim.3, Dim.4 & Dim.5), they would not be considered since they are not as important as contributions from Dim.1 & 2. The order of importance in the contribution for the dimensions are Dim.1 > Dim.2 > Dim.3 > Dim.4 > Dim.5. A variable with large contribution value contributes more to the component. Dim.1 which explains 72.4 % of the variation is represented in **Figure 4.60 b.** We can see the

bar chart for Dim.1 contributions arranged in descending order and the five best contributing variables were Cu5 (8.09%) > Cu15 (8.02%) > Pb5 (7.85%) > Cu25 (7.76%) > Pb15 (7.75%) . Dim.2 which explains 13.9 % of the variation is represented in **Figure 4.60 c.** We can see the bar chart for Dim.2 contributions also arranged in descending order and the best three contributing variables were Zn15 (28.88 %), Zn25 (28.75 %) and Zn5 (28.42 %). The best contributing variables for H_2O_2 effect from highest to lowest are in the order Cu5 > Cu15 > Pb5 > Cu25 > Pb15 > Zn15 > Zn25 > Zn5.

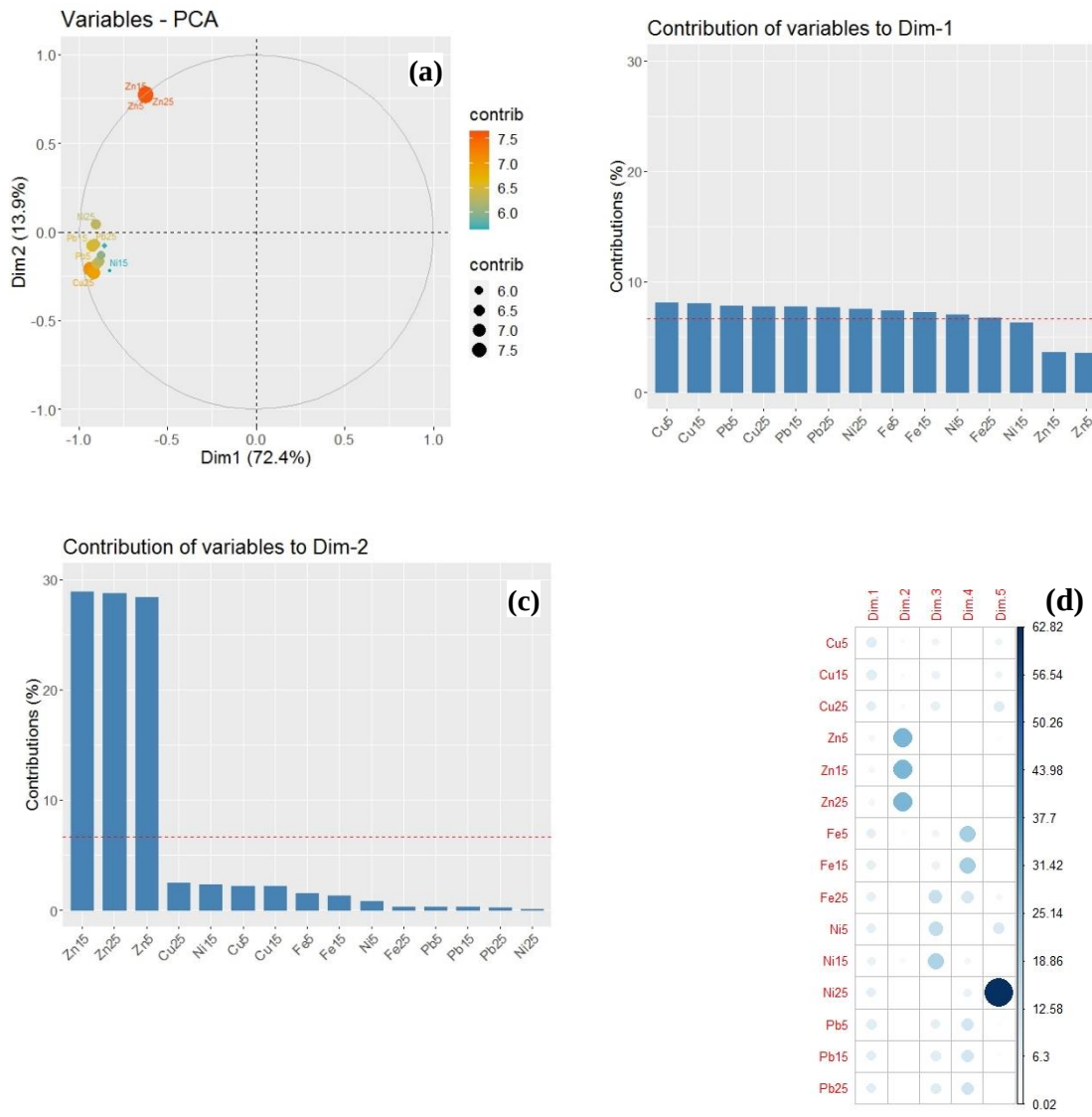

Figure 4.60: (a) Contribution of Variable Correlation Plot (H_2O_2 effect) (b) Dim.1 Contribution of Variable Bar Plots (H_2O_2 effect) (c) Dim.2 Contribution of Variable Bar Plots (H_2O_2 effect) (d) Variable Contribution Plot (H_2O_2 effect)

Table 4.38 Best Contributing Variables for H_2O_2 Effect (in bold)

	Dim 1 (%)	Dim 2 (%)
Cu 5	**8.09**	2.15
Cu 15	**8.02**	2.14
Cu 25	**7.76**	2.49
Zn 5	3.59	**28.42**
Zn 15	3.59	**28.88**
Zn 25	3.54	**28.75**
Fe 5	**7.41**	1.53
Fe 15	**7.21**	1.31
Fe 25	**6.73**	0.30
Ni 5	**6.99**	0.82
Ni 15	**6.29**	2.31
Ni 25	**7.51**	0.08
Pb 5	**7.85**	0.29
Pb 15	**7.75**	0.27
Pb 25	**7.68**	0.25

4.10.5 PCA Result for Observation Coordinates in H_2O_2 Effect

Figure 4.61 a shows the plot for the observation coordinates which are representing the position of the solvents used in H_2O_2 effect experiment for both the hotplate and microwave methods. **Figure 4.61 b - e** shows the three-dimensional plots of inorganic acids, organic acids, ionic liquid (a - c) and ionic liquid (d - g). Dim.1 on the x-axis, Dim.2 on the z-axis and Dim.3 on the y-axis. These three dimensional plots shows the coordinates or positioning of the solvents used for the H_2O_2 effect experiment. **Figure 4.62 a – d** shows the observation coordinate visualization plot for inorganic acids, organic acids, ionic liquid (a - c) and ionic liquid (d - g). In Dim.1, the observation coordinates for the inorganic acids showed very good negative correlation except NA4-6, HA4 – 6, SA1 – 6 which had correlation < 0.15. AQ1-3 (*aqua-regia* – hotplate method) had the strongest correlation values followed by NA1-3 (nitric acid – hotplate method), HA1 - 3 (hydrochloric acid – hotplate method), AQ4-6 (*aqua-regia* – microwave method). The strength of correlation can be seen on Dim.1 in **Figure 4.62** as very dark red colours. Dim.2 also had good correlation values (CA, MA, TA, ILs 1-3,).

The organic acid all showed strong correlation and the strength of correlation can be seen on Dim.1 in **Figure 4.62 b.**

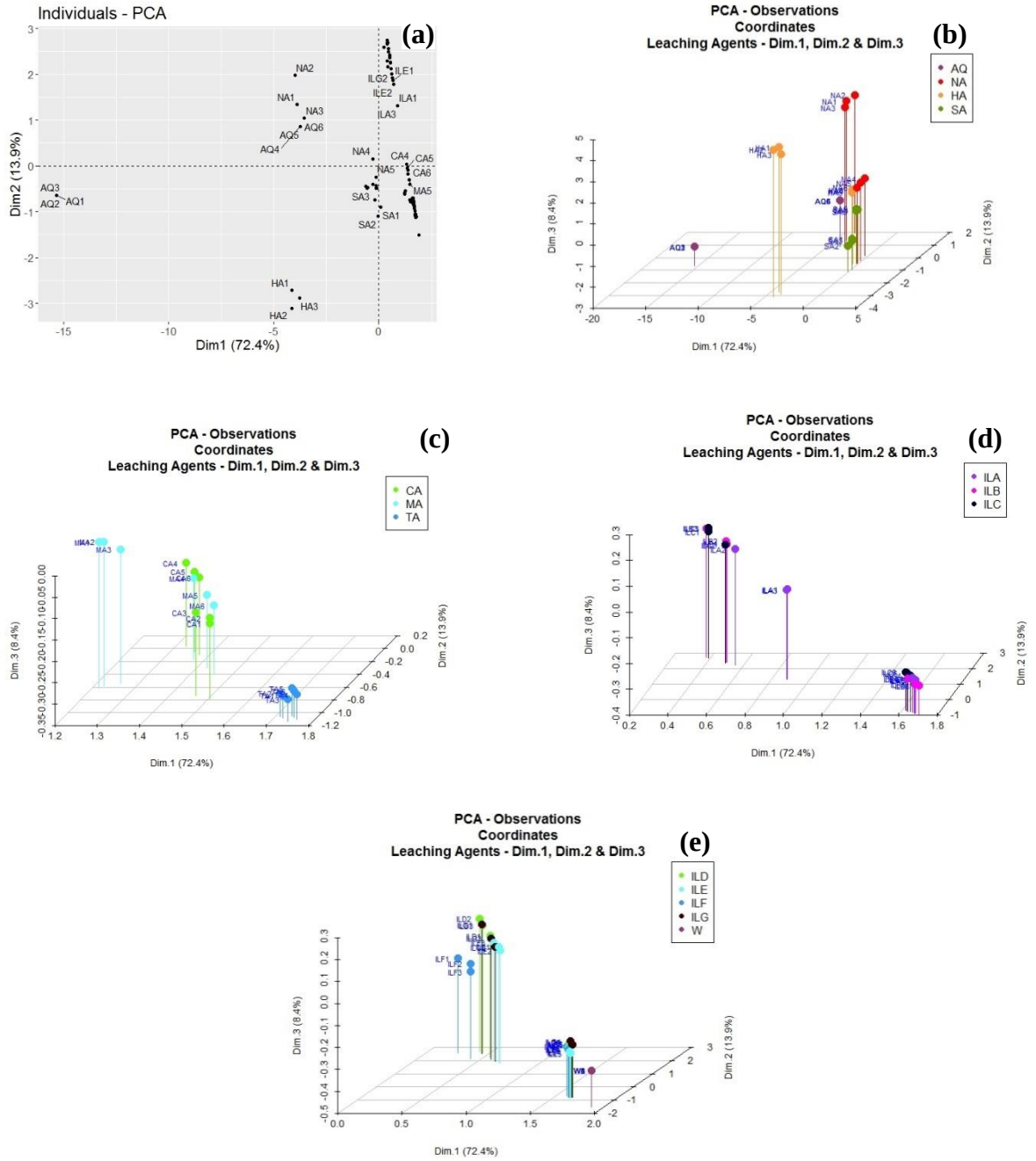

Figure 4.61: (a) observation coordinate correlation plot (H_2O_2 effect) (b) observation coordinate for inorganic acids (H_2O_2 effect) (c) observation coordinate for organic acids (H_2O_2 effect) (d) observation coordinate for IL a-c (H_2O_2 effect) (e) observation coordinate for IL d-g (H_2O_2 effect)

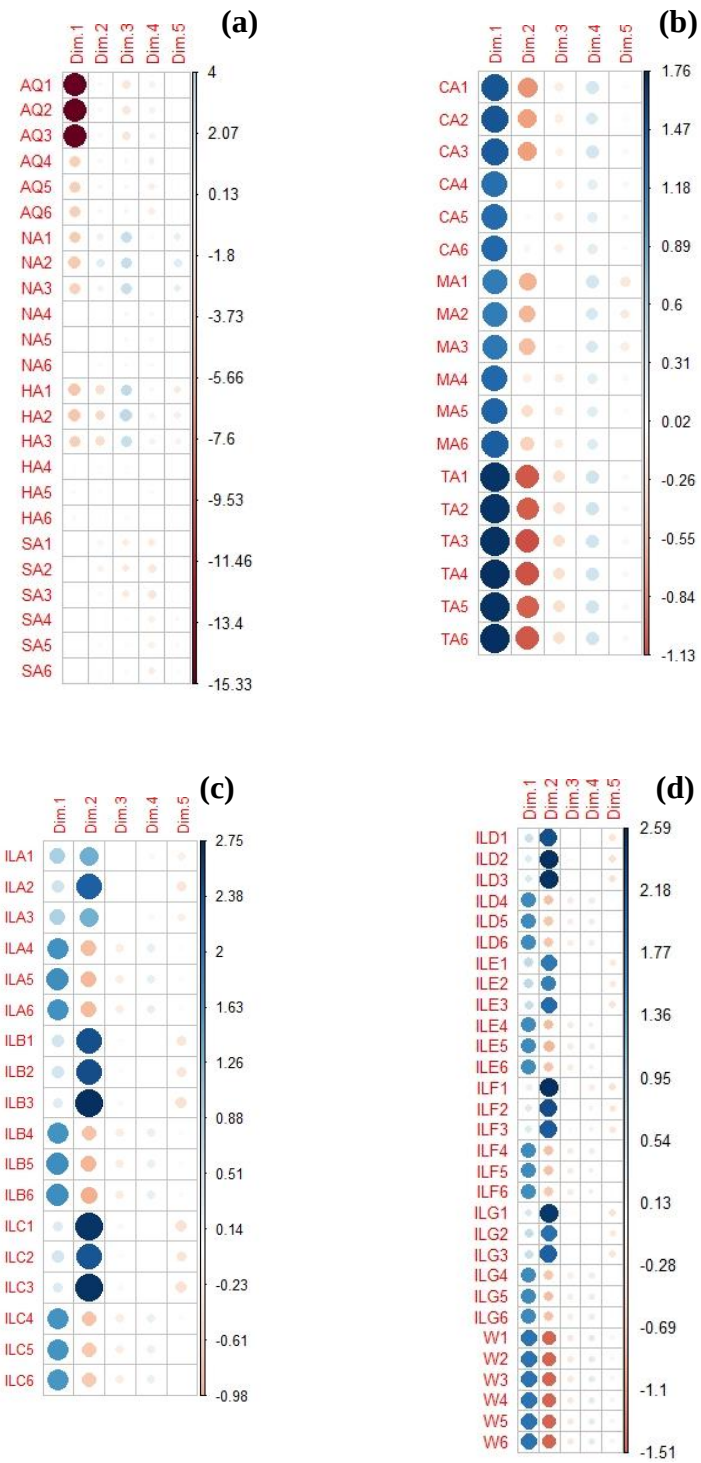

Figure 4.62: (a) Observation coordinate plot for inorganic acids (H_2O_2 effect) (b) observation coordinate plot for organic acids (H_2O_2 effect) (c) observation coordinate plot for IL a – c (H_2O_2 effect) (d) observation coordinate plot for IL d - g (H_2O_2 effect)

4.10.6 PCA Result for Observation Cos2 Quality of Representation in H_2O_2 Effect

Figure 4.63 a shows the Cos2 plot of observation with the highest Cos2 value which are in orange while the mid cos2 observation value are in blue. The observations in orange are the most represented in the plot as they have very high values and this is followed by the yellow and then the blue spots. **Figure 4.63 b - e** shows the three-dimensional plots Cos2 observation for inorganic acids, organic acids, ionic liquid (a - c) and ionic liquid (d - g). Dim.1 on the x-axis, Dim.2 on the z-axis and Dim.3 on the y-axis. These three dimensional plots shows the coordinates or positioning of the solvents used for the H_2O_2 effect experiment. Consequently, all negative values have been cancelled out and **Figure 4.64 a -d** shows the Cos2 observations visualization with spots of different colour intensity. The strongest or darkest colour represent the highest Cos2 observations and the Cos2 observations decreased with decrease in the colour intensity of the spots in the visualization. The quality of representation in Dim.1 showed good quality of representation. AQ1-6 had good quality of representation followed by NA1-3, HA1-3, CA4-6, MA4-6, TA4-6, ILs A-G (4-6). The poorest quality of representation were found in NA1-3, HA1-3, SA1-6. In Dim.2, only strong quality of representation were found in ILs A-G (1, 2 & 3).

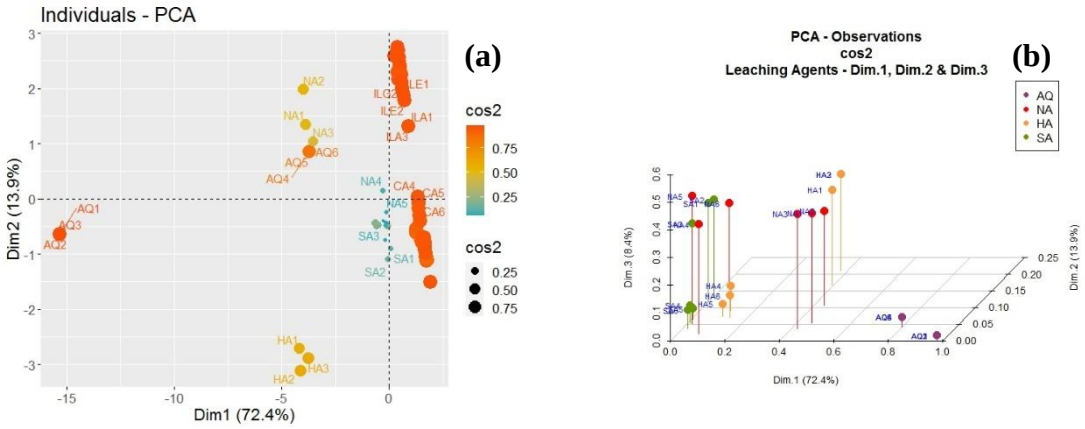

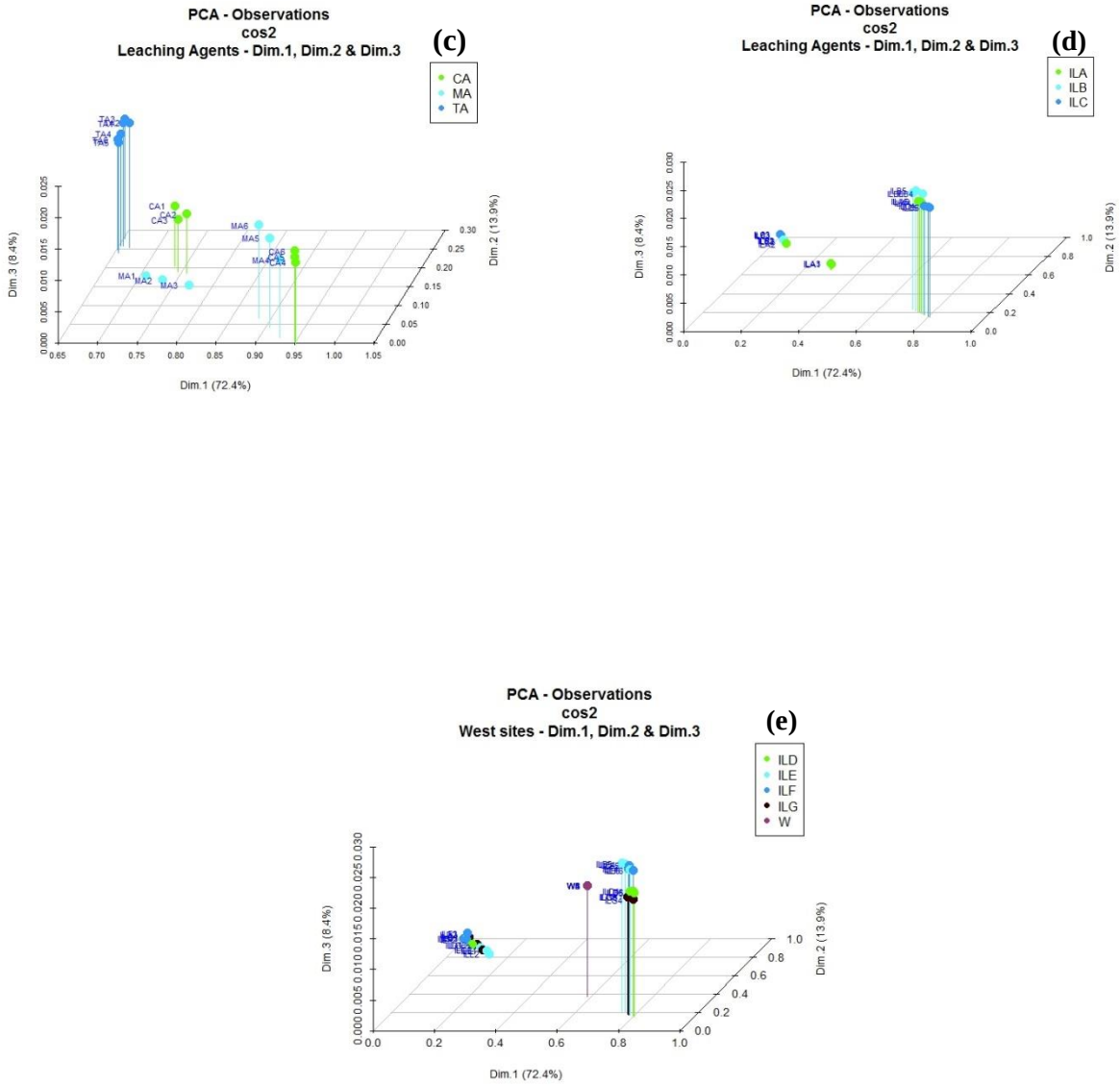

Figure 4.63: (a) Observation cos2 correlation plot (H_2O_2 effect) (b) Observation cos2 for inorganic acids (H_2O_2 effect)

(c) Observation cos2 for organic acids (H_2O_2 effect) (d) Observation cos2 for IL a-c (H_2O_2 effect)

(e) Observation cos2 for IL d-g (H_2O_2 effect)

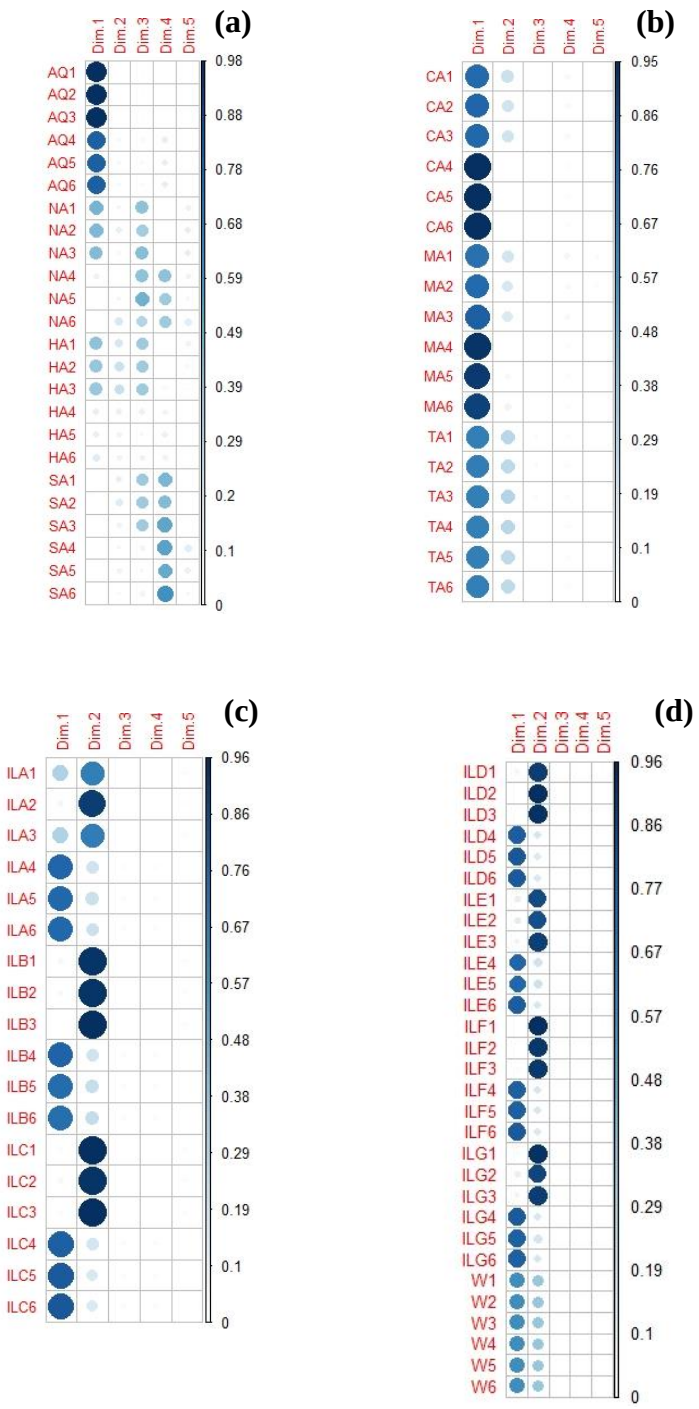

Figure 4.64: (a) Observation cos2 Dim plot for inorganic acids (H_2O_2 effect) (b) observation cos2 Dim plot for organic acids (H_2O_2 effect) (c) observation cos2 Dim plot for IL a – c (H_2O_2 effect) (d) observation cos2 Dim plot for IL d - g (H_2O_2 effect)

4.10.7 PCA Result for Observation Contribution in H_2O_2 Effect

Figure 4.65 a shows the contribution plot of observation with the highest contribution values which are in orange while the mid contribution value are in blue. The observations in orange are the most represented in the plot as they have very high values and this is followed by the yellow and then the blue spots. **Figure 4.65 b - e** shows the three-dimensional plots of observation contribution for inorganic acids, organic acids, ionic liquid (a - c) and ionic liquid (d - g). Dim.1 on the x-axis, Dim.2 on the z-axis and Dim.3 on the y-axis. These three dimensional plots shows the positioning of the solvents contribution on the plot. **Table 4.39** shows the observation contribution values in percentages. **Figure 4.66 a -d** shows the observation contribution visualization with spots of different colour intensity. The strongest or darkest colour represent the highest observation contribution and the observation contribution decreased with decrease in the colour intensity of the spots in the visualization. The observation contribution in Dim.1 (inorganic acids), shows observation contribution and the best five solvents that contributed to this Dim.1 were AQ1(26.1 %), AQ4(1.4 %), HA1(1.8 %), HA2(1.8 %) and NA2(1.6 %). In Dim.2 (inorganic acids), the best three observation contributions were HA2(5.2 %), HA3(4.4 %), HA1(4.0 %). The best observation contribution with strong colour intensity can be seen in Dim.1 (**Figure 4.66 a**). The best contributing solvents from highest to lowest are in the order AQ1 > AQ4 > HA1 > HA2 > NA2 > HA2 > HA3 > HA1. The observation contributions with strong colour intensity can be seen in Dim.1 & 2 (**Figure 4.66 b**).

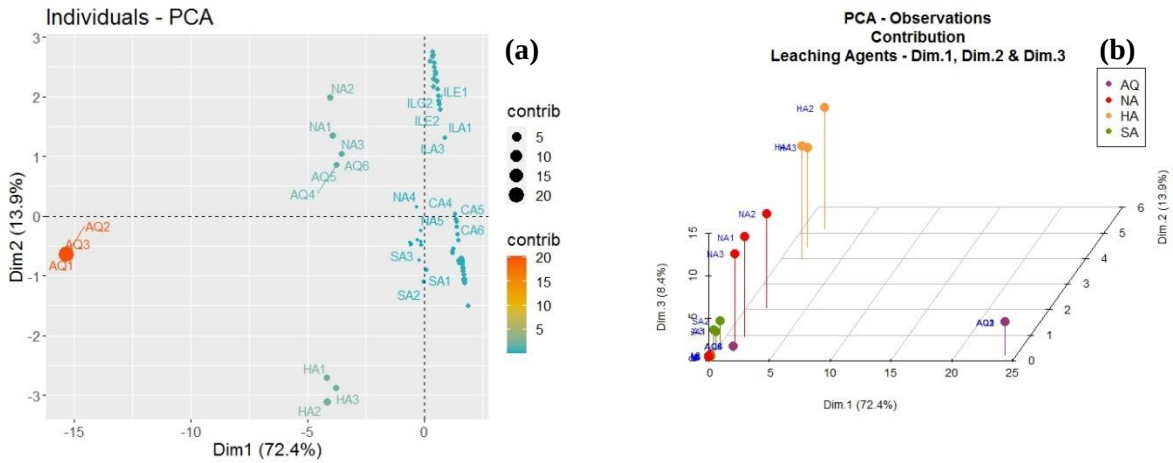

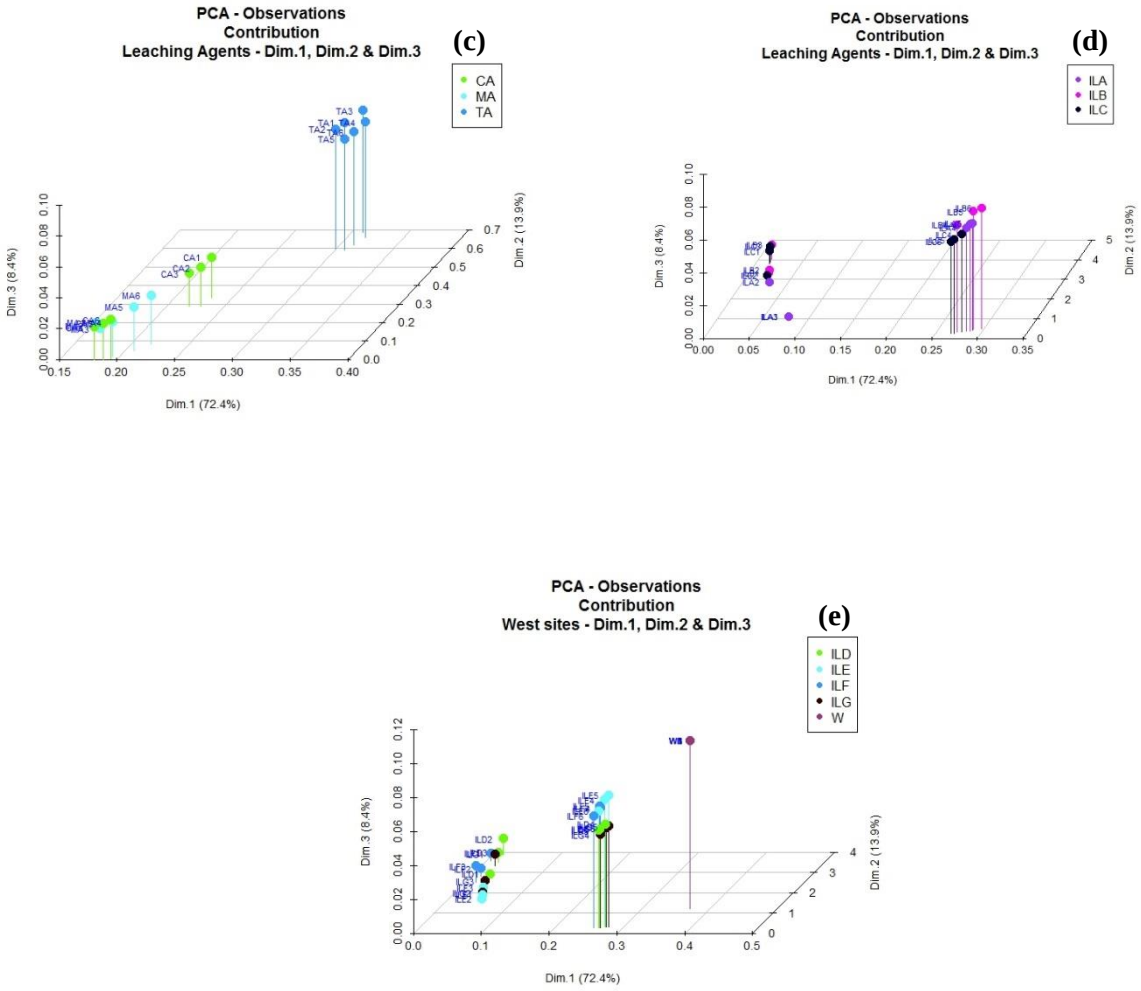

Figure 4.65: (a) Observation contribution plot (H_2O_2 effect) (b) Observation contribution for inorganic acids (H_2O_2 effect) (c) Observation contribution for organic acids (H_2O_2 effect) (d) Observation contribution for IL a-c (H_2O_2 effect) (e) Observation contribution for IL d-g (H_2O_2 effect)

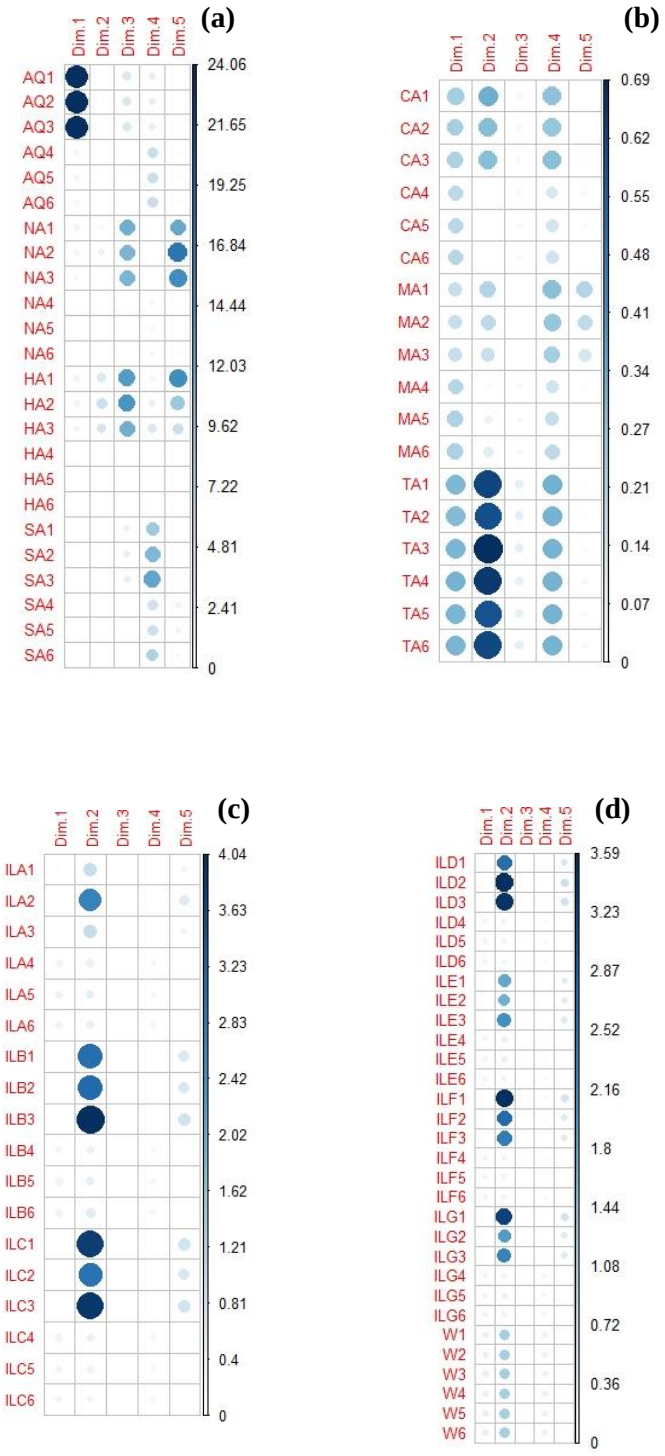

Figure 4.66: (a) Observation contribution Dim plot for inorganic acids (H_2O_2 effect) (b) observation contribution Dim plot for organic acids (H_2O_2 effect) (c) observation contribution Dim plot for IL a – c (H_2O_2 effect) (d) observation contribution Dim plot for IL d - g (H_2O_2 effect)

Table 4.39 Best Contributing Observations for H_2O_2 Effect

	Dim 1 (%)	Dim 2 (%)
AQ1	**24.06**	0.22
AQ4	**1.44**	0.39
NA1	**1.55**	0.97
NA2	**1.64**	**2.09**
NA3	**1.28**	0.57
HA1	**1.76**	**3.96**
HA2	**1.76**	**5.19**
HA3	0.03	0.12

4.11 Determination of Temperature Effect

Two methods, hotplate and microwave methods, were used to determine the effect of temperature (25, 40 and 70 ^{0}C) on the extraction of Cu, Zn, Fe, Ni and Pb. For the hotplate method, the experimental conditions were particle-size (4 mm), time (120 minutes), concentration (2 M for inorganic acids, 25 g/L for organic acids and 100 g/L for ionic liquids), sample weight (0.5 g) and rotation speed (340 rpm). **Appendices 4 a - e** shows tables of the mean concentrations of temperature effect for Cu, Zn, Fe, Ni and Pb (mg/g) with results from three different experiments and the standard deviation as the error bar.

4.11.1 Effect of temperature on Leaching Cu

Table 4.40 shows the percentage extraction of Cu and this is also represented in **Figure 4.67.** From **Figure 4.67** the temperature increased from 25 – 70 ^{0}C the Cu extraction also increased. The peak extractions were HA (58 % at 70 ^{0}C), NA (68 % at 70 ^{0}C), IL-G (33 % at 40 ^{0}C & 70 ^{0}C), SA (3 % at 70 ^{0}C) IL-E (3 % at 70 ^{0}C) and CA (1 % at 70 ^{0}C).

4.11.2 Effect of temperature on Leaching Zn

Table 4.41 shows the percentage extraction of Zn and this is also represented in **Figure 4.68.** From **Figure 4.68** the temperature increased from 25 – 70 ^{0}C the Zn extractions in the inorganic acids decreased while the organic acids increased. The peak extractions were NA (89 % at 25 ^{0}C), HA (86 % at 25 ^{0}C), SA (78 % at 25 ^{0}C), CA (48 % at 70 ^{0}C), TA (41 % at 70 ^{0}C), MA (26 % at 70 ^{0}C), ILs D, E, F & G were in the range of 8 – 10 % at 40 ^{0}C. ILs A, B & C extractions were < 1 %.

Table 4.40 Percentage concentration values for effect of temperature on leaching Cu

	Temperature (^{0}C)	Extraction (%)														
		AQ	NA	HA	SA	CA	MA	TA	IL-A	IL-B	IL-C	IL-D	IL-E	IL-F	IL-G	W
Hotplate Method	25.00	100.00	28.05	18.82	0.60	0.40	0.17	0.31	0.02	0.01	0.01	0.05	2.01	0.09	8.36	0.00
	40.00	100.00	52.38	34.13	1.52	0.40	0.16	0.36	0.06	0.01	0.01	0.14	2.63	0.34	33.14	0.00
	70.00	100.00	68.13	57.69	3.21	1.27	0.39	0.79	0.13	0.03	0.01	0.13	3.03	0.33	32.64	0.00

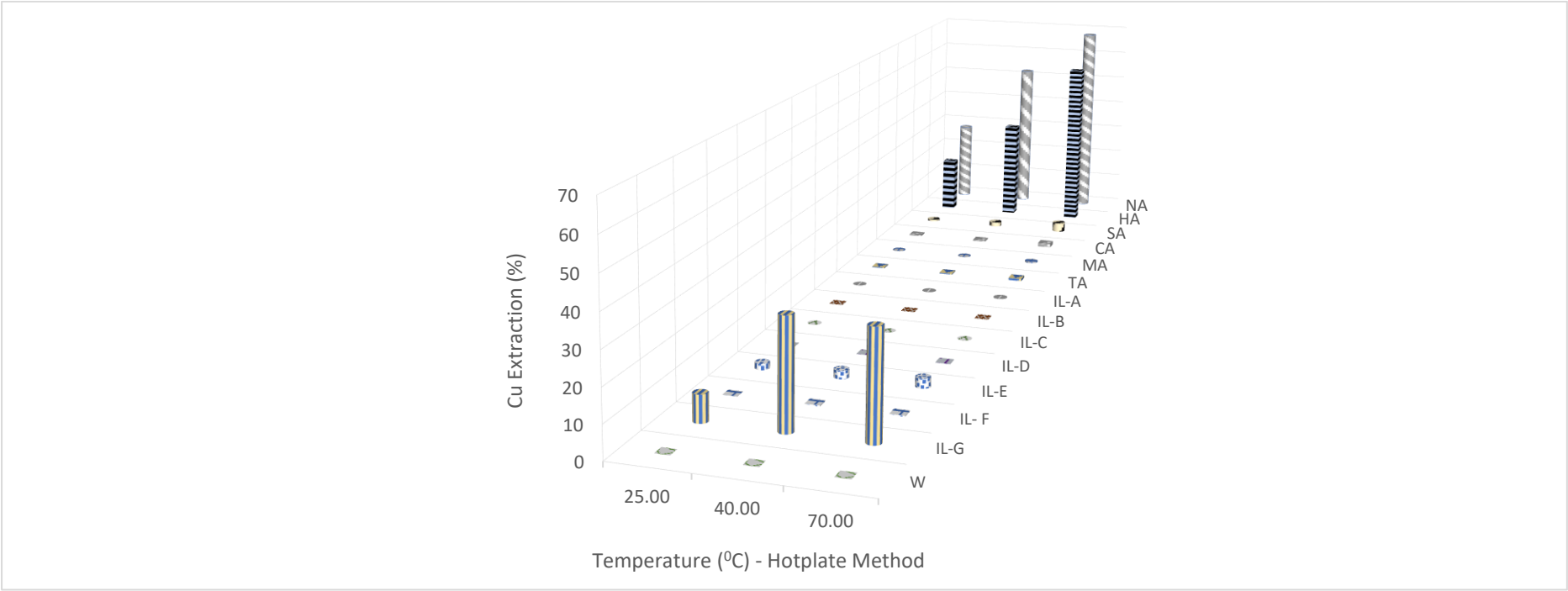

Figure 4.67 Percentage concentration for the effect of temperature on leaching Cu

Table 4.41 Percentage concentration values for effect of temperature on leaching Zn

	Temperature (^{0}C)	Extraction (%)														
		AQ	NA	HA	SA	CA	MA	TA	IL-A	IL-B	IL-C	IL-D	IL-E	IL-F	IL-G	W
Hotplate Method	25.00	100.00	88.89	85.60	78.35	27.06	7.21	13.93	0.41	0.36	0.33	0.81	0.40	0.04	0.30	0.21
	40.00	100.00	76.34	77.30	72.15	33.25	13.68	13.51	0.03	0.03	0.12	9.58	9.81	8.31	8.66	0.05
	70.00	100.00	55.45	55.87	58.84	48.25	26.24	41.14	0.10	0.06	0.08	8.04	8.80	7.79	6.94	0.01

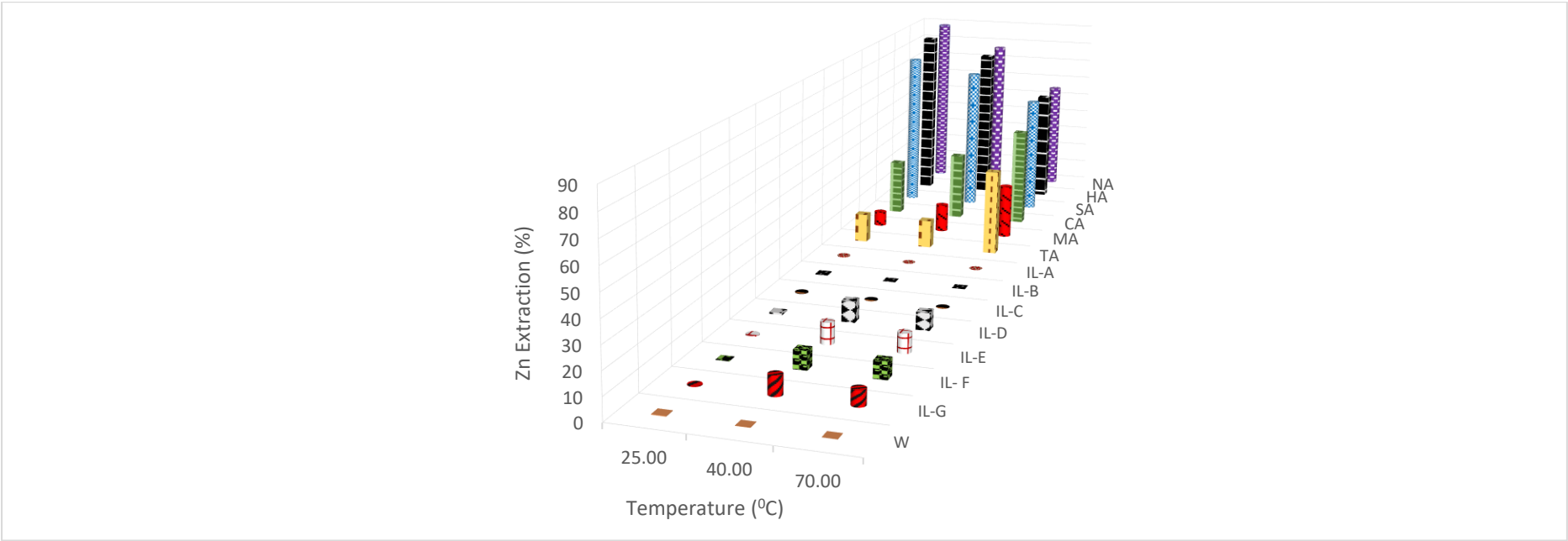

Figure 4.68 Percentage concentration for the effect of temperature on leaching Zn

4.11.3 Effect of temperature on Leaching Fe

Table 4.42 shows the percentage extraction of Fe and this is also represented in **Figure 4.69.** From **Figure 4.69** the temperature increased from 25 – 70 ^{0}C the Fe extractions also increased for the inorganic acids. The peak extractions were NA (36 % at 70^{0}C), HA (50 % at 70 ^{0}C), SA (28 % at 70 ^{0}C). There were no significant extractions for the organic acids and ILs A - G.

4.11.4 Effect of temperature on Leaching Ni

Table 4.43 shows the percentage extraction of Ni and this is also represented in **Figure 4.70.** From **Figure 4.70** the temperature increased from 25 – 70 ^{0}C the Ni extraction also increased. The solvents peak extractions were NA (5 % at 70 ^{0}C), HA (4 % at 70 ^{0}C), SA (3 % at 70 ^{0}C), CA (1 % at 70 ^{0}C), TA (3 % at 70 ^{0}C). ILs A - G did not show any significant extractions.

4.11.5 Effect of temperature on Leaching Pb

Table 4.44 shows the percentage extraction of Pb and this is also represented in **Figure 4.71.** From **Figure 4.71** the temperature increased from 25 – 70 ^{0}C the Pb extraction also increased. The solvents peak extractions were NA (54 % at 70 ^{0}C), HA (52 % at 70 ^{0}C), CA (4 % at 25 ^{0}C), MA (6 % at 40 ^{0}C), TA (9 % at 25 ^{0}C) and IL-D (3 % at 25 ^{0}C), ILs A, B, C, E, F & G did not show any significant extractions.

Table 4.42 Percentage concentration values for effect of temperature on leaching Fe

	Temperature (^{0}C)	Extraction (%)														
		AQ	NA	HA	SA	CA	MA	TA	IL-A	IL-B	IL-C	IL-D	IL-E	IL-F	IL-G	W
Hotplate Method	25.00	100.00	1.59	2.16	1.88	0.83	1.05	0.75	0.00	0.00	0.00	0.00	0.00	0.00	0.00	0.00
	40.00	100.00	2.29	4.25	3.14	0.61	0.77	0.60	0.00	0.00	0.00	0.00	0.00	0.00	0.00	0.00
	70.00	100.00	36.06	50.11	28.08	0.43	0.60	0.47	0.00	0.00	0.00	0.00	0.00	0.00	0.00	0.00

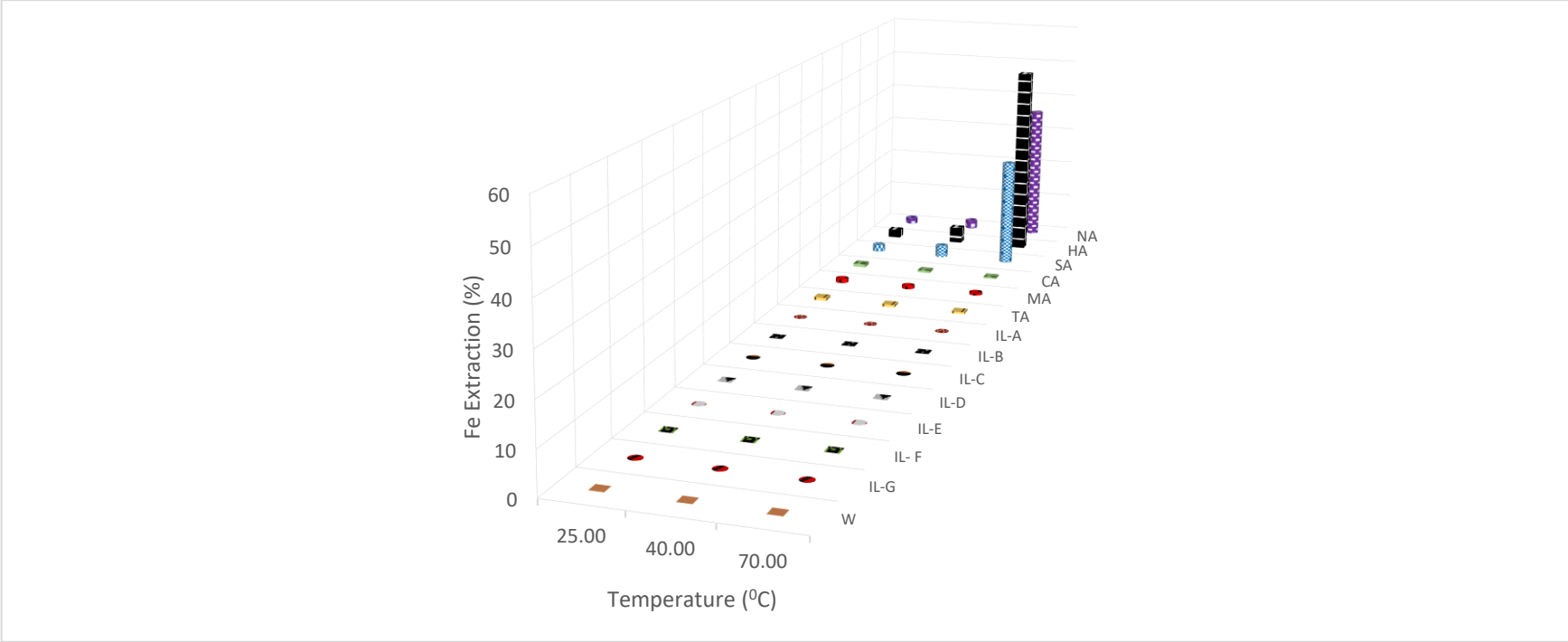

Figure 4.69 Percentage concentration for the effect of temperature on leaching Fe

Table 4.43 Percentage concentration values for effect of temperature on leaching Ni

	Temperature (^{0}C)	Extraction (%)														
		AQ	NA	HA	SA	CA	MA	TA	IL-A	IL-B	IL-C	IL-D	IL-E	IL-F	IL-G	W
Hotplate Method	25.00	100.00	2.73	2.50	1.08	0.03	0.03	0.03	0.01	0.01	0.01	0.01	0.01	0.01	0.01	0.01
	40.00	100.00	3.54	2.50	1.39	0.02	0.02	0.02	0.01	0.01	0.01	0.01	0.01	0.01	0.01	0.01
	70.00	100.00	4.66	3.55	3.19	2.21	1.13	3.31	0.01	0.01	0.01	0.01	0.01	0.01	0.01	0.01

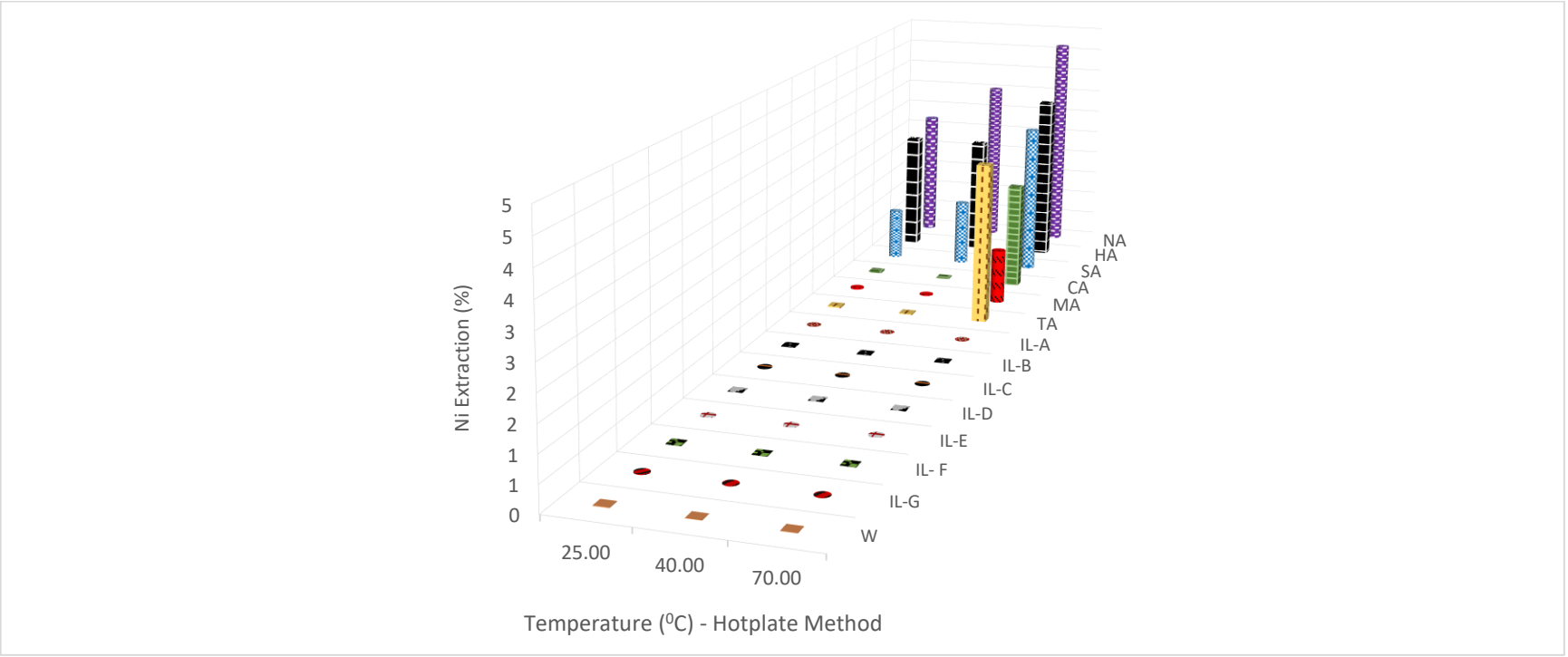

Figure 4.70 Percentage concentration for the effect of temperature on leaching Ni

Table 4.44 Percentage concentration values for effect of temperature on leaching Pb

	Temperature (^{0}C)	Extraction (%)														
		AQ	NA	HA	SA	CA	MA	TA	IL-A	IL-B	IL-C	IL-D	IL-E	IL-F	IL-G	W
Hotplate Method	25.00	100.00	42.86	27.43	0.81	3.71	3.71	9.14	0.23	0.23	0.23	3.43	0.26	0.24	1.18	0.09
	40.00	100.00	43.98	39.47	0.86	3.16	5.86	3.50	0.17	0.17	0.17	3.01	0.23	0.18	1.02	0.07
	70.00	100.00	53.57	52.02	0.78	3.67	4.59	1.91	0.12	0.11	0.11	2.04	0.15	0.12	0.69	0.05

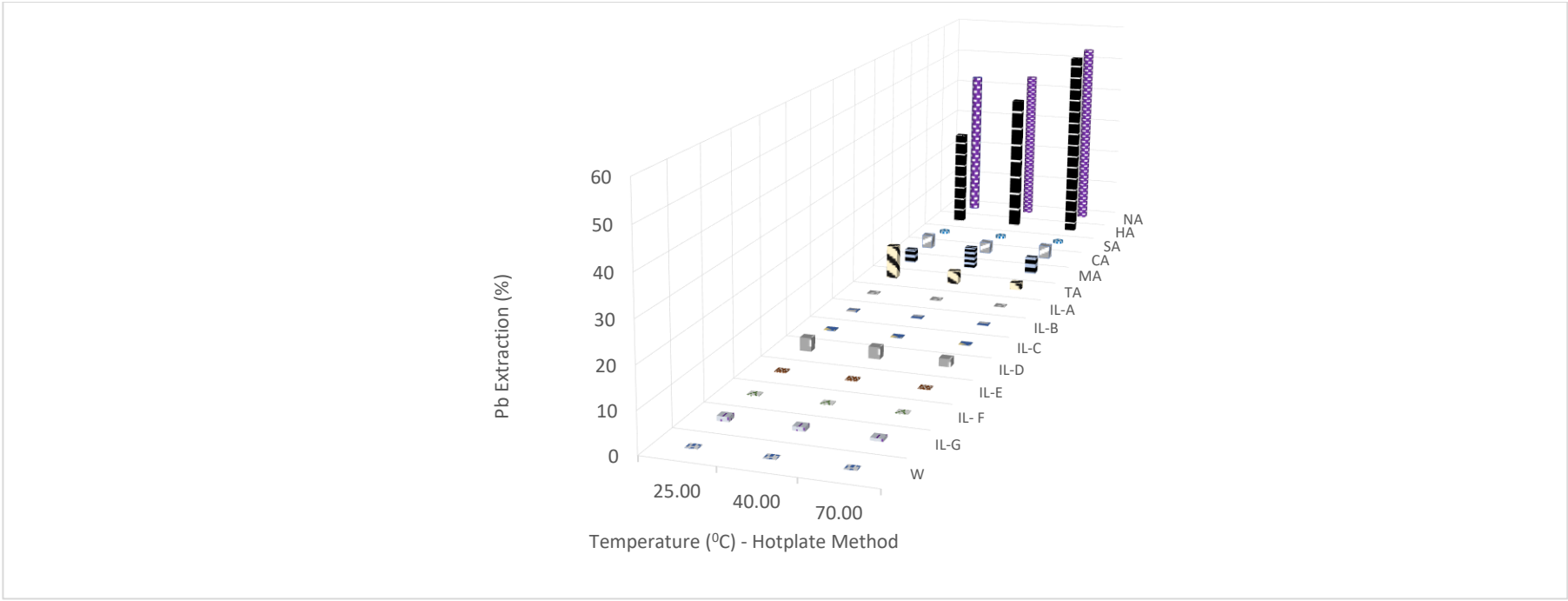

Figure 4.71 Percentage concentration for the effect of temperature on leaching Pb

4.12 PCA for Temperature Effect

4.12.1 PCA Scree Plot for Temperature Effect

The temperature effect experiment involved 15 variables and 45 observations. The variables were made up of five metals (Cu, Zn, Fe, Ni and Pb) with each of these metals having results from three expriments on effect of temperature (25, 40 and 70 ^{0}C). The observations were results from each of the fifteen solvents with three replicates each from the hotplate and microwave methods used in the experiment. **Table 4.45** shows the summarized data of the first six principal components extracted from only the hotplate method (mg/g) in **Appendices 4 a – e**. **Figure 4.72** shows the scree plot of variance for the dimensions from temperature effect data and they are in the order of highest to the lowest with Dim.1 as 83.8 %, Dim.2 as 10.6 % and Dim.3 as 3.3 %. From this scree plot we can infer that Dim.1 explains the most part of the temperature effect data as it is larger than the other dimensions. From **Table 4.43,** we can see that Dim.1 & 2 showed a SD > 1.0 as SD = 1 is the cutoff point. Therefore, we can accept the first two dimensions (Dim.1 & 2) with a proportion of variance of 83.8 & 10.6 % respectively. Consequently, the cumulative proportion in Dim.1 & 2 also showed 83.8 & 94.4 % respectively. This shows that with Dim.2 having a SD of 1.3, about 94.4 % of the data can be accounted for while the remaining 5.6 % of the data can be disregarded as they fall below SD < 1.0.

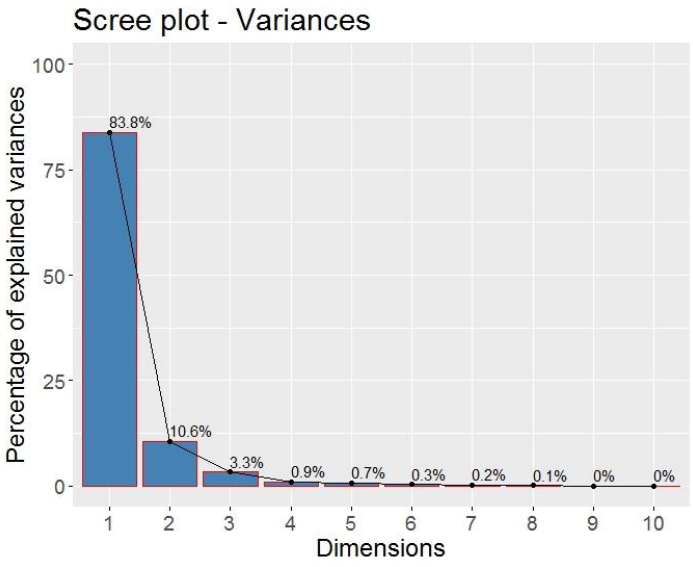

Figure 4.72 Scree plot for temperature effect

Table 4.45 Summarized principal components temperature effect

Principal Components	Dim.1	Dim.2	Dim.3	Dim.4	Dim.5	Dim.6
Standard deviation	3.545	1.263	0.702	0.374	0.328	0.222
Proportion of Variance	0.838	0.106	0.033	0.009	0.007	0.003
Cumulative Proportion	0.838	0.944	0.977	0.986	0.993	0.997

Figure 4.73 shows the biplot for temperature effect data which is the relationship between the variables and the observations in the temperature data. It also shows the structure of variables correlations and clustered observations. From the PCA plot, we can see the variables with the longest vector projections. They represent the highest variations in the data and they have occured in Ni25, Ni40, Ni70, Z25, Zn40 and Fe70. The replicate observations formed clusters, for example, in the hotplate method (1, 2 & 3) the observations AQ1, AQ2 & AQ3 which represents the hotplate result for *aqua-regia* formed a cluster which means that the three replicated experiments showed similarity in the result from temperature effect. Also, this behaviour was observed in other observation showing that the replicated results were similar. The *aqua-regia* observations AQ1-3 are considered outliers on the PCA as the cluster was clearly outside the group clustering and also far away from the other observations. However, they were not treated as outliers or removed as they were needed in this research inorder to clearly differentiate the best performing solvents or observations. Other observation clusters were seen in (NA1, NA2 & NA3), (HA1, HA2 & HA3), SA1, SA2 & SA3) and (CA1, CA2 & CA3). The above stated clusters had various degrees of euclidean distance (distance between observations) and the observations from *aqua-regia* (AQ1-3) was the farthest. Consequently, the organic acids and ionic liquids all seemed to have clustered together as their euclidean distance were relatively close.

We can see that the variables vectors were pointing towards AQ1-3, NA1-3 and HA1-3. This shows a high degree of association between the variables and the observations but the reverse was the case for the other observations such as SA1-3, CA1-3 the other organic acids and ionic liquids as the PCA plot (**Figure 4.73**) clearly shows the variable vectors pointing away from them and this implies very low association between the variables and these observations. Also, all the variables were pointing towards the hotplate method (red) showing high variable association with the hotplate method. The variable vectors closest to each other

showed high correlation amongst themselves, for example, Cu40 and Pb25, Zn40 and Fe70, Ni40 and Ni25 formed angles around 30 degrees. No correlation was observed between Zn70 and Ni70 as their vectors formed angle 90 degrees. The x-axis which is Dim.1 (83.8 % of variation explained) shows that all the variable vectors are positioned on the left side of the plot thereby revealing negative correlation for all variables. So we would expect that the lower the values of Dim.1 the higher high values for each of the variables. The y-axis which is Dim.2 (10.6 % of variation explained) shows that half of the variables postioned at the top were positive correlation and the other half at the bottom were negative correlation. (Kohla & Luniak, 2005; Reris & Brooks, 2015; Statisticshowto, 2021; STHDA, 2021; Towardsdatascience, 2021).

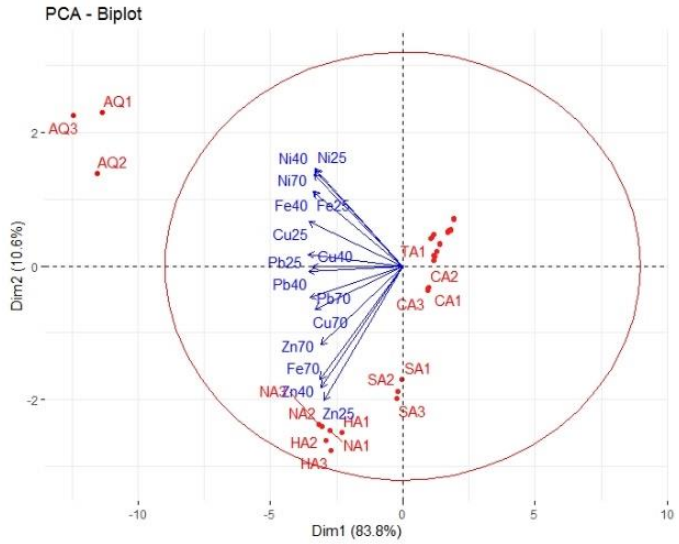

Figure 4.73 Biplot for temperature effect

4.12.2 PCA Result for Variable Coordinates in Temperature Effect

Figure 4.74 a shows the plot for the variable coordinates for Dim.1 & 2 which are representing of the position of the temperature effect variables on the plot. The coordinates are correlation between a variable and a dimension. **Figure 4.74 b** shows a three-dimensional view of variable coordinates for the three dimensions (Dim.1, 2 & 3) with Dim.1 (83.8 %) on the x-axis, Dim.2 (10.6 %) on the z-axis and Dim.3 (3.3 %) on the y-axis. **Figure 4.74 c** shows the variable coordinates visualization with spots of different colour intensity. The strongest or darkest colour represent the highest correlation values and the correlation values decreases with decrease in the colour intensity of the spots in the visualization. Also, the

positive correlated values are in blue while the negative correlated values are in red. Here, Dim.1, 2, 3, 4 & 5 are represented by Dim.1, 2, 3, 4 & 5. The order of importance decreased from Dim.1 to 5. We can see that Dim.1 showed the highest colour intensity and this was followed by Dim.2, 3, 4 & 5. However, all the coordinates in Dim.1 showed strong negative correlation. In Dim.2, moderately positive and negative correlation occurred in Zn25, Zn40 and Fe70. The other variables showed weak positive and negative correlation. Dim.3 showed relatively weak positive and negative correlations.

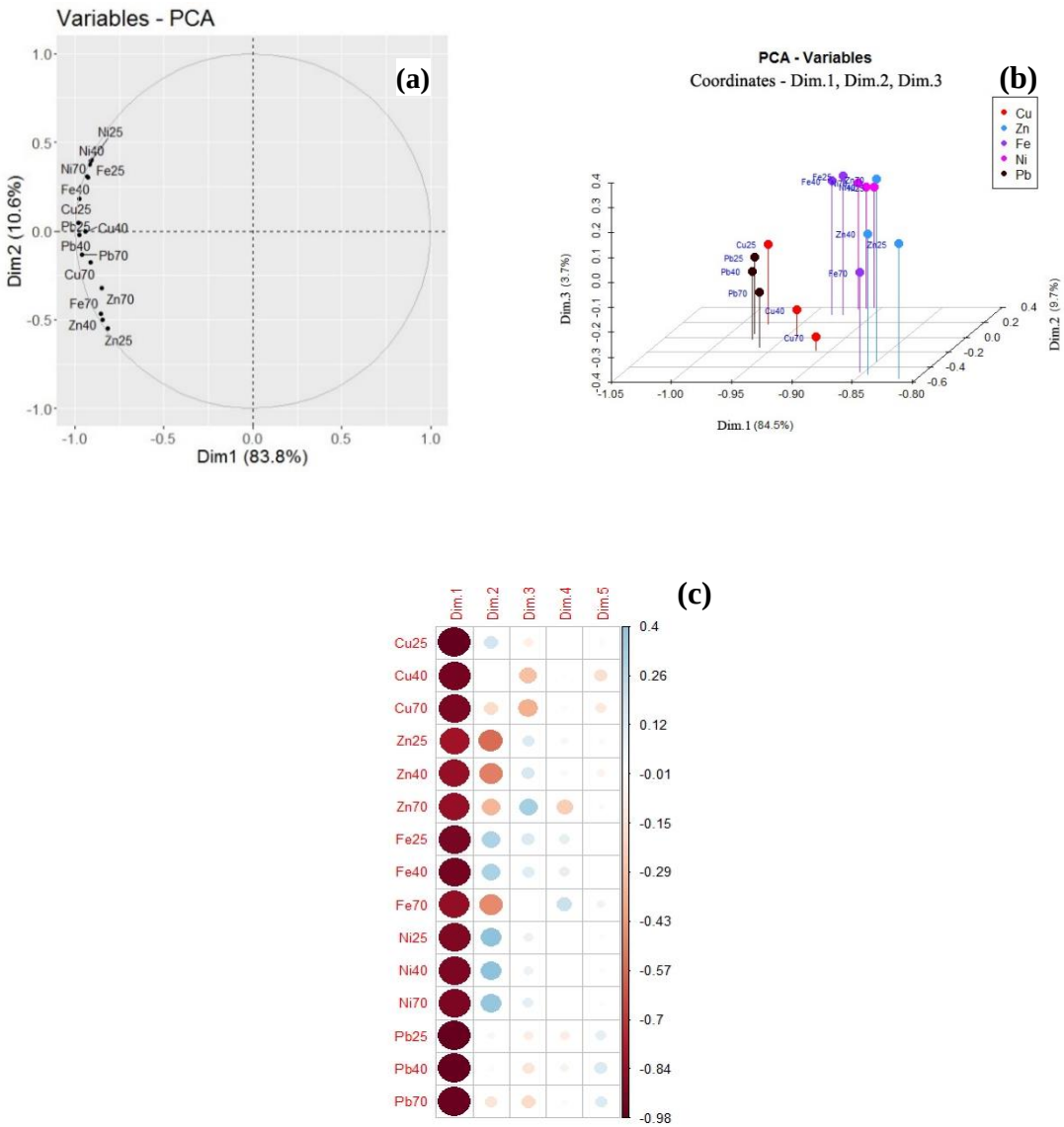

Figure 4.74: (a) Variable Coordinates Correlation Plot (temperature effect) (b) Variable Coordinates 3D Plot (temperature effect) (c) Variable Coordinates Dim Plot (temperature effect)

4.12.3 PCA Result for Variable Cos2 Quality of Representation in Temperature Effect

Figure 4.75 a shows the Cos2 plot of variable with the highest Cos2 value which are in orange while the mid cos2 variables value are in blue. The variables in orange are the most represented in the plot as they are closest to the circle of correlation with very high values and this is followed by the yellow and then the blue spots. All the variables indicated in this Cos2 plot **(Figure 4.75 a)** show very good representation for Dim.1 as all the variables are far from the centre of the circle and none is close to the centre of the circle. **Figure 4.75 b & c** shows another visualization of the Cos2 variables in the form of bar plots. We can see that the Cos2 variables for Dim.1 in **Figure 4.75 b** are the highest which also supports the fact that the quality of representation is good. The variables in the bar plots are arranged from highest to lowest. Consequently, all negative values have been cancelled out and **Figure 4.75 d** shows the Cos2 variables visualization with spots of different colour intensity. The strongest or darkest colour represent the highest Cos2 variables and the Cos2 variables decreased with decrease in the colour intensity of the spots in the visualization. We can see that Dim.1 variables showed the highest colour intensity and this was followed by Dim.2. In Dim.1 (**Figure 4.75 b**), the data visualized explains 83.8 % of the temperature effect experiment and the best five correlated variables were Pb25, Cu25, Pb40, Pb70 and Cu40. In Dim.2 (**Figure 4.75 c**), the visualized data explains 10.6 % of the temperature effect experiment and the best three represented variables were Zn25, Zn40 and Fe70.

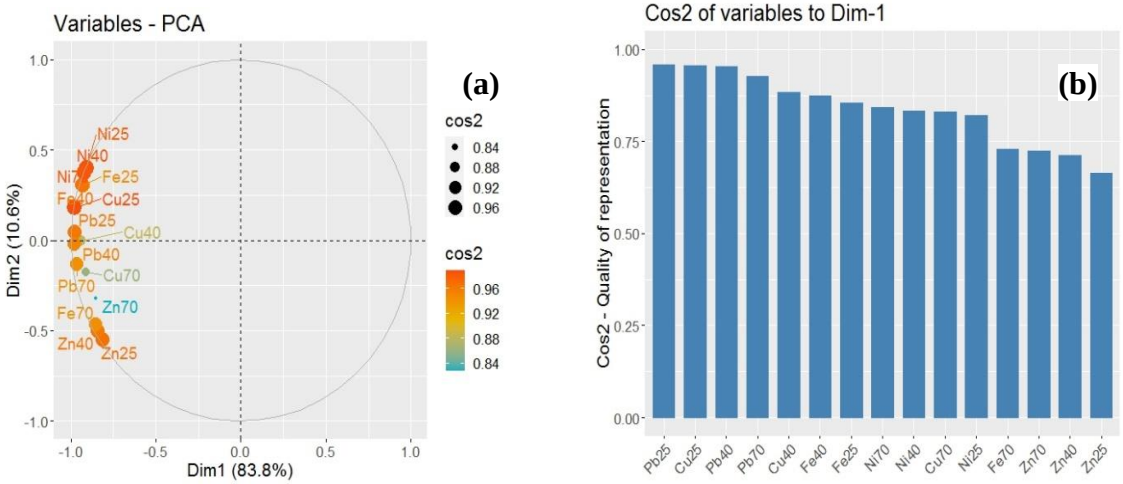

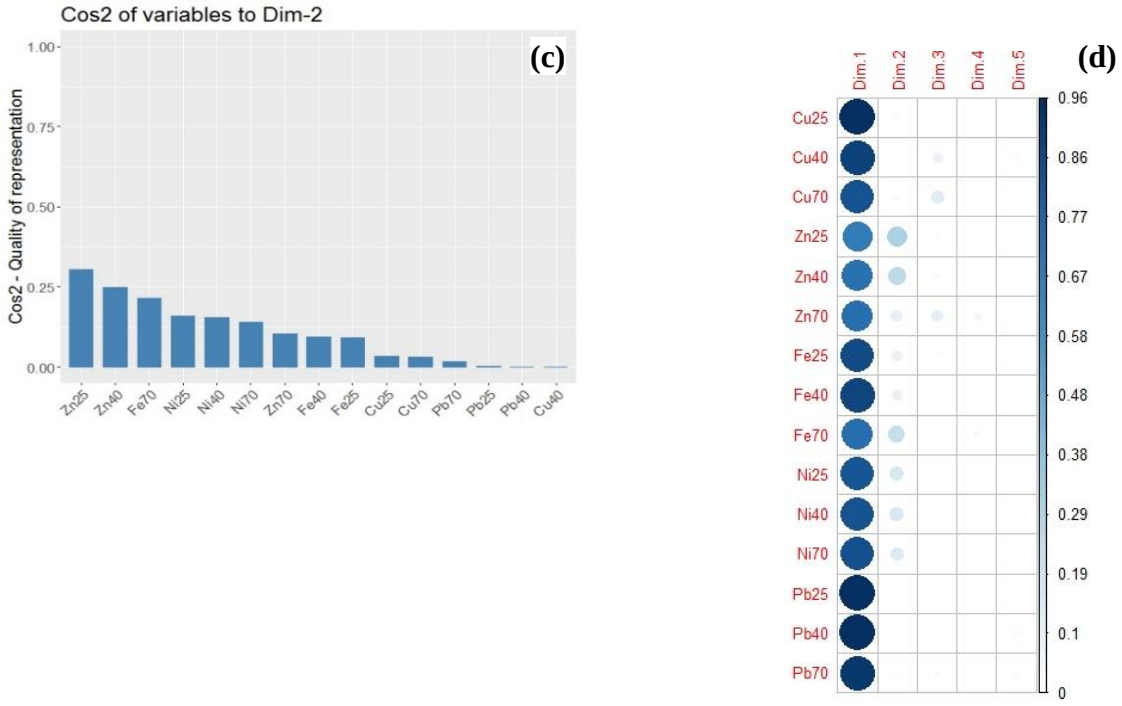

Figure 4.75: (a) Variable Cos2 quality of representation (temperature effect) (b) Dim.1 quality of representation (temperature effect) (c) Dim.2 quality of representation (temperature effect) (d) Cos2 quality of representation plot (temperature effect)

4.12.4 PCA Result for Variables Contribution in Temperature Effect

Figure 4.76 a shows the contribution of variable correlation plot with the most contributing variables indicated in red and the least contributing variables indicated in blue. From **Figure 4.76 b & c**, we can see the contribution of variables represented in bar plots with red dotted lines which indicates the expected average contribution. Dim.1 and Dim.2 are the most important to be considered in explaining the contribution while Dim.3, 4 & 5 are less important. In Dim.1 (**Figure 77 b**), most contribution of variables values were slightly above the expected average contribution. **Table 4.46** shows the actual values for contribution of variables and **Figure 4.76 g** shows the contribution of variables plot with spots of different colour intensity. The darker colours indicate higher contribution while the lighter color indicate low contribution. The contribution of variables for a particular dimension are measured in percentages. Correlated variables in the contribution of variables for Dim.1 & Dim.2 explains 83.8 % and 10.6 % respectively. Contributions from Dim.1 are the most important as they contribute more than other variables and this is followed by Dim.2. Even

though the contributions from other dimensions are high (Dim.3, Dim.4 & Dim.5), they would not be considered since they are not as important as contributions from Dim.1 & 2. The order of importance in the contribution for the dimensions are Dim.1 > Dim.2 > Dim.3 > Dim.4 > Dim.5. A variable with large contribution value contributes more to the component. Dim.1 which explains 83.8 % of the variation is represented in **Figure 4.76 b.** We can see the bar chart for Dim.1 contributions arranged in descending order and the best five contributing variables were Pb25(7.63 %), Cu25(7.61 %), Pb40(7.59 %), Pb70(7.37 %) and Cu40(7.03 %). Dim.2 which explains 10.6 % of the variation is represented in **Figure 4.76 c.** We can see the bar chart for Dim.2 contributions also arranged in descending order and the best three contributing variables were Zn25(19.01 %), Zn40(15.59) and Fe70(13.52 %). The best contributing variables for temperature effect from highest to lowest are in the order Pb25 > Cu25 > Pb40 > Pb70 > Cu40 > Zn25 > Zn40 > Fe70.

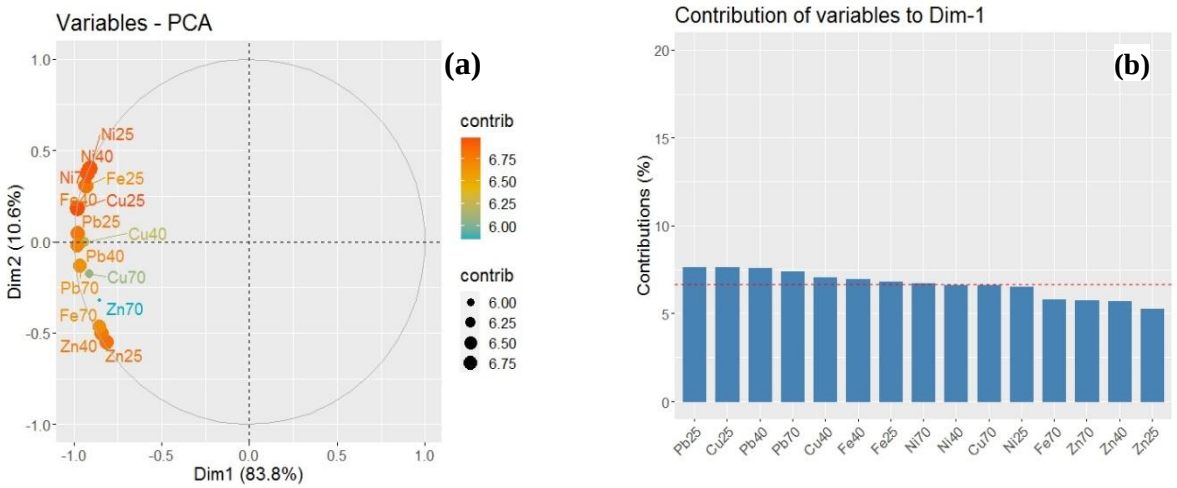

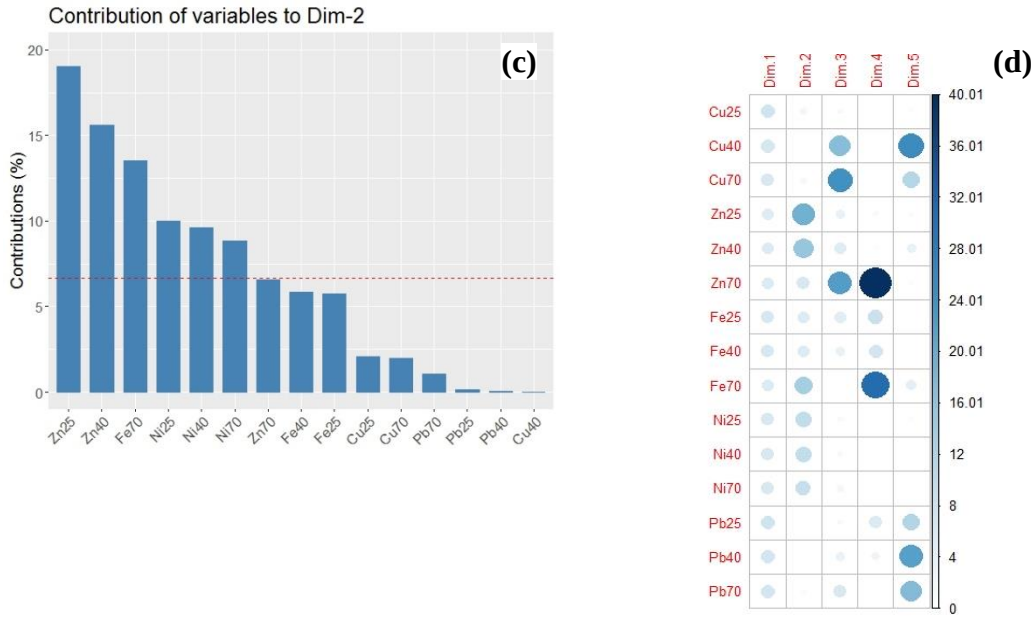

Figure 4.76: (a) Contribution of Variable Correlation Plot (temperature effect) (b) Dim.1 Contribution of Variable Bar Plots (temperature effect) (c) Dim.2 Contribution of Variable Bar Plots (temperature effect) (d) Variable Contribution Plot (temperature effect)

Table 4.46 Best Contributing Variables for Temperature Effect (in bold)

	Dim.1 (%)	Dim.2 (%)
Cu 25	**7.61**	2.06
Cu 40	**7.04**	0.00
Zn 25	5.28	**19.01**
Zn 40	5.68	**15.59**
Fe 70	5.80	**13.52**
Pb 25	**7.63**	1.78
Pb 40	**7.59**	0.03
Pb 70	**7.37**	1.07

4.12.5 PCA Result for Observation Coordinates in Temperature Effect

Figure 4.77 a shows the plot for the observation coordinates which are representing the position of the solvents used in temperature effect experiment for both the hotplate and microwave methods. **Figure 4.77 b - e** shows the three-dimensional plots of inorganic acids, organic acids, ionic liquid (a - c) and ionic liquid (d - g). Dim.1 on the x-axis, Dim.2 on the z-axis and Dim.3 on the y-axis. These three dimensional plots shows the coordinates or positioning of the solvents used for the temperature effect experiment. **Figure 4.78 a – d** shows the observation coordinate visualization plot for inorganic acids, organic acids, ionic liquid (a - c) and ionic liquid (d - g). In Dim.1, the observation coordinates for the inorganic acids all showed very good negative correlation except SA1 - 3 (sulphuric acid) which showed relatively weaker correlation. AQ1-3 (*aqua-regia*) had the strongest negative correlation values followed by NA1-3 (nitric acid) then HA 1-3 (hydrochloric acid). The strength of correlation can be seen on Dim.1 in **Figure 4.78 a** as very dark red colours. Dim.2 also had good correlation values between - 2.0 and - 3.0. The organic acid Dim.1 all showed strong positive correlation and the strength of correlation can be seen on Dim.1 in **Figure 4.78 b** while the Dim.2 showed good positive correlation. The coordinates in ionic liquids (a - c) all showed strong positive correlation in Dim.1 and the strength of correlation can be seen on Dim.1 in **Figure 4.78 c** while Dim.2 showed strong positive correlations. The coordinates in ionic liquids (d - g) in all showed strong positive correlation in Dim.1 and the strength of correlation can be seen on Dim.1 in **Figure 4.78 d** while Dim.2 showed moderate positive correlations.

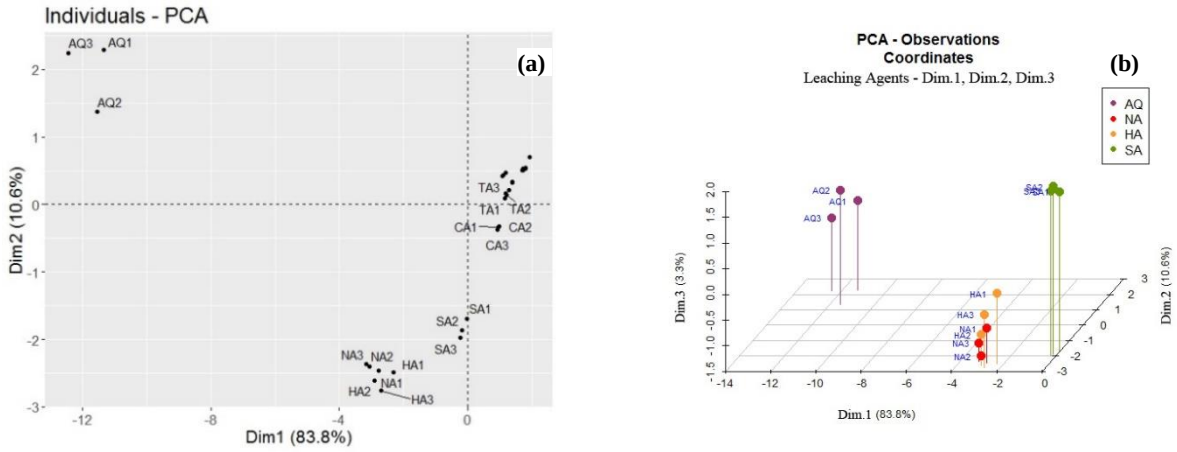

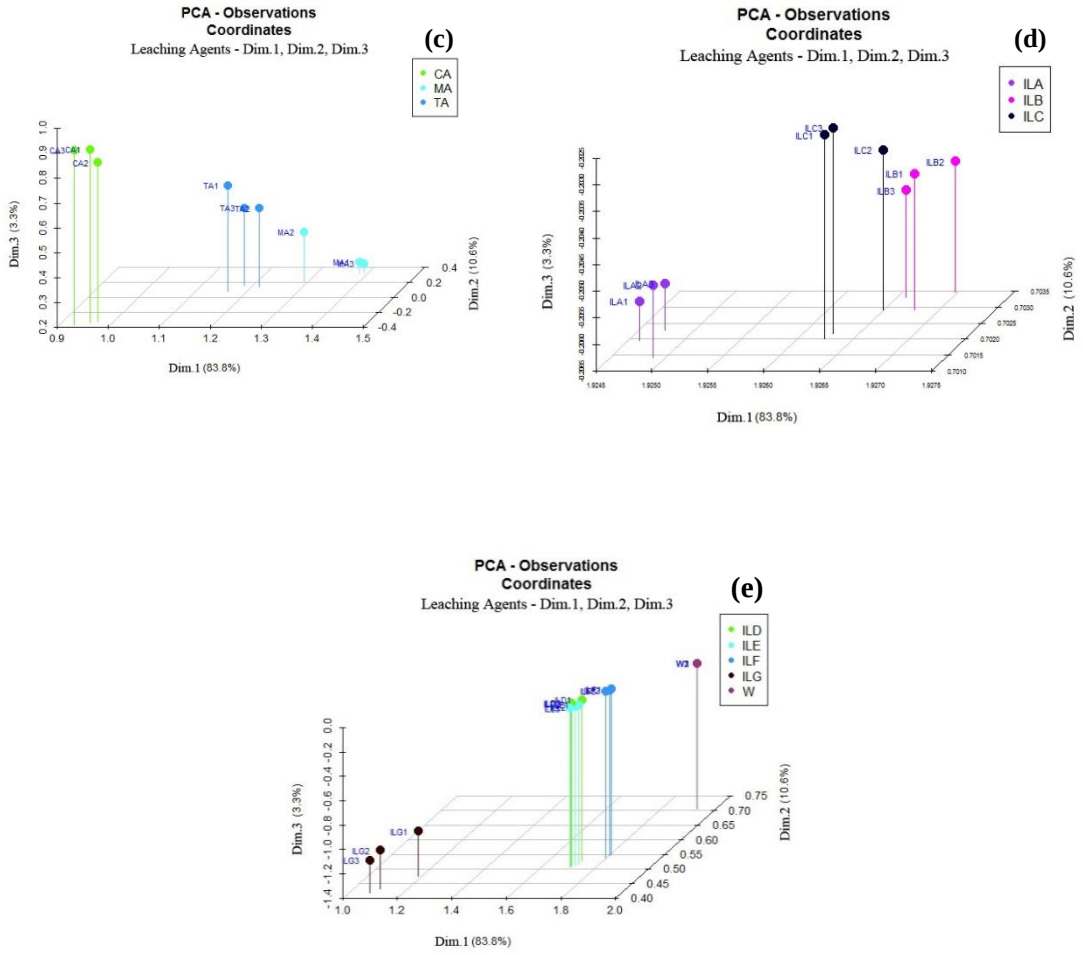

Figure 4.77: (a) observation coordinate correlation plot (temperature effect) (b) observation coordinate for inorganic acids (temperature effect) (c) observation coordinate for organic acids (temperature effect) (d) observation coordinate for IL a-c (temperature effect) (e) observation coordinate for IL d-g (temperature effect)

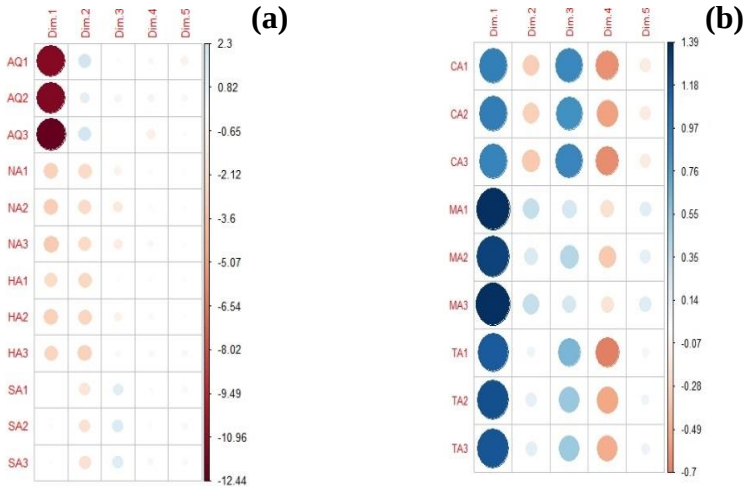

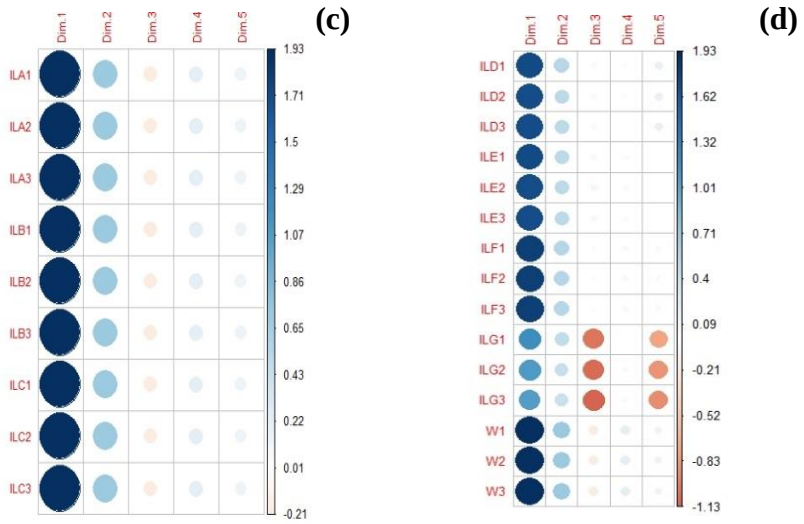

Figure 4.78: (a) Observation coordinate plot for inorganic acids (temperature effect) (b) observation coordinate plot for organic acids (temperature effect) (c) observation coordinate plot for IL a – c (temperature effect) (d) observation coordinate plot for IL d - g (temperature effect)

4.12.6 PCA Result for Observation Cos2 Quality of Representation in Temperature Effect

Figure 4.79 a shows the Cos2 plot of observation with the highest Cos2 value which are in orange while the mid cos2 observation value are in blue. The observations in orange are the most represented in the plot as they have very high values and this is followed by the yellow and then the blue spots. **Figure 4.79 b - e** shows the three-dimensional plots Cos2 observation for inorganic acids, organic acids, ionic liquid (a - c) and ionic liquid (d - g). Dim.1 on the x-axis, Dim.2 on the z-axis and Dim.3 on the y-axis. These three dimensional plots shows the coordinates or positioning of the solvents used for the temperature effect experiment. Consequently, all negative values have been cancelled out and **Figure 4.80 a - d** shows the Cos2 observations visualization with spots of different colour intensity. The strongest or darkest colour represent the highest Cos2 observations and the Cos2 observations decreased with decrease in the colour intensity of the spots in the visualization. Dim.1 in **Figure 4.80 a** (inorganic acids), showed good quality of representation. AQ1-3 had good quality of representation followed by NA1-3. In Dim.2 (inorganic acids), only moderate quality of representation were found except in QA1, 2 & 3. Dim.1 in **Figure 4.80 b** (organic acids), showed good quality of representation. In Dim.2 (organic acids), only relatively weak

correlation was observed. Dim.1 in **Figure 4.80 c** (IL (a - c)), showed good quality of representation. Dim.1 in **Figure 4.80 d** (IL (d - g)), showed good quality of representation.

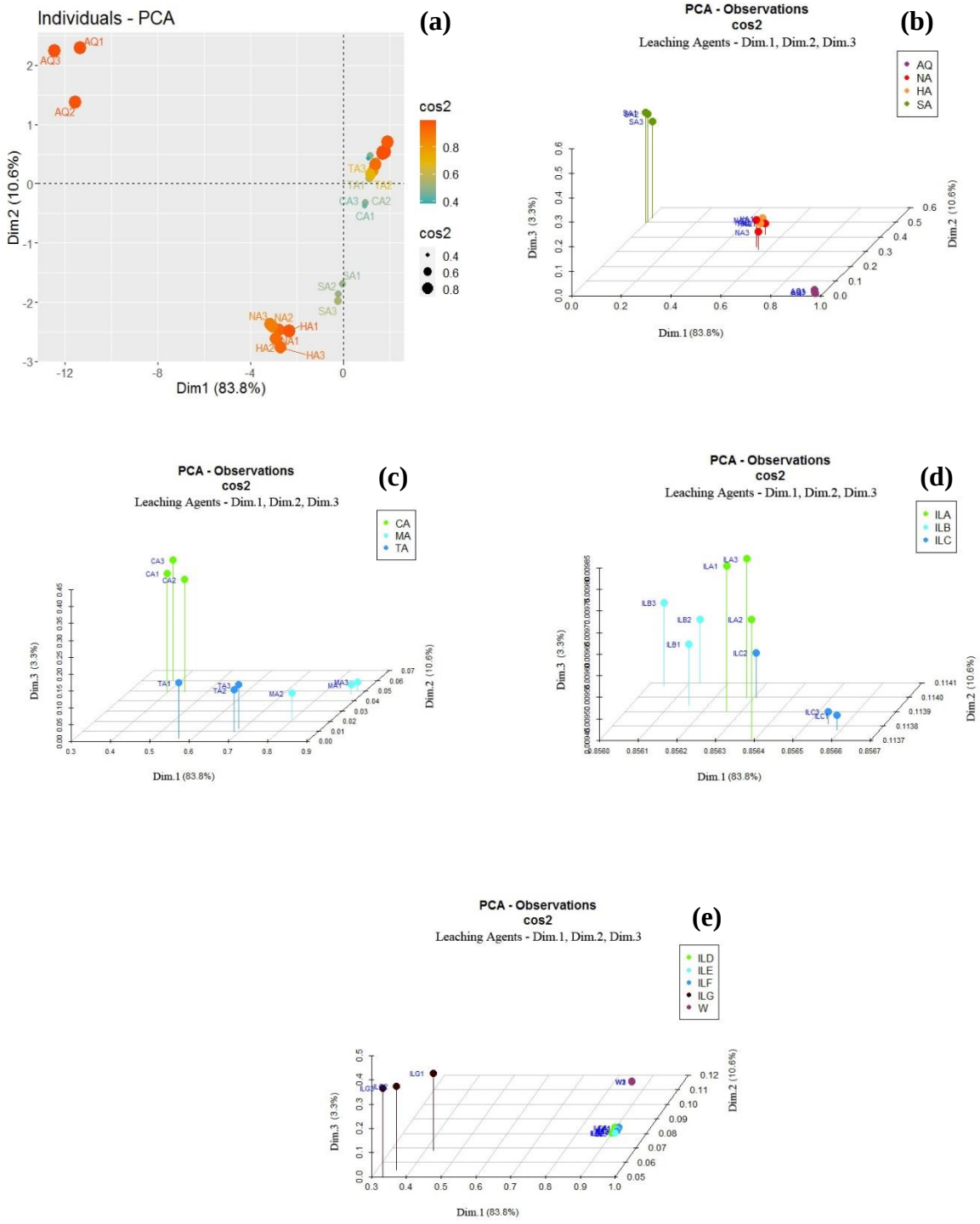

Figure 4.79: (a) Observation cos2 correlation plot (temperature effect) (b) Observation cos2 for inorganic acids (temperature effect) (c) Observation cos2 for organic acids (temperature effect) (d) Observation cos2 for IL a-c (temperature effect) (e) Observation cos2 for IL d-g (temperature effect)

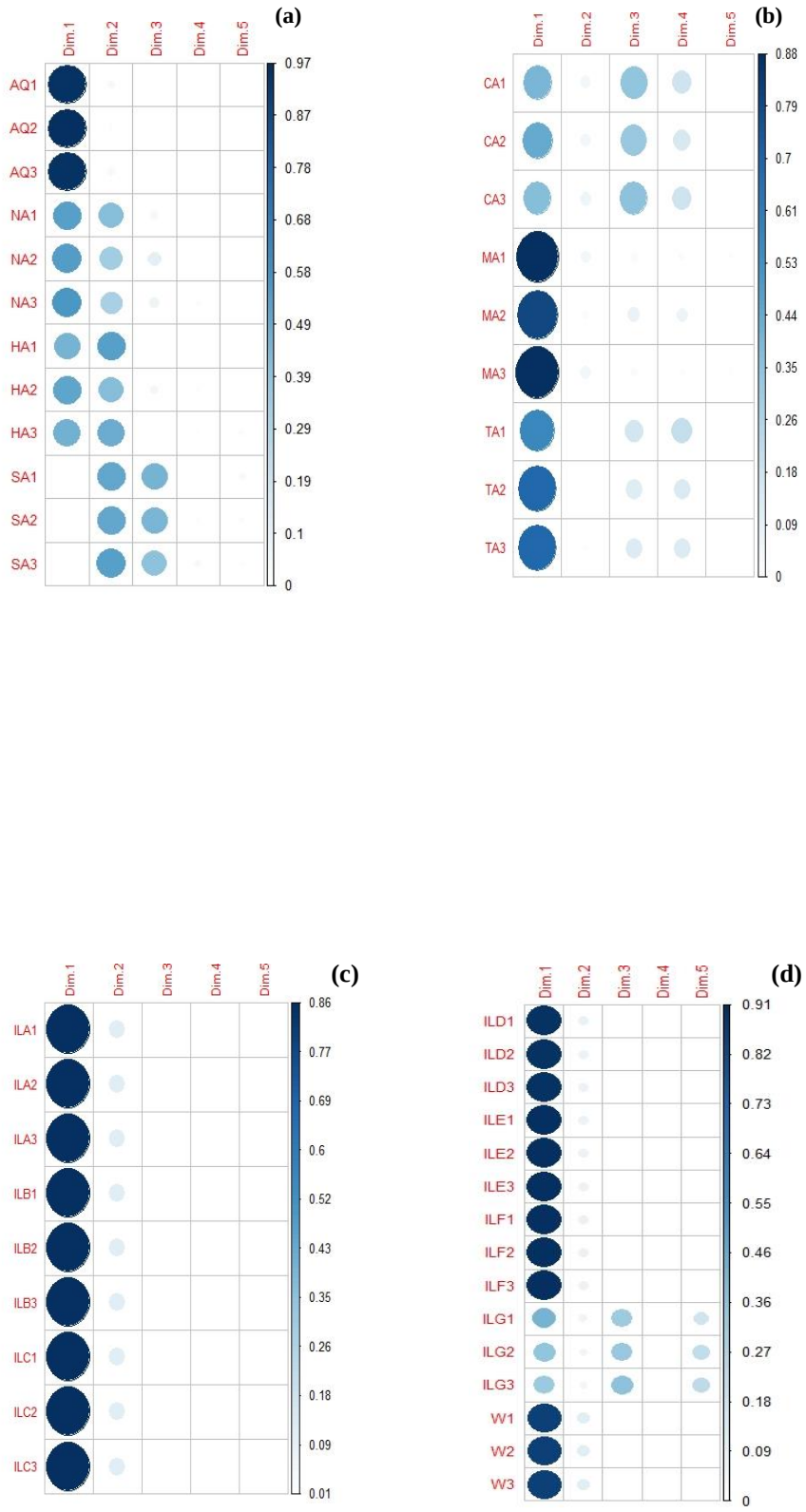

Figure 4.80: (a) Observation cos2 Dim plot for inorganic acids (temperature effect) (b) observation cos2 Dim plot for organic acids (temperature effect) (c) observation cos2 Dim plot for IL a – c (temperature effect) (d) observation cos2 Dim plot for IL d - g (temperature effect)

4.12.7 PCA Result for Observation Contribution in Temperature Effect

Figure 4.81 a shows the contribution plot of observation with the highest contribution values which are in orange while the mid contribution value are in blue. In the figure, more labelling priority is given to the highest contributing observation with the least contributing observations not appearing. The observations in orange are the most represented in the plot as they have very high values and this is followed by the yellow and then the blue spots. **Figure 4.81 b - e** shows the three-dimensional plots of observation contribution for inorganic acids, organic acids, ionic liquid (a - c) and ionic liquid (d - g). Dim.1 on the x-axis, Dim.2 on the z-axis and Dim.3 on the y-axis. These three dimensional plots shows the positioning of the solvents contribution on the plot. **Table 4.47** shows the observation contribution values in percentages. **Figure 4.82 a - d** shows the observation contribution visualization with spots of different colour intensity. The strongest or darkest colour represent the highest observation contribution and the observation contribution decreased with decrease in the colour intensity of the spots in the visualization. The observation contribution in Dim.1 for inorganic acids (**Table 4.47**), shows observation contribution and the best five were solvents that contributed to this Dim.1 were AQ3 (27.35 %), AQ2 (23.58 %), AQ1 (22.74 %), NA3 (1.77 %) and NA2 (1.65 %). In Dim.2 (inorganic acids), the best three observation contributions were HA3 (10.62 %), HA2 (9.50 %) and HA1 (8.63 %). The best observation contribution with strong colour intensity can be seen in Dim.1 (**Figure 4.82 a**). The best contributing solvents from highest to lowest are in the order AQ3 > AQ2 > AQ1 > NA3 > NA2 > HA3 > HA1 > NA1.

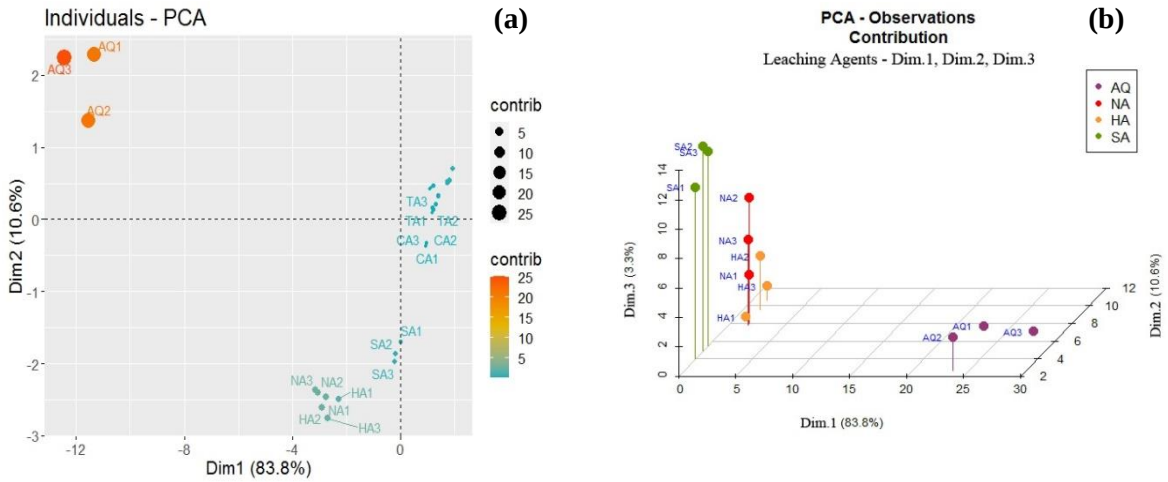

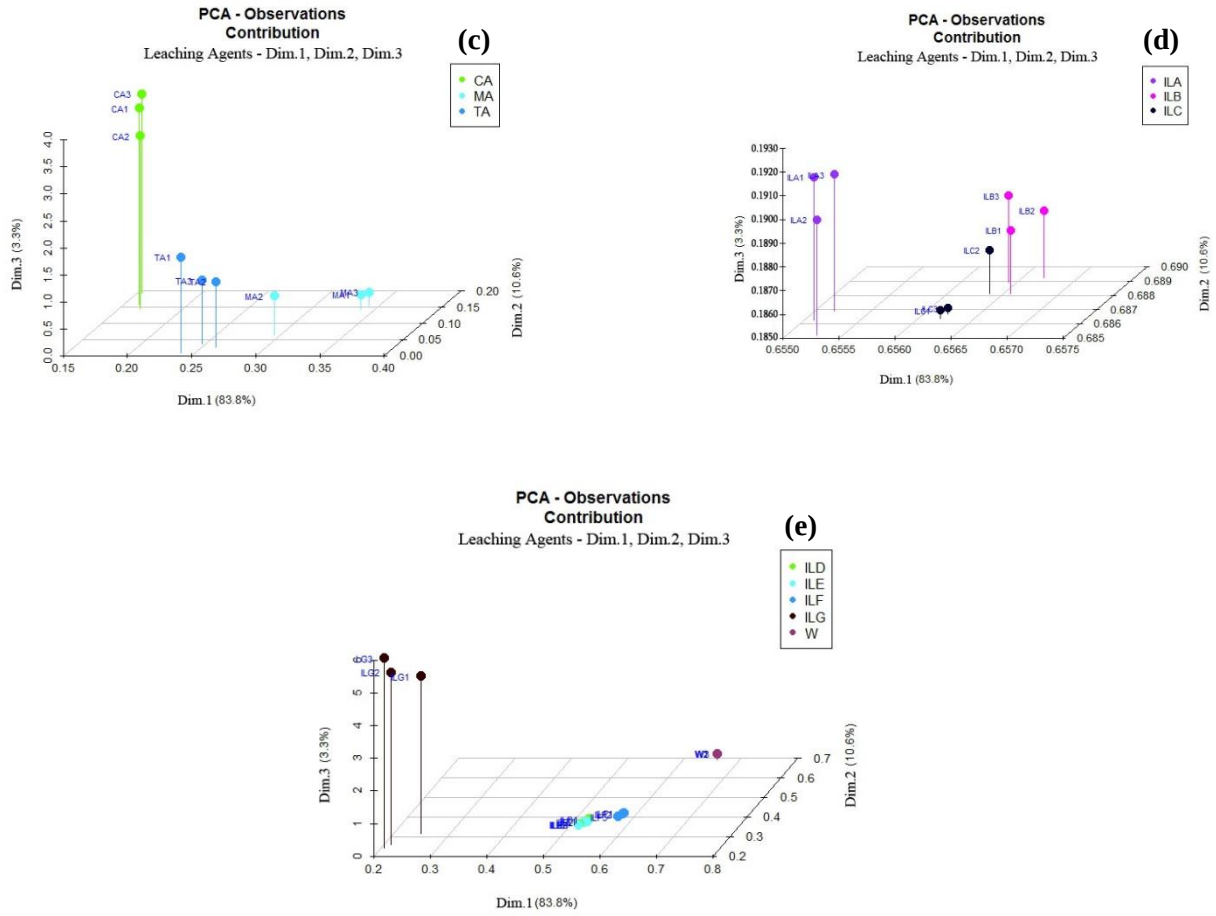

Figure 4.81: (a) Observation contribution plot (temperature effect) (b) Observation contribution for inorganic acids (temperature effect) (c) Observation contribution for organic acids (temperature effect) (d) Observation contribution for IL a-c (temperature effect) (e) Observation contribution for IL d-g (temperature effect)

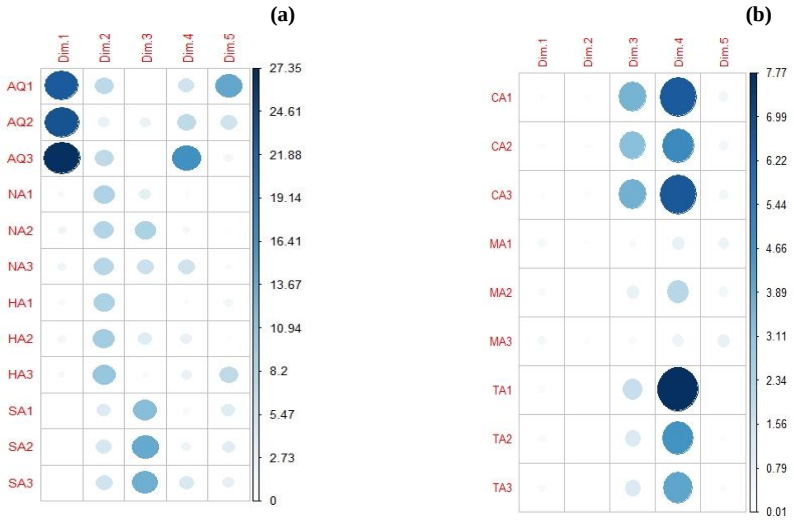

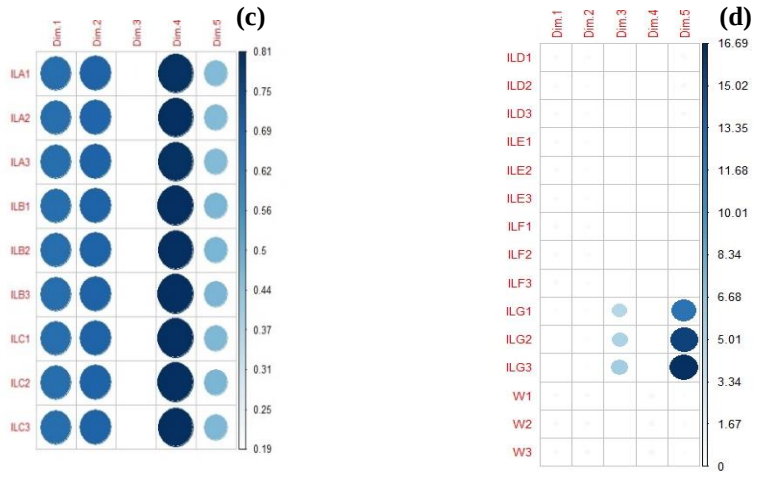

Figure 4.82: (a) Observation contribution Dim plot for inorganic acids (temperature effect) (b) observation contribution Dim plot for organic acids (temperature effect) (c) observation contribution Dim plot for IL a – c (temperature effect) (d) observation contribution Dim plot for IL d - g (temperature effect)

Table 4.47 Best Contributing Observations for Temperature Effect

	Dim 1 (%)	Dim 2 (%)
AQ1	**22.74**	7.34
AQ2	**23.58**	2.65
AQ3	**27.35**	7.04
NA1	1.35	8.43
NA2	**1.65**	8.01
NA3	**1.77**	7.80
HA1	0.94	**8.63**
HA2	1.50	**9.50**
HA3	1.29	**10.62**

4.13 Determination of time effect

One method, hotplate method, was used to determine the effect of time (30, 60, 90, 120, 150 and 180 minutes) on the extraction of Cu, Zn, Fe, Ni and Pb. For the hotplate method, the experimental conditions were particle-size (4 mm), temperature (70 ^{0}C), concentration (2 M for inorganic acids, 25 g/L for organic acids and 100 g/L for ionic liquids), sample weight (0.5 g) and rotation speed (340 rpm). **Appendices 5a - e** shows tables of the mean concentrations of time effect for Cu, Zn, Fe, Ni and Pb (mg/g) with dose from three different experiments and the standard deviation as the error bar. The time effect for the microwave method was not done as the microwave ran for a specified time (20 minutes).

4.13.1 Effect of time on Leaching Cu

Table 4.48 shows the percentage extraction of Cu with time and this is also represented in **Figure 4.83.** From **Figure 4.83** the time increased from 30 – 180 minutes the Cu extraction also increased. The peak extractions were NA (77 % at 180 minutes), HA (40 % at 180 minutes) and IL-G (25 % at 180 minutes). The other solvents had < 2 % Cu extraction.

4.13.2 Effect of time on Leaching Zn

Table 4.49 shows the percentage extraction of Zn with time and this is also represented in **Figure 4.84.** From **Figure 4.84** the time increased from 30 – 180 minutes the Zn extraction showed no significant increase except citric and malic acid which showed significant increase from 30 – 180 minutes. The peak extractions were NA (63 % at 180 minutes), HA (62 % at 180 minutes), TA (58 % at 180 minutes), SA (57 % at 180 minutes), CA (55 % at 180 minutes), MA (30 % at 180 minutes), ILs D - G had 8, 7, 9 & 9 % extractions at 180 minutes respectively. ILs A - C had < 1 % extractions.

Table 4.48 Percentage concentration values for effect of time on leaching Cu

	Time (minutes)	Extraction (%)														
		AQ	NA	HA	SA	CA	MA	TA	IL-A	IL-B	IL-C	IL-D	IL-E	IL-F	IL-G	W
Hotplate Method	30.00	100.00	6.08	3.60	0.09	0.05	0.02	0.08	0.00	0.01	0.02	0.02	0.11	0.03	0.21	0.00
	60.00	100.00	11.25	6.93	0.10	0.06	0.05	0.09	0.00	0.01	0.02	0.04	0.30	0.07	0.87	0.00
	90.00	100.00	21.67	9.60	0.10	0.11	0.08	0.18	0.00	0.01	0.02	0.06	0.38	0.08	2.27	0.00
	120.00	100.00	40.00	23.00	0.35	0.13	0.10	0.20	0.00	0.01	0.02	0.08	0.70	0.11	11.50	0.00
	150.00	100.00	55.00	32.54	0.67	0.24	0.17	0.31	0.00	0.02	0.02	0.13	0.80	0.14	13.87	0.00
	180.00	100.00	76.67	40.08	1.96	0.28	0.25	0.68	0.00	0.02	0.02	0.17	0.80	0.55	25.33	0.00

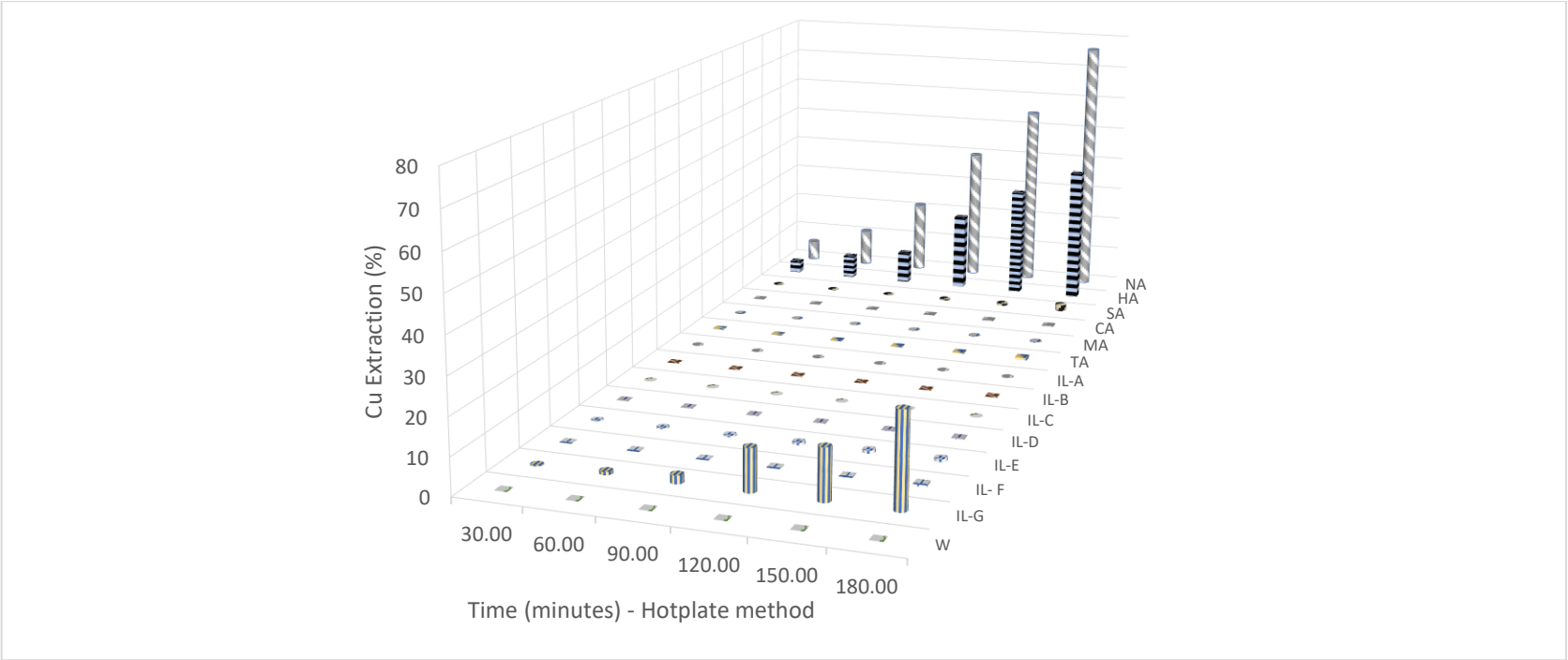

Figure 4.83 Percentage concentration for the effect of time on leaching Cu

Table 4.49 Percentage concentration values for effect of time on leaching Zn

	Time (minutes)	Extraction (%)														
		AQ	NA	HA	SA	CA	MA	TA	IL-A	IL-B	IL-C	IL-D	IL-E	IL-F	IL-G	W
Hotplate Method	**30.00**	100.00	50.41	57.05	49.09	28.75	12.99	52.80	0.01	0.02	0.10	7.52	5.84	6.46	6.90	0.00
	60.00	100.00	53.95	58.82	53.51	38.14	17.41	53.60	0.02	0.02	0.10	7.78	6.37	7.61	7.69	0.00
	90.00	100.00	56.61	60.14	54.16	42.29	21.48	54.66	0.02	0.02	0.10	8.05	7.96	8.14	8.31	0.00
	120.00	100.00	56.24	60.59	55.28	48.65	26.31	55.76	0.03	0.02	0.11	8.05	6.97	8.23	8.84	0.01
	150.00	100.00	58.82	60.40	55.65	54.45	26.76	56.52	0.03	0.02	0.11	8.31	7.20	9.20	9.02	0.01
	180.00	100.00	63.24	61.53	57.05	55.28	26.98	58.11	0.03	0.02	0.11	8.31	7.43	9.46	9.11	0.01

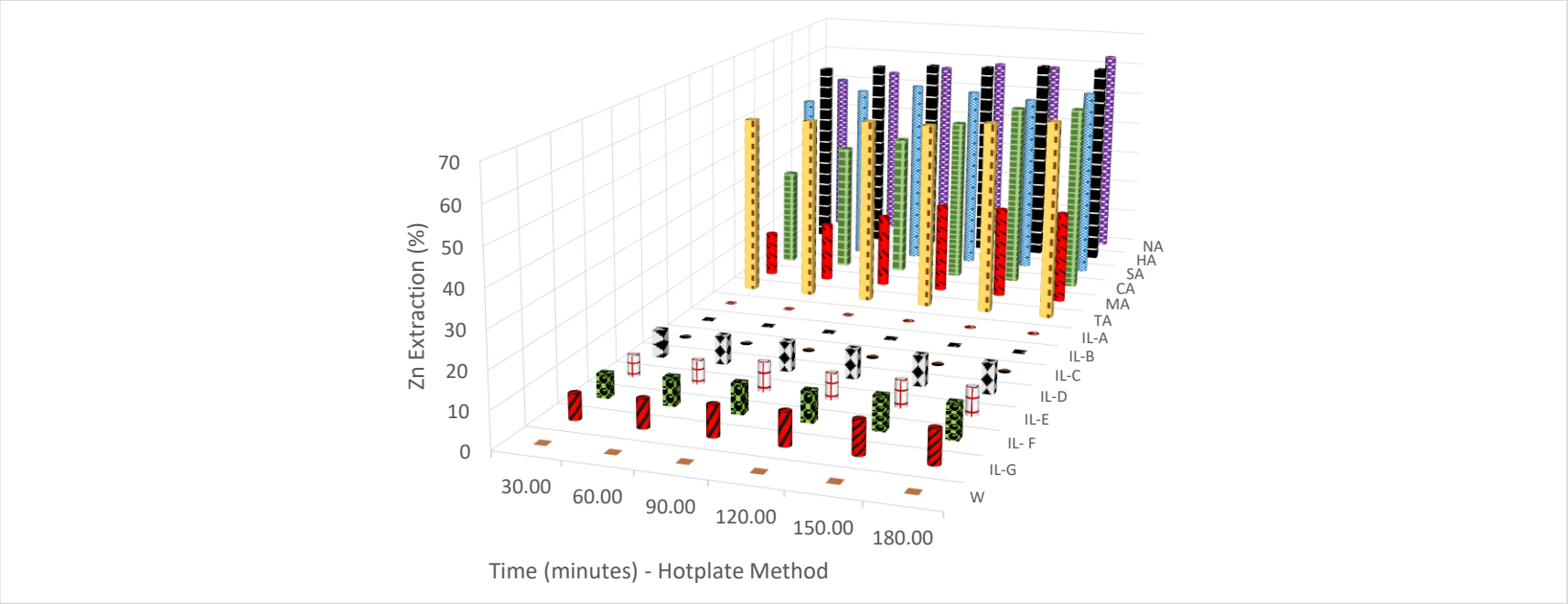

Figure 4.84 Percentage concentration for the effect of time on leaching Zn

4.13.3 Effect of time on Leaching Fe

Table 4.50 shows the percentage extraction of Cu with time and this is also represented in **Figure 4.85.** From **Figure 4.85** the time increased from 30 – 180 minutes the Cu extraction also increased. The peak extractions were NA (76 % at 150 minutes), HA (84 % at 180 minutes), SA (61 % at 180 minutes). The organic acids had extractions < 2 % and ionic liquids (ILs A – G) had extractions < 1 %.

4.13.4 Effect of time on Leaching Ni

Table 4.51 shows the percentage extraction of Ni with time and this is also represented in **Figure 4.86**. From **Figure 4.86** the time increased from 30 – 180 minutes the Ni extraction also increased. The solvents peak extractions was NA (4 % at 180 minutes). The extraction was genereally < 5 %.

4.13.5 Effect of time on Leaching Pb

Table 4.52 shows the percentage extraction of Pb with time and this is also represented in **Figure 4.87**. From **Figure 4.87** the time increased from 30 – 180 minutes the Pb extraction also increased. The solvents peak extractions were NA (59 % at 180 minutes), HA (70 % at 180 minutes), SA (1 % at 180 minutes), CA (4 % at 180 minutes), MA (11 % at 180 minutes), TA (4 % at 180 minutes) and IL D (2 % at 180 minutes). The other solvents did not show any significant extractions.

Table 4.50 Percentage concentration values for effect of time on leaching Fe

	Time (minutes)	Extraction (%)														
		AQ	NA	HA	SA	CA	MA	TA	IL-A	IL-B	IL-C	IL-D	IL-E	IL-F	IL-G	W
Hotplate Method	**30.00**	100.00	18.02	9.49	12.93	0.17	0.21	0.17	0.00	0.00	0.00	0.03	0.00	0.00	0.00	0.00
	60.00	100.00	21.16	23.31	14.06	0.30	0.42	0.36	0.00	0.00	0.00	0.16	0.00	0.00	0.00	0.00
	90.00	100.00	33.19	39.63	31.77	0.50	0.68	0.38	0.00	0.00	0.00	0.26	0.00	0.00	0.00	0.00
	120.00	100.00	62.27	69.91	39.10	0.75	0.91	0.58	0.00	0.00	0.00	0.33	0.00	0.00	0.00	0.00
	150.00	100.00	76.58	79.62	49.89	0.95	1.10	0.59	0.00	0.00	0.00	0.39	0.00	0.00	0.00	0.00
	180.00	100.00	77.03	83.87	60.81	1.32	1.28	0.86	0.00	0.00	0.00	0.51	0.00	0.00	0.00	0.00

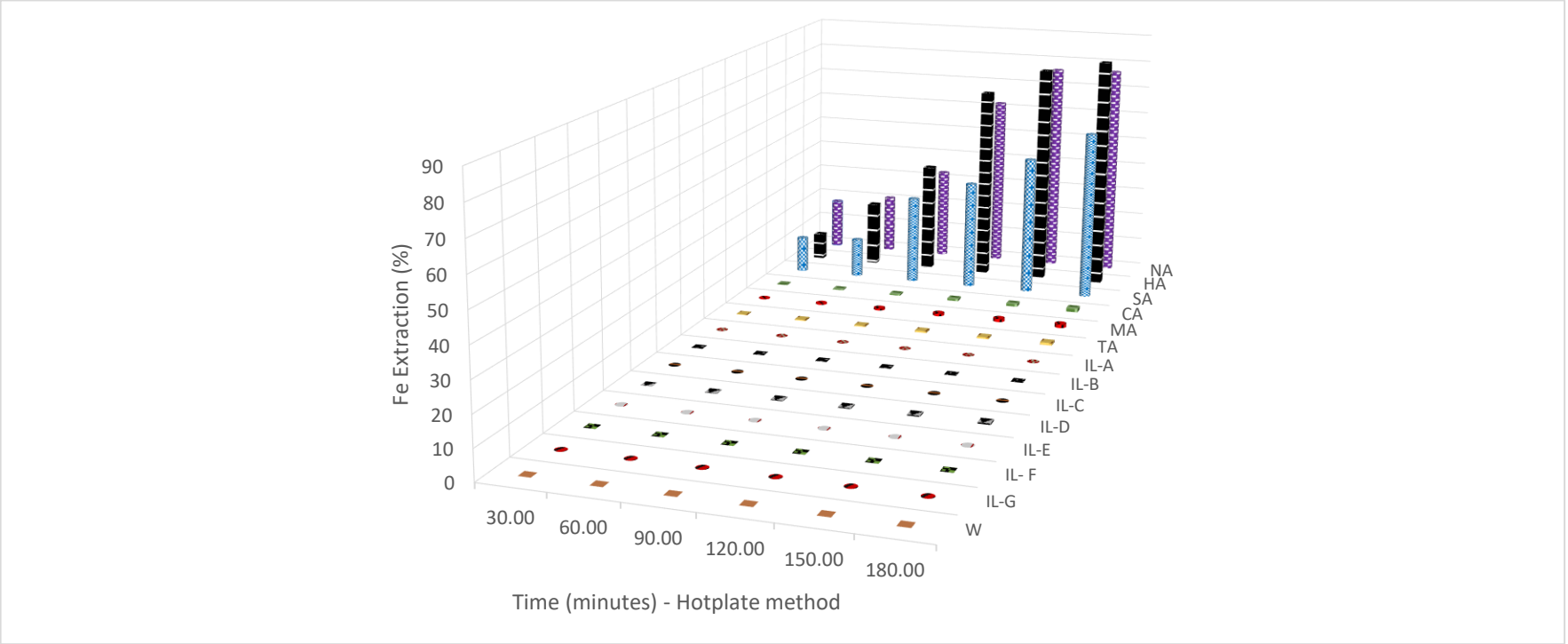

Figure 4.85 Percentage concentration for the effect of time on leaching Fe

Table 4.51 Percentage concentration values for effect of time on leaching Ni

	Time (minutes)	Extraction (%)														
		AQ	NA	HA	SA	CA	MA	TA	IL-A	IL-B	IL-C	IL-D	IL-E	IL-F	IL-G	W
Hotplate Method	30.00	100.00	1.92	0.57	1.02	1.52	0.14	1.31	0.01	0.01	0.01	0.01	0.01	0.01	0.01	0.01
	60.00	100.00	2.46	0.93	1.39	2.65	0.32	1.39	0.01	0.01	0.01	0.01	0.01	0.01	0.01	0.01
	90.00	100.00	3.79	1.45	1.20	2.90	0.58	1.20	0.01	0.01	0.01	0.01	0.01	0.01	0.01	0.01
	120.00	100.00	3.91	2.65	2.78	2.94	0.78	2.78	0.01	0.01	0.01	0.01	0.01	0.01	0.01	0.01
	150.00	100.00	4.29	3.16	3.16	2.92	0.78	3.16	0.01	0.01	0.01	0.01	0.01	0.01	0.01	0.01
	180.00	100.00	4.42	3.66	2.90	2.94	0.78	2.90	0.01	0.01	0.01	0.01	0.01	0.01	0.01	0.01

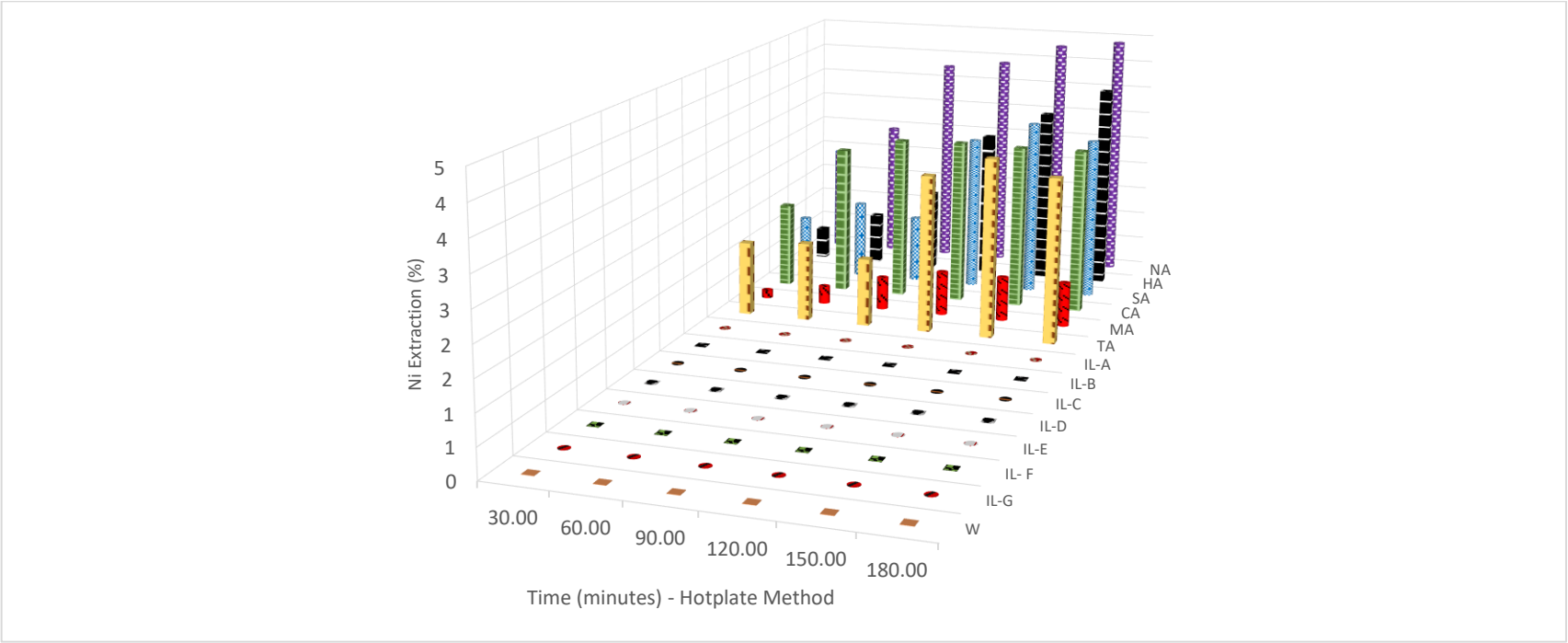

Figure 4.86 Percentage concentration for the effect of time on leaching Ni

Table 4.52 Percentage concentration values for effect of time on leaching Pb

	Time (minutes)	Extraction (%)														
		AQ	NA	HA	SA	CA	MA	TA	IL-A	IL-B	IL-C	IL-D	IL-E	IL-F	IL-G	W
Hotplate Method	30.00	100.00	13.49	8.84	0.26	1.40	1.30	0.74	0.07	0.06	0.07	0.12	0.07	0.05	0.22	0.05
	60.00	100.00	16.19	15.63	0.36	1.58	1.86	1.03	0.05	0.07	0.08	0.25	0.07	0.06	0.39	0.05
	90.00	100.00	26.05	23.02	0.57	1.81	2.23	1.22	0.09	0.08	0.09	1.12	0.08	0.08	0.44	0.05
	120.00	100.00	41.86	45.35	0.69	3.44	4.28	1.67	0.09	0.10	0.10	1.56	0.15	0.07	0.54	0.05
	150.00	100.00	51.63	57.21	0.94	3.35	5.95	3.26	0.10	0.11	0.10	1.56	0.16	0.10	0.60	0.05
	180.00	100.00	58.60	70.00	1.14	4.19	10.79	3.91	0.11	0.11	0.11	1.67	0.16	0.09	0.76	0.05

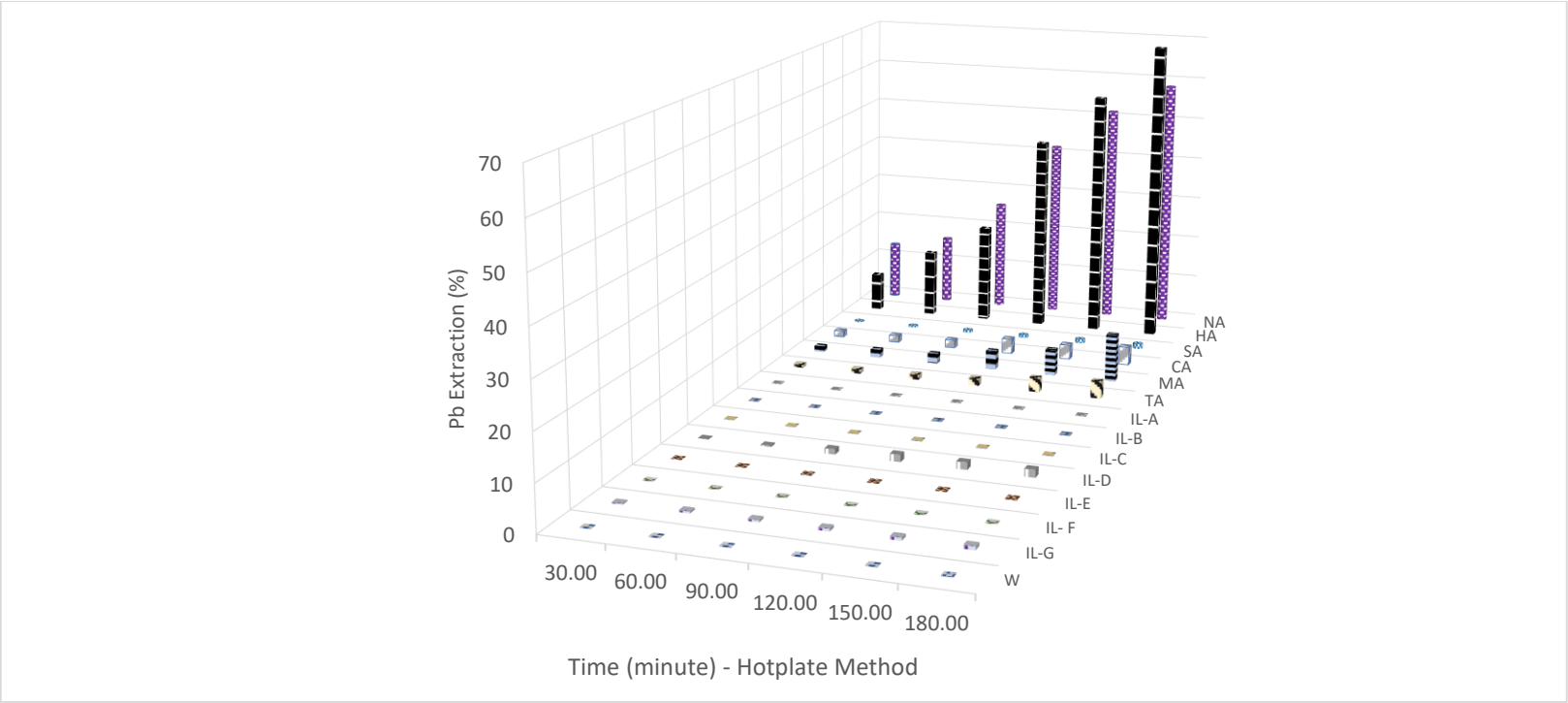

Figure 4.87 Percentage concentration for the effect of time on leaching Pb

4.14 PCA for Time Effect

4.14.1 Scree Plot Time Effect

This time effect experiment involved 30 variables and 45 observations. The variables were made up of five metals (Cu, Zn, Fe, Ni and Pb) with each of these metals having results from six different expriments on effect of time (30, 60, 90, 120, 150 and 180 minutes). The observations were results from each of the fifteen solvents with three replicates each from the hotplate and microwave methods used in the experiment. **Table 4.53** shows the summarized data of the first six principal components from only the hotplate method (mg/g) in **Appendices 5 a – e**. **Figure 4.88** shows the scree plot of variance for the dimensions from time effect data and they are in the order of highest to the lowest with Dim.1 as 84.5 %, Dim.2 as 9.7 % and Dim.3 as 3.7 %. From this scree plot we can infer that Dim.1 explains the most part of the time effect data as it is larger than the other dimensions. From **Table 4.51**, we can see that Dim.1, 2 & 3 showed a SD > 1.0 as SD = 1 is the cutoff point. Therefore, we can accept the first three dimensions (Dim.1, 2 & 3) with a proportion of variance of 84.5, 9.7 & 3.7 % respectively. Consequently, the cumulative proportion in Dim.1, 2 & 3 also showed 84.5, 94.2 & 97.9 % respectively. This shows that with Dim.3 having a SD of 1.1, about 97.9 % of the data can be accounted for while the remaining 4.3 % of the data can be disregarded as they fall below SD < 1.0.

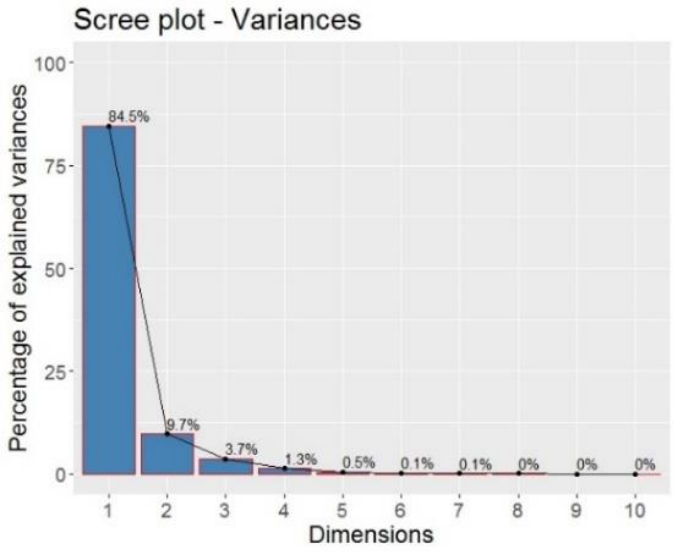

Figure 4.88 Scree plot for time effect

Table 4.53 Summarized principal components time effect

Principal Components	Dim.1	Dim.2	Dim.3	Dim.4	Dim.5	Dim.6
Standard deviation	5.034	1.704	1.056	0.621	0.380	0.192
Proportion of Variance	0.845	0.097	0.037	0.013	0.005	0.001
Cumulative Proportion	0.845	0.942	0.979	0.992	0.996	0.998

Figure 4.89 shows the biplot for time effect data which is the relationship between the variables and the observations in the time data. It also shows the structure of variables correlations and clustered observations. From the PCA plot, we can see the variables with the longest vector projections. They represent the highest variations in the data and they have occured in Cu90, Zn180, Fe120, Pb60 and Fe80. The replicate observations formed clusters, for example, in the hotplate method (1, 2 & 3) the observations AQ1, AQ2 & AQ3 which represents the hotplate result for *aqua-regia* formed a cluster which means that the three replicated experiments showed similarity in the result from time effect. Also, this behaviour was observed in other observation showing that the replicated results were similar. The *aqua-regia* observations AQ1-3 are considered outliers on the PCA as the cluster was clearly outside the group clustering and also far away from the other observations. However, they were not treated as outliers or removed as they were needed in this research inorder to clearly differentiate the best performing solvents or observations. Other observation clusters were seen in (NA1, NA2 & NA3), (HA1, HA2 & HA3), SA1, SA2 & SA3) and (CA1, CA2 & CA3), (TA1-3), (MA1-3). The above stated clusters had various degrees of euclidean distance (distance between observations) and the observations from *aqua-regia* (AQ1-3) was the farthest. Consequently, the organic acids and ionic liquids all seemed to have clustered together as their euclidean distance were relatively close.

We can see that half of the variables vectors were pointing towards AQ1-3 and a few more pointing towards NA1-3 and HA1-3. This shows a high degree of association between the variables and the observations but the reverse was the case for the other observations such as SA1-3, CA1-3 the other organic acids and ionic liquids as the PCA plot (**Figure 4.89**) clearly shows the variable vectors pointing away from them and this implies very low association between the variables and these observations. Also, all the variables were pointing towards the hotplate method (red) showing high variable association with the hotplate method. The variable vectors closest to each other showed high correlation amongst themselves, for

example, Fe120 and Pb150, Pb120 and Fe90, Pb60 and Pb90 formed angles around 30 degrees. No correlation was observed between Zn180 and Pb60 as their vectors formed angle 90 degrees. The x-axis which is Dim.1 (84.5 % of variation explained) shows that all the variable vectors are positioned on the left side of the plot thereby revealing negative correlation for all variables. So we would expect that the lower the values of Dim.1 the higher high values for each of the variables. The y-axis which is Dim.2 (9.7 % of variation explained) shows that half of the variables postioned at the top were positive correlation and the other half at the bottom were negative correlation. (Kohla & Luniak, 2005; Reris & Brooks, 2015; Statisticshowto, 2021; STHDA, 2021; Towardsdatascience, 2021).

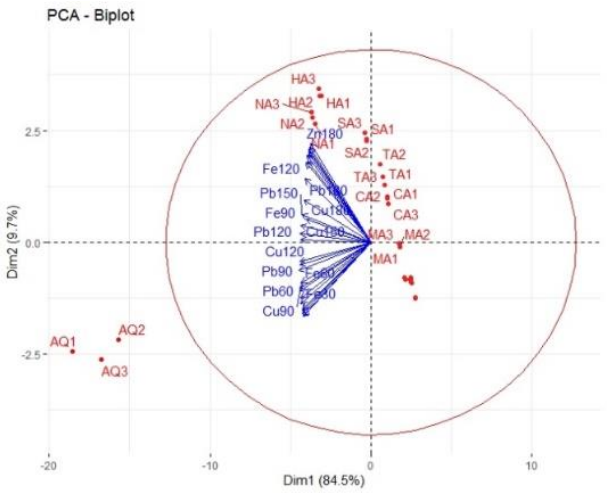

Figure 4.89 Biplot for time effect

4.14.2 PCA Result for Variable Coordinates in Time Effect

Figure 4.90 a shows the plot for the variable coordinates for Dim.1 & 2 which are representing of the position of the time effect variables on the plot. The coordinates are correlation between a variable and a dimension. **Figure 4.90 b** shows a three-dimensional view of variable coordinates for the three dimensions (Dim.1, 2 & 3) with Dim.1 (84.5 %) on the x-axis, Dim.2 (9.7 %) on the z-axis and Dim.3 (3.7 %) on the y-axis. **Figure 4.90 c** shows the variable coordinates visualization with spots of different colour intensity. The strongest or darkest colour represent the highest correlation values and the correlation values decreases with decrease in the colour intensity of the spots in the visualization. Also, the positive correlated values are in blue while the negative correlated values are in red. Here, Dim.1-5 are represented by Dim.1-5. The order of importance decreased from Dim.1 to 5. We can see that Dim.1 showed the highest colour intensity and this was followed by Dim.2, 3, 4 & 5.

However, all the coordinates in Dim.1 showed strong negative correlation. In Dim.2, both positive and negative correlation were moderate. Dim.3 showed relatively weak positive and negative correlations.

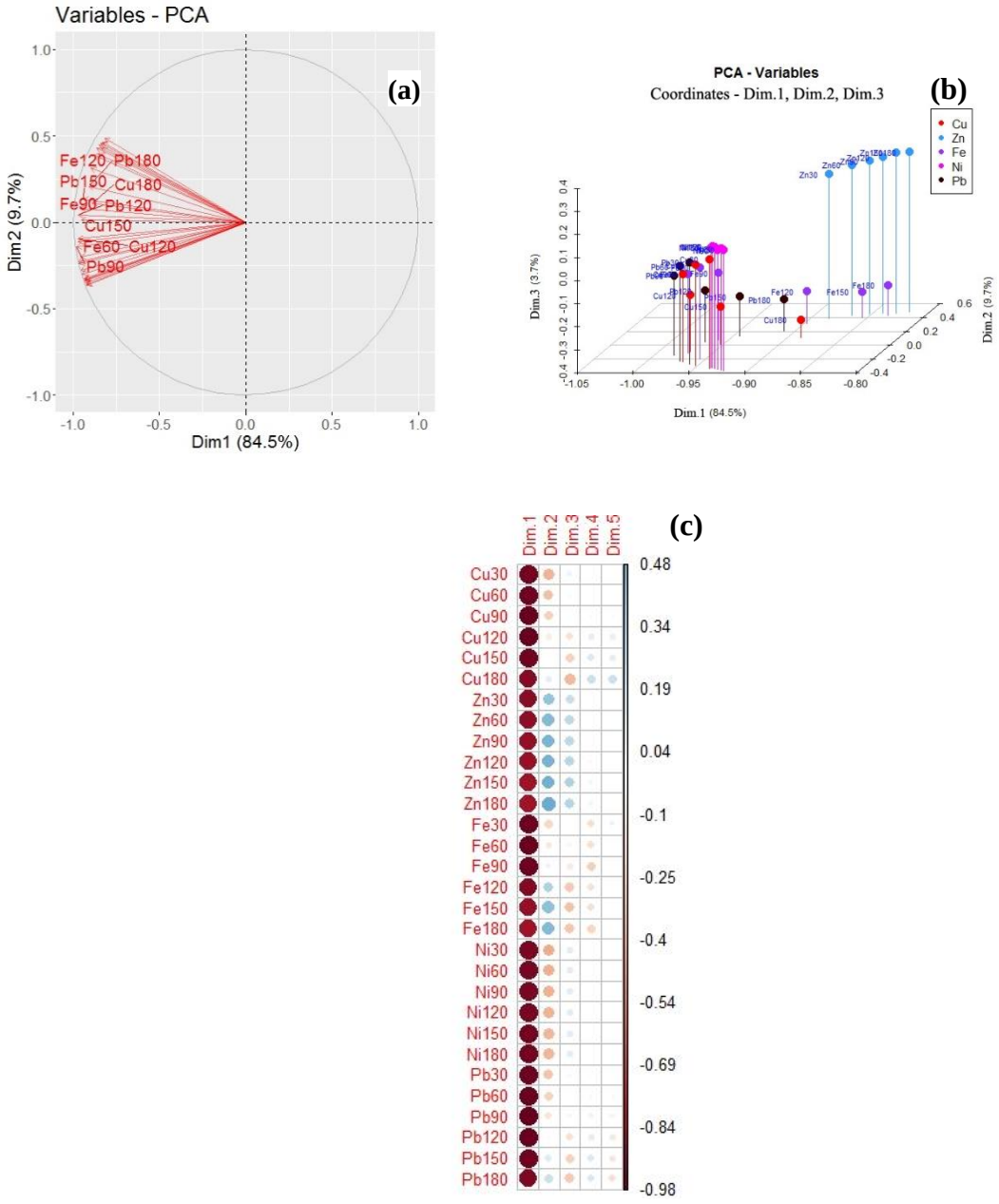

Figure 4.90 (a) Variable Coordinates Correlation Plot (time effect) (b) Variable Coordinates 3D Plot (time effect) (c) Variable Coordinates Dim Plot (time effect)

4.14.3 PCA Result for Variable Cos2 Quality of Representation in Time Effect

Figure 4.91 a shows the Cos2 plot of variable with the highest Cos2 value which are in orange while the mid cos2 variables value are in blue. The variables in orange are the most represented in the plot as they are closest to the circle of correlation with very high values and this is followed by the yellow and then the blue spots. All the variables indicated in this Cos2 plot **(Figure 4.91 a)** show very good representation for Dim.1 as all the variables are far from the centre of the circle and none is close to the centre of the circle. **Figure 4.91 b & c** shows another visualization of the Cos2 variables in the form of bar plots. We can see that the Cos2 variables for Dim.1 in **Figure 4.91 b** are the highest which also supports the fact that the quality of representation is good. The variables in the bar plots are arranged from highest to lowest. Consequently, all negative values have been cancelled out and **Figure 4.91 d** shows the Cos2 variables visualization with spots of different colour intensity. The strongest or darkest colour represent the highest Cos2 variables and the Cos2 variables decreased with decrease in the colour intensity of the spots in the visualization. We can see that Dim.1 variables showed the highest colour intensity and this was followed by Dim.2. In Dim.1 (**Figure 4.91 b**), the data visualized explains 84.5 % of the time effect experiment and the best five correlated variables were Pb90, Fe60, Cu120, Cu90 and Fe90. In Dim.2 (**Figure 4.91 c**), the visualized data explains 9.7 % of the time effect experiment and the best three represented variables were Zn180, Zn150 and Zn120.

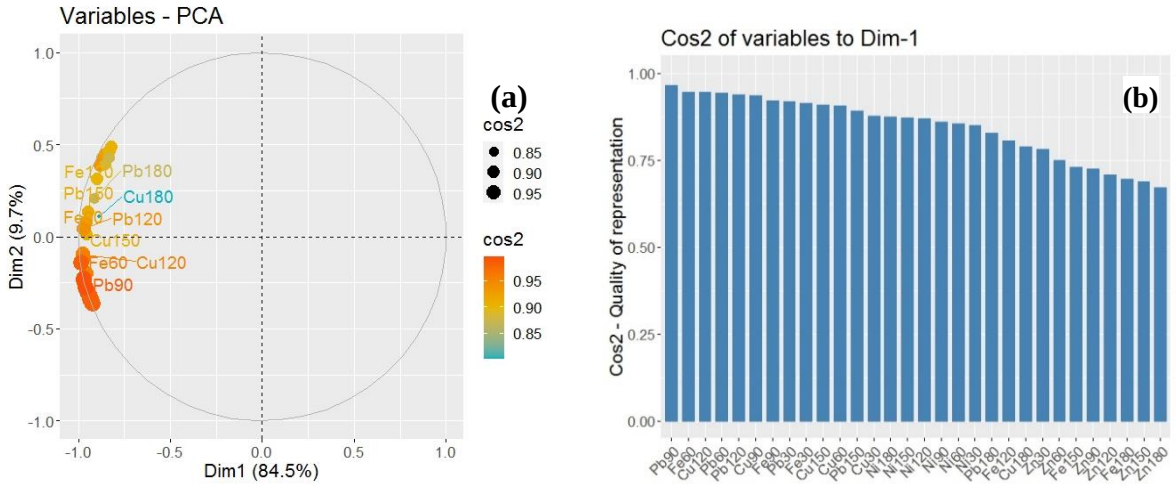

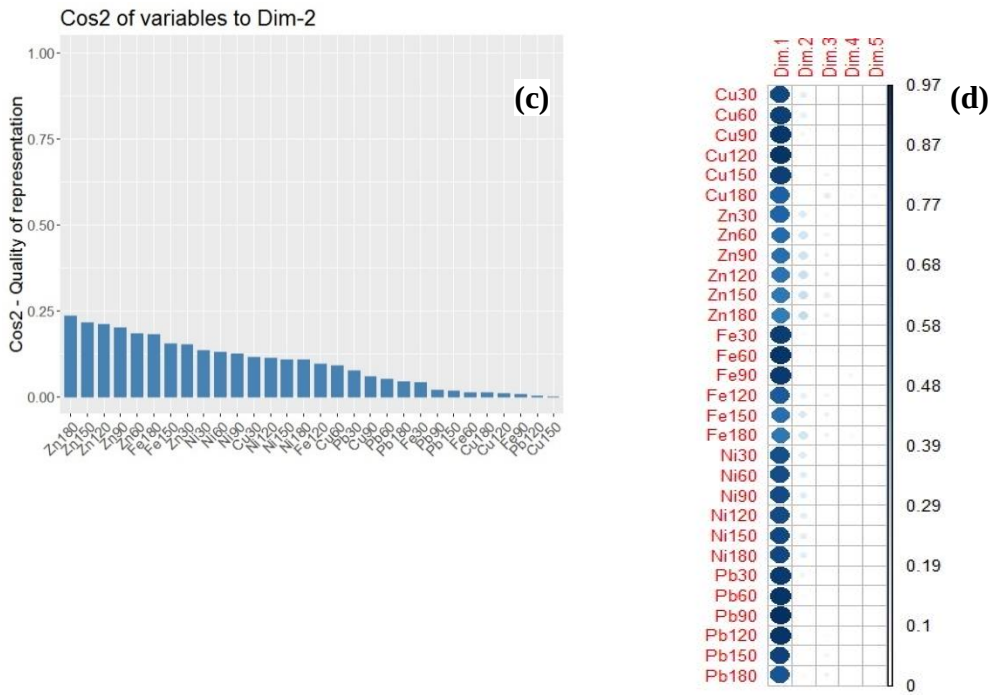

Figure 4.91 (a) Variable Cos2 quality of representation (time effect) (b) Dim.1 quality of representation (time effect) (c) Dim.2 quality of representation (time effect) (d) Cos2 quality of representation plot (time effect)

4.14.4 PCA Result for Variables Contribution in Time Effect

Figure 4.92 a shows the contribution of variable correlation plot with the most contributing variables indicated in red and the least contributing variables indicated in blue. From **Figure 4.92 b & c**, we can see the contribution of variables represented in bar plots with red dotted lines which indicates the expected average contribution. Dim.1 and Dim.2 are the most important to be considered in explaining the contribution while Dim.3, 4 & 5 are less important. In Dim.1 (**Figure 94 b**), most contribution of variables values were slightly above the expected average contribution. **Table 4.54** shows the actual values for contribution of variables and **Figure 4.92 d** shows the contribution of variables plot with spots of different colour intensity. The darker colours indicate higher contribution while the lighter color indicate low contribution. The contribution of variables for a particular dimension are measured in percentages. Correlated variables in the contribution of variables for Dim.1 & Dim.2 explains 84.5 % and 9.7 % respectively. Contributions from Dim.1 are the most important as they contribute more than other variables and this is followed by Dim.2. Even though the contributions from other dimensions are high (Dim.3, Dim.4 & Dim.5), they would not be considered since they are not as important as contributions from Dim.1 & 2.

The order of importance in the contribution for the dimensions are Dim.1 > Dim.2 > Dim.3 > Dim.4 > Dim.5. A variable with large contribution value contributes more to the component. Dim.1 which explains 84.5 % of the variation is represented in **Figure 4.92 b.** We can see the bar chart for Dim.1 contributions arranged in descending order and the best five contributing variables were Pb90(3.81 %), Fe60(3.73 %), Cu120(3.11 %), Cu90(3.69 %) and Fe90(3.63 %). Dim.2 which explains 9.7 % of the variation is represented in **Figure 4.92 c.** We can see the bar chart for Dim.2 contributions also arranged in descending order and the best three contributing variables were Zn180(8.10 %), Zn150(7.43 %) and Zn120(6.95 %). The best contributing variables for time effect from highest to lowest are in the order Pb90 > Fe60 > Cu120 > Cu90 > Fe90 > Zn180 > Zn150 > Zn120.

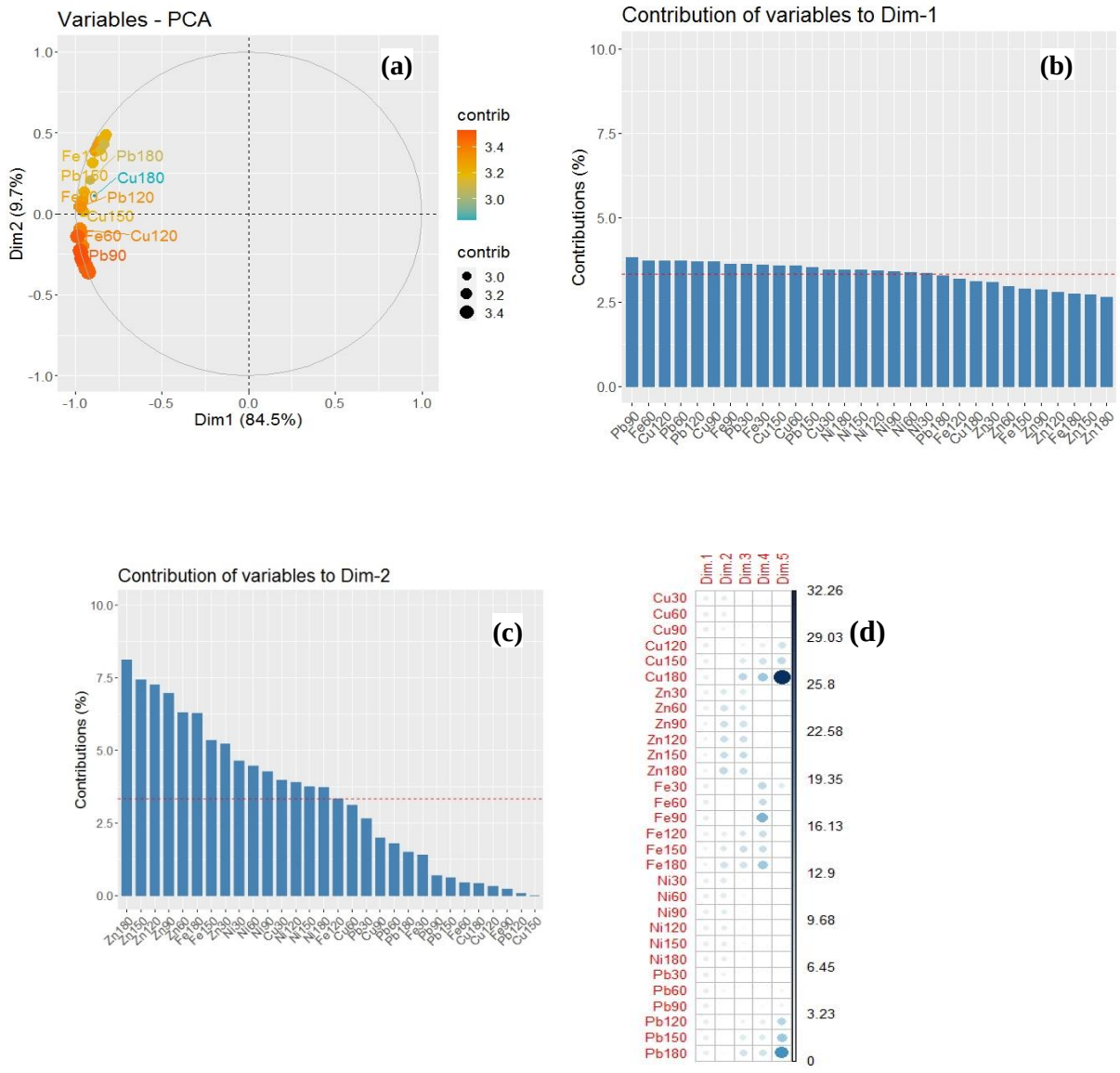

Figure 4.92 (a) Contribution of Variable Correlation Plot (time effect) (b) Dim.1 Contribution of Variable Bar Plots (time effect) (c) Dim.2 Contribution of Variable Bar Plots (time effect) (d) Variable Contribution Plot (time effect)

Table 4.54 Best Contributing Variables for Time Effect (in bold)

	Dim 1 (%)	Dim 2 (%)
Cu 90	**3.69**	1.99
Cu 120	**3.73**	0.32
Zn 120	2.79	**7.25**
Zn 150	2.71	**7.43**
Zn 180	2.64	**8.10**
Fe 60	**3.73**	0.43
Fe 90	**3.63**	0.23
Pb 90	**3.81**	0.69

4.14.5 PCA Result for Observation Coordinates in Time Effect

Figure 4.93 a shows the plot for the observation coordinates which are representing the position of the solvents used in time effect experiment for both the hotplate and microwave methods. **Figure 4.93 b - e** shows the three-dimensional plots of inorganic acids, organic acids, ionic liquid (a - c) and ionic liquid (d - g). Dim.1 on the x-axis, Dim.2 on the z-axis and Dim.3 on the y-axis. These three dimensional plots shows the coordinates or positioning of the solvents used for the time effect experiment. **Figure 4.94 a – d** shows the observation coordinate visualization plot for inorganic acids, organic acids, ionic liquid (a - c) and ionic liquid (d - g). In Dim.1, the observation coordinates for the inorganic acids all showed very good negative correlation. AQ1-6 (*aqua-regia*) had the strongest negative correlation values followed by NA1-3 (nitric acid) then HA 1-3 (hydrochloric acid). The strength of correlation can be seen on Dim.1 in **Figure 4.94 a** as very dark red colours. Dim.2 also had good positive and negative correlation between. The organic acid Dim.1 all showed strong positive correlation and the strength of correlation can be seen on Dim.1 in **Figure 4.94 b** while the Dim.2 showed good positive correlation. The coordinates in ionic liquids (a - c) seen in all showed strong positive correlation in Dim.1 and the strength of correlation can be seen on Dim.1 in **Figure 4.94 c** while Dim.2 showed strong negative correlations. The coordinates in ionic liquids (d - g) in all showed strong positive correlation in Dim.1 and the strength of correlation can be seen on Dim.1 in **Figure 4.94 d** while Dim.2 showed strong negative correlations.

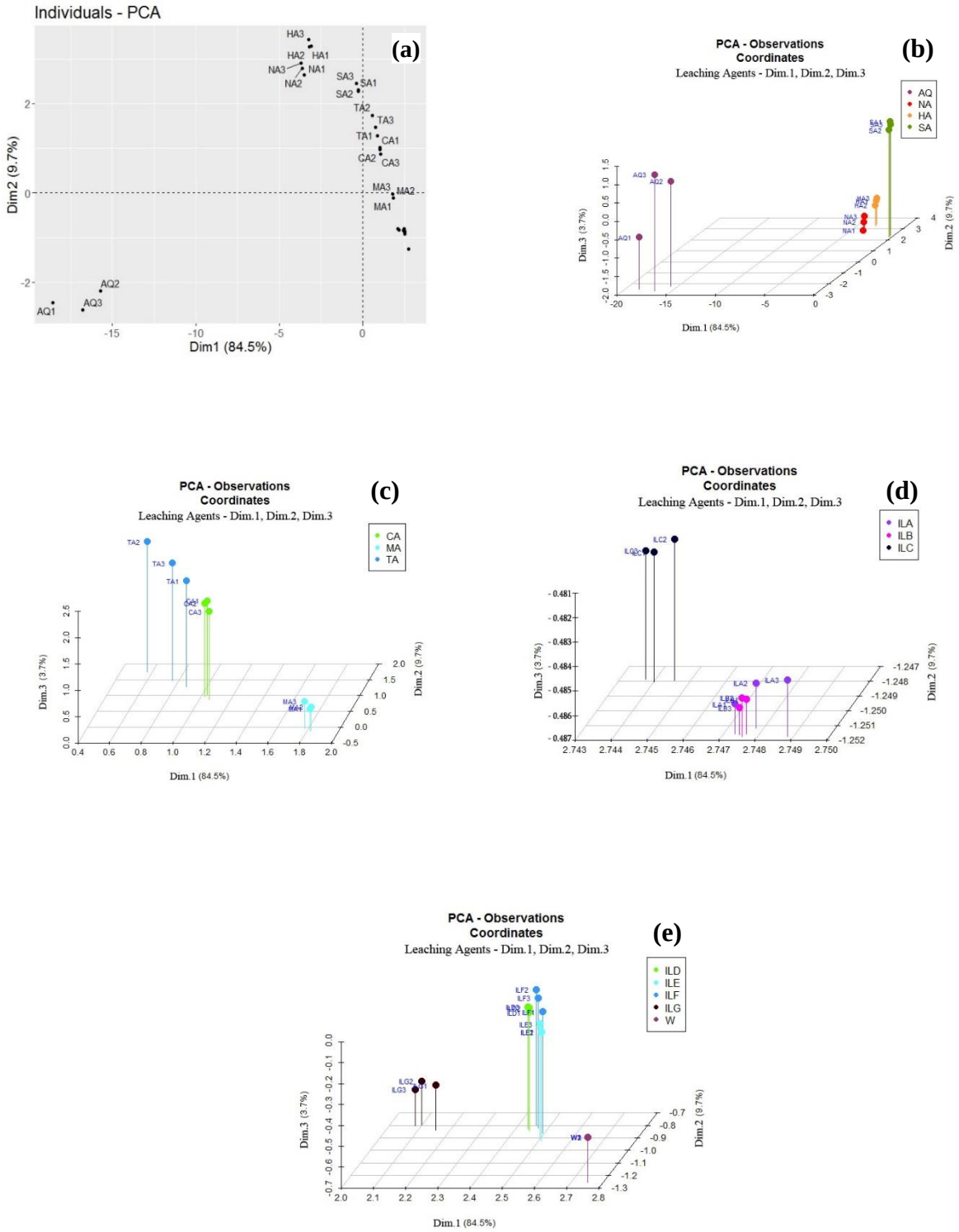

Figure 4.93 (a) observation coordinate correlation plot (time effect) (b) observation coordinate for inorganic acids (time effect) (c) observation coordinate for organic acids (time effect) (d) observation coordinate for IL a-c (time effect) (e) observation coordinate for IL d-g (time effect)

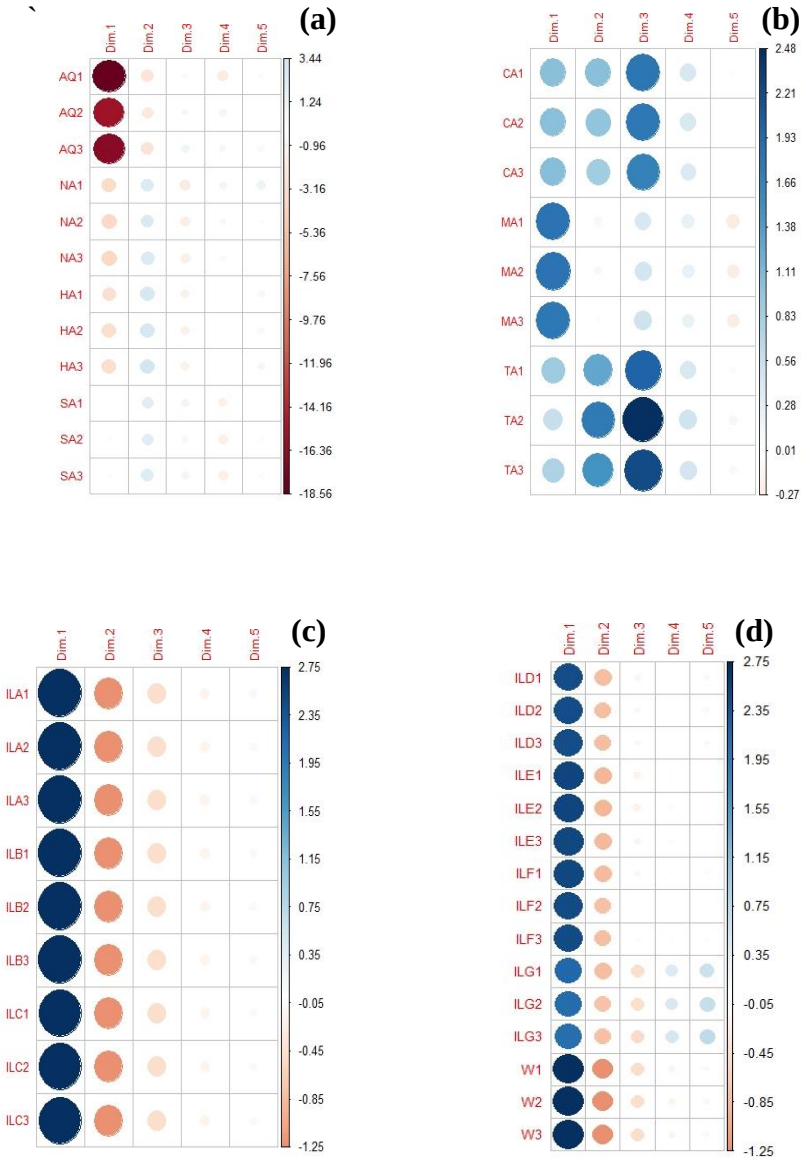

Figure 4.94 (a) Observation coordinate plot for inorganic acids (time effect) (b) observation coordinate plot for organic acids (time effect) (c) observation coordinate plot for IL a – c (time effect) (d) observation coordinate plot for IL d - g (time effect)

4.14.6 PCA Result for Observation Cos2 Quality of Representation in Time Effect

Figure 4.95 a shows the Cos2 plot of observation with the highest Cos2 value which are in orange while the mid cos2 observation value are in blue. The observations in orange are the most represented in the plot as they have very high values and this is followed by the yellow and then the blue spots. **Figure 4.95 b - e** shows the three-dimensional plots Cos2 observation for inorganic acids, organic acids, ionic liquid (a - c) and ionic liquid (d - g). Dim.1 on the x-axis, Dim.2 on the z-axis and Dim.3 on the y-axis. These three dimensional plots shows the coordinates or positioning of the solvents used for the time effect experiment.

Consequently, all negative values have been cancelled out and **Figure 4.96 a - d** shows the Cos2 observations visualization with spots of different colour intensity. The strongest or darkest colour represent the highest Cos2 observations and the Cos2 observations decreased with decrease in the colour intensity of the spots in the visualization. The quality of representation in Dim.1 (inorganic acids). AQ1-6 had good quality of representation (0.97) followed by NA1-3. The poorest quality of representation was in SA1 -3. In Dim.2 (inorganic acids), only moderate quality of representation were found in HA1-3 and SA1 - 3. The quality of representation with strong colour intensity can be seen in Dim.1 (**Figure 4.96 a**). In Dim.1 **Figure 4.96 b** (organic acids), only MA1-3 showed good quality of representation. In Dim.2 (organic acids), the only moderate quality of representation were found in TA1-3. Dim.1 **Figure 4.96 c** (IL (a - c)), showed good quality of representation. Dim.1 **Figure 4.96 d** (IL (d - g)), showed good quality of representation.

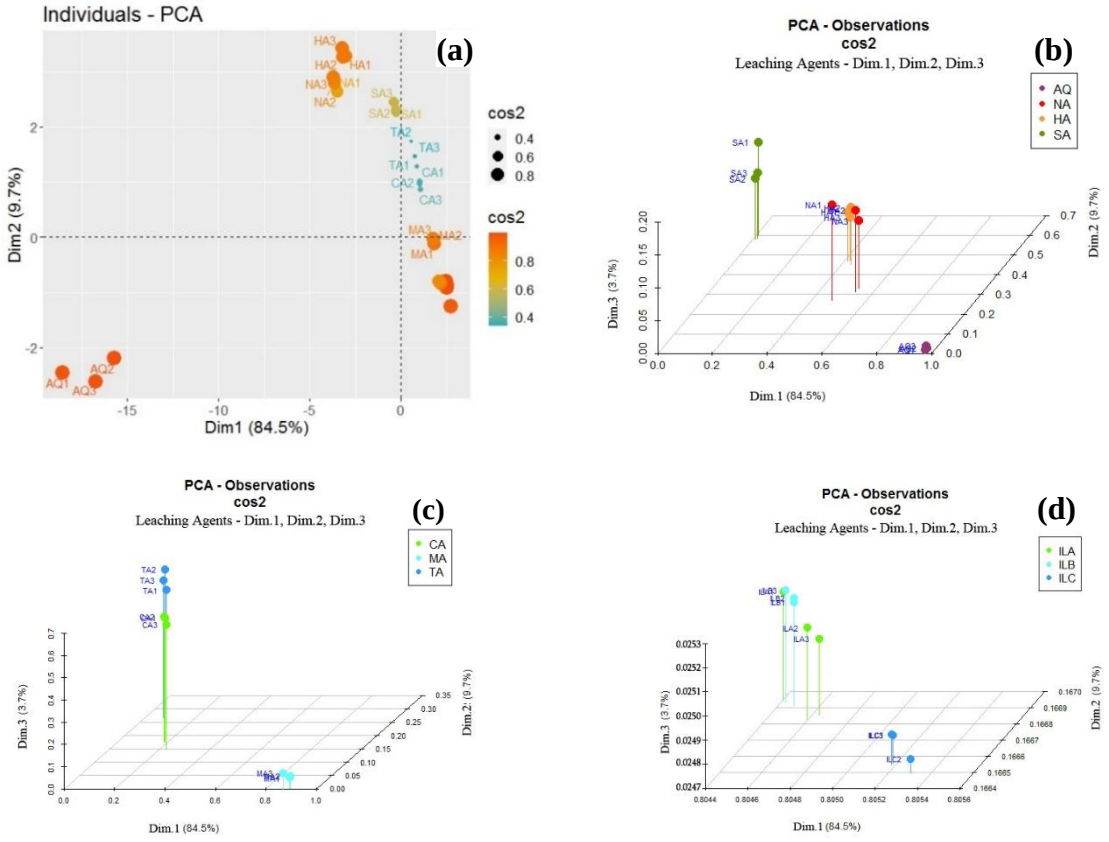

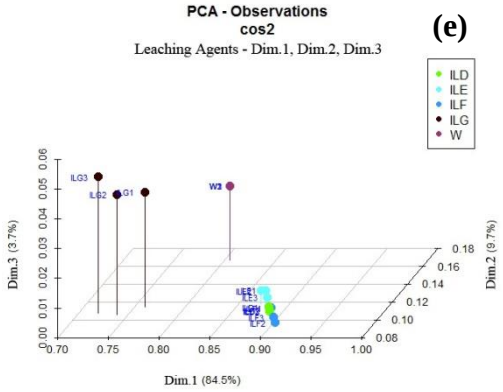

Figure 4.95 (a) Observation cos2 correlation plot (time effect) (b) Observation cos2 for inorganic acids (time effect) (c) Observation cos2 for organic acids (time effect) (d) Observation cos2 for IL a-c (time effect) (e) Observation cos2 for IL d-g (time effect)

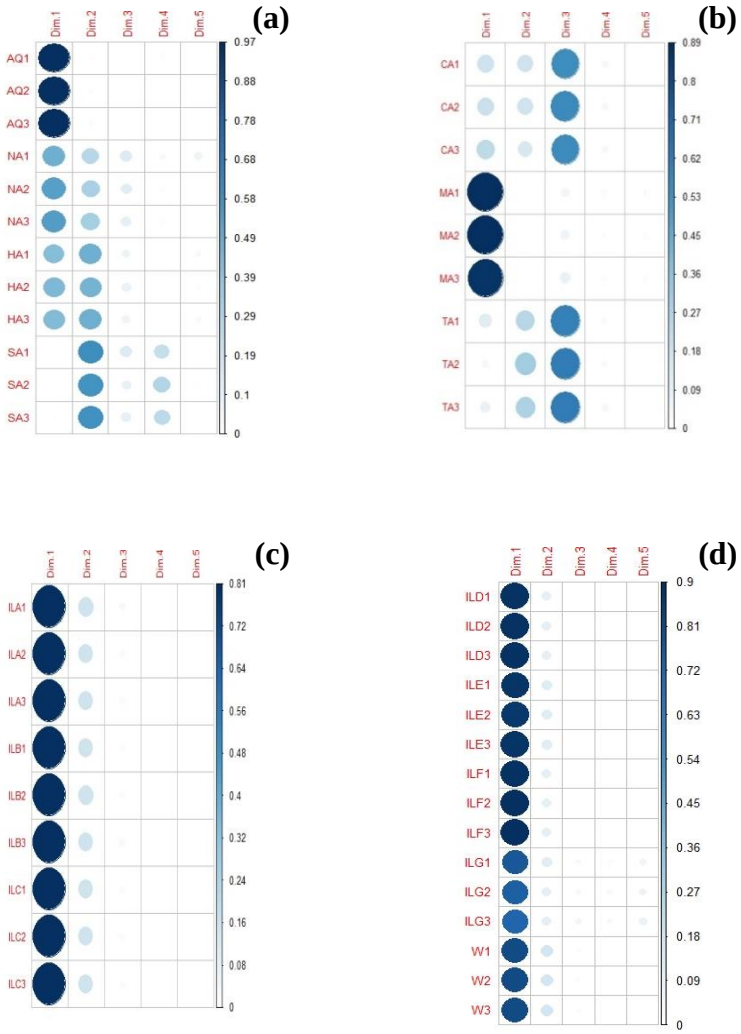

Figure 4.96: (a) Observation cos2 Dim plot for inorganic acids (time effect) (b) observation cos2 Dim plot for organic acids (time effect) (c) observation cos2 Dim plot for IL a – c (time effect) (d) observation cos2 Dim plot for IL d - g (time effect)

4.14.7 PCA Result for Observation Contribution in Time Effect

Figure 4.97 a shows the contribution plot of observation with the highest contribution values which are in orange while the mid contribution value are in blue. In the figure, more labelling priority is given to the highest contributing observation with the least contributing observations not appearing. The observations in orange are the most represented in the plot as they have very high values and this is followed by the yellow and then the blue spots. **Figure 4.97 b - e** shows the three-dimensional plots of observation contribution for inorganic acids, organic acids, ionic liquid (a - c) and ionic liquid (d - g). Dim.1 on the x-axis, Dim.2 on the z-axis and Dim.3 on the y-axis. These three dimensional plots shows the positioning of the solvents contribution on the plot. **Table 4.55** shows the observation contribution values in percentages. **Figure 4.98 a - d** shows the observation contribution visualization with spots of different colour intensity. The strongest or darkest colour represent the highest observation contribution and the observation contribution decreased with decrease in the colour intensity of the spots in the visualization. The observation contribution in Dim.1 for inorganic acids (**Table 4.53**), shows observation contribution and the best five were solvents that contributed to this Dim.1 were AQ1(30.19 %), AQ3(24.61 %), AQ2(21.63 %), NA3(1.21 %), NA2(1.16 %) and NA1(1.07 %). The other observations on Dim.1 were < 1.00 %. In Dim.2 (inorganic acids), the best three observation contributions were HA3(9.04 %), HA1(8.24 %) and HA2(8.20 %). The best observation contribution with strong colour intensity can be seen in Dim.1 (**Figure 4.98 a**). The best contributing solvents from highest to lowest are in the order AQ1 > AQ3 > AQ2 > NA3 > NA2 > NA1 > TA2 > TA3 > TA1. The observation in Dim.1 (organic acids) contributed (< 0.30 %) but in Dim.2 (organic acids), the highest contributors were in TA2(2.32), TA3(1.66) and TA1(1.26). The observation contributions with strong colour intensity can be seen in Dim.1 & 2 (**Figure 4.98 b**).

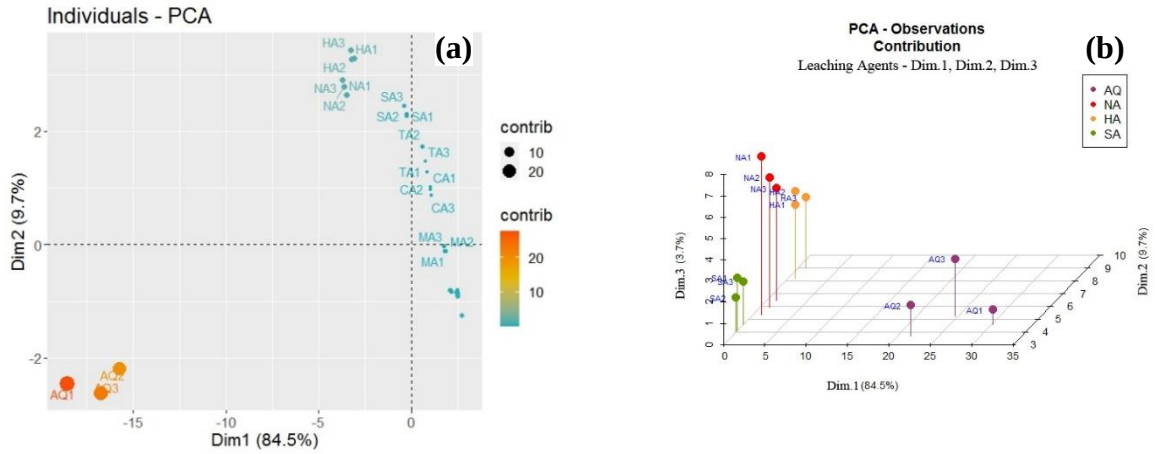

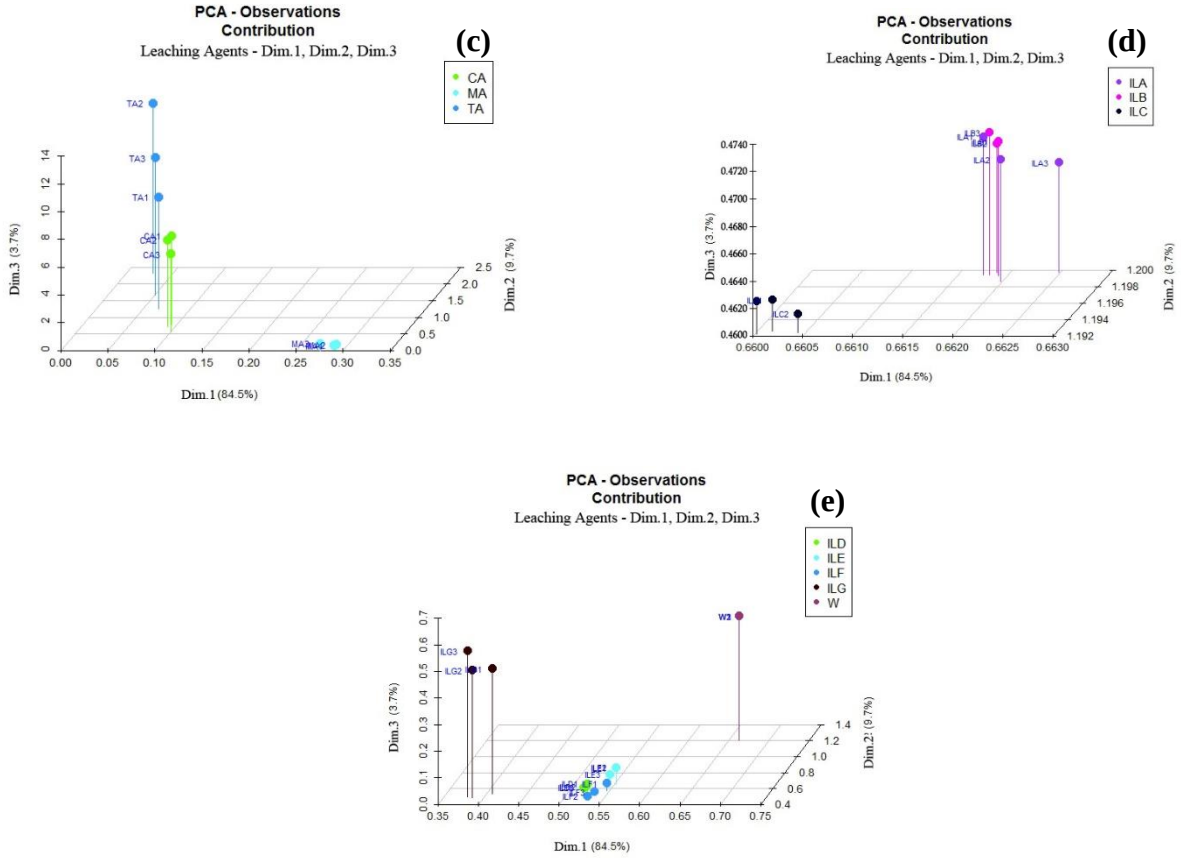

Figure 4.97: (a) Observation contribution plot (time effect) (b) Observation contribution for inorganic acids (time effect) (c) Observation contribution for organic acids (time effect) (d) Observation contribution for IL a-c (time effect) (e) Observation contribution for IL d-g (time effect)

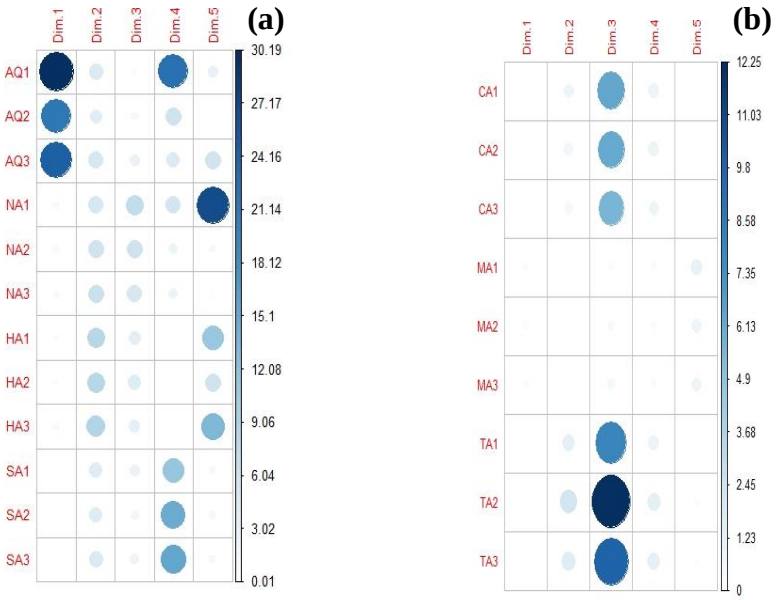

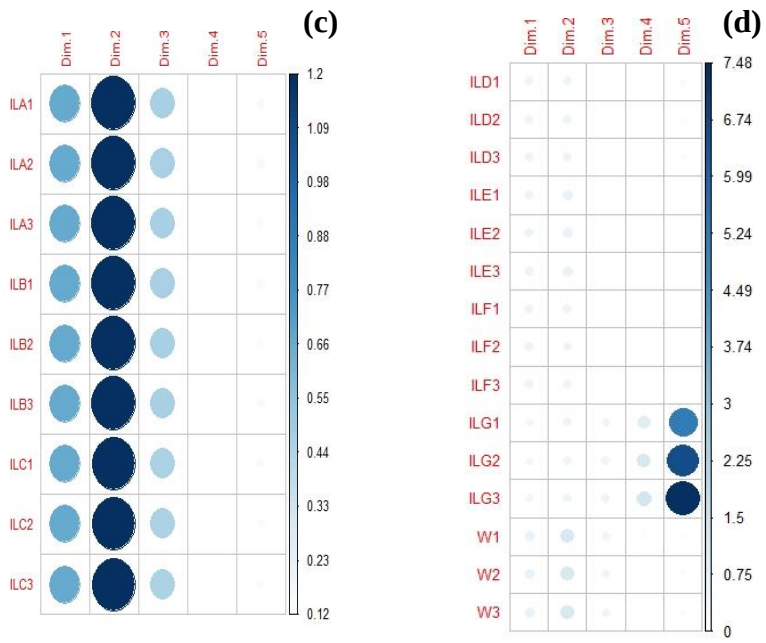

Figure 4.98: (a) Observation contribution Dim plot for inorganic acids (time effect) (b) observation contribution Dim plot for organic acids (time effect) (c) observation contribution Dim plot for IL a – c (time effect) (d) observation contribution Dim plot for IL d - g (time effect)

Table 4.55 Best Contributing Observations for Time Effect

	Dim 1 (%)	Dim 2 (%)
AQ1	**30.19**	4.60
AQ2	**21.63**	3.69
AQ3	**24.61**	5.26
NA1	**1.07**	5.34
NA2	**1.16**	5.96
NA3	**1.21**	6.46
HA1	0.83	**8.24**
HA2	0.90	**8.20**
HA3	0.93	**9.04**
TA1	0.07	1.26
TA2	0.03	2.32
TA3	0.05	1.66

4.15 Determination of concentration effect

Two methods, hotplate and microwave methods, were used to determine the effect of concentration. In order to extract the metals (Cu, Zn, Fe, Ni and Pb) different concentrations were used for inorganic acids (1, 2 & 3 mol/L), organic acids (15, 25 & 50 g/L) and the ionic liquids (50, 100 & 250 g/L). For the purpose of analysing the data, **Table 4.56** shows each of the solvents concentrations made into three groups (conc1, conc2 and conc3). Conc1 was the first group and it comprises the inorganic (1 mol/L), organic (15 g/L) and ionic liquids (50 g/L), conc2 was the second group and it comprises the inorganic (2 mol/L), organic (25 g/L) and ionic liquids (100 g/L) while conc3 was the third group and it comprises inorganic (3 mol/L), organic (50 g/L) and ionic liquids (250 g/L). For the hotplate method, the experimental conditions were particle-size (4 mm), time (120 minutes), temperature (70 ^{0}C), sample weight (0.5 g) and rotation speed (340 rpm). For the microwave method, the experimental conditions were particle-size (4 mm), time (20 minutes), temperature (150 ^{0}C) and sample weight (0.5 g). In this concentration experiment, *aqua-regia* concentration was not adjusted as it is a combination of NA and HA in a ratio of 1:3 and the experiment was conducted three different times. **Appendices 6 a - e** shows tables of the mean concentrations of extracted metals (Cu, Zn, Fe, Ni and Pb) in (mg/g) with three different experiments and the standard deviation as the error bar.

Table 4.56 Grouped concentrations

	Conc1	Conc2	Conc3
Inorganic acids	1 mol/L	2 mol/L	3 mol/L
Organic acids	15 g/L	25 g/L	50 g/L
Ionic liquids	50 g/L	100 g/L	250 g/L

4.15.1 Effect of concentration on Leaching Cu

Table 4.57 a shows the percentage extraction of Cu with different concentrations and this is also represented in **Figure 4.99**. In the hotplate method (**Figure 4.99**), the concentration increased from conc1 – conc3 Cu extraction increased for NA and IL-G except HA which decreased. The other solvents did not show much significant extractions. The peak extractions were NA (95 % at conc3), IL-G (85 % at conc3) and HA (16 % at conc1). The other solvents had < 2.5 % Cu extraction. In the microwave method (**Figure 4.99**), the

concentration increased from conc1 – conc3 the Cu extraction did not show any significant change in the leaching concentrations. The peak extraction for NA (48 % at conc3) and the other solvents had < 1.5 % Cu extraction.

Comparing the hotplate method with microwave method, two sample independent t-test was done for each of the solvents. The null hypothesis (H_0) stated that the mean of both methods are equal while the alternative hypothesis (H_1) stated that the mean of both methods are not equal. In **Table 4.57 b** it shows that at 95 % confidence level the independent t-test for NA, ILs G had p-values > 0.05 and this shows that the means for both methods are equal so the hotplate and microwave methods have the same efficiencies. However, HA had p-values < 0.05 meaning the hotplate method with the higher mean was better.

Table 4.57a Percentage concentration values for effect of concentration on leaching Cu

	Concentration	Extraction (%)													
		AQ	NA	HA	SA	CA	MA	TA	IL-A	IL-B	IL-C	IL-D	IL-E	IL-F	IL-G	W
Hotplate method	Conc1	100.00	51.51	15.45	0.23	1.00	1.01	0.90	0.04	0.01	0.01	0.19	2.15	0.10	21.54	0.00
	Conc2	100.00	70.33	13.52	0.49	1.05	0.98	0.86	0.04	0.03	0.01	0.17	2.11	0.32	26.92	0.00
	Conc3	100.00	95.05	9.75	1.23	1.10	0.94	0.82	0.10	0.04	0.02	0.13	0.32	0.48	84.62	0.00
Microwave method	Conc1	100.00	43.36	0.98	0.02	0.03	0.02	0.02	0.03	0.03	0.03	0.04	0.33	0.04	0.52	0.00
	Conc2	100.00	44.92	1.32	0.05	0.02	0.15	0.04	0.04	0.04	0.04	0.04	0.35	0.04	0.60	0.00
	Conc3	100.00	47.66	1.71	0.02	0.01	0.06	0.04	0.02	0.02	0.01	0.02	0.15	0.02	0.25	0.00

Where Conc1 = inorganic acid (1 M), organic acid (15 g/L) and ionic liquids (50 g/L), Conc2 = inorganic (2 M), organic (25 g/L) and ionic liquids (100 g/L), Conc3 = inorganic (3 M), organic (50 g/L) and ionic liquids (250 g/L).

Table 4.57b Independent t-test between hotplate and microwave methods at 95 % confidence level (concentration on Cu)

	NA	HA	IL-G
p-value	0.10	0.00	0.10
Hotplate Mean (%)	72.30	12.91	44.36
Microwave Mean (%)	45.31	1.34	0.46

Note: There were no t-tests for < 1.5 % extractions as they were considered insignificant

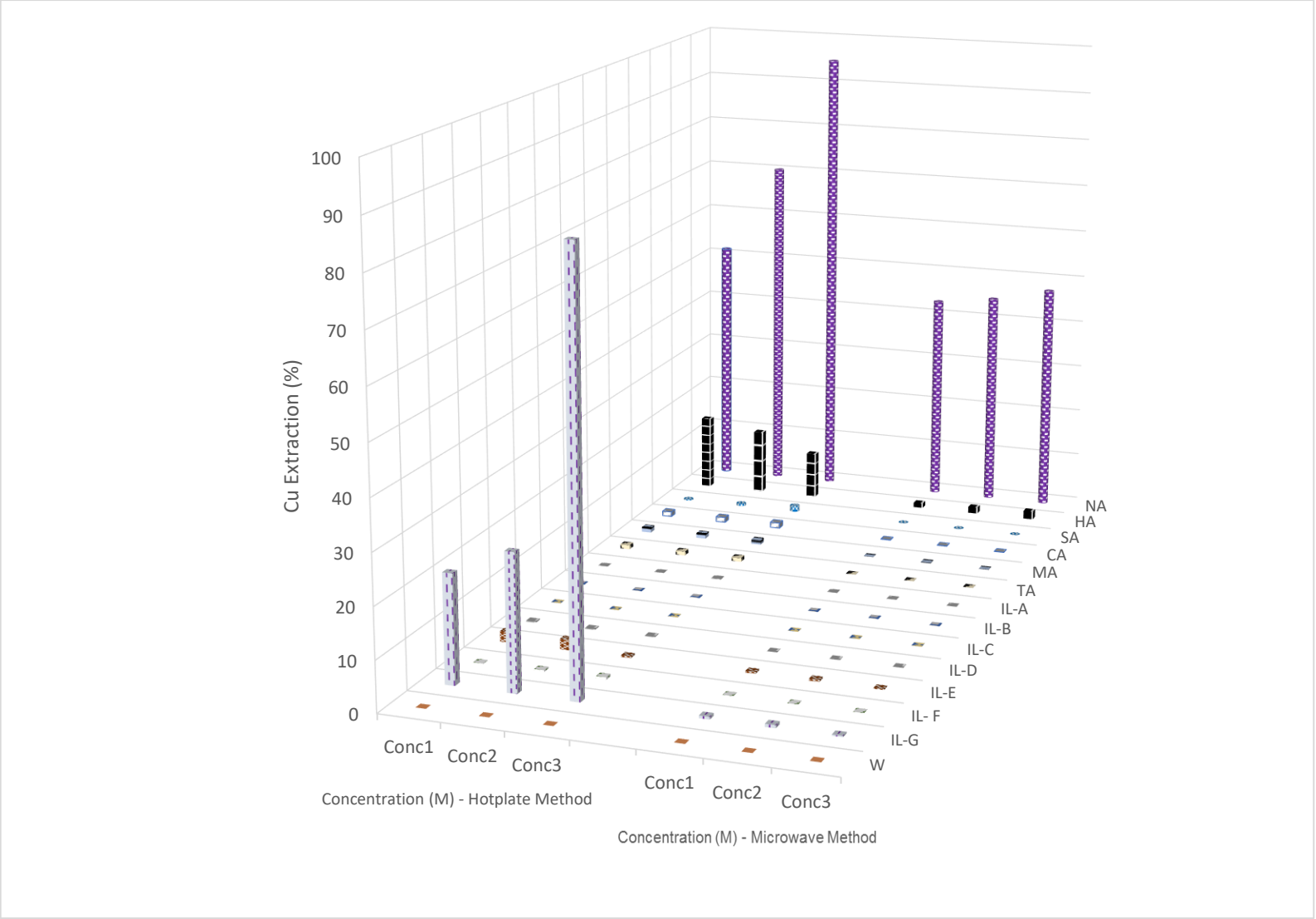

Figure 4.99 Percentage concentration for the effect of concentration on leaching Cu

4.15.2 Effect of concentration on Leaching Zn

Table 4.58 a shows the percentage extraction of Zn with concentration and this is also represented in **Figure 4.100**. In the hotplate method (**Figure 4.100**), the concentration increased from conc1 – conc3 the Zn extraction also increased except for malic acid which decreased. The peak extractions were NA (71 % at conc3), HA (67 % at conc3), SA (66 % at conc3), CA (55 % at conc3), TA (53 % at conc3), MA (36 % at conc1), ILs A-G were < 15 % extractions. In the microwave method (**Figure 4.100**), the concentration increased from conc1 – conc3 the Zn extraction increased for the inorganic acids while the other solvents peaked at conc2 and decreased. The peak extraction were NA (77 % at conc3), SA (76 % at conc3), HA (67 % at conc3), CA (19 % at conc2), TA (35 % at conc2), MA (23 % at conc1), IL-A (35 % at conc2), IL-B (44 % at conc2), IL-C (66 % at conc2), IL-D (65 % at conc2), IL-E (38 % at conc2), IL-F (61 % at conc2), IL-G (61 % at conc2).

Comparing the hotplate method with microwave method, two sample independent t-test was done for each of the solvents. The null hypothesis (H_0) stated that the mean of both methods are equal while the alternative hypothesis (H_1) stated that the mean of both methods are not equal. In **Table 4.58 b** it shows that at 95 % confidence level the independent t-test for for citric acid and tartaric acid had p-values < 0.05 and the hotplate method with higher mean was better while IL-A & IL-C also had p-values < 0.05 microwave method with higher mean was better. Consequently, other solvents had p-values > 0.05 and this shows that the means for both methods are equal so the hotplate and microwave methods have the same efficiencies.

Table 4.58a Percentage concentration values for effect of concentration on leaching Zn

	Concentration	Extraction (%)													
		AQ	NA	HA	SA	CA	MA	TA	IL-A	IL-B	IL-C	IL-D	IL-E	IL-F	IL-G	W
Hotplate method	Conc1	100.00	57.97	65.45	62.32	26.96	35.75	43.91	0.03	0.02	0.11	8.21	5.22	7.15	8.99	0.01
	Conc2	100.00	61.84	66.12	60.39	55.07	29.95	46.96	0.03	0.02	0.11	8.99	7.61	8.89	10.24	0.01
	Conc3	100.00	70.53	66.67	65.70	55.07	26.09	53.48	0.03	0.02	0.11	10.72	10.92	14.01	10.63	0.01
Microwave method	Conc1	100.00	57.30	40.11	48.90	16.55	22.92	22.16	24.45	28.52	40.75	38.96	26.49	39.47	43.29	0.00
	Conc2	100.00	66.21	57.56	66.21	19.10	21.01	34.63	34.97	44.14	66.21	64.52	37.69	61.12	60.78	0.00
	Conc3	100.00	76.91	67.23	76.40	6.73	3.46	4.98	8.27	8.53	13.97	13.65	7.63	12.82	13.40	0.00

Where Conc1 = inorganic acid (1 M), organic acid (15 g/L) and ionic liquids (50 g/L), Conc2 = inorganic (2 M), organic (25 g/L) and ionic liquids (100 g/L), Conc3 = inorganic (3 M), organic (50 g/L) and ionic liquids (250 g/L).

Table 4.58b Independent t-test between hotplate and microwave methods at 95 % confidence level (concentration on Zn)

	NA	HA	SA	CA	MA	TA	IL-A	IL-B	IL-C	IL-D	IL-E	IL-F	IL-G
p-value	0.65	0.22	0.91	0.04	0.10	0.04	0.04	0.06	0.06	0.11	0.15	0.12	0.10
Hotplate Mean (%)	63.45	66.51	62.80	45.70	30.60	48.12	0.03	0.02	0.11	9.31	7.92	10.02	9.95
Microwave Mean (%)	66.81	54.97	63.84	14.13	15.80	20.59	22.56	27.06	40.31	39.04	23.94	37.80	39.16

Note: There were no t-tests for < 0.5 % extractions as they were considered insignificant

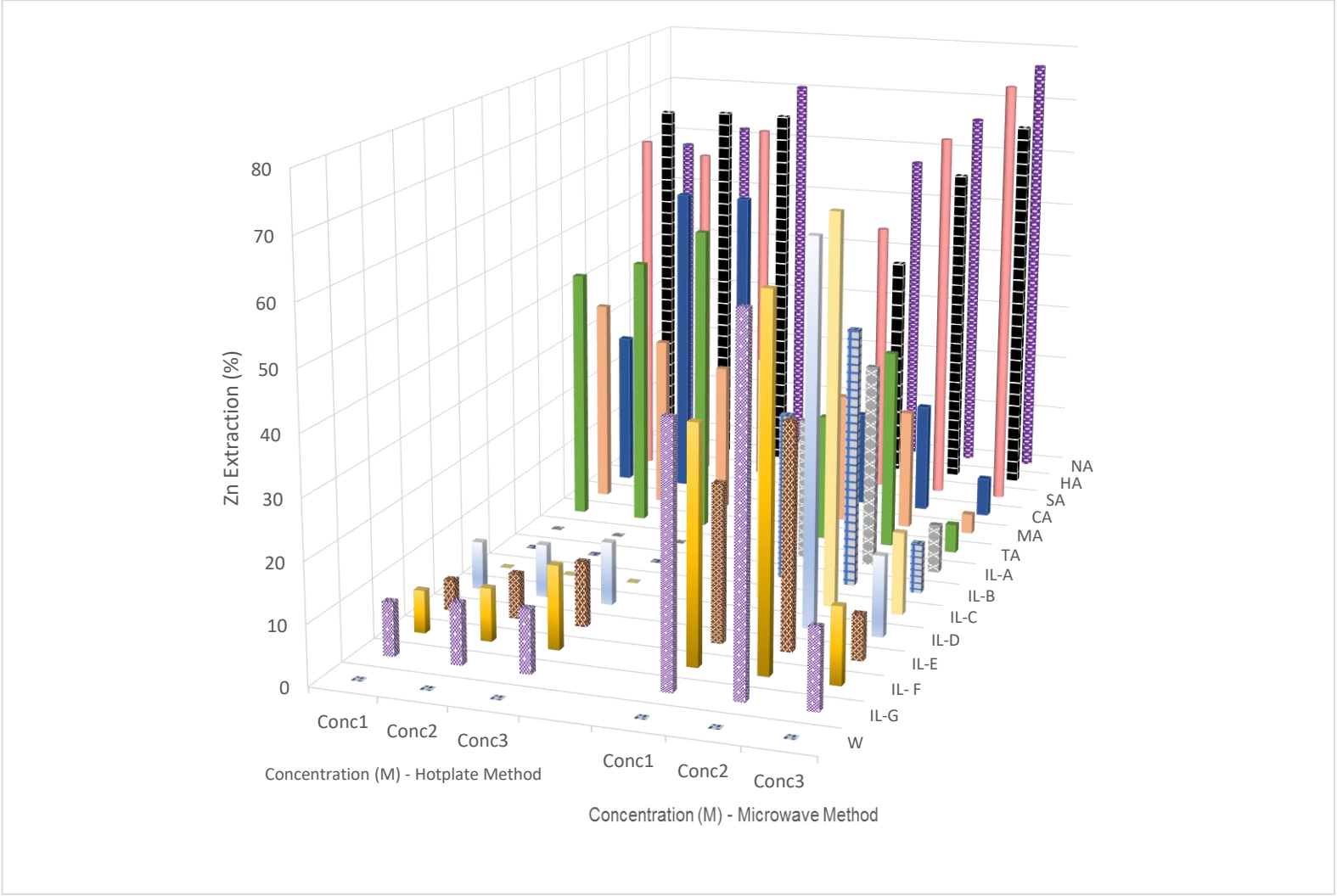

Figure 4.100 Percentage concentration for the effect of concentration on leaching Zn

4.15.3 Effect of concentration on Leaching Fe

Table 4.59 a shows the percentage extraction of Cu with concentration and this is also represented in **Figure 4.101**. In the hotplate method (**Figure 4.101**), the concentration increased from conc1 – conc3 the Fe extractions for the inorganic acids also increased. The solvents peak extractions were NA (89 % at conc3), HA (89 % at conc3), SA (78 % at conc3). The other solvents showed Fe extraction < 1.5 %. In the microwave method (**Figure 4.101**), the concentration increased from conc1 – conc3 the Fe extraction increased but HA peaked at conc2. The solvents peak extractions were NA (57 % at conc3), HA (62 % at conc2), SA (42 % at conc3). The other solvents had < 2.5 % Fe extraction.

Comparing the hotplate method with microwave method, two sample independent t-test was done for each of the solvents. The null hypothesis (H_0) stated that the mean of both methods are equal while the alternative hypothesis (H_1) stated that the mean of both methods are not equal. In **Table 4.59 b** it shows that at 95 % confidence level the independent t-test for NA, HA had p-values > 0.05 and this shows that the means for both methods are equal so the hotplate and microwave methods have the same efficiencies. However, SA had p-value < 0.05 showing that the means of both methods are not equal therefore the hotplate method was better for SA.

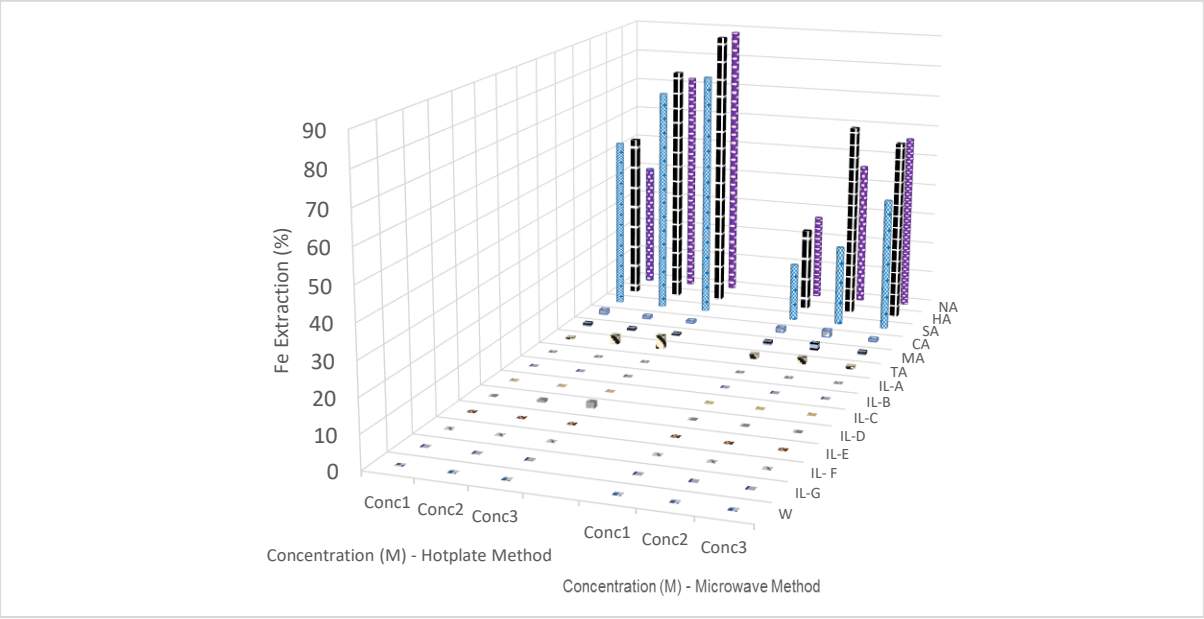

Figure 4.101 Percentage concentration for the effect of concentration on leaching Fe

Table 4.59a Percentage concentration values for effect of concentration on leaching Fe

	Concentration	Extraction (%)														
		AQ	NA	HA	SA	CA	MA	TA	IL-A	IL-B	IL-C	IL-D	IL-E	IL-F	IL-G	W
Hotplate method	Conc1	100.00	39.77	53.03	54.55	1.44	1.15	0.56	0.00	0.00	0.00	0.00	0.00	0.00	0.00	0.00
	Conc2	100.00	72.47	76.77	72.12	0.82	0.96	2.87	0.00	0.00	0.00	0.70	0.00	0.00	0.00	0.00
	Conc3	100.00	88.89	89.24	78.38	0.77	0.70	4.29	0.00	0.00	0.00	1.80	0.00	0.00	0.07	0.00
Microwave method	Conc1	100.00	27.42	26.38	18.44	1.45	1.25	1.60	0.01	0.01	0.01	0.01	0.01	0.01	0.01	0.00
	Conc2	100.00	46.10	62.03	25.59	2.10	2.22	2.10	0.01	0.01	0.01	0.01	0.01	0.01	0.01	0.00
	Conc3	100.00	56.55	57.92	42.24	0.87	1.09	0.93	0.00	0.00	0.00	0.00	0.00	0.00	0.00	0.00

Where Conc1 = inorganic acid (1 M), organic acid (15 g/L) and ionic liquids (50 g/L), Conc2 = inorganic (2 M), organic (25 g/L) and ionic liquids (100 g/L), Conc3 = inorganic (3 M), organic (50 g/L) and ionic liquids (250 g/L).

Table 4.59b Independent t-test between hotplate and microwave methods at 95 % confidence level (concentration on Fe)

	NA	HA	SA
p-value	0.23	0.19	0.017
Hotplate Mean (%)	67.04	73.01	68.35
Microwave Mean (%)	43.36	48.78	28.76

Note: There were no t-tests for < 5.0 % extractions as they were considered insignificant

4.15.4 Effect of concentration on Leaching Ni

Table 4.60 a shows the percentage extraction of Ni with concentration and this is also represented in **Figure 4.102**. In the hotplate method (**Figure 4.102)**, the concentration increased from conc1 – conc2 the Ni extraction decreased in HA while NA and SA did not show any significant change. The solvents peak extractions were NA (6 % at conc1), HA (15 % at conc1), SA (2 % at conc2). The other solvents were < 2 %. In the microwave method (**Figure 4.102)**, the concentration increased from conc1 – conc2 the Ni extraction increased in NA while Ni extraction in HA and SA did not show any significant change. The solvents peak extractions were NA (15 % at conc3), HA (4 % at conc2) and SA (5 % at conc3). The solvents were < 1.0 %.

Comparing the hotplate method with microwave method, two sample independent t-test was done for each of the solvents. The null hypothesis (H_0) stated that the mean of both methods are equal while the alternative hypothesis (H_1) stated that the mean of both methods are not equal. In **Table 4.60 b** it shows that at 95 % confidence level the independent t-test for NA, HA & SA had p-values > 0.05 and this shows that the means for both methods are equal so the hotplate and microwave methods have the same efficiencies.

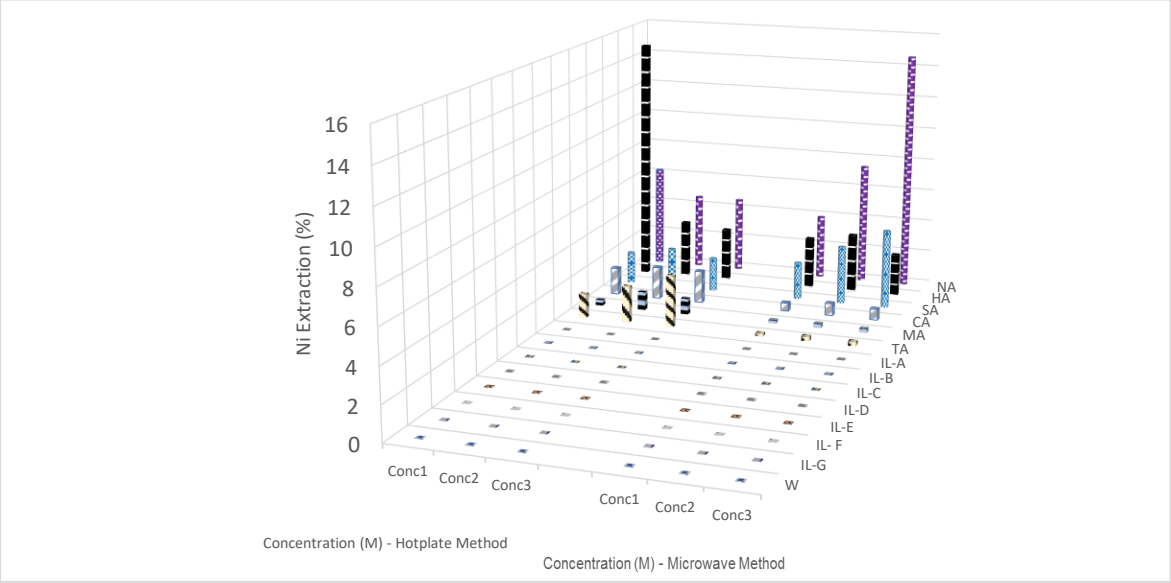

Figure 4.102 Percentage concentration for the effect of concentration on leaching Ni

Table 4.60a Percentage concentration values for effect of concentration on leaching Ni

	Concentration	Extraction (%)														
		AQ	NA	HA	SA	CA	MA	TA	IL-A	IL-B	IL-C	IL-D	IL-E	IL-F	IL-G	W
Hotplate method	Conc1	100.00	6.25	14.95	1.96	1.65	0.35	1.47	0.00	0.01	0.01	0.01	0.01	0.01	0.01	0.01
	Conc2	100.00	4.66	3.55	2.45	1.96	1.13	2.21	0.00	0.01	0.01	0.01	0.01	0.01	0.01	0.01
	Conc3	100.00	4.66	3.31	2.08	1.96	0.98	3.13	0.00	0.01	0.01	0.01	0.01	0.01	0.01	0.01
Microwave method	Conc1	100.00	3.98	3.21	2.29	0.49	0.18	0.17	0.01	0.01	0.01	0.01	0.01	0.01	0.01	0.01
	Conc2	100.00	7.50	3.67	3.57	0.73	0.26	0.28	0.01	0.01	0.01	0.01	0.01	0.01	0.01	0.01
	Conc3	100.00	14.69	2.65	4.82	0.66	0.24	0.27	0.01	0.01	0.01	0.01	0.01	0.01	0.01	0.01

Where Conc1 = inorganic acid (1 M), organic acid (15 g/L) and ionic liquids (50 g/L), Conc2 = inorganic (2 M), organic (25 g/L) and ionic liquids (100 g/L), Conc3 = inorganic (3 M), organic (50 g/L) and ionic liquids (250 g/L).

Table 4.60b Independent t-test between hotplate and microwave methods at 95 % confidence level (concentration on Ni)

	NA	HA	SA
p-value	0.33	0.35	0.13
Hotplate Mean (%)	5.19	7.27	2.16
Microwave Mean (%)	8.72	3.18	3.56

Note: There were no t-tests for < 3.0 % extractions as they were considered insignificant

4.15.5 Effect of concentration on Leaching Pb

Table 4.61 a shows the percentage extraction of Pb with concentration and this is also represented in **Figure 4.103**. In the hotplate method (**Figure 4.103)**, the concentration increased from conc1 - conc2 the Pb extraction increased for NA and HA. The solvents peak extractions were NA (59 % at conc3) and HA (67 % at conc3) while the other solvents all showed < 5 %. In the microwave method **(Figure 4.103)**, the concentration increased from conc1 - conc2 the Pb extraction increased. The solvents peak extractions were NA (68 % at conc3) and HA (37 % at conc3) while the other solvents all showed < 1 %.

To compare the hotplate method with microwave method, two sample independent t-test was done for each of the solvents. The null hypothesis (H_0) stated that the mean of both methods are equal while the alternative hypothesis (H_1) stated that the mean of both methods are not equal. In **Table 4.61 b** it shows that at 95 % confidence level the independent t-test had p-values > 0.05 and this shows that the means for both methods are equal so the hotplate and microwave methods have the same efficiencies.

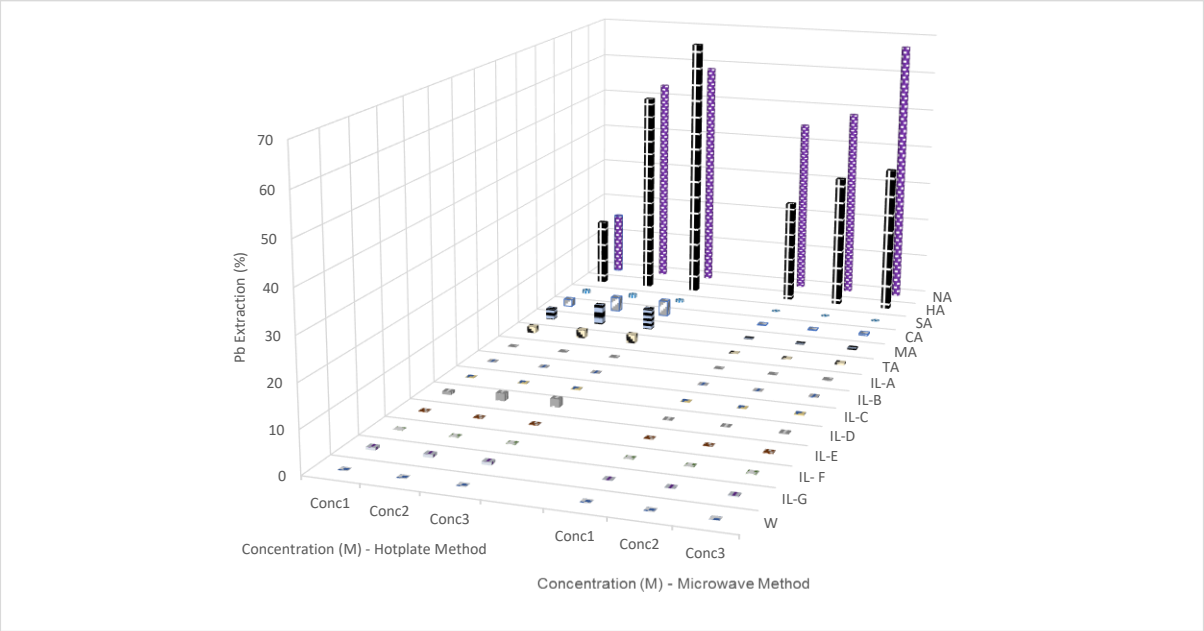

Figure 4.103 Percentage concentration for the effect of concentration on leaching Pb

Table 4.61a Percentage concentration values for effect of concentration on leaching Pb

	Concentration	Extraction (%)														
		AQ	NA	HA	SA	CA	MA	TA	IL-A	IL-B	IL-C	IL-D	IL-E	IL-F	IL-G	W
Hotplate method	Conc1	100.00	15.66	16.84	0.84	1.79	2.76	1.61	0.08	0.08	0.08	0.67	0.14	0.12	0.61	0.05
	Conc2	100.00	53.57	52.04	0.92	3.57	5.00	2.07	0.12	0.11	0.12	1.80	0.15	0.12	0.67	0.05
	Conc3	100.00	58.93	67.35	0.61	3.88	5.31	2.22	0.11	0.11	0.11	1.96	0.17	0.13	0.65	0.05
Microwave method	Conc1	100.00	45.00	26.25	0.08	0.13	0.10	0.12	0.08	0.08	0.08	0.08	0.08	0.08	0.08	0.05
	Conc2	100.00	48.75	33.91	0.08	0.14	0.14	0.13	0.08	0.08	0.08	0.08	0.08	0.08	0.08	0.05
	Conc3	100.00	67.50	37.19	0.08	0.41	0.41	0.47	0.22	0.22	0.22	0.22	0.22	0.22	0.22	0.05

Where Conc1 = inorganic acid (1 M), organic acid (15 g/L) and ionic liquids (50 g/L), Conc2 = inorganic (2 M), organic (25 g/L) and ionic liquids (100 g/L), Conc3 = inorganic (3 M), organic (50 g/L) and ionic liquids (250 g/L).

Table 4.61b Independent t-test between hotplate and microwave methods at 95 % confidence level (concentration on Pb)

	NA	HA
p-value	0.51	0.45
Hotplate Mean (%)	42.72	45.41
Microwave Mean (%)	53.75	32.45

Note: There were no t-tests for < 6.0 % extractions as they were considered insignificant

4.16 PCA for Concentration Effect

4.16.1 PCA Scree Plot for Concentration Effect

The concentration effect experiment involved 15 variables and 90 observations. The variables were made up of five metals (Cu, Zn, Fe, Ni and Pb) with each of these metals having results from six different expriments on effect of concentrations (inorganic acids (1, 2 & 3 M), organic acids (15, 25 & 50 g/L) and the ionic liquids (50, 100 & 250 g/L)). The observations were results from each of the fifteen solvents with three replicates each from the hotplate and microwave methods used in the experiment. **Table 4.62** shows the summarized data of the first six principal components extracted both the hotplate and microwave methods (mg/g) in **Appendices 6 a – e**. **Figure 4.104** shows the scree plot of variance for the dimensions from concentration effect data and they are in the order of highest to the lowest with Dim.1 as 67.1, Dim.2 as 19.9 % and Dim.3 as 7.5 %. From this scree plot we can infer that Dim.1 explains the most part of the concentration effect data as it is larger than the other dimensions. From **Table 4.62**, we can see that Dim.1, 2 & 3 showed a SD > 1.0 as SD = 1 is the cutoff point. Therefore, we can accept the first three dimensions (Dim.1, 2 & 3) with a proportion of variance of 67.1, 19.9 and 7.5 % respectively. Consequently, the cumulative proportion in Dim.1, 2 & 3 also showed 67.1, 87.0 and 94.5 % respectively. This shows that with Dim.3 having a SD of 1.1, about 94.5 % of the data can be accounted for while the remaining 5.5 % of the data can be disregarded as they fall below SD < 1.0.

Table 4.62 Summarized principal components for concentration effect

Principal Components	Dim.1	Dim.2	Dim.3	Dim.4	Dim.5	Dim.6
Standard deviation	3.172	1.730	1.059	0.679	0.473	0.216
Proportion of Variance	0.671	0.199	0.075	0.031	0.015	0.003
Cumulative Proportion	0.671	0.870	0.945	0.976	0.991	0.994

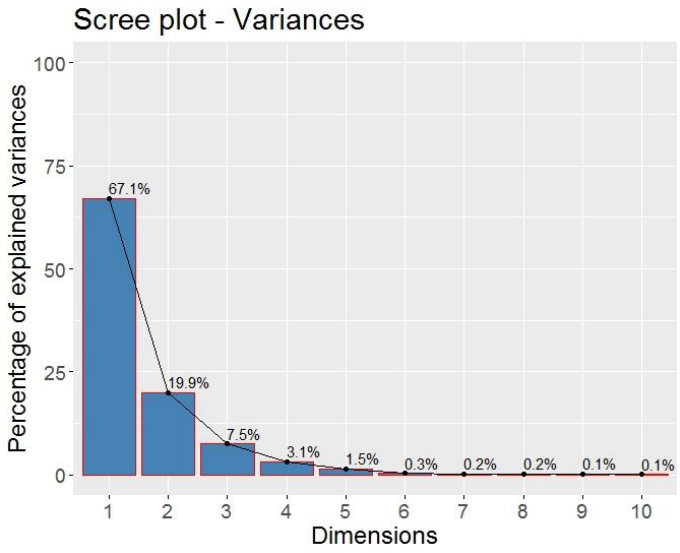

Figure 4.104 Scree plot for concentration effect

Figure 4.105 shows the biplot for concentration effect data which is the relationship between the variables and the observations in the concentration data. It also shows the structure of variables correlations and clustered observations. From the PCA plot, we can see the variables with the longest vector projections. They represent the highest variations in the data and they have occured in Pb_conc1, Pb_conc2, Pb_conc3, Zn_conc2 and Zn_conc1. The replicate observations formed clusters, for example, in the hotplate method (1, 2 & 3) the observations AQ1, AQ2 & AQ3 which represents the hotplate result for *aqua-regia* formed a cluster. This clustering also occurred in the microwave method (4, 5 & 6) the observations AQ4, AQ5 & AQ6. This means that the three replicated experiments showed similarity in the result from concentration effect. Also, this behaviour was observed in other observations showing that the replicated results were similar. The *aqua-regia* observations AQ1-3 and AQ4-6 are considered outliers on the PCA as their clusters were clearly outside the group clustering (in red and blue) and also far away from the other observations. However, they were not treated as outliers or removed as they were needed in this research inorder to clearly differentiate the best performing solvents or observations. Other observation clusters were seen in (NA1, NA2 & NA3), (HA1, HA2 & HA3), (SA1, SA2 & SA3). The above stated clusters had various degrees of euclidean distance (distance between observations) and the observations from *aqua-regia* (AQ1-3 and AQ4-6) were the farthest. Consequently, the organic acids and ionic liquids all seemed to have clustered together as their euclidean distance were relatively close.

We can see that more than half of the variables vectors were pointing towards AQ1-3 and the others pointing towards AQ4-6. This shows a high degree of association between the variables and those observations but the reverse was the case for the other observations such as the other organic acids and ionic liquids as the PCA plot (**Figure 4.105**) clearly shows the variable vectors pointing away from them and this implies very low association between the variables and these observations. Also, as more than half of the variables were pointing towards the hotplate method (red) it showed that there was high variable association with the hotplate method except for the varibles, Ni_conc3 and Ni_conc2, which were poitning away. Consequently, all the variables pointing towards the microwave method (blue) showed that there was high variable association between those variables and the microwave method. The variable vectors closest to each other showed high correlation amongst themselves, for example, Pb_conc1 and Pb_conc2, Cu_conc1 and Cu_conc2 formed angles around 30 degrees. No correlation was observed in Fe_conc2 and Pb_conc1, Pb_conc3 and Zn_conc1 as their vectors formed angle 90 degrees. The x-axis which is Dim.1 (67.1 % of variation explained) shows that all the variable vectors are positioned on the left side of the plot thereby revealing negative correlation for all variables. So we would expect that the lower the values of Dim.1 the higher high values for each of the variables. The y-axis which is Dim.2 (19.9 % of variation explained) shows that less than half of the variables positioned at the top were positive correlation and more than half of the variables positioned at the bottom were negative correlation (Kohla & Luniak, 2005; Reris & Brooks, 2015; Statisticshowto, 2021; STHDA, 2021; Towardsdatascience, 2021).

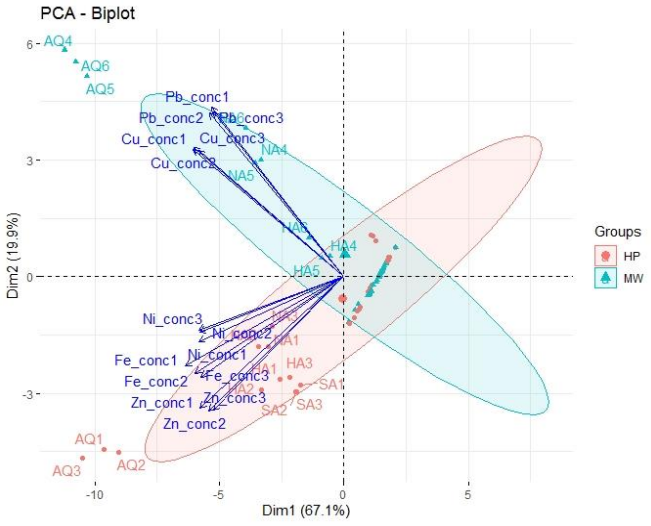

Figure 4.105 Biplot for concentration effect

4.16.2 PCA Result for Variable Coordinates in Concentration Effect

Figure 4.106 a shows the plot for the variable coordinates for Dim.1 & 2 which are representing the position of the concentration effect variables on the plot. The coordinates are correlation between a variable and a dimension. The variables have high negative correlation values as the fall around the circumference on the left side of the plot. **Figure 4.106 b** shows a three-dimensional view of variable coordinates for the three dimensions (Dim.1, 2 & 3) with Dim.1 (67.1 %) on the x-axis, Dim.2 (19.9 %) on the z-axis and Dim.3 (7.5 %) on the y-axis. **Figure 4.106 c** shows the variable coordinates visualization with spots of different colour intensity. The strongest or darkest colour represent the highest correlation values and the correlation values decreases with decrease in the colour intensity of the spots in the visualization. Also, the positive correlated values are in blue while the negative correlated values are in red. Here, Dim.1-5 are represented by Dim.1-5. The order of importance decreased from Dim.1 to 5. We can see that Dim.1 showed the highest colour intensity and this was followed by Dim.2. However, all the coordinates in Dim.1 showed strong negative correlation indicated in red colour. In Dim.1 (**Figure 4.106 c**), the data visualized explains 67.1 % of the concentration effect experiment and the best five correlated variables were Fe_conc1, Cu_conc2, Cu_conc1, Fe_conc2 and Cu_conc3. In Dim.2 (**Figure 4.106 c**), the visualized data explains 19.9 % of the concentration effect experiment and the best three correlated variables were Pb_conc1, Pb_conc3 and Pb_conc2.

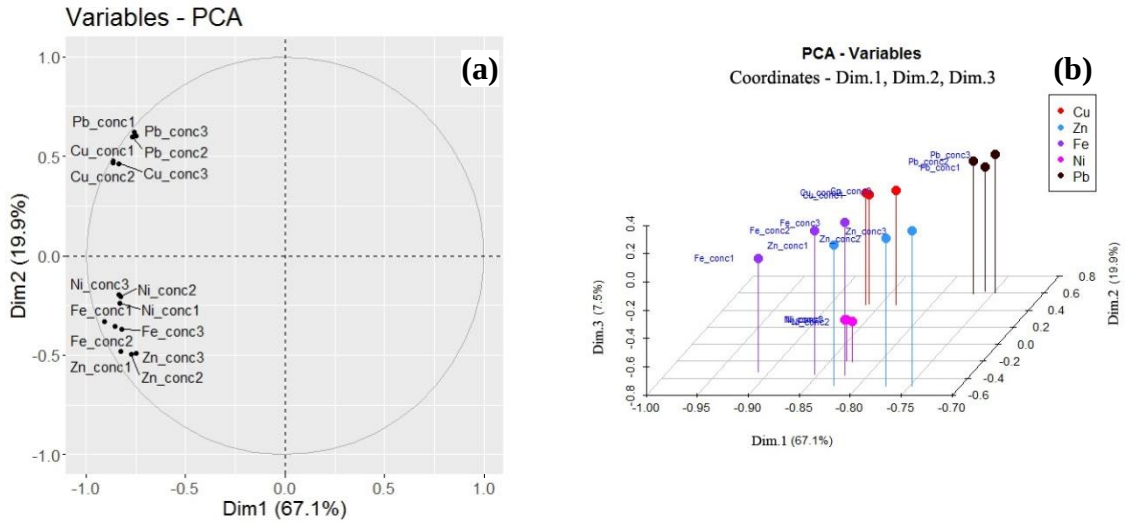

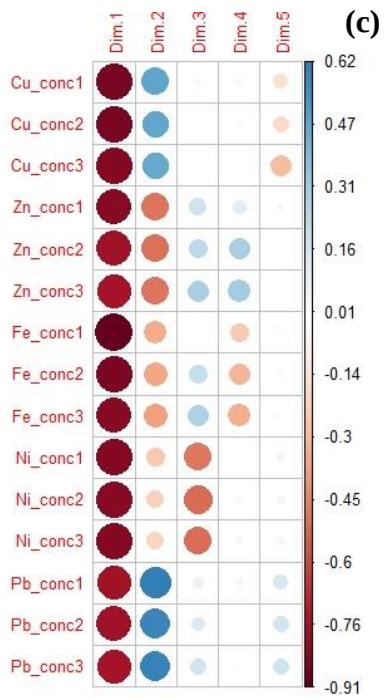

Figure 4.106: (a) Variable Coordinates Correlation Plot (concentration effect) (b) Variable Coordinates 3D Plot (concentration effect) (c) Variable Coordinates Dim Plot (concentration effect)

4.16.3 PCA Result for Variable Cos2 Quality of Representation in Concentration Effect

Figure 4.107 a shows the Cos2 plot of variable with the highest Cos2 value which are in orange and larger circles while the smallest cos2 variables value are in blue and smallest circles. The variables in orange are the most represented in the plot as they are closest to the circle of correlation with very high values and this is followed by the yellow and then the blue spots. All the variables indicated in this Cos2 plot **(Figure 4.107 a)** show very good representation for Dim.1 as all the variables are far from the centre of the circle and none is close to the centre of the circle. **Figure 4.107 b & c** shows another visualization of the Cos2 variables in the form of bar plots. We can see that the Cos2 variables for Dim.1 in **Figure 4.107 b** are the highest which also supports the fact that the quality of representation is good. The variables in the bar plots are arranged from highest to lowest. Cos2 variable are squared values of variable coordinates values. **Figure 4.107 d** shows the Cos2 variables visualization with spots of different colour intensity. The strongest or darkest colour represent the highest Cos2 variables and the Cos2 variables decreased with decrease in the colour intensity of the spots in the visualization. We can see that Dim.1 variables showed the highest colour intensity and this was followed by Dim.2. In Dim.1 (**Figure 4.107 b**), the data visualized

explains 67.1 % of the concentration effect experiment and the best five represented variables were Fe_conc1, Cu_conc2, Cu_conc1, Fe_conc2 and Cu_conc3. In Dim.2 (**Figure 4.107 c**), the visualized data explains 19.9 % of the concentration effect experiment and the best three represented variables were Pb_conc1, Pb_conc3 and Pb_conc2.

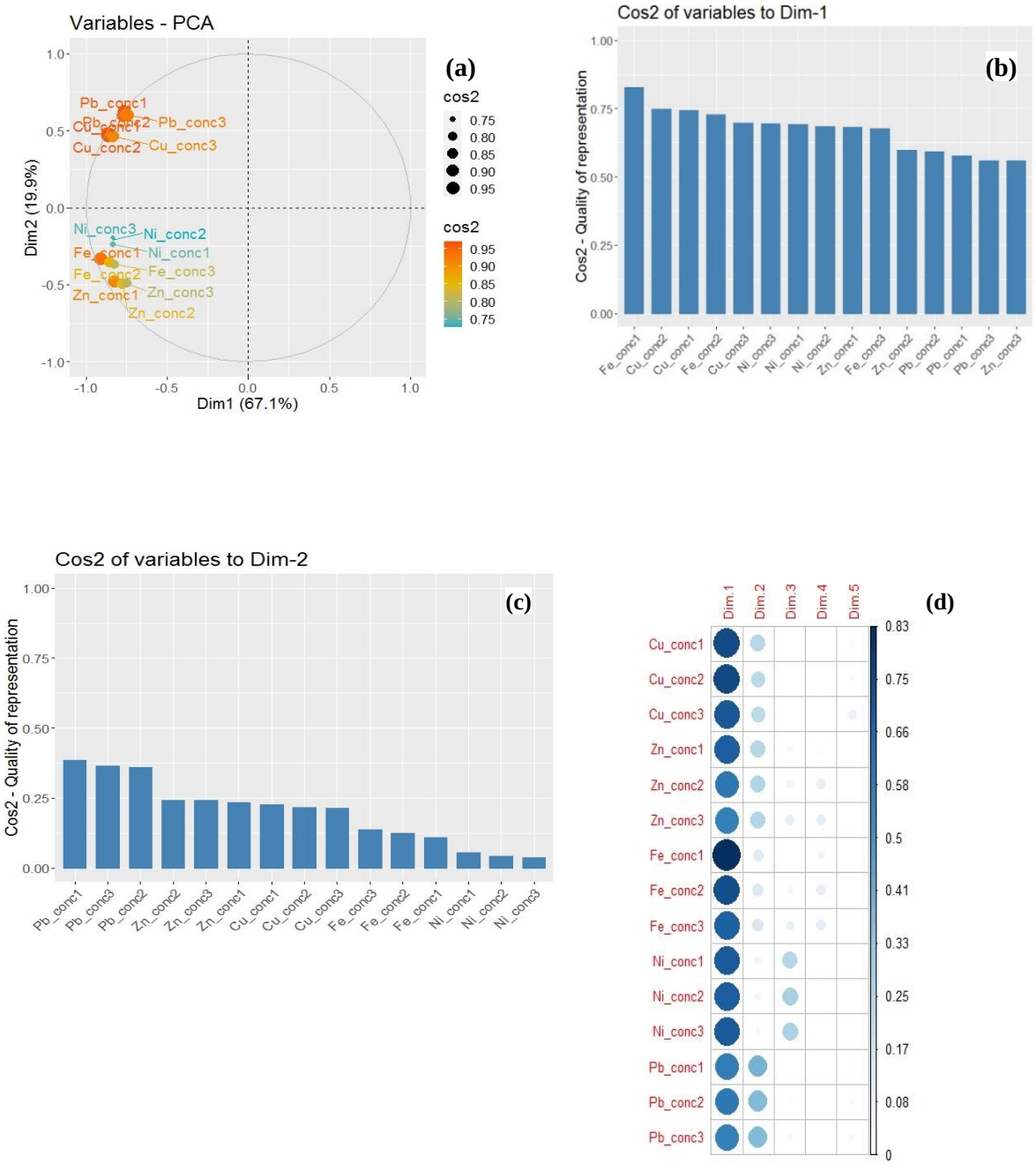

Figure 4.107: (a) Variable Cos2 quality of representation (concentration effect) (b) Dim.1 quality of representation (concentration effect) (c) Dim.2 quality of representation (concentration effect) (d) Cos2 quality of representation plot (concentration effect)

4.16.4 PCA Result for Variables Contribution in Concentration Effect

Figure 4.108 a shows the contribution of variable correlation plot with the most contributing variables indicated in red and the least contributing variables indicated in blue. From **Figure 4.108 b & c**, we can see the contribution of variables represented in bar plots with red dotted lines which indicates the expected average contribution. Dim.1 and Dim.2 are the most important to be considered in explaining the contribution while Dim.3, 4 & 5 are less important. In Dim.1 (**Figure 4.108 b**), most contribution of variables values were slightly above the expected average contribution. **Table 4.63** shows the actual values for contribution of variables and **Figure 4.108 d** shows the contribution of variables plot with spots of different colour intensity. The darker colours indicate higher contribution while the lighter color indicate low contribution. The contribution of variables for a particular dimension are measured in percentages. Correlated variables in the contribution of variables for Dim.1 & Dim.2 explains 67.1 % and 19.9 % respectively. Contributions from Dim.1 are the most important as they contribute more than other variables and this is followed by Dim.2. Even though the contributions from other dimensions are high (Dim.3, Dim.4 & Dim.5), they would not be considered since they are not as important as contributions from Dim.1 & 2. The order of importance in the contribution for the dimensions are Dim.1 > Dim.2 > Dim.3 > Dim.4 > Dim.5. A variable with large contribution value contributes more to the component. Dim.1 which explains 67.1 % of the variation is represented in **Figure 4.108 b.** We can see the bar chart for Dim.1 contributions arranged in descending order and the best five contributing variables were Fe_conc1 (8.2 %), Cu_conc2 (7.4 %), Cu_conc1 (7.4 %), Fe_conc2 (7.2 %) and Cu_conc3 (6.9 %). Dim.2 which explains 19.9 % of the variation is represented in **Figure 4.108 c.** We can see the bar chart for Dim.2 contributions also arranged in descending order and the best three contributing variables were Pb_conc1 (12.9 %), Pb_conc3 (12.2 %) and Pb_conc2 (12.0 %). The best contributing variables for concentration effect are in the order Fe_conc1 > Cu_conc2 > Cu_conc1 > Fe_conc2 > Cu_conc3 > Pb_conc1 > Pb_conc3 > Pb_conc2.

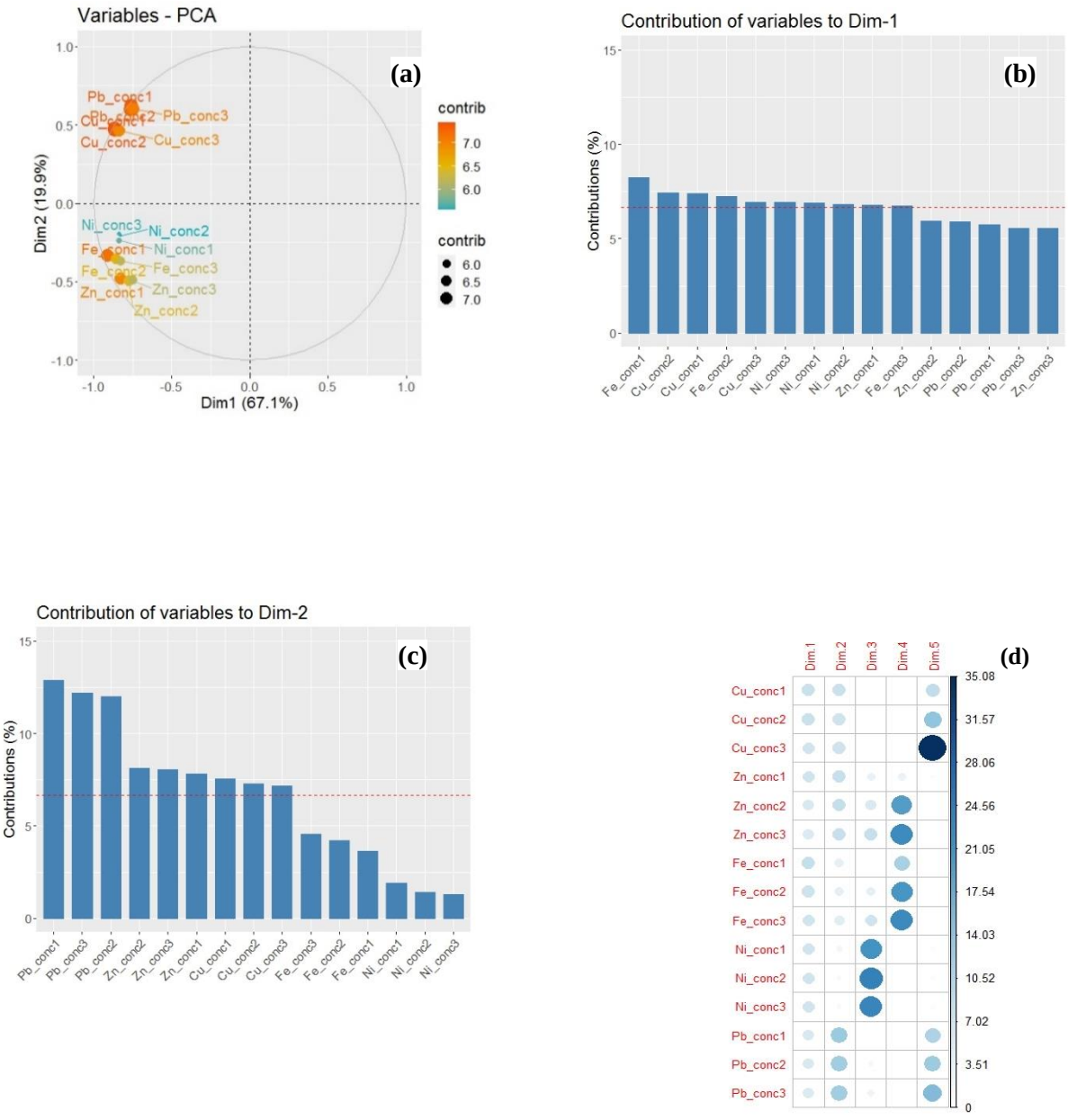

Figure 4.108: (a) Contribution of Variable Correlation Plot (concentration effect) (b) Dim.1 Contribution of Variable Bar Plots (concentration effect) (c) Dim.2 Contribution of Variable Bar Plots (concentration effect) (d) Variable Contribution Plot (concentration effect)

Table 4.63 Best contributing variables for concentration effect

	Dim1 (%)	Dim2 (%)
Cu_conc1	**7.4**	7.6
Cu_conc2	**7.4**	7.3
Cu_conc3	**6.9**	7.2
Fe_conc1	**8.2**	3.6
Fe_conc2	**7.2**	4.2
Pb_conc1	5.7	**12.9**
Pb_conc2	5.9	**12.0**
Pb_conc3	5.6	**12.1**

4.16.5 PCA Result for Observation Coordinates in Concentration Effect

Figure 4.109 a shows the plot for the observation coordinates which are representing the position of the solvents used in concentration effect experiment for both the hotplate and microwave methods. **Figure 4.109 b - e** shows the three-dimensional plots of inorganic acids, organic acids, ionic liquid (a - c) and ionic liquid (d - g). Dim.1 on the x-axis, Dim.2 on the z-axis and Dim.3 on the y-axis. These three dimensional plots shows the coordinates or positioning of the solvents used for the concentration effect experiment. **Figure 4.110 a – d** shows the observation coordinate visualization plot for inorganic acids, organic acids, ionic liquid (a - c) and ionic liquid (d - g). The observation coordinates for the inorganic acids all showed very good negative correlation indicated by the strong red colour. AQ1-6 (*aqua-regia*) had the strongest negative correlation values followed by NA1-3 (nitric acid) then HA1-3 (hydrochloric acid). The strength of correlation can be seen on Dim.1 in **Figure 4.110 a** as very dark red colours. Dim.2 also had good positive and negative correlation. The organic acid Dim.1 all showed strong positive correlation indicated in blue colour while the Dim.2 showed good positive correlation. The coordinates in ionic liquids (a - c) all showed strong positive correlation in Dim.1 while Dim.2 showed strong negative correlations. The coordinates in ionic liquids (d - g) all showed strong positive correlation in Dim.1 and Dim.2.

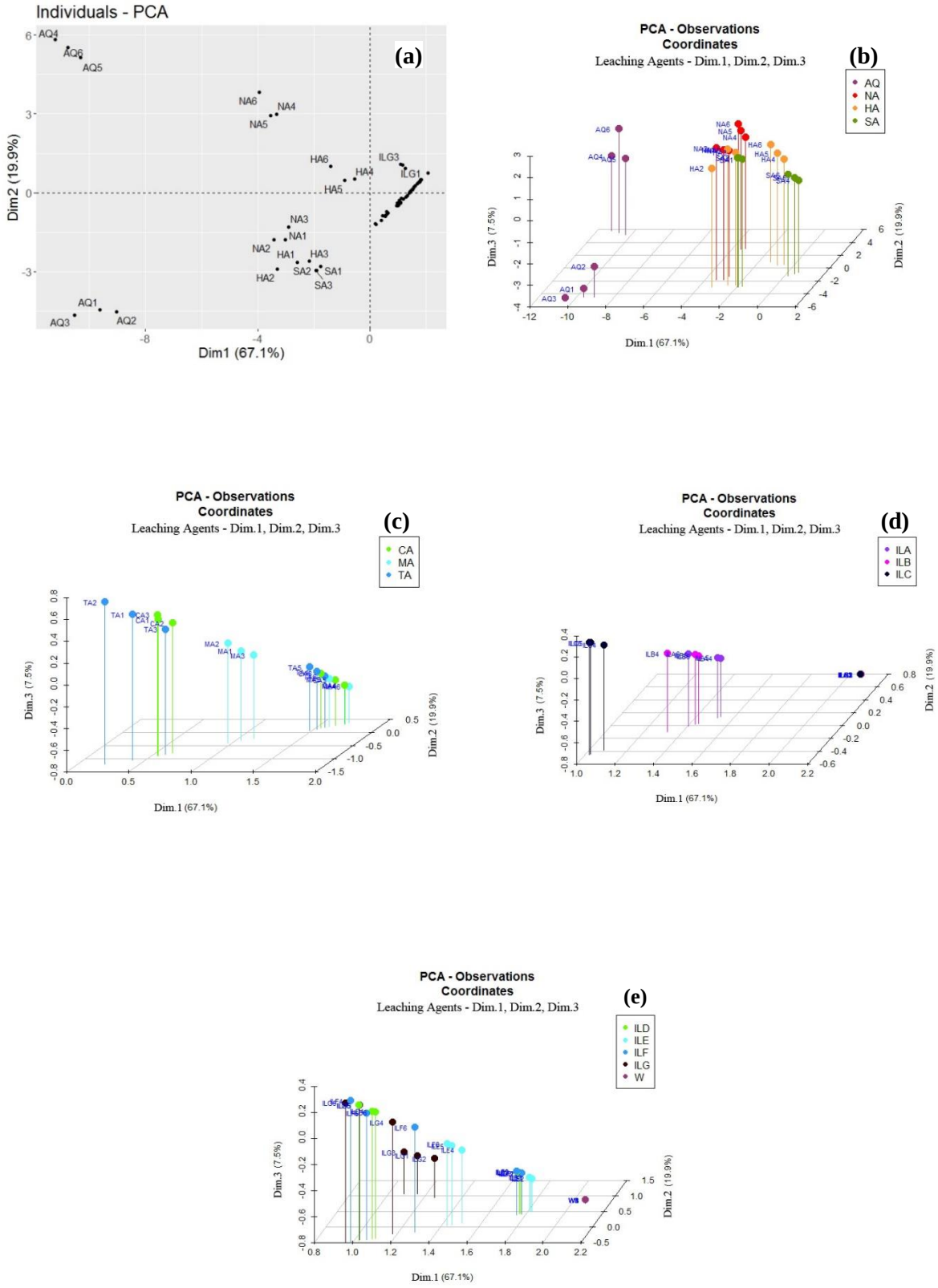

Figure 4.109: (a) observation coordinate correlation plot (concentration effect) (b) observation coordinate for inorganic acids (concentration effect) (c) observation coordinate for organic acids (concentration effect) (d) observation coordinate for IL a-c (concentration effect) (e) observation coordinate for IL d-g (concentration effect)

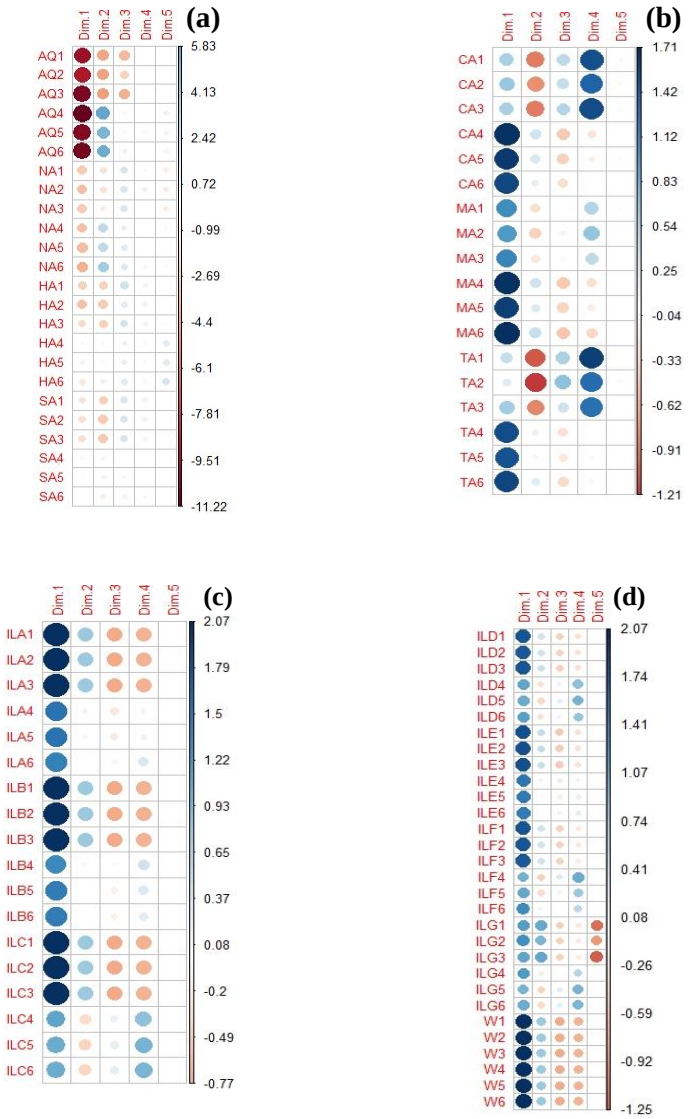

Figure 4.110: (a) Observation coordinate plot for inorganic acids (concentration effect) (b) observation coordinate plot for organic acids (concentration effect) (c) observation coordinate plot for IL a – c (concentration effect) (d) observation coordinate plot for IL d - g (concentration effect)

4.16.6 PCA Result for Observation Cos2 Quality of Representation in Concentration Effect

Figure 4.111 a shows the Cos2 plot of observation with the highest Cos2 value which are in orange and larger circles while the lowest cos2 observation value are in blue and smaller circles. The observations in orange are the most represented in the plot as they have very high values and this is followed by the yellow and then the blue spots. **Figure 4.111 b - e** shows the three-dimensional plots Cos2 observation for inorganic acids, organic acids, ionic liquid (a - c) and ionic liquid (d - g). Dim.1 on the x-axis, Dim.2 on the z-axis and Dim.3 on the y-axis. These three dimensional plots shows the coordinates or positioning of the solvents used for the concentration effect experiment. The Cos2 observation values which are squared

values of observation coordinates values. **Figure 4.112 a - d** shows the Cos2 observations visualization with spots of different colour intensity. The strongest or darkest colour represent the highest Cos2 observations and the Cos2 observations decreased with decrease in the colour intensity of the spots in the visualization. The quality of representation in Dim.1 (inorganic acids) showed good quality of representation. AQ1-6 had good quality of representation followed by NA1-6 and HA1-3, the rest were showed lower quality of representation. In Dim.2 (inorganic acids), the strongest quality of representation were found in SA1 – 6, NA4-6 and HA1-3. Dim.1 (organic acids) all showed good quality of representation while only CA1-3 and TA1-3 showed lower quality of representation. In Dim.2 (organic acids), the only moderate quality of representation were found in CA1-3 and TA1-3. The good quality of representation with strong colour intensity can be seen in Dim.1 (**Figure 4.112 b**). In IL (a - c) and IL (d - g), Dim.1 all showed good quality of representation.

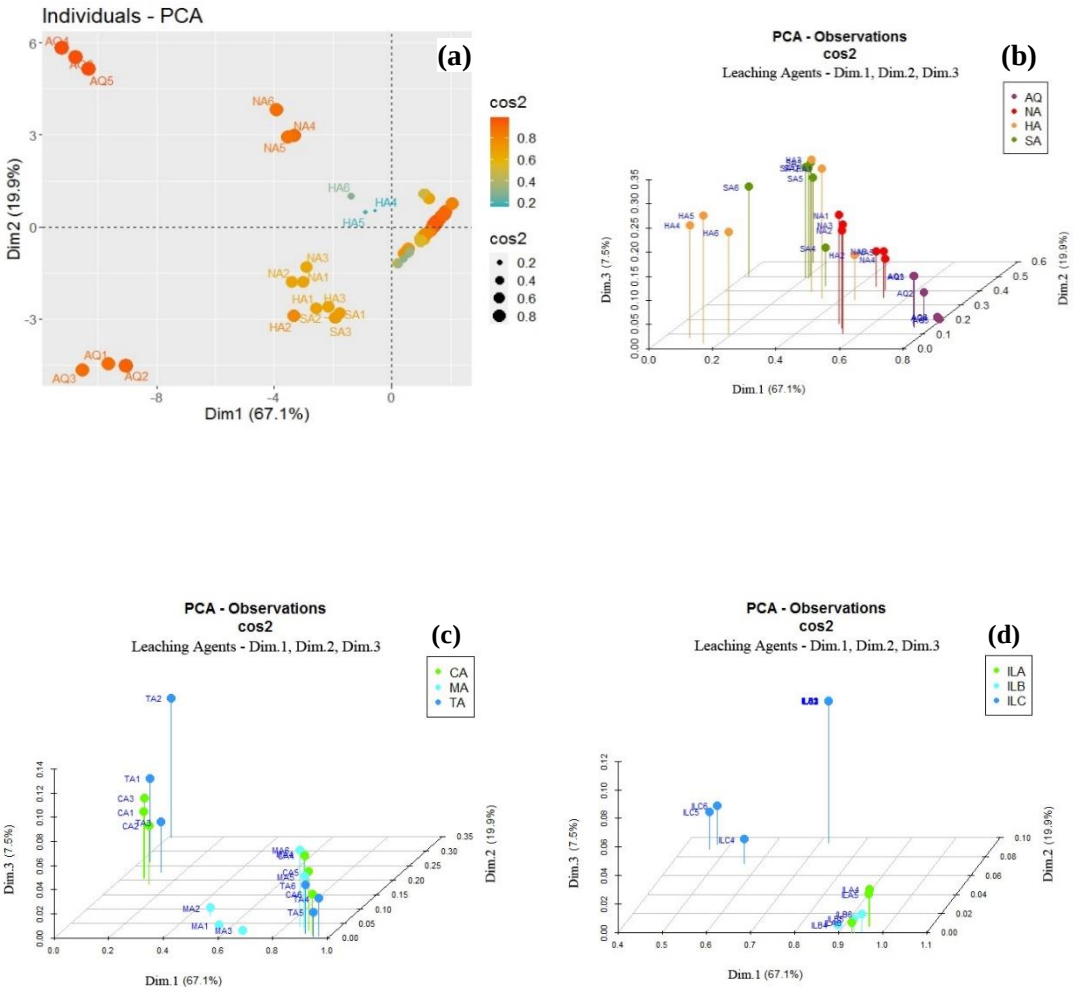

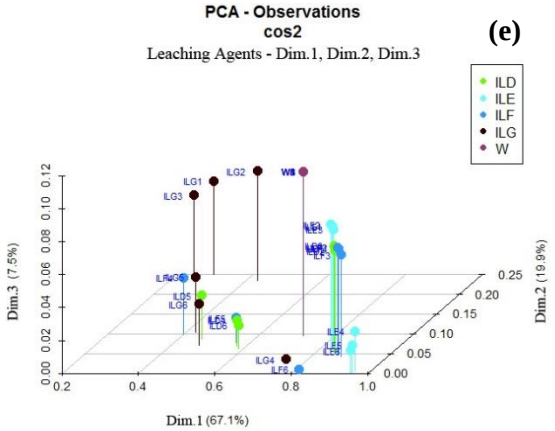

Figure 4.111: (a) Observation cos2 correlation plot (concentration effect) (b) Observation cos2 for inorganic acids (concentration effect) (c) Observation cos2 for organic acids (concentration effect) (d) Observation cos2 for IL a-c (concentration effect) (e)Observation cos2 for IL d-g (concentration effect)

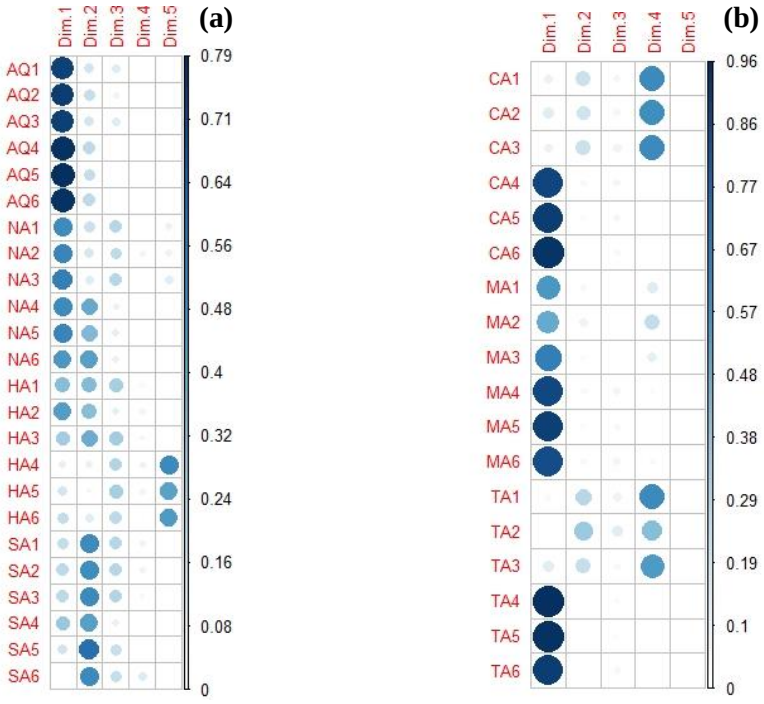

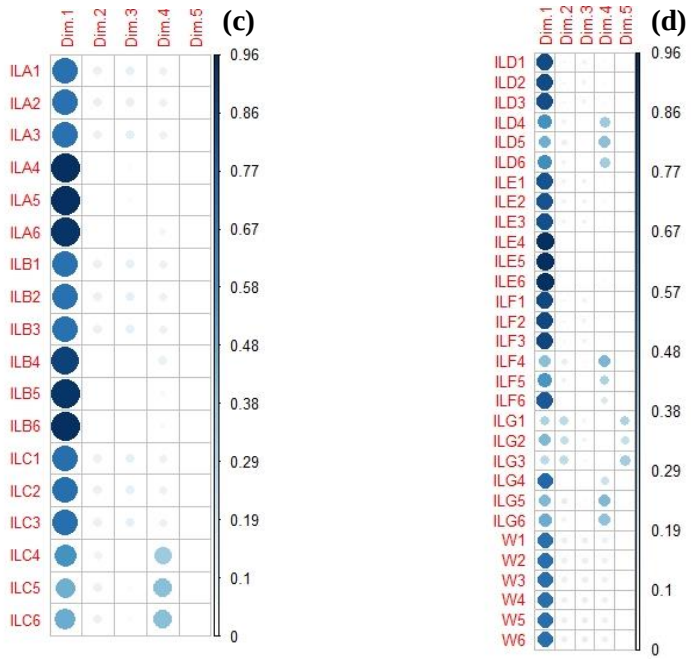

Figure 4.112: (a) Observation cos2 Dim plot for inorganic acids (concentration effect) (b) observation cos2 Dim plot for organic acids (concentration effect) (c) observation cos2 Dim plot for IL a – c (concentration effect) (d) observation cos2 Dim plot for IL d - g (concentration effect)

4.16.7 PCA Result for Observation Contribution in Concentration Effect

Figure 4.113 a shows the contribution plot of observation with the highest contribution values which are in orange and larger circles while the lowest contribution value are in blue and smaller circles. In the figure, more labelling priority is given to the highest contributing observation with the least contributing observations not appearing. The observations in orange are the most represented in the plot as they have very high values and this is followed by the yellow and then the blue spots. **Figure 4.113 b - e** shows the three-dimensional plots of observation contribution for inorganic acids, organic acids, ionic liquid (a - c) and ionic liquid (d - g). Dim.1 on the x-axis, Dim.2 on the z-axis and Dim.3 on the y-axis. These three dimensional plots shows the positioning of the solvents contribution on the plot. **Table 4.64** shows the observation contribution values in percentages. **Figure 4.114 a - d** shows the observation contribution visualization with spots of different colour intensity. The strongest or darkest colour represent the highest observation contribution and the observation contribution decreased with decrease in the colour intensity of the spots in the visualization. The observation contribution in Dim.1 for inorganic acids (**Table 4.62**), shows observation contribution. The solvents that contributed highest to Dim.1 were AQ4 (13.9 %), AQ6 (12.8 %), AQ3 (12.2 %), AQ5 (11.7 %), AQ1 (10.3 %), AQ2 (9.2 %), NA6 (1.7 %), NA5 (1.4 %),

NA2 (1.3 %), NA4 (1.2 %), NA1 (1.0 %), NA3 (0.9 %). In Dim.2 the best three contributing solvents were AQ4 (12.6 %), AQ6 (11.3 %), AQ5 (9.6 %). The best observation contribution with strong colour intensity can be seen in Dim1 (**Figure 4.114 a**). The best contributing solvents from highest to lowest are in the order AQ4 > AQ6 > AQ3 > AQ5 > AQ1 > AQ2 > NA6 > NA5 > NA2 > NA4 > NA1 > NA3.

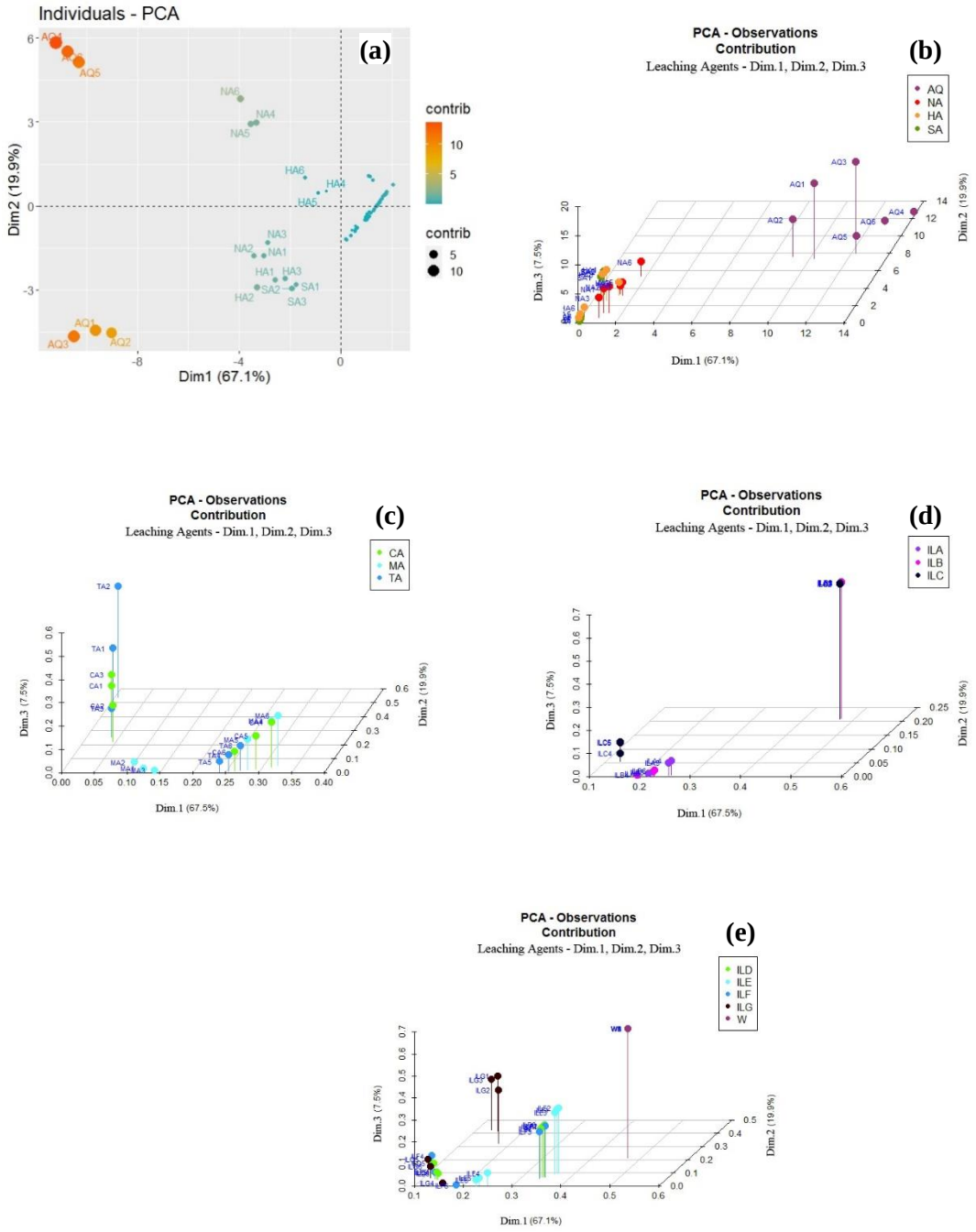

Figure 4.113: (a) Observation contribution plot (concentration effect) (b) Observation contribution for inorganic acids (concentration effect) (c) Observation contribution for organic acids (concentration effect) (d) Observation contribution for IL a-c (concentration effect) (e) Observation contribution for IL d-g (concentration effect)

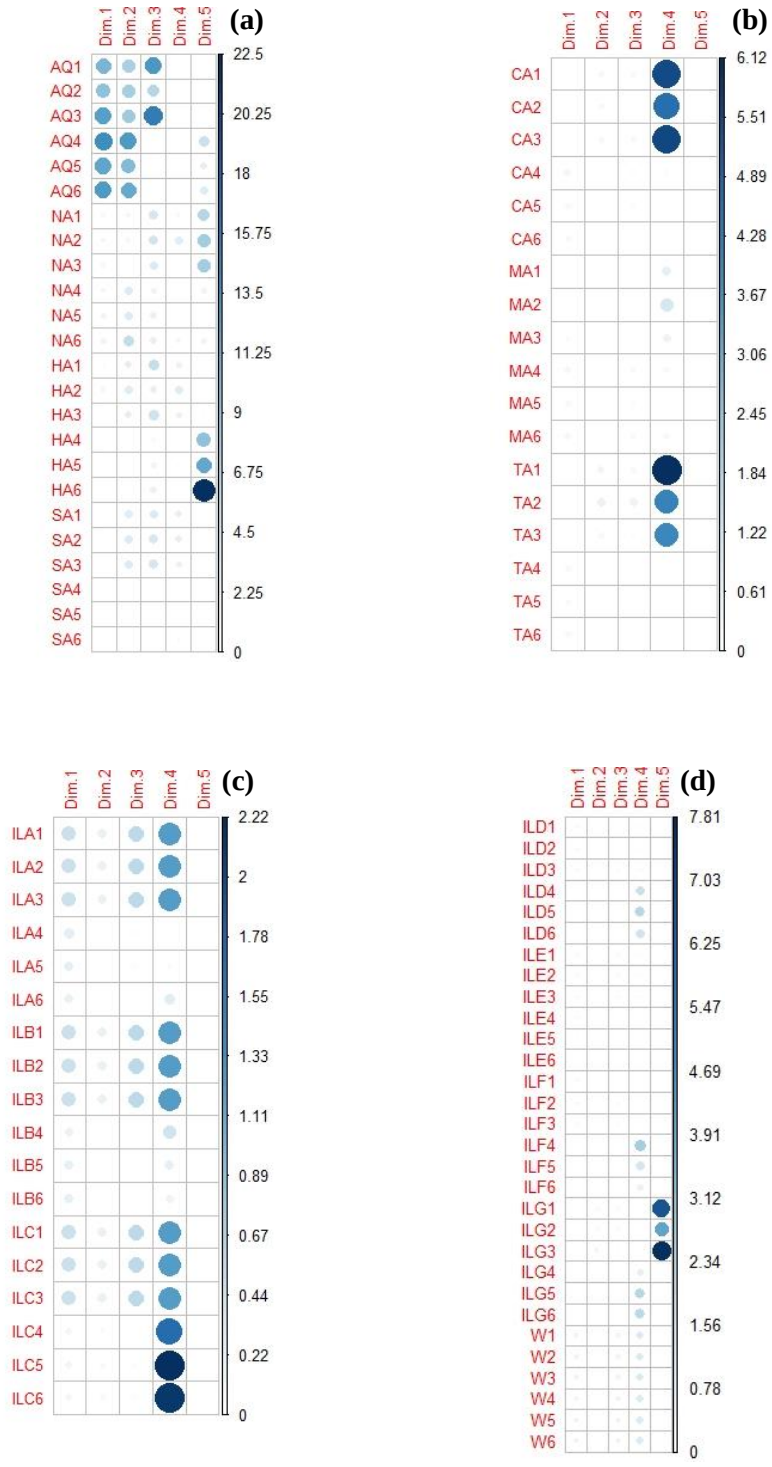

Figure 4.114: (a) Observation contribution Dim plot for inorganic acids (concentration effect) (b) observation contribution Dim plot for organic acids (concentration effect) (c) observation contribution Dim plot for IL a – c (concentration effect) (d) observation contribution Dim plot for IL d - g (concentration effect)

Table 4.64 Best Contributing Observations for Concentration Effect

	Dim 1 (%)	Dim 2 (%)
AQ1	**10.3**	7.4
AQ2	**9.2**	7.6
AQ3	**12.2**	8.1
AQ4	**13.9**	**12.6**
AQ5	**11.7**	**9.6**
AQ6	**12.8**	**11.3**
NA1	**1.0**	1.2
NA2	**1.3**	1.2
NA3	**0.9**	0.6
NA4	**1.2**	3.3
NA5	**1.4**	3.2
NA6	**1.7**	5.4

4.17 Energy Consumed by the Hotplate and Microwave Methods.

The amount of energy used by the hotplate and microwave methods are seen in Table 4.65. The Hotplate used was the MS-H280-Pro and the microwave was the MAR-6 CEM Microwave. The least energy consumed by the hotplate was 927 KJ within 30 minutes and the highest energy consumed was 5562 KJ within 180 minutes. The microwave consumed 1920 KJ within 20 minutes.

Table 4.65 Energy consumed by leaching with hotplate and microwave methods

	Power (watt)	Time (seconds)	Energy (KJ)
Microwave Method	**1600**	**1200**	**1920**
Hotplate Method	**515**	**1800**	**927**
	515	**3600**	**1854**
	515	**5400**	**2781**
	515	**7200**	**3708**
	515	**9000**	**4635**
	515	**10800**	**5562**

$$\text{Energy (KJ)} = \frac{Power\ (watt)\ \times Time\ (seconds)}{1000}$$

4.18 Electrochemical Recovery Experiment

The electrochemical recovery of metals from the NA leachate was carried out using the ISO-TECH (model number IPS-606D). The voltage (V) and current (A) were set to achieve the best results. Two anode electrodes and one cathode used were made of steel. The pH of the solution was adjusted using $Al(OH)_3$. The baseline concentration is the concentration of the solution before the experiment started and the final concentration is the concentration at the stop of the experiment. The recovered metal concentration was determined by subtracting the final recorded concentration from the baseline concentration.

4.18.1 Copper Recovery

Table 4.66 shows data from the recovery of copper as samples where taken every hour for a total period of 17 hours and this is represented in **Figure 4.115**. The concentration at 0 hour (1648 mg/L or 100 %) was used as baseline for this study at a pH of 1, current was set to 1.5 A and voltage was set to 2.9 V. At the 17th hour the concentration of copper left in solution was 295 mg/L (18 %) at a pH of 3.8, current of 2.5 A and voltage of 4.3 V. Therefore the recovered Cu was 1353 mg/L (82 %). Figure 4.116 (a & b) shows the recovered copper and **Figure 4.116 (c)** shows the presence of copper in the recovered sample.

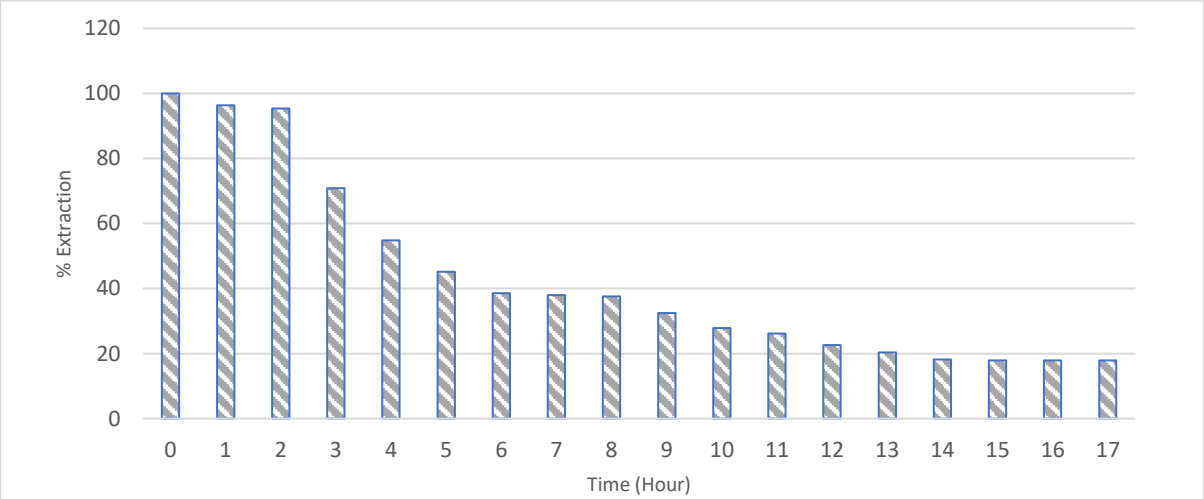

Figure 4.115 Cu left in Solution during Electrochemical Recovery

Table 4.66 Summary of electrochemical recovery of Cu

Conditions	Time (hour)	Baseline (mg/L)	Cu left in solution (mg/L)	Cu Recovered (mg/L)	Cu left in solution (%)	Cu recovered (%)	pH
1.5A, 2.9V	0	1648	1648	0	100	0	1.0
	1	1648	1588	60	96	4	1.0
	2	1648	1572	76	95	5	1.0
	3	1648	1168	480	71	29	1.0
	4	1648	904	744	55	45	1.0
	5	1648	744	904	45	55	1.0
	6	1648	636	1012	39	61	1.0
2.5A, 3.8V	7	1648	627	1022	38	62	1.0
	8	1648	620	1029	38	62	1.0
	9	1648	536	1113	32	67	1.0
	10	1648	459	1190	28	72	1.0
	11	1648	431	1218	26	74	1.0
2.5A, 4.3V	12	1648	372	1276	23	77	4.5
	13	1648	336	1312	20	80	4.7
	14	1648	300	1348	18	82	5.3
	15	1648	295	1353	18	82	3.8
	16	1648	294	1354	18	82	3.0
	17	1648	294	1354	18	82	3.0

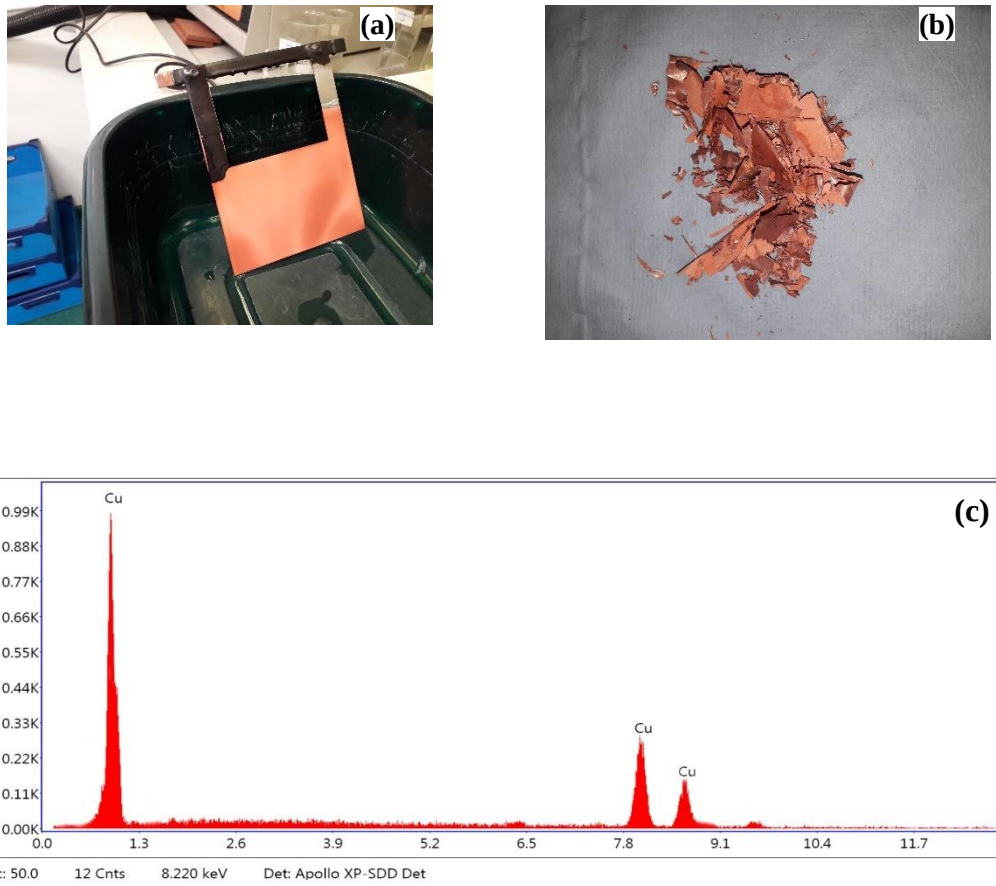

Figure 4.116 (a & b) Copper recovered from all leachates (b) SEM-EDS xray showing presence of copper in the recovery sample

4.18.2 Zinc Recovery

Table 4.67 shows data from the recovery of zinc as samples where taken every hour for a total period of 17 hours and this is represented in **Figure 4.117**. The concentration at 0 hour (1754 mg/L or 100 %) was used as baseline for this study at a pH of 1, current was set to 1.5A and voltage was set to 2.9V. At the 17th hour the concentration of zinc left in solution was 1224mg/L (70 %) at a pH of 3.0, current of 2.5A and voltage of 4.3V. Therefore the recovered zinc was 530mg/L (30 %).

Table 4.67 Summary of percentage Zn left after electrochemical recovery

Conditions	Time (hour)	Baseline (mg/L)	Zn left in solution (mg/L)	Zn recovered (mg/L)	Zn left in solution (%)	Zn recovered (%)	pH
1.5A, 2.9V	**0**	1754	1754	0	100	0	1.0
	1	1754	1740	14	99	1	1.0
	2	1754	1730	24	99	1	1.0
	3	1754	1723	31	98	2	1.0
	4	1754	1721	34	98	2	1.0
	5	1754	1651	103	94	6	1.0
	6	1754	1481	274	84	16	1.0
2.5A, 3.8V	**7**	1754	1474	281	84	16	1.0
	8	1754	1478	276	84	16	1.0
	9	1754	1464	290	83	17	1.0
	10	1754	1462	293	83	17	1.0
	11	1754	1459	295	83	17	1.0
2.5A, 4.3V	**12**	1754	1450	304	83	18	4.5
	13	1754	1440	314	82	18	4.7
	14	1754	1440	314	82	18	5.3
	15	1754	1440	314	82	18	3.8
	16	1754	1228	526	70	30	3.0
	17	1754	1224	530	70	30	3.0

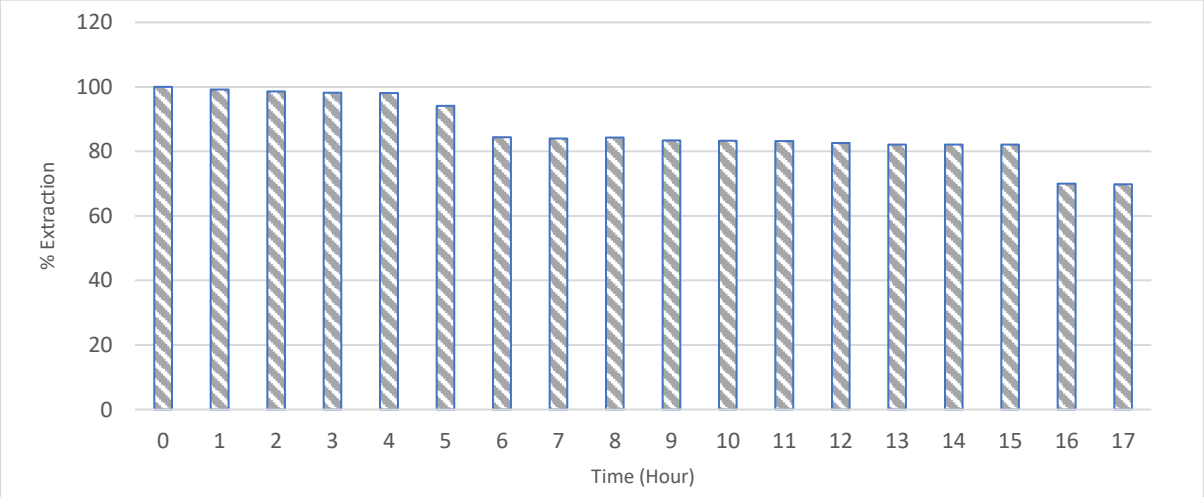

Figure 4.117 Zn left in Solution during Electrochemical Recovery

This research was impacted by Covid -19 as the laboratories were locked. I wanted to recover more metals but I was hindered by the lockdown and I could not continue much work on the electrochemical recovery.

4.19 Discussion

Nigeria is plagued with WEEE all over the country. Some of the WEEE still function and though they have reached their end-of-life, people still buy them because of the level of poverty as most people cannot afford new gadgets. Soon these second-hand products (WEEE) stop working and they are eventually discarded. The indescrimate dumping of WEEE in Nigeria could lead to leaching into the environment when it rains. Some of the locals resort to recovering metals from these wastes thereby dismantling and burning in the open indiscriminately and this affects the entire ecosystem as they could leach into the environment. This is a problem to the Nigerian government who has sponsored this research as a way of providing solution to the problem of WEEE amongst other environmental problems in Nigeria (Sum, 1991; Spalvins, 2008; Adediran & Abdulkarim, 2012; Damodaran *et al.*, 2013; Ghandi, 2014; He and Xu, 2014; Kumar *et al.*, 2014; Letsrecycle, 2020; Zhang & Xu, 2016).

This research focused on extracting five metals (Cu, Zn, Fe, Ni and Pb) from WEEE using traditional leaching solvents (inorganic and organic acids) and ionic liquids. The two methods used were namely: i) hotplate (HP) and ii) microwave methods (MW). Also, optimisation was done by investigating the effects of dose, particle-size, H_2O_2 amount, temperature, time and concentration. Principal component analysis (PCA) was done to understand the variation that occurred in the data amongst the metals (variables) and solvents (observations). All solvents used in this research where considered including aqua regia (AQ) which was used as the baseline. AQ was included in the PCA to see how well it varied from the other solvents and also to know how much it performed compared to the other solvents.

4.19.1 Discussion on Dose Effect

For Cu, the dose effect showed that Cu extraction (**Table 4.16 a**) in the HP method was significant in NA, HA, IL-E and IL-G and their peak extractions were 41, 10, 11 and 22 % respectively at 0.2 g each. As dose increased, Cu extraction in NA did not show any

significant change but it decreased in HA, IL-E and IL-G. Also, as dose increased, the MW method showed descrease in Cu extraction for NA with a peak extraction of 52 % at 0.2 g. Statistically, the mean extractions with respect to the dose effect for both HP and MW methods where the same for NA, HA, IL-E & IL-G. This implies that either the HP or MW methods when used would achieve similar results. The inorganic acids (NA & HA), especially NA, extracted Cu more than IL-E & IL-G. This was expected as the inorganic acids are more aggressive in leaching metals. The organic acids did not perform as aspected as their Cu extraction were significantly lower. However, the highest Cu extraction in this research was lesser than in Javaid 2006 and Faivre 2009 who extracted > 90 % of Cu from metal compounds (CuO and CuS) dissolved in IL. Consequently, the metals from the WEEE sample in this research were in elemental form and the highest Cu extraction (52% using the MW method) was lesser than in Javaid 2006 and Faivre 2009 who extracted > 90 % of Cu from metal compounds (CuO and CuS) dissolved in IL. However, Yang *et. al*., 2011 researched leaching Cu from shredded particles of PCBs using 15 % sulfuric acid and the result showed that as the amount of PCBs used decreased Cu extraction increased. Jadhao *et al*., 2021 research showed that when the dose was increased the extraction of Cu decreased and this was due to the higher amount of PCBs present. Cu extracted was 100 % when 1 g of PCBs was used with 20 ml of solvents used. Kavousi *et al.,* 2018 research showed that as the dose increased the amount of Cu extracted decreased. This showed that the smaller dose of PCBs were more effective as 92 % of Cu was extracted when 1 g was in in 20 ml of 0.4 mol/L of Tetrafluoroboric acid, HBF_4. The research revealed that as the dose increased the Cu extraction also increased and the best dose for leaching Cu was 20 g of the metal powder in 300 ml of solution used for leaching. The research by Janyasuthiwong *et al*., 2016 showed that the most effective solid dose to liquid ratio was 1g to 40 ml. Using 1 M HNO_3, 175 mg/g of Cu was extracted. Yazici & Deveci, 2016 research showed that as the dose of solids increased there was increase in the amount of Cu extracted. 1 % of the solid weight extracted more Cu (99.9 %) compared to 15 % of the solid weight which was the maximum used. It was expected in this research that as the dose of the PCBs increased, the extraction of Cu would also increase across all solvents used but this was not so. It was generally observed in this research that as the dose increased the Cu extraction decreased and this pattern was similar to the results obtained by Yang *et. al*., 2011. Consequently, the reason the Cu extraction decreased as the dose increased could be attributed to more contact between the lower PCB dose and the higher amount of solvent. There was also mass transfer efficiency leading to higher extraction at lower dose. Lower transmission efficiency and lower heat transfer occurred between higher

dose and the solvent thereby leading to reduced amount of Cu extraction. The result implies that using NA as the most suitable solvent at 0.2 g dose, Cu could be best extracted.

For Zn, the dose effect showed that Zn (**Table 4.17 a**) in the HP method was extracted by all solvents except ILs A-C and W. The highest of all peak extractions were seen at 0.7 g for HA (98 %) and the lowest of all peak extractions were in IL-E (10 %). As dose increased, Zn extraction in TA and ILs D-G decreased in the other solvents, Zn extraction increased before decreasing. Similar behaviour was seen in the MW method and the highest extraction was seen in IL-F (92 %) while the lowest was seen in IL-A (57 %). Generally, all the solvents extracted Zn in the MW method. Statistically, the mean Zn extraction of the MW method was better for TA and ILs A-G but it was the same for NA, HA, SA, CA and MA. However, Irannajad *et.al*., 2013 researched the leaching of Zn from low grade oxide ore using organic acid and the result revealed as dose increased the extraction of Zn decreased from 67% to 20% when citric acid was used. Chen *et al*., 2009 researched leaching Zn from Zn oxide ore using 0.5 mol/L of NaOH and the result showed that Zn extraction peaked at 42 % as the dose increased. The research by Janyasuthiwong *et al*., 2016 showed that the most effective solid dose to liquid ratio was 1g to 40 ml. Using 1 M HNO_3, 5 mg/g of Zn was extracted. It was expected in this research that as the dose of the PCBs increased, the extraction of Zn would also increase across all solvents used but this was not so for all solvents in the HP as only the inorganic acids and organic acids increased with increase in the dose before peaking and then decreasing in Zn extraction. However, TA and the ILs generally decreased steadily as the dose of PCbs increased. The result from this research is slightly different from those quoted from other researches. The research by Irannajad *et.al*., 2013 was similar to the IL results obtained in this research. The MW method showed that in the organic acids, the Zn extraction increased as the dose increased while there was decreasing Zn extraction as the dose increased in the ILs. Consequently, the reason the most solvents extracted Zn could be attributed to its position in the reactivity series. However, the reason the extractions in TA and ILs decreased as the dose increased could be attributed to more contact between the smaller PCB dose and the higher amount of solvent. Also, there was lesser contact between the higher PCB dose and the solvent which led to the lower extraction. This result means that Zn would be effectively extracted using any dose amount (0.2 – 3.0 g) However, the best extraction would be achieved using 0.7 g of HA (HP methods).

For Fe, the dose effect showed that Fe extraction (**Table 4.18 a**) in the HP method was significant in NA, HA and SA. Their peak extractions were 59, 68 and 46 % at 0.20, 0.50 & 0.50 g respectively. As the dose increased, Fe extraction was unstable. Also, the MW method showed significant extractions in NA, HA and SA. Their peak extraction were 46, 42 and 25 % at 0.20, 0.20 & 0.50 g respectively. Generally, as the dose increased Fe extraction decreased. Statistically, the HP and MW method were the same for NA and HA while the HP method was better for SA. However, Tao *et al*., 2021 researched the behaviour of Fe in copper tailings using 0.5 M sulfuric acid and the results revealed that with increase in dose the Fe extraction reduced and the peak extraction was 67 %. The study by Yazici & Deveci, 2013 revealed that 91 % of Fe was extracted when the ratio of solid dose of 1 g in 100ml of 0.5 H_2SO_4. The findings in the research by Tao *et al*., 2021 was similar to that in this research. The research by Tao *et al*., 2021 revealed that extraction of Fe decreased as the dose increased. 66.5 % of Fe was extracted when a dose was used in a ratio of 1 to 12 of liquid. Siaw et al., 2020 research showed that revealed that as the solid dose increased, amount of Fe extracted also increased and peak extraction of approximately 76 % Fe occurred when the dose used was in a ratio of 1 to 10 of liquid. It was expected in this research that the extraction of Fe would increase as the dose increased across all solvents used but this was not the case. The inorganic acids had the highest extraction of Fe amongst the solvents used. However, the Fe extractions in the organic acids were significantly low while the ILs dids not extract Fe the reason for this poor performance could be attributed to the fact that the organic acids and the ILs are not as aggressive as compared to the inorganic acids there is the possibility that the surface contact for the doses were not large enough. The reason the extraction of Fe was higher in the lower doses and lesser in the higher doses could be attributed to increased surface contact and increased heat transfer in the lower doses which aided the extraction. This result means that the lower dose of PCBs are better in extracting Fe using the inorganic acids especially NA & HA which was the best performing solvent at 0.20 g & 0.50 g respectively.

For Ni, the dose effect showed that Ni extraction (**Table 4.19 a**) in the HP method was significant in NA, HA, SA, CA and TA. Their peak extractions were 7, 7, 3, 5 and 2 % at 2.0,

2.0, 1.5, 2.0 & 0.5 g respectively. As the dose increased there was no significant increase in the extraction of Ni. Also, the MW method showed that Ni extraction was significant in NA, HA and SA. Their peak extractions are 12, 9 and 4 % at 3.0, 0.2 & 1.5 g respectively. As the dose increased there was no significant increase in the extraction of Ni except in HA where Ni decreased to 1 %. Statistically, the mean extraction for the HP and MW methods are the same for the inorganic acids. The research by Li *et al*., 2009 showed that using a microwave method, Ni extraction increased from 60 to 90 %. Jadhao *et al*., 2021 research showed that when the dose was increased the extraction of Ni decreased and this was due to the higher amount of PCBs present. Cu extracted was 85 % when 1 g of PCBs was used with 20 ml of solvents used. The research by Janyasuthiwong *et al*., 2016 showed that the most effective solid dose to liquid ratio was 1g to 40 ml. Using 1 M HNO_3, 9 mg/g of Ni was extracted. The research by Park & Fray, 2009 revealed that the extraction of Ni increased as the dose increased and 100 % of Ni was extracted when 5 g of PCBs was leached in 200 ml of *aqua-regia*. The study by Yazici & Deveci, 2013 revealed that 93 % of Ni was extracted when the ratio of solid dose of 1 g in 100ml of 0.5 H_2SO_4. It was expected in this research that Ni extraction would increase with increase in dose of PCBs but the increase observed was not significant and this could be attributed to the fact that surface area of the dose was not large enough to allow significant chemical acitivty. Another reason could be the amount of heat transferred in the lower and higher dose was not adequate to extract Ni. However, the ILs did not extract Ni and the reason for this could be attributed to the fact that the ILs are not as aggressive enough to extract Ni as compared to the inorganic acids. This result means that the any dose would be suitable to extract Ni both in the HP and MW methods. 3.0 g would be generally suitable.

For Pb, the dose effect showed that Pb extraction (**Table 4.20 a**) in the HP method was significant in NA, HA, SA, CA, MA, TA, IL-D and IL-G. Their peak extractions were 63, 55, 2, 6, 11, 4, 4 and 1 % at 3.0, 2.0, 0.2, 0.2, 0.2, 0.2, 0.2, 0.2 g respectively. As dose increased, there was significant increase in NA and HA. The MW method showed significant Pb extraction in NA and HA. Their peak extractions were 67 and 52 % at 0.2 g respectively. Statistically, the HP and MW methods are the same for NA and IL-G while the HP method was better for the other solvents. Jha *et.al*., 2012 researched the extraction of Pb from solder material of waste PCBs and the result showed that as the dose increased Pb extraction increased and peaked at 91 %. The research by Kamberovic *et al.*, 2018 revealed that increase in solid dose did not have any impact in the extraction of Pb. The best extraction obtained

was 98.5 % of Pb when 500 g was used in 1 litre. Kavousi *et al.,* 2018 research showed that as the dose increased the amount of Pb extracted decreased. This showed that the smaller dose of PCBs were more effective as 94 % of Pb was extracted when 1 g was in in 20 ml of 0.4 mol/L of Tetrafluoroboric acid, HBF_4. It was expected in this research that Pb extraction would increase with increase in dose and this was true for the inorganic solvents and the reason could be attributed to the fact that Pb has a physical property of beign soft with a low melting point which makes it relatively easy to extract from larger dose where the surface contact is reduced. 0.2 g was most suitable for extracting Pb in the HP method across the organic acids and ILs as the extraction of Pb in the higher dose was not significant. In the MW method, the reverse was the case as Pb was extracted by only NA and HA. Also, the Pb extraction decreased as the dose increased and the reason for this could be attributed to the reduced surface contact in the higher dose and the higher temperature used in the MW method. This result means that Pb extraction is most suitable using the HP method at 3.0 g dose of PCBs for the inorganic acids (NA & HA) while 0.2 g is most suitable for Pb extraction when using the MW method.

The PCA for dose effect revealed the best contributing metals (variables) which were in the order Pb 0.7 > Pb 0.5 > Fe 1.5 > Fe 3.0 > Pb 3.0 > … > Zn 0.7 > Zn 0.5 > Zn 1.5. These best contributing metals were the most extracted metals. The best contributing solvents (observations) which were in the order AQ2 > AQ3 > AQ1 > AQ5 > AQ6 > AQ4 > NA1 - 6 > HA1 – 3. This implies that AQ was the most outstanding solvent as it extracted the highest amount of metals each time it was used and this was followed by NA and HA. Consequently, as AQ is at the top of the descending order list for the best contributing solvents, it goes to show that AQ was suitable to use as baseline for the other solvents used in this research. Park et al., 2009 research also showed that aqua regia was very aggressive when used for PCBs and it dissolved most of the materials in few seconds. Furthermore, as earlier discussed above the most effective dose for extracting each of the metals can be seen in Table 4.68.

Table 4.68 Optimum dose

Metal	Cu	Zn	Fe	Ni	Pb
Dose (HP)	0.2 g	0.2 g	0.2 g	3.0g	3.0 g

4.19.2 Discussion on Particle-Size Effect

For Cu, the particle-size effect showed that Cu extraction (**Table 4.24 a**) in the HP method was also significant in NA, HA, IL-E and IL-G and their peak extractions were 66, 34, 3 and 29 % at 3, 34, 1 & 4 mm respectively. NA and IL-E did not show significant increase as particle-size increased. Also, as particle-size increased, the MW method did not show significant increase in Cu extraction in NA with a peak extraction of 49 % at 3 mm. Statistically, the HP method was better for NA, HA, IL-G and IL-E. Consequently, Zhang *et.al.,* 2018 researched the extraction of Cu from waste PCBs using acidic ionic liquids and the result showed that as particle-sizes increased from 0.100 – 0.250 mm Cu extraction also increased and peaked at 94 %. Similarly, Chen *et al.,* 2016a researched the extraction of Cu from waste PCBs by typical ionic liquid acids and the result showed that as particle-sizes increased from 0.075 – 0.500 mm Cu extraction also increased and peaked at 20 %. These results are similar to the leaching behaviour of Cu in the research by Park *et. al.,* 2013 when 212 – 300 μm particle-sizes were used to leach approximately 80 % of Cu from contaminated soil. However, Yang *et al.,* 2011 studied how copper is influenced by the particle-size of waste printed circuit boards and the research revealed that Cu extraction decreased as the particle-sizes increased. Over 96 % of Cu was extracted when a 0.5 mm particle-size was used. Oluokun & Otunniyi, 2020 revealed that Cu extraction decreased as the particle-sizes of PCBs increased. Sethurajan, & Hullebusch, 2019 research showed that particle-sizes 0 -500 µm were the most effective in extraction of Cu as 67 % of Cu when 50 mM ferric sulfate was used. However, above 500 µm there was significant reduction in the amount of Cu extracted. The research by Janyasuthiwong *et al.,* 2016 showed that the extraction of Cu decreased as the particle-sizes increased. When 0.5 – 1.0 mm and 1 M HNO_3 were used, 450 mg/g Cu was extracted. Kavousi *et al.,* 2018 research showed that as the particle-sizes increased, the amount of Cu extracted decreased meaning that the lower particle-sizes were more effective in extracting Cu as there was more availability of reactive surfaces. The research found 0.15 - 0.40 mm as the best particle-sizes for extracting more than 90 % of Pb. The research by Khalid *et al.,* 2019 showed that Cu extraction was better with smaller particle-sizes the two different paticle-sizes for sample A, (205 µm) and sample B (265 µm) were used in the research, sample A had Cu extraction increase from 50 – 100% while sample B had Cu extraction increase from 46 – 82 %. It was expected in this research that as the particle-sizes of the PCBs increased, the extraction of Cu would also increase across all solvents used and this was so for the HA and IL-G (HP) but this was not the case for the NA, IL-E (HP) and NA (MW).

Also, there were no significant extractions in SA, the organic acids and IL-A to IL-D and IL-F. It was generally observed in this research and other researches stated above that as the particle-sizes of the PCBs increased, the extraction of Cu also increased. Consequently, the reason for the increase in Cu extraction and also no significant change in Cu extraction in this research could be attributed to a decrease in surface area per unit mass. This means that the solvents were able to extract more Cu when the surface area was lesser. It is likely that there was severe attrition occurring at the lower particle-sizes which hindered the solvents from permeating through the smaller particle-sizes of the PCBs. This result means that particle-sizes (1.0 – 4.0 mm) would be suitable for Cu extraction using the inorganic acids.

For Zn, the particle-size effect showed that Zn (**Table 4.25 a**) in the HP method was extracted by all solvents except ILs A-C and W. The highest of all peak extractions was seen in HA (93 %) and the lowest of all peak extractions was in IL-D (9 %). As the particle-size increased, Zn extraction in HA decreased but it increased in NA, SA, CA, MA and TA. Similar behaviour was seen in the MW method and the highest of all peak extractions was seen in IL-F (84 %) while the lowest of all peak extractions was seen in CA (25 %). Statistically, MW methods was better for ILs A-G but it was the same for the others. Chen *et al*., 2009 researched leaching Zn from Zn oxide ore using 0.5 mol/L of NaOH and the result showed that Zn extraction increased and peaked at 79 % with increasing particle-size from 65 – 76 μm. Also, Irannajad *et.al*., 2013 researched the leaching of Zn from low grade oxide ore using organic acid and the result revealed that as the particle-size increased from 50 – 350 μm the extraction of Zn also increased from 34 – 42 %. The research by Janyasuthiwong *et al*., 2016 showed that the extraction of Zn decreased as the particle-sizes increased. When 0.5 – 1.0 mm and 1 M HNO_3 were used, approximately 300 mg/g Zn was extracted. It was generally observed in this research and other researches stated above that as the particle-sizes of the PCBs increased, the extraction of Zn also increased. The reason for the increase in Zn extraction in this research could be attributed to a decrease in surface area per unit mass. This means that the solvents were able to extract more Zn when the surface area was lesser. Amongst the lower particle-sizes there was attrition occurring which possibly prevented the solvents from permeating through the smaller particle-sizes of the PCBs. This result means that particle-sizes (1.0 – 4.0 mm) would effectively extract Zn.

The particle-size effect showed that Fe (**Table 4.26 a**) in the HP method was significant in NA, HA, SA, CA, MA and TA. Their peak extractions are 70, 98, 56, 4, 5 and 3 % respectively. As the particle-sizes increased, Fe extraction increased in NA, HA nad SA while CA, MA and TA decrsed. Similar behaviour was seen in the MW method which showed significant extraction in NA, HA, SA, CA, MA and TA. Their peak extractions were 52, 47, 24, 5, 5, 3 % respectively. Statistically, the HP method was better for HA while the rest solvents were considered the same for both methods. The research by Tao *et al*., 2021 researched the behaviour of Fe in copper tailings using 0.5 M sulfuric acid and the results revealed that as the particle-sizes increased Fe extraction decreased from 67 to 61 %. It was expected in this research that as the particle-sizes of the PCBs increased, the extraction of Fe would increase and this was true for the HP method. The reason for this could be attributed to lesser attrition in the lower particle-sizes and much lesser attrition in the larger particle-sizes thereby allowing more surface contact between the solvents and the PCB particles which then results in more Fe extraction. However, in the MW method the there was no significant change in Fe extraction as the particle-sizes increased and this could be attributed to the increased temperature in the MW method. This result implies that using the HP method, 4 mm particle-size is suitable for extracting Fe.

The particle-size effect showed that Ni extraction (**Table 4.27 a**) in the HP method was significant in NA, HA, SA, CA and TA. Their peak extractions were 5, 2, 3, 2 and 3 %. As the particle-size increased there was no significant increase in the extraction of Ni. Also, the MW method showed that Ni extraction was significant in NA, HA and SA. Their peak extractions are 10, 4 and 5 % respectively. As the dose increased there was no significant increase in the extraction. Statistically, HP and MW methods were the same for CA while HP method was better for TA and MW method was better for NA and HA. Gharabaghi *et al*., 2013 researched the extraction of Ni from hazardous waste using 8 % sulfuric acid and the result showed that 84 - 98 % Ni was extracted when particle-size increased. The research by Janyasuthiwong *et al*., 2016 showed that the extraction of Ni decreased as the particle-sizes increased. When 0.5 – 1.0 mm and 1 M HNO_3 were used, approximately 550 mg/g Ni was extracted. It was expected in this research that as the particle-sizes of the PCBs increased, the extraction of Ni would increase but this was not so for both the HP and MW methods. Generally, there was no significant increase in the extraction of Ni and this can be attributed to the surface contact not large enough to allow interaction between the solvents and the

particles. Another reason could that Ni reacts relatively slowly with acids this would mean more time would be needed to extract more Ni. This results implies that any particle-sizes (1.0 – 4. 0 mm) would be suitable for the extraction of Ni.

The particle-size effect showed that Pb extraction (**Table 4.28 a**) in the HP method was significant in NA, HA, SA, CA, MA, TA, IL-D and IL-G. Their peak extractions were 88, 73, 2, 13, 6, 5, 3 and 1 % respectively. As dose increased, there was no significant change in Pb extraction. The MW method showed significant Pb extraction in NA and HA. Their peak extractions were 70 and 37 % respectively. Statistically, the HP method was better for all the solvents. However, the research by Park *et. al*., 2013 showed that as the particle-sizes increased the extraction of Pb also increased when Pb was leached from soil 212 – 300 μm. The research by Chen *et al.*, 2015 showed that at as particle-sizes increased the extraction of Pb also increased and at particle-sizes 0.5 - 1.0 mm, 41.44 % of Pb was extracted using IL ([BSO3HMIm]OTf). Kavousi *et al.,* 2018 research showed that as the particle-sizes increased, the amount of Pb extracted decreased meaning that the lower particle-sizes were more effective in extracting Pb as there was more availability of reactive surfaces. The research found 0.15 - 0.40 mm as the best particle-sizes for extracting more than 85 % of Pb. It was expected in this research that as the particle-sizes of the PCBs increased, the extraction of Pb would increase. However, Pb extraction did not show any significant change for both HP and MW methods and this could be attributed to the fact that the surface contact was not large enough to allow form more interaction between the solvents and the particle-sizes. This result implies that particle-sizes (1.0 – 4.0 mm) is suitable for extracting Pb.

The PCA for particle-size effect revealed the best contributing metals (variables) which were in the order Fe2 > Pb3 > Pb2 > Pb4 > Fe3> Cu4 > Cu3 > Cu2. These best contributing metals were the most extracted metals. The best contributing solvents (observations) which were in the order AQ2 > AQ1 > AQ3 > AQ6 > AQ5 > AQ4 > NA2 > HA3 > HA2 > HA1 > NA3 > NA1. This implies that AQ was the most outstanding solvent as it extracted the highest amount of metals each time it was used and this was followed by NA and HA. Consequently, as AQ is at the top of the descending order list for the best contributing solvents, it goes to show that AQ was suitable to use as baseline for the other solvents used in this research. Park

et al., 2009 research also showed that aqua regia was very aggressive when used for PCBs and it dissolved most of the materials in few seconds. Furthermore, as earlier discussed above the most effective dose for extracting each of the metals can be seen in Table 4.69.

Table 4.69 Optimum particle-size

Metal	Cu	Zn	Fe	Ni	Pb
Particle-size (HP)	1.0 mm	1.0 mm	4.0 mm	1.0 mm	1.0 mm

4.19.3 Discussion on H_2O_2 Effect

For Cu, the H_2O_2 effect showed that Cu extraction (**Table 4.32 a**) in the HP method was significant in NA, HA, CA and MA and their peak extractions were 39, 77, 7 and 7 % at 15, 25, 5 & 5 % of H_2O_2 respectively but the extraction did not show any significant change with increase in H_2O_2 amount. Also the MW method showed significant Cu extraction in NA, HA, CA and MA and their peak extractions were 62, 74, 7 and 7 % at 25, 25, 5 & 5 % of H_2O_2 respectively. Statistically, HP method was better for NA, SA and CA while MW method was better for HA. However, Jadhav *et al*., 2016 researched leaching of Cu from large pieces of PCBs using H_2O_2 and citric acid. The results showed that using only H_2O_2 for leaching had little effect as 0.9 % of Cu was extracted but when 5.83 % of H_2O_2 was used with 0.5 M citric acid 100 % of Cu was extracted. Kumar *et al*., 2014 research also showed that combining 15 % H_2O_2 with 1.5 mol/L and 2.5 mol/L of sulfuric acid gave a Cu extraction of 69 and 82 % respectively. The research by Behera *et al*., 2020 observed that 99.99 % of copper was leached from spent catalyst when H_2O_2 was used. The research by Lisinka *et al.,* 2018 showed that Cu extraction increased when H_2O_2 was added. 6.4 g/dm^3 of Cu was extracted when 30 % of H_2O_2 was added to 5 M H_2SO_4 within 6 hours. Oluokun & Otunniyi, 2020 research revealed that 2 M NH_4OH combined with 10M of H_2O_2 extracted 85 % of Cu and above 10 M, there was significant drop in the extraction. Kavousi *et al.*, 2018 research showed that increasing the amount of H_2O_2 from 0.4 to 0.8 mol/L increased the extraction of Cu. Approximately 75 % of Cu was extracted when 0.8 mol/L of H_2O_2 was used with 1.5 mol/l of Tetrafluoroboric acid, HBF_4. The research by Wang *et al.,* 2016 revealed that with the addition of 0.05 – 0.4 M of H_2O_2 the extraction of Cu increased. The initial 0.8 % of Cu that was extracted increased to 60.8 % witihin 90 minutes when 0.05 M H_2O_2 was used. Also,

there was significant increase in Cu extraction as the concentration of H_2O_2 also increased. The research by Devecci, 2010 extracted 98 % of Cu when oxidant media was used on PCBs for 4 hours at 68 ^{0}C. The research by Oh *et al.*, 2003 extracted 100 % of Cu when sulfuric acid and hydrogen peroxide were combined for 12 hours at 85 ^{0}C. Zhang *et.al.*, 2018 researched the extraction of Cu from waste PCBs using acidic ionic liquids and the result showed that as H_2O_2 increased from 5 – 15 % Cu extraction also increased and peaked at about 80 %. However, further increase of H_2O_2 led to a decrease in the Cu extraction. Jadhao *et al.*, 2021 research showed that when 0.4 M of H_2O_2 and 90 g/L ammonia were used 100 % of Cu was extracted. It was expected in this research that with the addition of H_2O_2, the extraction of Cu would increase across all the solvents used but this was not the case. Cu extraction did not increase significantly and Cu extraction was highest in the inorganic acids (NA & HA) followed by the organic acids. The ILs did not perform as expected and were significantly lower. It was generally observed that the addition of H_2O_2 assisted with the extraction of Cu as this was seen in the results of this research and other researches stated above. The effect of H_2O_2 on Cu extraction in this research is also similar to that of Zhang *et.al.*, 2018. The reason Cu extraction increased and then peaked in this research can be attributed to the oxidation of Cu into ion in the solvent which was assisted by H_2O_2. Also, it is likely that the presence of excess amount of H_2O_2 oxidized the ILs leading to a significantly lower extraction of Cu. The result implies that 5 – 25 % of H_2O_2 could be used to extract Cu effectively when used with NA or HA. For best results, use HA.

For Zn, the H_2O_2 effect showed that Zn (**Table 4.33 a**) in the HP method was extracted by all solvents except W. The highest of all peak extractions was seen in HA (86 %) and the lowest of all peak extractions was in CA (16 %). As the H_2O_2 amount increased, Zn extraction in TA decreased but no significant change was seen in the other solvents. Similar behaviour was seen in the MW method and the highest of all peak extractions was seen in NA (51 %) while the lowest of all peak extractions was seen in IL-B (17 %). Statistically, both HP and MW method was the same for TA while MW methods was better for HA, SA, CA and MA and the HP was better for NA and ILs A – G. Jadhav *et al.*, 2016 researched leaching of Zn the result showed that < 1 % of Zn was extracted when 1 M citric acid was used within 4 hours. However, when 5.83 % of H_2O_2 was used with citric acid 100 % of Zn was extracted. Contrary to this research, Zarate *et al.*, 2015 researched leaching Zn from a lead-silver-zinc concentrate using 0.15 M H_2O_2 in citrate solutions and the result showed that 1.5 % of Zn was

extracted. Jadhao *et al*., 2021 research showed that Zn extracted was 75 % when the combination of 90 g/L ammonia concentration, 180 g/L ammonium sulfate concentration and 0.4 M H_2O_2 concentration were used. Oluokun & Otunniyi, 2020 research revealed that 2 M NH_4OH combined with 10M of H_2O_2 extracted 74 % of Zn and above 10 M, there was significant drop the extraction and the reason for this was attributed to the form in which zinc exists in PCBs. The research by Lisinka *et al.,* 2018 showed that Zn extraction increased when H_2O_2 was added. 0.45 g/dm^3 of Zn was extracted when 30 % of H_2O_2 was added to 5 M H_2SO_4 within 72 hours. Kilicarslan & Saridede, 2016 showed in their research that Zn dissolved in IL ($HmimHSO_4$) within 20 minutes and this was because ZnO has very high level of solubility. However, when 80 % of the IL and 20 % of H_2O_2 was added the amount of Zn extracted was not significant. Kilicarslan & Saridede, 2016 concluded that aqueous systems favor the dissolution of Zn. It was expected in this research that with the addition of H_2O_2, the extraction of Zn would increase across all the solvents used but this was not exactly the case. Although there were significant extraction of Zn observed in the solvents, it was also observed that there were no significant changes as the H_2O_2 concentration increased. It was generally observed that Zn extraction was increased with the application of H2O2 and this effect was seen across all solvents in this research and other researches stated above. The reason Zn was extracted by all solvents in this research can be attributed to the oxidation of Zn into ion in the solvent which was assisted by H_2O_2. Another reason there was no significant change in the concentration of Zn extracted as H_2O_2 concentration increased was because the reaction that occurred when H_2O_2 was added happened quick and and all the H_2O_2 was used up in the reaction. The result implies that 5 – 25 % of H_2O_2 could be used to extract Zn effectively when used with NA and ILs A – G for best results.

For Fe, the H_2O_2 effect showed that Fe extraction (**Table 4.34 a**) in the HP method was significant in NA, HA and SA. Their peak extractions are 6, 36 and 48 % respectively. As the H_2O_2 amount increased Fe extraction in HA decreased but NA and SA did not show any significant change. Similar behaviour was seen in the MW method which showed significant extraction in NA, HA and SA. Their peak extractions were 2, 85 and 85 % respectively. As the H_2O_2 amount increased Fe extraction in SA decreased but NA and HA were unstable. However, Jadhav *et al*., 2016 researched leaching of Fe and the result showed that 1.3 % of Fe was extracted when 1 M citric acid was used within 4 hours. However, when 5.83 % of H_2O_2 was used with citric acid 100 % of Fe was extracted. The research by Lisinka *et al.,*

2018 showed that Fe extraction increased when H_2O_2 was added. Approximately 0.9 g/dm^3 of Fe was extracted when 30 % of H_2O_2 was added to 5 M H_2SO_4 within 6 hours. It was expected in this research that with the addition of H_2O_2, the extraction of Fe would increase across all the solvents used but this was not exactly the case. The HP method did not show much significant change and this could be attributed to the oxidation of Fe into ion in the solvent which was assisted by H_2O_2. The result implies that 15 % of H_2O_2 when used with the inorganic acids could be used to extract Cu effectively when used with SA.

For Ni, the H_2O_2 effect showed that Ni extraction (**Table 4.35 a**) in the HP method was significant in NA and SA. Their peak extractions were 26 and 34 %. As the H_2O_2 amount increased, Ni extraction in NA did not change but HA was unstable. Also, the MW method showed that Ni extraction was significant in NA, HA and SA. Their peak extractions are 82, 78 and 96 % respectively. As the H_2O_2 amount increased Ni extraction was unstable. Statistically, the MW method was generally better. Jadhav *et al*., 2016 researched leaching of Ni which showed that < 1 % of Ni was extracted when 1 M citric acid was used within 4 hours. However, when 5.83 % of H_2O_2 was used with citric acid 100 % of Ni was extracted. Jadhao *et al.,* 2021 research showed that when 0.4 M of H_2O_2 and 90 g/L ammonia were used 80 % of Ni was extracted. It was expected in this research that with the addition of H_2O_2, the extraction of Ni would increase across all the solvents used but this was not the case. The HP method did not show any significant change and the MW method extracted significant amount of H_2O_2 at 15 %. The result generally implies that 15 % of H_2O_2 was observed to be the most suitable when used with the inorganic acids.

For Pb, the H_2O_2 effect showed that Pb extraction (**Table 4.36 a**) in the HP method was significant in NA and HA. Their peak extractions were 4 and 7 %. No significant change was observed as H_2O_2 amount increased. The MW method showed significant Pb extraction in NA and HA. Their peak extractions were 43 and 24 % respectively. Pb extractions increased as H_2O_2 amount increased. Statistically, the MW method was better for all the solvents. Jadhav *et al*., 2016 researched leaching of Pb showed that < 1 % of Pb was extracted when 1 M citric acid was used withing 4 hours. However, when 5.83 % of H_2O_2 was used with citric acid 100 % of Pb was extracted. The research by Zárate-Gutiérrez *et al*., 2015 revealed that

when 0.05M H_2O_2 100 % of Pb was extracted in 90 minutes. The use of H_2O_2 greatly increased the extraction of Pb. The research by Chen *et al.*, 2015 showed that at as H_2O_2 increased, the increase in extraction of Pb was significant when IL ([BSO3HMIm]OTf) was used. 26.67 % of Pb was extracted when 15ml of H_2O_2 was used. Kavousi *et al.*, 2018 research showed that increasing the amount of H_2O_2 from 0.4 to 0.8 mol/L increased the extraction of Pb. Approximately 75 % of Pb was extracted when 0.8 mol/L of H_2O_2 was used with 1.5 mol/l of Tetrafluoroboric acid, HBF_4. It was expected in this research that with the addition of H_2O_2, the extraction of Pb would increase across all the solvents used but this was not the case as the Pb extraction decreased with increase in H_2O_2 amount while the MW method increase with with H_2O_2 amount. The reason Pb extraction increased was observed in the inorganic acids in this research can be attributed to the oxidation of Pb into ion in the solvent which was assisted by H_2O_2 and the presence of excess amount of H_2O_2 oxidized the ILs leading to a significantly lower extraction of Pb. The result implies that 25 % of H_2O_2 could be used to extract Pb effectively when used with NA or HA (MW method).

The PCA for H_2O_2 effect revealed the best contributing metals (variables) which were in the order Cu5 > Cu15 > Pb5 > Cu25 > Pb15 > Zn15 > Zn25 > Zn5. These best contributing metals were the most extracted metals. The best contributing solvents (observations) which were in the order AQ1 > AQ4 > HA1 > HA2 > NA2 > HA2 > HA3 > HA1. This implies that AQ was the most outstanding solvent as it extracted the highest amount of metals each time it was used and this was followed by NA and HA. Consequently, as AQ is at the top of the descending order list for the best contributing solvents, it goes to show that AQ was suitable to use as baseline for the other solvents used in this research. Park et al., 2009 research also showed that aqua regia was very aggressive when used for PCBs and it dissolved most of the materials in few seconds. Furthermore, as earlier discussed above the most effective dose for extracting each of the metals can be seen in Table 4.70.

Table 4.70 Optimum H_2O_2

Metal	Cu	Zn	Fe	Ni	Pb
H_2O_2 (HP)	**5 %**	**5 %**	**15 %**	**15 %**	**25 %**

4.19.4 Discussion on Temperature Effect

For Cu, the temperature effect showed that Cu extraction (**Table 4.40**) in the HP method was significant in NA, HA, SA, CA, IL-E and IL-G and their peak extractions were 68, 58, 3, 1, 3, 33 % at 70 ^{0}C respectively. As the the temperature increased from 25 – 70 ^{0}C, Cu extraction also increased. There was no MW method as the microwave temperature was not adjustable. Hossain *et.al.*, 2018 researched the recovery of Cu from printed circuit boards of mobile phones when sulfuric acid was used and the result showed that temperature affects the leaching of Cu and as the temperature used increased from 40 – 80 ^{0}C, 138 mg/g peak concentration of Cu was extracted at 40 ^{0}C. Zhang *et.al.*, 2018 researched the extraction of Cu from waste PCBs using acidic ionic liquids and the result showed that as temperatue increased from 40 – 80 ^{0}C, Cu extraction also increased and peaked at 71 % at 80 ^{0}C. Biswas & Mulaba-Bafubiandi, 2016 extracted copper and cobalt from oxidized ore using organic acids at 60, 70 & 80 ^{0}C. The result showed that copper extracted using citric acid for 2 hours were 51, 79 & 84 % respectively. Kumar *et al*., 2014 studied leaching metals from waste printed circuit boards using sulfuric and nitric acids. The research showed that as temperature increased from 30 to 50 ^{0}C copper extraction also increased from 35 to 46 %. However, the extraction of copper reduced with temperatures above 50 ^{0}C. Oluokun & Otunniyi, 2020 revealed that Cu extraction of 85 % was maximum at 40 ^{0}C and above 40 ^{0}C there was no significant increase. The research by Khalid *et al*., 2019 on leaching Cu from rich converter slag using sulfuric acid showed that Cu extraction was $\geq$ 98 % at a temperature of 40 ^{0}C. Temperatures above 40 ^{0}C did not increase Cu extractions. Kavousi *et al.,* 2018 research showed that as the temperature increased the amount of Cu extracted also increased. 99 % of Cu was extracted when 75 ^{0}C temperature was used. Jadhao *et al*., 2021 research showed that when 90 g/L ammonia was used 100 % Cu was extracted at a temperature of 60 ^{0}C. The research by Wang *et al.*, 2016 showed that copper extraction was sensitive to temperature. The temperatures used were 25, 35, 45, 55 & 65 % and at 25 ^{0}C, 98 % of copper was extracted in 90 minutes while at 65 ^{0}C, 96 % of copper was extracted in 10 minutes. Mecucci & Scott, 2002 research showed that the amount of Cu extracted increased as the temperature increased. At 80 ^{0}C, 83 % of Cu was extracted when 4 M HNO_3 was used. It was expected in this research that as the temperature increased, the extraction of Cu would also increase across all solvents and this was the case for NA HA SA CA IL-E IL-G. This pattern was generally observed in this research and other researches stated above. The reason Cu extraction increased as the temperature increased could be attributed to a large increase in high energy collision which is equal to or greater than the

activation energy which led to the reaction. Another reason Cu extraction increased as temperature increased could be attributed increased mass transfer coefficient and diffusivity. The result implies that Cu extraction would be effective when 70 ^{0}C temperature is used on NA, HA & IL-G.

For Zn, the temperature effect showed that Zn (**Table 4.41**) in the HP method was extracted by all solvents except ILs A-C and W. The highest of all peak extractions was seen in HA (89 %) and the lowest of all peak extractions was in IL-F (8 %). As the temperature increased, Zn extraction in NA, HA and SA decreased while Zn extraction increased in the other solvents. Irannajad *et.al*., 2013 researched the leaching of Zn from low grade oxide ore using 0.5 M citric acid and the result revealed that as the temperature increased from 25 – 80 ^{0}C the extraction of Zn also increased from 42 - 65 %. Santos *et al.*, 2010 researched the extraction of Zn using 6 mol/L of NaOH and the result showed that as temperature increased from 60 – 90 ^{0}C, Zn extraction also increased and peaked at approximately 90 %. Nekouei *et al*., 2019 research revealed that 100 % of Zn was extracted when 2.7 M HNO3 was used at 25 ^{0}C. Oluokun & Otunniyi, 2020 revealed that Zn extraction of 55 % was maximum at 40 ^{0}C and above 40 ^{0}C there was no significant increase. It was expected in this research that as the temperature increased, the extraction of Zn would also increase across all solvents and this was the case for the organic acids but it was not the case for the inorganic acids. This increasing Zn extraction observed in the organic acids was generally observed in other researches stated above. The reason Zn extraction increased as the temperature increased in the organic acids could be attributed to a large increase in high energy collision which is equal to or greater than the activation energy which led to the reaction and extraction. Howevever, the reducing Zn extraction in the inorganic acids with increasing reaction temperature could be attributed to the decomposition of the inorganic acids. The result implies that Zn extraction would be most effective when 25 ^{0}C temperature is used on the inorganic acids or 70 ^{0}C temperature for the organic acids.

For Fe, the temperature effect showed that Fe extraction (**Table 4.42**) in the HP method was significant in NA, HA and SA. Their peak extractions are 36, 50 and 28 %. As the temperature increased, Fe extraction also increased. Tao *et al*., 2021 researched the behaviour of Fe in copper tailings and the results showed that as the temperature increased from 20 - 60 ^{0}C the extraction of Fe also increased and peaked at 69 %. The research by Xiao *et al*., 2021 extracted 90 % of Fe at a temperature of 220 ^{0}C. Nekouei *et al*., 2019 research revealed that 88.7 % of Fe was extracted when 2.4 M HNO3 was used at 26.9 ^{0}C. The research by Palden

et al., 2020 revealed that increasing the temperature did not have any significant increase on the extraction of Fe. However, the most suitable temperature was 25 ^{0}C. It was expected in this research that as the temperature increased, the extraction of Fe would also increase across all solvents and this was the case for the inorganic acids as peak Fe extraction was observed at 70 ^{0}C temperature. However, the reason for the increase in Fe extraction as the temperature increased could be attributed to a large increase in high energy collision which is equal to or greater than the activation energy which led to the reaction. This result implies that at 70 ^{0}C the extraction of Fe would be effective when the inorganic acids are used.

For Ni, the temperature effect showed that Ni extraction (**Table 4.43**) in the HP method was significant in NA, HA and SA. Their peak extractions were 5, 4 and 3 %. As temperature increased, Ni extraction did not show significant change. Gharabaghi *et al*., 2013 researched the extraction of Ni from hazardous waste using 8 % sulfuric acid and the result showed that when temperature increased from 25 – 75 ^{0}C Ni extraction was 52 – 70 %. Li *et.al.,* 2009 researched the extraction of Ni from spent battery material using 6 mol/L HCl and the result showed that as temperature increased from 20 - 90 ^{0}C Ni extraction (approximately 90 – 95 %) was not significantly. The research by Xiao *et al*., 2021 extracted 99 % of Ni at a temperature of 220 ^{0}C. The research by Mohammadreza *et al*., 2014 showed that 83 % of Ni was extracted when temperature increased to 95 ^{0}C. Jadhao *et al*., 2021 research showed that when 90 g/L ammonia was used 85 % Ni was extracted at a temperature of 60 ^{0}C. It was expected in this research that as the temperature increased, the extraction of Ni would also increase across all solvents and this was not the case for all the solvents. Although the inorganic acids extracted some Ni but it there was no significant change. However, the reason there was no significant change in Fe extraction as the temperature increased could be attributed slow reaction of Ni as it would require more time to react with the solvent. This result implies that at 25 - 70 ^{0}C temperature would be effective for Ni extraction when the inorganic acids are used.

For Pb, the temperature effect showed that Pb extraction (**Table 4.44**) in the HP method was significant in NA, HA, SA, CA, MA, TA, IL-D and IL-G. Their peak extractions were 54, 52, 1, 4, 4, 9, 3 and 1 % respectively. No significant change in Pb extraction was observed when temperature increased. However, the research by Jha *et al.*, 2012 also revealed that as

temperature increased from 60 – 90 ^{0}C, Pb extraction also increased from 42 – 100 % when 0.2 M nitric acid was used. The research by Palden et al., 2020 revealed that increasing the temperature did not have any significant increase on the extraction of Pb. However, the most suitable temperature was 25 ^{0}C. Kavousi *et al.,* 2018 research showed that as the temperature increased the amount of Pb extracted also increased. 90 % of Pb was extracted when 75 ^{0}C temperature was used. Zhang et al., 2019 research showed that the extraction of Pb increased as the temperature increased when 3.0 mol/L NaOH was used. 100 % of Pb was extracted within 80 ^{0}C. It was expected in this research that as the temperature increased, the extraction of Pb would also increase across all solvents and this was not the case for all the solvents. Although the inorganic acids extracted some Pb and showed some significant change, the organic acids and ILs extracted lower amount of Pb which also did not show much significant changes. However, the reason Pb extraction increased as the temperature increased in the inorganic acids could be attributed to high energy collision which is equal to or greater than the activation energy which led to the reaction. This result implies that at 70 ^{0}C the extraction of Pb would be effective when the inorganic acids are used.

The PCA for temperature effect revealed the best contributing metals (variables) which were in the order Pb25 > Cu25 > Pb40 > Pb70 > Cu40 > Zn25 > Zn40 > Fe70. These best contributing metals were the most extracted metals. The best contributing solvents (observations) which were in the order AQ3 > AQ2 > AQ1 > NA3 > NA2 > HA3 > HA1 > NA1. This implies that AQ was the most outstanding solvent as it extracted the highest amount of metals each time it was used and this was followed by NA and HA. Consequently, as AQ is at the top of the descending order list for the best contributing solvents, it goes to show that AQ was suitable to use as baseline for the other solvents used in this research. Park et al., 2009 research also showed that aqua regia was very aggressive when used for PCBs and it dissolved most of the materials in few seconds. Furthermore, as earlier discussed above the most effective dose for extracting each of the metals can be seen in Table 4.71.

Table 4.71 Optimum temperature

Metal	Cu	Zn	Fe	Ni	Pb
Temperature (HP)	70 ^{0}C	25 ^{0}C	70 ^{0}C	70 ^{0}C	70 ^{0}C

4.19.5 Discussion on Time Effect

For Cu, the time effect showed that Cu extraction (**Table 4.48**) in the HP method was significant in NA, HA and IL-G and the peak extractions were 77, 40 and 25 % respectively at 180 minutes each. As time increased from 30 – 180 minutes, Cu extraction also increased. Hossain *et.al.*, 2018 research also showed Cu extraction increased as the time increased from 15 – 90 minutes, 160 mg/g peak concentration of Cu was extracted at 75 minutes. The research by Behera *et al*., 2020 observed that 55 % of copper was leached within 300 minutes when microwave was used. The research by Xiao *et al*., 2021 extracted 93 % of Cu within 2 hours. Zhang *et.al.*, 2018 researched the extraction of Cu from waste PCBs using acidic ionic liquids and the result showed that as time increased from 90 – 120 minutes Cu extraction also increased and peaked at approximately 75 % and became stable above 120 minutes. Yang *et al*., 2011 research studied the influence of time extracting copper from waste printed circuit boards and the result showed that Cu extraction increased as time increased. The peak extraction of 87 % of Cu was extracted after 5 hours. Oluokun & Otunniyi, 2020 revealed that Cu extraction of 76 % was maximum at 3 hours. Nekouei *et al*., 2019 research revealed that 100 % of Cu was extracted when 2.7 M HNO3 was used in 20 minutes. The research by Ozbas et.al., 2013 revealed that 28 % of Cu was extracted within 100 minutes using 0.1 mol L−1 EDTA and no significant extraction was observed after 100 minutes. The research by Khalid *et al*., 2019 revealed that 60 minutes was sufficient enough to extract Cu as copper extraction did not increase after 30 minutes when 1 M of sulfuric acid was used. Jadhao *et al*., 2021 research showed that when 90 g/L ammonia and 180 g/L ammonium sulphate was used 85 % of Cu was extracted after 2 hours. It was expected in this research that as the reaction time of the PCBs increased, the extraction of Cu would also increase across all solvents used but this was not so as only NA, HA and IL-G increased Cu extraction as the reaction time increased. This means that the other solvents did not respond to the increase in time. Results from other researches as stated above revealed that there was an increased Cu extraction as the reaction time increased. However, in this research, the reason Cu extraction increased as the reaction time increased could be due to prolonged contact between solvents and the reacting materials (PCBs). As the reaction time increased, there was more contact for the reaction to occur thereby leading to more extraction of Cu. This result implies that using HA as the most suitable solvent at 180 minutes reaction time, Cu could be best extracted.

For Zn, the time effect showed that Zn (**Table 4.49**) in the HP method was extracted by all solvents except ILs A-C and W. The highest of all peak extractions was seen in HA (63 %) and the lowest was in IL-E (7%). As the temperature increased, Zn extraction in all the solvents also increased. Contrary to this research, Irannajad *et.al*., 2013 researched the leaching of Zn from low grade oxide ore using 0.5 M citric acid and the result revealed that time did not affect Zn extraction as there was no significant change in Zn extraction when time changed from 30 – 150 minutes. However, the research by Chen *et al*., 2016b on the effects of roasting pretreatment on zinc from complicated ores revealed that as the time increased from 10 – 60 minutes, the extraction of Zn increased from 77 – 85 % and no significant change till 150 minutes. Santos *et al.*, 2010 researched the extraction of Zn using 6 mol/L of NaOH and the result showed that as time increased from 25 – 300 minutes, Zn extraction also increased from approximately 20 - 90 %. The research by Ozbas et.al., 2013 revealed that 48 % of Zn was extracted within 100 minutes using 0.1 mol L−1 EDTA and no significant extraction was observed after 100 minutes. It was expected in this research that as the reaction time of the PCBs increased, the extraction of Zn would also increase across all solvents used but this was not so. It was only true for CA and MA. However, the other solvent did not show any significant changes in Zn extraction as the reaction time increased and this was also in line with the research by Irannajad *et.al*., 2013 stated above. However, in this research, the reason the Zn extraction increased in CA and MA as the reaction time increased could to be due to prolonged contact between solvents and the reacting materials (PCBs). As the time increased, there was more contact for the reaction to occur thereby leading to more extraction of Zn. The reason there was no significant difference in the Zn extraction as observed in the other solvents could be attributed to quick reaction occurring between the reactants. This result implies that 30 - 180 minutes would be suitable time for extracting Zn when the inorganic or organic acids are used. However, using NA as the most suitable solvent at 180 minutes reaction time, Zn could be best extracted.

For Fe, the Time effect showed that Fe extraction (**Table 4.50 a**) in the HP method was significant in NA, HA and SA. Their peak extractions are 77, 84 and 61 %. As the time increased, Fe extraction also increased. The research by Li *et al.*, 2009 on Fe extraction from spent battery material also revealed that as time increased from 10 – 60 minutes Fe extraction also increased to > 90 %. The research by Tao *et al.*, 2021 also revealed that as time increased from 10 – 180 minutes Fe extraction also increased. The research by Ozbas et.al.,

2013 revealed that 5 % of Fe was extracted within 100 minutes using 0.1 mol/L EDTA and no significant extraction was observed after 100 minutes. The research by Palden et al., 2020 revealed that 1.5 % of iron was extracted within 1 hour when 0.05 mol/L of EDTA was used. It was expected in this research that as the reaction time of the PCBs increased, the extraction of Cu would also increase across all solvents used. However, in this research, the reason Fe extraction increased as the reaction time increased could be due to prolonged contact between solvents and the reacting materials (PCBs). As the reaction time increased, there was more contact for the reaction to occur which led to more extraction of Fe. This result implies that using HA as the most suitable solvent at 180 minutes reaction time, Pb could be best extracted.

For Ni, the time effect showed that Ni extraction (**Table 4.51**) in the HP method was significant in NA, HA, SA, CA and TA. Their peak extractions were 4, 4, 3, 3 and 3 %. As time increased, Ni extraction also increased. Similarly, the research by Li *et al.*, 2009 revealed that as time increased from 10 – 60 minutes Ni extraction also increased to > 95 %. Gharabaghi *et al*., 2013 research showed that as time increased from 0 – 40 minutes, Ni extraction also increased rapidly and the peak extraction was 98 %.The research by Xiao *et al*., 2021 extracted 97 % of Ni within 2 hours. The research also showed that increase in temperature increased the extraction of Ni to 99 %. The research by Ozbas et.al., 2013 revealed that 13 % of Ni was extracted within 100 minutes using 0.1 mol/L EDTA and no significant extraction was observed after 100 minutes. Nekouei *et al*., 2019 research revealed that 95.6 % of Ni was extracted when 2.7 M HNO_3 was used in 41 minutes, 45 ^{0}C. Jadhao *et al*., 2021 research showed that when 90 g/L ammonia and 180 g/L ammonium sulphate was used 85 % of Ni was extracted after 4 hours. The research by Park & Fray, 2009 revealed that the extraction of Ni increased as the time increased and 100 % of Ni was extracted in 3 hours when *aqua-regia* was used. It was expected in this research that as the reaction time of the PCBs increased, the extraction of Ni would also increase across all solvents used. However, in this research, Ni extraction was not significant and also did not show significant changes. Consequently, the reason there was no significant change in Ni extraction as time increased could be attributed to a quick reaction which have occurred between the reactants. This result implies that using NA as the most suitable solvent at 180 minutes reaction time, Ni could be best extracted.

For Pb, the time effect showed that Pb extraction (**Table 4.52**) in the HP method was significant in NA, HA, SA, CA, MA, TA, IL-D and IL-G. Their peak extractions were 59, 70, 1, 4, 11, 4, 2, 1 % respectively. As time increased, Pb extraction also increased. Similarly, the research by Jha *et al.*, 2012 on the extraction of Pb from solder material of PCBs also revealed that as time increased from 10 – 120 minutes, Pb extraction increased from 17 – 100 % when 0.5 M nitric acid was used. However, <1% and 1 % of Pb was extracted when 0.5 M of sulfuric acid and 0.5 M of hydrochloric acid respectively were used. The research by Palden et al., 2020 revealed that 60 % of Pb was extracted within 60 minutes and further leaching showed that 74 % of Pb was extracted within 6 hours when 0.05 mol/L of EDTA was used. Nekouei *et al*., 2019 research revealed that 88.1 % of Pb was extracted when 2.6 M HNO_3 was used in 26 minutes. In the research by Zhang et al., 2019 the extraction of Pb increased as the temperature increased when 3.0 mol/L NaOH was used and 100 % of Pb was extracted within 120 minutes. Mecucci & Scott, 2002 research showed that the amount of Pb extracted within 2 hours was 50 %. However, after further leaching, 90 % of Pb was extracted within 6 hours. It was expected in this research that as the reaction time of the PCBs increased, the extraction of Pb would also increase across all solvents used and this was true for Pb extraction in inorganic and organic acids. The reason Pb extraction increased with increase in time could be attributed to to prolonged contact between solvents and the reacting materials (PCBs). As the reaction time increased, there was more contact for the reaction to occur which led to more extraction of Pb. This result implies that using HA as the most suitable solvent at 180 minutes reaction time, Pb could be best extracted.

The PCA for particle-size effect revealed the best contributing metals (variables) which were in the order Pb90 > Fe60 > Cu120 > Cu90 > Fe90 > Zn180 > Zn150 > Zn120. These best contributing metals were the most extracted metals. The best contributing solvents (observations) which were in the order AQ1 > AQ3 > AQ2 > NA3 > NA2 > NA1 > TA2 > TA3 > TA1. This implies that AQ was the most outstanding solvent as it extracted the highest amount of metals each time it was used and this was followed by NA and HA. Consequently, as AQ is at the top of the descending order list for the best contributing solvents, it goes to show that AQ was suitable to use as baseline for the other solvents used in this research. Park et al., 2009 research also showed that aqua regia was very aggressive when used for PCBs and it dissolved most of the materials in few seconds. Furthermore, as earlier discussed above the most effective dose for extracting each of the metals can be seen in Table 4.72.

Table 4.72 Optimum time

Metal	Cu	Zn	Fe	Ni	Pb
Time (HP)	180 minutes	180 minutes	180 minutes	180 minutes	180 minutes

4.19.6 Discussion on Concentration Effect

For Cu, the concentration effect showed that Cu extraction (**Table 4.57 a**) in the HP method was significant in NA, HA, IL-E and IL-G and their peak extractions were 95, 16, 2 and 85 % respectively. As the concentration increased, Cu extraction in NA and IL-G also increased but extraction in HA and IL-E decreased. Also, as concentration increased, the MW method did not show significant change in Cu extraction in NA with a peak extraction of 48 %. Statistically, the HP and MW methods were the same for NA and IL-G while the HP method was better for HA. Park *et. al*., 2013 researched the behaviour of Cu in contaminated soil by leaching with citric acid and the results showed that as the concentration increased from 0.1 – 2.0 kmol.m^{-3} the extraction of Cu also increased to 86.5 %. The research by Behera *et al*., 2020 observed that 87 % of copper was leached from spent catalyst when 3.0 M of H_2SO_4 was used in a microwave. The research by Li *et al.*, 2009 on the extraction of Cu from spent battery material showed that as the concentration of HCl increased from 4.0 - 7.0 mol/L, extraction also increased and reached a peak concentration of 98.5 % of Cu. Hossain *et.al.*, 2018 research also showed as the concentration of sulfuric acid increased from 0.1 M – 0.5 M, the extraction of Cu also increased. Kumar *et al*., 2014 studied leaching metals from waste printed circuit boards using sulfuric and nitric acids. The research revealed that as the concentration of sulfuric acid increased from 0.8 to 1.0 mol/L the percentage of Cu extracted increased from 34 to 55 %. Also, as nitric acid concentration also increased from 1.0 to 4.0 mol/L, Cu extracted increased from 63 - 96 %. Zhang *et.al.*, 2018 research showed that when the concentration of acid-functionalized ionic liquid ([CM-MIM]HSO_4) was increased from 10 - 90 %, the Cu extraction increased and peaked at 69 % with an IL concentration of 70 % but above 70 % IL concnetration, the Cu extraction was relatively thesame. The research by Khalid *et al*., 2019 using concentrations of 1, 2 & 3 M of sulfuric acid; the result showed 99% of copper extracted. Jadhao *et al*., 2021 research showed that when 90 g/L ammonia was used 70 % of Cu was extracted. The research by Wang *et al.*, 2016 showed that there was significant

increase in Cu extraction when HCl concentration increased from 0.05 – 0.8 M. When 0.05 M was used 49.7 % of Cu was extracted and when 0.8 M was used $\geq$ 80 % of copper was extracted. It was expected in this research that as the concentration of the solvents increased, the extraction of Cu would also increase across all solvents used but this was only so for NA, HA and IL-G. The reason the extraction of Cu increased with increase in solvent concentration could be attributed to rate law which states that the reaction rate would generally increase as the concentrations of the reactants increased. This means that there would be more extraction of Cu with increased solvent concentration. The result implies that using NA as the most suitable solvent at Conc 3, Cu could be best extracted.

For Zn, the concentration effect showed that Zn (**Table 4.58 a**) in the HP method was extracted by all solvents except ILs A-C and W. The highest of all peak extractions was seen in NA (71 %) and the lowest was in IL-G (11%). As the temperature increased, Zn extraction in NA and CA also increased but the other solvents did not show any significant change. Similar behaviour was seen in the MW method and the highest extraction was seen in IL-F (92 %) while the lowest was seen in IL-A (57 %). As the concentration increased, IL A-G extractions increased and then decreased while the others increased. Statistically, MW methods was better for IL-A and IL-C but it was the same for the other solvents. Park *et. al*., 2013 researched the behaviour of Zn in contaminated soil by leaching with citric acid and the results showed that as the concentration increased from 0.1 – 2.0 $kmol.m^{-3}$ the extraction of Zn also increased to 88.9 %. Silvas *et al*., 2015 research showed that 40% of Zn was extracted using sulfuric acid as zinc has a wide solubility range. Tao *et al*., 2021 researched the behaviour of Zn in copper tailings and the results showed that as the concentration increased from 0.10 – 0.53 mol L^{-1} the extraction of Zn also increased and peaked at 65 %. Ajiboye *et al*., 2019 researched the extraction of Zn from PCBs and as the concentration of hydrochloric acid increased from 0.5 – 2.5 M, the of extraction Zn did not show any significant increase from (59 – 62 %). It was expected in this research that as the concentration of the solvents increased, the extraction of Zn would also increase across all solvents used but this was only observed in the ILs (HP method) while the other solvents did not show significant changes in Zn extraction. Similar observation was seen in the (MW method) but conc3 Zn extraction were significantly lower. The reason the extraction of Zn increased with increase in solvent concentration could be attributed to rate law which states that the reaction rate would generally increase as the concentrations of the reactants

increased. This means that there would be more extraction of Cu with increased solvent concentration. The result implies that using NA as the most suitable solvent at Conc 3, Zn could be best extracted.

For Fe, the concentration effect showed that Fe extraction (**Table 4.59 a**) in the HP method was significant in NA, HA, SA and TA. Their peak extractions are 89, 89, 78 and 4 % respectively. As the time increased, Fe extraction also increased. Also, the MW method showed that Fe extraction was significant in NA, HA and SA. Their peak extractions are 57, 62 and 26 % respectively. As the time increased, Fe extraction in HA was unstable but NA and SA also increased. Consequently, The research by Li *et al.*, 2009 on the extraction Fe from spent battery material also showed that as the concentration of HCl increased from 4.0 - 7.0 mol/L, Fe extraction also increased and reached a peak concentration of 93.6 %. Similarly, Ajiboye *et al*., 2019 researched the extraction of Fe from PCBs and as the concentration of hydrochloric acid increased from 0.5 – 2.5 M, the extraction of Fe increased from < 15 % to approximately 65 %. Siaw et al., 2020 research showed that revealed that as the concentration of HCl increased the amount of Fe extracted also increased and peak extraction of approximately 65 % Fe occurred at 6M HCl. The research by Tao *et al*., 2021 revealed that 0.64 mol/L of sulfuric acid extracted 67.8 % of Fe. It was also observed that at a much lower concentration of 0.31 mol/L, the sulfuric acid concentration was not sufficient to extract Fe. It was expected in this research that as the concentration of the solvents increased, the extraction of Fe would also increase across all solvents used and this was true for the inorganic and organic acids. The reason the extraction of Fe increased with increase in solvent concentration could be attributed to rate law which states that the reaction rate would generally increase as the concentrations of the reactants increased. This means that there would be more extraction of Fe with increased solvent concentration. The result implies that using HA as the most suitable solvent at Conc 3, Fe could be best extracted.

For Ni, the concentration effect showed that Ni extraction (**Table 4.60 a**) in the HP method was significant in NA, HA, SA, CA and TA. Their peak extractions were 6, 15, 2, 2 and 3 %. As concentration increased, Ni extraction decreased in HA but the other solvents did not show any significant changes. Also, the MW method showed that Ni extraction was significant in NA, HA and SA. Their peak extractions are 15, 4 and 5 % respectively. As

concentration increased Ni extraction did not show significant changes but it increased in NA. Statistically, the HP and MW methods are the same. Similarly, the research by Li *et al.*, 2009 on the extraction of Ni from spent battery material also showed that as the concentration of HCl increased from 4.0 - 7.0 mol/L, extraction also increased and reached a peak concentration of 96.5 % of Ni. Also, Ajiboye *et al*., 2019 researched the extraction of Ni from PCBs and as the concentration of hydrochloric acid increased from 0.5 – 2.5 M, the extraction Ni increased from < 10 % to approximately 55 %. Jadhao *et al*., 2021 research showed that when 90 g/L ammonia was used 60 % of Ni was extracted. Hosseini *et al*., 2017 research showed that 23% of Ni was leached when 4 mol of sulfuric acid was used. It was expected in this research that as the concentration of the solvents increased, the extraction of Ni would also increase across all solvents used. It was generally observed that the Ni extractions were not significant and there was no significant differences as the concentrations increased. However, the reason there was no significant extraction of Ni could be attributed to the diluted acids used in the reaction. The result implies that using HA as the most suitable solvent at Conc 1, Ni could be best extracted.

For Pb, the concentration effect showed that Pb extraction (**Table 4.61 a**) in the HP method was significant in NA, HA, SA, CA, MA, TA, IL-D and IL-G. Their peak extractions were 59, 67, 1, 4, 5, 2, 2 and 1 % respectively. As dose increased, Pb extraction also increased. The MW method showed significant Pb extraction in NA and HA. Their peak extractions were 68 and 37 % respectively. Statistically, both HP and MW methods are the same for NA and HA. Consequently, Park *et. al*., 2013 researched the behaviour of Pb in contaminated soil by leaching with citric acid and the results showed that as the concentration increased from 0.1 – 2.0 $kmol.m^{-3}$ the extraction of Pb also increased to 83.3 %. Furthermore, the research by Jha *et al.*, 2012 revealed that as concentration increased from 0.1 - 0.4 M of nitric acid the Pb extraction increased from 66 – 100 %. However, Ajiboye *et al*., 2019 researched the extraction of Pb from PCBs and as the concentration of hydrochloric acid increased from 0.5 – 2.5 M, the extraction of Pb increase from approximately 55 % to 65 %. Mecucci & Scott, 2002 research showed that the amount of Pb extracted increased as the concentration increased. 90 % of Pb was extracted when 4 M HNO_3 was used. It was expected in this research that as the concentration of the solvents increased, the extraction of Pb would also increase across all solvents used. Significant increase in Pb extraction was observed in the inorganic and organic acids. The reason the extraction of Pb increased with increase in solvent concentration could be attributed to rate law which states that the reaction rate would

generally increase as the concentrations of the reactants increased. This means that there would be more extraction of Pb with increased solvent concentration. The result implies that using HA as the most suitable solvent at Conc 3, Pb could be best extracted.

The PCA for particle-size effect revealed the best contributing metals (variables) which were in the order Fe_conc1 > Cu_conc2 > Cu_conc1 > Fe_conc2 > Cu_conc3 > Pb_conc1 > Pb_conc3 > Pb_conc2. These best contributing metals were the most extracted metals. The best contributing solvents (observations) which were in the order AQ4 > AQ6 > AQ3 > AQ5 > AQ1 > AQ2 > NA6 > NA5 > NA2 > NA4 > NA1 > NA3. This implies that AQ was the most outstanding solvent as it extracted the highest amount of metals each time it was used and this was followed by NA and HA. Consequently, as AQ is at the top of the descending order list for the best contributing solvents, it goes to show that AQ was suitable to use as baseline for the other solvents used in this research. Park et al., 2009 research also showed that aqua regia was very aggressive when used for PCBs and it dissolved most of the materials in few seconds. Furthermore, as earlier discussed above the most effective dose for extracting each of the metals can be seen in Table 4.73.

Table 4.73 Optimum concentration

Metal	Cu	Zn	Fe	Ni	Pb
Concentration (HP)	Conc 3	Conc 3	Conc 3	Conc 1	Conc 3

4.19.7 Discussion on Electrochemical Recovery

Overall copper recovered was 1354 mg/L (82 %) from an initial 1648 mg/L (100 %). A current of 1.5 A was used for the first 6 hours with a recovery of 1012 mg/L of Cu. However, further recovery was done using a current of 2.5 A for another 11 hours and an additional 342 mg/L of Cu was recovered. It is expected that there would be a decrease in the concentration of the electrolyte as time progresses in the recovery and this was seen in the works of other researchers. Also, during the recovery, a cathodic and anodic reaction occured which led to the release of hydrogen. This process is represented by the following equations:

Cathode:

$Cu^{2+} + 2e^- = Cu$

$2H^+ + 2e^- = H_2$

Anode:

$2H_2O = O_2 + 4H^+ + 4e^-$

Huyen *et al*., 2016 researched the electrochemical recovery of Cu from galvanic sludge using 9 A for 2.5 hours and the results showed that all the Cu was recovered from solution. The research found that efficiency of current was low due to a side reaction occurring known as oxygen-induced corrosion or reduced dissolved oxygen. Consequently, Hatfield *et al*., 1996 researched the electrochemical remediation of metal-bearing wastewaters and corrosion-based inhibition of copper by iron (iii) and the results revealed that the presence of ferric ions in solution reduced the electrochemical recovery of Cu.

The electrochemical recovery of other metals such as Zn, Fe, Ni and Pb were hindered by the lock down in 2020 in the United Kingdom hence more work coud not be carried out. The overall zinc recovered was 530 mg/L (70 %) from an initial 1754 mg/L (100 %). A current of 1.5 A was used for the first 6 hours with a recovery of 274 mg/L of Cu. However, further recovery was done using a current of 2.5 A for another 11 hours and 256 mg/L of Cu was recovered. However, Carrilo *et al*., 2012 researched the electrochemical recovery of zinc from spent pickling solutions from hot dip in galvanizing industries and the results revealed that when -150 mA was used on a 0.1 M HCl solution containing 0.06 M $ZnCl_2$, approximately 0.055 M $ZnCl_2$ was still left in solution after 300 minutes. Consequently, when -700 mA was used on a 0.1 M HCl solution containing 0.06 M $ZnCl_2$, < 0.01 M $ZnCl_2$ was left in solution after 220 minutes. The research also revealed that as the current becomes more negative the amount of zinc left in the solution also gets lower. Carrilo *et al*., 2012 also revealed that the presence of iron in solution leads to reduced current efficiency. Furthermore, increasing current leads to decrease in current efficiency as a result of a side reaction known as hydrogen-reduction.

CHAPTER FIVE

5.0 Conclusion

The effect of dose showed significant metal extractions. Both the HP and MW methods were effective and the percentage extractions figures were relatively close to each other. The order of metal extractions for the dose effect from highest to lowest are as follows: Zn > Fe > Pb > Cu > Ni. The recommended optimized dose for extracting these metals can be seen in Table 5.1 as Cu (0.2 g), Zn (0.2 g), Fe (0.2 g), Ni (3.0 g), Pb (3.0 g). The effect of particle-size showed significant metal extractions. Both the HP and MW methods were effective and the extraction figures were relatively close to each other. The order of metal extractions for particle- size effect from highest to lowest are as follows: Fe > Zn > Pb > Cu > Ni. The recommended optimized particle-sizes for extracting these metals can be seen in Table 5.1 as Cu (1.0 mm), Zn (1.0 mm), Fe (4.0 mm), Ni (1.0 mm), Pb (1.0 mm). The effect of H_2O_2 showed significant metal extractions. Both the HP and MW methods were effective and the extraction figures were relatively close to each other except for Pb. However, all solvents extracted a significant amount of Zn and this shows that the addition of H_2O_2 was effective. All the ILs extracted Zn higher than HA and SA did. The order of metal extractions for H_2O_2 effect from highest to lowest are as follows: Zn > Cu > Pb > Fe > Ni. The recommended optimized amount of H_2O_2 for extracting these metals can be seen in Table 5.1 as Cu (5 %), Zn (5 %), Fe (15 %), Ni (15 %), Pb (25 %). The effect of temperature showed significant metal extractions. The HP method was effective. The order of metal extractions for temperature effect from highest to lowest are as follows: Zn > Cu > Pb > Fe > Ni. The recommended optimized temperature for extracting these metals can be seen in Table 5.1 as Cu (70 ^{0}C), Zn (25 ^{0}C), Fe (70 ^{0}C), Ni (70 ^{0}C), Pb (70 ^{0}C). The effect of time showed significant metal extractions. The HP method was effective. The order of metal extractions for time effect from highest to lowest are as follows: Fe > Cu > Pb > Zn > Ni. The recommended optimized time for extracting these metals can be seen in Table 5.1 as Cu (180 minutes), Zn (180 minutes), Fe (180 minutes), Ni (180 minutes), Pb (180 minutes). The effect of concentration showed significant metal extractions. Both the HP and MW methods were effective and the extraction values were relatively close to each other. The order of metal extractions for dose effect from highest to lowest are as follows: Cu > Fe > Zn > Pb > Ni. The recommended optimized concentration for extracting these metals can be seen in Table 5.1 as Cu (conc 3), Zn (conc 3), Fe (conc 3), Ni (conc 1), Pb (conc 3).

Table 5.1 Summarized optimum conditions

Metal	Cu	Zn	Fe	Ni	Pb
Dose (HP)	0.2 g	0.2 g	0.2 g	3.0g	3.0 g
Particle-size (HP)	1.0 mm	1.0 mm	4.0 mm	1.0 mm	1.0 mm
H_2O_2 (HP)	**5 %**	**5 %**	**15 %**	**15 %**	**25 %**
Temperature (HP)	70 ^{0}C	25 ^{0}C	70 ^{0}C	70 ^{0}C	70 ^{0}C
Time (HP)	180 minutes	180 minutes	180 minutes	180 minutes	180 minutes
Concentration (HP)	Conc 3	Conc 3	Conc 3	Conc 1	Conc 3

The efficiency of the solvents were in the order inorganic acids > organic acids > ionic liquids. AQ (Aqua-regia) was the best performing solvents; this was followed by NA (nitric acid) and then SA (sulfuric acid). The organic and ionic liquids were considered to have similar effects as they showed the same level contributions (PCA) in each of the experiments and the levels were relatively lower. However, with the use of H_2O_2, all the the solvents's extractions were relatively high for Zn extraction. Also, in certain experiments, 1-[2-(2-hydroxyethoxy)]-3-methylimidazolium chloride did show some significant extractions but not as compared to the inorganic acids which were the most aggressive amongst all solvents used in this research. It was expected that the ILs (Ionic liquids) would be able to extract most of the metals but this was not the case in this research.

5.1 Research Limitations and Recommendation

This research was impacted upon by the advent of covid-19 as all works (especially the electrochemical recovery) had to stop due to the lock down in 2020. All laboratories were locked and the experiments could not continue. Also, the various leaching parameters (effect of dose, particle-sizes, H_2O_2, temperature, time & concentration) discussed in this research faced some challenges with respect to the available publication on extraction of the metals (Cu, Zn, Fe, Ni & Pb). A good amount of research works have been published on extraction of Cu using the various parameter also used in this research. Consequently, the effect of dose on Zn, Fe, Ni & Pb extraction have relatively fewer publications and this shows that the extraction of these metals using dose effect has not been well researched as compared to the other parameters in the discussion hence there were fewer publications to discuss. Other

parameters affected were particle-size effect. Again, there were a reasonable amount of publication on the effect of particle-size on Cu extraction but there were fewer publications on the effect of particle-sizes for Zn, Fe, Ni & Pb and this also impacted on the discussion of the extraction of these metals. The effect of using oxidants had a reasonable amount of publications on Cu and Zn but there were fewer publications for the use of oxidants in the extraction of Fe, Ni & Pb. This also affected the discussion on the effect of oxidants in extraction of these metals. Further research could consider increasing the parameters (dose, particle-size, H_2O_2, temperature, time, concentration) used in this research to see if the results obtained would be different from those obtained in this research. Other ionic liquids could be considered based on their specific properties. As stated above, future researchers can focus more on using the effect of dose, particle-sizes and oxidants on the extraction of Fe, Ni & Pb. In this research, 1-[2-(2-hydroxyethoxy)]-3-methylimidazolium chloride showed signs of extracting Cu and Zn. Further research would be needed as it is promising IL. This would be an opportunity for future researchers to consider.

References

Adediran Y.A. & Abdulkarim A. 2012. Challenges of electronic wastes management in Nigeria. *International Journal of Advances of Engineering and Technology.* 4**(1):** 641 – 648.

Ajiboye A.E., Olasehinde F.E., Adebayo O.A., Ajayi O.J., Ghosh M.K. and Basu S., 2019. Extraction of Copper and Zinc from Waste Printed Circuit Boards. *Recycling*. 4 **(3)**: 36

Akbari, S. & Ahmadi A. 2019. Recovery of copper from a mixture of printed circuit boards (PCBs) and sulphidic tailings using bioleaching and solvent extraction processes. *Chemical Engineering & Processing: Process Intensification.* 142: 107584.

Akuru U.B. and Okoro O.I., 2010. *Electronic Wastes and the Nigerian Experience*. 18th International Conference on Domestic Use of Energy.

Arens V.Z. & Chernyak S.A., 2008. Hydrometallurgy in the mining industry. *Metallurgist.* 52: 3–10.

Astuti W., Hirajima T., Sasaki K. and Okibe N., 2016. Comparison of effectiveness of citric acid and other acids in leaching of low-grade Indonesian saprolitic ores. *Minerals Engineering*. 85: 1-16.

Baba Y., Kubota F., Kamiya N. & Goto M., 2011. Recent advances in extraction and separation of rare earth metals using ionic liquids. *Journal of Chemical Engineering*. 44**(10):** 679–685.

Behera S.S., Panda S.K., Das D., Mohapatra R.K., Kim H.I., Lee J.Y., Jyothi R.K. & Parhi P.K., 2020. Microwave assisted leaching investigation for the extraction of copper(II) and chromium(III) from spent catalyst. *Separation and Purification Technology*. 244: 116842

Berthod A., Angel M.J.R. & Broch S.C. 2008. Ionic liquids in separation techniques. *Journal of Chromatography A*, 1184: 6–18.

Binnemans, K., 2005. Ionic liquid crystals. *Chemical Review*. 105: 4148–4204.

Biswas S. & Mulaba-Bafubiandi A.F., 2016. Extraction of Copper and Cobalt from Oxidized Ore using Organic Acids. *Hydrometallurgy Conference 2016: Sustainable Hydrometallurgical Extraction of Metal, Cape Town, Southern African Institute of Mining and Metallurgy*.

Bizzo W.A., Figueiredo R.A., de Andrade V.F., 2014, Characterization of Printed Circuit Boards for Metal and Energy Recovery after Milling and Mechanical Separation. Materials. 7: 4555-4566. doi:10.3390/ma7064555.

Bonn, 2018. *Thousands of tonnes of e-waste is shipped illegally to Nigeria inside used vehicles*. United Nations University. Available on: https://ehs.unu.edu/media/press-releases/thousands-of-tonnes-of-e-waste-is-shipped-illegally-to-nigeria-inside-used-vehicles.html (Accessed on: 24th January 2021)

Bubalo M.C., Hanousek K., Radoševic K., Srcek, V.G., Jakovljevic T., Redovnikovic I.R., 2014. Imidiazolium Based Ionic Liquids: Effects of Different Anions and Alkyl Chains Lengths on the Barley Seedlings. *Ecotoxicology and Environmental Safety*. 101: 116–123.

Canal M.A., Cabrera J.-M. & Malfatti C.D.F., 2013. Printed circuit boards: a review on the perspective of sustainability. *Journal of Environmental Management*. 131: 298–306.

Carrilo A.J., Garcia G.M. and Perez H.V., 2012. Electrochemical Recovery of Zinc from the Spent Pickling Solutions Coming from Hot Dip Galvanizing Industries. Galvanostatic Operation. *International Journal of Electrochemical Science*. 7: 5442 - 5456.

Chen J.C., Lin S.R. & Tsai W.T., 2004. Effects of oxidizing agent and hydrodynamic condition on copper dissolution in chemical mechanical polishing electrolytes. *Applied Surface Science*. 233: 80-90.

Chen J.C. & Tsai W.T., 2004. Effects of hydrogen peroxide and alumina on surface characteristics of copper chemical-mechanical polishing in citric acid slurries. *Materials Chemistry & Physics*. 87: 387-393.

Chen J.P. & Lim L.L, 2005. Recovery of precious metals by an electrochemical deposition method. *Chemosphere.* 60: 1384–1392.

Chen M., Huang J., Ogunseitan O.A., Zhu N. & Wang Y., 2016a. Comparative study on copper leaching from waste printed circuit boards by typical ionic liquid acids. *Waste Management*. 41: 142 – 147.

Chen W., Zhang L., Peng J., Yin S., Ma A., Yang K., Li S. & Xie F., 2016b. Effects of roasting pretreatment on zinc leaching from complicated zinc ores. *Green Process and Synthesis*. 5: 41–47.

Chen A., Zhao Z.W., J X., Long S., H G. and Chen X., 2009. Alkaline leaching Zn and its concomitant metals from refractory hemimorphite zinc oxide ore. *Hydrometallurgy*. 97: 228–232.

Chen M., Zhang S., Huang J., Chen H., 2015. Lead during the leaching process of copper from waste printed circuit boards by five typical ionic liquid acids. *Journal of Cleaner Production*. 95: 142-147.

Conard B.R., 1992. The role of hydrometallurgy in achieving sustainable development. *Hydrometallurgy*. 30: 1–28.

Connell, L.H. & Moe, L.A., 1966. *Apparatus for treatment of ore*, USPatent No. 3261959.

Dalrymple I., Wright N., Bains N., Geraghty K., Goosey M. & Lightfoot L., 2007. An integrated approach to electronic waste (WEEE) recycling. *Circuit World.* 33: 52–58.

Damodaran D., Balakrishnan R.M. & Shetty V.K., 2013. The Uptake Mechanism of Cd(II), Cr(VI), Cu(II), Pb(II), and Zn(II) by Mycelia and Fruiting Bodies of Galerina vittiformis. *BioMed Research International*. 149120: 11.

Das D., Mukherjee S. & Chaudhuri M.G., 2021. Studies on leaching characteristics of electronic waste for metal recovery using inorganic and organic acids and base. *Waste Management & Research*. 39**(2)**: 242 - 249. https://doi.org/10.1177/0734242X20931929

Demim S., Drouiche N., Aouabed A., Benayad T., Dendene-Badache O., Semsari S., 2013a. Cadmium & nickel: Assessment of the Physiological Effects and Heavy Metal Removal using a Response Surface approach by L. Gibba. *Ecological Engineering*. 61: 426–435.

Demim S., Drouiche N., Aouabed A. & Semsari S., 2013b. CCD Study on The Ecophysiological Effects of Heavy Metals on Lemna Gibba. *Ecological Engineering*. 57: 302–313.

Demim S., Drouiche N., Aouabed A., Benayad T., Couderchet M. & Semsari S., 2014. Study of Heavy Metal Removal from Heavy Metal Mixture Using the Ccd Method. *Journal of Industrial & Engineering Chemistry*. 20: 512–520.

Devecci H., 2010. *Extraction of copper from scrap TV boards by sulphuric acid leaching under oxidising conditions. In: Extraction of copper from scrap TV boards by sulphuric acid leaching under oxidising conditions.* Going Green-Care Innovation 2010 Conference. 45. Viena.

Dhawan N., Wadhwa M., Kumar V., Kumar M., 2009. Recovery of Metals from Electronic Scrap by Hydrometallurgical. *Route, In: Proc. Annual Meeting & Exhibition, TMS 2009, Stanley M.H. (Ed.), EPD Congress, San Francisco, California, USA.* 1107–1109.

Domanska U. & Rekawek A. 2009. Extraction of Metal Ions from Aqueous Solutions Using Imidazolium Based Ionic Liquids. *Journal of Solution Chemistry*. 38: 739–751.

Du T., Vijayakumar A. & Desai V., 2004. Effect of hydrogen peroxide on oxidation of copper in CMP slurries containing glycine and Cu ions. *Electrochimica Acta*; 49: 4505-4512.

ETC-Brunel 2021, *Experimental Techniques Centre, Brunel University London*.

EU, 2003. Directive 2002/96/EC of the European Parliament and of the council of 27 January 2003 on waste electrical and electronic equipment (WEEE*). Official Journal of the European Union.* 37: 24 – 38.

Eswaraiah C., Kavitha T., Vidyasagar S. & Narayanan S.S., 2008. Classification of metals and plastics from printed circuit boards (PCB) using air classifier. *Chemical Engineering and Processing: Process Intensification.* 47: 565–576.

Faivre R., 2009. *Synthesis, Characterisation and Application of Ionic Liquids to Recover Materials from WEEE.* PhD Thesis, Brunel University.

Fleming, C.A., 1992. Hydrometallurgy of precious metals recovery. *Hydrometallurgy.* 30:127 – 162.

Freemantle M., 1998. *Ionic liquids show promise for clean separation technology*. Chemical Engineering News. 76: 12.

Gaines P., 2021. *Linearity and Detection Limits. ICP Operations Guide.* Inorganic Ventures Available at: https://www.inorganicventures.com/icp-guide/linearity-and-detection-limits (Accessed on: 3rd May 2021).

George S., 2019. *UK braced for tougher e-waste policies as impacts on human food chains revealed.* Edie Newsroom. Available on: https://www.edie.net/news/5/techUK-calls-for-tougher-e-waste-policies-after-illegal-exports-found-to-be-contaminating-food-chains/ (Accessed on: 25th April 2020).

Ghandi K., 2014. A Review of Ionic Liquids, Their Limits and Applications. *Green and Sustainable Chemistry*. 4: 44 – 53.

Gharabaghi M., Irannajad M. and Azadmehr A.R., 2013. Leaching kinetics of nickel extraction from hazardous waste by sulphuric acid and optimization dissolution conditions. *Chemical Engineering and Design.* 91: 325 - 331.

Ghosh B., Ghosh M.K., Parhi P., Mukherjee P.S. & Mishra B.K., 2015. Waste Printed Circuit Boards recycling: an extensive assessment of current status. *Journal of Cleaner Production*. 94: 5 -19.

Gonçalves A.R.P., Paredes X., Cristino A.F., Santos F.J.V., Queirós C.S.G.P., 2021. Ionic liquids—A Review of Their Toxicity to Living Organisms. *International Journal of Molecular Sciences*. 22: 5612. https://doi.org/10.3390/ijms22115612

Gordon C. M., Holbrey J.D., Kennedy A. R. & Seddon K. R., 1998. Ionic liquid crystals: hexafluorophosphate salts. *Journal of Materials Chemistry*. 8: 2627–2636.

Grossman E., 2007. *High Tech Trash: Digital Devices, Hidden Toxics, and Human Health*.

Habashi F., 1999. *A Textbook of hydrometallurgy*, 2nd edition. Métallurgie Extractive Québec.

Habbache N., Alane N., Djerad S. & Tifouti L., 2009. Leaching of copper oxide with different acid solutions. *Chemical Engineering Journal.* 152: 503–508

Hadi P., Xu M., Lin C.S.K., Hui C.-W. & McKay G., 2015. Waste printed circuit board recycling techniques and product utilization. *Journal of Hazardous Materials*. 283: 234 - 243.

Haqshenas M.A., 2018. *Faced with e-waste*. Tehran Times. Available at: https://www.tehrantimes.com/news/421667/Faced-with-e-waste (Accessed on 15th July 2020)

Hatfield, T.L., Kleven, T.L., Pierce, D.T., 1996. Electrochemical remediation of metal-bearing wastewaters. Part II: corrosion-based inhibition of copper removal by iron (III). *Journal of Applied Electrochemistry.* 28, 397–403.

Havlik T., Orac D., Berwanger M. & Anja M., 2014. The effect of mechanical–physical pretreatment on hydrometallurgical extraction of copper and tin in residue from printed circuit boards from used consumer equipment. Minerals Engineering 65: 163–171.

Havlik T., Turzakova M., Stopic S., Friedrich B., 2005. Atmospheric leaching of EAF dust with diluted sulphuric acid. *Hydrometallurgy*. 77:41–50.

He Y. & Xu Z., 2014. The status and development of treatment techniques of typical waste electrical and electronic equipment in China: a review. *Waste Management Resources*. 32: 254 - 269.

Hossain M, S., Yahaya A.N.A, Yacob L.S., Rahim M.Z.A, Yusof N.N.M. & Bachmann R.T., 2018. Selective recovery of Copper from waste mobile phone printed circuit boards using Sulphuric acid leaching. *Materials Today: Proceedings* 5: 21698–21702.

Hosseini S.A., Raygan S., Rezaei A. & Jafari A., 2017. Leaching of nickel from a secondary source by sulfuric acid. *Journal of Environmental Chemical Engineering*. 5: 3922 – 3929

HSE, 2021. Waste Electrical and Electronic Equipment recycling (WEEE). Available on: https://www.hse.gov.uk/waste/waste-electrical.htm (Assessed on: 13th October 2021)

Hsu E., Barmak K., Westa A.C. & Park A.A., 2019. Advancements in the treatment and processing of electronic waste with sustainability: a review of metal extraction and recovery technologies. *Green Chemistry.* 21: 919.

Huang K., Guo J. & Xu Z., 2009. Recycling of waste printed circuit boards: a review of current technologies and treatment status in China. *Journal of Hazardous Materials.* 164: 399-408.

Huyen P.T., Dang T.D., Tung M.T., Huyen N.T.T., Green T.A. and Roy S 2016. Electrochemical copper recovery from galvanic sludge. *Hydrometallurgy*. 164: 295 - 303.

Irannajad M., Meshkini M. & Azadmehr A.R., 2013. Leaching of zinc from low grade oxide ore using organic acid. *Physicochemical Problems of Mineral Processing.* 49**(2)**: 547−555.

Iwenwanne V., 2019. *Nigeria's e-waste mountain*. Resource. Available at: https://resource.co/article/nigerias-e-waste-mountain#:~:text=Nigeria%20is%20particularly%20burdened%20by,both%20local%20and%20imported%20EEE. (Accessed on: 24th January 2021).

Jadhao P.R., Pandey A., Pant K.K. & Nigam K.D.P., 2021. Efficient recovery of Cu and Ni from WPCB via alkali leaching approach. *Journal of Environmental Management.*296: 113154. https://doi.org/10.1016/j.jenvman.2021.113154

Jadhav U. & Hocheng H., 2015. Hydrometallurgical Recovery of Metals from Large Printed Circuit Board Pieces. *Scientific Reports*. 5: 14574.

Jadhav U., Su C. & Hocheng H., 2016. Leaching of metals from large pieces of printed circuit boards using citric acid and hydrogen peroxide. *Environmental Science Pollution Research.* 23: 24384–24392.

Janyasuthiwong S., Ugas R., Rene E.R., Alessandra C., Esposito G. & Lens P.N.L., 2016. Effect of operational parameters on the leaching efficiency and recovery of heavy metals from computer printed circuit boards. *Journal of Chemical Technology & Biotechnology*. 91: 2038–2046. DOI 10.1002/jctb.4798.

Javaid S., 2006. *Development and Optimisation of Treatment Technologies for Environmental Pollution Control.* PhD Thesis, Brunel University.

Jha M.K, Kumari, A., Choubey, P.K., Lee, J., Kumar, V. & Jeong, J., 2012. Leaching of lead from solder material of waste printed circuit boards (PCBs). *Hydrometallurgy* 121-124: 28–34.

Kamberovic Z., Ranitovic M., Korac M., Andjic Z., Gajic N., Djokic J. & Jevtic S., 2018. Hydrometallurgical Process for Selective Metals Recovery from Waste-Printed Circuit Boards. *Metals*. 8: 441. doi:10.3390/met8060441.

Kavousi M., Sattari A., Alamdari E.K. & Fatmehsari D.H., 2018. Leaching Studies for Copper and Solder Alloy Recovery from Shredded Particles of Waste Printed Circuit Boards *The Minerals, Metals & Materials Society and ASM International*. 1464: 49B. https://doi.org/10.1007/s11663-018-1243-6.

Khalid M.K., Hamuyuni J., Agarwal Vivek., Pihlasalo J., Haapalainen M. & Lundstrom M., 2019. Sulfuric acid leaching for capturing value from copper rich converter slag. *Journal of Cleaner Production*. 215: 1005 -1013.

Kiddee, P., Naidu, R. & Wong, M.H. 2013. Electronic waste management approaches: an overview. *Waste Management*. 33: 1237-1250.

Kilicarslan A., Saridede M.N., 2016. Leaching performance of imidazolium based ionic liquids in the presence of hydrogen peroxide for recovery of metals from brass waste. *Revista de Metalurgia*. 52(1): e063. http://dx.doi.org/10.3989/revmetalm.063.

Kohla, U. & Luniak, M., 2005. Data inspection using biplots. *The Stata Journal*. 5(**2**): 208–223.

Kubota, F., Shimobori, Y., Baba, Y., Koyanagi, Y. Shimojo, K., Kamiya, N., Goto, M., 2011. Application of ionic liquids to extraction separation of rare earth metals with an effective diglycol amic acid extractant. *Journal of Chemical Engineering*. 44: 307–312.

Kubota, F., Shimobori, Y., Koyanagi, Y., Shimojo, K., Kamiya, N., Goto, M., 2010. Uphill transport of rare earth metals through highly stable supported liquid membrane based on ionic liquid. *Analytical Sciences*. 26: 289–290.

Kumar M., Lee J., Kim M.S., Jeong J. & Yoo, K., 2014. Leaching of metals from waste printed circuit Boards (WPCBs) using sulfuric and nitric acids. *Environmental Engineering and Management Journal*. 13**(10):** 2601-2607.

Letsrecycle, 2020. *UK the 'second largest producer' of WEEE*. Available at: https://www.letsrecycle.com/news/latest-news/uk-the-second-largest-producer-of-weee/ (Accessed: 2nd April 2021).

Leyma R., Platzer S., Jirsa F., Kandiolla W., Krachler R. & Keppler B.K. 2016. Novel thiosalicylate-based ionic liquids for heavy metal extractions. *Journal of Hazardous Materials.* 314: 164 – 171.

Li L., Dunn J.B., Zhang X.X., Gaines L., Chen R.J., Wu F. & Amine K., 2013. Recovery of metals from spent lithium-ion batteries with organic acids as leaching reagents and environmental assessment. *Journal of Power Sources.* 233: 180–189.

Li L., Ge J., Wu F., Chen R., Chen S. & Wu B., 2010. Recovery of Cobalt and Lithium from spent lithium ion batteries using organic citric acid as leachant. *Journal of Hazardous Materials*. 176: 288 – 293.

Li L., Lu J., Ren Y., Zhang X.X., Chen R.J., Wu F. & Amine K., 2012. Ascorbic-acid-assisted recovery of cobalt and lithium from spent Li-ion batteries. *Journal of Power Sources.* 218: 21–27.

Li L., Li X., Wang Z., Zheng J., Wu L. & Zhang L., 2009. Study of extraction and purification of Ni, Co and Mn from spent battery material. *Hydrometallurgy*. 99**(1–2):** 7-12.

Li L., Qu W., Zhang X., Lu J., Chen R., Wu F. & Amine K., 2015. Succinic acid-based leaching system: a sustainable process for recovery of valuable metals from spent Li-ion batteries. *Journal of Power Sources.* 282: 544–551.

Lisinka M., Saternus M. & Willner J., 2018. Leaching Fe iron hydrogen peroxide H_2O_2 PCB. *Archives of Metallurgy and Materials*. 63(1): 143-147. DOI: 10.24425/118921.

Lister T.E., Wang P. & Andrerko A., 2014. Recovery of critical and value metals from mobile electronics enabled by electrochemical processing. *Hydrometallurgy*. 149: 228-237.

Liu J., Jonsson J.A. & Jiang G., 2005. Application of Ionic Liquids in Analytical Chemistry. *Trends in Analytical Chemistry*. 24 **(1).**

Manjanna J., Venkateswaran G., Sherigara B.S. & Nayak P.V., 2001. Dissolution studies of chromium substituted iron oxides in reductive-complexing agent mixtures. *Hydrometallurgy.* 60: 155–165.

Mecucci A. & Scott K., 2002. Leaching and electrochemical recovery of copper, lead and tin from scrap printed circuit boards. *Journal of Chemical Technology and Biotechnology*. 77: 449 - 457

Merck, 2021a. 00285 Sigma-Aldrich 1-Butylpyridinium bromide. Available at: https://www.sigmaaldrich.com/GB/en/product/sial/00285 (Accessed: 11th October 2021).

Merck, 2021b. 18122 Sigma-Aldrich 1-Butyl-3-methylimidazolium hexafluorophosphate. Available at: https://www.sigmaaldrich.com/GB/en/product/sial/18122 (Accessed: 11th October 2021).

Merck, 2021c. 95137 Sigma-Aldrich 1-Butyl-3-methylimidazolium bromide. Available at: https://www.sigmaaldrich.com/GB/en/product/sial/95137 (Accessed: 11th October 2021).

Mennea S., Anoutib M. & Balduccia A., 2013. Aprotic and protic ionic liquids in lithium ion batteries: a comparative study. 224th ECS Meeting. *The Electrochemical Society*. 1185.

Mohammadreza F., Mohammad N. & Ziaeddin S.S., 2014. Nickel extraction from low grade laterite by agitation leaching at atmospheric pressure. *International Journal of Mining Science and Technology.* 24: 543-548

Mooiman M.B., Sole K.C., Kinneberg D.J., 2005. Challenging the traditional hydrometallurgy curriculum—an industry perspective. *Hydrometallurgy*. 79: 80–88.

Naganawa H., Shimojo K., Mitamura H., Sugo Y., Noro J. & Goto M., 2007. A new Green Extractant of the diglycol amic acid type for lanthanides. *Solvent Extraction Resource Development.* 14: 151–160.

Nayaka G.P., Manjanna J., Pai K.V., Vadavi R., Keny J. & Tripathi V.S., 2015. Recovery of valuable metal ions from the spent lithium-ion battery using aqueous mixture of mild organic acids as alternative to mineral acids. *Hydrometallurgy.* 151: 73–77.

Nayaka G.P., Pai K.V., Manjanna J. & Keny S.J 2016. Use of mild organic acid reagents to recover the Co and Li from spent Li-ion batteries. *Waste Management.* 51: 234–238.

Nekouei R.K., Pahlevani F., Golmohammadzadeh R., Assefi M., Rajarao R., Chen Y. & Sahajwalla V., 2019. Recovery of heavy metals from waste printed circuit boards: statistical optimization of leaching and residue characterization. Environmental Science and Pollution Research. 26:24417–24429. https://doi.org/10.1007/s11356-019-05596-y

Neumann J., Steudte S.; Cho-Woong C., Thöming J., Stolte S., 2014. Biodegradability of 27 Pyrrolidinium, Morpholinium, Piperidinium, Imidazolium and Pyridinium Ionic Liquid Cations under Aerobic Conditions. *Green Chemistry*. 16: 2174–2184.

Ogunseitan O.A., 2013. The Basel Convention and e-waste: translation of scientific uncertainty to protective policy. *Lancet Global Health* 1: 313-314.

Oh C.J., Lee S.O., Yang H.S., Ha T.J. & Kim M.J., 2003. Selective Leaching of Valuable Metals from Waste Printed Circuit Boards. *Journal of the Air & Waste Management Association*. 53**(7):** 897-902.

Oishi T., Koyama K., Alam S., Tanaka M. & Lee J-C, 2007. Recovery of high purity copper cathode from printed circuit boards using ammoniacal sulfate or chloride solutions. *Hydrometallurgy.* 89: 82–88.

Okwu O., Hursthouse A., Viza E. & Idoko L., 2021. Enhancement of WEEE Management Practices in MTN Phone Village, Rumukurushi, Port Harcourt, Nigeria. *Recycling*. 6(4): 77. https://doi.org/10.3390/recycling6040077

Oluokun O.O. & Otunniyi I.O., 2020. Kinetic analysis of Cu and Zn dissolution from printed circuit board physical processing dust under oxidative ammonia leaching. *Hydrometallurgy*. 193: 105320

Oustadakis P., Tsakiridis P.E., Katsiapi A. & Agatzini-Leonardou S., 2010. Hydrometallurgical process for zinc recovery from electric arc furnace dust (EAFD). Part I: Characterization and leaching by diluted sulphuric acid. *Journal of Hazardous Materials*. 179: 1–7.

Ozbas E.E., Gokce C.E., Guneysu S., Ozcan H.S., Sezgin N., Aydin S. & Balkaya N., 2013. Comparative metal (Cu, Ni, Zn, total Cr, and Fe) removal from galvanic sludge by molasses Hydrolysate. *Journal of Chemical Technology & Biotechnology*. 88: 2046–2053. DOI 10.1002/jctb.4066

Palden T., Machiels L., Onghena B., Regadio M., Binnemans K., 2020. Selective leaching of lead from lead smelter residues using EDTA. *RSC Advances* 10: 42147

Pandija S., Roy D. & Babu SV., 2007. Chemical mechanical planarization of copper using abrasive-free solutions of oxalic acid and hydrogen peroxide. *Materials Chemistry & Physics*. 102: 144-151.

Park H., Jung K., Alorro R.D. & Yoo K., 2013. Leaching Behavior of Copper, Zinc and Lead from Contaminated Soil with Citric Acid. *Materials Transactions*. 54**(7):** 1220 – 1223.

Park J., Jung Y., Kusumah P., Lee J., Kwon K. & Lee C.K. 2014. Application of Ionic Liquids in Hydrometallurgy. *International Journal of Molecular Sciences*. 15: 15320-15343.

Park Y.J. & Fray D.J., 2009. Recovery of high purity precious metals from printed circuit boards. *Journal of Hazardous Materials*. 164(2–3): 1152-1158. https://doi.org/10.1016/j.jhazmat.2008.09.043

Patel M., Patel D.A & Gajra B., 2011. Validation of Analytical Procedure: Methodology. *International Journal of Review Article Pharmaceutical Innovations. Issn 2249 –1031*. 1**(2)**: 41 – 50.

Pawłowska B., Telesinski A., Biczak, R., 2019. Phytotoxicity of Ionic Liquids. *Chemosphere*. 237: 124436.

Ping Z., ZeYun F., Jie L., Qiang L., GuangRen Q. & Ming Z., 2009.. Enhancement of leaching copper by electro-oxidation from metal powders of waste printed circuit board. *Journal of Hazardous Materials*. 166(2–3): 746-750.

Qin H.S. & Ren Z.J., 2000. Cyanide waste pollution and prevention measures of rock heap leaching gold. *Journal of Qinghai Environment.* 10: 78–80.

Renner R., 2001. Ionic liquids: An industrial clean up solution. *Environmental Science Technology*. 35: 410A–413A.

Reris R & Brooks, J.P., 2015. Principal component analysis and optimization: A tutorial. *Statistical Sciences and Operations Research Publications*. 212 – 225.

Reuter M., Oyj O., Hudson C., Schaik A.V., Heiskanen K., Meskers C. & Hageluken C., 2013. Metal Recycling - Opportunities, Limits, Infrastrucuture. *United Nations Environment Programme*. 1 - 316.

RPA 2012. Stockpiling of Non-energy Raw Materials – Final Report. *Risk and Policy Analysts Limited*. 1 – 217.

Sabzkoohi H.A. & Kolliopoulos G., 2021. Green Zero-Waste Metal Extraction and Recycling from Printed Circuit Boards. *Material Proceedings*. 5**(1)**: 39. https://doi.org/10.3390/materproc2021005039.

Salgado A.L., Veloso A.M.O., Pereira D.D., Gontijo G.S., Salum A. & Mansur M.B., 2003. Recovery of zinc and manganese from spent alkaline batteries by liquid–liquid extraction with Cyanex 272. *Journal of Power Sources*. 115: 367–373.

Santos F.M.F., Pina P.S., Porcaro R., Oliveira V.A., Silva C.A. and Leao V.A., 2010. The kinetics of zinc silicate leaching in sodium hydroxide. *Hydrometallurgy*. 102: 43–49

Schaeffera N., Passosa H., Billardb I., Papaiconomoub N. and Coutinho J.A.P., 2018. Recovery of metals from waste electrical and electronic equipment (WEEE) using unconventional solvents based on ionic liquids. *Critical Reviews in Environmental Science and Technology*. 48**(13-15)**:1-64. DOI: 10.1080/10643389.2018.1477417

Shawabkeh RA., 2010. Hydrometallurgical extraction of zinc from Jordanian electric arc furnace dust. *Hydrometallurgy*. 104:61–65.

Seal S., Kuiry S.C. & Heinmen B., 2003. Effect of glycine and hydrogen peroxide on chemical-mechanical planarization of copper. *Thin Solid Films.* 423: 243-251.

Seddon K.R., 1997. Ionic Liquids for Clean Technology- Review. *Journal of Chemical Technology & Biotechnology.* 68: 351 – 356.

Sepulveda A., Schluep M., Renaud F.G., 2010. A review of the environmental fate and effects of hazardous substances released from electrical and electronic equipments during recycling: examples from China and India. *Environmental Impact Assessment Review*. 30**(1):** 28–41

Sethurajan M., & Hullebusch E.D.V., 2019. Leaching and Selective Recovery of Cu from Printed Circuit Boards. *MDPI*. Metals, 9: 1034. doi:10.3390/met9101034

Shimojo K., Naganawa H., Noro J., Kubota F. & Goto M., 2007. Extraction behavior and separation of lanthanides with a diglycol amic acid derivative and a nitrogendonor ligand. *Analytical Sciences.* 23: 1427–1430.

Siaw W.C., Rakunman M.R.M., Kamaruzaman N., Tsuji T. & Manaf N.A., 2020. Metal Removal from Industrial Waste by Hydrochloric Acid. *IOP Conference Series: Materials Science and Engineering.* 808: 012008. doi:10.1088/1757-899X/808/1/012008

Silvas F.P.C., Correa M.M. J., Caldas M.P.K., de Moraes V.T., Espinosa D.C.R. & Tenório J.A.S., 2015. Printed circuit board recycling: Physical processing and copper extraction by selective leaching. *Waste Management*. 46: 503–510

Sonmez M.S. & Kumar R.V., 2009. Leaching of waste battery paste components. Part 1: Lead citrate synthesis from PbO and PbO2. *Hydrometallurgy.* 95 53–60.

Spalvins E., Dubey B. & Townsend T., 2008. Impact of electronic waste disposal on lead concentrations in landfill leachate. *Environmental Science & Technology.* 42: 7452–7458.

Statista, 2021. *Electronic waste generated worldwide from 2010 to 2019 (in million metric tons).* Available at: https://www.statista.com/statistics/499891/projectionewaste-generationworldwide/#:~:text=Since%202010%2C%20the%20volume%20of,be%20collected%20and%20properly%20recycled (Accessed: 2nd April 2021).

Statisticshowto, 2021. *Principal Component Analysis (PCA), Regression & Parafac.* Available at: https://www.statisticshowto.com/principal-component-analysis-2/ (Accessed: 1st March 2021).

Stepnowski P., 2006. Review: Application of Chromatographic and Electrophoretic Methods for the Analysis of Imidazolium and Pyridinium Cations as Used in Ionic Liquids. *International Journal of Molecular Science*. 7: 497-509.

STHDA, 2021. *Principal Component Methods in R: Practical Guide. PCA - Principal Component Analysis Essentials.* Available at: http://www.sthda.com/english/articles/31-principal-component-methods-in-r-practical-guide/112-pca-principal-component-analysis-essentials/ (Accessed: 1st March 2021).

Suarez P.A.Z., Einloft S., Dullius J.E.L., Souza R.F. & Dupont J., 1998. Synthesis and physical-chemical properties of ionic liquids based on l -n-butyl-3-methylimidazolium cation. *Journal de Chimie Physique*. 95: 1626 – 1639.

Sum E.Y.L., 1991. The recovery of metals from electronic scrap. *Journal of the Minerals, Metals and Materials Society*. 43: 53–61.

Sun L. & Qiu K., 2012. Organic oxalate as leachant and precipitant for the recovery of valuable metals from spent lithium-ion batteries. *Waste Management*. 32: 1575–1582.

Sun X., Luo S. & Dai S., 2012. Ionic liquids-based extraction: a promising strategy for the advanced nuclear fuel cycle. *Chemical Review*. 112: 2100–2128.

Tao L., Wang L., Tang K., Wang X., Chen L. and Ning P., 2021. Leaching of iron from copper tailings by sulfuric acid: behavior, kinetics and mechanism. *Royal Society of Chemistry*. 11: 5741. DOI: 10.1039/d0ra08865j

Terada C., 2012. Recycling Electronic Wastes in Nigeria: Putting Environmental and Human Rights at Risk. *Northwestern Journal of International Human Rights*. 10**(3):** 153 - 172

Thawarkar S., Khupse N.D. & Kumar A., 2016. Comparative Investigation of the Ionicity of Aprotic and Protic Ionic Liquids in Molecular Solvents by using Conductometry and NMR Spectroscopy. *Chemical Physics and Physical Chemistry*. 17: 1006 – 1017.

Towardsdatascience, 2021. *Principal Component Analysis (PCA) 101, using R.* Available at: https://towardsdatascience.com/principal-component-analysis-pca-101-using-r-361f4c53a9ff (Accessed: 1st March 2021).

Tribuneonlineng, 2018. *Open Burning Of E-Waste: Recyclers, Residents At Risk Of Cancer, Study Shows*. Nigerian Tribune. Available at: https://tribuneonlineng.com/open-burning-e-waste-recyclers-residents-risk-cancer-study-shows/ (Accessed on 15th July 2020)

Tripathi A., Kumar M., Sau D. C., Agrawal A., Chakravarty S. & Mankhand T. R., 2012. Leaching of Gold from the Waste Mobile Phone Printed Circuit Boards (PCBs) with Ammonium Thiosulphate. *International Journal of Metallurgical Engineering*. 17-21.

Tuncuk A., 2019. Lab scale optimization and two-step sequential bench scale reactorleaching tests for the chemical dissolution of Cu, Au & Ag from wasteelectrical and electronic equipment (WEEE). *Waste Management* 95: 635 - 643

Tuncuk A., Stazi V., Akcil A., Yazici E.Y. & Deveci H., 2012. Aqueous metal recovery techniques from e-scrap: Hydrometallurgy in recycling. *Minerals Engineering*. 25: 28 – 37.

Varma R.S. & Namboodiri V.V., 2001. Solvent-free preparation of ioni liquids using a household microwave oven. *Pure & Applied Chemistry.* 73, 1309

Vehlow J., Bergfeldt B., Jay K., Seifert H., Wanke T. & Mark F.E., 2000. Thermal treatment of electrical and electronic waste plastics. *Waste Management Resources*. 18: 131–140.

Veit H. M., Diehl T.R., Salami A.P., Rodrigues J.S., Bernardes A. M. & Tenorio J. A. S., 2005. Utilisation of magnetic and electrostatic separation in the recycling of printed circuit boards scrap. *Waste Management*. 25: 67–74.

Velis C. & Cook E., 2021. *Health crisis: up to a billion tonnes of waste potentially burned in the open every year.* The Conversation. Available on: https://theconversation.com/health-crisis-up-to-a-billion-tonnes-of-waste-potentially-burned-in-the-open-every-year-152778 (Accessed on: 20th April 2021)

Visser A.E., Swatlowski R.P., Griffin S.T., Hartman D.H. & Rogers R.D., 2001a. Liquid/liquid extraction of metal ions in room temperature ionic liquids. *Separation Science & Technology.* 36: 785–804.

Visser A.E., Swatlowski R.P., Reichert W.M., Mayton R., Sheff S., Wierzbicki A., Davis J.H. Jr. & Rogers R.D. 2001b. Task-specific ionic liquids for the extraction of metal ions aqueous solutions. *Chemical Communications*. 135–136.

Wang Z., Guo S. & Ye C., 2016. *Leaching of copper from metal powders mechanically separated from waste printed circuit boards in chloride media using hydrogen peroxide as oxidant.* The Tenth International Conference on Waste Management and Technology (ICWMT). Procedia Environmental Sciences. 31: 917 – 924

Wang J. & Xu Z., 2015. Disposing and recycling waste printed circuit boards: disconnecting, resource recovery, and pollution control. *Environmental Science & Technology*. 49: 721-733.

Wang J., Wang Z., Zhang Z. & Zhang G., 2019. Removal of zinc from basic oxygen steelmaking filter cake by selective leaching with butyric acid. *Journal of Cleaner Production* 209: 1 – 9.

WEEE Directive, 2012. Directive 2012/19/EU of the European Parliament And Of The Council of 4 July 2012 on waste electrical and electronic equipment (WEEE). *Official Journal of the European Union.* 197: 38 – 70.

WEEE Regulations, 2013. WEEE Regulations Government Guidance Notes. *Department for Business Innovation & Skills.*

Wei G., Yang Z. & Chen C. 2003. Room temperature ionic liquid as a novel medium for liquid/liquid extraction of metal ions. *Analytical Chimica Acta*. 488: 183 – 192.

Welton T.,1999. Room-Temperature Ionic Liquids. Solvents for Synthesis and Catalysis. *Chemical Review*. 99 **(8):** 2071–2084.

Witt K., Urbaniak W., Kaczorowska M.A. & Bozejewicz D., 2021. Simultaneous Recovery of Precious and Heavy Metal Ions from Waste Electrical and Electronic Equipment (WEEE) Using Polymer Films Containing Cyphos IL 101. Polymers. 13(9): 1454; https://doi.org/10.3390/polym13091454

Wu J., Li J. & Xu Z., 2008. Electrostatic separation for multisize granule of crushed printed circuit board waste using two-roll separator. *Journal of Hazardous Materials*. 159: 230–234.

Wu J-Y., Chang F., Wang H.P., Tsai M.J., Ko C. & Chen C., 2015. Selective leaching process for the recovery of copper and zinc oxide from copper-containing dust. *Environmental Technology*. 36**(23):** 2952-2958.

Xiao T., Mu W., Shi S., Xin H., Xu X., Cheng H., Luo S. & Zhai Y., 2021. Simultaneous extraction of nickel, copper, and cobalt from low–grade nickel matte by oxidative sulfation roasting-water leaching process. *Minerals Engineering.* 174: 107254

Xie F., Zhang T.A., Dreisinger D. & Doyle F., 2014. A critical review on solvent extraction of rare earths from aqueous solutions. *Minerals Engineering.* 53: 10-28.

Yang F., Baba Y., Kubota F., Kamiya N. & Goto M., 2012. Extraction and separation of rare earth metal ions with DODGAA in ionic liquids. *Solvent Extraction Resource Development Japan.* 19: 69–76.

Yang F., Kubota F., Baba Y., Kamiya N. & Goto M., 2013. Selective extraction and recovery of rare earth metals from phosphor powders in waste fluorescent lamps using an ionic liquid system. *Journal of Hazardous Materials*. 254– 255: 79– 88.

Yang H., Liub J. & Yang J., 2011. Leaching copper from shredded particles of waste printed circuit boards. *Journal of Hazardous Materials*. 187: 393–400.

Yang K., Li S., Zhang L., Peng G., Chen W., Xie F. & Ma A., 2016. Microwave roasting and leaching of an oxide-sulphide zinc ore. *Hydrometallurgy*. 166: 243 -251.

Yazici E.Y & Deveci H., 2013. Extraction of metals from waste printed circuit boards (WPCBs) in H_2SO_4–$CuSO_4$–NaCl solutions. *Hydrometallurgy*. 139: 30-38.

Yazici E.Y. & Deveci H., 2016. Ferric sulphate leaching of metals from waste printed circuit boards. *International Journal of Mineral Processing*. 133: 39 -45.

Yordanov A.T. & Roundhill D.M., 1998. "Solution extraction of transition and post-transition heavy and precious metals by chelate and macrocyclic ligands". *Coordination Chemistry Reviews.* 170**(1):** 93-124.

Yuan C., Zhang H., McKenna G., Korzeniewski C. & Li J., 2007. Experimental studies on cryogenic recycling of printed circuit board. *International Journal of Advanced Manufacturing Technology.* 34: 657 - 666.

Zarate R.Z., Gregorio L.G., & Lapidus G.T., 2015. Selective leaching of lead from a lead–silver–zinc concentrate with hydrogen peroxide in citrate solutions. *Canadian Metallurgical Quarterly*. 54**(3)**: 305-309.

Zhang D., Dong L., Li Y., Wu Y., Ma Y. & Yang B., 2018. Copper leaching from waste printed circuit boards using typical acidic ionic liquids recovery of e-wastes' surplus value. *Waste Management.* 78: 191–197.

Zhang J., Lan X.Z., Song Y.H., Wang B.X. & Xing, X.D., 2009. Study on the extraction of gold with acidic thiourea. *Precious Metals*. 2**(30)**: 75–82

Zhang L. & Xu Z., 2016. A review of current progress of recycling technologies for metals from waste electrical and electronic equipment. *Journal of Cleaner Production*. 127: 19 – 36.

Zhang X., Zhang C., Zheng F., Ma E., Wang R., Bai J., Yuan W. & Wang J., 2019. Alkaline electrochemical leaching of Sn and Pb from the surface of waste printed circuit board and the stripping of gold by methanesulfonic acid. *Environmental Progress & Sustainable Energy*. 39:e13324. https://doi.org/10.1002/ep.13324

Zhang Y., Liu S., Xie H., Zeng X. & Li J., 2012. Current status on leaching precious metals from waste printed circuit boards. *Procedia Environmental Sciences*. 16: 560 – 568

Appendices

Appendix 1a Summarized dose effect for Cu

	Dose (g)	Extraction (mg/g)														
		AQ	NA	HA	SA	CA	MA	TA	IL-A	IL-B	IL-C	IL-D	IL-E	IL-F	IL-G	W
Hotplate Method	0.20	504.17 ±21.63	206.67 ±20.55	48.37 ±3.59	0.91 ±0.08	6.85 ±0.70	2.00 ±0.08	0.79 ±0.04	0.05 ±0.00	0.05 ±0.01	0.43 ±0.02	1.20 ±0.00	55.83 ±3.12	3.33 ±0.31	113.33 ±10.27	0.00 ±0.00
	0.50	506.00 ±18.09	176.00 ±13.06	15.49 ±0.67	0.46 ±0.03	2.58 ±0.13	0.31 ±0.03	0.24 ±0.02	0.03 ±0.00	0.09 ±0.01	0.18 ±0.01	0.70 ±0.00	7.25 ±0.40	1.52 ±0.07	93.33 ±6.80	0.00 ±0.00
	0.70	490.48 ±26.94	178.57 ±5.83	6.19 ±0.67	0.35 ±0.02	0.70 ±0.09	0.18 ±0.03	0.16 ±0.01	0.02 ±0.00	0.06 ±0.00	0.13 ±0.01	0.60 ±0.00	4.33 ±0.09	0.59 ±0.06	47.33 ±3.40	0.00 ±0.00
	1.50	524.44 ±22.81	177.78 ±8.31	1.35 ±0.06	0.10 ±0.00	0.14 ±0.00	0.06 ±0.00	0.02 ±0.00	0.01 ±0.00	0.03 ±0.00	0.06 ±0.00	0.28 ±0.00	1.81 ±0.10	0.27 ±0.02	6.67 ±0.44	0.00 ±0.00
	2.00	526.67 ±32.86	187.50 ±8.06	0.31 ±0.02	0.05 ±0.00	0.11 ±0.00	0.04 ±0.00	0.02 ±0.00	0.01 ±0.00	0.10 ±0.11	0.05 ±0.00	0.18 ±0.00	1.44 ±0.13	0.12 ±0.01	2.27 ±0.21	0.00 ±0.00
	3.00	443.11 ±25.68	176.94 ±11.99	0.18 ±0.02	0.07 ±0.01	0.08 ±0.00	0.02 ±0.00	0.01 ±0.00	0.00 ±0.00	0.02 ±0.00	0.03 ±0.00	0.15 ±0.00	0.40 ±0.02	0.04 ±0.01	0.74 ±0.06	0.00 ±0.00
Microwave Method	0.20	1340.00 ±37.42	700.00 ±65.32	15.00 ±3.43	0.27 ±0.02	0.22 ±0.04	2.01 ±0.14	0.89 ±0.07	0.60 ±0.07	0.63 ±0.05	0.70 ±0.07	0.71 ±0.15	7.47 ±1.05	0.71 ±0.09	10.40 ±1.13	0.01 ±0.00
	0.50	645.33 ±32.88	322.67 ±16.44	5.20 ±1.13	0.13 ±0.01	0.10 ±0.01	0.80 ±0.07	0.30 ±0.04	0.25 ±0.01	0.23 ±0.03	0.28 ±0.04	0.30 ±0.04	2.77 ±0.42	0.30 ±0.03	4.16 ±0.45	0.02 ±0.01
	0.70	626.67 ±67.99	317.14 ±7.00	1.28 ±0.10	0.18 ±0.01	0.10 ±0.01	0.48 ±0.04	0.22 ±0.04	0.17 ±0.00	0.18 ±0.01	0.17 ±0.02	0.22 ±0.02	1.98 ±0.22	0.20 ±0.03	3.31 ±0.40	0.03 ±0.00
	1.50	300.00 ±48.99	108.44 ±20.69	0.46 ±0.10	0.19 ±0.02	0.09 ±0.02	0.18 ±0.02	0.05 ±0.01	0.08 ±0.01	0.08 ±0.01	0.09 ±0.01	0.10 ±0.01	1.01 ±0.12	0.10 ±0.01	1.39 ±0.15	0.04 ±0.01
	2.00	244.00 ±24.66	38.00 ±2.94	0.34 ±0.07	0.21 ±0.03	0.08 ±0.01	0.05 ±0.00	0.03 ±0.00	0.07 ±0.00	0.06 ±0.00	0.06 ±0.00	0.07 ±0.01	0.76 ±0.09	0.07 ±0.01	1.14 ±0.13	0.04 ±0.01
	3.00	220.00 ±43.20	21.11 ±4.16	0.23 ±0.04	0.13 ±0.02	0.08 ±0.01	0.02 ±0.00	0.02 ±0.00	0.04 ±0.00	0.05 ±0.00	0.04 ±0.00	0.05 ±0.01	0.46 ±0.05	0.05 ±0.01	0.71 ±0.09	0.14 ±0.04

Appendix 1b Summarized dose effect for Zn

	Dose (g)	Extraction (mg/g)														
		AQ	NA	HA	SA	CA	MA	TA	IL-A	IL-B	IL-C	IL-D	IL-E	IL-F	IL-G	W
Hotplate Method	0.20	886.67 ±16.50	382.50 ±12.25	442.75 ±37.40	305.00 ±7.07	253.33 ±41.10	313.33 ±63.42	170.00 ±123.56	0.53 ±0.02	0.41 ±0.03	1.61 ±0.13	113.33 ±4.99	85.17 ±14.66	106.67 ±4.99	106.67 ±6.80	0.06 ±0.01
	0.50	522.00 ±25.46	378.93 ±24.36	485.33 ±19.96	341.33 ±7.54	277.33 ±15.98	170.67 ±21.00	73.33 ±9.09	0.20 ±0.01	5.54 ±7.62	0.61 ±0.02	35.20 ±1.50	35.47 ±4.76	45.87 ±3.02	62.93 ±2.00	0.03 ±0.00
	0.70	458.57 ±6.06	341.14 ±9.53	448.00 ±26.67	240.00 ±16.16	240.00 ±29.14	281.90 ±27.34	69.52 ±9.29	0.14 ±0.00	3.39 ±4.63	0.43 ±0.02	17.33 ±0.71	26.67 ±2.49	35.81 ±1.08	46.48 ±1.94	0.03 ±0.00
	1.50	218.00 ±2.83	143.20 ±8.70	187.20 ±9.27	116.44 ±5.03	112.00 ±13.60	135.11 ±16.05	28.89 ±20.61	2.07 ±2.84	1.58 ±2.16	0.32 ±0.15	3.31 ±0.09	17.07 ±1.15	16.18 ±0.25	21.69 ±0.50	0.02 ±0.00
	2.00	358.50 ±2.12	169.33 ±13.97	187.00 ±7.88	110.83 ±4.25	95.33 ±4.11	96.00 ±17.20	24.00 ±16.99	0.05 ±0.00	0.03 ±0.00	0.16 ±0.00	0.94 ±0.01	13.87 ±1.32	12.40 ±3.12	35.73 ±1.00	0.01 ±0.00
	3.00	410.00 ±7.07	167.20 ±6.71	165.33 ±2.49	93.33 ±1.89	66.22 ±7.88	72.00 ±6.06	14.44 ±10.30	0.03 ±0.00	0.02 ±0.00	0.11 ±0.00	0.22 ±0.01	6.58 ±2.77	9.87 ±1.43	24.00 ±2.18	0.00 ±0.00
Microwave Method	0.20	457.33 ±23.49	185.00 ±30.82	230.00 ±14.14	146.00 ±14.99	56.00 ±9.90	50.00 ±7.48	212.33 ±13.11	261.33 ±26.55	296.33 ±28.19	361.67 ±23.65	245.00 ±15.61	324.33 ±18.37	420.00 ±37.15	326.67 ±32.31	6.50 ±1.87
	0.50	263.47 ±35.29	174.40 ±18.52	178.40 ±7.92	147.20 ±4.53	60.00 ±9.80	66.00 ±10.32	99.20 ±14.55	108.80 ±13.58	147.20 ±13.83	198.40 ±18.84	170.67 ±15.08	139.73 ±21.12	229.33 ±32.88	165.33 ±19.96	6.83 ±1.60
	0.70	211.43 ±24.24	171.43 ±24.40	177.14 ±8.08	137.14 ±5.60	66.29 ±8.55	73.14 ±11.65	71.62 ±15.08	98.29 ±30.03	100.57 ±9.88	125.71 ±16.16	118.10 ±14.25	99.05 ±14.97	148.57 ±23.64	129.52 ±19.42	16.19 ±3.56
	1.50	116.36 ±6.03	85.33 ±3.99	93.87 ±3.02	52.00 ±17.78	70.40 ±7.27	78.93 ±14.39	80.00 ±14.97	38.80 ±2.26	52.40 ±5.57	68.40 ±12.28	62.40 ±8.02	54.80 ±4.63	72.00 ±9.80	70.00 ±11.31	19.56 ±2.51
	2.00	92.00 ±5.63	70.40 ±2.26	63.60 ±11.13	33.00 ±5.16	69.60 ±13.58	58.40 ±9.86	36.00 ±14.70	33.30 ±5.74	39.60 ±2.55	52.80 ±1.70	48.00 ±4.24	41.10 ±6.79	61.50 ±10.61	42.00 ±12.90	21.00 ±2.45
	3.00	69.44 ±5.50	45.87 ±1.51	44.24 ±2.00	20.40 ±3.92	53.33 ±3.77	39.20 ±6.88	28.00 ±7.48	25.20 ±7.70	30.40 ±4.53	35.00 ±6.16	33.40 ±4.53	25.60 ±0.57	36.00 ±4.90	35.00 ±3.74	16.33 ±1.91

Appendix 1c Summarized dose effect for Fe

	Dose (g)	Extraction (mg/g)														
		AQ	**NA**	**HA**	**SA**	**CA**	**MA**	**TA**	**IL-A**	**IL-B**	**IL-C**	**IL-D**	**IL-E**	**IL-F**	**IL-G**	**W**
Hotplate Method	**0.20**	142.92 ±10.91	85.00 ±6.37	60.23 ±2.47	54.17 ±3.12	3.03 ±0.09	1.06 ±0.04	2.40 ±1.66	0.01 ±0.00	0.01 ±0.00	0.01 ±0.00	0.01 ±0.00	0.01 ±0.00	0.01 ±0.00	0.01 ±0.00	0.01 ±0.00
	0.50	109.33 ±8.22	61.83 ±7.19	74.13 ±4.20	50.40 ±2.29	2.13 ±0.10	1.35 ±0.11	2.15 ±1.49	0.00 ±0.00	0.00 ±0.00	0.00 ±0.00	0.00 ±0.00	0.00 ±0.00	0.00 ±0.00	0.00 ±0.00	0.00 ±0.00
	0.70	148.81 ±4.45	42.48 ±3.34	87.42 ±2.92	39.41 ±2.85	1.92 ±0.07	1.37 ±0.13	1.17 ±0.82	0.00 ±0.00	0.00 ±0.00	0.00 ±0.00	0.00 ±0.00	0.00 ±0.00	0.00 ±0.00	0.00 ±0.00	0.00 ±0.00
	1.50	79.02 ±3.44	37.33 ±1.09	18.40 ±1.34	26.80 ±0.89	1.28 ±0.04	1.21 ±0.04	1.14 ±0.80	0.00 ±0.00	0.00 ±0.00	0.00 ±0.00	0.00 ±0.00	0.00 ±0.00	0.00 ±0.00	0.00 ±0.00	0.00 ±0.00
	2.00	56.67 ±2.49	15.75 ±1.84	28.91 ±2.01	19.11 ±1.04	1.05 ±0.04	0.53 ±0.01	0.98 ±0.69	0.00 ±0.00	0.00 ±0.00	0.00 ±0.00	0.00 ±0.00	0.00 ±0.00	0.00 ±0.00	0.00 ±0.00	0.00 ±0.00
	3.00	56.67 ±1.36	18.05 ±1.04	34.45 ±2.14	8.98 ±0.90	0.80 ±0.05	0.20 ±0.01	0.51 ±0.36	0.00 ±0.00	0.00 ±0.00	0.00 ±0.00	0.00 ±0.00	0.00 ±0.00	0.00 ±0.00	0.00 ±0.00	0.00 ±0.00
Microwave Method	**0.20**	165.33 ±3.77	76.19 ±2.56	70.27 ±2.88	40.27 ±1.32	4.03 ±0.12	4.23 ±0.17	2.87 ±0.21	0.01 ±0.00	0.01 ±0.00	0.01 ±0.00	0.01 ±0.00	0.01 ±0.00	0.01 ±0.00	0.01 ±0.00	0.01 ±0.00
	0.50	85.87 ±2.73	39.00 ±8.49	36.08 ±5.61	21.65 ±1.40	2.56 ±0.12	2.02 ±0.17	2.40 ±0.10	0.00 ±0.00	0.00 ±0.00	0.00 ±0.00	0.00 ±0.00	0.00 ±0.00	0.00 ±0.00	0.00 ±0.00	0.00 ±0.00
	0.70	75.43 ±2.42	22.81 ±0.61	31.08 ±3.88	15.77 ±1.14	1.92 ±0.07	1.83 ±0.12	1.43 ±0.05	0.00 ±0.00	0.00 ±0.00	0.00 ±0.00	0.00 ±0.00	0.00 ±0.00	0.00 ±0.00	0.00 ±0.00	0.00 ±0.00
	1.50	50.40 ±0.98	14.58 ±0.25	21.45 ±1.04	10.72 ±0.36	1.23 ±0.04	1.16 ±0.02	1.34 ±0.07	0.00 ±0.00	0.00 ±0.00	0.00 ±0.00	0.00 ±0.00	0.00 ±0.00	0.00 ±0.00	0.00 ±0.00	0.00 ±0.00
	2.00	108.33 ±1.18	20.17 ±1.30	30.98 ±2.15	19.11 ±1.04	2.10 ±0.08	8.53 ±0.19	2.34 ±0.10	0.00 ±0.00	0.00 ±0.00	0.00 ±0.00	0.00 ±0.00	0.00 ±0.00	0.00 ±0.00	0.00 ±0.00	0.00 ±0.00
	3.00	39.60 ±1.04	7.44 ±0.16	13.78 ±0.85	3.59 ±0.36	0.64 ±0.04	3.25 ±0.14	0.35 ±0.03	0.00 ±0.00	0.00 ±0.00	0.00 ±0.00	0.00 ±0.00	0.00 ±0.00	0.00 ±0.00	0.00 ±0.00	0.00 ±0.00

Appendix 1d Summarized dose effect for Ni

	Dose (g)	Extraction (mg/g)														
		AQ	NA	HA	SA	CA	MA	TA	IL-A	IL-B	IL-C	IL-D	IL-E	IL-F	IL-G	W
Hotplate Method	**0.20**	63.33 ±4.71	1.75 ±0.35	1.92 ±0.31	1.50 ±0.20	1.17 ±0.16	0.53 ±0.06	1.25 ±0.20	0.01 ±0.00	0.01 ±0.00	0.01 ±0.00	0.01 ±0.00	0.01 ±0.00	0.01 ±0.00	0.01 ±0.00	0.01 ±0.00
	0.50	53.33 ±1.89	1.93 ±0.47	1.67 ±0.25	1.47 ±0.25	1.23 ±0.12	0.32 ±0.03	1.33 ±0.09	0.00 ±0.00	0.00 ±0.00	0.00 ±0.00	0.00 ±0.00	0.00 ±0.00	0.00 ±0.00	0.00 ±0.00	0.00 ±0.00
	0.70	51.19 ±1.68	3.05 ±0.49	2.57 ±0.23	1.43 ±0.12	0.95 ±0.09	0.25 ±0.03	1.10 ±0.07	0.00 ±0.00	0.00 ±0.00	0.00 ±0.00	0.00 ±0.00	0.00 ±0.00	0.00 ±0.00	0.00 ±0.00	0.00 ±0.00
	1.50	25.56 ±0.79	1.83 ±0.36	1.61 ±0.08	0.78 ±0.08	0.42 ±0.06	0.12 ±0.01	0.58 ±0.03	0.00 ±0.00	0.00 ±0.00	0.00 ±0.00	0.00 ±0.00	0.00 ±0.00	0.00 ±0.00	0.00 ±0.00	0.00 ±0.00
	2.00	22.92 ±0.65	1.70 ±0.28	1.65 ±0.12	0.60 ±0.07	1.25 ±1.24	0.10 ±0.01	0.47 ±0.02	0.00 ±0.00	0.00 ±0.00	0.00 ±0.00	0.00 ±0.00	0.00 ±0.00	0.00 ±0.00	0.00 ±0.00	0.00 ±0.00
	3.00	17.67 ±0.47	1.20 ±0.22	1.20 ±0.08	0.42 ±0.04	0.23 ±0.04	0.08 ±0.01	0.33 ±0.03	0.00 ±0.00	0.00 ±0.00	0.00 ±0.00	0.00 ±0.00	0.00 ±0.00	0.00 ±0.00	0.00 ±0.00	0.00 ±0.00
Microwave Method	**0.20**	31.67 ±2.36	2.27 ±0.50	2.80 ±0.29	1.00 ±0.16	0.28 ±0.12	0.17 ±0.04	0.11 ±0.02	0.01 ±0.00	0.01 ±0.00	0.01 ±0.00	0.01 ±0.00	0.01 ±0.00	0.01 ±0.00	0.01 ±0.00	0.01 ±0.00
	0.50	24.00 ±0.85	1.87 ±0.07	0.96 ±0.10	0.75 ±0.17	0.12 ±0.07	0.07 ±0.02	0.05 ±0.01	0.00 ±0.00	0.00 ±0.00	0.00 ±0.00	0.00 ±0.00	0.00 ±0.00	0.00 ±0.00	0.00 ±0.00	0.00 ±0.00
	0.70	22.52 ±0.74	2.40 ±0.14	0.64 ±0.06	0.67 ±0.17	0.10 ±0.05	0.05 ±0.01	0.04 ±0.01	0.00 ±0.00	0.00 ±0.00	0.00 ±0.00	0.00 ±0.00	0.00 ±0.00	0.00 ±0.00	0.00 ±0.00	0.00 ±0.00
	1.50	12.27 ±0.38	1.40 ±0.08	0.27 ±0.02	0.44 ±0.03	0.07 ±0.01	0.04 ±0.00	0.03 ±0.00	0.00 ±0.00	0.00 ±0.00	0.00 ±0.00	0.00 ±0.00	0.00 ±0.00	0.00 ±0.00	0.00 ±0.00	0.00 ±0.00
	2.00	10.83 ±0.31	1.25 ±0.10	0.15 ±0.02	0.30 ±0.02	0.05 ±0.01	0.03 ±0.00	0.02 ±0.00	0.00 ±0.00	0.00 ±0.00	0.00 ±0.00	0.00 ±0.00	0.00 ±0.00	0.00 ±0.00	0.00 ±0.00	0.00 ±0.00
	3.00	8.24 ±0.22	1.00 ±0.07	0.07 ±0.01	0.19 ±0.02	0.03 ±0.01	0.02 ±0.00	0.01 ±0.00	0.00 ±0.00	0.00 ±0.00	0.00 ±0.00	0.00 ±0.00	0.00 ±0.00	0.00 ±0.00	0.00 ±0.00	0.00 ±0.00

Appendix 1e Summarized dose effect for Pb

	Dose (g)	Extraction (mg/g)														
		AQ	NA	HA	SA	CA	MA	TA	IL-A	IL-B	IL-C	IL-D	IL-E	IL-F	IL-G	W
Hotplate Method	0.20	77.50 ±9.35	17.09 ±2.55	15.83 ±3.12	1.25 ±0.20	4.83 ±0.62	8.83 ±0.62	2.83 ±0.31	0.27 ±0.05	0.19 ±0.01	0.19 ±0.00	3.47 ±0.34	0.28 ±0.02	0.18 ±0.02	1.13 ±0.12	0.00 ±0.00
	0.50	62.67 ±6.80	25.96 ±2.86	30.00 ±2.45	0.63 ±0.12	2.07 ±0.25	3.20 ±0.16	1.17 ±0.12	0.09 ±0.02	0.07 ±0.00	0.08 ±0.00	1.19 ±0.16	0.11 ±0.01	0.07 ±0.01	0.48 ±0.07	0.00 ±0.00
	0.70	47.14 ±4.01	22.23 ±2.65	21.43 ±1.75	0.33 ±0.09	1.48 ±0.07	1.48 ±0.18	0.74 ±0.09	0.07 ±0.01	0.07 ±0.01	0.06 ±0.00	0.65 ±0.10	0.07 ±0.00	0.05 ±0.00	0.30 ±0.05	0.00 ±0.00
	1.50	22.78 ±2.08	13.63 ±1.98	11.67 ±1.70	0.23 ±0.05	0.73 ±0.05	0.67 ±0.11	0.32 ±0.06	0.03 ±0.01	0.03 ±0.00	0.03 ±0.00	0.28 ±0.05	0.03 ±0.00	0.02 ±0.00	0.09 ±0.02	0.00 ±0.00
	2.00	19.25 ±1.12	10.79 ±0.87	10.50 ±0.71	0.18 ±0.03	0.33 ±0.04	0.33 ±0.03	0.25 ±0.02	0.03 ±0.00	0.02 ±0.00	0.02 ±0.00	0.10 ±0.02	0.02 ±0.00	0.00 ±0.00	0.06 ±0.02	0.00 ±0.00
	3.00	16.67 ±0.47	10.50 ±1.22	6.42 ±0.48	0.14 ±0.03	0.22 ±0.02	0.23 ±0.02	0.15 ±0.01	0.02 ±0.00	0.01 ±0.00	0.01 ±0.00	0.07 ±0.01	0.01 ±0.00	0.01 ±0.00	0.01 ±0.00	0.00 ±0.00
Microwave Method	0.20	60.00 ±9.80	40.00 ±4.08	31.47 ±2.64	0.08 ±0.00	0.10 ±0.02	0.10 ±0.02	0.10 ±0.02	0.27 ±0.05	0.31 ±0.02	0.27 ±0.05	0.21 ±0.15	0.30 ±0.00	0.34 ±0.01	0.33 ±0.02	0.27 ±0.05
	0.50	36.27 ±3.99	21.60 ±1.96	14.47 ±2.38	0.03 ±0.00	0.06 ±0.02	0.06 ±0.02	0.06 ±0.01	0.12 ±0.01	0.13 ±0.02	0.12 ±0.00	0.08 ±0.05	0.13 ±0.00	0.13 ±0.00	0.13 ±0.00	0.12 ±0.00
	0.70	34.29 ±4.67	17.71 ±2.14	9.14 ±1.07	0.02 ±0.00	0.06 ±0.01	0.06 ±0.01	0.07 ±0.01	0.09 ±0.01	0.09 ±0.01	0.10 ±0.01	0.06 ±0.04	0.09 ±0.00	0.10 ±0.00	0.10 ±0.01	0.10 ±0.01
	1.50	22.40 ±1.31	13.01 ±1.38	4.56 ±0.68	0.01 ±0.00	0.05 ±0.01	0.05 ±0.01	0.05 ±0.01	0.04 ±0.01	0.04 ±0.00	0.04 ±0.00	0.03 ±0.02	0.04 ±0.00	0.04 ±0.00	0.04 ±0.00	0.04 ±0.00
	2.00	20.37 ±1.23	10.80 ±0.98	2.57 ±0.12	0.01 ±0.00	0.04 ±0.01	0.04 ±0.01	0.04 ±0.01	0.03 ±0.00	0.03 ±0.00	0.03 ±0.00	0.02 ±0.02	0.03 ±0.00	0.03 ±0.00	0.03 ±0.00	0.03 ±0.00
	3.00	16.83 ±0.62	8.18 ±0.67	2.28 ±0.21	0.01 ±0.00	0.03 ±0.01	0.03 ±0.01	0.03 ±0.01	0.02 ±0.00	0.02 ±0.00	0.02 ±0.00	0.01 ±0.01	0.02 ±0.00	0.02 ±0.00	0.02 ±0.00	0.02 ±0.00

Appendix 2a Summarized Particle-size effect for Cu

	Particle-size (mm)	Extraction (mg/g)														
		AQ	**NA**	**HA**	**SA**	**CA**	**MA**	**TA**	**IL-A**	**IL-B**	**IL-C**	**IL-D**	**IL-E**	**IL-F**	**IL-G**	**W**
Hotplate Method	**1.00**	373.33 ±20.55	205.67 ±13.07	41.83 ±4.25	0.37 ±0.05	1.21 ±0.16	0.54 ±0.10	0.28 ±0.04	0.02 ±0.00	0.01 ±0.00	0.01 ±0.00	0.06 ±0.00	12.13 ±0.82	0.45 ±0.03	31.00 ±2.94	0.00 ±0.00
	2.00	326.33 ±10.34	181.67 ±16.50	52.00 ±5.89	0.49 ±0.15	0.94 ±0.10	0.56 ±0.07	0.26 ±0.04	0.02 ±0.00	0.02 ±0.00	0.01 ±0.01	0.12 ±0.03	8.64 ±1.40	0.48 ±0.02	36.40 ±1.50	0.00 ±0.00
	3.00	261.33 ±15.11	172.33 ±18.52	74.17 ±10.07	0.83 ±0.26	0.60 ±0.16	0.81 ±0.08	0.94 ±0.20	0.02 ±0.00	0.02 ±0.00	0.01 ±0.00	0.08 ±0.03	5.68 ±0.49	0.12 ±0.02	41.60 ±6.91	0.00 ±0.00
	4.00	247.00 ±16.87	156.67 ±15.46	84.17 ±10.47	1.43 ±0.23	0.50 ±0.16	1.17 ±0.12	1.49 ±0.21	0.03 ±0.00	0.02 ±0.00	0.02 ±0.00	0.32 ±0.01	5.52 ±0.39	0.28 ±0.03	72.00 ±5.88	0.00 ±0.00
Microwave Method	**1.00**	704.00 ±34.56	328.00 ±11.31	3.52 ±0.63	0.08 ±0.00	0.11 ±0.01	0.48 ±0.05	0.28 ±0.03	0.18 ±0.01	0.18 ±0.02	0.19 ±0.01	0.22 ±0.02	2.96 ±0.17	0.29 ±0.02	3.36 ±0.20	0.01 ±0.00
	2.00	672.00 ±26.13	320.00 ±5.31	3.12 ±0.20	0.09 ±0.00	0.10 ±0.01	0.50 ±0.06	0.31 ±0.01	0.19 ±0.01	0.20 ±0.03	0.21 ±0.02	0.24 ±0.02	2.72 ±0.23	0.26 ±0.01	3.44 ±0.23	0.02 ±0.01
	3.00	624.00 ±13.06	306.67 ±9.98	2.72 ±0.30	0.09 ±0.01	0.09 ±0.00	0.60 ±0.07	0.32 ±0.00	0.21 ±0.02	0.22 ±0.02	0.22 ±0.02	0.26 ±0.01	2.53 ±0.10	0.26 ±0.01	3.88 ±0.20	0.03 ±0.00
	4.00	613.33 ±19.96	290.67 ±9.98	2.80 ±0.57	0.10 ±0.01	0.09 ±0.00	0.63 ±0.06	0.33 ±0.01	0.23 ±0.02	0.24 ±0.02	0.26 ±0.01	0.26 ±0.02	2.40 ±0.13	0.22 ±0.05	4.08 ±0.17	0.04 ±0.01

Appendix 2b Summarized Particle-size effect for Zn

	Particle-size (mm)	Extraction (mg/g)														
		AQ	NA	HA	SA	CA	MA	TA	IL-A	IL-B	IL-C	IL-D	IL-E	IL-F	IL-G	W
Hotplate Method	**1.00**	600.00 ±32.66	166.67 ±4.99	560.00 ±65.32	150.67 ±8.22	133.33 ±9.98	138.67 ±4.99	146.00 ±6.00	0.07 ±0.01	0.05 ±0.01	0.19 ±0.01	44.27 ±3.29	40.53 ±2.00	51.73 ±3.29	54.40 ±4.71	0.03 ±0.00
	2.00	517.33 ±19.96	394.67 ±24.73	341.33 ±41.99	354.67 ±26.40	146.67 ±4.99	144.00 ±3.27	200.00 ±8.00	0.09 ±0.01	0.07 ±0.01	0.42 ±0.04	43.73 ±2.00	43.20 ±1.31	44.80 ±2.61	52.80 ±3.92	0.03 ±0.00
	3.00	496.00 ±19.60	392.00 ±22.63	354.67 ±26.40	362.67 ±22.94	197.40 ±9.07	140.00 ±3.27	218.40 ±8.40	0.12 ±0.01	0.12 ±0.02	0.52 ±0.03	43.73 ±1.51	45.87 ±2.00	38.40 ±2.61	44.80 ±2.61	0.03 ±0.00
	4.00	482.67 ±16.44	376.00 ±22.63	317.33 ±14.78	373.33 ±9.98	304.00 ±11.31	165.33 ±24.73	259.20 ±28.80	0.17 ±0.01	0.12 ±0.02	0.61 ±0.02	41.60 ±1.31	45.87 ±2.00	38.40 ±2.26	36.27 ±3.02	0.03 ±0.00
Microwave Method	**1.00**	164.27 ±41.24	105.33 ±4.99	126.40 ±12.60	131.20 ±11.97	41.60 ±5.99	48.00 ±4.49	92.80 ±12.80	115.20 ±18.29	94.93 ±27.69	132.27 ±3.99	88.53 ±62.73	117.33 ±7.98	138.67 ±15.08	96.00 ±11.39	6.50 ±1.87
	2.00	208.67 ±40.54	161.60 ±31.68	131.20 ±12.60	152.00 ±19.33	49.60 ±3.57	69.60 ±3.39	115.20 ±9.60	117.33 ±7.54	117.33 ±7.54	169.60 ±29.44	106.67 ±75.42	110.93 ±7.98	165.33 ±7.54	102.40 ±6.91	6.83 ±1.60
	3.00	257.33 ±36.12	184.00 ±11.31	149.60 ±17.12	161.60 ±28.35	59.20 ±2.99	75.60 ±2.94	104.00 ±8.00	133.33 ±3.99	122.67 ±18.90	171.73 ±24.28	131.20 ±95.39	123.73 ±3.02	208.00 ±13.06	122.67 ±10.56	7.15 ±1.32
	4.00	281.20 ±37.75	212.80 ±20.11	172.80 ±5.18	176.00 ±16.32	56.80 ±6.88	73.20 ±7.40	115.20 ±12.80	138.67 ±15.08	126.93 ±18.90	183.47 ±16.80	140.80 ±100.79	119.47 ±6.58	226.13 ±3.02	144.00 ±14.55	7.48 ±1.05

Appendix 2c Summarized Particle-size effect for Fe

	Particle-size (mm)	Extraction (mg/g)														
		AQ	NA	HA	SA	CA	MA	TA	IL-A	IL-B	IL-C	IL-D	IL-E	IL-F	IL-G	W
Hotplate Method	**1.00**	61.00 ±6.16	11.40 ±1.53	34.13 ±9.83	9.80 ±0.00	2.63 ±0.21	2.91 ±0.20	1.57 ±0.43	0.00 ±0.00	0.00 ±0.00	0.00 ±0.00	0.00 ±0.00	0.00 ±0.00	0.00 ±0.00	0.00 ±0.00	0.00 ±0.00
	2.00	86.33 ±1.65	38.27 ±3.49	47.00 ±4.30	15.00 ±0.00	2.19 ±0.14	2.67 ±0.20	1.50 ±0.45	0.00 ±0.00	0.00 ±0.00	0.00 ±0.00	0.00 ±0.00	0.00 ±0.00	0.00 ±0.00	0.00 ±0.00	0.00 ±0.00
	3.00	103.83 ±4.37	56.10 ±8.08	85.00 ±7.07	48.87 ±6.65	1.66 ±0.10	2.02 ±0.16	1.36 ±0.26	0.00 ±0.00	0.00 ±0.00	0.00 ±0.00	0.00 ±0.00	0.00 ±0.00	0.00 ±0.00	0.00 ±0.00	0.00 ±0.00
	4.00	122.67 ±6.80	86.33 ±7.19	120.53 ±6.58	68.13 ±11.73	1.04 ±0.07	1.47 ±0.08	1.13 ±0.11	0.00 ±0.00	0.00 ±0.00	0.00 ±0.00	0.00 ±0.00	0.00 ±0.00	0.00 ±0.00	0.00 ±0.00	0.00 ±0.00
Microwave Method	**1.00**	60.27 ±3.29	23.60 ±1.50	27.20 ±2.04	9.20 ±0.28	2.76 ±0.30	2.97 ±0.16	1.64 ±0.45	0.00 ±0.00	0.00 ±0.00	0.00 ±0.00	0.00 ±0.00	0.00 ±0.00	0.00 ±0.00	0.00 ±0.00	0.01 ±0.00
	2.00	73.20 ±2.24	27.73 ±1.60	29.76 ±1.75	11.28 ±1.22	2.77 ±0.29	2.81 ±0.16	1.60 ±0.42	0.00 ±0.00	0.00 ±0.00	0.00 ±0.00	0.00 ±0.00	0.00 ±0.00	0.00 ±0.00	0.00 ±0.00	0.00 ±0.00
	3.00	81.33 ±1.89	33.44 ±2.48	35.84 ±2.77	16.25 ±1.15	2.76 ±0.28	2.65 ±0.17	1.55 ±0.39	0.00 ±0.00	0.00 ±0.00	0.00 ±0.00	0.00 ±0.00	0.00 ±0.00	0.00 ±0.00	0.00 ±0.00	0.00 ±0.00
	4.00	87.27 ±2.48	45.00 ±1.47	40.96 ±2.09	21.28 ±0.91	2.48 ±0.20	2.46 ±0.17	1.67 ±0.52	0.00 ±0.00	0.00 ±0.00	0.00 ±0.00	0.00 ±0.00	0.00 ±0.00	0.00 ±0.00	0.00 ±0.00	0.00 ±0.00

Appendix 2d Summarized Particle-size effect for Ni

	Particle-size (mm)	Extraction (mg/g)														
		AQ	NA	HA	SA	CA	MA	TA	IL-A	IL-B	IL-C	IL-D	IL-E	IL-F	IL-G	W
Hotplate Method	1.00	46.67 ±3.77	1.60 ±0.33	0.40 ±0.08	0.56 ±0.10	0.23 ±0.06	0.25 ±0.04	0.23 ±0.03	0.00 ±0.00	0.00 ±0.00	0.00 ±0.00	0.00 ±0.00	0.00 ±0.00	0.00 ±0.00	0.00 ±0.00	0.00 ±0.00
	2.00	56.00 ±3.46	2.07 ±0.41	0.63 ±0.12	0.67 ±0.17	0.51 ±0.10	0.40 ±0.07	0.65 ±0.15	0.00 ±0.00	0.00 ±0.00	0.00 ±0.00	0.00 ±0.00	0.00 ±0.00	0.00 ±0.00	0.00 ±0.00	0.00 ±0.00
	3.00	60.00 ±5.66	2.33 ±0.25	0.90 ±0.12	1.10 ±0.19	0.77 ±0.26	0.44 ±0.07	1.05 ±0.30	0.00 ±0.00	0.00 ±0.00	0.00 ±0.00	0.00 ±0.00	0.00 ±0.00	0.00 ±0.00	0.00 ±0.00	0.00 ±0.00
	4.00	62.13 ±3.34	2.87 ±0.25	1.33 ±0.25	1.73 ±0.25	1.13 ±0.25	0.44 ±0.09	1.60 ±0.40	0.00 ±0.00	0.00 ±0.00	0.00 ±0.00	0.00 ±0.00	0.00 ±0.00	0.00 ±0.00	0.00 ±0.00	0.00 ±0.00
Microwave Method	1.00	18.20 ±1.14	1.73 ±0.07	0.60 ±0.08	0.72 ±0.10	0.11 ±0.01	0.05 ±0.01	0.05 ±0.00	0.00 ±0.00	0.00 ±0.00	0.00 ±0.00	0.00 ±0.00	0.00 ±0.00	0.00 ±0.00	0.00 ±0.00	0.01 ±0.00
	2.00	20.27 ±1.72	2.01 ±0.07	0.75 ±0.11	0.90 ±0.10	0.15 ±0.01	0.05 ±0.01	0.05 ±0.00	0.00 ±0.00	0.00 ±0.00	0.00 ±0.00	0.00 ±0.00	0.00 ±0.00	0.00 ±0.00	0.00 ±0.00	0.00 ±0.00
	3.00	22.96 ±2.10	2.01 ±0.17	0.96 ±0.10	1.09 ±0.11	0.17 ±0.01	0.09 ±0.01	0.06 ±0.00	0.00 ±0.00	0.00 ±0.00	0.00 ±0.00	0.00 ±0.00	0.00 ±0.00	0.00 ±0.00	0.00 ±0.00	0.00 ±0.00
	4.00	25.20 ±1.47	2.05 ±0.17	1.04 ±0.11	1.07 ±0.13	0.22 ±0.01	0.08 ±0.01	0.06 ±0.00	0.00 ±0.00	0.00 ±0.00	0.00 ±0.00	0.00 ±0.00	0.00 ±0.00	0.00 ±0.00	0.00 ±0.00	0.00 ±0.00

Appendix 2e Summarized Particle-size effect for Pb

	Particle-size (mm)	Extraction (mg/g)														
		AQ	NA	HA	SA	CA	MA	TA	IL-A	IL-B	IL-C	IL-D	IL-E	IL-F	IL-G	W
Hotplate Method	1.00	20.00 ±3.27	17.50 ±1.87	14.50 ±2.55	0.41 ±0.01	2.67 ±0.25	1.20 ±0.16	0.85 ±0.15	0.03 ±0.00	0.03 ±0.00	0.03 ±0.00	0.24 ±0.03	0.04 ±0.01	0.03 ±0.00	0.09 ±0.01	0.03 ±0.00
	2.00	31.67 ±4.25	23.33 ±1.89	20.00 ±1.63	0.48 ±0.02	2.60 ±0.16	1.33 ±0.12	1.05 ±0.15	0.07 ±0.00	0.07 ±0.00	0.07 ±0.00	0.47 ±0.05	0.09 ±0.00	0.04 ±0.01	0.16 ±0.01	0.03 ±0.00
	3.00	40.00 ±3.74	30.00 ±3.54	28.33 ±3.12	0.50 ±0.01	2.47 ±0.25	2.27 ±0.19	1.10 ±0.20	0.07 ±0.00	0.08 ±0.00	0.08 ±0.00	0.99 ±0.14	0.10 ±0.00	0.08 ±0.01	0.21 ±0.00	0.03 ±0.00
	4.00	52.00 ±8.64	35.00 ±3.74	34.45 ±1.41	0.51 ±0.02	2.40 ±0.33	3.00 ±0.28	1.25 ±0.05	0.08 ±0.00	0.07 ±0.00	0.07 ±0.00	1.33 ±0.10	0.10 ±0.00	0.08 ±0.01	0.45 ±0.04	0.03 ±0.00
Microwave Method	1.00	10.13 ±2.00	4.53 ±0.75	3.20 ±0.28	0.03 ±0.00	0.03 ±0.00	0.03 ±0.00	0.03 ±0.00	0.03 ±0.00	0.03 ±0.00	0.03 ±0.00	0.02 ±0.02	0.03 ±0.00	0.03 ±0.00	0.03 ±0.00	0.04 ±0.00
	2.00	22.40 ±2.99	8.40 ±1.70	6.40 ±0.65	0.03 ±0.00	0.03 ±0.00	0.03 ±0.00	0.03 ±0.00	0.03 ±0.00	0.03 ±0.00	0.03 ±0.00	0.02 ±0.02	0.03 ±0.00	0.03 ±0.00	0.03 ±0.00	0.03 ±0.00
	3.00	32.67 ±3.49	12.80 ±2.61	10.00 ±1.50	0.03 ±0.00	0.03 ±0.00	0.03 ±0.00	0.03 ±0.00	0.03 ±0.00	0.03 ±0.00	0.03 ±0.00	0.02 ±0.02	0.03 ±0.00	0.03 ±0.00	0.03 ±0.00	0.02 ±0.00
	4.00	35.20 ±2.61	24.80 ±4.08	13.07 ±1.32	0.03 ±0.00	0.03 ±0.00	0.03 ±0.00	0.03 ±0.00	0.03 ±0.00	0.03 ±0.00	0.03 ±0.00	0.02 ±0.02	0.03 ±0.00	0.03 ±0.00	0.03 ±0.00	0.02 ±0.00

Appendix 3a Summarized H_2O_2 effect for Cu

	H_2O_2 Amount (%)	Extraction (mg/g)														
		AQ	**NA**	**HA**	**SA**	**CA**	**MA**	**TA**	**IL-A**	**IL-B**	**IL-C**	**IL-D**	**IL-E**	**IL-F**	**IL-G**	**W**
Hotplate Method	**5**	1680.00 ±21.12	640.00 ±12.26	1130.67 ±65.75	18.42 ±0.81	109.87 ±10.56	100.27 ±9.18	4.75 ±0.19	1.50 ±0.08	1.08 ±0.08	4.60 ±0.43	2.37 ±0.26	9.07 ±0.82	3.39 ±0.16	8.36 ±0.62	0.01 ±0.00
	15	1680.00 ±21.12	661.33 ±54.39	1173.33 ±18.78	19.50 ±0.92	26.28 ±3.56	113.07 ±12.35	4.10 ±0.31	1.27 ±0.12	1.15 ±0.07	4.93 ±0.38	2.43 ±0.09	9.60 ±0.33	3.47 ±0.16	9.12 ±0.31	0.02 ±0.01
	25	1680.00 ±21.12	640.00 ±52.26	1290.67 ±13.90	21.02 ±1.10	13.87 ±1.36	122.67 ±9.89	3.70 ±0.55	1.23 ±0.12	1.20 ±0.04	5.27 ±0.25	2.63 ±0.12	10.40 ±0.00	3.49 ±0.10	10.01 ±0.47	0.03 ±0.00
Microwave Method	**5**	384.00 ±11.23	221.87 ±3.02	260.27 ±6.03	2.67 ±0.10	25.60 ±1.57	25.81 ±1.32	0.53 ±0.06	0.27 ±0.02	0.31 ±0.04	0.20 ±0.04	0.28 ±0.03	0.58 ±0.06	0.07 ±0.00	0.55 ±0.04	0.01 ±0.00
	15	384.00 ±11.23	226.13 ±7.98	275.20 ±13.83	2.43 ±0.10	3.67 ±0.34	22.83 ±1.84	0.35 ±0.04	0.37 ±0.02	0.27 ±0.02	0.22 ±0.03	0.33 ±0.01	0.61 ±0.05	0.07 ±0.00	0.58 ±0.06	0.02 ±0.01
	25	384.00 ±11.23	236.80 ±5.23	285.87 ±7.98	1.89 ±0.16	1.87 ±0.27	5.67 ±0.68	0.27 ±0.03	0.55 ±0.04	0.26 ±0.02	0.24 ±0.03	0.36 ±0.02	0.67 ±0.02	0.07 ±0.00	0.63 ±0.06	0.03 ±0.00

Appendix 3b Summarized H_2O_2 effect for Zn

	H_2O_2 Amount (%)	Extraction (mg/g)														
		AQ	**NA**	**HA**	**SA**	**CA**	**MA**	**TA**	**IL-A**	**IL-B**	**IL-C**	**IL-D**	**IL-E**	**IL-F**	**IL-G**	**W**
Hotplate Method	**5**	1013.33 ±34.77	853.33 ±12.24	240.00 ±13.25	161.33 ±5.21	160.00 ±6.15	183.00 ±4.24	170.83 ±3.88	562.67 ±5.41	710.67 ±14.21	716.00 ±17.25	718.33 ±6.82	592.00 ±5.78	673.33 ±18.25	635.00 ±12.94	6.50 ±1.85
	15	1013.33 ±20.23	866.67 ±23.21	216.67 ±15.21	209.83 ±4.56	153.67 ±4.54	196.60 ±5.58	69.07 ±2.19	551.33 ±10.23	708.67 ±20.10	730.00 ±21.25	690.00 ±12.23	584.00 ±9.45	686.67 ±17.54	641.67 ±15.25	6.83 ±1.40
	25	1013.33 ±31.23	860.00 ±14.12	220.50 ±9.31	241.03 ±3.54	130.67 ±5.44	199.67 ±3.69	0.07 ±0.01	538.67 ±12.21	696.00 ±15.32	700.00 ±17.88	697.33 ±3.45	616.33 ±16.21	695.00 ±14.65	670.00 ±12.55	7.15 ±1.32
Microwave Method	**5**	667.33 ±46.31	296.13 ±21.33	287.47 ±18.63	275.03 ±17.71	248.12 ±6.68	196.00 ±10.20	204.67 ±10.87	118.40 ±4.71	115.47 ±11.69	143.67 ±0.47	143.20 ±2.36	127.00 ±6.16	142.13 ±5.85	134.67 ±10.50	6.50 ±1.87
	15	667.33 ±46.31	325.07 ±14.42	329.19 ±10.53	295.07 ±9.22	260.13 ±12.94	224.33 ±18.55	37.00 ±2.16	116.80 ±4.66	113.40 ±6.04	138.00 ±12.96	146.00 ±10.20	128.33 ±10.87	141.73 ±8.80	137.33 ±3.77	6.83 ±1.60
	25	667.33 ±46.31	343.53 ±19.10	332.73 ±11.97	299.20 ±11.26	284.92 ±8.75	245.33 ±10.96	0.01 ±0.00	123.27 ±3.06	111.67 ±3.37	139.47 ±5.89	140.00 ±4.08	134.00 ±7.48	139.20 ±7.95	139.00 ±13.93	7.15 ±1.32

Appendix 3c Summarized H_2O_2 effect for Fe

	H_2O_2 Amount (%)	Extraction (mg/g)														
		AQ	NA	HA	SA	CA	MA	TA	IL-A	IL-B	IL-C	IL-D	IL-E	IL-F	IL-G	W
Hotplate Method	5	231.00 ±8.23	10.60 ±0.86	83.20 ±4.93	70.67 ±4.11	0.01 ±0.00	1.17 ±0.13	0.54 ±0.04	0.01 ±0.00	0.01 ±0.00	0.27 ±0.04	0.01 ±0.00	0.01 ±0.00	7.92 ±0.72	0.60 ±0.13	0.00 ±0.00
	15	231.00 ±8.23	11.99 ±0.95	63.00 ±5.30	85.60 ±6.88	0.01 ±0.00	0.31 ±0.01	0.13 ±0.02	0.01 ±0.00	0.01 ±0.00	0.30 ±0.02	0.01 ±0.00	0.01 ±0.00	8.92 ±1.05	0.64 ±0.03	0.00 ±0.00
	25	231.00 ±8.23	14.31 ±1.40	10.80 ±0.88	111.00 ±6.48	0.01 ±0.00	0.34 ±0.02	0.14 ±0.00	0.01 ±0.00	0.01 ±0.00	0.33 ±0.02	0.01 ±0.00	0.01 ±0.00	9.67 ±0.47	0.76 ±0.04	0.00 ±0.00
Microwave Method	5	105.60 ±7.12	2.10 ±0.15	8.13 ±0.84	89.63 ±7.46	0.00 ±0.00	0.00 ±0.00	0.00 ±0.00	0.05 ±0.00	0.67 ±0.10	0.12 ±0.01	0.42 ±0.05	1.50 ±0.08	1.41 ±0.04	0.10 ±0.01	0.00 ±0.00
	15	105.60 ±7.12	2.38 ±0.07	90.13 ±6.49	59.40 ±5.30	0.00 ±0.00	0.03 ±0.01	0.03 ±0.00	0.06 ±0.00	0.71 ±0.11	0.13 ±0.01	0.44 ±0.01	1.70 ±0.15	1.63 ±0.07	0.12 ±0.01	0.00 ±0.00
	25	105.60 ±7.12	0.03 ±0.01	1.76 ±0.12	31.67 ±2.87	0.00 ±0.00	0.00 ±0.00	0.00 ±0.00	0.07 ±0.00	0.71 ±0.10	0.14 ±0.01	0.48 ±0.02	1.97 ±0.12	1.80 ±0.14	0.15 ±0.01	0.00 ±0.00

Appendix 3d Summarized H_2O_2 effect for Ni

	H_2O_2 Amount (%)	Extraction (mg/g)														
		AQ	NA	HA	SA	CA	MA	TA	IL-A	IL-B	IL-C	IL-D	IL-E	IL-F	IL-G	W
Hotplate Method	5	61.10 ±3.21	15.60 ±2.06	14.30 ±2.22	0.40 ±0.57	0.02 ±0.03	0.22 ±0.31	0.01 ±0.00	0.01 ±0.00	0.01 ±0.00	0.01 ±0.00	0.01 ±0.00	0.01 ±0.00	0.01 ±0.00	0.01 ±0.00	0.00 ±0.00
	15	61.10 ±3.21	14.40 ±0.36	20.80 ±2.42	0.30 ±0.43	0.03 ±0.05	0.00 ±0.00	0.01 ±0.00	0.01 ±0.00	0.01 ±0.00	0.01 ±0.00	0.01 ±0.00	0.01 ±0.00	0.01 ±0.00	0.01 ±0.00	0.00 ±0.00
	25	61.10 ±3.21	13.60 ±2.23	0.40 ±0.57	0.24 ±0.34	0.01 ±0.01	0.08 ±0.11	0.01 ±0.00	0.01 ±0.00	0.01 ±0.00	0.01 ±0.00	0.01 ±0.00	0.01 ±0.00	0.01 ±0.00	0.01 ±0.00	0.00 ±0.00
Microwave Method	5	19.20 ±1.30	15.77 ±1.37	12.27 ±0.75	5.73 ±0.68	0.01 ±0.00	0.03 ±0.00	0.00 ±0.00	0.00 ±0.00	0.03 ±0.00	0.00 ±0.00	0.00 ±0.00	0.00 ±0.00	0.01 ±0.00	0.03 ±0.00	0.00 ±0.00
	15	19.20 ±1.30	12.30 ±1.12	15.03 ±1.37	18.40 ±0.57	0.01 ±0.00	0.03 ±0.00	0.00 ±0.00	0.00 ±0.00	0.03 ±0.00	0.00 ±0.00	0.00 ±0.00	0.00 ±0.00	0.01 ±0.00	0.03 ±0.00	0.00 ±0.00
	25	19.20 ±1.30	10.64 ±1.64	9.33 ±0.87	8.63 ±1.19	0.00 ±0.00	0.03 ±0.00	0.00 ±0.00	0.00 ±0.00	0.02 ±0.00	0.00 ±0.00	0.00 ±0.00	0.00 ±0.00	0.01 ±0.00	0.03 ±0.00	0.00 ±0.00

Appendix 3e Summarized H_2O_2 effect for Pb

	H_2O_2 Amount (%)	Extraction (mg/g)														
		AQ	NA	HA	SA	CA	MA	TA	IL-A	IL-B	IL-C	IL-D	IL-E	IL-F	IL-G	W
Hotplate Method	5	108.00 ±2.24	4.00 ±0.65	7.50 ±1.22	0.40 ±0.08	0.30 ±0.08	0.53 ±0.12	0.30 ±0.08	0.58 ±0.02	0.42 ±0.08	0.48 ±0.09	0.37 ±0.05	0.45 ±0.11	0.58 ±0.06	0.28 ±0.10	0.04 ±0.00
	15	108.00 ±2.24	2.33 ±0.24	5.20 ±1.50	0.47 ±0.12	0.27 ±0.09	0.37 ±0.05	0.35 ±0.04	0.45 ±0.04	0.47 ±0.05	0.47 ±0.12	0.40 ±0.08	0.47 ±0.05	0.60 ±0.08	0.23 ±0.05	0.03 ±0.00
	25	108.00 ±2.24	2.00 ±0.41	3.50 ±0.71	0.57 ±0.12	0.23 ±0.05	0.37 ±0.05	0.40 ±0.00	0.40 ±0.08	0.47 ±0.05	0.40 ±0.14	0.40 ±0.14	0.47 ±0.05	0.33 ±0.05	0.27 ±0.09	0.02 ±0.00
Microwave Method	5	18.00 ±1.21	5.07 ±0.68	0.20 ±0.03	0.24 ±0.04	0.12 ±0.02	0.20 ±0.03	0.10 ±0.02	0.11 ±0.02	0.08 ±0.02	0.02 ±0.00	0.02 ±0.00	0.02 ±0.00	0.03 ±0.00	0.03 ±0.00	0.04 ±0.00
	15	18.00 ±1.21	6.50 ±0.41	3.40 ±0.28	0.20 ±0.02	0.12 ±0.03	0.17 ±0.03	0.07 ±0.01	0.11 ±0.01	0.07 ±0.02	0.02 ±0.00	0.02 ±0.00	0.02 ±0.00	0.03 ±0.00	0.03 ±0.00	0.03 ±0.00
	25	18.00 ±1.21	7.67 ±0.24	4.30 ±0.51	0.19 ±0.03	0.06 ±0.02	0.09 ±0.01	0.06 ±0.02	0.07 ±0.02	0.07 ±0.02	0.02 ±0.00	0.01 ±0.01	0.02 ±0.00	0.03 ±0.00	0.03 ±0.00	0.02 ±0.00

Appendix 4a Summarized temperature effect for Cu

	Temperature (^{0}C)	Extraction (mg/g)														
		AQ	NA	HA	SA	CA	MA	TA	IL-A	IL-B	IL-C	IL-D	IL-E	IL-F	IL-G	W
Hotplate Method	25.00	191.33 ±7.36	53.67 ±5.79	36.00 ±7.35	1.15 ±0.23	0.77 ±0.05	0.32 ±0.02	0.59 ±0.03	0.03 ±0.01	0.01 ±0.00	0.01 ±0.00	0.09 ±0.02	3.84 ±0.26	0.17 ±0.00	16.00 ±0.00	0.00 ±0.00
	40.00	210.00 ±15.30	110.00 ±10.80	71.67 ±12.47	3.20 ±0.65	0.84 ±0.04	0.33 ±0.02	0.75 ±0.07	0.12 ±0.01	0.02 ±0.00	0.02 ±0.00	0.30 ±0.04	5.52 ±0.39	0.71 ±0.08	69.60 ±3.39	0.00 ±0.00
	70.00	242.67 ±25.84	165.33 ±19.96	140.00 ±24.83	7.80 ±1.07	3.09 ±0.34	0.96 ±0.82	1.92 ±0.36	0.32 ±0.01	0.08 ±0.01	0.03 ±0.00	0.31 ±0.03	7.36 ±0.23	0.80 ±0.02	79.20 ±5.88	0.00 ±0.00

Appendix 4c Summarized temperature effect for Fe

	Temperature (^{0}C)	Extraction (mg/g)														
		AQ	**NA**	**HA**	**SA**	**CA**	**MA**	**TA**	**IL-A**	**IL-B**	**IL-C**	**IL-D**	**IL-E**	**IL-F**	**IL-G**	**W**
Hotplate Method	**25.00**	46.00 ±5.89	3.03 ±0.25	4.13 ±0.12	3.60 ±0.16	1.59 ±0.08	2.02 ±0.06	1.44 ±0.31	0.00 ±0.00	0.00 ±0.00	0.00 ±0.00	0.00 ±0.00	0.00 ±0.00	0.00 ±0.00	0.00 ±0.00	0.00 ±0.00
	40.00	87.50 ±6.12	4.80 ±0.59	8.93 ±0.41	6.60 ±0.49	1.28 ±0.06	1.63 ±0.07	1.26 ±0.19	0.00 ±0.00	0.00 ±0.00	0.00 ±0.00	0.00 ±0.00	0.00 ±0.00	0.00 ±0.00	0.00 ±0.00	0.00 ±0.00
	70.00	129.33 ±9.11	87.50 ±5.72	121.60 ±13.83	68.13 ±9.24	1.04 ±0.07	1.47 ±0.08	1.13 ±0.11	0.00 ±0.00	0.00 ±0.00	0.00 ±0.00	0.00 ±0.00	0.00 ±0.00	0.00 ±0.00	0.00 ±0.00	0.00 ±0.00

Appendix 4b Summarized temperature effect for Zn

	Temperature (^{0}C)	Extraction (mg/g)														
		AQ	**NA**	**HA**	**SA**	**CA**	**MA**	**TA**	**IL-A**	**IL-B**	**IL-C**	**IL-D**	**IL-E**	**IL-F**	**IL-G**	**W**
Hotplate Method	**25.00**	405.00 ±14.70	360.00 ±13.06	346.67 ±9.98	317.33 ±9.98	109.60 ±4.08	29.20 ±3.96	56.40 ±8.40	1.64 ±0.16	1.45 ±0.11	1.34 ±0.12	3.26 ±0.05	1.62 ±0.30	0.17 ±0.01	1.20 ±0.04	0.84 ±0.10
	40.00	462.00 ±30.59	357.33 ±9.98	357.33 ±3.77	333.33 ±9.98	153.60 ±3.92	63.20 ±4.93	62.40 ±2.40	0.16 ±0.01	0.12 ±0.00	0.56 ±0.07	44.27 ±2.00	45.33 ±2.00	38.40 ±1.31	40.00 ±1.31	0.25 ±0.02
	70.00	630.00 ±53.48	349.33 ±21.00	352.00 ±11.31	370.67 ±9.98	304.00 ±11.31	165.33 ±24.73	259.20 ±28.80	0.60 ±0.08	0.36 ±0.05	0.48 ±0.07	50.67 ±2.00	55.47 ±0.75	49.07 ±1.51	43.73 ±8.40	0.07 ±0.01

Appendix 4d Summarized temperature effect for Ni

	Temperature (^{0}C)	Extraction (mg/g)														
		AQ	NA	HA	SA	CA	MA	TA	IL-A	IL-B	IL-C	IL-D	IL-E	IL-F	IL-G	W
Hotplate Method	25.00	29.33 ±4.11	0.80 ±0.16	0.73 ±0.12	0.32 ±0.06	0.01 ±0.00	0.01 ±0.00	0.01 ±0.00	0.00 ±0.00	0.00 ±0.00	0.00 ±0.00	0.00 ±0.00	0.00 ±0.00	0.00 ±0.00	0.00 ±0.00	0.00 ±0.00
	40.00	48.00 ±4.90	1.70 ±0.25	1.20 ±0.24	0.67 ±0.10	0.01 ±0.00	0.01 ±0.00	0.01 ±0.00	0.00 ±0.00	0.00 ±0.00	0.00 ±0.00	0.00 ±0.00	0.00 ±0.00	0.00 ±0.00	0.00 ±0.00	0.00 ±0.00
	70.00	54.40 ±4.43	2.53 ±0.52	1.93 ±0.47	1.73 ±0.47	1.20 ±0.08	0.61 ±0.05	1.80 ±0.60	0.00 ±0.00	0.00 ±0.00	0.00 ±0.00	0.00 ±0.00	0.00 ±0.00	0.00 ±0.00	0.00 ±0.00	0.00 ±0.00

Appendix 4e Summarized temperature effect for Pb

	Temperature (^{0}C)	Extraction (mg/g)														
		AQ	NA	HA	SA	CA	MA	TA	IL-A	IL-B	IL-C	IL-D	IL-E	IL-F	IL-G	W
Hotplate Method	25.00	35.00 ±3.74	15.00 ±2.45	9.60 ±0.98	0.28 ±0.02	1.30 ±0.08	1.30 ±0.08	3.20 ±0.20	0.08 ±0.00	0.08 ±0.00	0.08 ±0.00	1.20 ±0.07	0.09 ±0.00	0.08 ±0.00	0.41 ±0.02	0.03 ±0.00
	40.00	44.33 ±7.19	19.50 ±1.22	17.50 ±1.87	0.38 ±0.02	1.40 ±0.08	2.60 ±0.16	1.55 ±0.05	0.08 ±0.00	0.07 ±0.00	0.07 ±0.00	1.33 ±0.10	0.10 ±0.00	0.08 ±0.01	0.45 ±0.04	0.03 ±0.00
	70.00	65.33 ±4.99	35.00 ±3.74	35.00 ±1.41	0.51 ±0.02	2.40 ±0.33	3.00 ±0.28	1.25 ±0.05	0.08 ±0.00	0.07 ±0.00	0.07 ±0.00	1.33 ±0.10	0.10 ±0.00	0.08 ±0.01	0.45 ±0.04	0.03 ±0.00

Appendix 5a Summarized time effect for Cu

	Time (minutes)	Extraction (mg/g)														
		AQ	NA	HA	SA	CA	MA	TA	IL-A	IL-B	IL-C	IL-D	IL-E	IL-F	IL-G	W
Hotplate Method	**30**	800.00 ±22.66	48.67 ±5.73	28.80 ±2.61	0.69 ±0.06	0.41 ±0.05	0.19 ±0.04	0.61 ±0.04	0.01 ±0.00	0.05 ±0.02	0.17 ±0.01	0.15 ±0.01	1.01 ±0.14	0.23 ±0.03	1.65 ±0.20	0.00 ±0.00
	60	800.00 ±22.66	90.00 ±8.16	55.47 ±4.42	0.81 ±0.03	0.49 ±0.06	0.39 ±0.06	0.74 ±0.03	0.02 ±0.00	0.05 ±0.02	0.18 ±0.01	0.32 ±0.01	2.72 ±0.35	0.52 ±0.03	6.93 ±0.54	0.00 ±0.00
	90	800.00 ±22.66	173.33 ±9.43	76.80 ±4.49	0.82 ±0.04	0.84 ±0.07	0.61 ±0.04	1.43 ±0.08	0.03 ±0.00	0.08 ±0.00	0.18 ±0.01	0.50 ±0.02	3.53 ±0.41	0.60 ±0.03	18.13 ±1.64	0.00 ±0.00
	120	800.00 ±22.66	320.00 ±26.13	184.00 ±6.53	2.80 ±0.20	1.07 ±0.10	0.80 ±0.05	1.61 ±0.08	0.03 ±0.00	0.09 ±0.02	0.19 ±0.01	0.67 ±0.03	5.79 ±0.13	0.90 ±0.04	92.00 ±6.53	0.00 ±0.00
	150	800.00 ±22.66	440.00 ±32.66	260.33 ±10.37	5.33 ±0.33	1.94 ±0.12	1.39 ±0.08	2.46 ±0.20	0.03 ±0.00	0.12 ±0.00	0.19 ±0.01	1.00 ±0.03	6.93 ±0.40	1.09 ±0.10	110.93 ±6.49	0.00 ±0.00
	180	800.00 ±22.66	613.33 ±120.37	320.67 ±12.26	15.67 ±2.49	2.22 ±0.13	2.03 ±0.10	5.44 ±0.34	0.04 ±0.00	0.16 ±0.00	0.20 ±0.01	1.36 ±0.07	6.93 ±0.54	4.37 ±0.33	202.67 ±13.60	0.00 ±0.00

Appendix 5b Summarized time effect for Zn

	Time (minutes)	Extraction (mg/g)														
		AQ	NA	HA	SA	CA	MA	TA	IL-A	IL-B	IL-C	IL-D	IL-E	IL-F	IL-G	W
Hotplate Method	**30.00**	603.00 ±14.70	304.00 ±17.28	344.00 ±13.06	296.00 ±9.73	173.33 ±18.41	78.33 ±3.12	318.40 ±21.59	0.08 ±0.01	0.13 ±0.01	0.62 ±0.01	45.33 ±2.00	34.67 ±2.00	38.93 ±5.28	41.60 ±2.61	0.02 ±0.00
	60.00	603.00 ±14.70	325.33 ±13.60	354.67 ±7.54	322.67 ±13.60	230.00 ±14.72	105.00 ±2.45	323.20 ±23.95	0.10 ±0.02	0.13 ±0.01	0.62 ±0.01	46.93 ±2.00	37.87 ±2.00	45.87 ±3.02	46.40 ±4.71	0.02 ±0.00
	90.00	603.00 ±14.70	341.33 ±13.20	362.67 ±15.08	338.67 ±13.60	255.00 ±24.49	129.50 ±2.86	329.60 ±19.73	0.14 ±0.02	0.14 ±0.01	0.63 ±0.01	48.53 ±2.00	42.67 ±3.99	49.07 ±3.02	50.13 ±3.77	0.03 ±0.00
	120.00	603.00 ±14.70	354.67 ±3.77	365.33 ±7.54	333.33 ±9.98	293.33 ±26.56	158.67 ±6.80	336.23 ±13.03	0.17 ±0.02	0.15 ±0.00	0.64 ±0.01	48.53 ±0.75	44.33 ±3.30	49.60 ±2.26	53.33 ±0.75	0.03 ±0.00
	150.00	603.00 ±14.70	354.67 ±7.54	373.33 ±13.60	325.33 ±7.54	328.33 ±6.24	161.33 ±4.99	340.80 ±17.96	0.18 ±0.01	0.15 ±0.01	0.66 ±0.01	50.13 ±0.75	47.13 ±5.28	55.47 ±6.03	54.40 ±2.26	0.05 ±0.01
	180.00	603.00 ±14.70	381.13 ±16.44	371.08 ±13.60	344.00 ±6.53	333.33 ±6.24	162.67 ±6.80	350.40 ±19.60	0.20 ±0.04	0.15 ±0.00	0.66 ±0.01	50.13 ±1.51	34.53 ±14.52	57.07 ±6.03	54.93 ±0.75	0.06 ±0.01

Appendix 5c Summarized time effect for Fe

	Time (minutes)	Extraction (mg/g)														
		AQ	NA	HA	SA	CA	MA	TA	IL-A	IL-B	IL-C	IL-D	IL-E	IL-F	IL-G	W
Hotplate Method	30.00	296.00 ±8.98	53.34 ±2.12	28.09 ±2.87	38.27 ±1.68	0.51 ±0.03	0.63 ±0.02	0.51 ±0.35	0.00 ±0.00	0.00 ±0.00	0.00 ±0.00	0.10 ±0.00	0.00 ±0.00	0.00 ±0.00	0.00 ±0.00	0.00 ±0.00
	60.00	296.00 ±8.98	62.62 ±4.54	69.00 ±6.48	41.61 ±2.98	0.89 ±0.08	1.24 ±0.12	1.08 ±0.63	0.00 ±0.00	0.00 ±0.00	0.00 ±0.00	0.47 ±0.03	0.00 ±0.00	0.00 ±0.00	0.00 ±0.00	0.00 ±0.00
	90.00	296.00 ±8.98	98.25 ±10.38	117.32 ±13.58	94.05 ±8.35	1.48 ±0.20	2.02 ±0.17	1.14 ±0.60	0.00 ±0.00	0.00 ±0.00	0.00 ±0.00	0.77 ±0.05	0.00 ±0.00	0.00 ±0.00	0.00 ±0.00	0.00 ±0.00
	120.00	296.00 ±8.98	184.33 ±8.73	206.93 ±13.15	115.73 ±11.51	2.21 ±0.10	2.69 ±0.16	1.71 ±0.83	0.00 ±0.00	0.00 ±0.00	0.00 ±0.00	0.97 ±0.02	0.00 ±0.00	0.00 ±0.00	0.00 ±0.00	0.00 ±0.00
	150.00	296.00 ±8.98	226.67 ±21.00	235.67 ±11.90	147.66 ±6.50	2.80 ±0.16	3.27 ±0.17	1.75 ±0.74	0.00 ±0.00	0.00 ±0.00	0.00 ±0.00	1.17 ±0.06	0.00 ±0.00	0.00 ±0.00	0.00 ±0.00	0.00 ±0.00
	180.00	296.00 ±8.98	228.00 ±4.24	248.27 ±15.62	180.00 ±17.64	3.92 ±0.30	3.80 ±0.37	2.55 ±0.86	0.00 ±0.00	0.00 ±0.00	0.00 ±0.00	1.50 ±0.13	0.00 ±0.00	0.00 ±0.00	0.00 ±0.00	0.00 ±0.00

Appendix 5d Summarized time effect for Ni

	Time (minutes)	Extraction (mg/g)														
		AQ	NA	HA	SA	CA	MA	TA	IL-A	IL-B	IL-C	IL-D	IL-E	IL-F	IL-G	W
Hotplate Method	30.00	52.80 ±3.39	1.01 ±0.10	0.30 ±0.07	0.54 ±0.07	0.80 ±0.07	0.07 ±0.01	0.69 ±0.11	0.00 ±0.00	0.00 ±0.00	0.00 ±0.00	0.00 ±0.00	0.00 ±0.00	0.00 ±0.00	0.00 ±0.00	0.00 ±0.00
	60.00	52.80 ±3.39	1.30 ±0.08	0.49 ±0.10	0.73 ±0.05	1.40 ±0.16	0.17 ±0.02	0.73 ±0.05	0.00 ±0.00	0.00 ±0.00	0.00 ±0.00	0.00 ±0.00	0.00 ±0.00	0.00 ±0.00	0.00 ±0.00	0.00 ±0.00
	90.00	52.80 ±3.39	2.00 ±0.99	0.77 ±0.09	0.63 ±0.05	1.53 ±0.09	0.31 ±0.04	0.63 ±0.05	0.00 ±0.00	0.00 ±0.00	0.00 ±0.00	0.00 ±0.00	0.00 ±0.00	0.00 ±0.00	0.00 ±0.00	0.00 ±0.00
	120.00	52.80 ±3.39	2.07 ±0.90	1.40 ±0.28	1.47 ±0.09	1.55 ±0.11	0.41 ±0.07	1.47 ±0.09	0.00 ±0.00	0.00 ±0.00	0.00 ±0.00	0.00 ±0.00	0.00 ±0.00	0.00 ±0.00	0.00 ±0.00	0.00 ±0.00
	150.00	52.80 ±3.39	2.27 ±1.05	1.67 ±0.09	1.67 ±0.09	1.54 ±0.10	0.41 ±0.07	1.67 ±0.09	0.00 ±0.00	0.00 ±0.00	0.00 ±0.00	0.00 ±0.00	0.00 ±0.00	0.00 ±0.00	0.00 ±0.00	0.00 ±0.00
	180.00	52.80 ±3.39	2.33 ±0.96	1.93 ±0.25	1.53 ±0.09	1.55 ±0.11	0.41 ±0.07	1.53 ±0.09	0.00 ±0.00	0.00 ±0.00	0.00 ±0.00	0.00 ±0.00	0.00 ±0.00	0.00 ±0.00	0.00 ±0.00	0.00 ±0.00

Appendix 5e Summarized time effect for Pb

	Time (minutes)	Extraction (mg/g)														
		AQ	NA	HA	SA	CA	MA	TA	IL-A	IL-B	IL-C	IL-D	IL-E	IL-F	IL-G	W
Hotplate Method	30.00	71.67 ±2.87	9.67 ±1.25	6.33 ±1.25	0.19 ±0.01	1.00 ±0.16	0.93 ±0.12	0.53 ±0.05	0.05 ±0.01	0.04 ±0.00	0.05 ±0.01	0.09 ±0.01	0.04 ±0.01	0.03 ±0.00	0.16 ±0.00	0.03 ±0.00
	60.00	71.67 ±2.87	11.60 ±2.04	11.20 ±0.57	0.26 ±0.05	1.13 ±0.12	1.33 ±0.12	0.74 ±0.04	0.04 ±0.02	0.05 ±0.00	0.06 ±0.00	0.18 ±0.02	0.05 ±0.00	0.04 ±0.00	0.28 ±0.00	0.03 ±0.00
	90.00	71.67 ±2.87	18.67 ±3.29	16.50 ±2.45	0.41 ±0.01	1.30 ±0.08	1.60 ±0.08	0.87 ±0.05	0.06 ±0.01	0.06 ±0.00	0.07 ±0.01	0.80 ±0.07	0.05 ±0.01	0.06 ±0.01	0.32 ±0.00	0.03 ±0.00
	120.00	71.67 ±2.87	30.00 ±4.08	32.50 ±2.04	0.49 ±0.02	2.47 ±0.34	3.07 ±0.09	1.20 ±0.08	0.07 ±0.01	0.07 ±0.00	0.07 ±0.01	1.12 ±0.07	0.10 ±0.00	0.05 ±0.02	0.39 ±0.02	0.03 ±0.00
	150.00	71.67 ±2.87	37.00 ±2.83	41.00 ±1.41	0.67 ±0.02	2.40 ±0.16	4.27 ±0.38	2.33 ±0.19	0.07 ±0.02	0.08 ±0.00	0.07 ±0.01	1.12 ±0.07	0.11 ±0.01	0.07 ±0.01	0.43 ±0.01	0.03 ±0.00
	180.00	71.67 ±2.87	42.00 ±2.86	50.17 ±5.95	0.82 ±0.07	3.00 ±0.16	7.73 ±0.38	2.80 ±0.33	0.08 ±0.02	0.08 ±0.01	0.08 ±0.00	1.20 ±0.07	0.11 ±0.01	0.07 ±0.01	0.55 ±0.05	0.03 ±0.00

Appendix 6a Summarized concentration effect for Cu

	Concentration	Extraction (mg/g)														
		AQ	NA	HA	SA	CA	MA	TA	IL-A	IL-B	IL-C	IL-D	IL-E	IL-F	IL-G	W
Hotplate Method	Conc1	242.67 ±25.84	125.00 ±20.41	37.50 ±21.31	0.57 ±0.05	2.42 ±0.28	2.44 ±0.25	2.18 ±0.24	0.09 ±0.01	0.03 ±0.00	0.03 ±0.00	0.47 ±0.01	5.23 ±0.70	0.23 ±0.02	52.27 ±3.49	0.00 ±0.00
	Conc2	242.67 ±31.44	170.67 ±9.98	32.80 ±17.73	1.20 ±0.07	2.54 ±0.30	2.38 ±0.24	2.08 ±0.31	0.11 ±0.01	0.08 ±0.02	0.03 ±0.00	0.42 ±0.13	5.12 ±0.30	0.77 ±0.02	65.33 ±4.99	0.00 ±0.00
	Conc3	242.67 ±28.74	230.67 ±12.36	23.67 ±16.13	2.99 ±0.20	2.68 ±0.20	2.28 ±0.13	2.00 ±0.33	0.25 ±0.01	0.10 ±0.02	0.04 ±0.00	0.31 ±0.06	0.77 ±0.07	1.17 ±0.16	205.33 ±33.52	0.00 ±0.00
Microwave Method	Conc1	682.67 +12.39	296.00 ±7.76	6.72 ±1.30	0.13 ±0.06	0.18 ±0.01	0.17 ±0.06	0.12 ±0.06	0.24 ±0.02	0.23 ±0.02	0.23 ±0.03	0.24 ±0.02	2.24 ±0.07	0.25 ±0.01	3.56 ±0.11	0.00 ±0.00
	Conc2	682.67 +12.39	306.67 ±4.94	9.04 ±1.23	0.33 ±0.08	0.16 ±0.02	0.99 ±0.17	0.27 ±0.07	0.25 ±0.01	0.25 ±0.01	0.24 ±0.02	0.25 ±0.02	2.40 ±0.13	0.28 ±0.03	4.08 ±0.52	0.00 ±0.00
	Conc3	682.67 +12.39	325.33 ±3.99	11.67 ±0.87	0.12 ±0.04	0.16 ±0.04	0.95 ±0.12	0.67 ±0.15	0.28 ±0.01	0.28 ±0.00	0.26 ±0.02	0.28 ±0.01	2.59 ±0.14	0.29 ±0.04	4.24 ±0.57	0.00 ±0.00

Where Conc1 = inorganic acid (1 M), organic acid (15 g/L) and ionic liquids (50 g/L), Conc2 = inorganic (2 M), organic (25 g/L) and ionic liquids (100 g/L),

Conc3 = inorganic (3 M), organic (50 g/L) and ionic liquids (250 g/L).

Appendix 6b Summarized concentration effect for Zn

	Concentration (M)	Extraction (mg/g)													
		AQ	NA	HA	SA	CA	MA	TA	IL-A	IL-B	IL-C	IL-D	IL-E	IL-F	IL-G	W
Hotplate Method	Conc1	552.00 ±11.22	320.00 ±13.06	361.33 ±8.60	344.00 ±19.60	148.80 ±7.84	197.33 ±8.22	242.40 ±7.20	0.15 ±0.01	0.12 ±0.03	0.61 ±0.10	45.33 ±2.00	28.80 ±0.98	39.47 ±2.00	49.60 ±3.92	0.07 ±0.01
	Conc2	552.00 ±11.22	341.33 ±16.44	365.00 ±11.31	333.33 ±9.98	304.00 ±11.31	165.33 ±24.73	259.20 ±28.80	0.15 ±0.02	0.12 ±0.02	0.59 ±0.08	49.60 ±1.31	42.00 ±2.29	49.07 ±2.72	56.53 ±2.72	0.07 ±0.01
	Conc3	552.00 ±11.22	389.33 ±9.98	368.00 ±13.06	362.67 ±3.77	304.00 ±4.53	144.00 ±6.53	295.20 ±16.80	0.18 ±0.01	0.13 ±0.02	0.61 ±0.08	59.20 ±1.31	60.27 ±0.75	77.33 ±2.00	58.67 ±2.00	0.07 ±0.01
Microwave Method	Conc1	314.13 ±20.85	180.00 ±14.49	126.00 ±14.88	153.60 ±10.65	52.00 ±3.15	72.00 ±1.03	69.60 ±1.00	76.80 ±5.18	89.60 ±17.12	128.00 ±5.66	122.40 ±3.39	83.20 ±4.93	124.00 ±34.41	136.00 ±14.97	0.07 ±0.01
	Conc2	314.13 ±20.85	208.00 ±19.87	180.80 ±14.66	59.87 ±19.67	60.00 ±4.49	66.00 ±1.81	108.80 ±1.00	109.87 ±10.88	138.67 ±10.88	208.00 ±13.06	202.67 ±15.08	118.40 ±4.53	192.00 ±26.13	190.93 ±24.83	0.07 ±0.01
	Conc3	314.13 ±20.85	41.60 ±12.92	211.20 ±13.56	48.99 ±12.47	112.00 ±3.41	57.60 ±1.70	82.80 ±2.00	137.60 ±15.89	141.87 ±5.44	232.53 ±6.58	227.20 ±4.53	126.93 ±6.58	213.33 ±30.17	222.93 ±27.44	0.07 ±0.01

Where Conc1 = inorganic acid (1 M), organic acid (15 g/L) and ionic liquids (50 g/L), Conc2 = inorganic (2 M), organic (25 g/L) and ionic liquids (100 g/L),

Conc3 = inorganic (3 M), organic (50 g/L) and ionic liquids (250 g/L).

Appendix 6c Summarized concentration effect for Fe

	Concentration	Extraction (mg/g)													
		AQ	NA	HA	SA	CA	MA	TA	IL-A	IL-B	IL-C	IL-D	IL-E	IL-F	IL-G	W
Hotplate Method	**Conc1**	132.00 ±3.27	52.50 ±7.36	70.00 ±4.08	72.00 ±3.92	1.90 ±0.10	1.52 ±0.19	0.73 ±0.20	0.00 ±0.00	0.00 ±0.00	0.00 ±0.00	0.00 ±0.00	0.00 ±0.00	0.00 ±0.00	0.00 ±0.00	0.00 ±0.00
	Conc2	132.00 ±3.27	95.67 ±7.19	101.33 ±3.99	95.20 ±2.29	1.08 ±0.06	1.27 ±0.19	3.78 ±4.40	0.00 ±0.00	0.00 ±0.00	0.00 ±0.00	0.92 ±0.03	0.00 ±0.00	0.00 ±0.00	0.00 ±0.00	0.00 ±0.00
	Conc3	132.00 ±3.27	117.33 ±13.20	117.80 ±8.21	103.47 ±5.44	1.01 ±0.04	0.92 ±0.07	5.67 ±6.60	0.00 ±0.00	0.00 ±0.00	0.00 ±0.00	2.38 ±0.12	0.00 ±0.00	0.00 ±0.00	0.09 ±0.01	0.00 ±0.00
Microwave Method	**Conc1**	84.60 ±6.15	23.20 ±2.99	22.32 ±1.18	15.60 ±0.90	1.23 ±0.11	1.06 ±0.00	1.36 ±0.28	0.00 ±0.00	0.00 ±0.00	0.00 ±0.00	0.00 ±0.00	0.00 ±0.00	0.00 ±0.00	0.00 ±0.00	0.00 ±0.00
	Conc2	84.60 ±6.15	39.00 ±8.49	52.48 ±8.16	21.65 ±1.40	1.78 ±0.12	1.88 ±0.24	1.77 ±0.57	0.00 ±0.00	0.00 ±0.00	0.00 ±0.00	0.00 ±0.00	0.00 ±0.00	0.00 ±0.00	0.00 ±0.00	0.00 ±0.00
	Conc3	84.60 ±6.15	47.84 ±3.00	49.00 ±3.02	35.73 ±2.00	2.11 ±0.23	2.64 ±0.02	2.25 ±0.89	0.00 ±0.00	0.00 ±0.00	0.00 ±0.00	0.00 ±0.00	0.00 ±0.00	0.00 ±0.00	0.00 ±0.00	0.00 ±0.00

Where Conc1 = inorganic acid (1 M), organic acid (15 g/L) and ionic liquids (50 g/L), Conc2 = inorganic (2 M), organic (25 g/L) and ionic liquids (100 g/L),

Conc3 = inorganic (3 M), organic (50 g/L) and ionic liquids (250 g/L).

Appendix 6d Summarized concentration effect for Ni

	Concentration	Extraction (mg/g)													
		AQ	NA	HA	SA	CA	MA	TA	IL-A	IL-B	IL-C	IL-D	IL-E	IL-F	IL-G	W
Hotplate Method	**Conc1**	54.40 ±4.93	3.40 ±0.16	8.13 ±9.52	1.07 ±0.19	0.90 ±0.08	0.19 ±0.04	0.80 ±0.10	0.00 ±0.00	0.00 ±0.00	0.00 ±0.00	0.00 ±0.00	0.00 ±0.00	0.00 ±0.00	0.00 ±0.00	0.00 ±0.00
	Conc2	54.40 ±4.93	2.53 ±0.52	1.93 ±0.47	1.33 ±0.09	1.07 ±0.12	0.61 ±0.05	1.20 ±0.00	0.00 ±0.00	0.00 ±0.00	0.00 ±0.00	0.00 ±0.00	0.00 ±0.00	0.00 ±0.00	0.00 ±0.00	0.00 ±0.00
	Conc3	54.40 ±4.93	2.53 ±0.25	1.80 ±0.16	1.13 ±0.81	1.07 ±0.12	0.53 ±0.05	1.70 ±0.10	0.00 ±0.00	0.00 ±0.00	0.00 ±0.00	0.00 ±0.00	0.00 ±0.00	0.00 ±0.00	0.00 ±0.00	0.00 ±0.00
Microwave Method	**Conc1**	26.15 ±1.04	1.04 ±0.07	0.84 ±0.10	0.60 ±0.08	0.13 ±0.02	0.05 ±0.01	0.04 ±0.00	0.00 ±0.00	0.00 ±0.00	0.00 ±0.00	0.00 ±0.00	0.00 ±0.00	0.00 ±0.00	0.00 ±0.00	0.00 ±0.00
	Conc2	26.15 ±1.04	1.96 ±0.11	0.96 ±0.10	0.93 ±0.17	0.19 ±0.03	0.07 ±0.02	0.07 ±0.01	0.00 ±0.00	0.00 ±0.00	0.00 ±0.00	0.00 ±0.00	0.00 ±0.00	0.00 ±0.00	0.00 ±0.00	0.00 ±0.00
	Conc3	26.15 ±1.04	3.84 ±0.20	0.69 ±0.10	1.26 ±0.11	0.21 ±0.02	0.08 ±0.02	0.08 ±0.01	0.00 ±0.00	0.00 ±0.00	0.00 ±0.00	0.00 ±0.00	0.00 ±0.00	0.00 ±0.00	0.00 ±0.00	0.00 ±0.00

Where Conc1 = inorganic acid (1 M), organic acid (15 g/L) and ionic liquids (50 g/L), Conc2 = inorganic (2 M), organic (25 g/L) and ionic liquids (100 g/L),

Conc3 = inorganic (3 M), organic (50 g/L) and ionic liquids (250 g/L).

Appendix 6e Summarized concentration effect for Pb

	Concentration (M)	Extraction (mg/g)														
		AQ	NA	HA	SA	CA	MA	TA	IL-A	IL-B	IL-C	IL-D	IL-E	IL-F	IL-G	W
Hotplate Method	Conc1	65.33 ±4.99	10.23 ±0.92	11.00 ±1.40	0.55 ±0.02	1.17 ±0.12	1.80 ±0.16	1.05 ±0.05	0.05 ±0.00	0.05 ±0.01	0.05 ±0.01	0.44 ±0.03	0.09 ±0.00	0.08 ±0.01	0.40 ±0.03	0.00 ±0.00
	Conc2	65.33 ±4.99	35.00 ±3.74	34.00 ±1.41	0.60 ±0.08	2.33 ±0.25	3.27 ±0.25	1.35 ±0.05	0.08 ±0.00	0.07 ±0.00	0.08 ±0.00	1.17 ±0.10	0.10 ±0.00	0.08 ±0.01	0.44 ±0.03	0.00 ±0.00
	Conc3	65.33 ±4.99	38.50 ±2.86	44.00 ±0.00	0.40 ±0.08	2.53 ±0.25	3.47 ±0.50	1.45 ±0.05	0.07 ±0.01	0.07 ±0.01	0.07 ±0.01	1.28 ±0.13	0.11 ±0.00	0.09 ±0.01	0.43 ±0.04	0.00 ±0.00
Microwave Method	Conc1	426.67 ±8.06	192.00 ±9.80	112.00 ±9.90	0.33 ±0.00	0.56 ±0.03	0.44 ±0.01	0.49 ±0.04	0.33 ±0.00	0.33 ±0.00	0.33 ±0.00	0.33 ±0.02	0.33 ±0.00	0.03 ±0.00	0.33 ±0.00	0.03 ±0.00
	Conc2	426.67 ±8.06	208.00 ±5.66	144.67 ±5.95	0.33 ±0.00	0.61 ±0.05	0.61 ±0.03	0.56 ±0.04	0.33 ±0.00	0.33 ±0.00	0.33 ±0.00	0.33 ±0.02	0.33 ±0.00	0.03 ±0.00	0.33 ±0.00	0.02 ±0.00
	Conc3	426.67 ±8.06	288.00 ±8.80	158.67 ±6.50	0.33 ±0.00	0.61 ±0.02	0.61 ±0.04	0.70 ±0.03	0.33 ±0.00	0.33 ±0.00	0.33 ±0.00	0.33 ±0.02	0.33 ±0.00	0.03 ±0.00	0.33 ±0.00	0.02 ±0.00

Where Conc1 = inorganic acid (1 M), organic acid (15 g/L) and ionic liquids (50 g/L), Conc2 = inorganic (2 M), organic (25 g/L) and ionic liquids (100 g/L),

Conc3 = inorganic (3 M), organic (50 g/L) and ionic liquids (250 g/L).